Trinity College Dublin
Coláiste na Tríonóide, Baile Átha Cliath
The University of Dublin

Targeting the Prostate Cancer Metabolome with Novel Trojan Horse Compounds.

Ms. Laura Bogue Edgerton BSc BScHons AMRSC

Molecular Pathology Research Group

The Coombe Women and Infants University Hospital and Trinity College Dublin

A thesis submitted to Trinity College Dublin, the University of Dublin

for the award of Doctor of Histopathology and Morbid Anatomy

March 2023

Under the supervision of:

Professor John O'Leary, Professor Doug Brooks, and Doctor Prerna Tewari

Declaration

I declare that this thesis has not been submitted as an exercise for a degree at this or any other university and it is entirely my own work. I agree to deposit this thesis in the University's open access institutional repository or allow the library to do so on my behalf, subject to Irish Copyright Legislation and Trinity College Library conditions of use and acknowledgement. I have read and I understand the plagiarism provisions in the General Regulations of the University Calendar for the current year, found a http://www.tcd.ie/calendar.

I have also completed the Online Tutorial on avoiding plagiarism 'Ready Steady Write', located at http://tcd-ie.libguides.com/plagiarism/ready-steady-write.

Acknowledgements

Firstly, I must thank my supervisors, Prof. John O'Leary, and Dr. Prerna Tewari from TCD and Prof. Doug Brooks from UniSA for the opportunity to pursue a PhD in a field I have become so passionate about, allowing my knowledge and love for science to grow and expand. John, I wish you good health and happiness in your future, I known the past year has been quite the curveball. I'd also like to thank Envision Biosciences for funding my studentship, throughout a global pandemic, and for the past 4.5 years. From UniSA I would also like to thank Dr. Brooks and Ms. Eva Hayball for all of the hard work in preparing and synthesizing the novel compounds for this work to be achieved. I'd also like to send a thanks to Prof. Cara Martin for her support since day one and for helping me get things done. I'd like to thank Prof. Stavros Selemidis for his kindness and extensive knowledge in all things related to ROS. I'd like to thank Dr. Sharon O'Toole, Dr. Lucy Norris, Dr Christine White, Dr Stephen Reynolds, Dr. Mark Ward, Dr. Tanya Kelly, Dr. Bashir Mohammed, Dr. Ola Ibrahim, and Dr. Roisin O'Connor of the molecular pathology research group here in TCD for the kindness, reassurance, support, and advice throughout these tough 4.5 years. Coming from a non-biology background, the understanding and patience you have all shown me has allowed me to grow as a scientist and as a person. I have enjoyed learning new things from and with you all.

Next, I must thank my beautiful giant family, without you I would not be here, nor would I have had the strength, and belief in myself to continue through this challenging process. To my parents, Ron and Louise, your faith and love for me forever blows my mind. I could never ask for better, more supportive parents, but I also have grown to love the ways in which you challenge me (dad specifically) to keep me on my toes, it's definitely made me the strong young woman that I can say I am very proud to be. Thank you for teaching me to take no nonsense from anyone and to believe in myself. The fact that both of you are cancer survivors pushed me on the days I wanted to quit, I would remember the challenges you both faced throughout your journeys, and it inspired me to continue to push myself with the hopes of improving even the life of one person with cancer.

Thank you to my brother Graham for helping me achieve this PhD studentship. Our relationship may not always be dandy, but I always love you and your beautiful children, nonetheless. To my sisters, Cara, Sarah, Jill, and Nicole. Your eternal

confidence in my abilities in everything I do still takes me by surprise, every time it crosses my path.

Cara, thank you for being one I can talk to, you have been a vital support during the toughest times in my life especially over the past few years, thank you for being so open with me and for sharing your beautiful family with me, they light up my life.

SJ, the fact you seem to think I am the smartest human on the planet makes me laugh and helps with my undeniable imposter syndrome. Your girls bring me so much joy and bring sunshine to my tough days, I can't wait to meet Sebby.

Jill, for all the cups of tea, and chats about life to help from the stress of thesis writing. I love you and your beautiful family so much; my best pals Luan and Evan have become my solace and safe place when I am stressed and sad and just need some cuddles, I hope my relationship with your boys continues to bloom and grow.

Finally, Nicki… what can I say about you. Your ridiculous charm and humor has been the light of my life ever since you were born. You are my best friend and my baby sister, yet you have been the one to 'big sister' me, just when I needed it, Thank you.

I'd also like to acknowledge my beautiful pupper 'Stinky' Hopie. I know your time is limited on this earth, with the end getting ever nearer, but you have been my rock through the 17.5 amazing years we have had together. Through my junior cert, leaving cert, undergrad and now my PhD and I have loved having you live with me while writing my thesis.

To my 'mom' Aunt Iris, you are the best second mum a girl could ask for, thank you for housing me, feeding me, and loving me in between late nights and weekend timepoints in the lab and treating me like your daughter. I will forever be grateful.

To my dearest grandad Paddy, we lost you last year to cancer. I know how proud you were of me and how you learned some science mumbo jumbo to tell everyone about your granddaughter who was becoming a doctor. I'm sorry you aren't here to see my dreams come true, but I know you are with me in spirit. I am so grateful that I was placed in James's as you became sicker, and I could spend my lunch time visiting you. You were such a gentle giant, and we miss you dearly.

I want to thank my beautiful nieces Holly and Suzie. You both have no idea how much you inspire me to be a strong woman in a world where things may be improving but being a woman can still be very hard. I want you to live in a world where you can be powerful in everything that you do and to have as few obstacles reaching all of your goals. I didn't know love until you two came along. Please continue to be incredible and individual, that is hard to find these days.

To my incredible, science sisters; Fiona O'Connell, Laura Kane, and Eimear Mylod… or should I say Doctors. One of the best things about this PhD has been meeting you guys. Through thick and thin, you have all been the best friends a girl could ask for. You took me under your wings when I was a lost soul in TTMI. You treated me like family from the get-go and for that, I can never thank you enough. You are all incredible strong women who I admire so greatly, without you all I question my strength to continue through the tough times of the PhD. I have learned so much from you all and I cannot wait to see the greatness that comes from you all next. Friends are your chosen family, and my god, did I win the lottery.

Oh Lady La! Your patience, humor and your infectious laugh are some of my favorite memories from the PhD. Our Raura walks (or walking rants) were like therapy during tough times. Thank you for being such a beautiful human and friend and thank you for your incredible formatting skills! I'm so lucky to have a friend like you and I am so beyond proud of how you have become stronger and stronger fighting your own corner and demanding the respect you so deserve. Eimear our love of trash TV and the zara app has just brought us closer and closer and I can certainly say you are in my inner circle and one of the best people ever! Thank you for being hilarious, strong, and inspiring throughout our time together in and out of the lab. Your use of the word "violent" for the things you dislike have brought all of us so much laughter, you are a shining star, and I am so grateful to have a friend like you. Finally, I want to add an extra little thank you to Fi. My god Fi your unbelievable patience to help me both in the lab and out is beyond comprehension. You are the kindest soul I have ever encountered; no task is too big; you are always there with bells on (and with a coffee or Fanta in hand). I can't say thank you enough, you are going to do incredible things in this world, and I cannot wait to see them.

Thank you to Christine Butler for your kindness and support throughout the PhD.

Chonaill and Dr. Laura, I can’t leave you guys out of here. Thank you for being like family to me, your offers of dinners, wine, being a model for my presentations (Chonaill), board games, Buddy cuddles and sorting giant data files are just some of the incredible things you have done even in just the last few months of thesis writing.

Ryan, you came into my life at a pinnacle moment, the PhD was getting tougher and tougher, the world was in chaos with a global pandemic, but you made me forget all of that and turned everything golden. I thought I was happy until I met you, but you radiate sunshine, like no one I’ve ever seen and to get to spend my days with you, I can’t be anything but content. You are the best thing I have gotten from these difficult 4.5 years, and it was worth every second, just to have met you. Your goodness and strength is inconceivable and I hope I can continue to learn from you. Thank you for choosing me, I love you.

To end, my final thank you goes to my examiners, for taking the time out of their busy schedules to read my research and to attend my viva.

Abstract

Prostate cancer (PCa) is the second most common cancer diagnosed in males worldwide, and the incidence of this disease is predicted to double globally by 2030. In Ireland, PCa accounts for nearly 16% of all invasive cancers diagnosed annually. While approximately 70% of all prostate cancer patients display an initial response to androgen ablation therapy, eventually patients become unresponsive to further anti-androgen therapy. With this, the androgen independent prostate cancer is considered incurable.

Cancer cells tend to employ aerobic glycolysis, the "Warburg effect" to meet their energy demands. Although, much more inefficient in terms of ATP production when compared to Oxidative Phosphorylation (OxPhos) employed by normal cells, this process is quicker and tends to use glucose 100 times faster. Our group in collaboration with University of South Australia has developed a unique 'Trojan Horse' chemotherapeutic strategy that exploits the Warburg effect to target the prostate cancer metabolome and multiple aspects of the disease biology. The approach involves generating a series of compounds by complexing Vitamin C and Vitamin K3 with sugars and lipids.

A panel of prostate cancer cell lines (LNCAP, PC3, DU154) representing varying stages of disease progression and a non-malignant cell line (PNT-1a) were tested with 10 Trojan Horse (TH) compounds to determine the cytotoxicity of the compounds under 3 physiological glucose conditions. Three TH compounds; two glucose Menadione and one lipid Menadione based demonstrated significant cytotoxic effects. To evaluate the effects of these compounds on the PCa metabolome, the metabolic bioenergetic profiles of the panel of cell lines mentioned above were examined with the seahorse XFe2 Bioanalyzer following treatments with the three TH compounds. Flow cytometry and immunofluorescence-based assays were performed in parallel to determine levels of reactive oxygen species (ROS) and measure changes in mitochondrial membrane potential. LC-MS analysis was also performed to identify metabolites which could map specific metabolic phenotypes displayed by the cell lines.

The androgen independent cell lines PC3 and Du145 displayed a greater reliance on glycolysis for ATP production which shifted marginally towards energy production by OxPhos following treatment with TH compounds. LNCAP the androgen dependent cell line was heavily dependent on OxPhos, and no change was observed in its metabolic capacity following treatment with TH compounds. An increase in reactive oxygen species (ROS) levels and alterations in mitochondrial membrane potential (MMP) were observed following TH treatments, but not to the levels expected. The results of the metabolomic analysis were in agreement with the metabolic bioenergetic profiles displayed by the cell lines pre and post TH treatment. LC-MS analysis also identified a significant increase in ROS scavenging amino acids which would account for the lower ROS levels and changes in MMP following TH treatments.

The findings highlight the differences in metabolic phenotypes between androgen dependent and independent PCa and indicate a role for metabolic targeting by TH compounds.

Presentations, Publications, Awards and Outreach

Poster Presentations:

- Irish Association of Cancer Research (IACR), 30/03/2022, Little Island, Co. Cork – Varying Levels of Physiological Glucose Affects the Metabolic Bioenergetics of Prostate Cancer Cells.
- Cancer Metabolism Showcase and Workshop Meeting, Virtual, 04/04/2022 – Varying Levels of Glucose Affects the Metabolic Bioenergetics Profiles of Prostate Cancer Cells.
- Keystone Symposia Tumour Metabolism 2022, Banff Canada – Varying Levels of Physiological Glucose Affects the Metabolic Bioenergetics Profiles of Prostate Cancer Cells.
- European Association of Cancer Research, Seville Spain, 20/06/2022- Varying Levels of Physiological Glucose Affects the Metabolic Bioenergetics Profiles of Prostate Cancer Cells.
- 12th International Cancer Conference, Trinity Biomedical Science Institute, Dublin, 13/10/2022- The Impact of Varying Glucose milieu on the Metabolic Bioenergetic Profiles of Prostate Cancer Cells.
- 12th International Cancer Conference, Trinity Biomedical Science Institute, Dublin, 13/10/2022- Targeting Cancers Sweet Tooth with Novel Trojan Horse Compounds.

Oral Presentations:

- International Conference for Healthcare and Medical Students, 2022, Virtual, 11/02/2022- Varying Levels of Physiological Glucose Affects the Metabolic Bioenergetics Profiles of Prostate Cancer Cells.
- IACR 2022, Patrick G Johnston Presentation, Little Island Cork, 30/03/2022- Targeting Cancers Sweet Tooth with Novel Trojan Horse Compounds.

Publications:

- Lazniewska J, Lok Li K, Johnson I, Sorvina A, Logan J, Martini C, Moore C, Ung B, Hickey S, Karageorgos L, Prabhakaran S, Heatlie J, Brooks R, Huzzell C, Warnock N, Ward M, Mohammed B, Tewari P, Martin C, O'Toole S, Bogue Edgerton L, Bates M, Moretti P, Pitson S, Selemidis S, Butler L, O'Leary J, and Brooks D - Sortilin and syndecan-1 drive a metabolic switch during prostate cancer progression

Publications in progress:

- Bogue Edgerton L, O'Connell F, Martin C, O'Toole S, Selemidis S, Brooks D, O'Leary J, Tewari P - A varied glucose milieu alters the prostate cancer metastatic potential and metabolism.
- Bogue Edgerton L, O'Connell F, Martin C, O'Toole S, Brooks R, Selemidis S , Brooks D, O'Leary J, Tewari P - Vitamin C and Menadione in a varying glucose milieu alters the prostate cancer mitochondrial metabolism.
- Bogue Edgerton L, O'Connell F, Martin C, O'Toole S, Hayball E, Brooks R, Selemidis S, Brooks D, O'Leary J, Tewari P – Targeting the prostate cancer cell metabolome with novel trojan horse compounds.
- Bogue Edgerton L, O'Connell F, Martin C, O'Toole S, Hayball E, Brooks R, Selemidis S, Brooks D, O'Leary J, Tewari P – No kill switch: Warburg metabolism in prostate cancer cells persists in a varying glucose milieu.

Awards:

- Top 6 nomination for Patrick G. Johnston award: IACR 2022, Patrick G Johnston Presentation, Little Island Cork, 30/03/2022- Targeting Cancers Sweet Tooth with Novel Trojan Horse Compounds.

- Top Poster in category: 12th International Cancer Conference, Trinity Biomedical Science Institute, Dublin, 13/10/2022- The Impact of Varying Glucose milieu on the Metabolic Bioenergetic Profiles of Prostate Cancer Cells.

Outreach

Volunteer for Homeless period Ireland 4 years. 2019 - current

Table of Contents

List of Figures

List of Tables

List of Appendices

Abbreviations

4K - 4- kallikrein Score

ADT - Androgen deprivation therapy.

AP-1 - activator protein-1

AR - Androgen receptor

ATP - Adenosine triphosphate

BMI - Body Mass Index

BRCA - Breast Cancer Gene

CAFs – Cancer associated fibroblasts

CTCs - Circulating tumour cells

DHA - dehydroascorbate

DHT - 5α-dihydrotestosterone

DRE - Digital rectal examination

EBRT - External beam radiotherapy

EMT - Epithelial–mesenchymal transition

FDA - Food and Drug Administration

GnRH - gonadotropin-releasing hormone

GSH - Glutathione

HB-EGF - Heparin binding epidermal growth factor like growth factor

HDB - High-dose brachytherapy

HIF-1α - Hypoxia-inducible factor-1α

HRR - Homologous recombination repair

ISUP - International Society of Urological Pathology

KLF - Krüppel-like factor

LDB - Low-dose brachytherapy

LH - Luteinizing Hormone

LuPSMA - Lutetium-117

LUTS - Lower urinary tract symptoms

mCRPC – Metastatic castrate resistant prostate cancer

MRI - Magnetic Resonance Imaging

NF-κB - nuclear factor kappa-light-chain-enhancer of activated B cells

Oxphos – Oxidative phosphorylation

PARP - Poly [ADP-ribose] polymerase

PCa - Prostate cancer

PCA3 - Prostate cancer antigen 3

PHI - Prostate Health Index

PIN - Prostate Intraepithelial Neoplasia.

PSA - Prostate Specific Antigen

PSMA - Prostate Specific Membrane Antigen

PSMA-PET - PSMA-Positron Emission Tomography

PTEN - Phosphate and tension homologues

ROS – Reactive oxygen Species

SHBG- Sex hormone binding globulin

STAT-3 - signal transducer and activator of transcription 3

SVCT - Sodium dependent vitamin C transporter

TCA - Tricarboxylic acid

TGF- β - Transforming growth factor beta

TH – Trojan Horse

TNBC - Triple negative breast cancer

TURS - Transrectal ultrasound

VEGF - Vascular Endothelial Growth Factor

Chapter 1. Introduction

1.1 General Introduction

Prostate cancer is the second most common form of cancer in males worldwide[1], and the incidence of this disease is predicted to double globally by 2030. [2] The growth and survival of early-stage prostate cancer relies on androgens. Due to this fact many therapeutic methods have been designed to target this with the likes of hormone therapies like androgen ablation therapy. Prostate cancer cells can become androgen independent if not treated early rendering the use of androgen therapy to be futile. The intermediate/late-stage androgen independent prostate cancers (AIPCs) are considered at this time to be incurable. We propose to create a solution to this problem with the synthesis of novel therapeutics that will take a different approach, targeting the prostate cancer metabolism rather than the hormone cycle.

We have developed a unique approach which specifically targets different parts of the cancer cells metabolic pathway, using a 'Trojan horse' metabolic targeting event. The approach involves the use of Vitamin C and Menadione, complexed to simple sugars and lipids which demonstrates significant anti-reactive oxygen species activity, without causing environmental apoptosis: resulting in the direct killing of cancer cells, with no effect on normal cells. With the ever-increasing incidence in cancer cases and resulting deaths, this novel approach is of great relevance and importance.

It is safe to consider cancer is one of the most lethal and dangerous health issues faced by modern medicine. Several hallmarks of cancer cell biology have been recognised and many current therapeutic strategies have aimed to exploit these commonalities in cancer pathogenesis in order to find a cure to this disease. However, most of these strategies remain ineffective as they target a mechanism that the cancer cells can adapt to, in order to survive. Consequently, a treatment regimen that does not consider the variable nature of cancer cell biology and the adaptability of cancer cells is destined for failure, leaving a huge burden for patients, families, and health care systems. There is an urgent need for a therapeutic strategy that effectively targets cancers at multiple mechanistic and metabolic endpoints, and that utilises novel approaches to limit cancer cell adaptability. We will achieve this important outcome by exploiting the Warburg effect to target prostate cancers metabolism and develop compounds that target multiple aspects of cancer biology.

The prevalence, risk factors, current diagnosis and treatments, upcoming treatments, disease biology and the vitamins of interest are discussed here, to lend insight

into the thought process for the development of the novel compounds and why they are an important step forward in the field of cancer research.

1.2 Epidemiology

1.2.1 Global

Prostate Cancer (PCa) is one of the most common cancers diagnosed in men, with over 1,276,106 new cases and 358,989 related deaths reported worldwide in 2018.[1] The disease burden associated with PCa is expected to rise globally to ~2.3 million new cases and 750,000 related deaths by 2040[1, 2] The risk of developing PCa severely increases with age.[2,16] Mortality rates increase with age with approximately 55% of all PCa related deaths occurring after the age of 65 years.[3,4]

1.2.2 Ireland

PCa accounts for 29.2% of all invasive cancers diagnosed annually with one in three men at risk of developing this disease during their lifetime.[5]

On an average 3,474 cases of prostate cancer were diagnosed per year 2012-2014 with an increase in incidence rate observed between 1994-2010.[5] Figure 1.1 illustrates the PCa incidence and mortality rates in Ireland from the years 1994 to 2015, from the National Cancer Registry Ireland.

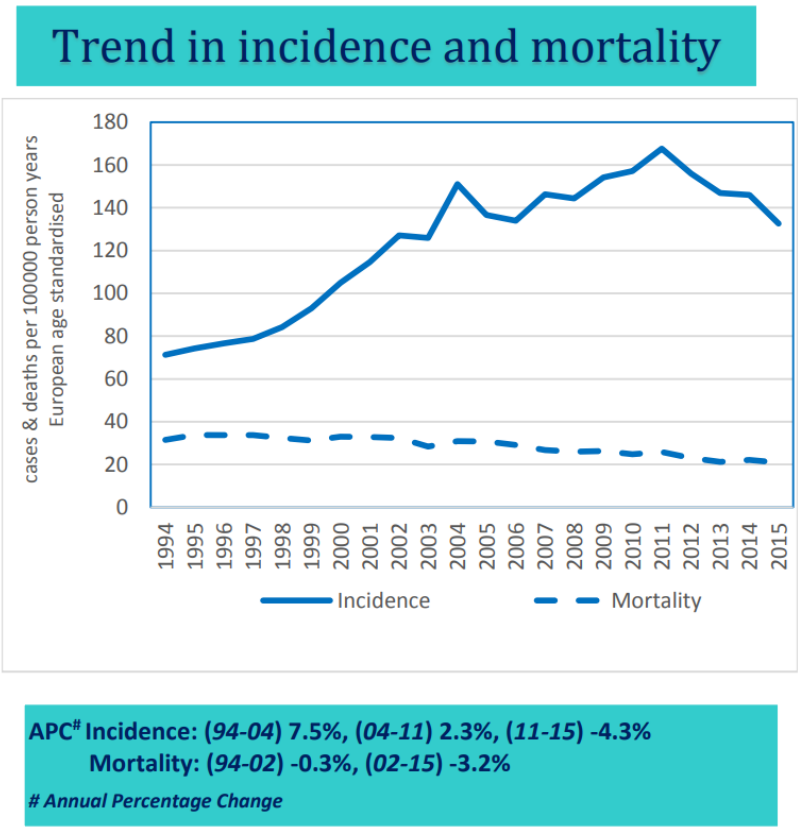

Figure 1. 1 Trends in PCa incidence and mortality in Ireland from 1994 to 2015 (most recent figures) detailing the annual PCa (APC) incidence, from the National Cancer Registry Ireland.[5]

1.3 Risk Factors

The main risk factors include diet, age, and genetic predisposition.

1.3.1 Diet, Obesity, and Diabetes

Obesity and diabetes are distinct conditions, but both can have an impact on the development and progression of PCa.[6] Obesity is a condition characterised by an elevated visceral fat accumulation.[7] Obesity is associated with an increased risk of developing aggressive forms of PCa and a higher likelihood of disease recurrence following treatment.[8,9] The high levels of adipose tissue found in an obese patient can produce oestrogen and inflammatory molecules, which may promote the growth and progression of PCa cells. Further, insulin resistance and chronic low-grade inflammation, that can be found in patients with obesity, may result in a tumour-promoting environment.[10,11] Associations between obesity and alterations in sex hormone levels, including a decrease in testosterone and an increase in oestrogen, which may affect prostate cancer growth have been reported in the literature.[11,12]

While diabetes is often found in those with high levels of obesity, diabetes is a metabolic disorder described by an elevated blood sugar levels due to insufficient insulin production or impaired insulin function.[13] Diabetes is associated with an increased risk of developing advanced and aggressive prostate cancer.[14–16] Type 2 diabetes is often associated with insulin resistance, which leads to increased insulin production, resulting in elevated insulin levels and insulin and insulin-like growth factors may promote tumour growth and therefore the progression of PCa.[17,18] Increased inflammation and oxidative stress have been linked to diabetes in patients, which can create a tumour-promoting environment and overall increase the risk of cancer progression.[10,19] Finally, diabetes is known to result in issues with vasculature, including impaired blood flow and reduced oxygen supply to tissues, which may affect tumour growth and response to treatment, due to tumours ability to survive in an hypoxic environment.[15,20,21]

A typical western diet, is implicated in the stimulation of oestrogen receptors mediating oestrogen's harmful effects, due to the presence of animal derived oestrogen in the diet.[22] Many studies have associated high concentrations of circulating oestrogens to increased PCa risk.[23–26] The highest global PCa incidence rates are seen in Australia, Europe and the US where a western diet predominates, in comparison to nations that have a diet lower in animal products. [27, 22]

While, there is no conclusive evidence at present linking obesity and PCa, nevertheless, lack of exercise and/ or a western diet may increase concentrations of serum adipokines, which have been adversely linked to PCa disease.[28] Adipokines are cytokines produced from adipose tissue and are known to stimulate proliferation, metastasis, alterations of sex steroid hormone levels and angiogenesis.[29,30] They disseminate through the blood and interact through ligand receptor endocrine mechanisms. Adipokines such as Leptin, Vascular Endothelial Growth Factor (VEGF), Heparin binding epidermal growth factor like growth factor (HB-EGF), interleukin-6 and adiponectin are heavily implicated in PCa carcinogenesis. Leptin disrupts insulin signalling in metabolic syndrome and type 2 diabetes, where it plays a role in lipid metabolism, while adiponectin regulates blood sugars and its levels are inversely associated with the grade of PCa disease. [9,28,29,31,32] Increased concentrations of Leptin, HB-EGF, IL-6 and VEGF have been recorded along with a concurrent decrease in adiponectin concentrations in obese patients.[33,34]

Patient body mass index (BMI) levels have been shown to be inversely proportional to total serum and free testosterone concentrations due to decreased sex hormone binding globulin (SHBG). SHBG is a glycoprotein that binds to sex hormones androgens and oestrogens, controlling their bioavailability.[35,36] The presence of SHBG is reported to decrease with increasing adiposity correlating to decreased testosterone levels, this trend is linked to insulin resistance as seen in metabolic syndrome.[36] Low levels of SHBG have been associated with an increased risk of PCa, with increased circulating oestrogens introducing an additional risk factor.[37] Obesity is also associated with decreased testosterone levels, observed in more advanced disease stages and poor prognosis.[38, 39]

Overall, the management of diabetes and maintaining optimal blood sugar levels is critical for patients with prostate cancer to mitigate the potential adverse effects due to obesity and diabetes both in combination and respectively.

1.3.2 Age

The risk of developing PCa dramatically increases with age.[2,16] 1 in 350 men under 50 years of age will be diagnosed with prostate cancer, the rate of incidence increases to 1 in 52 for the age range of 50 - 59 years of age. For men aged 65 and over, the incidence rate of PCa is 60%.[40] Mortality rates also increase with age with nearly 55% of all PCa related deaths occurring after the age of 65 years.[3,4] Figure 1.2 illustrates the age of diagnosis and death from PCa in Ireland from the years 1994 to 2015, with a

median age of diagnosis being 65-69 years of age and the median age of PCa related death being 80-84 years of age.

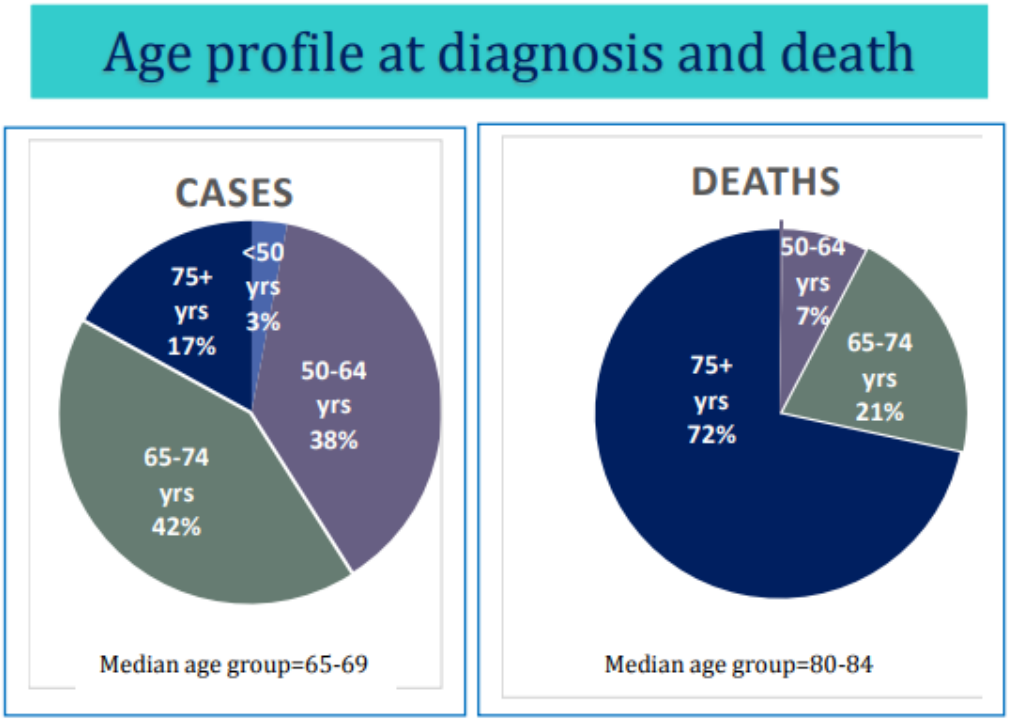

Figure 1. 2: Age Profile at diagnosis and death in Ireland from 1994 to 2015 (most recent figures) from the National Cancer Registry Ireland, with median age of diagnosis being 65-69 years of age and the median age of PCa related death being 80-84 years of age.[5]

1.3.3 Genetics and Familial Risk

The risk of disease increases if a first degree relative has been diagnosed with PCa allowing for risk stratification for those with genetic predisposition of the diesease.[2] A family history of breast and/or ovarian cancer is associated with a three-fold increase in risk of PCa, possibly due to germ-line mutations of BRCA1 and 2 genes.[3,4,41] In addition, men that present with BRCA 1 and 2 mutations have a much more aggressive disease phenotype. Moreover PALB2, a breast cancer susceptibility gene that encodes BRCA2-interacting protein, is altered in patients with a family history of PCa, leading to BRCA2 mutations and corresponds to higher incidence of PCa.[18,42]

The X chromosome plays a role in contributing towards familial disposition to PCa. The androgen receptor is located on the X chromosome (Xq 11-12) and small deletions within Xq27-q28 (16%) region of the X chromosome can be found in hereditary PCa cases.[2,43,44]

Genetic variation also plays a significant role in conferring susceptibility to PCa. Single-nucleotide polymorphisms identified at the 8q24 locus, 17q, 17q12, and 17q24.3 are strongly associated with PCa.[45,46]

1.3.4 Smoking

Although smoking has not been conclusively identified as a risk factor for PCa, heavy smokers are at a greater risk of dying due to PCa than non-smokers.[47, 27] Exposure to smoking related carcinogens can affect sex steroid levels and lead to mutations in the TP53 gene leading to the development of a more aggressive, hormone independent disease phenotype.[47] Around 64% of smokers will present with TP53 mutations when compared to 36% in non-smokers, which can be a considerable disadvantage to the patient. Mutations of TP53 in exon 7 and 8 can play a significant role in PCa progression and recurrence.[48]

1.4 The Diagnosis, Histology and Staging

1.4.1 Diagnosis

In cases of an abnormal growth in the prostate, a digital rectal examination (DRE) and Prostate Specific Antigen (PSA) blood test is first carried out by a physician and patients with suspect diagnosis are referred for further investigation. DRE generally detects peripheral zone cancers, although cancer can arise in other zones and become significantly advanced before palpable by DRE.[49,50] Further investigations involve a transrectal ultrasound (TURS) examination and acquisition of guided biopsies for histopathological evaluation. The procedure involves extraction of 10 to 12 prostate tissue cores through a rectal probe.[51] The associated side effects of this procedure include; sepsis, bleeding and urinary retention.[42] There is also a relatively high risk of a false negative result.[52]

Patients with a negative result from the initial biopsy, may undergo a repeat biopsy or Magnetic Resonance Imaging (MRI) in cases of suspected disease.[51,53] Multiparametric MRI has now become a standard method of detection, prior to biopsy with a greater associated accuracy (85%) and sensitivity (93%) in the detection of clinically significant prostatic disease. MRI in combination with biopsy has greatly increased the detection rate of PCa.[54]

1.4.2 Histology

Gleeson grading was established by Donald F. Gleeson in the 1970's and is the conventional technique used in the classification of prostate adenocarcinoma into different histological growth patterns to determine a prognosis and guide decisions on treatmentintervention.[55] In 2004 the World Health Organisation (WHO) approved the Gleason grading system for the Histopathological grading of PCa. Using the Gleason grading system, PCa's can be classified as G1 (well differentiated), G2 (moderately differentiated) or a G3 (poorly differentiated or undifferentiated).[56]

The Gleason system is based on architectural differences in the prostatic glands and does not evaluate nuclear atypia. The primary and secondary patterns should be reported and added to give the tissue pathology a score.[55–57]

In 2014, modifications to the grading system were proposed by the International Society of Urological Pathology (ISUP) due to the limitations presented by Gleeson grading, such as poor differentiation and prognosis prediction.[26] These changes included the assignment of all cribriform and glomeruloid glands to pattern 4. Regardless of

morphology, grading of mucinous carcinoma should not all be graded as a pattern 4 but should be based on its growth pattern, and intraductal carcinoma without invasive carcinoma should not be assigned a Gleason grade and a comment should be made as to its association with aggressive cancer. [49,58]

The ISUP grade groups divided Gleason grading into 5 groups with a consensus by expert pathologists and clinicians at the ISUP conference. These grade groups provide a standardised approach to management and prognosis. Grade groups are defined as:

ISUP Group 1: Gleason score ≤ 6

ISUP Group 2: Gleason score 3 + 4 = 7

ISUP Group 3: Gleason score 4 + 3 = 7

ISUP Group 4: Gleason score 8 (4+4. 3+5, and 5+3)

ISUP Group 5: Gleason score 9-10

Although, improvements have been made through the introduction of ISUP grades, limitation still arise due to the complexity of the modified system. For example, Gleason 3 + 4 carries a much more favourable prognosis than Gleason 4 + 3. This can be confusing for patients and clinicians and one cannot confidently place an intermediate risk on a Gleason score of 7.[59,60]

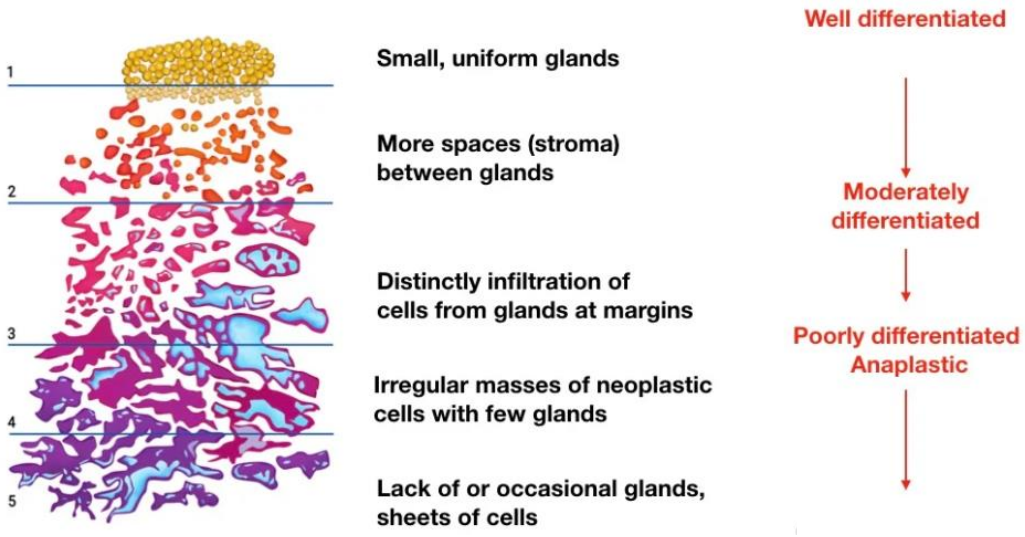

Figure 1. 3: Gleason Grading: A grade of 5 corresponds to a highly aggressive or malignant cell pattern. A grade of 3 is also regarded as malignant, without an aggressive pattern. Depending on their frequency, cells with a Gleason score of 4 may tend toward tumours with a Gleason score of 6. Tumours with a Gleason score of 7 are regarded as intermediate-grade tumours. Image from ALTA KLINIK

1.4.3 Tumour Staging and Risk Stratification

There are 3 main categories in which the disease is typically classified into based on: T; size of the primary tumour and invasion of nearby tissue or not. N; the degree of spread to regional lymph nodes. M; metastasis to other sites in the body.[53,61]

- Localised disease (T1/2 N-M-)
- Locally Advanced (T1/2 N+M-) or (T3/4 N-/+M-) and
- Metastatic disease (any T/NM+)

The localised and locally advanced disease are split into 3 further categories:

- Low risk
- Intermediate risk and
- High risk

Risk stratification is dependent on the disease stage and the treatment is guided by the risk category established. An overview of this is seen in Figure 1.4.

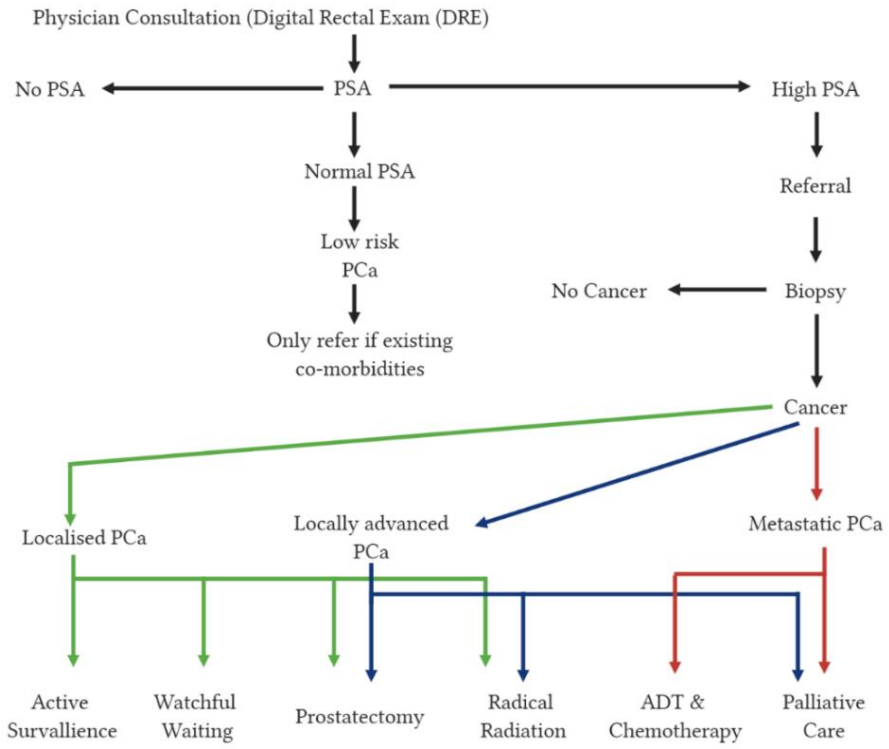

Figure 1. 4: Current patient diagnosis, disease staging, and treatment schematic. The patient is sent to their general practitioner (GP) for a DRE. Here PSA levels may be determined by blood test. If the PSA is normal, the patient is sent home, however, there may be a referral to an oncologist and or urologist, if there are existing co-morbidities. If PSA readings are high, the patient is sent for a referral to an oncologist and or urologist, where a biopsy would be taken. If the patient is cancer positive, their disease will be stratified into; localised PCa, where active surveillance, watchful waiting, prostatectomy, or radiation therapy will be utilised as the treatment regimen. Locally advanced PCa where a prostatectomy, radiation therapy, or palliative care will be utilised as the treatment regimen. For metastatic PCa, ADT and chemotherapy or palliative care will be utilised as the treatment regimen for the patient.

1.5 Current strategies in clinical management

The treatment options for PCa are guided by disease severity and tend to be either curative or palliative. Palliative options are advised for patients with existing comorbidities, and for older patients who are likely to die of unrelated causes. [57] To undergo radical curative treatment, the patient must have a life expectancy of more than 10 years due to the severity of treatment and inherent risk involved. [53,61]

1.5.1 Watchful Waiting

This is a method of treatment typically undertaken for elderly patients or those with serious comorbidities. This involves infrequent PSA checks and disease monitoring; it is typically considered within the palliative route of care.[61]

1.5.2 Active Surveillance:

Patients with low or intermediate risk localised disease are often placed under active surveillance. It is also referred to as a "delayed radical treatment" and is set in place to avoid overtreatment of localised tumours with low chance of progression.[62,63] Active surveillance involves the bi-annual reassessment by the patients' medical team, where examination of the patients PSA levels and possible repeat biopsy are conducted if required. During active surveillance, more radical treatment such as radiotherapy can be investigated, with further intervention decided by the patient or based upon the results of a repeat biopsy.[64,65] However, there is an inherent risk involved as once progression of disease is detected, and radical treatment is undertaken. Overall, active surveillance has proven to be effective and results in the best quality of life for the low risk patients.[66,67]

1.5.3 Radiotherapy

Radiotherapy can be considered as a treatment option alone, or in combination with brachytherapy, hormone therapy or chemotherapy for localised and locally advanced disease patients.

The recommendations for treatment are guided by risk category. The recommendations for low risk PCa patients are treatment with either external beam radiotherapy or brachytherapy. Presently there is no as yet proven benefit in combining external beam radiotherapy (EBRT) or brachytherapy with hormonal therapy for low- risk disease.[51,68,69] Intermediate risk category patients undergo EBRT in combination with hormonal therapy such as androgen deprivation therapy (ADT). For this stage of disease, a treatment regimen involves several months of both radical therapies is advised.[70,71] High risk PCa is managed by long term EBRT in combination with ADT or a combination of

EBRT and brachytherapy with or without ADT, depending on patient and doctor choice. For high-risk patients, a combination of EBRT and long term ADT is recommended.[7270,73,74]

The negative side effects associated with radiotherapy, both internal and external include, haematuria, incontinence, radiation proctitis, erectile dysfunction and radiation cystitis. [54]

1.5.4 Brachytherapy

Brachytherapy is a method of internal radiative treatment. A radioactive source is inserted directly into the prostate. In low-dose brachytherapy (LDB) the radioactive source contains either $^{(125)}$Iodine or $^{(103)}$Palladium and involves permanent seed implantation to the prostate.[54] High-dose brachytherapy (HDB) is typically preformed with $^{(192)}$Iridium under local anaesthetic and the patient remains in hospital for the duration of the treatment. Brachytherapy can be performed in combination with external radiation treatment.[75–79] Side effects include; lower urinary tract symptoms (LUTS), urinary incontinence, perineal haematoma, erectile dysfunction and seed migration.[54]

1.5.5 Prostatectomy

Prostatectomy is the surgical removal of either the entire prostate gland or part of the gland. The neck of the bladder is then connected to the urethra.[80] This method of treatment is undertaken for locally advanced disease. There are two main methods of prostatectomy including perineal and retropubic (most common). Following the procedure, PSA levels are expected to fall to an undetectable level. PSA levels are subsequently regularly monitored to detect biochemical recurrence. [80–83] A spike in PSA often leads to further radical intervention. Side effects can include; incontinence and erectile dysfunction.[54]

1.5.6 Hormonal therapy (ADT)

Hormonal therapy is the mainstay treatment for metastatic disease or disease relapse. This involves the reduction of the concertation of circulating androgens in which prostate cells are dependent upon for growth.[84] There are two primary forms of ADT, chemical and surgical castration. Medical castration tends to target the production of Luteinizing Hormone (LH) in the pituitary gland.[84, 54] The different forms of ADT include;

1.5.6.1 LHRH Agonist

This involves lowering the concentration of LH released from the pituitary gland, resulting in a corresponding decrease in testosterone secretion. This can result in an initial increase in testosterone serum levels two weeks after treatment and is referred to as a tumour flare.[80,84,85]

1.5.6.2 Anti-androgen treatment

This is a chemical non-steroidal agent, that blocks the production of androgen. This can be in combination with LHRH agonist treatment and is then referred to as a maximum androgen blockade. It prevents flare reactions if used prior to LHRH agonist treatment. [68,80,82,84,85]

1.5.6.3 LHRH antagonist

This is another form of chemical castration. It does not result in an initial surge of testosterone but can be associated with anaphylaxis. This is often considered a palliative method of treatment or for patients who will not undergo surgical intervention or if the initial increase in testosterone is harmful, due to existing comorbidities. [69,86,87]

1.5.6.4 Surgical castration:

Involves the surgical removal of the testicles, to stop the production of androgens. For years, this was the standard ADT treatment for PCa patients. [84,85] This method of treatment is still used for patients who do not want to undergo frequent injections of drugs or those with severe underlying cardiac conditions, that may be affected by the other treatment options. [54 80,81]

1.5.7 Androgen deprivation therapy and metabolic syndrome

ADT is a primary, globally utilised treatment for advanced or metastatic prostate cancer. It works to suppress the production or to stop the action of androgens, to prevent further disease promotion.[84] While ADT is effective in disease control for patients with PCa, it can also lead to various side effects, including the development of metabolic syndrome.[88]

Metabolic syndrome is a set of conditions that occur together and have been shown to increase the risk of cardiovascular disease, stroke, and type 2 diabetes.[18] It is characterized by many factors, including high visceral fat in the abdomen, high blood pressure, high blood sugar levels, high triglycerides, and low levels of high-density lipoprotein (HDL) cholesterol.[18,38]

ADT can result in an increase in visceral body fat and the redistribution of fat, with an accumulation primarily at the abdomen. This increase in abdominal fat is associated with insulin resistance, where cells become less responsive to the effects of insulin, leading to elevated blood sugar levels and an increased risk of type 2 diabetes.[89,90] Androgens play a role in regulating insulin sensitivity and glucose metabolism. ADT-induced androgen suppression can disrupt this balance, resulting in insulin resistance. This impairs glucose uptake from the bloodstream, resulting in elevated blood sugar levels, where prolonged insulin resistance can promote the development of type 2 diabetes.[88,91,92] ADT has also been linked to an increased risk of hypertension in patients. The exact mechanism behind this yet to be determined in definite, it is thought that ADT-induced changes in hormone levels, vascular function, and fluid balance which may result in the development of hypertension.[93,94]

While not all patients will develop metabolic syndrome following ADT, metabolic syndrome is reported in approximately 50% of men undergoing long-term ADT in the United States, and thus it is important to consider when considering the patient's treatment regimen.[91] Exercise interventions have been shown to improve metabolic syndrome variables in insulin-resistant, however more research is required in the field of PCa.[95,96] However, a regular exercise regimen has been shown to improve some ADT-related adverse effects, including metabolic syndrome.[17 95,96]

1.5.8 Chemotherapy

Docetaxel is the classic chemotherapeutic used in the treatment of metastatic prostate cancer.[42] It is administered intravenously and is an option for patients who have androgen independent disease phenotype.[97] A combination of chemotherapy and hormonal therapy has been shown to have a better disease prognosis throughout studies (STAMPEDE). However, this has been reassessed due to the severe adverse effects on the patient, following treatment.[42,61,98–100]

Over a period of treatment, patients can develop docetaxel resistance, thus other drugs such as Abiraterone and Enzalutamide are advised. At this point the disease is considered incurable and these therapies are to increase survival time.[61,98,101,102]

Abiraterone inhibits adrenal gland production of androgens. Abiraterone is an irreversible inhibitor of CYP17 (17α hydroxylase), that blocks the processes involved in the synthesis of testosterone. Phase III clinical trials of 1195 participants resulted in a

median time of deterioration of 59.9 weeks versus 36.1 weeks and with this, Abiraterone is now used in the clinical treatment of PCa. [102–104,105]

Enzalutamide is an oral androgen receptor inhibitor that blocks androgen from entering the cell's nucleus to activate DNA. The PREVAIL phase III Clinical study of 1717 patients received either Enzalutamide (160 mg) or placebo daily. Radiographic progression free survival was seen in 65% of Enzalutamide treated patients compared to 14% in the placebo group.[106–109]

Cabazitaxel, is a semi-synthetic derivative of a natural taxoid and is a microtubule inhibitor.[110] Treatment is administered by injection with prednisone (steroid) for patients with mCRPC.[111,112] In Germany, guidelines allow for Cabazitaxel for docetaxel-pre-treated patients with a good performance status, however strict monitoring is required.[110] Cabazitaxel has been approved for use by the FDA.[113]

1.6 Recent developments in the treatment of PCa

With mCRPC being considered incurable at this time, research is continuing to investigate new avenues of treatment to prolong and improve the quality of life of patients.

1.6.1 Poly [ADP-ribose] polymerase (PARP) Inhibitors

Research has shown that many patients with mCRPC hold the germline mutations in BRCA1 and BRCA2. In ovarian cancer, PARP inhibitors such as Olaparib have been very successful for the treatment of patients with these germline mutations. PARP inhibitors are pharmacological inhibitors of the enzyme poly ADP ribose polymerase.[114–116]

In 2020, Olaparib was approved by the FDA and the EMA for men with deleterious germline or somatic homologous recombination repair (HRR) gene-mutated mCRPC who have progressed following prior treatment with Enzalutamide or Abiraterone based on the phase III PROfound study of 4425 patients.[116] Treatment with olaparib resulted in a 66% reduction in the risk of disease progression or death in comparison to Abiraterone or Enzalutamide in BRCA1/2 mCRPC patients. The study highlighted an overall survival improvement in BRCA1/2 patients of 19.1 months with olaparib compared with 14.7 months with Enzalutamide or Abiraterone.[116] Other studies have noted similar outcomes.[110,116–119]

On May 15th, 2020, Rucaparib (RUBRACA, Clovis Oncology, Inc.) was approved by the FDA for treatment of patients with a BRCA mutation (germline and/or somatic)-associated mCRPC who have been treated with androgen receptor-directed therapy and a taxane-based chemotherapy. A cohort of 115 patients with BRCA mutated mCRPC were treated with 600mg orally twice daily with gonadotropin-releasing hormone (GnRH) analogue simultaneously. Patients were evaluated radiographically every 8 weeks for 24 weeks, and then every 12 weeks. PSA was measured every 4 weeks. Overall, the 62 patients who remained in the study, with BRCA1/2-mutant mCRPC had a 44% response rate with a duration of response of 1.7-24+ months. Additionally, 56% of the patients had a duration of response of ≥6 months.[120]

1.6.2 Novel Radiotherapies

There are many advances in novel radiotherapeutics for prostate cancer with many clinical trials ongoing.[121–124]

LuPSMA (lutetium-117) is a small novel radiolabelled molecule that binds with PSMA, in mCRPC patients who have already undergone docetaxel treatment. It emits predominantly low energy beta but also gamma photons particles which can be used to kill cancerous cells.[125]

In a Phase II randomized TheraP trial of 200 participants established the effectiveness of LuPSMA in comparison to Cabazitaxel. LuPSMA was given by I.V. every 6 weeks for up to 6 cycles (6-8.5 GBq) until unreasonable toxicity in the patient was reached, the patient was not benefiting, or post-therapy imaging showed complete resolution of PSMA uptake.[126] The TheraP trial concluded with LuPSMA improving PSA progression free survival in comparison to Cabazitaxel after 13 months follow up.[126]

50 patients under LuPSMA therapy for an 18-month study, underwent 132 cycles of treatment. Patients underwent a median 3 cycles of 3.5–8.2 GB q IV doses. PSA decline could be calculated for 49 of the 50 patients, with a PSA decline of ≥ 50% in 44.9% of patients.[127] Additional studies of LuPSMA have shown similar results to that of these trials.[126,128,129]

Actinium-225 (Ac-225) is an alpha particle emitting isotope emerging due to its high toxicity to cancer tissue and relative lack of toxicity towards normal tissue.[130] It has been used as a potent anticancer drug and is currently used in the treatment against acute myelogenous leukaemia. Alpha radiation does present some advantages over beta radiation as a treatment option due to the linear energy transfer capabilities.[131,132] It has a 100 keV/μm range resulting in more lethal double strand DNA breaks per alpha track than beta particles when traversing a cell nucleus. [130–132]

Some studies have reported that nearly 80% of patients with advanced PCa treated with Ac-225 showed notable decrease in PSA levels post-treatment, though adverse effects including; xerostomia, renal insufficiency, anaemia and thrombocytopenia were also reported.[111,133]

A combination of radiotherapies is of growing interest with a combination of radium-223 and simultaneous EBRT under trial for prostate and pelvic lymph node disease in patients with metastasis to the skeleton, following conventional treatment with ADT, and docetaxel.[134] This therapy has the potential to deliver radiation to all disease sites, with the EBRT reaching the primary and pelvic lymph node sites and the Radium-

223 addressing the metastasis in the bones, this is proven to be safe for the patients involved.[134]

1.6.3 Immunotherapies

1.6.3.1 Immune checkpoint Inhibitors

Immune checkpoint inhibitors are a growing form of cancer immunotherapy. It involves the targeting of key regulators of the immune system that during disease can cause a decreased response. Some cancers have been shown to protect themselves through the stimulation of these checkpoint targets such as CTLA4, programmed death protein-1 (PD-1) and its ligand-1 (PDL-1). [135–137]

Ipilimumab is a monoclonal antibody targeted at the CTLA4 protein receptor that blocks the CTLA-4/B7 pathway. Ipilimumab was the first immunotherapy approved by the FDA in the treatment of metastatic melanoma with studies then conducted in PCa from 2010-15 (Bristol-Myers Squibb).[138] Results yielded detectable anti-tumour effects radiographically at high doses (greater than 3 mg/kg). Studies have shown increased efficiency when in combination with prostate GVAX.[139,140] Early clinical trials revealed decreased PSA readings in patients along with a desired response by the disease. However, adverse immune effects were observed in some patients.[140] Overall, a study by the American Society of Clinical Oncology in 2016 demonstrated that Ipilimumab produces clinical activity in patients with CRPC, including very long responders with no detectable residual disease.[141] From the phase III clinical trials preformed, long term remission was found to be rare in CRPC patients resulting in 32 months of progression-free survival rates of less than 5 - 10%. [141,142]

Another emerging target for immune checkpoint therapies is the immune checkpoint proteins PD-1 and PDL-1. Studies have shown that the interactions between PD1 and PDL-1 can result in the inhibition of T-cell functions and that the blockade of PD-1 can potentate anti-tumour responses. Increased PDL-1 expression in human studies was associated with a poorer outcome in several cancers. [143–146]

FDA approved anti PD-1 therapies include; nivolumab and pembrolizumab.[144] They have shown very promising results in many cancers including; melanoma, non-small cell lung cancer (NSCLC), urothelial cancer, renal cell carcinoma (RCC) and head and neck cancer. Thus, it would be rational to consider these treatments for the currently untreatable mCRPC.[144–146]

Nivolumab in combination with Ipilimumab phase II trials showed that 10% of patients had a 30-100% reduction from baseline PSA was encountered in patients with somatic BRCA1/2 or ATM mutations, with only 5% resulting in a radiographic response. In earlier studies nivolumab alone showed little response. [144,145]

A clinical trial (NCT04019964, Sidney Kimmel Comprehensive Cancer Centre at Johns Hopkins, January 2020- 2025) of Nivolumab in biochemically recurrent PCa is commencing with an aim to reduce PSA>50% from baseline levels and to increase the overall survival or participants.

1.6.3.2 Cancer Vaccines

Cancer vaccines are an emerging and promising treatment option for PCa, with many studies showing potential in trials for advanced cancer patients. [135,136,147]

Sipuleucel-T is a therapeutic dendritic-cell vaccine, autologous cellular immunological agent. These therapies are derived from the patient' s blood, incubated with the fusion protein (PA2024) incorporating the prostate tumour-associated antigen prostatic acid phosphatase (PAP) and granulocyte-macrophage colony- stimulating factor, the immune cells are infused into the patient with the goal of generating an antitumor immune response.[148,149] Phase III IMPACT clinical trial of 512 patients, resulted in substantial improvements in patients with mCRPC. Patients showed a 22% reduction in mortality risk in comparison to the placebo group and 4.1 months overall survival increase in comparison to the placebo group.[150] This study highlighted the possible benefits of immuno-vaccines in the prolonging of life for terminal PCa patients.[150] Sipuleucel-T has been approved by the U.S. FDA in 2010 for the treatment of metastatic prostate cancer.[149,151,152]

PROSTVAC is a prostate-specific antigen (PSA)-targeted recombinant viral vaccine with additional monthly recombinant fowl pox boosts.[139,153,154] Phase II trial of PROSTVAC conducted on 125 patients with minimal symptom mCRPC, involved 82 patients received PROSTVAC and 40 received a control vector. Initially, the results of the study were very similar, however after 3 years the overall survival of the PROSTVAC patients was a median of 8.5-months greater than the placebo. Overall, there was a reported 44% reduction in mortality rate and an 8.5-month improvement overall survival.[155] In Phase III clinical trials, PROSTVAC was found to be well tolerated by patients but had minimal effect on overall survival in patients with mCRPC.[156,157]

One of the most interesting effects of immunotherapy is the potentially long duration of remission in responders, observed in PCa, melanoma, lung cancer and renal cell carcinoma, with some patients still in complete remission years later.[135,136,147]

1.7 Prostate physiology and disease pathogenesis

1.7.1 Normal Prostate

The prostate is a small secretory gland located at the neck of the urinary bladder. The prostate, the seminal vesicle and Cowper's gland produce seminal fluid, composed of zinc, citrate and kallikreins, secreted by the prostate luminal cells.[158,159] These secretions play an important role in the stabilisation of the cell membrane and nuclear chromatin of spermatozoa that are imperative for sperm motility and maturation.[159] Fibromuscular prostatic stroma lies ventrally, and the glandular tissue is located at the dorsal aspect. The glandular tissue is divided into three zones.[160] The peripheral zone, which makes up approximately 70% of the prostatic tissue, the transition zone, which surrounds the urethra and a central zone, which receives the ejaculatory ducts.

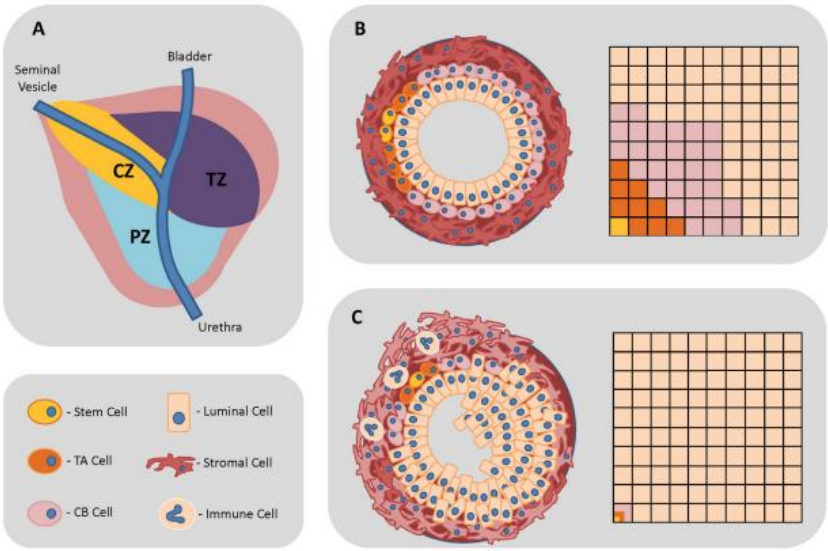

Figure 1. 5: The human prostate anatomy and epithelial cell makeup. (A.) The prostate and its 3 distinct zones; the central zone (CZ) that contains the ductal tube from the seminal vesicle to where it meets the urethra, the peripheral zone (PZ) which is situated at the posterior of the gland and is the region from where the vast majority of PIN and cancer arises, and the transitional zone (TZ) that is directly below the bladder and surrounds the transitional urethra. (B.) A normal prostatic acinus; the epithelial bilayer of basal and luminal cells, surrounded by fibromuscular stroma. The relative content of different epithelial cells in the normal prostate includes luminal (60%), basal (40%) with the stem cells comprising ~1% of total epithelia. (C.) The cellular arrangement of a cancerous acinus. Luminal hyperproliferation is a characteristic of PCa along with the loss of the basal layer, breakdown of basement membrane, immune cell infiltration and stromal reactivity. Cancer alters the epithelial cell percentages where the luminal cells make up 99% of tumours. Image from Packer J.R. et al.[161]

1.7.2 Disease initiation and pathogenesis

The majority of early PCa is reported as adenocarcinoma, originating from the glandular structure of the prostate epithelium. The surrounding stroma facilitates malignant growth and proliferation, through an increase in the concentration of inflammatory cells and promotion of angiogenesis and extracellular matrix remodelling.[54,162] Initial organ specific disease can take up to 15 years to develop within the prostate gland with early proliferation and neoplastic growth seen in the glandular

epithelium, defined as Prostate Intraepithelial Neoplasia (PIN).[54,163] Cells from the original tumour site with high metastatic potential migrate to the surrounding lymph nodes where lymphatic disease establishes.[54,164]

Dissemination of disease is facilitated through the lymphatic and circulatory systems, to the surrounding iliac and obturator nodes.[54,42,165] The growth factor VEGF is a signal protein from cells that stimulate the production of vasculature, and has been shown to play a vital role in this process, which is believed to be essential for angiogenesis during disease migration from the prostate glandular site.[166] An increase in the expression of VEGF-C, a form of VEGF, has been observed in tumour tissues of patients with lymph node metastases suggesting a role for VEGF in facilitating lymph angiogenesis. Evidence suggests that the primary tumour site becomes a source of growth factors such as VEGF, which can prepare the lymph nodes for tumour invasion. [164,167] Not all PCa patients present with lymph node enlargement, however, through histopathological examination signs of nodal involvement is often observed.[167–169] Lymph node immune function appears to be impaired before the spread of PCa to the lymph nodes resulting in an altered lymph node architecture, that would typically be affected during disease proliferation. [164] [167–169]

The most common sites for metastasis for PCa are in the lower axial skeleton, presenting with sclerotic (bone forming) lesions, and possible further progression to other sites including the brain. [42,165,170] Metastatic PCa can involve an osteoblastic process, resulting in sclerotic lesion on the bone, detected through CT and MRI imaging. The sclerotic lesions transpire through the bone matrix remodelling by osteoclasts and osteoblasts.[171,172] Osteoclasts are large bone cells that absorb bone tissue and osteoblasts are bone forming cells.[173] Normally the bones will present with continuous growth turnover, however in PCa there is an equilibrium imbalance. This presents as exaggerated stimulation of soluble osteoblasts and bone specific proteins, inducing the production of abnormal bone lesions. As a result, the cancer cells can metastasise to further sites and this event is often considered terminal.[171,172] [164]

Metastasis from the primary disease site to the bone microenvironment is thought to involve mediators such as the growth factor Endothelin-1, transforming growth factor beta (TGF- β). Endothelin-1 stimulates the production of bone and osteoblastic proliferation and is found to be increased in patients with PCa. TGF-β is recognised as a

stimulator of bone formation in vivo in PCa. High expression of TGF-β2 is reported in the PCa cell line PC3, which are developed from isolated human prostate epithelial cells from metastatic bone tissue.[174] The mechanism of PCa disease initiation and progression is illustrated in Figure 1.6.

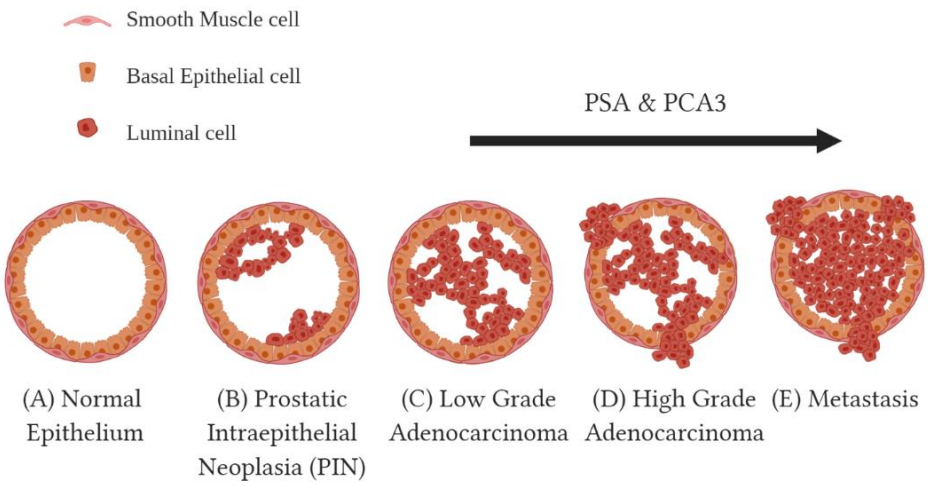

Figure 1. 6: Prostate cancer disease initiation and progression (A.) Prostate normal epithelium. (B.) Prostatic Intraepithelial Neoplasia (PIN) "defined by neoplastic growth of epithelial cells within pre-existing benign prostatic acini or ducts and can be considered a precursor to PCa". – hyperproliferation of the prostatic luminal cells occurs. (C.) Low Grade Adenocarcinoma neoplastic proliferation of the luminal cells with the loss of defined basal cell layer. (D.) High Grade Adenocarcinoma further neoplastic proliferation of the luminal cells with the loss of defined basal cell layer. (E.) Metastasis: further neoplastic proliferation of the luminal cells with the loss of defined basal cell layer. Image created with Biorender.

1.8 Molecular drivers of prostate cancer development and progression

Prostate cancer is a complex disease influenced by various molecular drivers that contribute to its development and progression. The following details just some of the molecular drivers implicated in PCa disease development and progression.

1.8.1 Androgen receptor (AR):

The androgen receptor plays a crucial role in the development and growth of the prostate. Androgens, such as testosterone and dihydrotestosterone (DHT), bind to the androgen receptor, leading to the activation of downstream signalling pathways that promote cell proliferation and survival.[175,176] In prostate cancer, alterations in AR signalling can occur, including amplification of the AR gene, mutations in the AR gene, or increased sensitivity of the receptor to androgens.[177] These alterations can result in persistent androgen receptor activity, even in the absence of normal levels of androgens, encouraging prostate cancer cell growth.[177,178]

In prostate cancer, amplification of the AR gene is a common genetic alteration resulting in an increased number of AR receptors expressed by the prostate cancer

cells.[179,180] Consequently, the cells become more responsive to androgens, promoting the growth of the tumour growth and, further progression. Amplification of the AR gene can result from genomic instability and can occur in different stages of prostate cancer, including early-stage disease and castration-resistant prostate cancer (CRPC).[179,181,182]

Mutations in the AR gene in prostate cancer, has been shown to lead to altered AR protein function. These mutations are found in the different regions of the AR gene, including the DNA-binding domain, ligand-binding domain, and transactivation domain.[183,184] Mutations in the DNA-binding domain are shown to affect the AR's ability to bind to androgen response elements (AREs) in target genes, resulting in dysregulated gene expression. Mutations in the ligand-binding domain can result in altered ligand binding affinity and specificity, allowing the receptor to be activated by alternative ligands, even in the absence of androgens.[184–186] Such mutations can lead to AR signalling activation, promoting prostate cancer growth even in low androgen environments, for example during ADT. [184–186]

Alterations of the AR protein can result in increased sensitivity to androgens, which can lead to enhanced activation of AR signalling, even during times of low androgen concentrations.[187] Various molecular mechanisms contribute to increased sensitivity, including changes in AR co-regulators, post-translational modifications, and alterations in AR protein conformation which all can promote AR signalling, thereby promoting prostate cancer growth and survival.[178 187,188]

These molecular alterations collectively contribute to the dysregulation of AR signalling in prostate cancer resulting in sustained androgen-driven growth and survival of prostate cancer cells.[177,188,189] Understanding these molecular alterations is crucial for developing targeted therapies to effectively inhibit AR signalling and overcome resistance mechanisms by the disease.

1.8.2 Phosphate and tension homologues (PTEN)

PTEN is a tumour suppressor gene frequently lost in human cancers. Its plays a key role in the regulation of many biological processes such as the maintenance of genomic stability, cell survival, migration, proliferation and metabolism, linked to the development and progression of disease.[190,191] A decline in the function of PTEN is due to a combination of genetic and epigenetic mechanisms such as; chromosomal deletions, point mutations, post-translational modifications and promoter hypermethylation.[192–194]

In PCa, the loss of PTEN function leads to the activation of the phosphoinositide-3-kinase (PI3K) signalling pathways involved in, cell growth, proliferation, and metastasis along with the inhibition of the AR signalling pathway.[190,195] PTEN acts as a negative regulator of the PI3K/AKT/mTOR signalling pathway. Dysregulation promotes prostate cancer cell survival and growth by enhancing protein synthesis, cell cycle progression, and inhibiting apoptosis. The dysregulation of PI3K/AKT/mTOR signalling pathway enhances the expression of anti-apoptotic proteins, such as Bcl-2, and suppresses pro-apoptotic factors, shifting the balance towards cell survival.[192–194,196] This resistance to apoptosis allows prostate cancer cells to evade cell death signals and promote their survival and progression.[193,194]

PTEN loss has also been linked to genomic instability as typically PTEN contributes to maintaining genomic integrity by regulating DNA repair mechanisms and cell cycle checkpoints.[192,195] PTEN function loss can disrupt these processes, resulting in DNA damage accumulation, chromosomal aberrations, and genomic instability. Genomic instability can drive further genetic alterations, including additional mutations in cancer-related genes, promoting prostate cancer development and progression.[195,197]

PTEN deactivation is associated with the development of hormone-independent phenotype, poor prognosis and shorter progression free survival.[192,198] PTEN loss, in combination with other molecular alterations such as AR amplification or mutations, can promote the reactivation of androgen receptor (AR) signalling and can result in resistance to ADT. The dysregulated PI3K/AKT/mTOR pathway downstream of PTEN loss can heighten AR signalling and promote the survival and growth of prostate cancer cells under low androgen conditions. This loss of function is identified in ~20% of PCa prostatectomy samples and ~50% found in mCRPC samples.[192,199] The deletion or mutation of PTEN is shown to promote malignancy and induce metabolic reprogramming of PCa, through the alteration of glycolysis, glutaminolysis, fatty acid metabolism and branched chain amino acid catabolism pathways.[195] Overall, PTEN loss is likely to induce an immunosuppressant tumour microenvironment and its tumour suppression proficiencies, along with the aforementioned factors highlight possible disease vulnerabilities that have potential as a therapeutic target.[91,96,97]

MicroRNAs (miRNAs) are essential in the expression of PTEN and can influence PTEN concentrations.[202]. Currently, investigations into the viability of PTEN as a diagnostic, prognostic and therapeutic biomarker for PCa are underway.[203]

1.8.3 MicroRNAs

MicroRNAs are endogenous, short (~22 nucleotides), non-coding RNAs that mediate gene expression and are emerging as diagnostic and prognostic biomarkers as well as and potential therapeutic targets in PCa due to their role in disease progression.[204,205] The deregulation of several miRNAs is reported in PCa is thought to function as tumour suppressors or oncogenes, due to the apoptotic evasion resulting in carcinogenesis.[205,206]

Numerous microRNAs act as tumour suppressors through the inhibition of the expression of oncogenes or genes involved in promoting cancer progression. These miRNAs are often downregulated in prostate cancer, and their reduced expression contributes to enhanced cell proliferation, invasion, and metastasis.[207,208] Conversely, some microRNAs act as oncogenes through the promotion of tumour growth, metastasis, and therapy resistance. MiR-21 and miR-155 have been found to be frequently upregulated in prostate cancer and have been associated with increased cell proliferation, migration, and resistance to apoptosis.[209–211] These oncogenic miRNAs are found to target tumour suppressor genes, resulting in downregulation, and the promotion of PCa progression.[212]

Patient studies have indicated miRNA signatures involving; miR-17, miR-20a, miR-20b, miR-106a and miR-182-5p, that can distinguish between high and low risk patients with malignant and non- malignant disease phenotypes who have undergone radical prostatectomy, with a high specificity.[195,213] MiR-185 is important in the development of PCa to an androgen independent disease phenotype.[213] It binds to the 3′ untranslated region (UTR) of AR mRNA and its coactivator, bromodomain and results in a decreased expression.[202] High expression of the miRNAs studied were associated with shorter time to biochemical recurrence in the TCGA dataset, and confer an aggressive phenotype upon overexpression in vitro.[195]

Overall, it is important to note that miRNA regulation is complex, and miRNAs can have multiple targets and functions depending on the context. Further research is required to elucidate the precise mechanisms of miRNA involvement in PCa development and progression.[205]

1.8.4 DNA

DNA repair pathway alterations have been implicated in prostate cancer development and response to treatment. Mutations in genes involved in DNA repair, such as BRCA1, BRCA2, and ATM, can impair the ability of cells to repair DNA damage.[214] These mutations are more commonly associated with aggressive forms of prostate cancer and may confer sensitivity to certain therapies, such as PARP inhibitors.[214,215]

Homologous recombination (HR) deficiency is involved in repairing double-strand breaks in DNA.[216] Mutations or epigenetic silencing of HR-associated genes, such as BRCA1 and BRCA2 are thought to lead to HR deficiency in prostate cancer cells. This deficiency impairs the ability of cells to correctly repair double strand breaks, making them more susceptible to genomic alterations and promoting tumorigenesis.[216–218] HR deficiency has important implications for prostate cancer treatment, as it can result in increased sensitivity to therapies that target DNA repair, such as PARP inhibitors.[216–218]

Non-Homologous End Joining (NHEJ) dysregulation is a major DNA repair pathway involved in repairing DSBs, particularly in the absence of a sister chromatid template.[219] Dysregulation of NHEJ components, have been shown in prostate cancer, where alterations in the expression or the activity of these proteins can lead to defects in NHEJ-mediated DNA repair, contributing to genomic instability and potentially promoting prostate cancer progression.[220,221]

1.8.5 Prostate cancer antigen 3 (PCA3)

PCA3 is a urinary biomarker and a non-coding RNA expressed by the prostate during disease progression. Although the exact function of PCA3 in disease progression is not known, it is shown to control the survival of PCa through regulation of AR signalling and epithelial–mesenchymal transition (EMT) markers.[190] PCA3 may contribute to cancer development and progression through various mechanisms, as its been shown to interact with and to modulate the activity of androgen receptor (AR), a critical driver of prostate cancer. It may promote AR signalling, leading to enhanced cell growth, survival, and resistance to therapy.[220,221] Furthermore, PCA3 may play a role in the regulation of genes involved in cellular proliferation, apoptosis, and invasion. PAC3 has been detected at low levels in benign prostatic hyperplasia but found in higher concentrations in PCa tissue.[64,77,80] Due to its high expression in PCa (95%), it can serve as a useful biomarker for disease. In 2012 the FDA approved the use of PCA3 test (Progensa and GenProbe) for

clinical use for patients based on negative biopsy result, negative PSA results and or DRE results.[106,107]

1.9 Androgen Receptor Signalling and its role in Prostate Cancer

Androgens are a group of steroidal analogues of the hormone testosterone, which play an essential role in normal prostate development, growth and the sexual development and differentiation in males. The androgen receptor (AR) is a steroidal receptor and a transcription factor for testosterone and 5α-dihydrotestosterone (DHT).[176,226] AR is a ligand dependent transcription factor which translocates to the nucleus via androgen binding and switches on the transcription of genes, such as KLF4, involved in cell differentiation to maintain prostate homeostasis.[227,228] KLF4 is a zinc finger Krüppel-like factor that regulates stomatic cell reprogramming and has been shown to play an important role in cancer pathogenesis.[229] It is shown to be overexpressed in murine prostate stem cells to regulate homeostasis, to block malignant transformation, and to control the renewal of tumour-initiating cells.[228]

1.9.1 Androgen Dependency

AR signalling plays a critical role in the establishment and progression of PCa.[175] Cells in the basal layer have been shown to express an increased concentration of AR in PIN and the early stages of PCa.[163,230] With disease progression, the cancer cells become more sensitised to the presence of androgens.[42,227] The establishment of prostatic adenocarcinoma involves switching of AR transcription in the luminal cells from the regulation of cell differentiation to proliferation, aiding in disease progression.[227] Early stage PCa is androgen dependent, but progression often results in the initiation of an androgen independent phenotype.

1.9.2 Androgen Independency

Metastatic castrate resistance PCa (mCRPC) is the androgen independent disease phenotype and is considered incurable at present. This is perhaps due to changes in androgen receptors (e.g. mutations, amplification, splice variants) changes in steroid metabolism or changes in signalling pathways.[231–234]

Androgen is known to bypass pathways that promote AR-dependent cancer growth and the cancer cells no longer require the use of androgen for progression. [42,170,171] With progression to androgen independence, an alteration in the AR signalling cascade results in amplification of the AR gene, AR gene mutations, modifications in the

expression of steroid-generating enzymes and ligand-independent activation of AR through “outlaw” pathways, and AR-independent “bypass” pathways. These alterations induce the androgen-independent phenotype seen in late stage PCa.[228,44,175,235] Patients with mCRPC and amplification of the AR gene survive longer than patients without amplification of this gene. Approximately one third of patients with androgen-independent disease, display an amplification of the AR gene, which is not present when the tumours are hormone-dependent. This amplification leads to an increase in the expression of the AR and enhanced activation of the receptor by low levels of androgens.[236,237] Blockade of AR can delay disease progression and is the recommended treatment for patients who are unable to undergo radical surgery or where disease has spread from the prostate to other sites.[238,170] The PCa disease progression from the androgen dependent (localised) to androgen independent (metastatic) disease, illustrated in Figure 1.7.

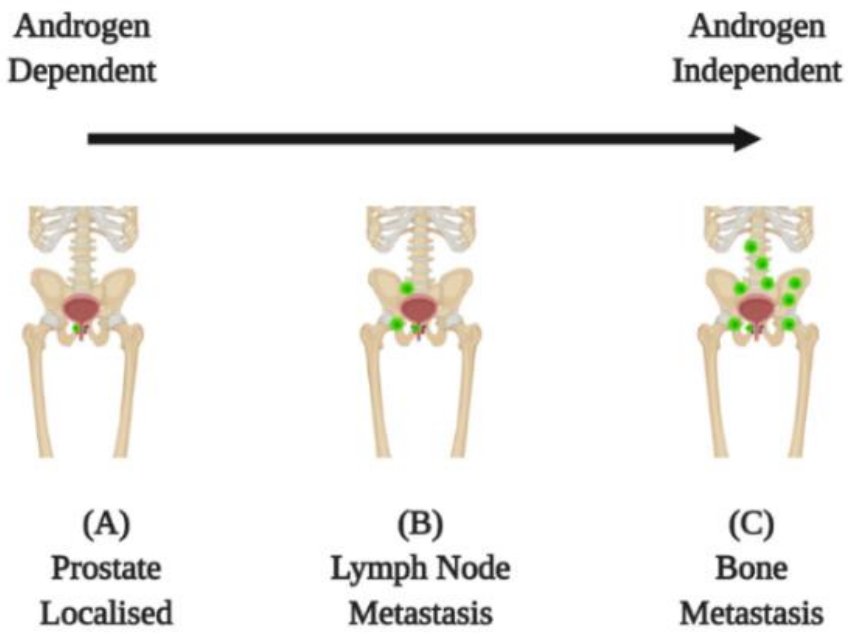

Figure 1. 7 (A)Disease is localised to the prostate gland itself in the early stages of androgen dependent PCa establishment. (B) Disease dissemination through the circulatory and the lymphatic system results in metastasis to the surrounding lymph nodes with decreasing androgen dependency (C) Further disease progression classically spreads to the lower axial skeleton where it is considered androgen independent and fatal, this can then further metastasise to the brain. Image created with Biorender.

1.10 The Hallmarks of Cancer

The Hallmarks of Cancer are a collection of biological mechanisms by which normal cells transform to malignancy, focusing on the different aspects of tumourigenesis.[239] Initially starting as 6 hallmarks, then expanding later to 8 in 2011 with further considerations in recent years.[240] Unaccompanied, the hallmark's do not account for cancers complexities in tumour development and malignant progression.[240] With this, the enabling characteristics of the hallmarks of cancer have been proposed, addressing the conditions of neoplasia by which cancer assume these traits as seen in Figure 1.8.[240]

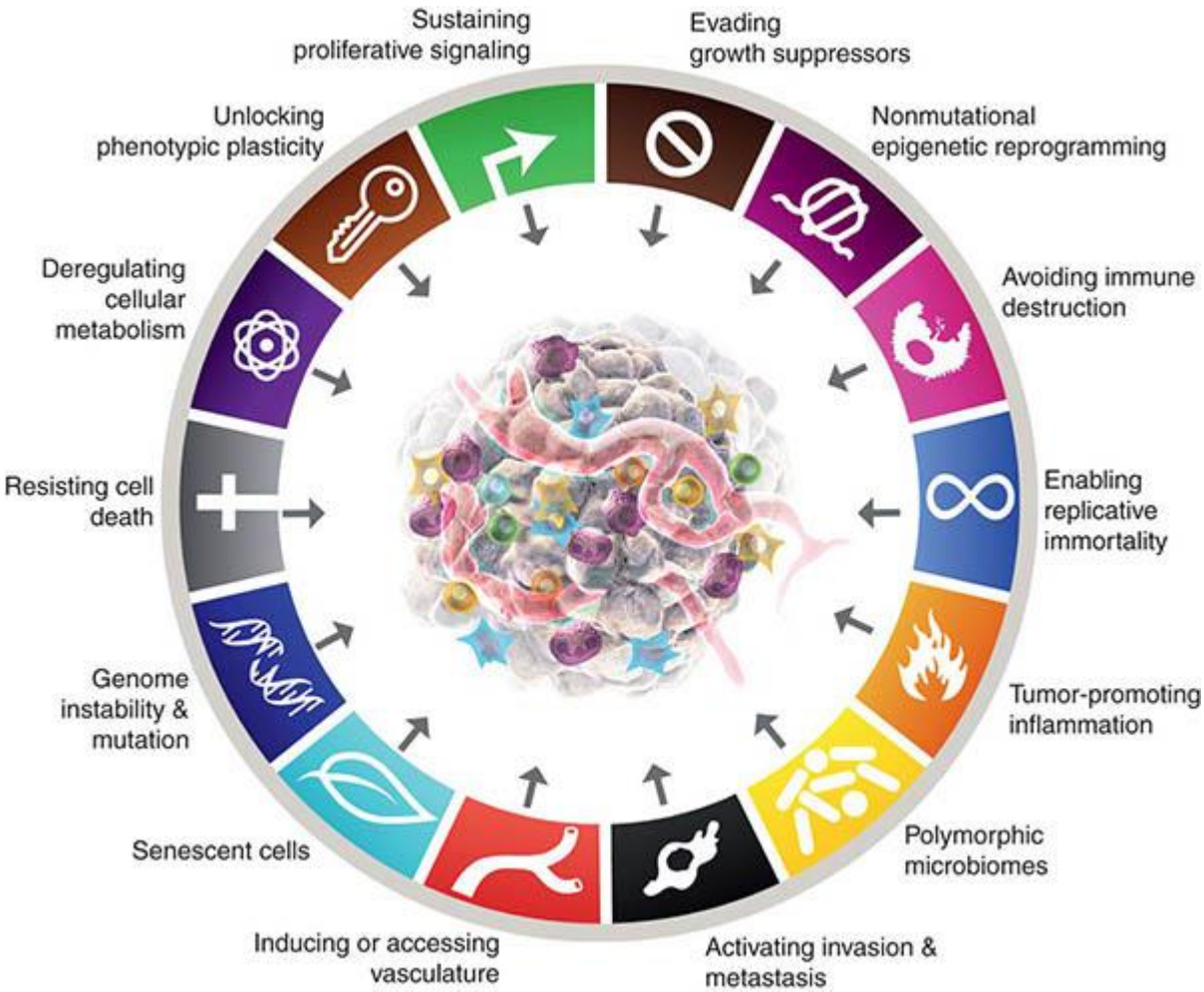

Figure 1. 8: The hallmarks of cancer, new dimensions from the American Association of Cancer Research..[241]

In 2011, the reprogramming of energy metabolism was listed as an emerging hallmark of cancer; recognising in cancer, the unregulated control of cell proliferation, paired with the modifications to the cell's metabolism for fuelling cell growth and division.[240,242,243] This is thought to lead to the glycolytic switch of cancer cells from Oxidative Phosphorylation (OxPhos) to aerobic glycolysis to fuel energy

demands.[240,242,243] The fuelling of cancer cells by glycolysis has been linked to activated oncogenes (e.g., RAS, MYC) and mutant tumour suppressors (e.g., TP53), with further links to the hallmarks of cell proliferation, avoidance of cytostatic controls, and a reduction of apoptosis.[240]

These ever-expanding hallmarks of cancer are advancing the growing understanding of the disease with the hallmarks growing in interest as therapeutic targets. In this study the reprogramming of energy metabolism is of therapeutic interest with our novel metabolic targeting event.

1.11 Energy Metabolism and Metabolic Pathways

The normal prostate exhibits an unusual metabolic signature. The metabolic processes account for an accumulation of zinc in the mitochondria, which results in the inhibition of the enzyme mitochondrial aconitase, which catalyses the oxidation of citrate in the mitochondria, cutting the Krebs cycle short.[244,245] Furthermore, citrate is secreted into the prostatic fluid. Thus, a normal benign prostate relies on cytosolic metabolic processes, such as aerobic glycolysis for its ATP production.[175,244]

OxPhos is the metabolic phenotype hypothesised for the early-stage prostatic disease.[244] OxPhos involves the production of ATP in the mitochondria through the Krebs cycle and oxygen consumption processes of the electron transport chain.[246,247] OxPhos is thought to be the most efficient method of energy production for the cell, with 36 ATP molecules produced per glucose molecule.[246,248] Details of OxPhos and the Krebs cycle are expanded on in Figure 1.9.

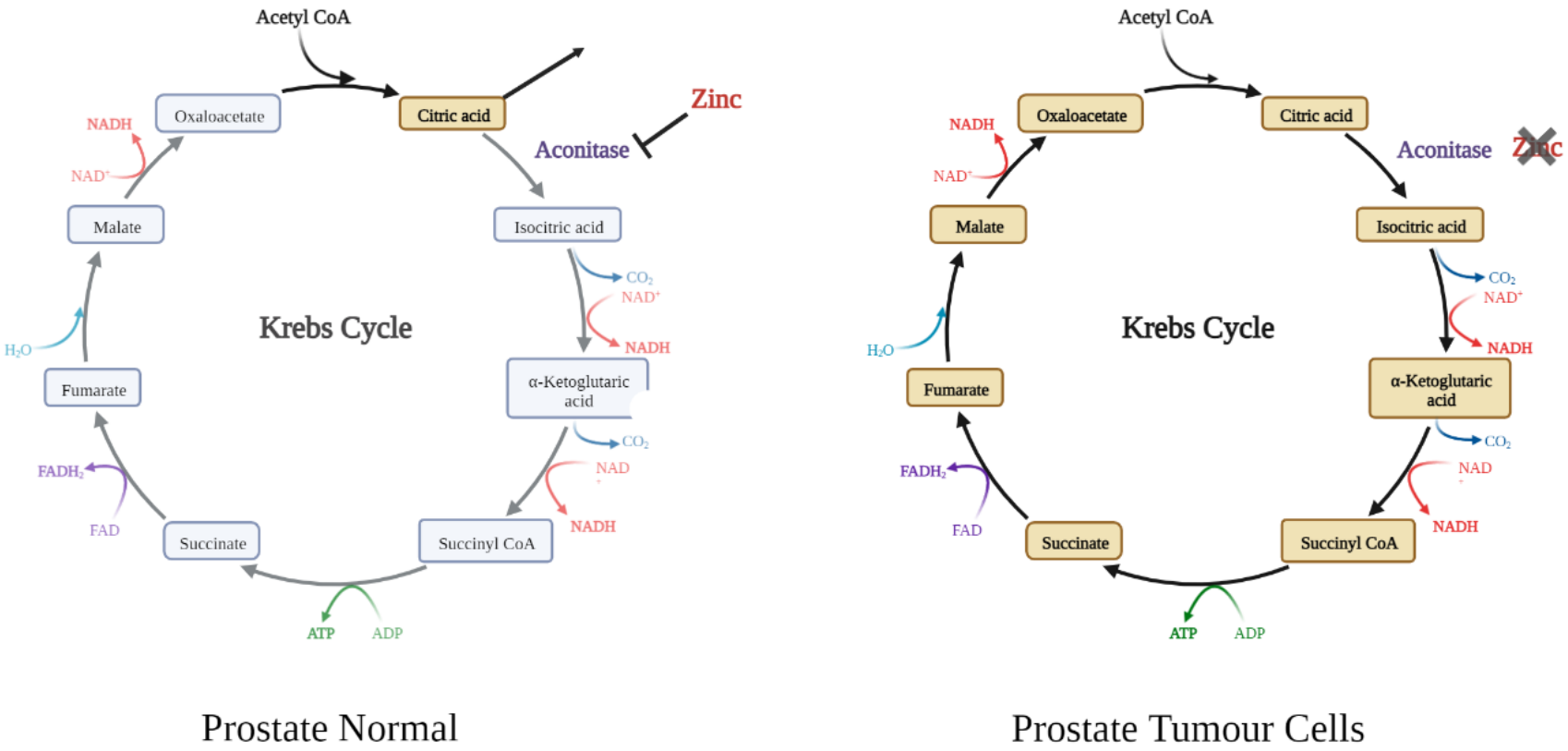

Figure 1. 9: Oxidative Phosphorylation and the Krebs Cycle: In OxPhos, glucose is broken down into pyruvate, this pyruvate is converted to acetyl co-A through the decarboxylation, reduction of NAD+ and finally the addition of coenzyme-A to the molecule. Acetyl co-A is added to oxaloacetate through an enzymatic aldol reaction resulting in citrate. Iso-citric acid is formed through the dehydration-hydration reaction of citrate. The decarboxylation and oxidation of iso-citric acid results in the production of 2-ketoglutaric acid. Another decarboxylation and oxidation take place resulting in succinyl CoA. The hydrolysis of 2-ketoglutaric acid to succinyl CoA, is coupled to the phosphorylation of guanosine diphosphate (GDP) to guanosine triphosphate (GTP). The enzymatic desaturation by flavin adenine dinucleotide (FAD)-dependent succinate dehydrogenase yields fumarate. Following the hydration reaction, fumarate is catalysed by fumarase and converted to L-malate. Finally, NAD-coupled oxidation of L-malate to oxaloacetate is catalysed by malate dehydrogenase. This ends the cycle. Image curated in Biorender online.

Glycolysis is a process of energy production that takes place in the cell's cytoplasm, where glucose is oxidised to generate pyruvate. Depending on the oxygen levels present, these pyruvate molecules hold different fates.[246,248]

In the presence of oxygen, pyruvate is produced, where it can then follow on to the Krebs cycle for further metabolism, or further to the anaerobic glycolysis process to produce lactate.[242,249] Ultimately, a large output of lactate is reported during the process of aerobic glycolysis with the production of 4 ATP molecules/glucose for net gain.[242,249] This method of aerobic glycolysis is thought to be favoured by cancer cells and referred to as the Warburg effect.[250,251] Under the presence of oxygen, it is thought cells would preferentially produce energy through the efficient process of OxPhos, however, the Warburg effect has been characterised in many cancer cells and is illustrated in Figure 1.10.[250–255] It is known that the method of glucose metabolism undertaken by cancer cells, works under this less efficient manner of metabolism, even with more than sufficient levels of oxygen.[256]

Anaerobic glycolysis takes place in the absence of oxygen. Pyruvate is reduced to lactate as NADH is oxidized to NAD+ by lactate dehydrogenase. [257,258] During aerobic glycolysis, NADH is transported by the malate aspartate shuttle to the mitochondria where it is oxidized to NAD+ while it participates in the electron transport chain to produce ATP.[257,258] In the process of anaerobic glycolysis, considerably lower levels of ATP production occur. [257,258]

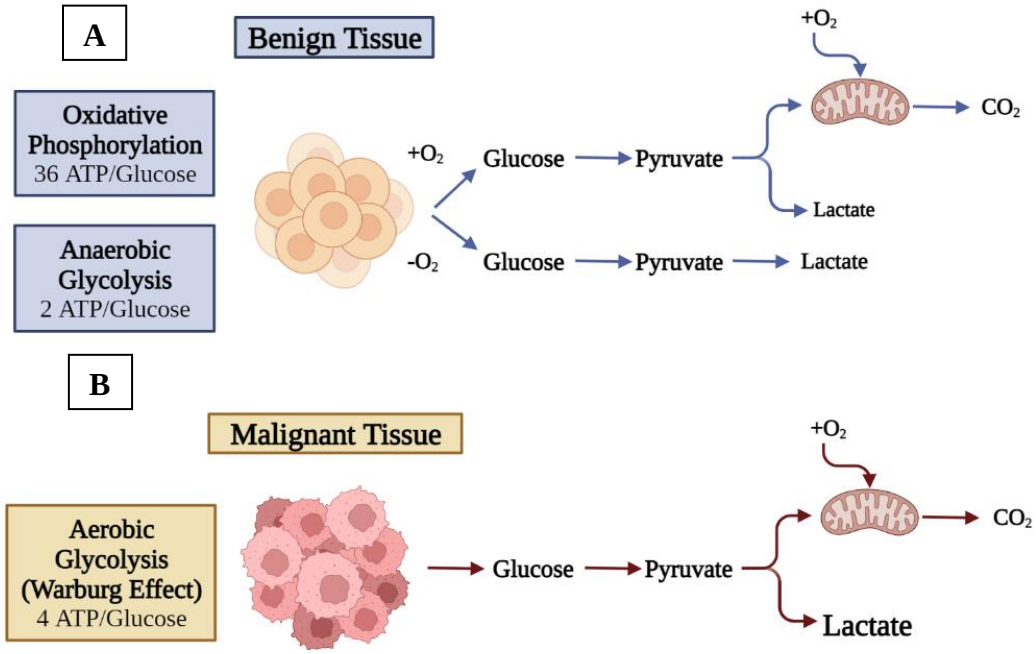

Figure 1. 10: OxPhos vs Glycolysis in the cell: (A.) In benign tissue, OxPhos results in the production of 36 molecules of ATP/glucose in the presence oxygen. It takes place in the mitochondria and results in an output of ATP and CO_2. Anaerobic glycolysis is the production of ATP on the cytosol in the absence of oxygen, with an output of 2 ATP/glucose and a small concentration of lactate. (B.) In malignant tissue, aerobic glycolysis, referred to as the Warburg effect, is the process of ATP production in the cytoplasm in the presence of oxygen. It results in the production of 4 ATP/glucose with very large outputs of lactate into the cytoplasm and potential for further mitochondrial metabolic processes. Image made with Biorender.

The Warburg effect is a recognised hallmark of cancer and has been a topic of vast interest within the cancer research community. It is defined as an increased use of the process glycolysis rather than oxidative phosphorylation by tumour cells to meet energy requirements under normoxia. This phenomenon was first notarised by Otto Warburg in the 1920's when an increased uptake of glucose was observed in cancer cells and with the secretion of lactic acid . This aerobic fermentation is a signature of cancer metabolism.[250,259] Even in the presence of high levels of oxygen, cancer cells will select the metabolism pathway of Warburg's glycolysis. This is a far less efficient manner of ATP production when compared to that of oxidative phosphorylation, yet it is still chosen as the metabolic pathway for glucose in cancer cells.[253]

The rate of glucose metabolism through aerobic glycolysis is believed to be up to100 times faster than that of complete oxidation in the mitochondria.[260] Some studies suggest that this rate could in fact be even higher due to the limited diffusion of oxygen and the allosteric regulation of glycolysis. This rate limiting energy production may be the reason cancer cells utilise glucose in this manner.[260]

The Warburg effect may in fact be advantageous to cancer cell growth due to the kinetic difference when compared to that of oxidative phosphorylation, especially when in times of limited energy resources.[251,260,261] The limited availability of glucose in tumour microenvironments may cause a competitiveness for resources such as glucose especially for the immune system and stromal cells.[251] Thus, the altered metabolism for cancer cells allows a selective advantage for survival and proliferation.[251]

.

1.12 Vitamins in cancer treatment

1.12.1 Ascorbic Acid in Cancer Treatment

Vitamin C is a small, water-soluble, polar molecule required by human and animal systems.[262] It is a glucose derivative which is transported in the human body via sodium transporters SVCT1 and 2 as well as the glucose carrier molecules GLUT.[263] In its natural state, it is considered an antioxidant molecule but, studies have shown it to act as a pro-oxidant at high concentrations, producing hydrogen peroxide (H_2O_2) in-vitro and in-vivo, inducing selective toxicity to cancerous cells with negligible effects to normal cells.[264] Vitamin C is transported through the circulatory system to individual cells, and intracellular concentration of ascorbate can be as high as 50µM greater than that in the plasma, through uptake by the sodium dependant Vitamin C transporters, SVCT1 and 2.[262,264,265] However, red blood cells accumulate ascorbate in the form of dehydroascorbate (DHA) by the glucose transporters (GLUTs), due to the lack of SVCT2 expression.[262,264,265] Concentrations of ascorbate vary by tissue type and high intracellular concentrations are believed to be due to tissues demand as an essential enzyme cofactor.[266] The water-soluble nature of ascorbate means, that the compound can be readily circulated and attained, however, it cannot be stored and is therefore in constant demand. The human body, along with other mammals, cannot produce its own Vitamin C, due to the lack of l -gluconolactone - oxidase in the liver; hence it is required in the diet.[267] Existing studies have determined that plasma Vitamin C half-life is approximately 2hrs after administration.[268]

Growing evidence indicates that ascorbate in pharmacologic concentration could be significant in cancer treatment, showing selective killing of various cancer cells.[269] Although pharmacological ascorbic acid concentrations are not achievable through oral administration. I.V. administration has been shown to be the most successful route of administration. Several clinical trials on the effects of high dose Vitamin C by IV

administration, have shown to improve and prolong the life span of terminal cancer patients, where the oral administration resulted in no effect.[270–273] IV administration has shown to result in plasma concentrations of Vitamin C ~25 times higher than that of oral administration. The cytotoxic effects demonstrated by Vitamin C in many studies has been found to be both in combination with other therapies and when alone.[270,271,273,274]

1.12.1.1 Anticancer oxidative pathways of Ascorbate

Ascorbic acid, a key nutrient in human nutrition is a concentration dependent; pro-oxidant and an antioxidant, increasing its possible drug interaction ability.[275] Due to these properties, the pathway for cell killing is known to be through the depletion of intracellular thiols and production of H_2O_2.[276]

1.12.1.2 Antioxidant Pathways

At low concentrations ascorbate will act as an antioxidant undergoing a one or two electron oxidation, resulting in an ascorbate radical or DHA.[262,263,276,277] In the cell, DHA is very unstable at neutral pH and will be reduced by intracellular thiols such as glutathione (GSH) or thioredoxin, to generate a more stable molecule, reduced ascorbate.[262,276,278] This results in a depletion of antioxidant species in the intracellular space, increasing endogenous ROS.[277,278] The reduced ascorbate goes on to forms oxalic, diketoglonic and threonic acid, which are excreted by the kidneys.[277,278] The antioxidant mechanisms of vitamin C in producing DHA are illustrated in Figure 1.11.

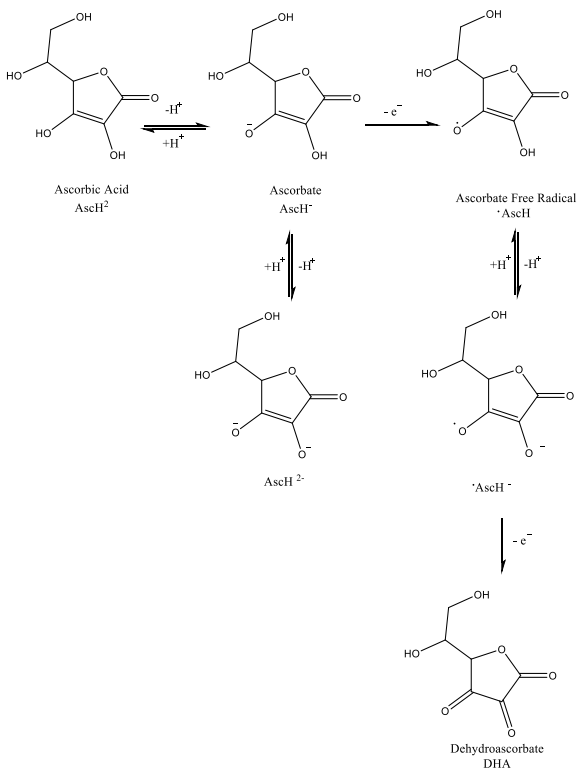

Figure 1. 11: Antioxidant mechanism of Vitamin C. The 2-electron oxidation of Ascorbic Acid with the formation of a stable DHA molecule. Images made in ChemDraw Professional 16.0.

DHA can be taken up by the GLUT transporters, due to its similar chemical structure to that of glucose, resulting in accumulation in red blood cells.[262,279] DHA is reduced by glutathione (GSH), NADH and NADPH- dependent enzymes, in response to oxidative stress, and reducing thiol concentrations.[278,280,281] Reducing the cell's ability to equilibrate its redox balance, in turn overthrowing the ROS quenching abilities and increasing sensitivity to prooxidant mechanisms.[262]

DHA exists in competitive concentrations to that of glucose for uptake by GLUTs, and hence is readily taken up by cancer cells. Studies of the effects of pharmacological Vitamin C on colon cancer have been found to increase the cytotoxicity of chemotherapeutics, reversing the Warburg phenotype in the meantime.[282]

Whether Vitamin C has a net pro-oxidant or antioxidant effect depends on the cell's concentration gradient and redox state. Due to the reduced blood flow and oxygen present in the tumour microenvironment, Vitamin C more often acts as a prooxidant, producing hydrogen peroxide and resulting in cell damage.

1.12.1.3 Prooxidant Pathway

The chelation properties of ascorbate enable its pro-oxidant activity at high concentrations, through the recycling of Fe^{2+}.[188–191] When in the presence of oxygen, produces H_2O_2 and hydroxyl radicals ($^{\bullet}OH$) through Fenton's reactions and Haber Weiss chemistry.[277,287] The autoxidation of ascorbate is reduced when chelators of iron and copper are added to cell culture media, and this supports the dependency on transition metals to produce H_2O_2. [277,287] Hence, the reducing abilities of Vitamin C on transition metals are thought to be the source of its anticancer properties.[277,287] This process explains the ability to promote iron uptake from dietary intake. The Fenton's mechanism of Vitamin C and ascorbate are illustrated in Equation 1.1 and

.

$$AscH^{-} + Fe^{3+} \rightarrow Asc^{\bullet -} + Fe^{2+} + H^{+}$$

$$Fe^{2+} + H_2O_2 + H^{+} \rightarrow Fe^{3+} + H_2O + HO^{\bullet}$$

Equation 1.1: Trace transition metals such as iron are reduced by ascorbate, through Fenton's reaction and Haber Weiss chemistry producing ascorbate radicals then producing H_2O_2, which is cytotoxic. This can then undergo further reduction with the iron 2+ that is recycled to produce hydroxyl radicals and upsurge oxidative stress mechanism.

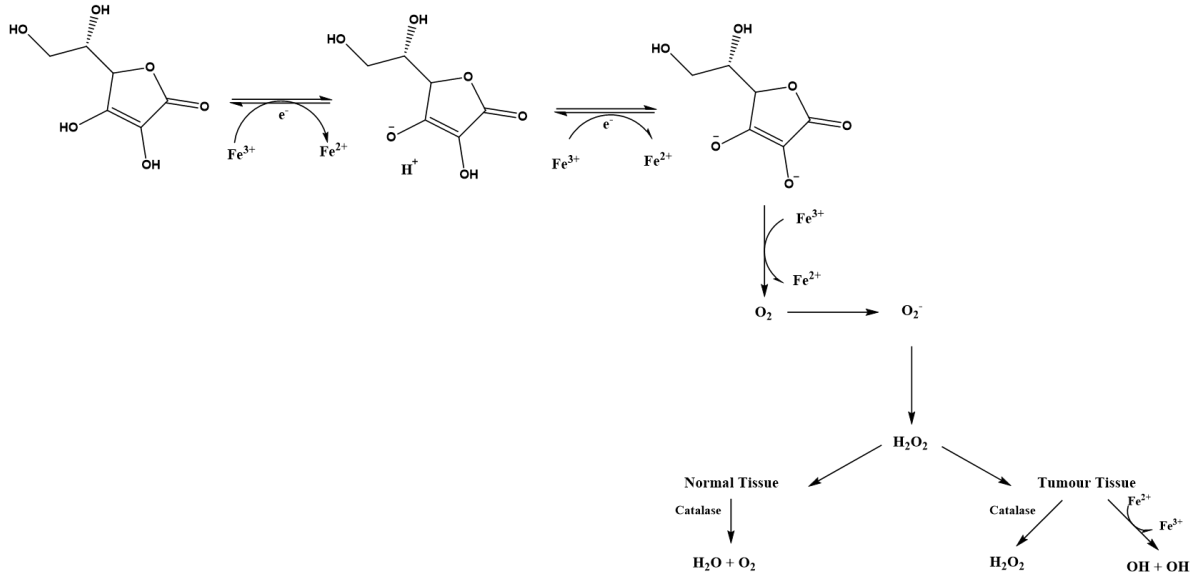

Figure 1. 12: Ascorbic acid radical formation: After ionization of ascorbic acid, the ionized form loses an electron to form the ascorbate radical Asc• - and hydrogen peroxide. Images made in ChemDraw Professional 16.0.

Ascorbic acid is the pro-drug of hydrogen peroxide (H_2O_2). Achieved through the formation of the ionized ascorbate molecule followed by steady state formation of the ascorbate free radical and H_2O_2 in extracellular matrix.[266] The concentration of hydrogen peroxide becomes too high for the cells antioxidant enzymes such as GSH present in the mitochondria, to regulate and results in cytotoxic effects and eventually cell death.[266]

At concentrations of 1mM and greater, cytotoxicity is demonstrated in cancer cells by increased cell cycle arrest, p53 uptake, decreased ATP concentration, compromised mitochondrial function and the suppression of NrF-2, all resulting in apoptosis.[288,289] Effects on cancer cells have been noted at concentrations lower than 1mM, resulting in enhanced vulnerability to conventional chemotherapeutics.[288,289]

I.V administration of ascorbic acid allows for pharmacological ascorbate concentrations to be achieved, where it acts as a prodrug for H_2O_2 formation.[283,284] This mechanism of cell death is dependent on H_2O_2 formation. H_2O_2 scavengers have been used to demonstrate how they are protective of the cellular redox balance and how H_2O_2 is an effector species that mediates the pharmacological ascorbate induced death of cancer cells.[283,284]

In vitro preclinical studies of 43 tumour and 5 normal cell lines involved exposure to Vitamin C. The resultant tumour xenograft showed that pharmacologic concentrations of ascorbate decreased tumour volumes by 41–53% in the different cancer types, including aggressive disease. [273,283–285]

The H_2O_2 produced by the metabolism of ascorbate, causes a depletion of cellular ATP inducing autophagy.[279] This has been demonstrated in prostate cancer cells resulting in cell death. ATP depletion has been recognised as a possible mechanism of preferential cell death; this is unlike normal cells.[279] Malignant cells depend on glycolysis for ATP, in the Warburg effect. Warburg metabolism results in the uptake of glucose at a rate of 100 times that of non-malignant cells.[242] The uptake and transport of Vitamin C by GLUT may cause the increased uptake of Vitamin C by cancerous cells, hence showing a far greater toxicity to cancer cells than non- cancerous cells by greater intracellular concentration accumulations.[264,279] Thus, some cancer cells have a greater sensitivity to pharmacologic ascorbate concentrations in comparison to normal cells that would use oxidative phosphorylation pathways for energy production.[262,279] Studies have demonstrated significantly lower levels of ATP for cancer cells exposed to pharmacologic concentrations of ascorbic acid, supporting the dependence on Warburg metabolism.[279,285,290] This mechanism of ascorbate induced oxidative stress could illustrate the difference between normal cell and tumour cell metabolism.[279,285,290]

The low oxygen concentrations found in the tumour microenvironment, due to the lack of circulation and rapid cell division present in tumour tissue, has been questioned in altering the ability of Vitamin C to express its anticancer properties.[291]

1.12.2 Menadione in Cancer treatment

Menadione is a water soluble polycyclic aromatic ketone, and a synthetic analogue of vitamin K.[292] It is a quinone derivative, formed in the body from catabolic reactions from the intestinal absorption of vitamin K.[292,293] Menadione, along with other quinone derivatives has been found to demonstrate cytotoxicity in many different forms of cancer cells, without effect on normal cells.[292,293] Menadione is a derivative of vitamin K_3 and studies show it can interfere with the body's antioxidant levels resulting in damage to cell membranes.[293]

Proteins responsible for blood clotting, bone mineralization and the development of the nervous system require vitamin K_3.[294] These properties of vitamin K_3 have steered

investigations towards its possible therapeutic capabilities.[294–296] Studies have demonstrated the possible anti-carcinogenic effects of dietary vitamin K_3, causing a stir in its possible uses as a combination treatment with conventional chemotherapeutics.[295]

Menadione has been identified to increase the expression of pro-apoptotic proteins and a simultaneous decrease in anti- apoptotic proteins in different forms of human cancer cells.[294,297] However, the primary mechanism of cell death by Menadione is thought to be due to its redox cycling capabilities, forming mitochondrial ROS at high concentration and inducing oxidative stress.[295]

1.12.2.1 Anticancer Mechanisms of Action:

Menadione is thought to have many different possible mechanisms resulting in its anticancer effects.

1.12.2.2 Oxidative Stress Pathways:

I. Redox Cycling and Oxidative Stress:

Menadione has been linked to the alteration of the body's natural antioxidant effects, resulting in membrane damage, DNA damage, inhibition of blood vessel formation, altered proliferation, cell shrinkage, and the activation of capsase-3.[292]

The cytotoxicity of Menadione is due to the redox cycling of the quinone moiety resulting in the production of reactive oxygen species (ROS).[292] The type of cell death typically observed by Menadione oxidative stress process is oncosis (swelling), leading to further necrosis or when combined with Vitamin C, autoschizis.[298] Menadione will kill cancerous cells with negligible effects on normal cells, by this oxidative stress mechanism.[299–302] Menadione cytotoxicity involves redox cycling of the benzoquinone moiety with production of reactive oxygen species (ROS).[299,303] Redox cycling of the quinone moiety of Menadione results in the induction of oxidative stress by the production of high concentrations of ROS, exceeding the oxidative capacity of the cancer cell and resulting in cell death.[299,303] The electrophilic quinone component of Menadione undergoes the process of either; one electron reduction, generating semiquinone radical species, which may cause lipid peroxidation and cell death or; two electron reduction forming a hydroquinone species.[297]

The spin restricted oxidation of hydroquinone species is slow. Thus, the presence of trace metals, such as iron and copper, aids in the suppression of spin restrictions, by readily transferring one electron to O_2, directly oxidizing hydroquinone.[304] This pathway

results in the reduction of the trace metal present with a simultaneous production of hydrogen peroxide and other ROS that may hinder DNA.[304] These reactions occur with the depletion of superoxide radicals and other reducing species.[304] The redox cycling properties of Menadione, causing reduction in reducing species is thought to be the mechanism behind its cancer supressing activities.[305]

Semiquinone radicals of K_3 can reduce transition metals through intracellular chelation of iron, triggering Fenton's reaction ($Fe^{2+} \rightarrow Fe^{3+}$) producing highly reactive oxygen species (hydroxyl and hydroperoxyl radicals).[254,306] These hydroxyl radicals can result in DNA strand breaks.[254,306] This is a potential mechanism that could result in hazardous side effects on normal cells. Oxidative stress mechanisms have shown to result in single (ss) and double (ds) strand DNA breaks but, after 6hrs in drug free media, significant repair is found, but not total.[254,306] Figure 1.13 demonstrates the one electron reduction of Menadione to semiquinone inducing Fenton's reaction resulting in hydroxyl, per-hydroxyl) and hydrogen peroxide radicals. With further two-electron reduction of Menadione resulting in the formation of hydroquinone through the equilibrium shift by γ-carboxylation.

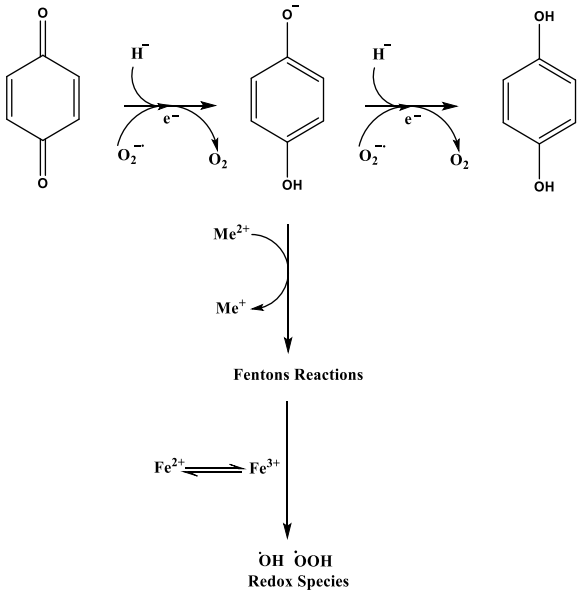

Figure 1. 13: One electron reduction of Menadione: The one electron reduction to semiquinone induces Fenton's reaction producing hydroxyl, per-hydroxyl) and hydrogen peroxide radicals. The two-electron reduction of Menadione results in the formation of hydroquinone through the equilibrium shift by γ-carboxylation favouring its production. Images made in ChemDraw Professional 16.0.

Menadione is thought to result in a decrease in oncogenic superoxide leading to apoptosis through the generation of onco-suppressive hydroperoxides and cytotoxic hydroxyl radicals.[295,297] Antioxidants such as GSH and antioxidant enzymes; catalase and superoxide dismutase quench ROS, decreasing the oxidative stress capabilities of Menadione reducing its anticancer effects.[305,307–309] However, if high enough concentrations of Menadione are achieved, the capability of antioxidant enzymes to eliminate ROS is exceeded and results in redox related death.[305,307–309]

Phase I clinical trials of 40 men with PCa were given a (1–5 h) intravenous infusion every 3 weeks, starting at 40 mg/m2 - 1360 mg/m of Menadione[2].[310] Plasma Menadione concentrations peaked at 1.9–7.4 µM during the infusion in 3 patients receiving 1360 mg/m.[310] Menadione was found to be not cytotoxic and was safe, however no objective partial or complete responses were observed.[310]

Mitomycin C in combination with Menadione for the treatment of lung cancer was observed through a Phase II Trial of 23 patients with advanced disease. Menadione was administered (2.5 gm/m2) by I.V. infusion over 48 hours followed by mitomycin C (10-20 mg/m2) by I.V. bolus, every 4 to 6 weeks.[311] 2 of 23 participants had an objective response of 3.5 months and 13 months with a median survival of 5.5 months.[311] Overall, 28% of patients with non-small cell lung carcinoma, demonstrated tumour regression on a single occasion but were lost to follow up.[311]

Evidence suggests that at high concentrations of Menadione, anticancer mechanisms occur by these oxidative stress mechanisms as well as direct arylation.

II. Direct Arylation:

Arylation is the addition of electrophilic aromatic hydrocarbon (aryl) group to nucleophilic organic molecules and is mediated by the presence of trace metals.[304] Direct arylation of thiols by Menadione involves the addition of the aromatic from Menadione to molecules such as GSH forming a Menadione-glutathione complex.[295] Once oxidative stress occurs, GSH is typically the first line of defence as a ROS quencher, however once this is overwhelmed the depletion of sulfhydryl-containing proteins and GSH is thought to occur.[277,303] This can alter the function of protein thiol groups that cause, regulation of metabolism, protein folding, regulatory pathways, and antioxidant defence.[277,303] This synthetic form of the vitamin has been shown to then bond to peptides directly at the cysteine sulphur group.[308]

Many anticancer studies of Menadione have supported the mechanism of direct arylation, being the cause of the anticancer effects demonstrated. However, most are reported to be due to the redox cycling pathways.[299]

1.12.2.3 Non-Oxidative pathways

There are many methods of Menadione metabolism; those linked to anticancer effects are that of the oxidative pathways, however, Menadione does also result in some non-oxidative mechanisms. These non-oxidative pathways are associated with the natural forms of Vitamin K (K_1 and K_2) however, Menadione is also linked to Calcium (II) homeostasis.[297,308]

1.12.3 Apatone

The increased effectiveness of Menadione when in combination with ascorbate, demonstrates the requirement for a reducing agent with the quinone moiety for the optimum effect. Studies of breast, prostate, and bladder carcinoma to name a few, have shown great success in the use of Vitamin C and Menadione at a ratio of 100:1 (Apatone).[310,312] The synergistic effects of the vitamins in combination induce mechanisms of oxidative stress, resulting in a unique type of cell death called autoschizis.[313]

Autoschizis is a novel form of necrosis. It has been identified through the loss of the organelle free cytoplasm through self-expurgation due to hyperbolic damage to the membrane of the cell.[314] The nucleus and cell also reduce to between one half to one third of its usual size. There are also some organelle-based alterations within this process, but overall tumour cell death does not result from ATP depletion.[298]

Possible mechanisms of the vitamin combination include free radical production, thiol depletion, induction of lipid peroxidation, modulation of ATP, calcium regulation, activation of NF-kB and depletion of GSH by oxidative stress mechanism.[315] These mechanisms are orchestrated through the pathways detailed in the sections above; however, the method of radical production is different, as there is a synergistic mechanism between Menadione and Vitamin C.

The redox cycling of Vitamin C and Menadione are known to involve an overlapping process. Vitamin C non-enzymatically reduces Menadione with the subsequent production of H_2O_2.[298] Vitamin C is oxidised to DHA and semiquinone free radicals.[298] The semiquinone is re-oxidised to its quinone form by molecular

oxygen.[298,316] This generates hydroxyl, perhyroxide and hydrogen peroxide radicals, resulting in oxidative stress mediated cell death.[312] This has been confirmed through the addition of the ROS suppressor; catalase, to the culture media of Apatone treated cells, where the cytotoxic effects are seen to be dramatically reduced as the redox species are mopped up by the free radical scavenger.[298,315]

A 12 Week, phase I/IIa trial of Apatone in the treatment of prostate cancer patients who have failed standard treatment was conducted with 17 patients.[310] Participants were treated with Vitamin C (5,000mg) and $VitK_3$ (50mg) daily for 12 weeks.[310] Patients PSA was recorded at 6 and 12 weeks resulting in; 15 of the 17 patients continuing treatment for 6-24 months.[310] Overall, PSA velocity and PSA doubling time decreased in 13 of the 17 patients with no adverse effects observed.[310]

Cells treated with Apatone show an increased production of ATP in the mitochondria, to defective areas of complex III of the electron transport chain.[301,316] Ensuing a shift from anaerobic glycolysis to aerobic oxidative metabolisms with reduction in hypoxia and lactic acid. [310,301,316] In the likes of prostate cancer, the late-stage metastatic disease holds a glycolytic phenotype, pushing this back to the oxidative lipid metabolism is significant in the regression of the disease.[317]

1.13 Hypothesis and project aims

This research project has multiple strands of innovation using a combination of approaches and intelligent design to synthesise and develop novel cancer therapeutics. The primary aim is to develop a strategy where cancer cells have a restricted capacity to adapt to the treatment, limiting their capacity for survival, as well as taking advantage of their critical need to function using metabolic pathways. This project has designed and synthesised a set of innovative compounds that aim to provide an effective cancer therapy to address the major issue of the prevalence of PCa and of patient survival.

This project presents many novel ideas, with the final objective of optimizing a therapeutic agent to target the Warburg effect to eradicate cancer cells present in a tissue and to visualize this resulting effect within the tissue cells. With this a hypothesis and numerous research aims present themselves.

Overall, we hypothesise that the Trojan horse principle will create the ability to trick cancer cells into the continued uptake of Vitamin C and Menadione via a highly desirable fuel moiety (simple sugars and lipids), through increasing endogenous ROS and resulting in cell death. Overall improving the burden on patients and the healthcare system by providing an effective treatment and further insight into PCa's biology.

The following aims are reflected in each results chapter.

- To develop and synthesise a set of unique compounds to result in an optimum drug structure and characteristics, to target the Warburg effect of PCa cells.
- To investigate if the Warburg effect can be targeted in an effort to target a weakness in cancer cell metabolism to achieve apoptosis and cell death.
- To investigate if cancer cells can be 'tricked' into internalising a toxic moiety increasing cytoplasmic ROS concentration to a level that will induce apoptosis.
- To investigate the effects of the TH compounds on the PCa metabolome.

Chapter 2. Materials and Methods

2.1 Materials and Methods

This chapter provides a full description of the various cell and molecular techniques that were employed to deliver the aims of this thesis. For novel methodologies, detailed background information is provided. Techniques that pertain to the following chapters are detailed in full within this chapter, with relevant details limited to individual chapters. Herein, the methodologies required to analyse the efficacy of the TH compounds in a panel of prostate cell lines are described (Figure 2.1).

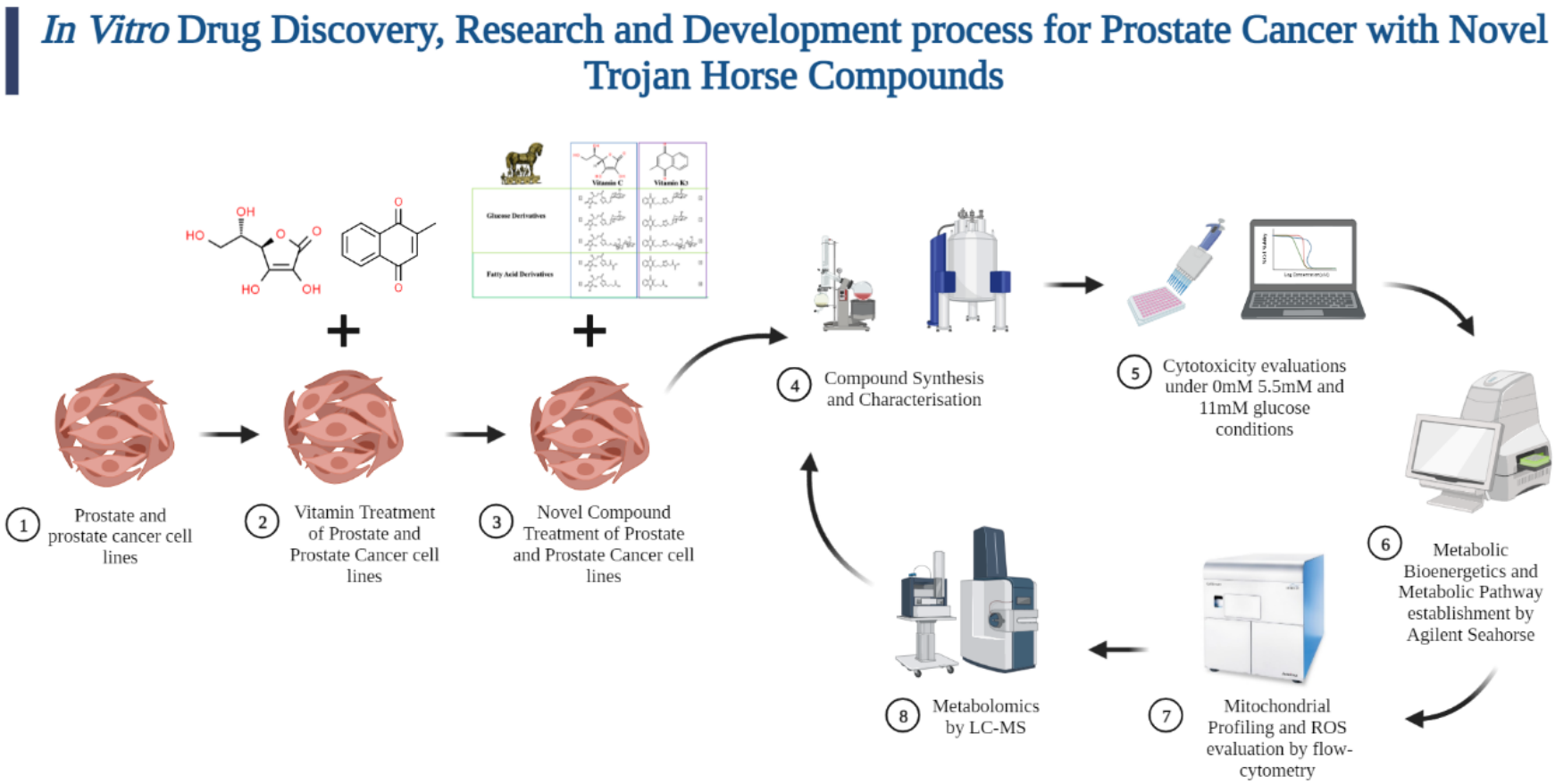

Figure 2. 1: The invitro drug discovery process, detailing the manner by which the TH compounds were examined in a panel of prostate cell lines under zero, 5.5mM and 11mM glucose conditions. This image was made in Biorender online.

2.2 Synthesis of the novel Trojan Horse (TH) compounds

The compound synthesis was conducted by Ms Eva Hayball and Dr. Robert Brooks in the University of South Australia (UniSA). The methods below were provided by Ms Hayball and Dr. Brooks. The compounds include conjugating a substrate used for cellular metabolism, such as glucose, to Menadione which is toxic to the cells at high concentrations, to increase uptake by the cancer cells and induce cell death.

I. <u>Menadione-amine</u>

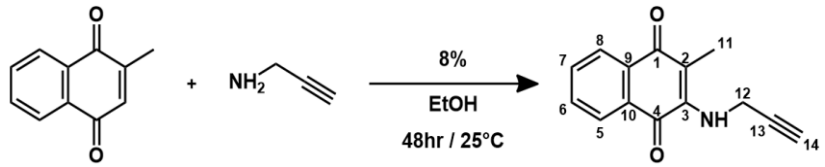

Figure 2. 2: Menadione-amine compound backbone synthesis.

To a solution of Menadione (1.000 g, 5.81 x 10^{-3} mol, 1 eq) in ethanol (EtOH) (30 mL) was added propargylamine (391 µL, 6.10 x 10^{-3} mol, 1.05 eq). The reaction mixture was allowed to stir at room temperature for 48 hours, after which it was concentrated under reduced pressure. The resulting dark red solid was redissolved in 50% ethyl acetate (EtOAc) / hexane and isolated by column chromatography (50% EtOAc / hexane). The combined fractions were concentrated under reduced pressure and the resulting red solid was then recrystallised from hot ethanol (10 mL) to obtain fibrous orange crystals. The crystals were isolated by filtration through a sintered glass funnel, washed with cold hexane (15 mL) and dried under high vacuum to yield pure orange crystals (113 mg, 8 %).

II. <u>Menadione-amine-glucose- Trojan Horse 1</u>

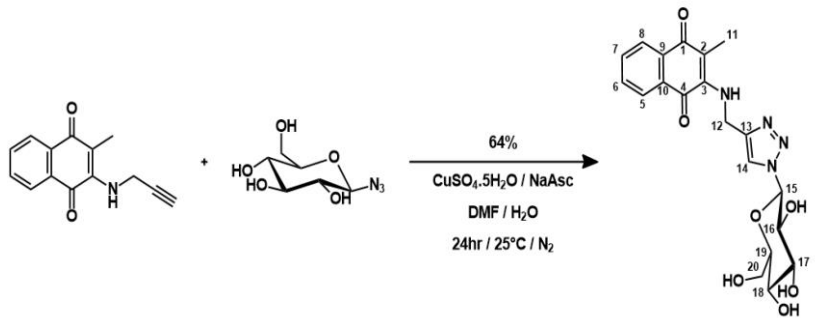

Figure 2. 3: Menadione-amine-glucose compound synthesis.

Dimethyl formamide (DMF) (1 mL) was added to a solution of β-D-Glucopyranosyl azide (111 mg, 5.4 x 10-4 mol, 1 eq) in H2O (1 mL), which was then

added to a stirred solution of 20190730-9-38-RG01R10 (146 mg, 6.48 x 10-4 mol, 1.2 eq) in DMF (7 mL).

Copper sulfate pentahydrate ($CuSO_4.5H_2O$) (67 mg, 2.7 x 10^{-4} mol, 0.5 eq) and sodium ascorbate (NaAsc) (161 mg, 8.1 x 10^{-4} mol, 1.5 eq) were separately dissolved in H_2O (1 mL respectively), then DMF (1 mL) was added to each solution. The $CuSO_4.5H_2O$ and NaAsc solutions were then combined and added to the reaction mixture, which was allowed to stir at room temperature in a nitrogen (N_2) atmosphere for 24 hours. The reaction mixture was then dried under a stream of N_2 gas and the oily residue was purified by column chromatography (15% Methanol (MeOH) / Dichloromethane (DCM)) (RF = 0.3 in 15% MeOH / DCM) to yield a dark red oil (151 mg, 64 %).

Solubility of product - Water, DMSO, DMF, Methanol.

III. <u>Menadione-alkyl</u>

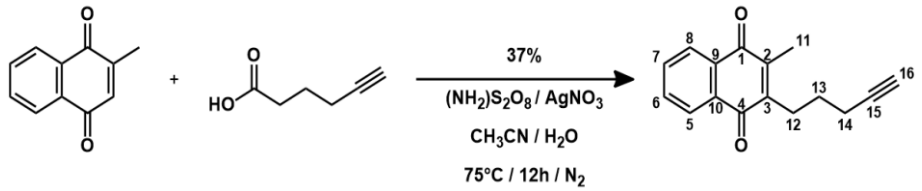

Figure 2. 4: Menadione-alkyl backbone synthesis.

A solution of ammonium persulfate (795 mg, 3.48 x 10^{-3} mol, 1.2 eq) in H_2O (30 mL) was added dropwise over 1 h to a stirred suspension of 5-hexynoic acid (391 mg, 3.48 x 10^{-3} mol, 1.2 eq), silver nitrate (493 mg, 2.90 x 10^{-3} mol, 1 eq) and Menadione (500 mg, 2.90 x 10^{-3} mol, 1 eq) in 50% acetonitrile (CH_3CN) / H_2O (60 mL) at 75 °C while protected from light. The reaction mixture was then allowed to stir in the dark at 75 °C for 20 hours then allowed to cool to ~40 °C. The CH_3CN was removed under reduced pressure and the remnant aqueous mixture was extracted with diethyl ether (3 x 90 mL). The organic layers were combined and washed with saturated sodium hydrogen carbonate solution (2 x 90 mL) and saturated sodium chloride solution (1 x 90 mL). The organic layer was dried over sodium sulfate, filtered through cotton wool and dried under reduced pressure to yield a red brown residue. The residue was then purified by column chromatography on silica gel (100% DCM) and dried in vacuo to yield a yellow solid (255 mg, 37 %).

Solubility of product - DMSO, DMF, $CDCl_3$, EtOH, EtOAc, Acetone.

IV. Menadione-alkyl-glucose - Trojan Horse 4

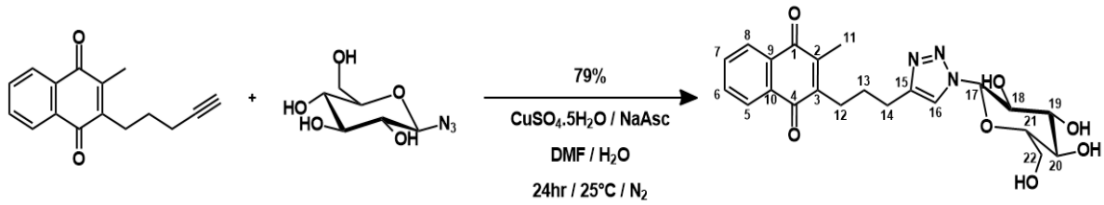

Figure 2. 5: Menadione-alkyl-glucose compound synthesis.

To a solution of β-D-Glucopyranosyl azide (95 mg, 4.62 x 10^{-4} mol, 1 eq) in H_2O (1 mL) was added DMF (1mL), the resulting solution was added to the solution of 20200114-10-109-RB52R1 (115 mg, 5.08 x 10^{-4} mol, 1.1 eq) in DMF (8 mL) with stirring under a N_2 atmosphere. $CuSO_4.5H_2O$ (58 mg, 2.31 x 10^{-4} mol, 0.5 eq) and NaAsc (137 mg, 6.93 x 10^{-4} mol, 1.5 eq) were separately dissolved in H2O (1 mL respectively), then DMF (1 mL) was added to each solution. The solutions of $CuSO_4.5H_2O$ and NaAsc were combined and added to the reaction mixture, which was allowed to stir overnight at room temperature in a N_2 atmosphere. The reaction mixture was then concentrated under a stream of N_2 gas whilst heated by a warm water bath until ~5 mL of the suspension remained. The suspension was filtered through a sintered glass funnel and the filtrate was then heated by a warm water bath and dried under a stream of N_2 gas. The resulting brown wax was redissolved in methanol (2 mL) forming a suspension which was filtered through cotton wool. The resulting brown wax was purified by column chromatography on silica gel (15% MeOH / DCM) to yield a yellow-brown oil (163 mg, 79 %).

Solubility of product - Water, DMSO, DMF, Methanol.

V. <u>Menadione-amine-azido hexanoic acid - Trojan Horse 6</u>

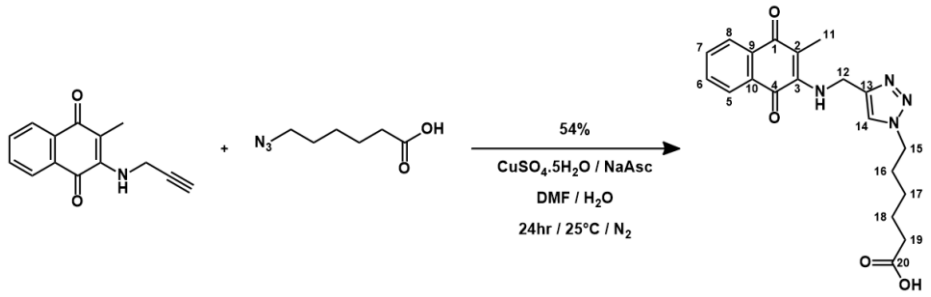

Figure 2. 6: Menadione-amine-azido hexanoic acid

DMF (1 mL) was added to a solution of 6-azido hexanoic acid (48 mg, 3.30 x 10^{-4} mol, 1 eq) in H_2O (1 mL), which was then added to a stirred solution of 20190528-9-28-RG01R7 (75 mg, 3.33 x 10^{-4} mol, 1.1 eq) in DMF (7 mL). $CuSO_4.5H_2O$ (38 mg, 1.51 x 10^{-4} mol, 0.5 eq) and NaAsc (90 mg, 4.54 x 10^{-4} mol, 1.5 eq) were separately dissolved in H2O (1 mL respectively), then DMF (1 mL) was added to each solution. The catalyst solutions were then combined and added to the reaction mixture, which was allowed to stir at room temperature in a N_2 atmosphere for 24 hours. The reaction mixture was then dried under a stream of N_2 gas, and the resulting red solid was purified by column chromatography on silica gel (DCM to 5% MeOH / DCM to 15% MeOH / DCM) (RF = 0.48 in 10% MeOH / DCM) to yield a dark red oil (63 mg, 54 %).

Solubility of product - DMSO, DMF, DCM, $CDCl_3$.

2.3 Cell culture:

Four model prostate cell lines were selected for metabolic analysis in this thesis: PNT1a (Sigma-Aldrich), LNCaP (ATCC, Manassas, VA, USA), PC3, and Du145 (ATCC). PNT1a is the human post-pubertal prostate normal cell line immortalised with SV40. LNCaP is from a prostate supraclavicular lymph node metastasis and is androgen dependent. PC3 is a prostate bone metastasis cell line and is androgen independent. Du145 is a prostate brain metastasis cell line and is androgen independent (Table 2.1). These cell lines were used to represent the different stages of prostate non-malignant (PNT1a) and prostate cancer from the androgen dependent (LNCaP) to the androgen independent (PC3 and Du145) disease All cell lines were cultured in Roswell Park Memorial Institute (RPMI)-1640 media (Sigma–Aldrich) supplemented with 10% dialysed foetal bovine serum (Sigma–Aldrich) and 5 mM pen-strep (Sigma–Aldrich), at 37 ℃ and 5 % CO_2. PNT1a was selected as a control cell line, and LNCaP, PC3 and Du145 cell lines were chosen to represent the different metabolic states of metastatic cancers.

Table 2.1: Description of the panel of prostate cell lines used in the study. Where PNT1a is the non-malignant model, LNCaP is the lymph node metastasis model, PC3 is the bone metastasis model and Du145 is the brain metastasis model.

Cell Line	Cell Morphology	Description	Androgen Status
PNT1a	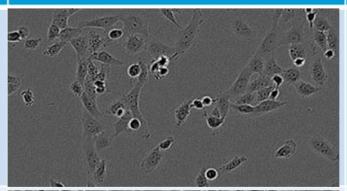	Non-Malignant Prostate Epithelial Cell line	Androgen Dependent
LNCaP	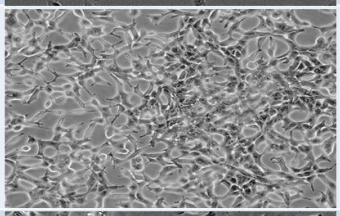	Lymph Node Metastasis Prostate epithelial carcinoma cancer cell line	Androgen Dependent
PC3	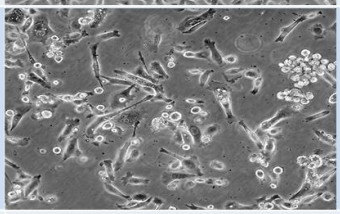	Bone Metastasis Prostate epithelial adenocarcinoma; Grade IV cancer cell line	Androgen Independent
Du145	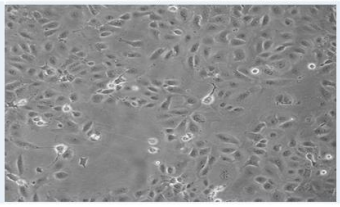	Brain Metastasis Prostate epithelial carcinoma cancer cell line	Androgen Independent

Cell culturing protocol Cells were removed from liquid nitrogen storage and thawed gently in a water bath at 37 °C. They were then transferred into a sterile 15 mL centrifuge tube with 2 mL of complete RPMI and centrifuged at 300 xg for 10 minutes (mins). The supernatant was aspirated, and the cell pellet resuspended in 5 mL of complete RPMI media and transferred into a new 25 cm^2 cell culture flask. Once the cells had adhered, the media was removed and fresh complete RPMI-1640 was added to the cells. After the cells reached a confluency of 80%, they were transferred into a 75 cm^2 cell culture flask.

From the 75 cm^2 flask, culture media was removed, cells were washed with 3 mL of Dulbecco's phosphate buffered saline (DPBS) solution. DPBS was then aspirated from the flask and 2.5 mL of trypsin-EDTA (0.05 mg/mL) was added to the cells and incubated for 5 mins at 37 °C. 5 mL of complete RPMI-1640 media was then added to the cells and transferred into a 15 mL centrifuge tube and centrifuged at 300 xg for 5 mins. The supernatant was then aspirated, and the cell pellet was resuspended in 2 mL of fresh complete RPMI-1640 medium. For routine maintenance, cells were split in a 1:4 ratio (cells: media) and transferred to a new 75 cm^2 flask with 10 mL of fresh complete media. Cells were only used for experiments between 3 – 30 passages after revival from liquid nitrogen storage.

2.3.1 Cell counting protocol

Cell counts were performed using a haemocytometer. Trypan blue (Sigma Aldrich) was used to stain the dead cells present in the solution, allowing for the visual distinction between dead and live cells. The cells in RPMI media (50 µL) were combined with trypan blue (10 µL, a dilution factor of 1.2). The cell/trypan blue mixture was placed into the haemocytometer where the number of live cells in 1 mL was determined (Figure 2.7).

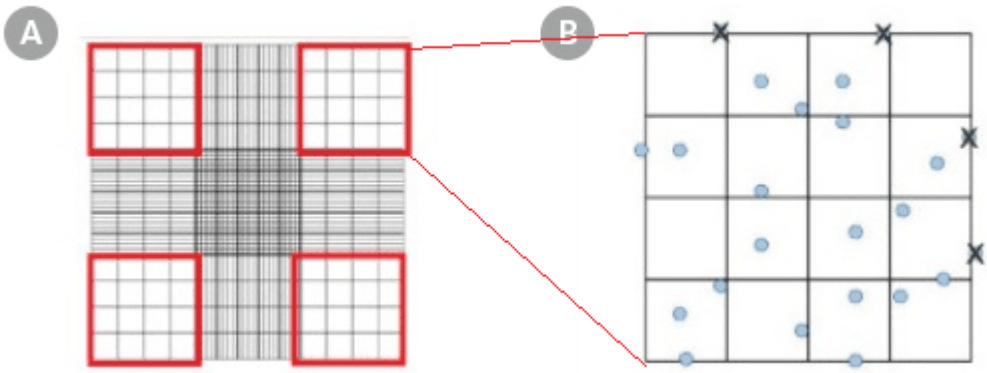

Figure 2. 7: Cell counting: The haemocytometer is used to calculate the number of cells present in a cell solution. It is comprised of 9 squares of 1 mm^2. Dead cells are stained blue and alive/viable cells remain unstained. The unstained cells are counted within the outer 4 squares of the haemocytometer, averaged, and then multiplied by the cell conversion factor of $1x10^4$ mL . As a result, the number of cells in 1 mL has been determined. Image by Stemcell Technologies.[318]

2.3.2 Cell storage protocol

Cells were stored for extended periods of time between experiments and revived as needed. The storage of cell lines followed the above cell culturing procedure, however, after pelleting , cells were resuspended in 2 mL of freezing media (90 % foetal bovine serum (FBS), 9 % dimethyl sulfoxide (DMSO), 1 % RPMI-1640), then split in a 1:4 ratio (cells: media) into labelled cryovials. Cryovials were placed into -80 ºC storage overnight, then stored long-term in a liquid nitrogen storage tank.

2.4 Alamar Blue cell viability

The viability of the cells under examination must be determined in order to establish the cytotoxicity and IC_{50} concentrations of the compounds of interest in the study. Alamar blue is a fluorometric and colorimetric assay designed for use in the quantitative determination of cell proliferation and is frequently used in the cytotoxic determination of chemical substances. In the assay, a redox reaction involving the chemical reduction of the resazurin (a blue dye with low fluorescence), to resorufin (a pink dye with high fluorescence), a reaction that only occurs in viable healthy cells. As the cells proliferate, their metabolic capabilities allow for the reduction of resazurin (Figure 2.8), where NADH is oxidised to NAD^- and water, resulting in a fluorescent, pink solution. This reduction does not occur in non-proliferating resting stage cells, and therefore the cell solution remains blue. Alamar blue was determined as the optimal assay for this work as the vitamins examined are not typical cytotoxic compounds as they are required by the cells in small amounts and the Alamar blue would allow for more consistent results than other tests.

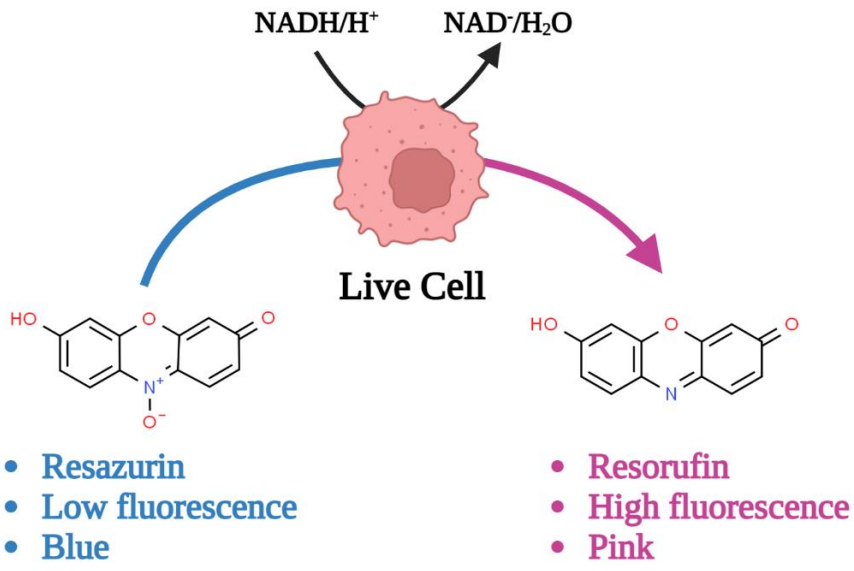

Figure 2. 8: The reduction of Resazurin to Resorufin in the Alamar blue cytotoxicity assay. NADH is oxidised to NAD^- and water while resazurin is reduced to resorufin. Viable cells present as a pink, fluorescent cell solution, whereas non-viable cells will remain a blue low-fluorescence solution. Image created in Biorender online.

2.4.1 Alamar Blue cell viability assay protocol

Cells at 80-90 % confluency were plated in a 96-well black, fluorescent plate (Fisher Scientific, Ireland) at a density of $20x10^4$ in complete media, and then incubated at 37 °C for 24 h. The next day, the complete media was washed out with the Dulbecco's phosphate-buffered saline (DPBS) and replenished with 90 µL of the desired glucose media concentration, made with dialysed FBS and the compound under investigation dissolved in 10 µL of sterile water. A death control of 20 % DMSO was used to ensure 100 % cell death in the cell lines. Cells were then incubated for either 2, 24 or 48 h. Following treatment, cells were washed with 100 µL phosphate-buffered saline (PBS) and replenished with 90 µL of their respective glucose media. For each time point, alamar blue (10 µL) (10 %) was added to each well for 4 h at 37 °C. Plates were refrigerated

overnight at 4 °C, and then their fluorescent emission at 604 nm (578 nm excitation) was recorded on the GloMax microplate reader (Promega, Madison WI, USA). The values obtained were normalised by the blank well readings and used to plot the dose response curves to determine the IC_{50} values.

2.5 Extracellular flux and cell bioenergetics analysis

The Agilent Seahorse XFe24 analyser was used to perform cellular bioenergetics experiments in real time which is advantages in determining the effects of the glucose milieu and the novel compounds on the live prostate cells. The XFe24 analyser measures the cellular bioenergetics through the measurement of the cells oxygen consumption rate (OCR) and the extracellular acidification rate (ECAR). The OCR measure is linked to mitochondrial respiration, whereas the ECAR is due to the production of lactic acid by the process of glycolysis. Cells metabolic dependencies can be determined in real-time. The Seahorse analyser allows for the injection of up to 4 drugs or inhibitors into each cell well. Appropriate inhibitors are used for specific assays and serially injected. The instantaneous reaction to the inhibitors is measured by the Seahorse analyser, allowing for the determination of metabolic endpoints.[319]

The inhibitors used for the extracellular flux assays (MitoStress and ATP Rate) was injected serially and include oligomycin, carbonyl cyanide 4-(trifluoromethoxy)phenylhydrazone (FCCP) and antimycin A. Oligomycin inhibits ATP synthase through mitochondrial complex V and decreases the flow of electrons through the electron transport chain, resulting in a decrease in mitochondrial respiration or OCR.[319] FCCP is an uncoupling agent that disrupts the proton gradient and mitochondrial membrane potential in the mitochondria. It is then injected after oligomycin resulting in removal of the inhibition on electron flow through the electron transport chain, which subsequently causes oxygen consumption by complex IV until the upper limit is achieved.[319] Antimycin A, a complex III inhibitor, shuts down mitochondrial respiration and therefore enables the calculation of respiration driven by processes outside the mitochondria.[319]

The impacts of the inhibitors on the cellular bioenergetics are illustrated below (Figure 2.9).

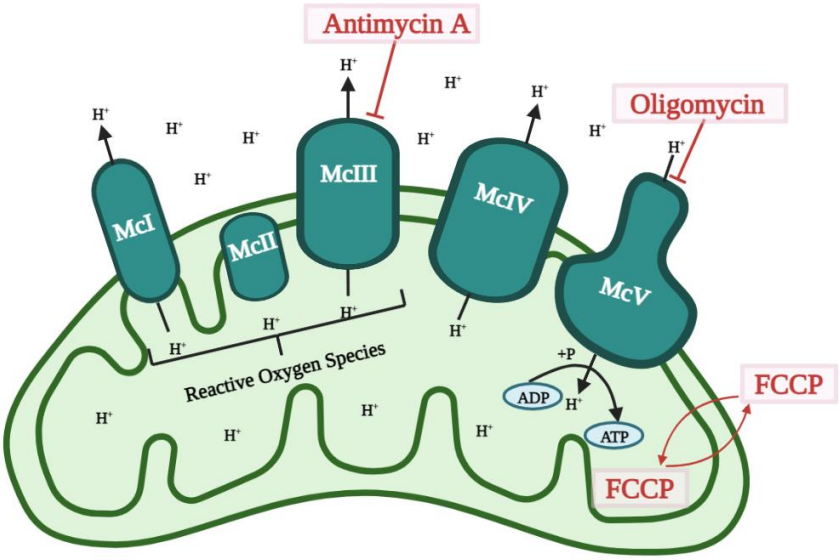

Figure 2. 9: The Seahorse inhibitors and their effects on the mitochondria. Oligomycin inhibits mitochondrial complex V, inhibiting ATP synthase in the mitochondria. Finally, injection of FCCP an oxidative phosphorylation uncoupler, allows maximum non-mitochondrial respiration to occur. Antimycin A inhibits the mitochondrial complex III in turn, inhibiting the electron transport chain. Image made in Biorender online.

2.5.1 Mitochondrial stress (MitoStress)Test

The MitoStress test is an assay that determines the mitochondrial metabolic endpoints of live cells (Figure 2.10).

The basal OCR is a measure of the amount of oxygen required for ATP production in the mitochondria under basal conditions. Proton leak depicts the basal respiration not coupled to ATP production and is an indicator of mitochondrial dysfunction. All cells would have a baseline level of proton leak for regulation of mitochondrial ATP production, but alteration of levels may indicate mitochondrial dysfunction. Maximal respiration is the maximum rate of oxygen consumption after the stimulation of the high energy demands with the addition of the uncoupler FCCP. This results in generating an environment in which the cells maximum respiration rate can be determined. Non-mitochondrial respiration is the respiration that occurs outside of the mitochondria, such as fatty acid oxidation, glycolysis, and the use of glycogen stores. Overall, the use of the MitoStress test allows for respiration in the mitochondria to be examined and can indicate if mitochondrial dysfunction has occurred.

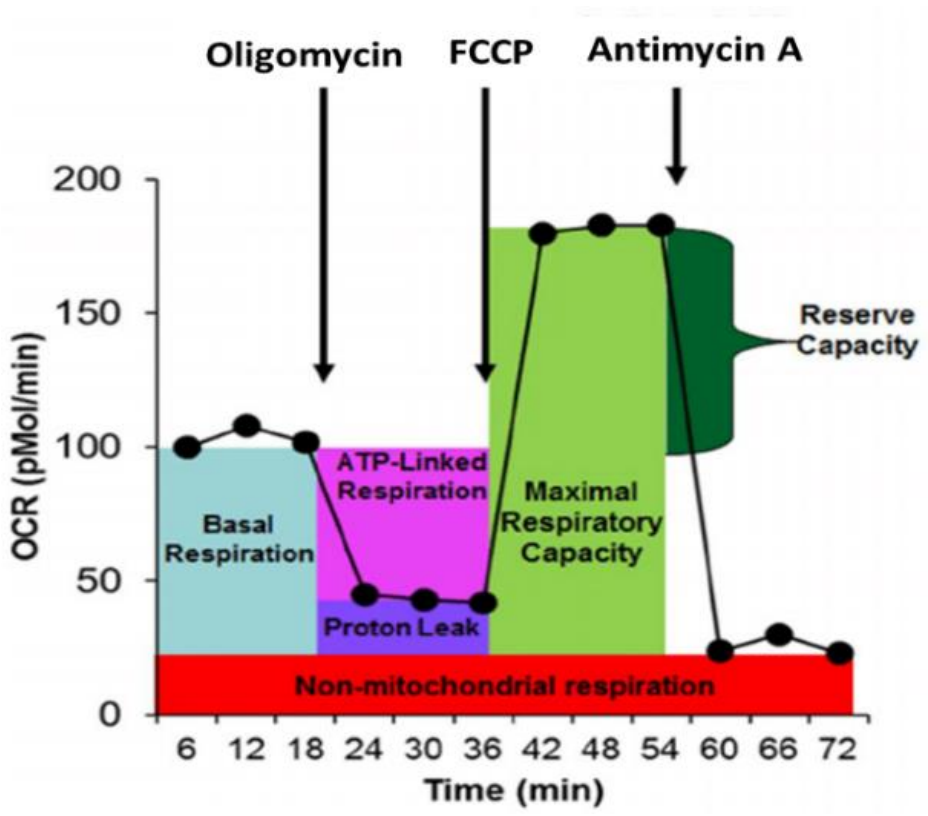

Figure 2. 10: Mitochondrial Stress (MitoStress) Assay: The MitoStress assay identifies the elements of mitochondrial metabolism. Basal OCR is measured before the addition of any inhibitors. Oligomycin is added to the cells, decreasing OCR allowing for the ATP linked respiration and the proton leak to be calculated. FCCP is added to increase the OCR, from this the spare respiratory capacity and maximal respiration of the cell is calculated. The addition of Antimycin A causes the OCR to plummet allowing for non-mitochondrial respiration to be calculated.[319] *Image by Agilent Technologies.*

2.5.1.1 MitoStress test protocol

Cells were seeded at $6x10^4$ cells/well in duplicate in the 24-well XF microplate (Agilent Technologies, Santa Clara, CA, USA) at a volume of 100 µL and incubated for 24 h at 37 °C and 5 % CO_2/95 % air. Cells were washed with glucose-free seahorse XF assay medium (Agilent Technologies, Santa Clara, CA, USA.) supplemented with 11 mM, 5.5 mM, and 0 mM D-(+)-glucose (Sigma-Aldrich) respectively and 5 mM sodium pyruvate. To each well, 500 µL of the supplemented glucose-free seahorse XF assay medium (Agilent Technologies, Santa Clara, CA, USA) was added. Specific inhibitors and uncouplers were prepared in XF assay media, supplemented with 0 mM D-(+)-glucose for sequential addition at the appropriate final concentrations of oligomycin A (1.8 µM), FCCP (4 µM) and antimycin A (5 µM) (all Sigma-Aldrich). Cells were placed in a non-CO_2 incubator at 37 °C for 1 h prior to the assay. Basal respiration (OCR) and extracellular acidification rate (ECAR) were measured by the Seahorse Biosciences XFe24 Extracellular Flux Analyser (Agilent Technologies, Santa Clara, CA, USA). All recorded measurements were normalised to cell number using the crystal violet assay in Section 4.3.2. The metabolic endpoints were calculated as described in Table 2.2, below.

Table 2.2: Metabolic Endpoint Calculations from the MitoStress Test

Metabolic Parameters	**Calculations**
Basal Respiration (OCR)	OCR = Baseline OCR - OCR after Antimycin A
Proton Leak	Proton Leak = OCR after Oligomycin - OCR after Antimycin A
Maximal Respiration	Maximal Respiration = OCR after FCCP - OCR after Antimycin A
Non-Mitochondrial Respiration	Non-Mitochondrial Respiration = OCR after Antimycin A
ATP Production	ATP Production = Baseline OCR - OCR after Oligomycin

2.5.2 ATP rate test

The adenosine triphosphate (ATP) rate assay allows the determination of the amount of ATP produced through both OxPhos and glycolysis . The distinction between these processes can be made through the measurement of OCR, which indicates mitochondrial respiration and EACR indicates glycolysis. ATP in the cell is the predominant glucose-derived energy source in the process of metabolism. The metabolic regulation of the cell can alter the demands of the ATP required for regular function; thus, its production is vital for normal cellular processes.[320]

The ATP rate assay takes a basal reading of OCR and EACR prior to the serial injection of the mitochondrial inhibitors, oligomycin and antimycin A. The initial OCR decreases with the addition of oligomycin, and this allows for the determination of mitochondrial ATP and glycolytic ATP. The later addition of antimycin A causes further drop in OCR due to the complete inhibition of oxidative phosphorylation, which allows for the determination of the mitochondrial-associated acidification in the cell media. The remaining acidification is due to lactic acid production, derived from the production of glycolytic ATP by glycolysis.[321,320] Representative ATP rate assay outputs from the seahorse are presented in Figure 2.11.

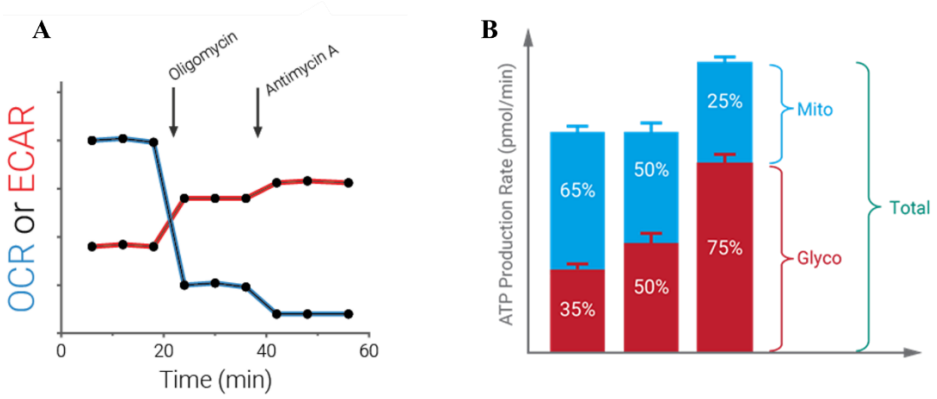

Figure 2. 11: ATP Rate Assay outputs: (A.) The extracellular acidification measured due to the addition of oligomycin allows for the determination of the mitochondrial ATP. With the addition of antimycin A, oxidative phosphorylation is completely inhibited, and the remaining acidification can be attributed to lactic acid production by glycolysis (glycolytic ATP). (B.) The ATP rate assay distinguishes the amount of ATP produced through oxidative phosphorylation and glycolysis respectively. This can be converted to the %oxidative phosphorylation and the %glycolysis.[320] Images by Agilent Technologies.

2.5.2.1 <u>ATP rate test protocol</u>

Cells were seeded at $6x10^4$ cells / well in duplicate in the 24-well XF microplate (Agilent Technologies, Santa Clara, CA, USA) at a volume of 100 µL and incubated for 24 h at 37 °C and 5 % CO_2/95 % air. Cells were washed with glucose-free seahorse XF assay medium (Agilent Technologies, Santa Clara, CA, USA.) supplemented with 11 mM, 5.5 mM and 0 mM D-(+)-glucose (Sigma-Aldrich) respectively and 5 mM sodium pyruvate. To each well, 500 µL of the supplemented glucose-free seahorse XF assay medium (Agilent

Technologies, Santa Clara, CA, USA) was added. Specific inhibitors were prepared in XF assay media supplemented with 0 mM D-(+)-glucose for sequential addition at the appropriate final concentrations of oligomycin A (1.8 µM) and antimycin A (5 µM) (all Sigma-Aldrich). Cells were placed in a non-CO_2 incubator at 37 °C for 1 h prior to the assay. OCR and ECAR were measured by the Seahorse Biosciences XFe24 Extracellular Flux Analyser (Agilent Technologies, Santa Clara, CA, USA). All recorded measurements were normalised to cell number using the crystal violet assay.

2.5.3 Crystal violet normalisation

The crystal violet assay was used to normalise the number of cells undergoing the extracellular flux assays described above. This is vital to allow comparisons of the cell lines and the treatments as they are all normalised to a cell value and thus can be compared. Cells were fixed in 99.9 % ice-cold methanol for 15 mins on ice. The fixative was removed, and cells were washed with PBS and stained with 0.1 % crystal violet for 20 mins at room temperature. Crystal violet was removed, and cells were washed twice with water, air dried overnight, then placed in 1% Triton X-100 on a plate shaker for 1 h. Absorbance was recorded at 595 nm on the GloMax plate reader.

2.6 Flowcytometry and mitochondrial profiling.

Mitochondrial profiling examines the functional and structural properties of mitochondria, which have important implications for number of disease states, including cancer, neurodegenerative disorders, and metabolic disorders. To profile mitochondria from prostate cell lines, flowcytometry is required, hence the Amins Cell Stream was selected. The Amins Cell Stream allows for the real time examination of a single tube in addition to a 96-well plate of samples, yielding multiparametric single-cell data results. The Amins Cell Stream holds up to 7 lasers (Figure 2.8), which allow for a wide range of endpoint examinations such as, cell identification, cell counting, cell viability, cell cycle analysis and apoptosis analysis.[322] The cellular mitochondrial health can be determined through flow analysis of reactive oxygen species (ROS) in the cells, mitochondrial membrane potential, and the apoptosis and DNA damage markers. The Amins Cell Stream lasers used for examination of cells in this study are detailed in Figure 2.14 and Figure 2.15.

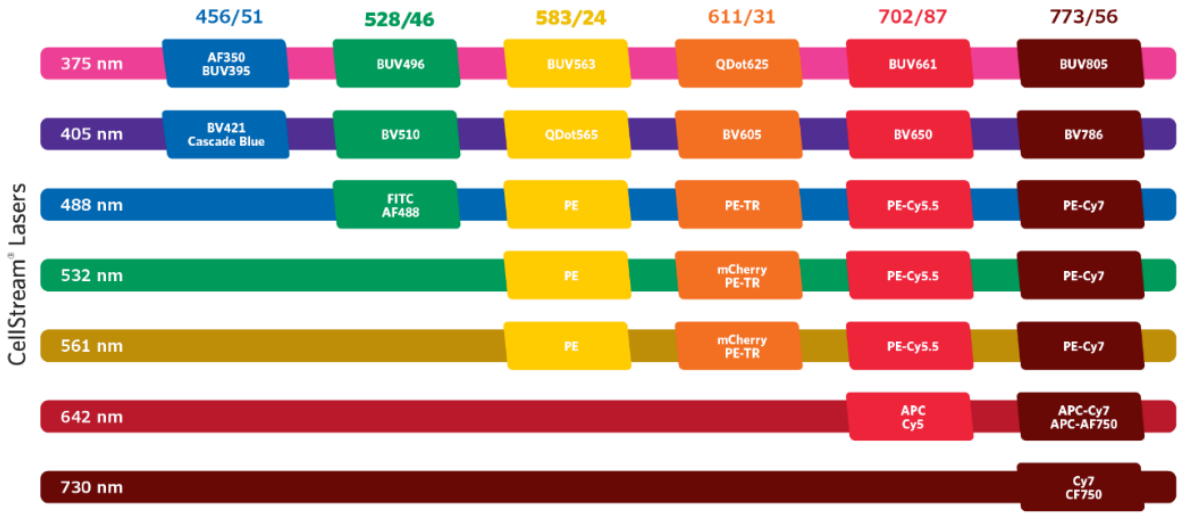

Figure 2. 12: The Amins Cell Stream Laser Channels: The cell stream covers the wavelengths of 375 – 730 nm, allowing for the examination of multiple endpoints. The cell stream holds lasers including a pink, violet, blue (pacific blue), green (FitC), yellow (PE), red (APC) and deep red(Cy7). Image by Amnis by Luminex.[322]

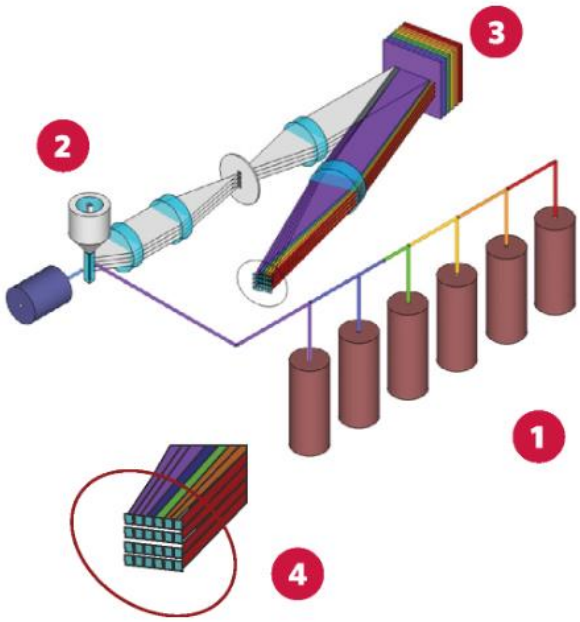

Figure 2. 13: The Cell Stream components: (1.) The lasers of the cell stream as detailed in Figure 2.14 (2.) The cells pass through the lasers where the fluorophores on the cells under examination generate emissions, and the fluorescence is collected and directed to the image pane. (3.) The filter deconvolutes the discrete vertical positions from the image pane into 22 data channels. (4.) The 22 data channels fit onto the charged coupled device array, where the sensor then interprets the data. Image by Amnis by Luminex.[322]

2.6.1 Oxyburst Green H2DCFDA (Thermofisher):

Oxyburst Green H_2DCFDA succinimidyl ester (2',7'-dichlorodihydrofluorescein diacetate, SE) is an amine-reactive assay reagent that can be used to prepare oxidation-sensitive conjugates of a wide variety of biomolecules and particles, including antibodies, antigens, peptides, proteins, dextrans, bacteria, yeast, and polystyrene microspheres. Following conjugation to amines, the two acetates of Oxyburst Green H_2DCFDA can be removed by treatment with hydroxylamine at neutral pH to yield the dihydrofluorescein conjugate. Oxyburst Green H_2DCFDA conjugates are nonfluorescent until they are oxidized to the corresponding fluorescein derivatives.[161] The range of concentrations used for carrying out the experiments is detailed in Chapter 2, Table 2.1. For the Oxyburst assay, hydrogen peroxide (H2O2) is used as a control molecule. The representative fluorocytogram of Oxyburst is presented in Figure 2.16.

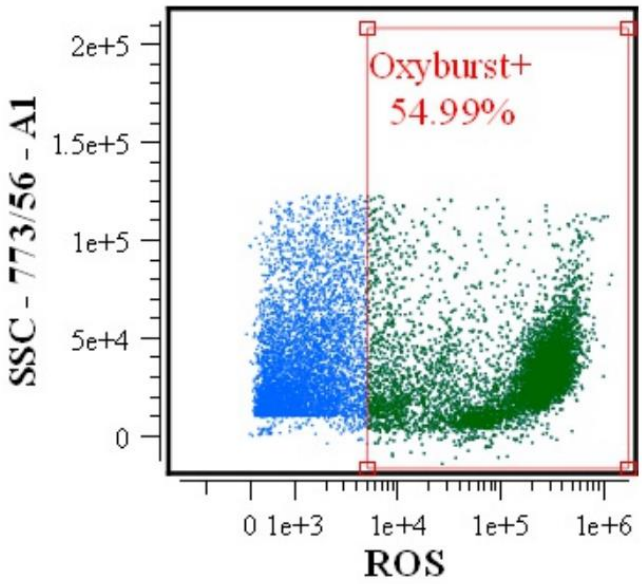

Figure 2. 14: Representative fluorocytograms of ROS analysis of PNT1a cells. The Oxyburst negative cells are in the left quadrant (blue) and the Oxyburst positive cells are in the right quadrant (green). Oxyburst positive cells indicate ROS positivity in the cell.

2.6.2 JC-1 Dye (Thermofisher)

5′,6,6′-tetrachloro-1,1′,3,3′-tetraethylbenzimidazolylcarbocyanine iodide (JC-1) is a mitochondrial membrane potential probe. It is a cationic carbocyanine dye that is known to accumulate in the mitochondria

The membrane-permeant JC-1 dye is widely used in apoptosis studies to monitor mitochondrial health JC-1 dye exhibits potential-dependent accumulation in mitochondria, indicated by a green fluorescence emission at (~529 nm) for the monomeric form of the probe, which shifts to red (~590 nm) with a concentration-dependent formation of red fluorescent J-aggregates. Consequently, mitochondrial depolarization is indicated by a decrease in the red/green fluorescence intensity ratio.[323]

At higher concentrations (aqueous solutions above 0.1 µM) or higher potentials, JC-1 dye monomer forms red fluorescent "J-aggregates" where it has accumulated within the mitochondria. The J-aggregates exhibit a broad excitation spectrum and an emission maximum at ~590 nm. At lower internal mitochondrial concentrations or low membrane potential, the JC-1 dye is present as monomers, exhibiting an emission of 529 nm.[323] FCCP is used as a control molecule in this assay. The colour change seen with the JC1 assay is illustrated in Figure 2.17 with the representative fluorocytogram for the JC1 assay presented in Figure 2.18.

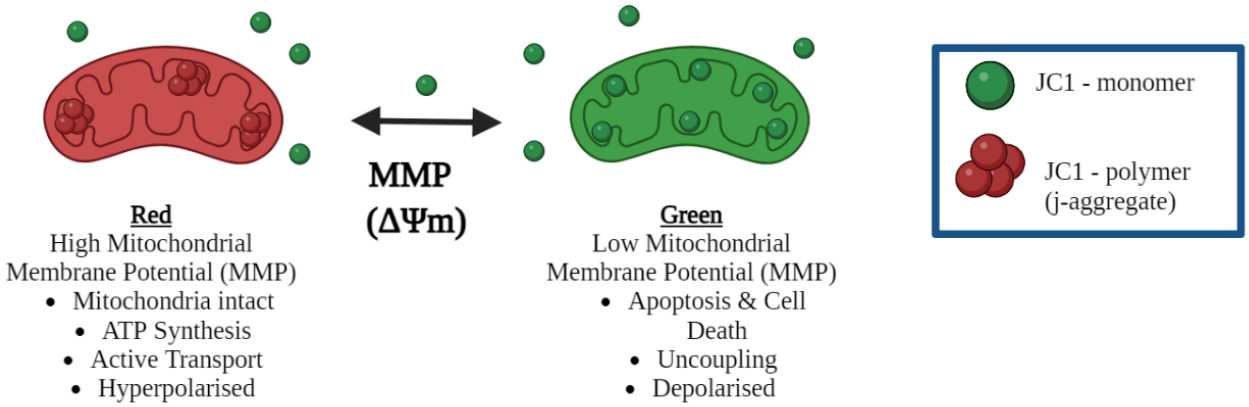

Figure 2. 15: JC-1 assay monomeric form and its j-aggregates. JC-1 Red (j-aggregate) indicates healthy mitochondria, with high MMP, healthy intact mitochondria with functional ATP synthesis and hyperpolarised mitochondria. JC-1 Green (monomer) indicates unhealthy mitochondria, with low MMP, high apoptosis and cell death, metabolic uncoupling and increased mitochondrial depolarisation. Image made in Biorender.

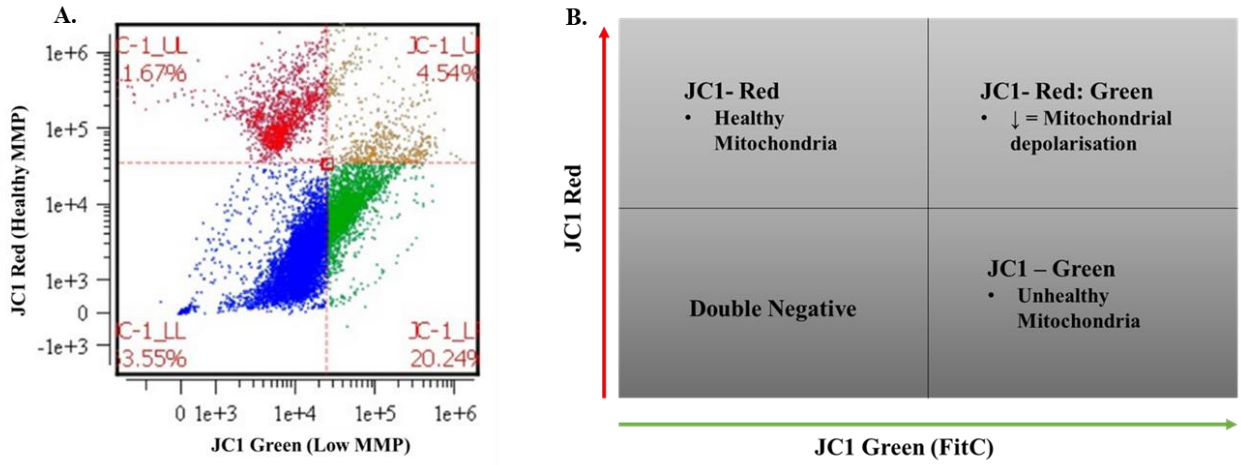

Figure 2. 16: JC-1 MMP fluorocytograms: (A) Representative fluorocytograms of MMP analysis of LNCaP cells under 5.5mM glucose. Viable/healthy cells are in the lower left quadrant (blue). Cells with healthy and or high MMP are in the upper left quadrant (red). Cells with dual staining of JC-1 are in the upper right quadrant (yellow). The cells with unhealthy/ low MMP are in the lower right quadrant (green). The data from the 5.5mM untreated conditions are shown here in all 4 cell lines used. (B) JC-1 MMP quadrants from the fluorocytograms.

2.6.3 Annexin AV-Pacific Blue (BioLegend) and Propidium Iodide

Annexin V (Av) is used to determine cell death by apoptosis. It is an intracellular protein that binds in a calcium dependant binding process to phosphatidylserine (PS). PS is typically located in the intracellular leaflet in healthy cells, but during apoptosis it is found in the external leaflet, due to membrane asymmetry. Av is often combined with a DNA binding dye to confirm cell death and further, DNA damage. See the representative fluorocytogram in Figure 2.19 for further details.

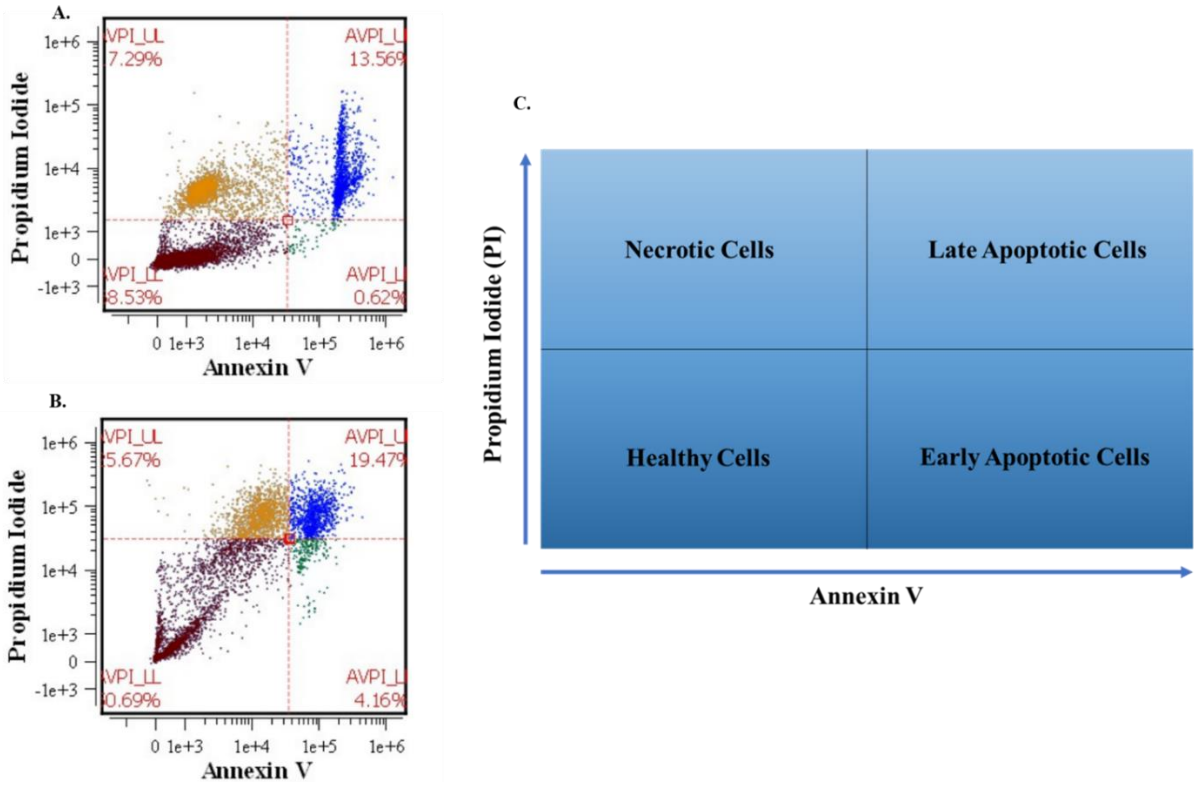

Figure 2. 17: Av PI fluorocytograms : (A)Representative fluorocytograms of Apoptosis analysis of PC3 cells under 5.5mM glucose. (B) Representative fluorocytograms of Apoptosis analysis of Du145 untreated cells under 5.5mM glucose conditions. Viable/healthy cells are in the lower left quadrant (brown). Necrotic cells are in the upper left quadrant (yellow). Cells in late apoptosis are in the upper right quadrant (blue). The cells in early apoptosis are in the lower right quadrant (green). (C) Av PI quadrants from the fluorocytograms.

Propidium Iodide (PI) is a DNA and RNA binding agent, that binds to dead or dying cells to allow for the determination of cell viability and DNA damage. PI can be used along with Av to determine between the stages of apoptosis, DNA quantification and chromosomal analysis. PI can be excited through the blue, green, and yellow-green laser channels in flowcytometry analysis.

2.6.4 Gating Strategy

The single cell population was identified in the unstained cell population. From this, the alive single cell population was identified to allow the determination of the %gated cells positive for the individual cell markers examined. All markers were checked to be negative in the unstained cell population. The Oxyburst population was identified under the FitC channel. The JC-1 populations identified with the FitC vs PE channel. The Av PI populations were identified through the D4 and A2 channels. The marker quadrants were set due to the cell populations present in the flow-cytogram. This is detailed in Figure 2.20.

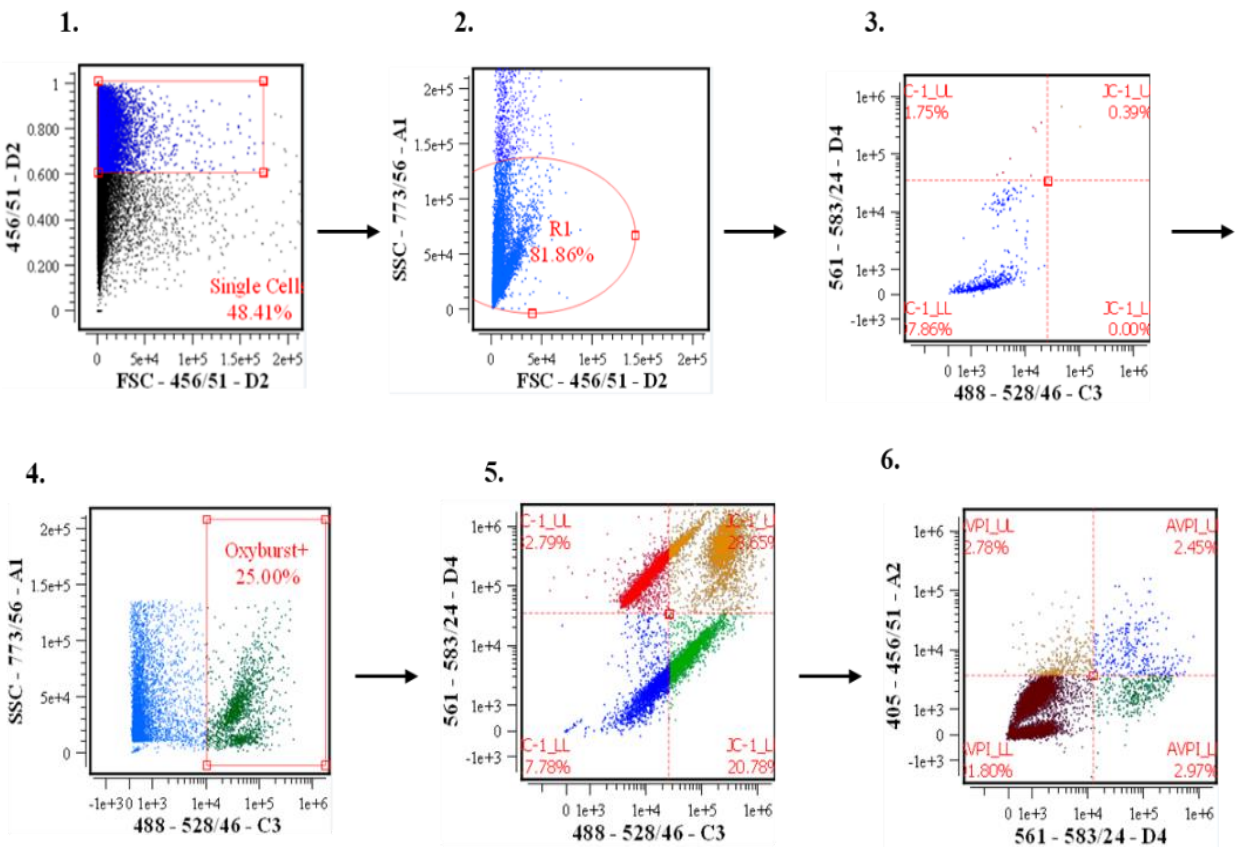

*Figure 2. 18: Gating strategy used in the experimental design . (**1.**) Single cell population identified in the unstained cell population. (**2.**) from this, the alive single cell population, R1 was identified to allow the determination of the %gated cells positive for the individual cell markers examined. (3.) All marker checked to be not positive in the unstained cell population. (4.) Oxyburst population identified under the FitC channel. (5.) JC-1 populations identified with the FitC vs D4 (FIND NAME) channel. (6.) Av PI populations identified through the D4 and A2 channels. Quadrants set due to the populations present in the flow-cytogram.*

2.6.5 The flow cytometry protocol

Cells were seeded at 6 x 10^4 cells per well for 24 h in a 96-well plate. Following 24 h incubation at 37 °C, cells were placed under three different glucose conditions; 0 mM, 5.5 mM and 11 mM glucose and treated with compounds; menadione, TH4 and TH6 treatments for 24 h. Following 24 h treatment the cells were centrifuged at 200 xg for 3 mins. Media was aspirated from each well, cells were trypsinised using 50 µL of trypsin EDTA and incubated at 37 °C for 10 mins. 50 µL of warm RPMI media was subsequently added to the trypsinised cells and the cells were centrifuged again at 200 xg for 3 mins. Supernatant aspirated from the plate. Cells were washed with 100 µL of warm DPBS. Cells centrifuged at 200 xg for 3 mins. PBS aspirated. Annexin binding buffer was added to the required wells. Cells were centrifuged at 200 xg for 3 mins. The binding buffer was removed. Fluorescent dyes were added to the plate for 30 mins at room temperature in foil. Cells were centrifuged at 200 xg for 3 mins. Cells were washed in 100 µL of warm PBS then, 100 µL Flow Cytometry Staining Buffer (FACS). Cells then centrifuged at 200 xg for 3 mins and the buffer removed. Cells were all resuspended in 60 µL of FACS. Compensation was performed with positive and negative compensation beads. Gating and analysis were performed using the CellStream Analysis software.

Details of the fluorescent dyes used in the cell stream analysis of the cell lines are presented in

Table *2.3*.

Table 2.3: Cell Stream Fluorescent dyes

Fluorescent Dye	Excitation	Laser Channel	Concentration	Purpose
Oxyburst - Green	492-495 nm	FitC	0.01 µM	Reactive oxygen species production
JC-1	590 nm	FitC-APC	0.01 µM	Mitochondrial Membrane potential
Mito Tracker – Deep Red	644/655 nm	Allophycocyanin (APC)	0.01 µM	Mitochondrial Tracker in live cells
Annexin AV-Pacific Blue		Pacific Blue (PacBlue)	0.05 µM	Apoptosis identifier
Propidium Iodide (PI)	561-488 nm	FitC/Phycoerythrin (PE) /PacBlue	0.05 µM	Cell Viability
H_2O_2 Standard	-	-	10 %	ROS production Standard

2.7 Metabolomics

The metabolomic analysis by Liquid Chromatography (LC) tandem Mass Spectrum (MS) was performed with the QTRAP 6500 LC-MS/MS system with a multi-component Ion Drive. This method combines high sensitivity and performance, with the SCIEX patented Ion Drive technology increases the number of ions produced while enhancing the way ions are transmitted and detected in the machine.[324] This machine has improved polarity switching and multiple reaction monitoring (MRM) speeds, allowing for faster chromatography and better throughput. The built-in QTRAP allows for quantitative MRMs and qualitative QTRAP scans in the same injection to maximize throughput.[324]

2.7.1 Sample Preparation

PNT1a, LNCaP, PC3 and Du145 cells were plated at 5×10^6 cells/well in a T75 flask for 24 h. Cells were washed with DPBS, then 8 mL of RPMI assay medium with the required glucose concentration (0 – 11 mM glucose) (Sigma Aldrich), supplemented with 10 % dialysed FBS (Sigma Aldrich), was added to each flask. Vitamins solutions were prepared using sterile water at the IC_{50} concentrations of the; Menadione, Trojan Horse 4 and Trojan Horse 6 compounds. To each flask 1 mL of each treatment was added respectively, then each cells flask was incubated for 24 h. A negative control containing the cell lines in RPMI-1640 medium in all three glucose conditions (0 mM, 5.5 mM, and 11 mM glucose) was also prepared under the same conditions as the treated cells. After 24 h, the cells were gently trypsinised to detach them from the flask, then centrifuged at 300 xg to pellet the cells. The supernatant was removed and discarded, then the cells were washed with PBS, resuspended in PBS and placed into labelled cryovials. The samples were quickly flash-frozen in liquid nitrogen and stored at -80 °C. Cells were sent to the University College Dublin (UCD) Metabolomics core facility for preparation and examination.

2.7.2 Metabolomics Analysis

This experimental work was carried out by Dr. Xiaofei Yin and Dr. Lorraine Brennan of the Conway Institute, University College Dublin and the methods above were provided by Dr. Yin. Dr. Brennan's group is well known for their metabolomic works and are the gold standard used in Ireland for metabolomic analysis.

Cell lysate samples were analysed using a targeted metabolomic platform and were prepared according to the MxP® Quant 500 assay manual (Biocrates Life Sciences, Innsbruck, Austria). 10 µL of each sample (in a 96-well format) was dried and derivatised using 50 µL of derivatization solution (5% phenyl isothiocyanate in ethanol/water/pyridine (volume ratio 1:1:1)) and incubated for 60 mins at room temperature. The plate was then dried for 60 mins under nitrogen. Following addition of 300 µL of 5 mM ammonium acetate in methanol to each well the plate was left to shake for 30 mins. In the next step, the plate was centrifuged at 500 xg for 2 mins, and 150 µL of high-performance liquid chromatography (HPLC)-grade water was added for analysis by liquid chromatography tandem mass spectrometry (LC-MS/MS). Additionally, 10 µL of eluate was diluted with 490 µL of methanol running solvent for flow injection analysis tandem mass spectrometry (FIA-MS/MS) analysis.

The prepared 96-well plate was analysed by a Sciex ExionLC series UHPLC system coupled to a Sciex QTRAP 6500+ mass spectrometer. The UHPLC column,

provided by Biocrates Life Sciences were installed and mobile phase A and B were 100 % water and 95 % acetonitrile (both added 0.2 % formic acid), respectively. In the LC-MS/MS analysis, amino acids (n = 20), amino acid related (n = 30), bile acids (n = 14), biogenic amines (n = 9), carboxylic acids (7), hormones and related (n=4), indoles and derivatives (n = 4), nucleobases and related (n = 2), fatty acids (n = 12), trigonelline, trimethylamine N-oxide, p-Cresol sulfate, and choline were quantified. Lipid classes such as lysophosphatidylcholines (n = 14), phosphatidylcholines (n = 76), sphingomyelins (n = 15), ceramides (n = 28), dihydroceramides(n = 8), hexosylceramides (n = 19), dihexosylceramides (n = 9), trihexosylceramides (n = 6), cholesteryl esters (n = 22), diglycerides (n = 44), triglycerides (n = 242) were quantified in FIA-MS/MS analysis, furthermore acylcarnitines (n = 40) and the sum of hexose were also quantified in FIA-MS/MS analysis. The multiple reaction monitoring (MRM) method, which was optimized by Biocrates Life Sciences, was applied to identify, and quantify all of the metabolites.

2.7.3 Data processing and metabolite quantification

Once more, the preliminary data processing and metabolite quantification was carried out by Dr. Xiaofei Yin and Dr. Lorraine Brennan of the Conway Institute, University College Dublin and the methods above were provided by Dr. Yin.

Data were processed using MetIDQ software provided by Biocrates Life Sciences. Amino acids and part of amino acid related metabolites and biogenic amines were quantified based on isotopically labelled internal standards and seven-point calibration curves. All other metabolites were semi-quantified by using internal standards. Data quality was assessed by investigating the accuracy and reproducibility of QC sample, provided with Quant 500 assay.

The dataset including metabolite concentrations in micromolar were exported. Metabolites were included for further statistical analyses only when their concentrations were above the limit of detection (LOD) in more than 50 % of samples.

2.7.4 Data and statistical analysis of metabolite concentrations:

The raw data was reordered to match the technical and biological replicates, cell lines and glucose conditions. Two hundred and eleven metabolites were detected above the LOD of the five hundred examined. A two tailed-t-test was performed in Excel between the groups of interest, where metabolites of significance were identified ($p \leq 0.05$). Following identification of significant metabolites, each significant metabolite was graphed in GraphPad prism for each cell line, treatment, and glucose condition, where a repeated measure (Bonferroni) 1-way ANOVA was conducted with multiple comparisons applied. Data was presented as mean ± SEM in the graphs in Section Results

Chapter 3.

a) The synthesis and characterisation of Trojan Horse compounds

b) Determining the cytotoxicity of Vitamin C, Menadione and Trojan Horse compounds

3.1 Introduction

Current treatment regimens do not consider the variable nature of cancer cell biology and the adaptability of cancer cells. There is an urgent need for a therapeutic strategy that effectively targets cancers at multiple mechanistic and metabolic endpoints, and that utilises novel approaches to limit cancer cell adaptability. We aim to achieve this important outcome by exploiting the Warburg effect to target cancer cell metabolism and develop compounds that target multiple aspects of cancer biology.

The majority of anticancer agents are hydrophilic molecules; they rely on active ligand transport mechanisms to be efficiently internalized into cells (e.g., folate receptor, nucleoside transporters). However, rapid development of resistance to therapy often occurs via downregulation of these receptors. Lipid modification can enhance passive transport of these hydrophilic drugs mediated by the lipid moiety.[325,326] The resultant drugs no longer require active ligand transport mechanisms and are therefore able to overcome transport resistance barriers. Lipid conjugation can also lead to a reduction in the amount of drug effluxes out of the cell by these transporters, resulting in increased accumulation compared to the free drug.[325,326] Therefore, increased antitumor efficacy can be achieved using lipid conjugation strategies by increasing cell permeability and retention of anticancer agent.

We propose that the selective delivery of a toxic moiety to cancer cells is possible when coupled to a “natural substrate”. In this regard, a Trojan Horse (TH) principle was used to trick the cancer cells into taking up Vitamin C and Menadione, attached to a substrate such as simple sugars and lipids which are highly sought-after by proliferative cancer cells, with prospects of achieving ideal candidates for a selective range of attractive, yet toxic TH compounds which are presented in Figure 3.1.

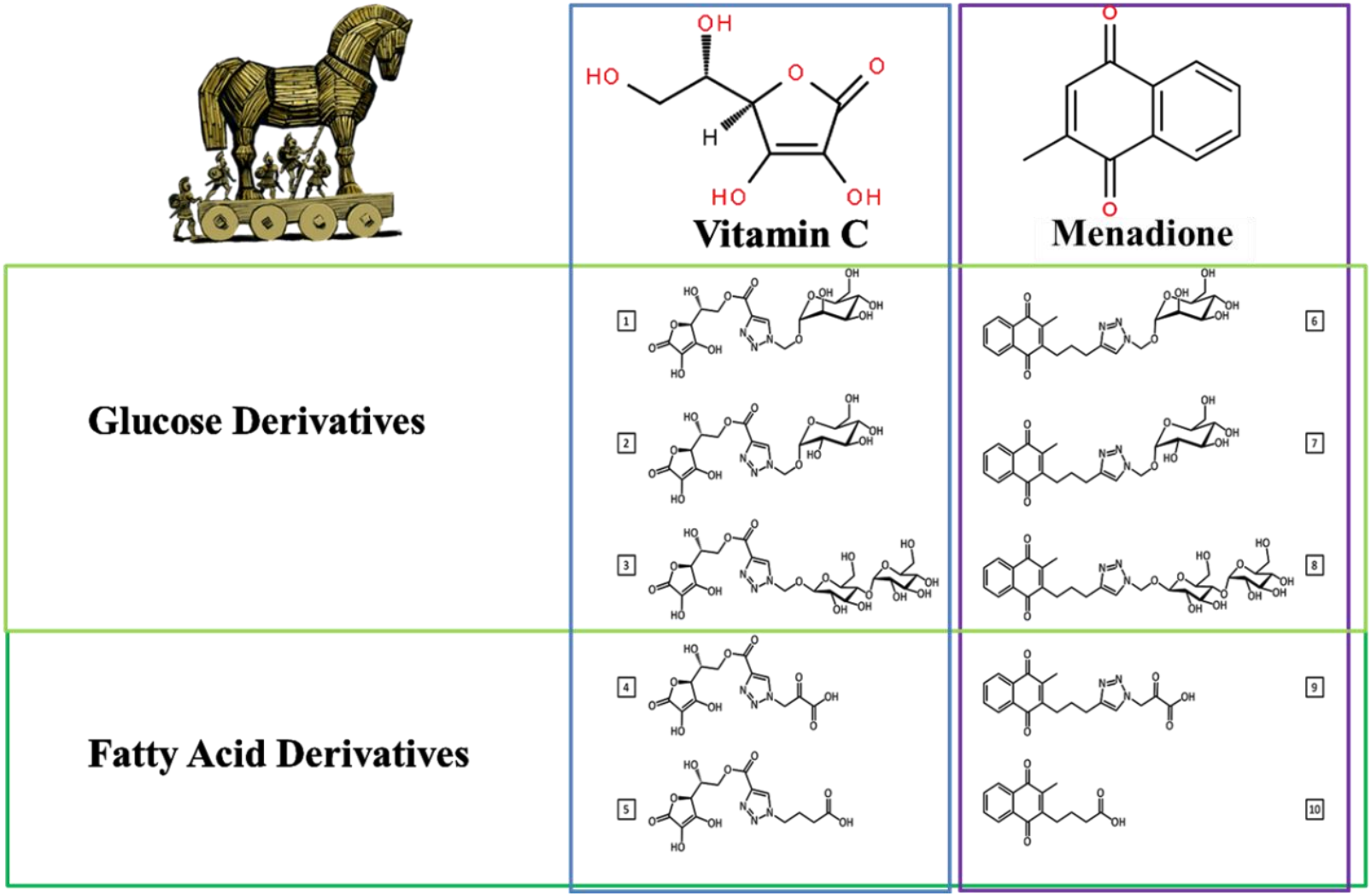

Figure 3.1: The TH Strategy: Coupling of Vitamin C and Menadione with simple sugars and lipids. Image made in PowerPoint.

Vitamin C has shown some success as a cancer therapeutic, but it has been found that the cancer cells tend to develop resistance to this therapeutic approach through upregulation of efflux mechanisms often resulting in this treatment being non-viable.[262] Our approach will couple Vitamin C to simple sugars and lipids to target selective cellular uptake of an antioxidant in cancer cells. It is expected to remove cancer's ability to adapt to Vitamin C antioxidant treatment by employing the TH principle to trick the cancer cells into a continued uptake of Vitamin C coupled to a highly desirable target fuel moiety like glucose.

Alterations to the levels of cellular ROS modifies the signalling pathways required for cell division and rapid proliferation, but can also be used to trigger apoptosis in cancer cells.[327] Endogenous ROS in proliferative cancer cell lines can be altered depending on the redox capabilities of the moiety bound to the natural substrate. Accordingly, by binding a ROS generator, such as Menadione to a natural substrate, the cancer cell will be tricked into internalizing a toxic moiety capable of increasing ROS concentration and inducing apoptosis.[304]

Dr. Barry Sharpless' introduced the theory of click chemistry in 1999 at the 217th American Chemical Society annual meeting.[328] Click chemistry describes the functional groups on a compound that rapidly and selectively react with each other in an aqueous environment. The concept of Click Chemistry has been transformed into convenient, versatile and reliable two step coupling procedure of two molecules and is particularly used in drug discovery.[328] In pharmaceutical chemistry, the discovery of compounds with specific properties is always a necessity. Once the compound is identified, it is important to establish an efficient method of synthesis and purification.[329]

Click chemistry is growing in popularity for the synthesis of simple molecules by connecting two existing molecules to each other through the addition of a triazole linker group.[328,330] In click chemistry, the copper(I)-catalyzed 1,2,3-triazole-forming reaction between azides and terminal alkynes is now the gold-standard reaction.[329] This reaction involves the use of the triazole linker. These linkers not only work to conjugate two existing molecules, it also readily associates with biological targets, through interactions such as hydrogen-bonding and dipole interactions possibly adding to the action of the conjugated compound.[329]

Many applications of click chemistry are apparent in the drug discovery field, with novel compound synthesis being the main application.[330] The characteristics increasing the popularity and prevalence of click chemistry in drug discovery includes high compound yield, high compound specificity, and the simplicity of reactions.[331] In some applications, click chemistry has been used in the modification of biological ligands, after nanoparticles production without altering functions of the nano-particle while enhancing the process of drug delivery to a biological site. This is greatly important to maintain the function of the nano-particle.[332] Click chemistry was utilized in the synthesis of the novel TH compounds, due to the aforementioned benefits in the method of synthesis and the high compound yield and compound specificity.

Glucose is an essential energy source in cells, with significant implications in many cellular processes. In PCa, glucose can directly and indirectly impact cancer progression and development.[317] In this study we examine the relationship between prostate cancer progression, metabolism, and the effects of the range of novel compounds on the glucose milieu in which the cells are present, due to the role of glucose in the disease progression and survival.

Cancer cells require high energy levels to support their rapid growth, where glucose serves as a primary energy source. PCa cells have been shown to exhibit heightened glucose uptake and utilisation compared to that of normal prostate cells. This metabolic alteration, the Warburg effect or aerobic glycolysis, enables cancer cells to generate energy efficiently, even in the presence of sufficient oxygen.[253,333] High availability of glucose provides the fuel required for the growth and proliferation of PCa cells. The PCa cells can adapt their metabolism to efficiently utilise glucose through increased expression of glucose transporters (such as GLUT1 and GLUT4) and other biomolecules involved in glucose metabolism to allow an adequate supply of glucose to quench their high energy demands.[334,335] This metabolic adaptation contributes to the survival and growth of PCa cells in high glucose environments, as seen in patients with unmanaged insulin resistance or diabetes.[336]

Glucose metabolism can influence signalling pathways involved in prostate cancer growth and progression, where increased glucose uptake and metabolism have been shown to activate pathways like PI3K, AKT and mTOR, which promote cell growth, survival, and proliferation.[336] These pathways are known to contribute to the aggressive behaviour of

prostate cancer cells and aid in their resistance to therapy.[337,338] The implications of glucose metabolism on androgen signalling is important in PCa where studies have shown that high glucose concentrations can influence the activity of the AR.[339] These high glucose levels can enhance AR-mediated gene expression, promoting growth and survival of PCa cells.[340,341]

The maintenance of optimal blood glucose in individuals with diabetes or insulin resistance may aid in managing the metabolic aspects of prostate cancer. However, further research is necessary to understand the intricate interactions between glucose metabolism and PCa and in the development of effective targeted therapies. This work aims to bridge this knowledge gap, through examining the effect of the glucose milieu on PCa metabolism and how effective glycoconjugated compounds can be in the targeting of PCa metabolism and the treatment of the disease.

3.2 Hypothesis and Aims

We propose to synthesise novel Trojan Horse compounds through the application of 'click chemistry' by coupling simple sugars and lipids with native Vitamin C and Menadione and evaluate these agents for their ability to specifically target cancer cell metabolism and cause cell death.

- To synthesise and characterize the structure of the novel TH compounds designed by the University of South Australia (UniSA) team and the Trinity College Dublin Molecular Pathology (TCD) Research group.
- To determine the cytotoxicity of Vitamin C and Menadione in a panel of prostate cell lines, under 0mM, 5.5mM and 11mM glucose conditions. From this an IC_{50} concentration can be determined for further experiments.
- To determine the cytotoxicity of the novel TH compounds and select compounds for further downstream cellular evaluations.
- To determine the cytotoxicity of two glucose-Menadione compounds and 1 fatty acid-Menadione compound in a panel of prostate cell lines, under 0mM, 5.5mM and 11mM glucose conditions.

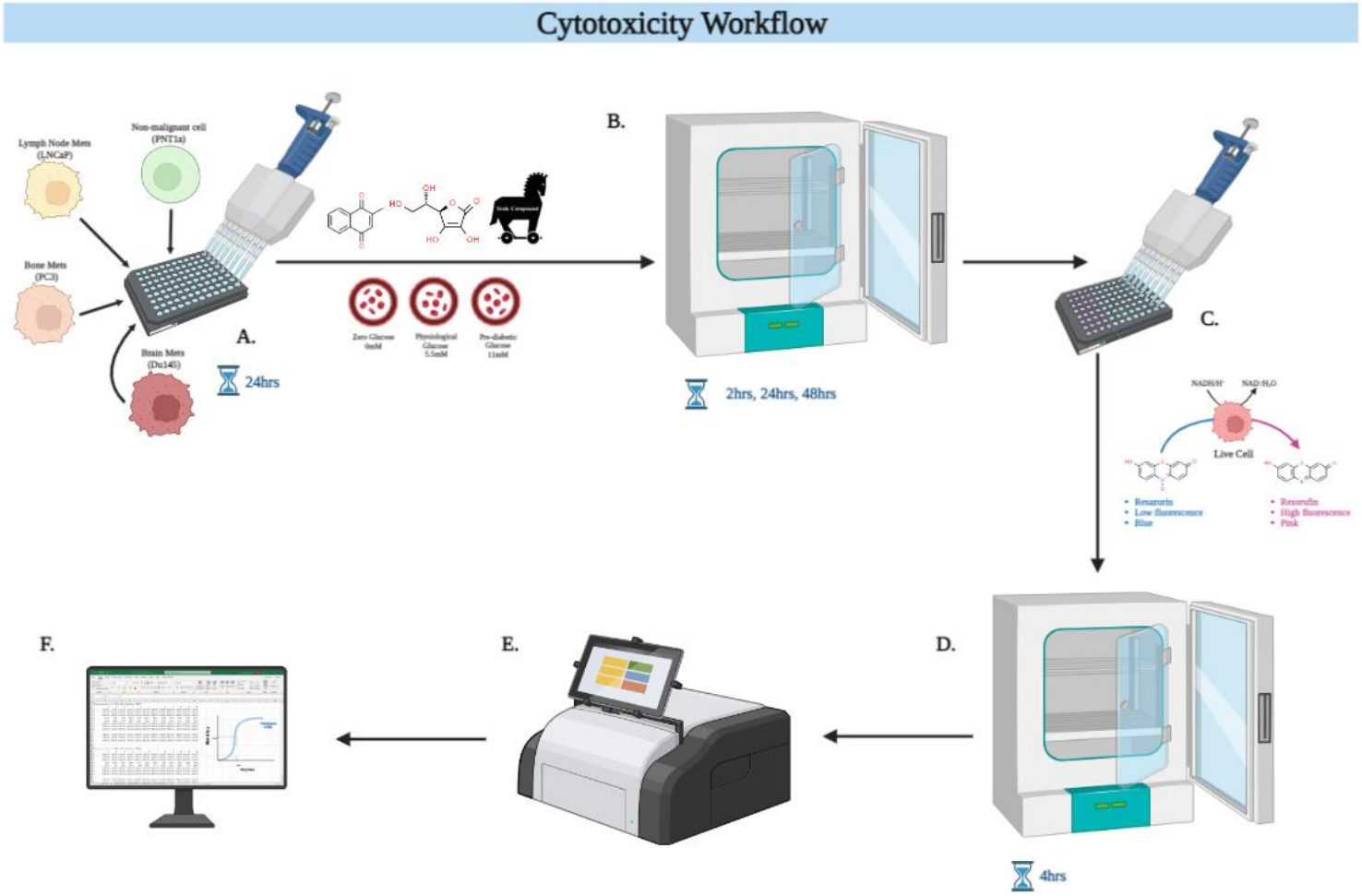

Figure 3.2: Experimental workflow (A.) The panel of cell lines were plated for 24hrs, following this, cells were washed and placed in 0mM. 5.5mM and 11mM glucose conditions respectively. Cells were treated with native vitamins, and novel TH compounds. (B.) Treated cells were incubated for; 2hrs, 24hrs and 48hrs respectively in the different glucose conditions. (C.) Cells were washed and 10% alamar blue was added to each well. (D.) Cells were incubated for 4hrs to allow the dye to develop. (E.) The cells were read on the GloMax fluorescent reader at emission 604nm, and excitation 578nm (F.) Data was analysed and IC_{50} concentrations were determined. Image made in Biorender.

3.3 Methods and Materials

3.3.1 Novel Trojan Horse Synthesis:

The full details of the TH compound synthesis are detailed in Chapter 2, Section 2.2.

3.3.2 Cell culture:

The full details of the cell lines and the methods for the culturing of the cell lines is detailed in Chapter 2, Section 2.3.

3.3.3 Alamar blue cell viability

Alamar blue assay was used to determine the viability of the cell lines detailed in Chapter 2 Section 2.4.

3.3.4 Statistical Analysis

Statistical analysis was performed using GraphPad Prism version 9.0. The results were expressed as mean ± SEM. Data was log transformed, normalised, and plotted on a non-linear regression graph, using GraphPad Prism version 9.0 and $p < 0.05$ was considered significant.

3.4 Results:

3.4.1 Optimisation of cell seeding density of prostate cancer cell lines at 24hr by alamar blue assay

Cells were seeded in a 96 well plate at various cell densities with 11mM glucose RPMI media. The density range was 10– $1x10^5$ cells/well. Cell viability was determined after 24 hours to mimic treatment times. After 24 hours the cells were stained with alamar blue (10% v/v) and incubated for 4hrs at 37°C in the dark. The cell viability was determined through UV/Vis spectroscopy, at 595nm. The results are summarised in Figure 3.3.

A linear correlation was observed between cell density and absorbance in the cells. A cell seeding density of $2x10^4$ cells per well was determined to be optimal for performing subsequent drug treatment experiments for all 4 cell lines. A representative graph for the seeding densities is presented in Figure 3.3.

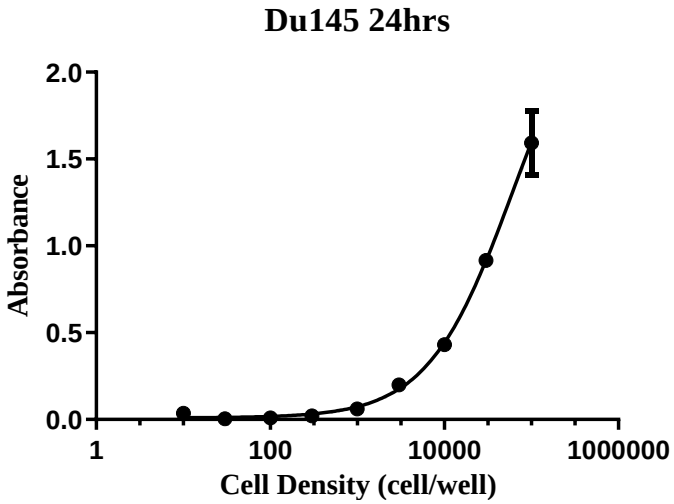

Figure 3. 3: Determination of optimum seeding density for Du145 cells by alamar blue assay. Du145 cells were seeded at different densities ranging from 10– $1x10^5$ cells/well. Alamar blue dye was added after 24hrs, and absorbance determined after four hours of incubation. Values represent the mean ± S.E.M of three independent experiments. Results were plotted using GraphPad Prism 9.0.

Initial experiments included time points of 2hrs, 4hrs, 8hrs, 16hrs, 24hrs and 48hrs, this was reduced down to 24hrs and 48hrs shortly after the commencement of the study. Further, from the results obtained, the time point of 24hrs treatment was taken forward for all further experiments. Treatments less than 24hrs required very high concentrations of the novel compound, in which we did not have, to obtain sufficient cell death. However, treatments greater than 24hrs under glucose starvation posed the

question, if cell death was in fact due to the novel compound treatment, or that of the starvation of a vital fuel source for the proliferating cancer cells.

3.4.2 Trojan Horse Compound 1 (TH1)

3.4.2.1 The effect of varying glucose concentrations on the cytotoxicity of the TH 1 compound in the PC3 cell line under 11mM glucose.

Trojan Horse 1 is a Menadione-amine-glucose compound, as detailed in Chapter 2.

Preliminary cytotoxicity analysis was carried out on TH1 compound in the PC3 cells under media glucose conditions (11mM) there was very little cell kill, and the IC_{50} values were high, as shown in Figure 3.4. This suggested that perhaps due to the glucose molecule conjugated to Menadione, the uptake of the compound was being inhibited and therefore it prompted us to consider the impact of the glucose milieu on the uptake of the Trojan horse compounds and the role of media glucose in modulating cytotoxicity. We therefore examined varying glucose conditions to represent glucose starvation (0mM), normal physiological glucose (5.5mM), and pre-diabetic glucose (11mM) conditions as detailed in Figure 3.5.

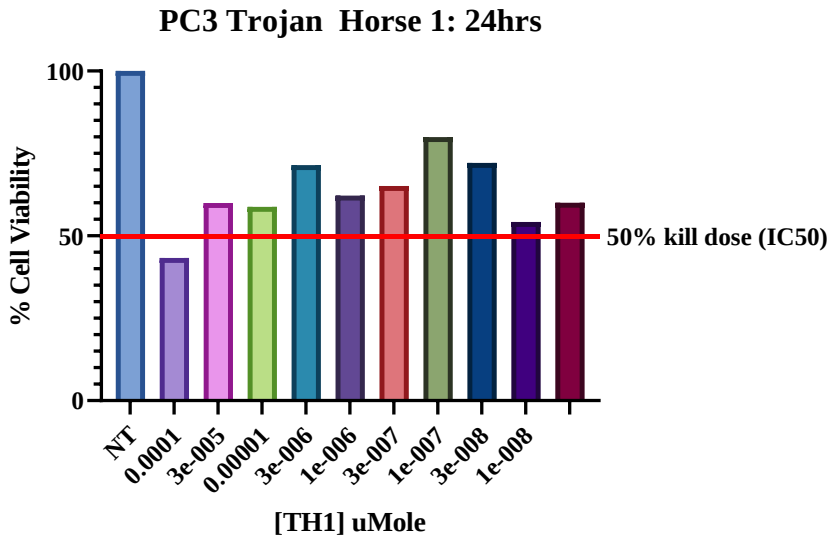

Figure 3. 4: Early examination of TH1 compound effects on PC3 cells in 11mM Glucose media after 24hrs treatment.

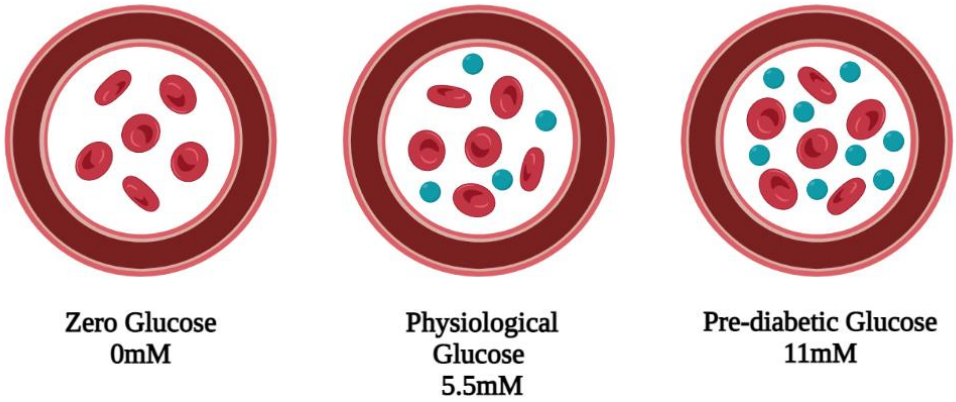

Figure 3. 5: The Glucose milieu: The cellular experiments were conducted under 3 glucose milieus, to represent: glucose starvation, normal physiological glucose, and pre-diabetic glucose.

The preliminary cytotoxicity experiments to follow are conducted under 3 different glucose milieus, due to the results obtained in Figure 3.4. The time points of 24hrs and 48hrs were continued in the examination of the cytotoxicity of the novel compounds.

3.4.2.2 The effect of the varying glucose conditions on the IC_{50} values of TH1 in the PNT1a cell line.

PNT1a cells under glucose starvation treated with TH1 resulted in IC_{50} values of 14.4µM under 24hrs incubation and 405.3µM under 48hrs incubation. Under normoglycemia of 5.5mM glucose and TH1 treatment, cells presented with IC_{50} values of 148.0µM after 24hrs and 393.6µM after 48hrs. Finally, PNT1a cells treated with TH1 under 11mM glucose media resulted in IC_{50} values of 284.5µM after 24hrs and 208.1µM after 48hrs. The results for all IC_{50} determinations are summarised in Table 3.4.

Table 3.4: IC_{50} values for TH1 treated PNT1a cells under 3 glucose RPMI conditions and 3 time points

Media glucose concentration	24 hours	48 hours
	IC_{50} (µM)	**IC_{50} (µM)**
0mM	14.4µM	405.3µM
5.5mM	148.0µM	393.6µM
11mM	284.5µM	208.1µM

An overlay of the 3 response curves for 24hr treatments in PNT1a cells is shown in Figure 3.6 depicting the effect of varying glucose conditions on the IC_{50} values of TH1.

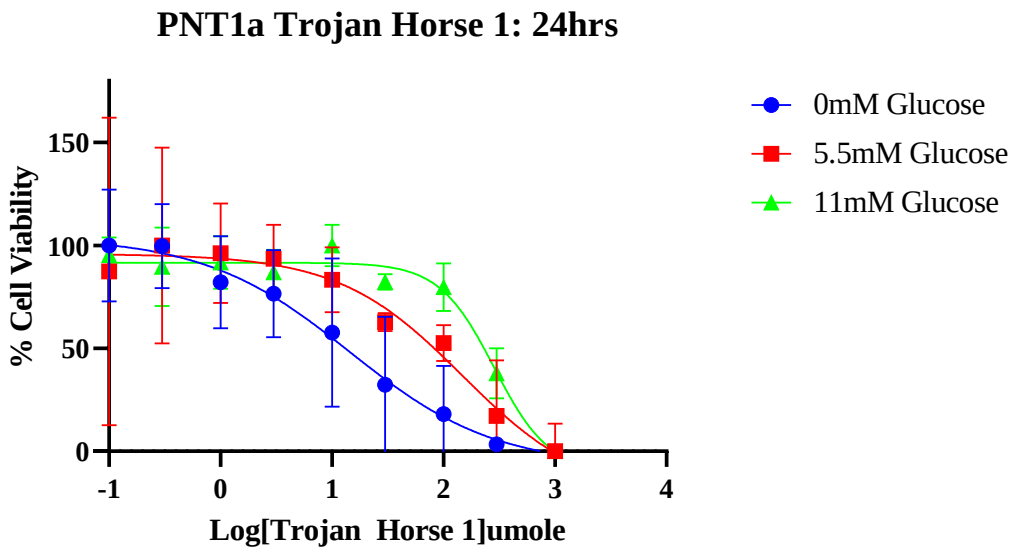

Figure 3. 6: Effect of TH1 on PNT1a cell line viability cells under 3 different glucose RPMI conditions at 24 hours. The data shown is expressed as mean ± SEM. Each experiment is in technical replicate of 3 and biological replicate of 3.

3.4.2.3 The effect of the varying glucose conditions on the IC_{50} values of TH1 in the LNCaP cell line.

LNCaP cells under glucose starvation treated with TH1 resulted in IC_{50} values of 339.8µM under 24hrs incubation and 194.7µM under 48hrs incubation. Under normoglycemia of 5.5mM glucose and TH1 treatment, cells presented with IC_{50} values of 368.8µM after 24hrs and 428.8µM after 48hrs. Finally, LNCaP cells treated with TH1 under 11mM glucose media resulted in IC_{50} values 377.5µM after 24hrs and 538.6µM after 48hrs. The results for all IC_{50} determinations are summarised in Table 3.5.

Table 3.5: IC_{50} values for TH1 treated LNCaP cells under 3 glucose RPMI conditions and 3 time points

Media glucose concentration	24 hours	48 hours
	IC_{50} (µM)	**IC_{50} (µM)**
0mM	339.8µM	194.7µM
5.5mM	368.8µM	428.8µM
11mM	377.5µM	538.6µM

An overlay of the 3 response curves for 24hr treatments in LNCaP cells is shown in Figure 3.7, depicting the effect of varying glucose conditions on the IC_{50} values of TH1.

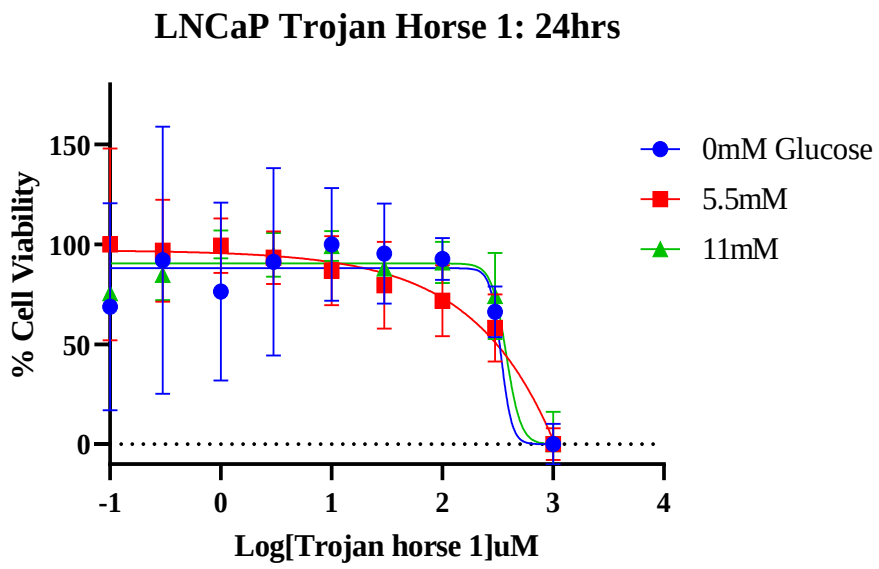

Figure 3. 7: Effect of TH1 on LNCaP cell line viability cells under 3 different glucose RPMI conditions at 24 hours. The data shown is expressed as mean ± SEM. Each experiment is in technical replicate of 3 and biological replicate of 3.

3.4.2.4 The effect of the varying glucose conditions on the IC50 values of TH1 in the PC3 cell line.

PC3 cells were tested under the outlined conditions, however no response to the TH1 compound was reported. From this, 1000µM of TH1 was tested on the PC3 cell lines in further experiments, in the hopes of seeing some drug activity.

3.4.2.5 The effect of the varying glucose conditions on the IC_{50} values of TH1 in the Du145 cell line.

Du145 cells under glucose starvation treated with TH1 resulted in IC_{50} values 37.7µM under 24hrs incubation and 6.5µM under 48hrs incubation. Under normoglycemia of 5.5mM glucose and TH1 treatment, cells presented with IC_{50} values of 241.1µM after 24hrs and 95.75µM after 48hrs. Finally, Du145 cells treated with TH1 under 11mM glucose media resulted in IC_{50} values of 214.5µM after 24hrs and 230.4µM after 48hrs. The results for all IC_{50} determinations are summarised in Table 3.6.

Table 3.6: IC_{50} values for TH1 treated Du145 cells under 3 glucose RPMI conditions and 3 time points

Media glucose concentration	**24 hours**	**48 hours**
	IC_{50} (µM)	**IC_{50} (µM)**
0mM	37.7 µM	6.5µM
5.5mM	241.1 µM	95.75µM
11mM	214.5 µM	230.4µM

An overlay of the 3 response curves for 24hr treatments in Du145 cells is shown in Figure 3.8 depicting the effect of varying glucose conditions on the IC_{50} values of TH1.

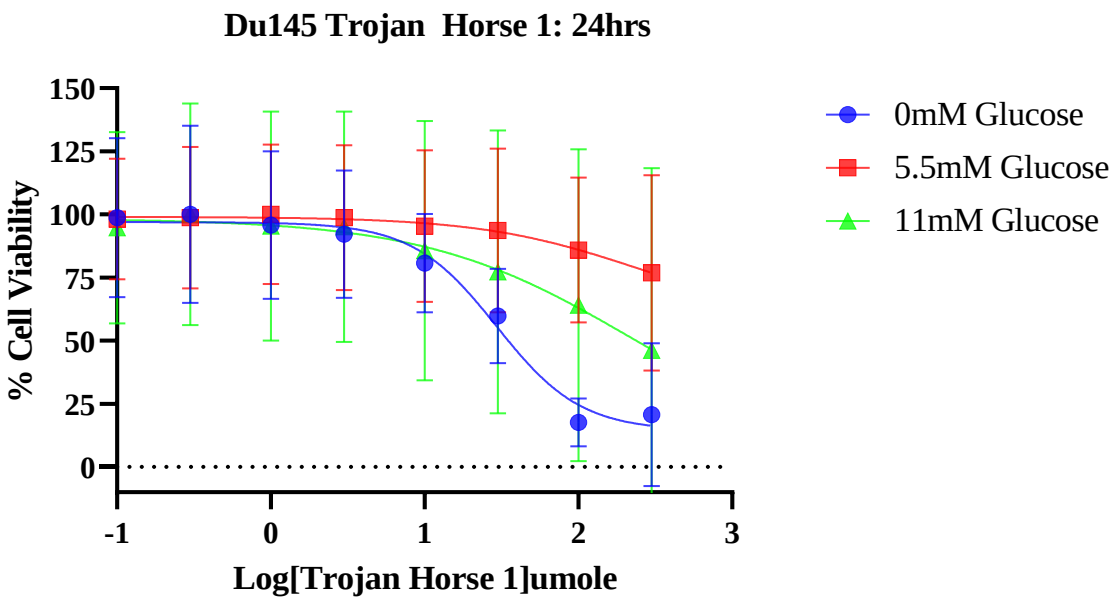

Figure 3. 8: Effect of TH1 on Du145 cell line viability cells under 3 different glucose RPMI conditions at 24 hours. The data shown is expressed as mean ± SEM. Each experiment is in technical replicate of 3 and biological replicate of 3.

3.4.3 Effect of Vitamin C cytotoxicity on panel of prostate cell line viability under varying glucose conditions

A range of Vitamin C concentrations (1-1x10^4 µM) were tested to determine an optimal cytotoxicity concentration, that would not cause total cell death, but demonstrate the anticancer effects of the substance. Vitamin C treatments decreased the viability of the cell lines in a dose dependent manner and time dependent manner when the treatments were carried out under three different glucose RPMI conditions. The IC_{50} values were determined from the response graphs and were plotted as % cell viability.

3.4.3.1 The effect of the varying glucose conditions on the IC_{50} values of Vitamin C in the PNT1a cell line.

PNT1a cells under glucose starvation treated with Vitamin C resulted in IC_{50} values of 1035µM under 2hrs incubation, 201.7µM under 24hrs incubation and 264.1µM under 48hrs incubation. Under normoglycemia of 5.5mM glucose and Vitamin C treatment, cells presented with IC_{50} values of 958µM after 2hrs, 333.8µM after 24hrs and 346.4µM after 48hrs. Finally, PNT1a cells treated with Vitamin C under 11mM glucose media resulted in IC_{50} values of 1013µM after 2hrs, 347.7µM after 24hrs and 1912µM after 48hrs. The results for all IC_{50} determinations are summarised in Table 3.7.

Table 3.7: IC_{50} values for Vitamin C treated PNT1a cells under 3 glucose RPMI conditions and 3 time points

Media glucose concentration	**2 hours**	**24 hours**	**48 hours**
	IC_{50} (µM)	**IC_{50} (µM)**	**IC_{50} (µM)**
0mM	1035µM	201.7µM	264.1µM
5.5mM	958µM	333.8µM	346.4µM
11mM	1013µM	347.7µM	1912µM

An overlay of the 3 response curves for 24hr treatments in PNT1a cells is shown in Figure 3.9, depicting the effect of varying glucose conditions on the IC_{50} values of Vitamin C.

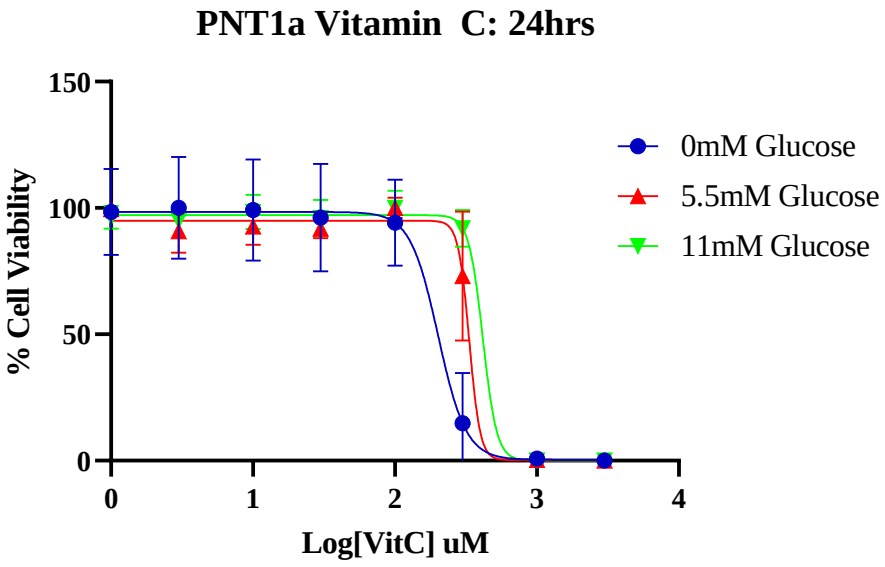

Figure 3. 9: Effect of Vitamin C on PNT1a cell line viability under 3 glucose conditions at 24 hours. The data shown is expressed as mean ± SEM. Each experiment is in technical replicate of 3 and biological replicate of 3.

3.4.3.2 The effect of the varying glucose conditions on the IC_{50} values of Vitamin C in the LNCaP cell line.

LNCaP cells under glucose starvation treated with Vitamin C resulted in IC_{50} values of 1038.1µM under 2hrs incubation, 521.9µM under 24hrs incubation and 782.1µM under 48hrs incubation. Under normoglycemia of 5.5mM glucose and Vitamin C treatment, cells presented with IC_{50} values of 3481.6µM after 2hrs, 2098µM after 24hrs and 3039µM after 48hrs. Finally, LNCaP cells treated with Vitamin C under 11mM glucose media resulted in IC_{50} values of 3562.8µM after 2hrs, 33357µM after 24hrs and 3419µM after 48hrs. The results for all IC_{50} determinations are summarised in Table 3.8.

Table 3.8: IC_{50} values for Vitamin C treated LNCaP cells under 3 glucose RPMI conditions and 3 time points

Media glucose concentration	2 hours	24 hours	48 hours
	IC_{50} (µM)	IC_{50} (µM)	IC_{50} (µM)
0mM	1038.1µM	521.9µM	782.1µM
5.5mM	3481.6µM	2098µM	3039µM
11mM	3562.8µM	3357µM	3419µM

An overlay of the 3 response curves for 24hr treatments is shown in Figure 3.10, depicting the effect of varying glucose conditions on the IC_{50} values of Vitamin C.

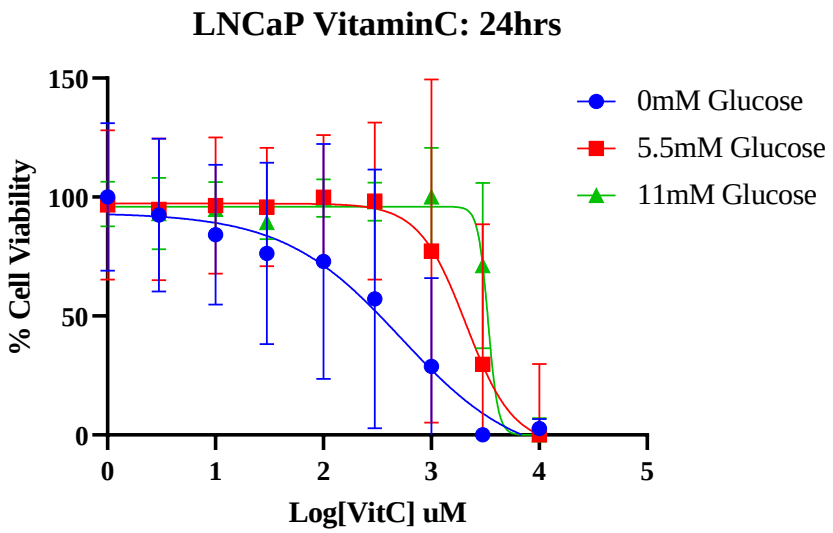

Figure 3. 10: Effect of Vitamin C on LNCaP cell line viability under 3 glucose conditions at 24 hours. The data shown is expressed as mean ± SEM. Each experiment is in technical replicate of 3 and biological replicate of 3.

3.4.3.3 The effect of the varying glucose conditions on the IC50 values of Vitamin C in the PC3 cell line.

PC3 cells under glucose starvation treated with Vitamin C resulted in IC_{50} values of 332.5µM under 2hrs incubation, 243.3uM under 24hrs incubation and 306.7µM under 48hrs incubation. Under normoglycemia of 5.5mM glucose and Vitamin C treatment, cells presented with IC_{50} values of 1079µM after 2hrs, 905.7uM after 24hrs and 1834.2µM after 48hrs. Finally, PNT1a cells treated with Vitamin C under 11mM glucose media resulted in IC_{50} values of 2116µM after 2hrs, 1001.0µM after 24hrs and 2281.6µM after 48hrs. The results for all IC_{50} determinations are summarised in Table 3.9.

Table 3.9: IC_{50} values for Vitamin C treated PC3 cells under 3 glucose RPMI conditions and 3 time points

Media glucose concentration	2 hours	24 hours	48 hours
	IC_{50} (µM)	**IC_{50} (µM)**	**IC_{50} (µM)**
0mM	332.5µM	243.3µM	306.7µM
5.5mM	1079µM	905.7µM	1834.2µM
11mM	2116µM	1001.0µM	2281.6µM

An overlay of the 3 response curves for PC3 under 24hr treatment is shown in Figure 3.11 depicting the effect of varying glucose conditions on the IC_{50} values of Vitamin C.

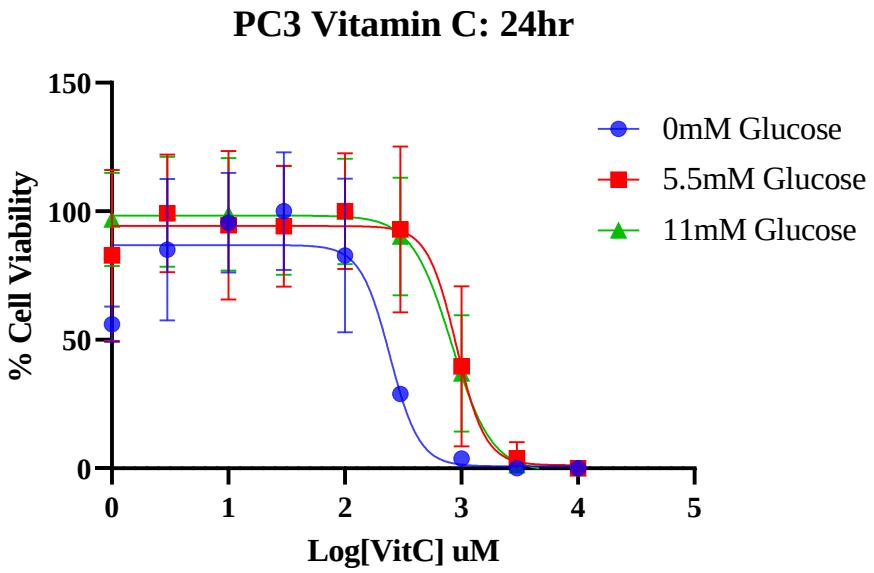

Figure 3. 11: Effect of Vitamin C on PC3 cell line viability under 3 glucose conditions at 24 hours. The data shown is expressed as mean ± SEM. Each experiment is in technical replicate of 3 and biological replicate of 3.

3.4.3.4 The effect of the varying glucose conditions on the IC_{50} values of Vitamin C in the Du145 cell line.

In Du145 cells, Vitamin C at physiological glucose (5.5mM) was found to be comparable to that of existing literature. With an IC_{50} concentration of 3197µM at 2 hours, decrease 3-fold to 1002µM at 24hrs and 2980.6µM at 48hrs (n=3).[342] In high glucose conditions (11mM), the IC_{50} for Vitamin C was determined to be 432.2µM at 2 hours with a 3-fold decrease to 114.3µM after 24 hours and 433.7µM at 48hrs (n=3). An emerging trend was observed, with the IC_{50} concentration 3-fold decreasing by 3fold between 2 hours and 24 hours, in the presence of glucose. Conversely, Du145 cells treated with Vitamin C in 0mM glucose conditions saw an opposite effect, with lower IC_{50} concentrations of 206.4µM at 2 hours and 900.9µM at 24 hours and 1032.1µM at 48hrs.The results for all IC_{50} determinations are summarised in Table 3.10.

Table 3.10: IC_{50} values for Vitamin C treated Du145 cells under 3 glucose RPMI conditions and 3 time points

Media glucose concentration	**2 hours**	**24 hours**	**48 hours**
	IC_{50} (µM)	**IC_{50} (µM)**	**IC_{50} (µM)**
0mM	206.4µM	900.9µM	1032.1µM
5.5mM	3197µM	1002µM	2980.6µM
11mM	432.2µM	114.3µM	433.7µM

An overlay of the 3 response curves for 24hr treatments is shown in Figure 3.12, depicting the effect of varying glucose conditions on the IC_{50} values of Vitamin C on Du145 cells.

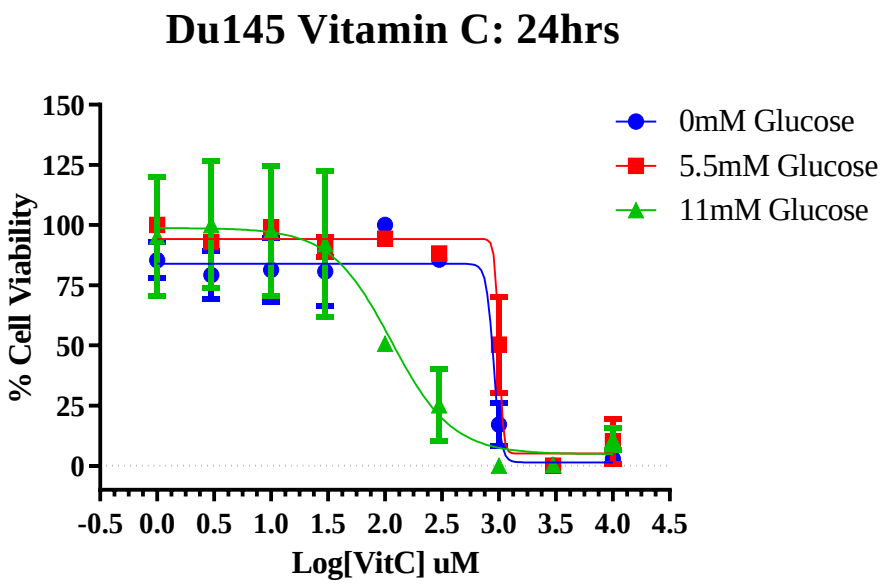

Figure 3. 12: Effect of Vitamin C on Du145 cell line viability under 3 glucose conditions at 24 hours. The data shown is expressed as mean ± SEM. Each experiment is in technical replicate of 3 and biological replicate of 3.

3.4.4 Effect of Menadione on cell line viability relative to the untreated under 3 glucose conditions

In this study, a range of concentrations of Menadione from 0.1-1x10^3 µM were tested to determine a concentration, that would not cause total cell death, but illustrate the anticancer effects of the substance. IC_{50} values were determined following Menadione treatment at two different time points 2 hours and 24 hours and three different RPMI glucose conditions; 0mM, 5.5mM and 11mM.

3.4.4.1 The effect of the varying glucose conditions on the IC50 values of Menadione in the PNT1a cell line.

PNT1a cells under glucose starvation treated with Menadione resulted in IC_{50} values of 147.1µM under 2hrs incubation, 10.6µM under 24hrs incubation and 16.9µM under 48hrs incubation. Under normoglycemia of 5.5mM glucose and Menadione treatment, cells presented with IC_{50} values of 95.9µM after 2hrs, 24.2µM after 24hrs and 37.6µM after 48hrs. Finally, PNT1a cells treated with Menadione under 11mM glucose media resulted in IC_{50} values of 101.3µM after 2hrs, 24.4µM after 24hrs and 147.0µM after 48hrs. The results for all IC_{50} determinations are summarised in Table 3.8.

Table 3.11: IC_{50} values for Menadione treated PNT1a cells under 3 glucose RPMI conditions and 3 time points

Media glucose concentration	**2 hours**	**24 hours**	**48 hours**
	IC_{50} (µM)	**IC_{50} (µM)**	**IC_{50} (µM)**
0mM	147.1µM	10.6µM	16.9µM
5.5mM	95.9µM	24.2µM	37.6µM
11mM	101.3µM	24.4µM	147.0µM

An overlay of the 3 response curves for 24hr treatments in PNT1a cells is shown in Figure 3.13, depicting the effect of varying glucose conditions on the IC_{50} values of Menadione.

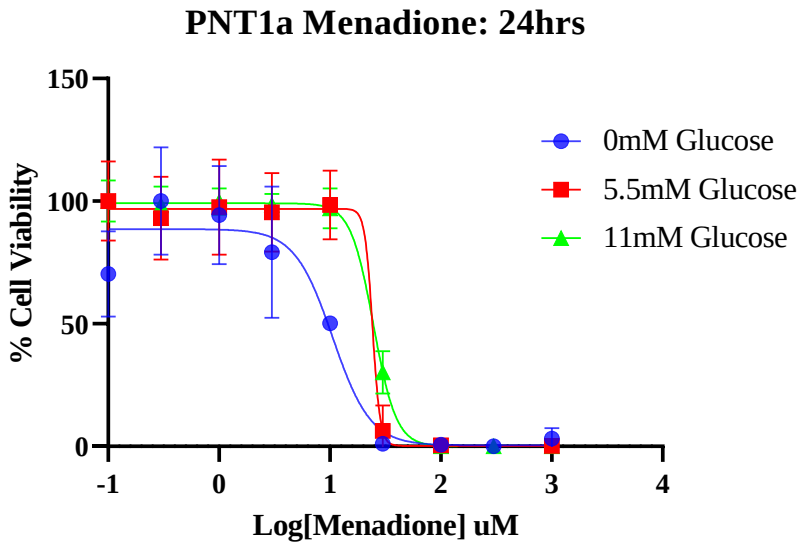

Figure 3. 13: Effect of Menadione on PNT1a cell line viability under 3 glucose conditions at 24 hours. The data shown is expressed as mean ± SEM. Each experiment is in technical replicate of 3 and biological replicate of 3.

3.4.4.2 The effect of the varying glucose conditions on the IC_{50} values of Menadione in the LNCaP cell line.

LNCaP cells under glucose starvation treated with Menadione resulted in IC_{50} values of 121.2µM under 2hrs incubation, 26.4µM under 24hrs incubation and 23.5µM under 48hrs incubation. Under normoglycemia of 5.5mM glucose and Menadione treatment, cells presented with IC_{50} values of 201.3µM after 2hrs, 30.1µM after 24hrs and 30.2µM after 48hrs. Finally, LNCaP cells treated with Menadione under 11mM glucose media resulted in IC_{50} values of 203.4µM after 2hrs, 40.4µM after 24hrs and 35.8µM after 48hrs. The results for all IC_{50} determinations are summarised in Table 3.12.

Table 3.12: IC_{50} values for Menadione treated LNCaP cells under 3 glucose RPMI conditions and 3 time points

Media glucose concentration	2 hours	24 hours	48 hours
	IC_{50} (µM)	IC_{50} (µM)	IC_{50} (µM)
0mM	121.2µM	26.4µM	23.5µM
5.5mM	201.3µM	30.1µM	30.2µM
11mM	203.4µM	40.4µM	35.8µM

An overlay of the 3 response curves for 24hr treatments in LNCaP cells is shown in Figure 3.14, depicting the effect of varying glucose conditions on the IC_{50} values of Menadione.

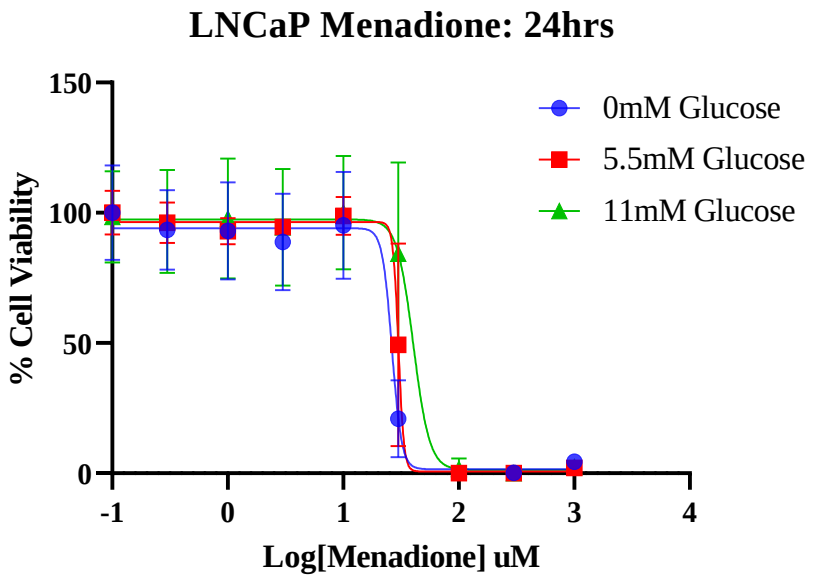

Figure 3. 14: Effect of Menadione on LNCaP cell line viability under 3 glucose conditions at 24 hours. The data shown is expressed as mean ± SEM. Each experiment is in technical replicate of 3 and biological replicate of 3.

3.4.4.3 The effect of the varying glucose conditions on the IC_{50} values of Menadione in the PC3 cell line.

PC3 cells under glucose starvation treated with Menadione resulted in IC_{50} values of 78.7µM under 2hrs incubation, 19.3µM under 24hrs incubation and 10.4µM under 48hrs incubation. Under normoglycemia of 5.5mM glucose and Menadione treatment, cells presented with IC_{50} values of 83.7µM after 2hrs, 26.0µM after 24hrs and 14.7µM after 48hrs. Finally, PC3 cells treated with Menadione under 11mM glucose media resulted in IC_{50} values of 71.3µM after 2hrs, 26.7µM after 24hrs and 25.9µM after 48hrs. The results for all IC_{50} determinations are summarised in Table 3.13.

Table 3.13: IC_{50} values for Menadione treated PC3 cells under 3 glucose RPMI conditions and 3 time points

Media glucose concentration	2 hours	24 hours	48 hours
	IC_{50} (µM)	IC_{50} (µM)	IC_{50} (µM)
0mM	78.7µM	19.3µM	10.4µM
5.5mM	83.7µM	26.0µM	14.7µM
11mM	71.3µM	26.7µM	25.9µM

An overlay of the 3 response curves for 24hr treatments is shown in Figure 3.15, depicting the effect of varying glucose conditions on the IC_{50} values of Menadione in PC3 cells.

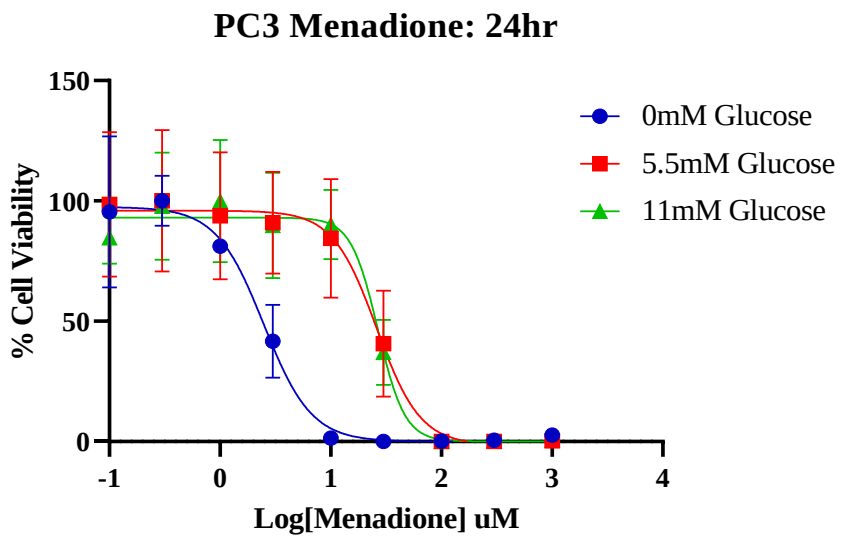

Figure 3. 15: Effect of Menadione on PC3 cell line viability under 3 glucose conditions at 24 hours. The data shown is expressed as mean ± SEM. Each experiment is in technical replicate of 3 and biological replicate of 3.

3.4.4.4 The effect of the varying glucose conditions on the IC_{50} values of Menadione in the Du145 cell line.

IC_{50} values changed in a time dependent manner when Du145 cells were treated in 0mM RPMI glucose conditions from 12.33µM at 2 hours to 5.68µM at 24 hours. However, the was no noticeable time dependent change in IC_{50} values when cells were plated in 5.5mM RPMI glucose and 11mM RPMI glucose (P=0.93). Although it was interesting to note, that for 2-hour treatment the IC_{50} values increased from 12.44µM in 0mM RPMI glucose conditions, to nearly three times that at 30.43µM and 35.66µM in 5.5mM and 11mM RPMI glucose concentrations respectively. The results are presented in Table 3.11.

Table 3.14: IC_{50} values for Menadione treated Du145 cells under 3 different glucose RPMI conditions and 3 time points

Glucose Condition	2 hours	24 hours	48hrs
	IC_{50} (µM)	**IC_{50} (µM)**	**IC_{50} (µM)**
0mM	12.2µM	5.7µM	10.1µM
5.5mM	30.4µM	34.8µM	30.4µM
11mM	35.7µM	30.8µM	30.6µM

An overlay of the 3 response curves for 24hr treatments in 3 glucose different conditions is shown in Figure 3.16. The change in IC_{50} values for Menadione is influenced by glucose conditions.

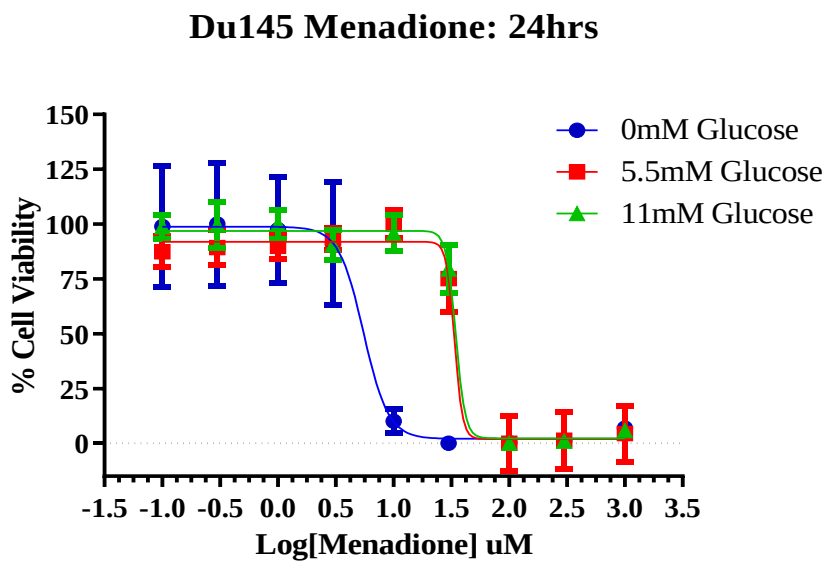

Figure 3. 16: Effect of Menadione on Du145 cell line viability under 3 different glucose conditions at 24 hours. The data shown is expressed as mean ± SEM. Each experiment is in technical replicate of 3 and biological replicate of 3.

3.4.5 The Trojan Horse Compounds

3.4.5.1 The pre-screening of the range of Menadione TH compounds in the prostate cell lines under 5.5mM glucose conditions.

A panel of novel compounds were sent from the UniSA lab to the molecular pathology lab, the coombe hospital in November 2020 for analysis. Initially, 20 Menadione and Vitamin C compounds had been discussed for synthesis, but in total 6 compounds were received. These compounds included 5 Menadione – glucose compounds and one Menadione – fatty acid compound. These 6 novel compounds were pre-screened to determine which of the novel compounds were best to take forward for full analysis in this study. TH compound 1 was received year 2 of the study, in 2019 and thus was not included in the pre-screening but has undergone full analysis. No Vitamin C compounds were received for analysis in this study as per November 2022.

Table 3.15: Novel Trojan Horse Compound Pre-Screening under 5.5mM Glucose RPMI

Compound	PNT1a	LNCaP	PC3	Du145
TH2	1131µM	1129.3µM	No response	1275µM
TH3	557.8µM	988.9µM	No response	2535µM
TH4	151.2µM	90.1µM	729.6µM	86.5µM
TH5	171.5µM	306.7µM	999.6µM	316.0µM
TH6	1106µM	30.95µM	75.47µM	426.2µM

The pre-screening of the compounds found glucose compound TH4 and the fatty acid compound TH6, the optimum compounds to take forward for further analysis.

3.4.5.2 The synthesis and characterisation of the TH compounds.

The compounds were synthesized as per Chapter 2. Following synthesis, the compound structures were confirmed through many spectroscopic methods.

3.4.5.2.1 Menadione-Amine Backbone

The Electrospray Ionisation -Mass Spectrometer (ESI-MS) had a calculated mass: charge (*m/z*) mass ion peak $[M+H]^+$ of 226.087g/mol with a *m/z* of 226.220 found for the TH1 amine backbone structure seen in Figure 3.17.

The Proton Non-Magnetic Resonance (^{1}H NMR) determined the compound structure through the determination of the number protons (hydrogens) present, their nearest proton neighbours, and their location in the compound. This confirms the compound backbone has been achieved. ^{1}H NMR (500 MHz, $CDCl_3$): δ 8.07 (1H, dd, *J* = 8, 1 H-z, **H8**), 8.00 (1H, dd, *J* = 7.5, 1 Hz, **H5**), 7.68 (1H, td, *J* = 7.5, 1.5 Hz, **H7**), 7.59 (1H, td, *J* = 8, 1.5 Hz, **H6**), 5.76 (1H, bs, N**H**), 4.27 (2H, dd, *J* = 6.5, 2.5 Hz, **H12**), 2.33 (1H, t, *J* = 2.5 Hz, **H14**), 2.27 (3H, s, **H11**). The ^{1}H NMR is found in Figure 3.18.

The Carbon-13 NMR (^{13}C NMR) determines the placement of the carbons present in the compound, with signals indicating the number of carbons present, their number of nearest neighbours and also the location of the carbons within the compound. ^{13}C NMR (125 MHz, $CDCl_3$): δ 184.1 (**C1**), 182.3 (**C4**), 145.6 (**C3**), 134.5 (**C7**), 133.3 (**C9**), 132.4 (**C6**), 130.5 (**C10**), 126.5 (**C8**), 126.3 (**C7**), 115.6 (**C2**), 80.2 (**C13**), 73.3 (**C14**), 35.4 (**C12**), 11.1 (**C11**). This technique confirms the structure required, as seen in Figure 3.19.

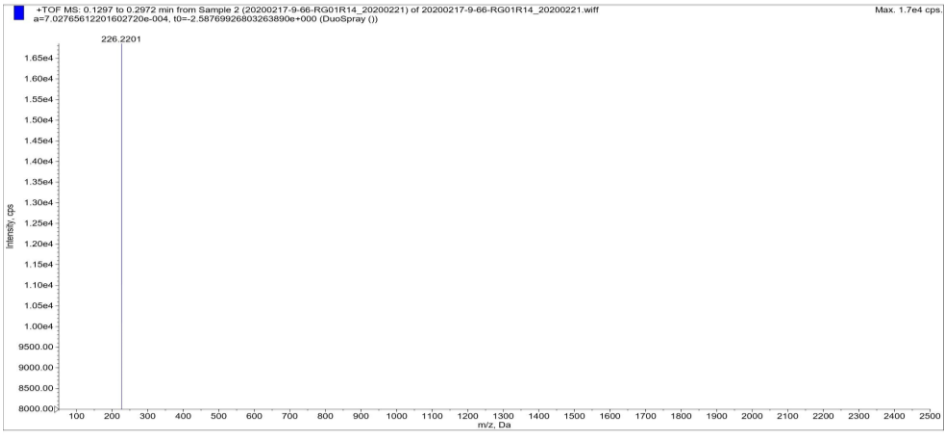

Figure 3. 17: Mass Spectrum of the glucose Amine compound backbone: ESI-MS, m/z: calculated, $[M+H]^+$ 226.087; found 226.220.

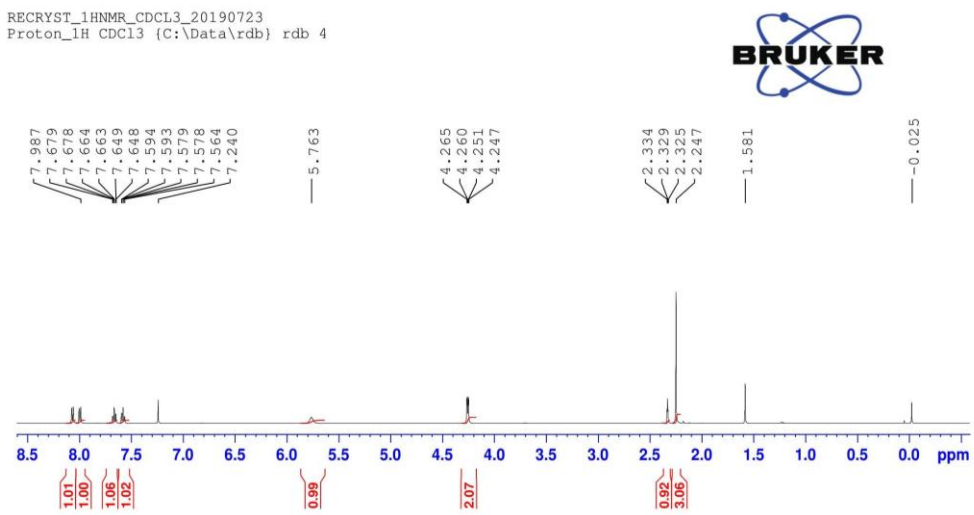

Figure 3. 18: The Proton NMR of the Menadione-Amine backbone : ^{1}H NMR (500 MHz, CDCl3): δ 8.07 (1H, dd, J = 8, 1 H-z, H8), 8.00 (1H, dd, J = 7.5, 1 Hz, H5), 7.68 (1H, td, J = 7.5, 1.5 Hz, H7), 7.59 (1H, td, J = 8, 1.5 Hz, H6), 5.76 (1H, bs, NH), 4.27 (2H, dd, J = 6.5, 2.5 Hz, H12), 2.33 (1H, t, J = 2.5 Hz, H14),2

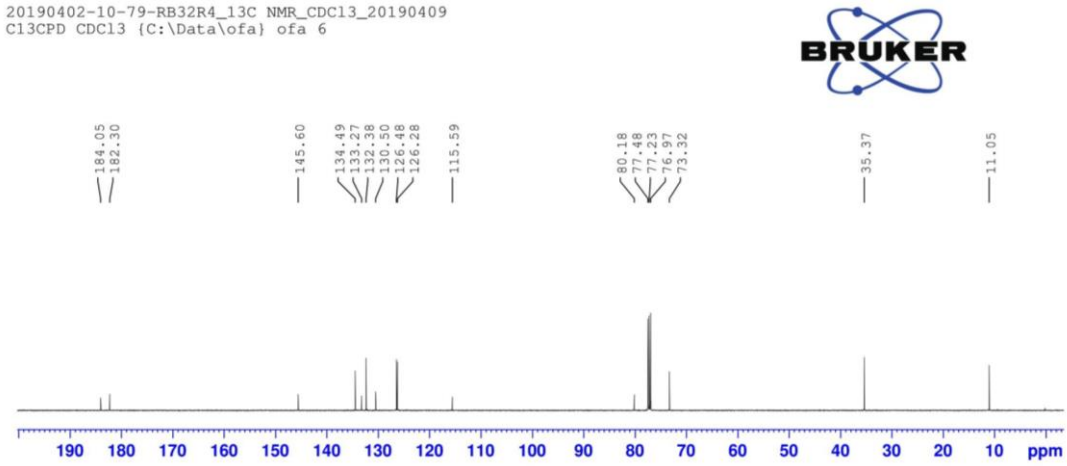

Figure 3. 19: The Carbon NMR of the Menadione-amine backbone. ^{13}C NMR (125 MHz, CDCl3): δ 184.1 (C1), 182.3 (C4), 145.6 (C3), 134.5 (C7), 133.3 (C9), 132.4 (C6), 130.5 (C10), 126.5 (C8), 126.3 (C7), 115.6 (C2), 80.2 (C13), 73.3 (C14), 35.4 (C12), 11.1 (C11).

3.4.5.2.2 Menadione-amine-glucose (Trojan Horse 1)

The Electrospray Ionisation -Mass Spectrometer (ESI-MS) had a calculated mass: charge (*m/z*) mass ion peak $[M+H]^+$ of 431.1567g/mol with a *m/z* of 431.1734 found for the TH1 structure seen in Figure 3.20.

The Proton Non-Magnetic Resonance (^{1}H NMR) determined the compound structure through the determination of the number protons (hydrogens) present, their nearest proton neighbour and their location in the compound. This confirms the compound backbone has been achieved. ^{1}H NMR (500 MHz, D_2O): δ 8.18 (1H, s, **H14**), 7.32 (4H, m, **H5,6,7,8**), 5.76 (1H, d, *J* = 9 Hz, **H15**), 4.58 (2H, s, **H12**), 4.05 (1H, t, *J* = 9 Hz, **H16**), 3.90 (1H, d, *J* = 10.5 Hz, **H20**), 3.79 (3H, m, **H17, H19, H20**), 1.60 (3H, s, **H11**). The ^{1}H NMR is Figure 3.21.

The Carbon-13 NMR (^{13}C NMR) determines the placement of the carbons present in the compound, with signals indicating the number of carbons present, their number of nearest neighbours and also the location of the carbons within the compound. ^{13}C NMR (125 MHz, D_2O): δ 183.5 (**C1**), 181.5 (**C4**), 146.5 (**C13**), 146.3 (**C3**), 134.6 (**C6**), 132.3 (**C7**), 131.7 (**C9**), 129.2 (**C10**), 125.7 (**C5**), 125.2 (**C8**), 123.1 (**C14**), 112.2 (**C2**), 87.5 (**C15**), 78.9 (**C19**), 76.0 (**C17**), 72.3 (**C16**), 68.9 (**C18**), 60.4 (**C20**), 39.6 (**C12**), 9.8 (**C11**). This technique confirms the structure required, as seen in Figure 3.22.

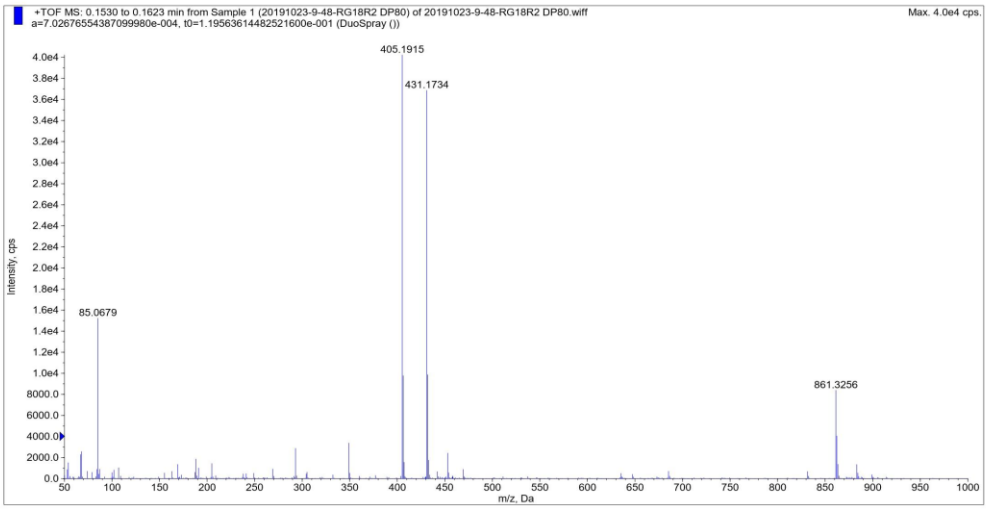

Figure 3. 20: ESI-MS of trojan horse compound 1: m/z: calculated, $[M+H]^+$ 431.1567; found 431.1734.

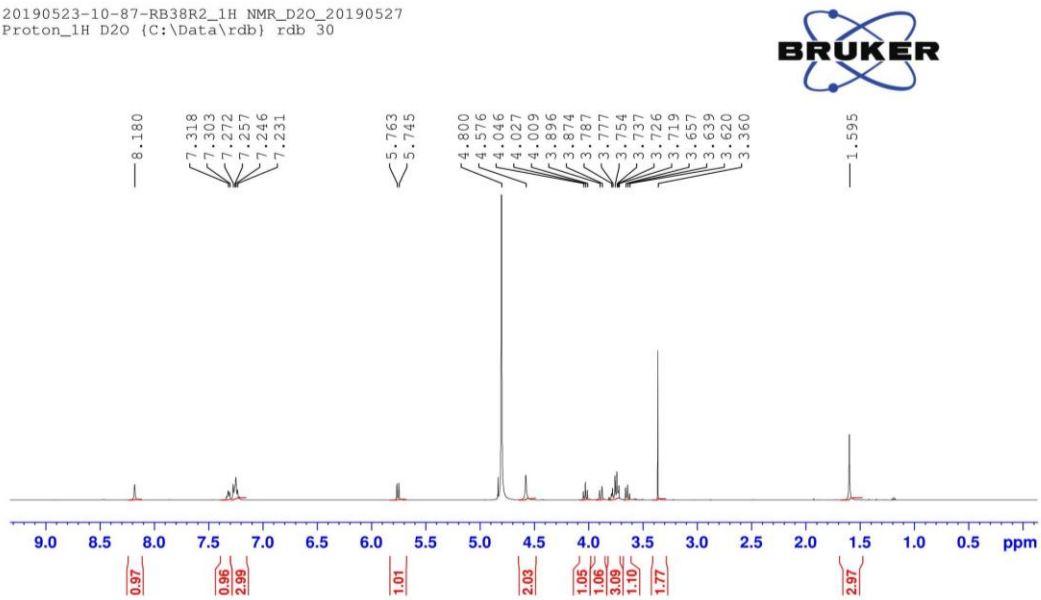

Figure 3. 21: ^{1}H NMR (500 MHz, D2O): δ 8.18 (1H, s, H14), 7.32 (4H, m, H5,6,7,8), 5.76 (1H, d, J = 9 Hz, H15), 4.58 (2H, s, H12), 4.05 (1H, t, J = 9 Hz, H16), 3.90 (1H, d, J = 10.5 Hz, H20), 3.79 (3H, m, H17, H19, H20), 1.60 (3H, s, H11).

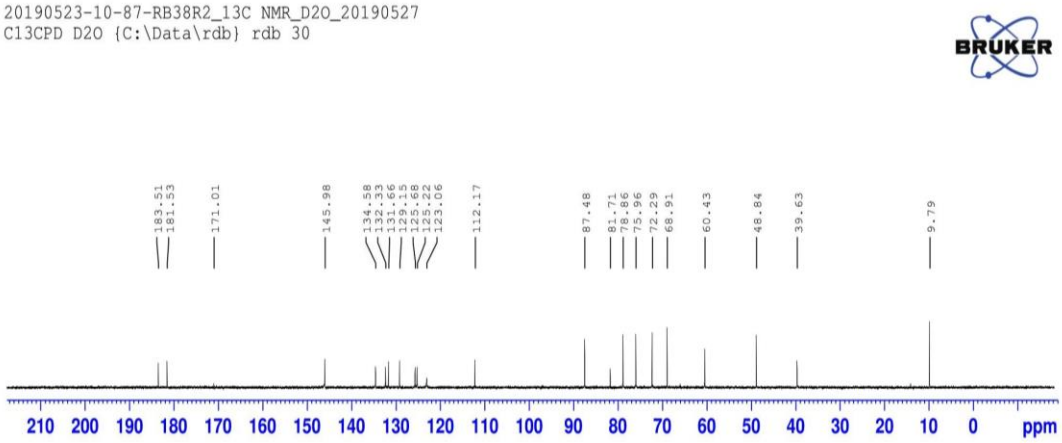

*Figure 3. 22: ^{13}C NMR (125 MHz, D_2O): δ 183.5 (**C1**), 181.5 (**C4**), 146.5 (**C13**), 146.3 (**C3**), 134.6 (**C6**), 132.3 (**C7**), 131.7 (**C9**), 129.2 (**C10**), 125.7 (**C5**), 125.2 (**C8**), 123.1 (**C14**), 112.2 (**C2**), 87.5 (**C15**), 78.9 (**C19**), 76.0 (**C17**), 72.3 (**C16**), 68.9 (**C18**), 60.4 (**C20**), 39.6 (**C12**), 9.8 (**C11**).*

3.4.5.2.3 Menadione-alkyl

Making the backbone of TH4

The ESI-MS had a calculated *m/z* mass ion peak $[M+H]^+$ of 239.1072g/mol with a *m/z* of 239.3654 found for the Menadione-alkyl structure seen in Figure 3.23.

The Proton Non-Magnetic Resonance (^{1}H NMR) Figure 3.24, determined the compound structure through the determination of the number protons (hydrogens) present, their nearest proton neighbours, and their location in the compound. This confirms the compound backbone has been achieved. ^{1}H NMR (500 MHz, $CDCl_3$): δ 8.06 (2H, t, *J* = 3.25 Hz, **Ar-H**),7.69 (2H, t, *J* = 4.25 Hz, **Ar-H**), 2.77 (2H, t, *J* = 8 Hz, **H12**), 2.31 (2H, td, *J* = 6.75 Hz, **H14**), 2.21 (3H, s, **H11**), 2.00 (1H, s, **H16**), 1.74 (2H, p, *J* = 7.38 Hz, **H13**).

The Carbon-13 NMR (^{13}C NMR) determines the placement of the carbons present in the compound, with signals indicating the number of carbons present, their number of nearest neighbours and also the location of the carbons within the compound. ^{13}C NMR (125 MHz, $CDCl_3$): δ 185.4 (**C1/C4),** 184.8 (**C1/C4**), 146.6 (**C3**), 144.0 (**C2**), 133.6 (**C5,C8**), 132.3 (**C9,C10**), 126.5 (**C6/C7**), 126.4 (**C6/C7**), 83.9 (**C15**), 69.3 (**C16**), 27.6 (**C13**), 26.4 (**C12**), 18.9 (**C14**), 12.9 (**C11**).This technique confirms the structure required, as seen in Figure 3.25.

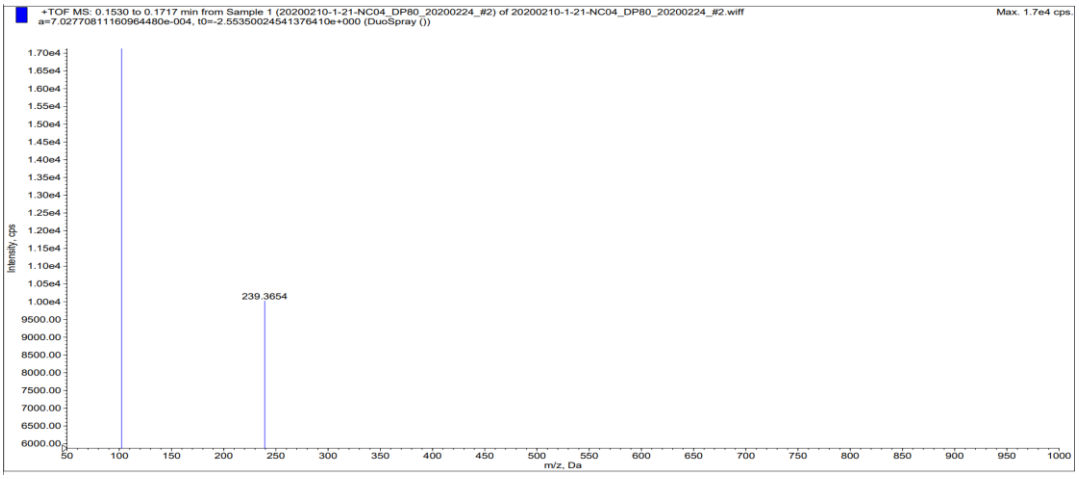

Figure 3. 23: ESI-MS , m/z: calculated, $[M+H]^+$ 239.1072; found 239.3654.

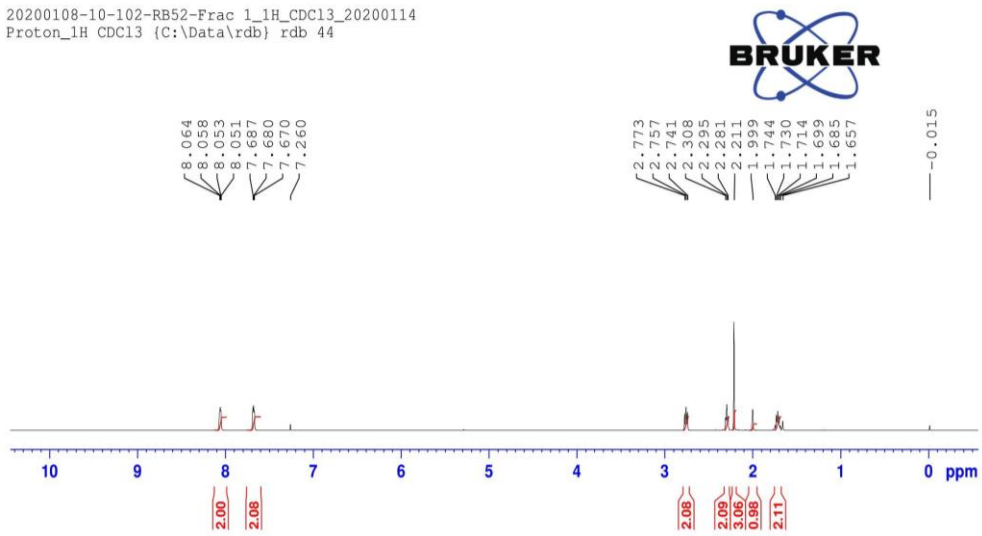

*Figure 3. 24: ^{1}H NMR (500 MHz, $CDCl_3$): δ 8.06 (2H, t, J = 3.25 Hz, **Ar-H**),7.69 (2H, t, J = 4.25 Hz, **Ar-H**), 2.77 (2H, t, J = 8 Hz, **H12**), 2.31 (2H, td, J = 6.75 Hz, **H14**), 2.21 (3H, s, **H11**), 2.00 (1H, s, **H16**), 1.74 (2H, p, J = 7.38 Hz, **H13**).*

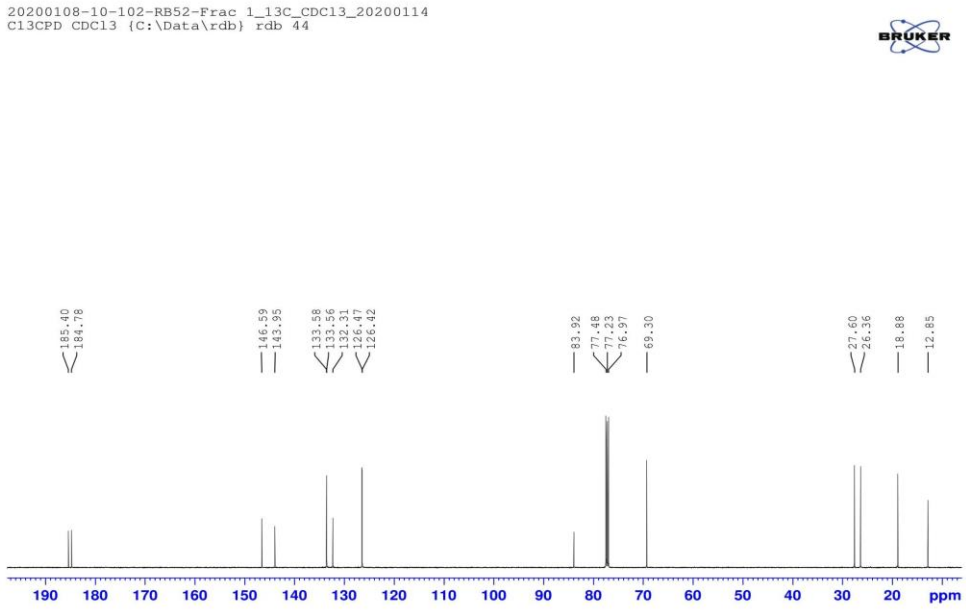

*Figure 3. 25: ^{13}C NMR (125 MHz, $CDCl_3$): δ 185.4 (**C1/C4**), 184.8 (**C1/C4**), 146.6 (**C3**), 144.0 (**C2**), 133.6 (**C5,C8**), 132.3 (**C9,C10**), 126.5 (**C6/C7**), 126.4 (**C6/C7**), 83.9 (**C15**), 69.3 (**C16**), 27.6 (**C13**), 26.4 (**C12**), 18.9 (**C14**), 12.9 (**C11**).*

3.4.5.2.4 Menadione-alkyl-glucose -Trojan Horse 4

The ESI-MS had a calculated *m/z* mass ion peak $[M+H]^+$ of 444.1771g/mol with a *m/z* of 444.2313g/mol found for the Menadione-alkyl-glucose structure seen in Figure 3.26.

The Proton Non-Magnetic Resonance (^{1}H NMR) Figure 3.27, determined the compound structure through the determination of the number protons (hydrogens) present, their nearest proton neighbours, and their location in the compound. This confirms the compound backbone has been achieved. ^{1}H NMR (500 MHz, DMSO): δ 8.07 (1H, s, **H16**), 8.01 (2H, q, *J* = 3.75 Hz, **H5,8**), 7.84 (2H, m, **H6,7**), 5.47 (1H, d, *J* = 8.5 Hz, **H17**), 5.34 (1H, d, *J* = 6 Hz, **OH**), 5.30 (1H, bs, **OH**), 5.16 (1H, d, *J* = 4.5 Hz, **OH**), 4.62 (1H, t, *J* = 5 Hz, **OH**), 3.73 (2H, m, **Sugar-H**, **H22**), 3.43 (2H, m, **Sugar-H**, **H22**), Obscured (1H, **Sugar-H**), 3.21 (1H, d, *J* = 4.5 Hz, **Sugar-H**), 2.73 (2H, t, *J* = 7.75 Hz, **H12**), 2.68 (2H, t, *J* = 7.75 Hz, **H14**), 2.11 (3H, s, **H11**), 1.79 (3H, qui, *J* = 7.5 Hz, **H13**).

The Carbon-13 NMR (^{13}C NMR) determines the placement of the carbons present in the compound, with signals indicating the number of carbons present, their number of nearest neighbours and the location of the carbons within the compound. ^{v13}C NMR (125 MHz, DMSO): δ 184.6 (**Carbonyl**), 184.1 (**Carbonyl**), 146.4 (**Ar-C**), 146.1 (**Ar-C**), 143.3 (**Ar-C**), 133.8 (**C5,8**), 131.7 (**Ar-C**), 131.6 (**Ar-C**), 125.9 (**C6/7**), 125.8 (**C6/7**), 121.0 (**C16**), 87.4 (**C17**), 79.9 (**Sugar-C**), 77.0 (**Sugar-C**), 72.1 (**Sugar-C**), 69.6 (**Sugar-C**), 60.8 (**C22**), 27.9 (**C13**), 26.3 (**C14**), 25.2 (**C12**), 12.5 (**C11**). This technique confirms the structure required, as seen in Figure 3.28.

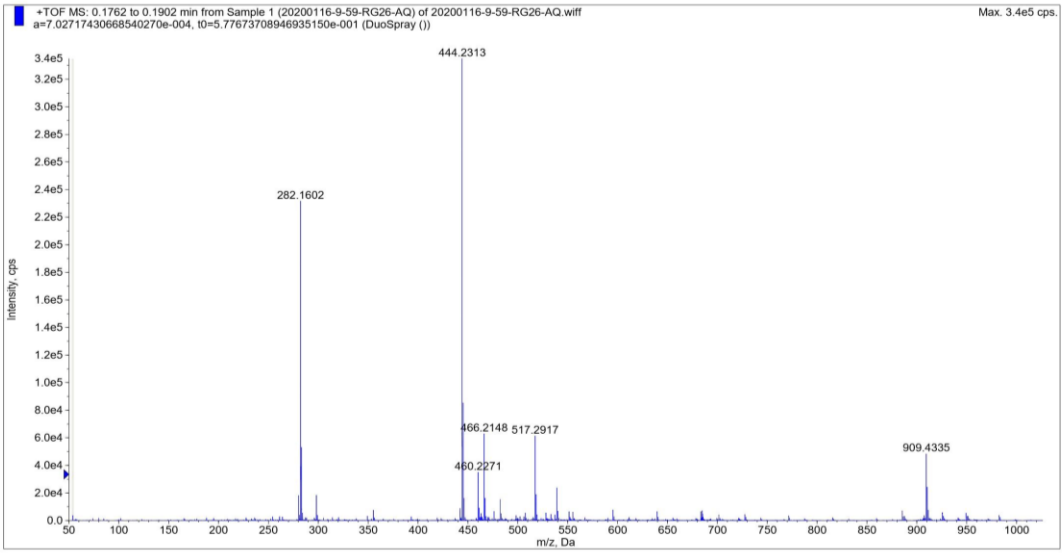

Figure 3. 26: ESI-MS, m/z: calculated, $[M+H]^+$ 444.1771; found 444.2313.

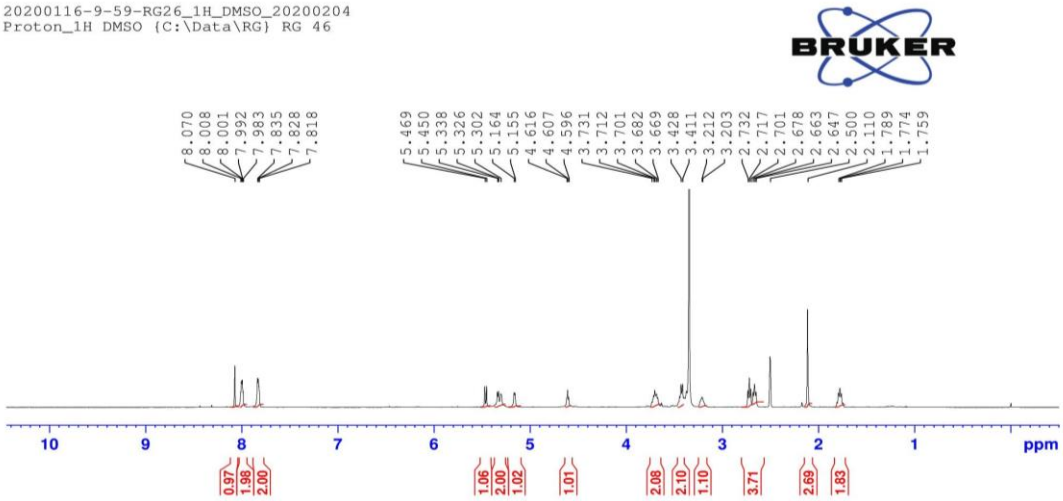

*Figure 3. 27: ^{1}H NMR (500 MHz, DMSO): δ 8.07 (1H, s, **H16**), 8.01 (2H, q, J = 3.75 Hz, **H5,8**), 7.84 (2H, m, **H6,7**), 5.47 (1H, d, J = 8.5 Hz, **H17**), 5.34 (1H, d, J = 6 Hz, **OH**), 5.30 (1H, bs, **OH**), 5.16 (1H, d, J = 4.5 Hz, **OH**), 4.62 (1H, t, J = 5 Hz, **OH**), 3.73 (2H, m, **Sugar-H**, **H22**), 3.43 (2H, m, **Sugar-H**, **H22**), Obscured (1H, **Sugar-H**), 3.21 (1H, d, J = 4.5 Hz, **Sugar-H**), 2.73 (2H, t, J = 7.75 Hz, **H12**), 2.68 (2H, t, J = 7.75 Hz, **H14**), 2.11 (3H, s, **H11**), 1.79 (3H, qui, J = 7.5 Hz, **H13**).*

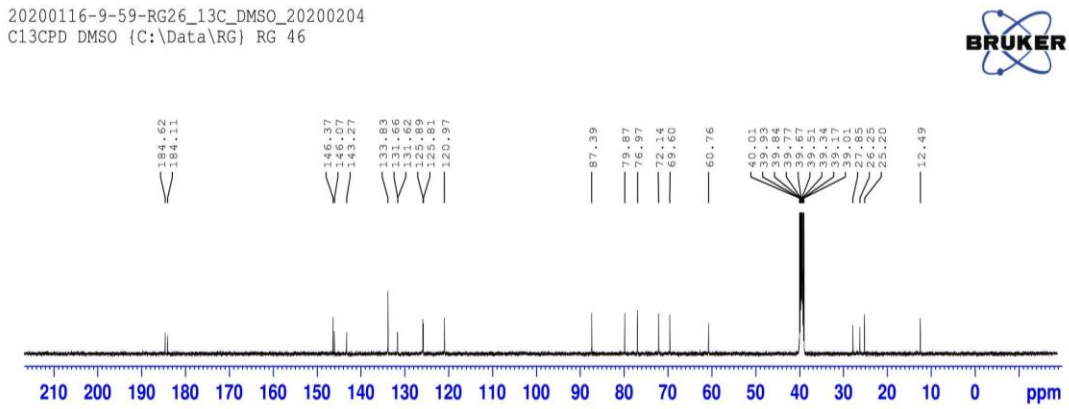

*Figure 3. 28: ^{13}C NMR (125 MHz, DMSO): δ 184.6 (**Carbonyl**), 184.1 (**Carbonyl**), 146.4 (**Ar-C**), 146.1 (**Ar-C**), 143.3 (**Ar-C**), 133.8 (**C5,8**), 131.7 (**Ar-C**), 131.6 (**Ar-C**), 125.9 (**C6/7**), 125.8 (**C6/7**), 121.0 (**C16**), 87.4 (**C17**), 79.9 (**Sugar-C**), 77.0 (**Sugar-C**), 72.1 (**Sugar-C**), 69.6 (**Sugar-C**), 60.8 (**C22**), 27.9 (**C13**), 26.3 (**C14**), 25.2 (**C12**), 12.5 (**C11**).*

3.4.5.2.5 Menadione-amine-Azido hexanoic acid – Trojan Horse 6

The ESI-MS had a calculated *m/z* mass ion peak $[M+H]^+$ of 383.1719g/mol with a *m/z* of 383.1982g/mol found for the Menadione-alkyl-glucose structure seen in Figure 3.29.

The Proton Non-Magnetic Resonance (^{1}H NMR) Figure 3.30, determined the compound structure through the determination of the number protons (hydrogens) present, their nearest proton neighbours, and their location in the compound. This confirms the compound backbone has been achieved. ^{1}H NMR (500 MHz, DMSO): δ 7.98 (1H, s, **H14**), 7.93 (2H, d, *J* = 8 Hz, **H5/8**), 78.79 (1H, t, *J* = 7.5 Hz, **H6/7**), 7.71 (1H, t, *J* = 7.5 Hz, **H6/7**), 7.05 (1H, t, *J* = 7 Hz, **NH**), 4.81 (2H, d, *J* = 6.5 Hz, **H12**), 4.31 (2H, t, *J* = 7 Hz, **H15**), 2.16 (2H, t, *J* = 7.5 Hz, **H19**), 2.08 (3H, s, **H11**), 1.79 (2H, qui, *J* = 7.38 Hz, **H16**), 1.50 (2H, qui, *J* = 7.5 Hz, **H18**), 1.21 (2H, qui, *J* = 7.63 Hz, **H17**).

The Carbon-13 NMR (^{13}C NMR) determines the placement of the carbons present in the compound, with signals indicating the number of carbons present, their number of nearest neighbours and the location of the carbons within the compound. ^{13}C NMR (125 MHz, DMSO): δ 181.2 (**Carbonyl**), 180.9 (**Carbonyl**), 173.3 (**C20**), 145.4 (**Ar-C**), 144.7 (**Ar-C**), 133.4 (**C6/7**), 131.6 (**Ar-C**), 131.2 (**C6/7**), 129.4 (**Ar-C**), 124.6 (**C5/8**), 124.4 (**C5/8**), 121.5 (**C14**), 111.1 (**Ar-C**), 48.2 (**C15**), obscured (**C12**), 32.4 (**C19**), 28.5 (**C16**), 24.4 (**C17**), 22.8 (**C18**), 9.4 (**C11**). This technique confirms the structure required, as seen in Figure 3.31.

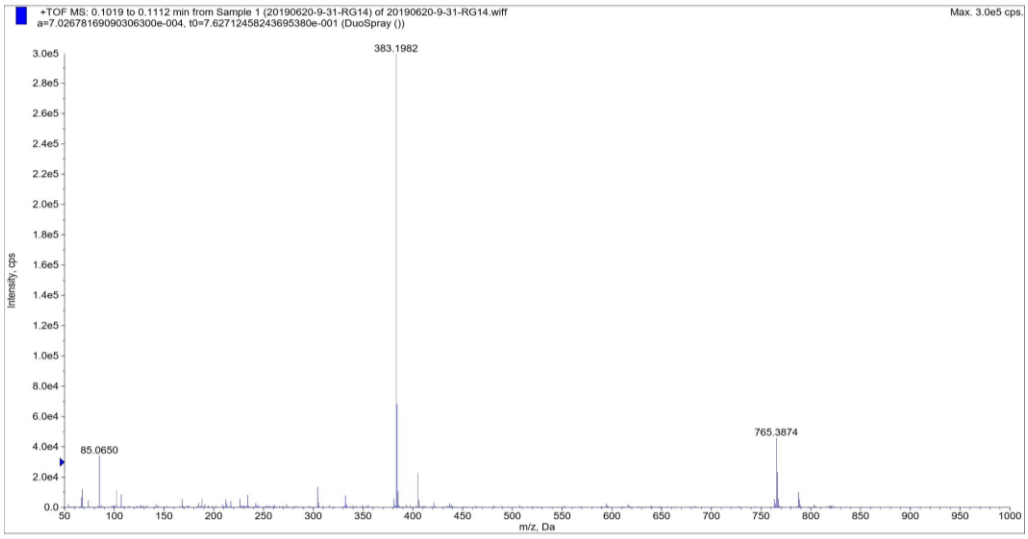

Figure 3. 29: ESI-MS , m/z: calculated, $[M+H]^+$ 383.1719; found, 383.1982

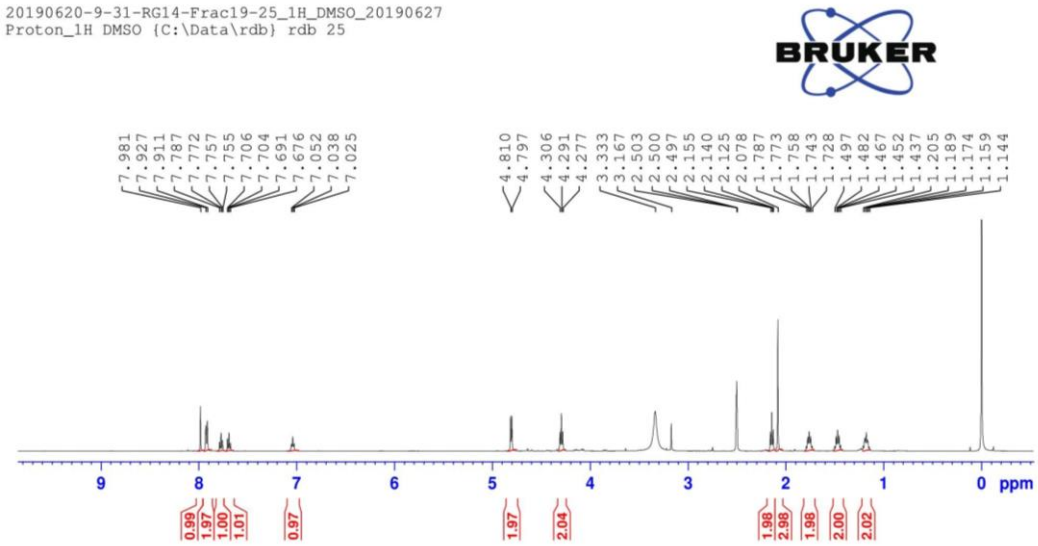

*Figure 3. 30: ^{1}H NMR (500 MHz, DMSO): δ 7.98 (1H, s, **H14**), 7.93 (2H, d, J = 8 Hz, **H5/8**), 78.79 (1H, t, J = 7.5 Hz, **H6/7**), 7.71 (1H, t, J = 7.5 Hz, **H6/7**), 7.05 (1H, t, J = 7 Hz, **NH**), 4.81 (2H, d, J = 6.5 Hz, **H12**), 4.31 (2H, t, J = 7 Hz, **H15**), 2.16 (2H, t, J = 7.5 Hz, **H19**), 2.08 (3H, s, **H11**), 1.79 (2H, qui, J = 7.38 Hz, **H16**), 1.50 (2H, qui, J = 7.5 Hz, **H18**), 1.21 (2H, qui, J = 7.63 Hz, **H17**).*

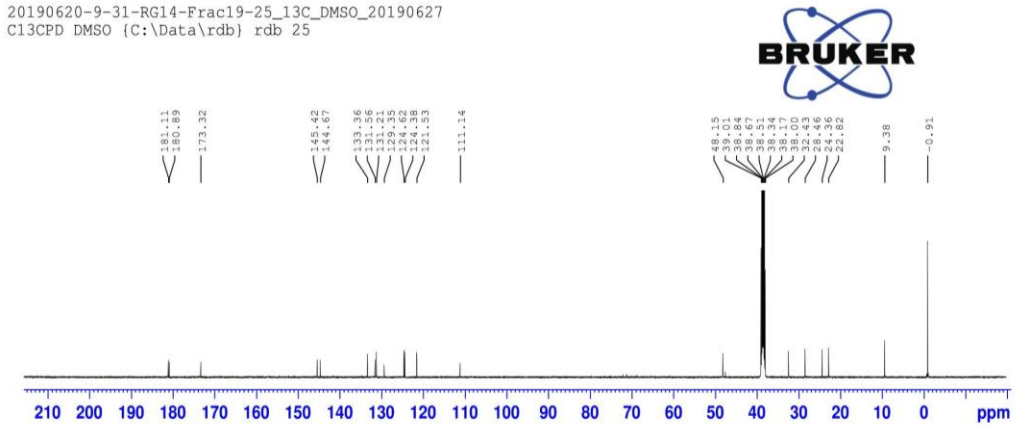

*Figure 3. 31: ^{13}C NMR (125 MHz, DMSO): δ 181.2 (**Carbonyl**), 180.9 (**Carbonyl**), 173.3 (**C20**), 145.4 (**Ar-C**), 144.7 (**Ar-C**), 133.4 (**C6/7**), 131.6 (**Ar-C**), 131.2 (**C6/7**), 129.4 (**Ar-C**), 124.6 (**C5/8**), 124.4 (**C5/8**), 121.5 (**C14**), 111.1 (**Ar-C**), 48.2 (**C15**), obscured (**C12**), 32.4 (**C19**), 28.5 (**C16**), 24.4 (**C17**), 22.8 (**C18**), 9.4 (**C11**).*

3.4.6 Trojan Horse Compound 4 (TH4)

Trojan Horse 4 is a Menadione-alkyl-glucose compound, as detailed in Chapter 2.

3.4.6.1 The effect of the varying glucose conditions on the IC_{50} values of TH4 in the PNT1a cell line.

PNT1a cells under glucose starvation treated with TH4 resulted in IC_{50} values of 27.7µM under 24hrs incubation and 25.9µM under 48hrs incubation. Under normoglycemia of 5.5mM glucose and TH4 treatment, cells presented with IC_{50} values of 323.8µM after 24hrs and 301.2µM after 48hrs. Finally, PNT1a cells treated with TH4 under 11mM glucose media resulted in IC_{50} values of 338.2µM after 24hrs and 305.4µM after 48hrs. The results for all IC_{50} determinations are summarised in Table 3.16.

Table 3.16: IC_{50} values for TH4 treated PNT1a cells under 3 glucose RPMI conditions and 3 time points

Media glucose concentration	24 hours	48 hours
	IC_{50} (µM)	**IC_{50} (µM)**
0mM	27.7µM	25.9µM
5.5mM	323.8µM	301.2µM
11mM	338.2µM	305.4µM

An overlay of the 3 response curves for 24hr treatments in PNT1a cells is shown in Figure 3.32, depicting the effect of varying glucose conditions on the IC_{50} values of TH4.

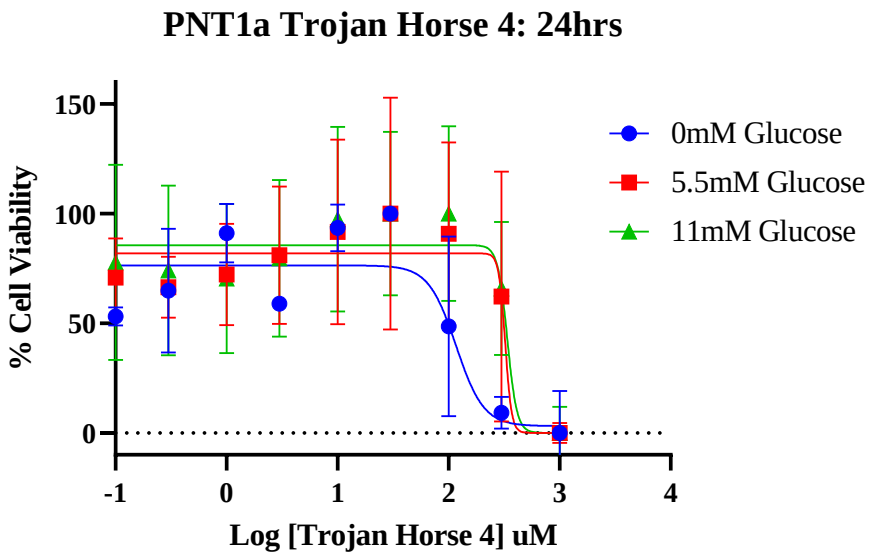

Figure 3. 32: Effect of TH4 on PNT1a cell line viability cells under 3 different glucose RPMI conditions at 24 hours. The data shown is expressed as mean ± SEM. Each experiment is in technical replicate of 3 and biological replicate of 3.

3.4.6.2 The effect of the varying glucose conditions on the IC_{50} values of TH4 in the LNCaP cell line.

LNCaP cells under glucose starvation treated with TH4 resulted in IC_{50} values of 82.4µM under 24hrs incubation and 90.1µM under 48hrs incubation. Under normoglycemia of 5.5mM glucose and TH4 treatment, cells presented with IC_{50} values of 179.6µM after 24hrs and 72.8µM after 48hrs. Finally, LNCaP cells treated with TH1 under 11mM glucose media resulted in IC_{50} values of 86.6µM at 24hrs and 100.6µM after 48hrs. The results for all IC_{50} determinations are summarised in Table 3.17.

Table 3.17: IC_{50} values for TH4 treated LNCaP cells under 3 glucose RPMI conditions and 3 time points

Media glucose concentration	24 hours	48 hours
	IC_{50} (µM)	IC_{50} (µM)
0mM	82.4 µM	90.1µM
5.5mM	79.6 µM	72.8µM
11mM	86.6 µM	100.6µM

An overlay of the 3 response curves for 24hr treatments in LNCaP cells is shown in Figure 3.33, depicting the effect of varying glucose conditions on the IC_{50} values of TH4.

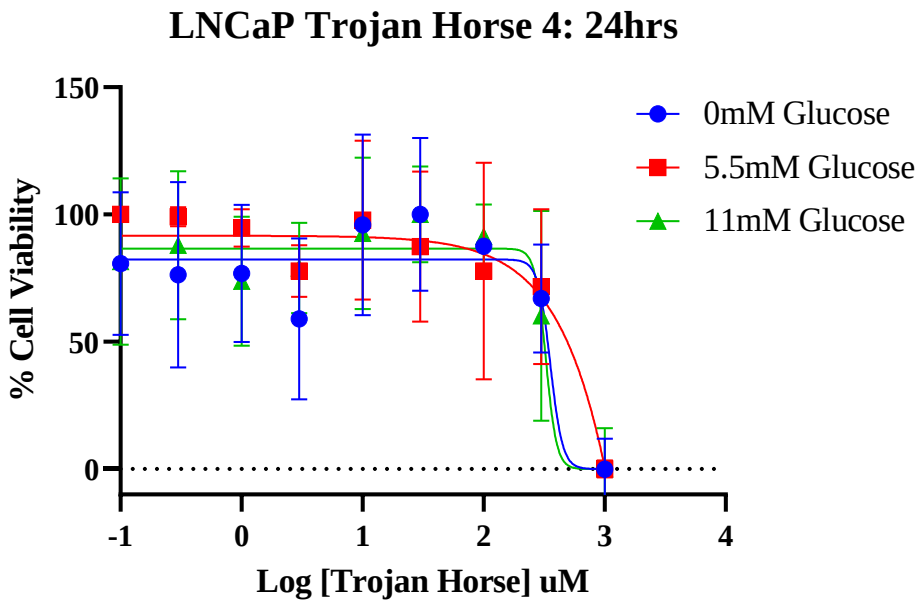

Figure 3. 33: Effect of TH4 on LNCaP cell line viability cells under 3 different glucose RPMI conditions at 24 hours. The data shown is expressed as mean ± SEM. Each experiment is in technical replicate of 3 and biological replicate of 3.

3.4.6.3 The effect of the varying glucose conditions on the IC_{50} values of TH4 in the PC3 cell line.

PC3 cells under glucose starvation treated with TH4 resulted in IC_{50} values of 317.5µM under 24hrs incubation and 512.9µM under 48hrs incubation. Under normoglycemia of 5.5mM glucose and TH4 treatment, cells presented with IC_{50} values of 1537µM after 24hrs and 869.7µM after 48hrs. Finally, cells treated with TH4 under 11mM glucose media resulted in IC_{50} values of 2085µM after 24hrs and 1137.0µM after 48hrs. The results for all IC_{50} determinations are summarised in Table 3.18.

Table 3.18: IC_{50} values for TH4 treated PC3 cells under 3 glucose RPMI conditions and 3 time points

Media glucose concentration	24 hours	48 hours
	IC_{50} (µM)	**IC_{50} (µM)**
0mM	317.5µM	512.9µM
5.5mM	1537.0µM	869.7µM
11mM	2085.0µM	1137.0µM

An overlay of the 3 response curves for 24hr treatments in PC3 cells is shown in Figure 3.34 depicting the effect of varying glucose conditions on the IC_{50} values of TH4.

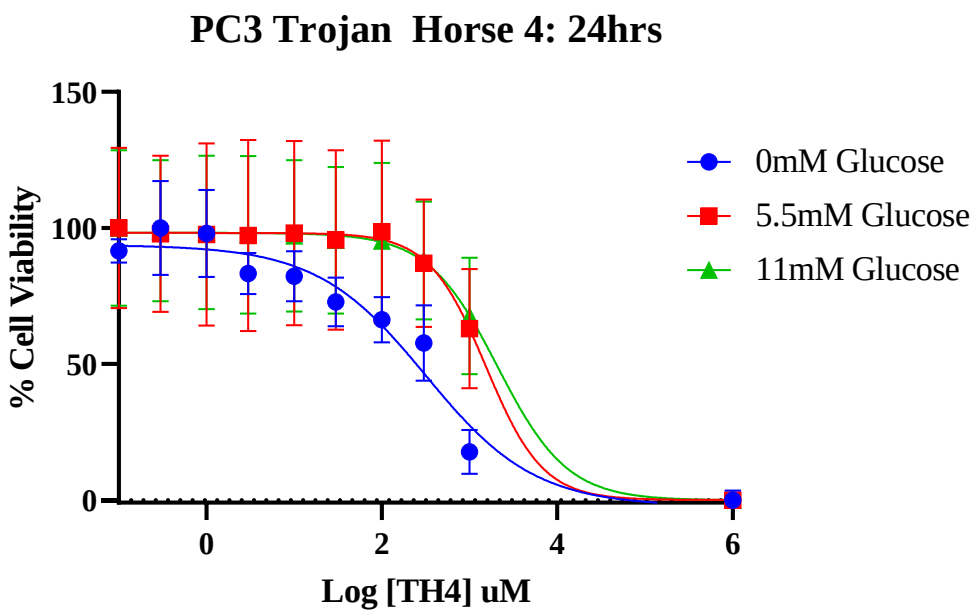

Figure 3. 34: Effect of TH4 on PC3 cell line viability cells under 3 different glucose RPMI conditions at 24 hours. The data shown is expressed as mean ± SEM. Each experiment is in technical replicate of 3 and biological replicate.

3.4.6.4 The effect of the varying glucose conditions on the IC_{50} values of TH4 in the Du145 cell line.

Du145 cells under glucose starvation treated with TH4 resulted in IC_{50} values of 103.6µM under 24hrs incubation and 133.7µM under 48hrs incubation. Under normoglycemia of 5.5mM glucose and TH4 treatment, cells presented with IC_{50} values of 162.8µM after 24hrs and 163.8µM after 48hrs. Finally, Du145 cells treated with TH4 under 11mM glucose media resulted in IC_{50} values of 241.6µM following 24hrs treatment and 194.1µM after 48hrs. The results for all IC_{50} determinations are summarised in Table 3.19.

Table 3.19: IC_{50} values for TH4 treated Du145 cells under 3 glucose RPMI conditions and 3 time points

Media glucose concentration	24 hours	48 hours
	IC_{50} (µM)	**IC_{50} (µM)**
0mM	103.6µM	133.7µM
5.5mM	162.8µM	163.8µM
11mM	241.6µM	194.1µM

An overlay of the 3 response curves for 24hr treatments in Du145 cells is shown in Figure 3.35 depicting the effect of varying glucose conditions on the IC_{50} values of TH4.

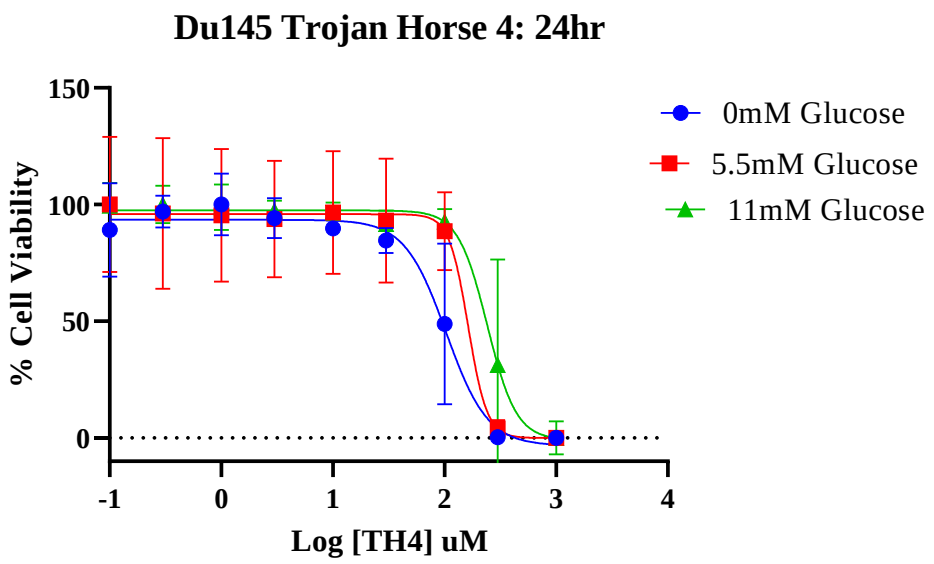

Figure 3. 35: Effect of TH4 on Du145 cell line viability cells under 3 different glucose RPMI conditions at 24 hours. The data shown is expressed as mean ± SEM. Each experiment is in technical replicate of 3 and biological replicate of 3.

3.4.7 Trojan Horse Compound 6 (TH6)

Trojan Horse 6 is a Menadione-amine-fatty acid compound, as detailed in Chapter 2.

3.4.7.1 The effect of the varying glucose conditions on the IC50 values of TH6 in the PNT1a cell line.

PNT1a cells under glucose starvation treated with TH6 resulted in IC_{50} values 92.8µM under 24hrs incubation. Under normoglycemia of 5.5mM glucose and TH6 treatment, cells presented with IC_{50} values of 341.0µM after 24hrs. Finally, PNT1a cells treated with TH6 under 11mM glucose media resulted in IC_{50} values of 315.2µM after 24hrs. The results for all IC_{50} determinations are summarised in Table 3.20.

Table 3.20: IC_{50} values for TH6 treated PNT1a cells under 3 glucose RPMI conditions and 3 time points

Media glucose concentration	24 hours
	IC_{50} (µM)
0mM	92.8µM
5.5mM	341.0µM
11mM	315.2µM

An overlay of the 3 response curves for 24hr treatments in PNT1a cells is shown in Figure 3.36, depicting the effect of varying glucose conditions on the IC_{50} values of TH6.

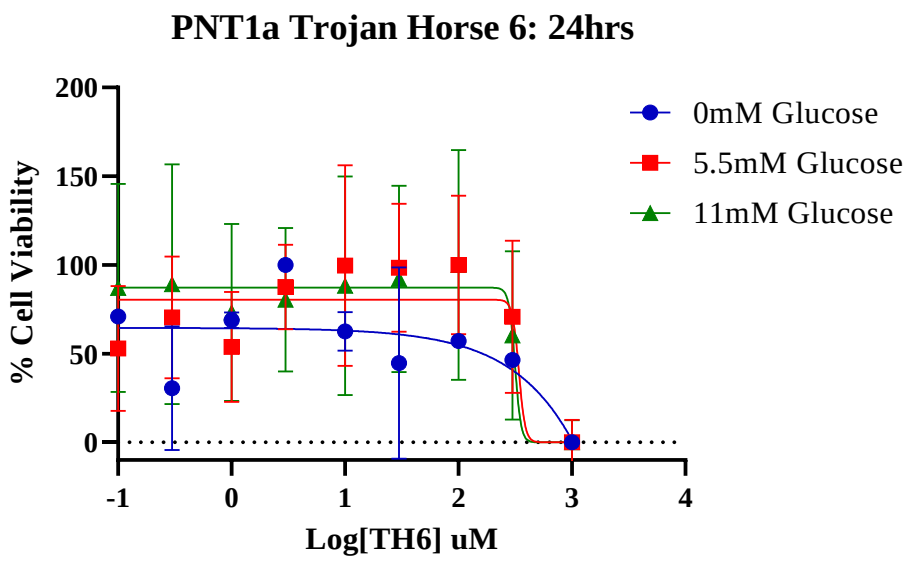

Figure 3. 36: Effect of TH6 on PNT1a cell line viability cells under 3 different glucose RPMI conditions at 24 hours. The data shown is expressed as mean ± SEM. Each experiment is in technical replicate of 3 and biological replicate of 3.

3.4.7.2 The effect of the varying glucose conditions on the IC_{50} values of TH6 in the LNCaP cell line.

LNCaP cells under glucose starvation treated with TH6 resulted in IC_{50} values of 297.7µM under 24hrs incubation. Under normoglycemia of 5.5mM glucose and TH6 treatment, cells presented with IC_{50} values of 295.7µM after 24hrs. Finally, LNCaP cells treated with TH6 under 11mM glucose media resulted in IC_{50} values of 344.9µM after 24hrs. The results for all IC_{50} determinations are summarised in Table 3.21.

Table 3.21: IC_{50} values for TH6 treated LNCaP cells under 3 glucose RPMI conditions and 3 time points

Media glucose concentration	24 hours
	IC_{50} (µM)
0mM	297.7µM
5.5mM	295.7µM
11mM	344.9µM

An overlay of the 3 response curves for 24hr treatments in LNCaP cells is shown in Figure 3.37, depicting the effect of varying glucose conditions on the IC_{50} values of TH6.

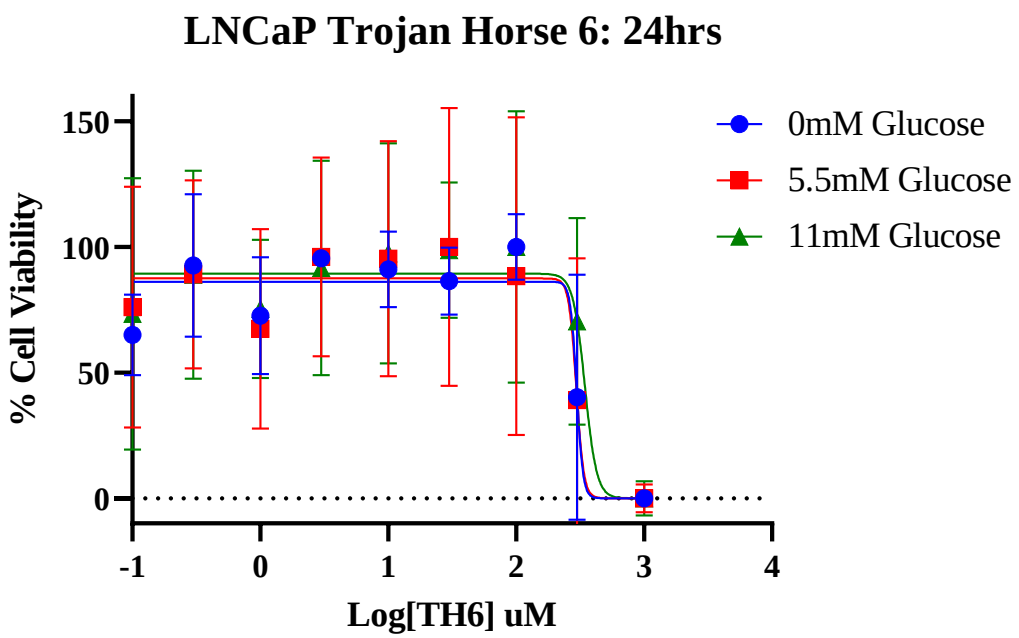

Figure 3. 37: Effect of TH6 on LNCaP cell line viability cells under 3 different glucose RPMI conditions at 24 hours. The data shown is expressed as mean ± SEM. Each experiment is in technical replicate of 3 and biological replicate of 3.

3.4.7.3 The effect of the varying glucose conditions on the IC_{50} values of TH6 in the PC3 cell line.

PC3 cells under glucose starvation treated with TH6 resulted in IC_{50} values of 113.8µM under 24hrs incubation. Under normoglycemia of 5.5mM glucose and TH6 treatment, cells presented with IC_{50} values of 329.8µM after 24hrs. Finally, PC3 cells treated with TH6 under 11mM glucose media resulted in IC_{50} values of 309.9µM after 24hrs. The results for all IC_{50} determinations are summarised in Table 3.22.

Table 3.22: IC_{50} values for TH6 treated PC3 cells under 3 glucose RPMI conditions and 3 time points

Media glucose concentration	24 hours
	IC_{50} (µM)
0mM	113.8µM
5.5mM	326.8µM
11mM	309.9µM

An overlay of the 3 response curves for 24hr treatments in PC3 cells is shown in Figure 3.38 depicting the effect of varying glucose conditions on the IC_{50} values of TH6.

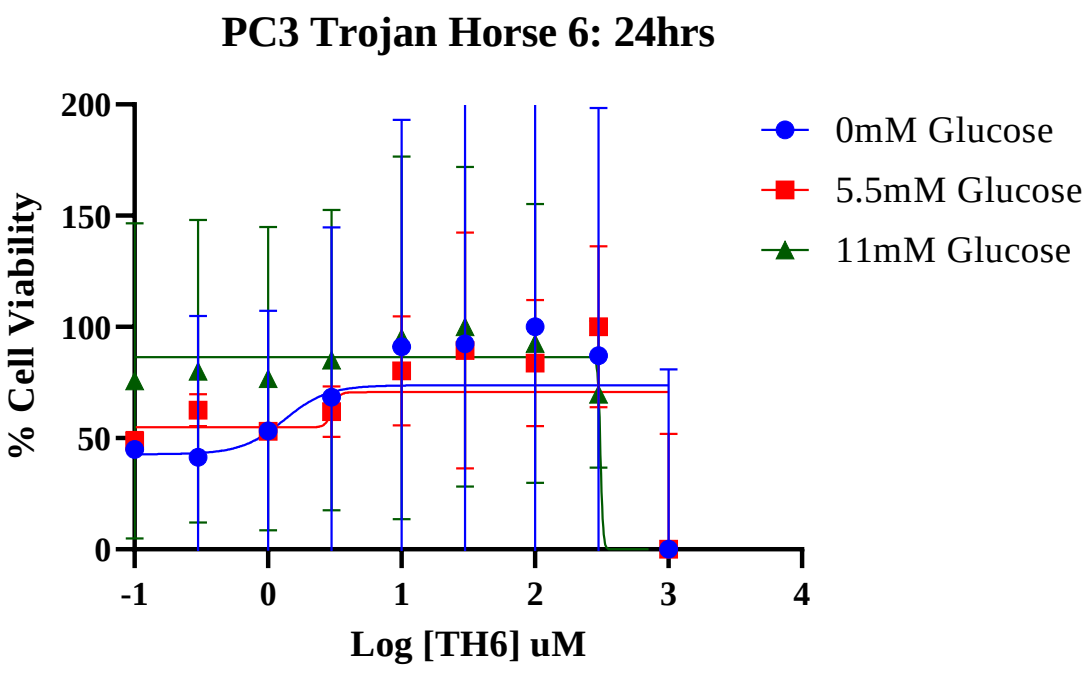

Figure 3. 38: Effect of TH6 on PC3 cell line viability cells under 3 different glucose RPMI conditions at 24 hours. The data shown is expressed as mean ± SEM. Each experiment is in technical replicate of 3 and biological replicate of 3.

3.4.7.4 The effect of the varying glucose conditions on the IC_{50} values of TH6 in the Du145 cell line.

Du145 cells under glucose starvation treated with TH6 resulted in IC_{50} values of 29.9µM under 24hrs incubation. Under normoglycemia of 5.5mM glucose and TH6 treatment, cells presented with IC_{50} values of 305.9µM after 24hrs. Finally, Du145 cells treated with TH6 under 11mM glucose media resulted in IC_{50} values of 317.2µM after 24hrs. The results for all IC_{50} determinations are summarised in Table 3.23.

Table 3.23: IC_{50} values for TH6 treated Du145 cells under 3 glucose RPMI conditions and 3 time points

Media glucose concentration	24 hours
	IC_{50} (µM)
0mM	29.9µM
5.5mM	305.9µM
11mM	317.2µM

An overlay of the 3 response curves for 24hr treatments in Du145 cells is shown in Figure 3.39 depicting the effect of varying glucose conditions on the IC_{50} values of TH6.

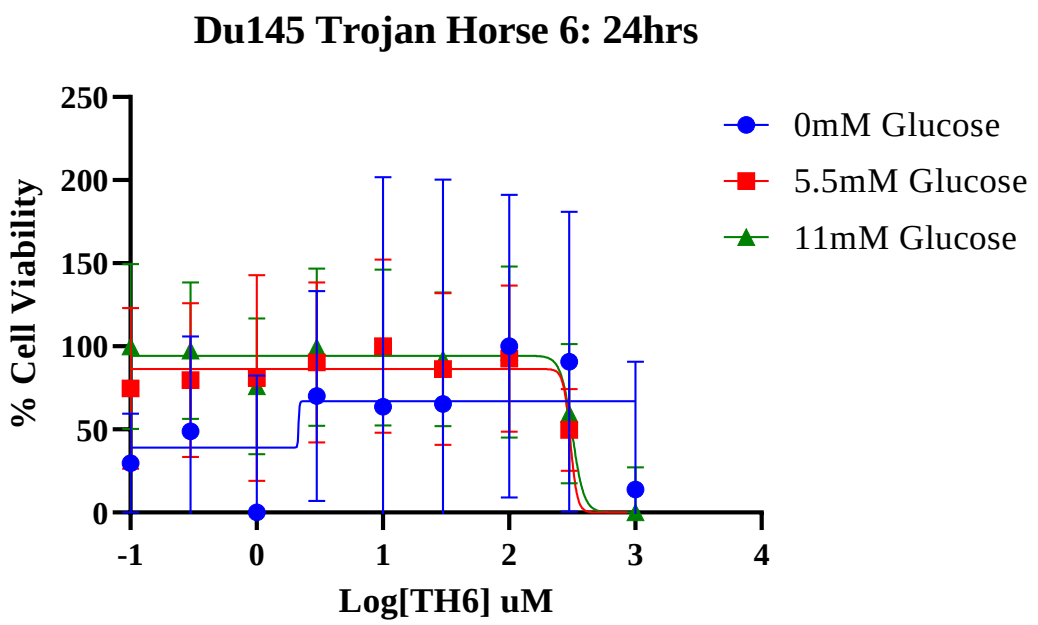

Figure 3.39: Effect of TH6 on Du145 cell line viability cells under 3 different glucose RPMI conditions at 24 hours. The data shown is expressed as mean ± SEM. Each experiment is in technical replicate of 3 and biological replicate of 3.

3.4.7.5 The selectivity of the TH compounds in the LNCaP, PC3 and Du145 cell lines in the zero, 5.5mM and 11mM glucose conditions.

The selectivity index (SI) is a ratio that measures the cytotoxic activity of a compound by dividing the IC_{50} of the non-malignant cells by the IC_{50} of the malignant cells. The higher the SI ratio in *vitro*, the theoretically more effective and safe a drug would be in *vivo*.

The selectivity of TH compounds was calculated to determine the compound with the optimal selectivity towards the killing of the PCa cells.

TH4 has shown greater selectivity than TH1 in all of the PCa cell lines in the zero, 5.5mM and 11mM glucose conditions, with TH6 performing similarly to that of TH4 in the cells across the glucose milieu, as presented in Table 2.21 below.

Table 2.21: The SI of TH1, TH4 and TH6 in the PCa cell lines in the zero, 5.5mM and 11mM glucose conditions.

Cell Line	**zero Glucose**					**5.5mM Glucose**					**11mM Glucose**				
	VC	**K3**	**TH1**	**TH4**	**TH6**	**VC**	**K3**	**TH1**	**TH4**	**TH6**	**VC**	**K3**	**TH1**	**TH4**	**TH6**
LNCaP	0.4	0.4	0.04	0.3	0.3	0.2	0.8	0.4	1.8	1.2	0.1	0.6	0.8	1.8	0.9
PC3	0.8	0.6	N/A	0.09	0.8	0.4	0.9	N/A	0.2	1.0	0.4	0.9	N/A	0.2	1.0
Du145	0.2	1.7	0.3	0.3	3.1	0.3	0.7	0.6	2.0	1.1	3.0	0.8	1.3	1.4	0.99

3.5 Summary of results

Chapter 3 Highlights.
• Vitamin C presents with a glucose dependent cytotoxicity in the cell lines. • Menadione does not present with a glucose dependent cytotoxicity in the cell lines. • TH1 and TH4 present with a glucose dependent cytotoxicity in the cell lines. • All of the cell lines present with an IC_{50} of ~300µM across the three glucose conditions, treated with TH6. • TH4 and TH6 present with an increased SI in LNCaP and Du145 cell lines compared to the Menadione treatment

3.6 Discussion

The TH strategy aims to create a novel treatment that exploits the Warburg effect to target PCa metabolism and to target multiple aspects of the cancer biology, by complexing Menadione and Vitamin C to simple sugars and lipids required by the cell for normal growth and proliferation. This method of cancer targeting is a unique approach, creating a therapeutic compound that is comprised of molecules required by the cell, but at a high enough dosage to induce cell death. The approach of coupling the vitamins to sugars and lipids aims to increase the overall uptake of the compound into the cell, due to the cancers unrelenting need for fuel to meet the high energy demands.

First and foremost, cell viability was examined through the use of an alamar blue viability assay, which indirectly determines cell viability through measuring the reduction of resazurin to resorufin, through cellular metabolism. However, it does not provide specific information about the underlying mechanisms of cell death, or the precise cellular processes affected.[343] The performance of the alamar blue assay can be influenced by various experimental conditions. Experimental factors such as pH, temperature, and the addition of some compounds or drugs can affect the accuracy and reliability of the dye reduction reaction.[344] With this, in some situations, alamar blue may not accurately reflect cell viability, for example if autophagy is induced or if particular compounds, such as reducing agents are used. Autophagy can impact cellular metabolic activity and alter the reduction of resazurin, leading to misleading viability measurements.[343,345] In the case of this study, vitamin C is a reducing agent, thus would affect the colour changes determined with the alamar blue assay, to combat this, following treatment the cells were washed twice with PBS in an attempt to reduce the interferences caused. [262] Consequently, the use of additional assays or techniques would be more optimal in the cytotoxicity determination of the vitamin-based compounds in future works. Despite the limitations, an alamar blue viability assay remains a widely used method for assessing cell viability and metabolic activity in many research applications, which lent to its use in this study. However, further knowledge of the benefits and limitations of the assay and further understanding of when it is appropriate would have been beneficial prior to study commencement.

Initial testing of TH1 in PC3 cells was not very promising, with a low cytotoxicity profile displayed by the compound. Following the analysis of the experimental conditions, it was concluded that the media glucose concentration (11mM) may play a role in inhibiting the uptake of the compound. It was therefore decided to consider media glucose

concentrations as a factor in mediating the uptake of these compounds. Therefore, all further evaluations were undertaken in the zero, 5.5mM and 11mM glucose conditions.

Since these are novel compounds, and we can only infer about their potential to kill cells, we first wanted to determine the cytotoxicity profiles of these compounds to evaluate their potential for therapeutic efficacy. Interestingly when we tested our first compound, we observed very limited cytotoxicity effects from the TH1 compound on the PC3 cells under 11mM glucose conditions following 24hrs incubation.

Vitamin C and glucose have very similar chemical structures (see Figure 3.40), allowing both to be transported into the cell by the glucose (GLUT) and sodium Vitamin C transporters,[262,269]

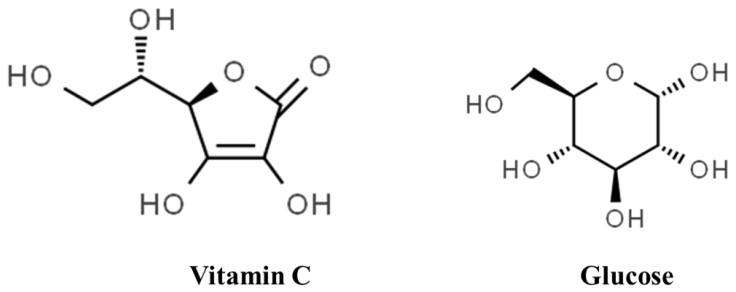

Figure 3. 40: Vitamin C vs Glucose chemical structure.

Previous studies evaluating the anti-cancer effects of Vitamin C in PCa cell lines have reported cytotoxicity values similar to our findings, and are within the range of 1.9 to 3.5 mM [346,279] In the zero glucose media conditions, Vitamin C treatment resulted in low IC_{50} values in all the cell lines. In zero glucose, the cells would likely be more vulnerable to drug treatment due to the lack of glucose present for conventional glycolytic energy production by cancer cells.[317,347] Nevertheless, the absence of glucose for transport by SVCT and GLUT into the cell, would reduce competitive uptake between glucose and Vitamin C.[262,269] When glucose was reintroduced in the 5.5mM and in the 11mM glucose media conditions, the IC_{50} values increased, perhaps[298] due to the cells being in more favourable conditions to undergo glucose metabolism for energy production.[298,282, 348] Our macroscale study of Vitamin C is in agreement with the existing literature, where similar cytotoxicity is observed, however the existing studies were conducted only in normal media glucose conditions.

Menadione has also sparked interest in the cancer therapeutics community, due to its high ROS generating abilities.[292,299,342] The TH strategy which we have outlined

complexes Menadione to the sugar and lipid molecules to induce Menadione uptake in the cell. This would result in an increase in intracellular ROS production by Menadione resulting in cell death.[294,299] Existing research has shown some promise in the use of Menadione as a cancer killing compound, with cytotoxicity reached at ~40μM within *in vitro* studies of pancreatic cancer, with Menadione examined in many other cancer types.[349,304,305,308,309,312,350] Once more, the existing literature has not determined the cytotoxicity of the native vitamins across a range of glucose milieu which is unique to this study.

With Menadione we do not see a strong effect of the glucose conditions on the IC_{50} values in the cell lines. Yet, lower concentrations of Menadione are required to achieve cell death in zero glucose across the cell lines. This may be a result of the vulnerable nature of the cells in these undesirable conditions. We do examine the effect of the zero-glucose condition on the cell lines, without the addition of a drug treatment in Chapters 4 and 5 to assure the cell death observed is not due to the glucose starvation. In the presence of glucose (5.5mM and 11mM glucose) the cytotoxicity outcomes determined for the cell lines showed a plateau effect. This is indicative of how menadione uptake is not glucose dependent, unlike vitamin C which has proven to be glucose dependent, likely due to their similarities in structure and in cellular uptake mechanisms

Overall, the findings indicate that in the presence of glucose, Vitamin C is required at higher concentrations to achieve cell kill, due to the structural similarities between glucose and Vitamin C, resulting in competitive cellular uptake. This effect is less apparent in the Menadione treated cells, with very low concentrations resulting in cell death. When comparing the cytotoxicity values achieved for Vitamin C and Menadione. Menadione was pursued for the TH strategy due to the improved cytotoxicity profiles in the cancer cells.

A panel of six novel TH Menadione compounds were received by the TCD laboratory for analysis consisting of five glucose compounds and one fatty acid compound. Due to the nature of the project, a screening process was undertaken where preliminary cytotoxicity examinations allowed the elimination of the less optimal compounds and the superlative compounds were taken forward including, two glucose TH compounds (TH1 and TH4) and the one fatty acid compound (TH6).

TH1 is comprised of Menadione and glucose with an amine linker group. This structure aims to allow the continuous uptake of the high volumes of Menadione, resulting

in cell death. The amine linker group comprised of a nitrogenous backbone aims to allow the compound to stay intact during cellular uptake allowing for the generation of high levels of ROS and promoting cell kill within the cancer cells. TH4, the second Menadione glucose compound in the study is comprise of an aryl linker group which contains a long carbon chain linker group. Little is known regarding stability of these compounds once entering the cell, but overall, the stability and cytotoxicity profiles appeared improved with the TH4 treatments, compared to TH1. This work aims to enlighten future discovery with the novel compounds to inform which of the linker groups is optimal for the greatest drug efficacy.

The practice of conjugating a natural substrate to a toxic compound is seen across the literature, with Glufosfomide (D-glucose isophosphoramide mustard) entering stage III clinical trials in patients with metastatic pancreatic adenocarcinoma in 2013. The study found an 18% increase in overall survival with the Glufosfomide treatment but overall, it was found that low activity of glufosfamide was found patient population.[351] These early clinical trials lead the way for the use of natural compounds, coupled to glucose to be trialed as new chemotherapeutics.

Glycoconjugation is a means by which compounds are combined with a glucose molecule, this is used in the therapeutic space to enhance uptake of the conjugated toxic moiety by the cells of interest. Annunziata A. Et al have shown that glycoconjugated platinum compounds exhibit high in vitro cytotoxicity and malignant cell selectivity when compared to non-glycoconjugated versions of the platinum compounds.[352] Supporting the use of glycosylation in the design of novel cancer therapeutics. Our work aimed to improve the cytotoxicity and the selectivity of the native menadione, through glycoconjugation seen in TH1 and TH4. In the evaluation of the TH compounds, an improvement in SI was noted in the 5.5mM glucose conditions where SI is higher in the LNCaP cells treated with TH4 than the menadione treated cells, and in the Du145 cells treated with TH4. TH4 again out preformed Menadione in the LNCaP and the Du145 cells compared to the native menadione with improved SI established. Some studies call an SI of greater than 1 to be a good selectivity index, however, the highest possible SI is desired as low cell death is required in the non-malignant cells versus the malignant cells.[353]

On the other hand, the exploration into the clinical relevance of quinone derivatives in cancer treatment is rising showing some success both in *vitro* and in *vivo*.[354–359] Many novel quinone derivatives have been explored in cancer with one study examining the

effects of chromenopyrazolediones (a combination of a quinone and a cannabinoid) in PCa with the aim to exhibit the toxicity of the quinone and the anti-cancer activities of the cannabinoid. This study showed success in the LNCaP cells and PC3 cell lines generated in mice, with significant growth hindrance observed due to the chromenopyrazoledione treatment, with the significant success attributed to the quinone toxicity.[360] A study of the effectiveness of nonglycoside quinones in HeLa and normal mouse JB6 P+ Cl41 cells was undertaken where p53-independent cell death was observed in the cells treated with the novel quinones. The selectivity index determined for these novel quinone compounds ranged from 1.67 in the unsubstituted 1,4-Naphthoquinone derivatives to 4.71 in the hydroxyderivative 1,4-Naphthoquinone. This study found that the group attached to the carbon-2 (C2) of the quinone carbon ring determined the cytotoxicity of the compound in the cells through structure activity relationship (SAR) analysis.[355] Our novel compounds are glycoconjugated on C2 of the quinone ring of Menadione, with this existing work highlighting the importance of this choice in stereochemistry. However, the linker group used in the work by N. Pelageev et al is a much shorter hydrocarbon chain than used in our TH technique, which may improve the cytotoxicity of the menadione and also a smaller molecule would have preferential uptake by GLUT into the cell.

Further examinations of the cytotoxicity of glycoconjugated naphthoquinones in PCa showed some success in LNCaP, PC3, Du145 and PNT2 cell lines, with SI ranging from 0.7 to 2.8 following 48hrs treatments.[361] These compounds were substituted at C6 of the glucose molecule and was found to be optimal for uptake by GLUT1.[361] With some structural similarities to the quinone compounds in this study, one could propose similar uptake by the GLUT1 of our novel compounds, however the work we have performed was across a glucose milieu but this study was conducted only in normal media glucose which would also impact the uptake by GLUT1 and requires further investigation.

The results obtained in this chapter highlight a glucose dependent uptake of the glucose conjugated compound thus it is important to note, that all of the studies discussed from the literature were only conducted in cellular media glucose. Unique to our study, the effect of three glucose conditions was also examined on the efficacy of our novel TH compounds, which is important in the examination and further improvement of the novel compounds and their cellular uptake.

While we examined two glucose Menadione compounds, we wanted to look at the impact of a lipid based Menadione compound, to examine its role in promoting cell death. TH6 is comprised of Menadione complexed to 6-azidohexanoic acid by an amine linker group. This compound aims to target the fatty acid metabolic pathways utilised by the cell for ATP production during intermediate/late-stage prostate cancer.[362–365] Breyer et al examined the conjugation of thymoquinone to fatty acid conjugates to determine the effects in HL-60 leukemia, 518A2 melanoma, KB-V1/Vbl cervix, and MCF-7/Topo breast carcinoma cells.[361] The study found that the unsaturated side chains of the fatty acid used showed greater activities than that of saturated chains of equal length, with the number of carbon to carbon double bonds being less significant than the fatty acid carbon chain length.[361] The use in this work of the 6-azidohexanoic acid is comprised of a 6 carbon chain with no additional saturated or unsaturated side chains. Examining the makeup of the fatty acid used in the novel TH compound construction may be useful in improving the compound selectivity. The use of fatty acid conjugation has not only occurred with natural moieties but with conventional therapies with aims to improve the selectivity once more. Mice studies of docosahexaenoic acid and paclitaxel, the anticancer drug, with aims to target tumours and reduce toxicity to normal tissues, with the conjugated compound presenting itself as less toxic than paclitaxel alone with a 4.4-fold higher molar doses tolerated in the mice.[361] The evidence of the impact of fatty acid conjugation, from these studies and others highlights the potential for the fatty acid menadione compound in achieving selective cell death to the cancer cells. In our work the SI of the TH compounds and Menadione were similar across the zero glucose conditions, however in Du145 cells the SI of TH6 was 3.1, which is greatly improved from the SI of 1.7 seen in the Menadione treated Du145 cells. Improvement in SI was noted in the 5.5mM glucose conditions where SI is higher in the LNCaP cells treated with TH6 than the menadione cells. Although the IC_{50} values achieved with the TH6 compound is greater than that of the Menadione, an improvement in selective killing of the cancer cells is observed which is important.

Overall, the findings indicate that some of the microscale TH compounds are displaying cytotoxic effects in the prostate cell lines. For the glucose-Menadione TH compounds TH1 and TH4, cytotoxicity was achieved in the PNT1a, LNCaP and the Du145 cell lines, with TH4 showing an increased SI than TH1. In the PC3 cell line, TH1 showed no cytotoxic effects, with cytotoxicity achieved with TH4 treatments, but the values were very high to achieve an IC_{50} value. Interestingly, in the presence of 5.5mM and 11mM

glucose, all the cells resulted with an IC_{50} of ~300µM when treated with TH6, indicating that the uptake of TH6 is not impeded by the glucose gradient. TH4 and TH6 are showing some promise in the LNCaP and Du145 cell lines, with increased selectivity compared to the Menadione treatment.

Chapter 4. An investigation into the effects of Vitamin C, Menadione and the TH compounds on the metabolic phenotypes and the cellular bioenergetics profiles of a panel of prostate cell lines under varying glucose conditions.

4.1 Introduction:

The reprogramming of metabolic pathways is now considered an emerging hallmark of cancer.[240,366,367] Further investigations into the mechanisms adopted by cancer cells to fulfil their energy requirements to sustain and support their growth and proliferation could lead to potential new avenues of treatment.

This chapter examines the metabolic bioenergetic profiles and the AR status of a panel of prostate cell lines during exposure to different glucose substrate concentrations. Furthermore, the impact on the cellular bioenergetic profiles was also determined after treating the prostate cell lines with Vitamin C, Menadione and the TH compounds.

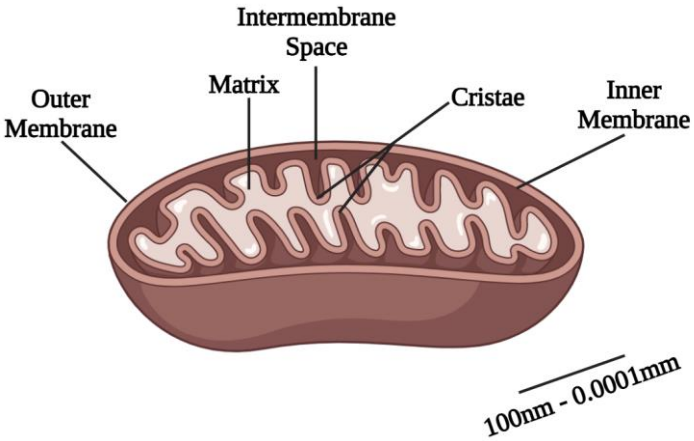

Figure 4. 1: The structure of the mitochondrion. The mitochondrion is made up of an outer membrane, which differentiates the cytoplasm from an inner membrane. The inner membrane encloses the internal matrix and cristae of the mitochondrion where the large surface area allows for efficient ATP production.

4.1.1 The Mitochondrion

The powerhouse of the cell, the mitochondrion is the organelle responsible for the majority of energy production in normal cells. It is home to many important cellular processes, such as bioenergetics, metabolism, and oxidative stress regulation.[368]

The mitochondrion occurs as a large tubular network, throughout the cytosol and close to the nucleus, the Endoplasmic Reticulum, the Golgi network, as well as interacting with the cytoskeleton of the cell for motility.[369] It is comprised of an inner boundary membrane, an outer membrane, and the cristae.[369,370] The cristae are structural invaginations of the mitochondrial matrix that provide an increased surface area for metabolic processes.[370,371] Within the cristae, multiple protein complexes (such as caspases) play an important role in mediating metabolic and apoptotic pathways.[369, 372]

The mitochondrial membrane potential (MMP) is located in the space between the inner and outer mitochondrial membranes and allows the movement of ions to and from the mitochondria.[371,373] Within the inner membrane the mitochondrial matrix is where metabolic processes such as the TCA cycle occur. [373] Mitochondria play a large role in cancer metabolism with some of these processes illustrated in Figure 4.2.

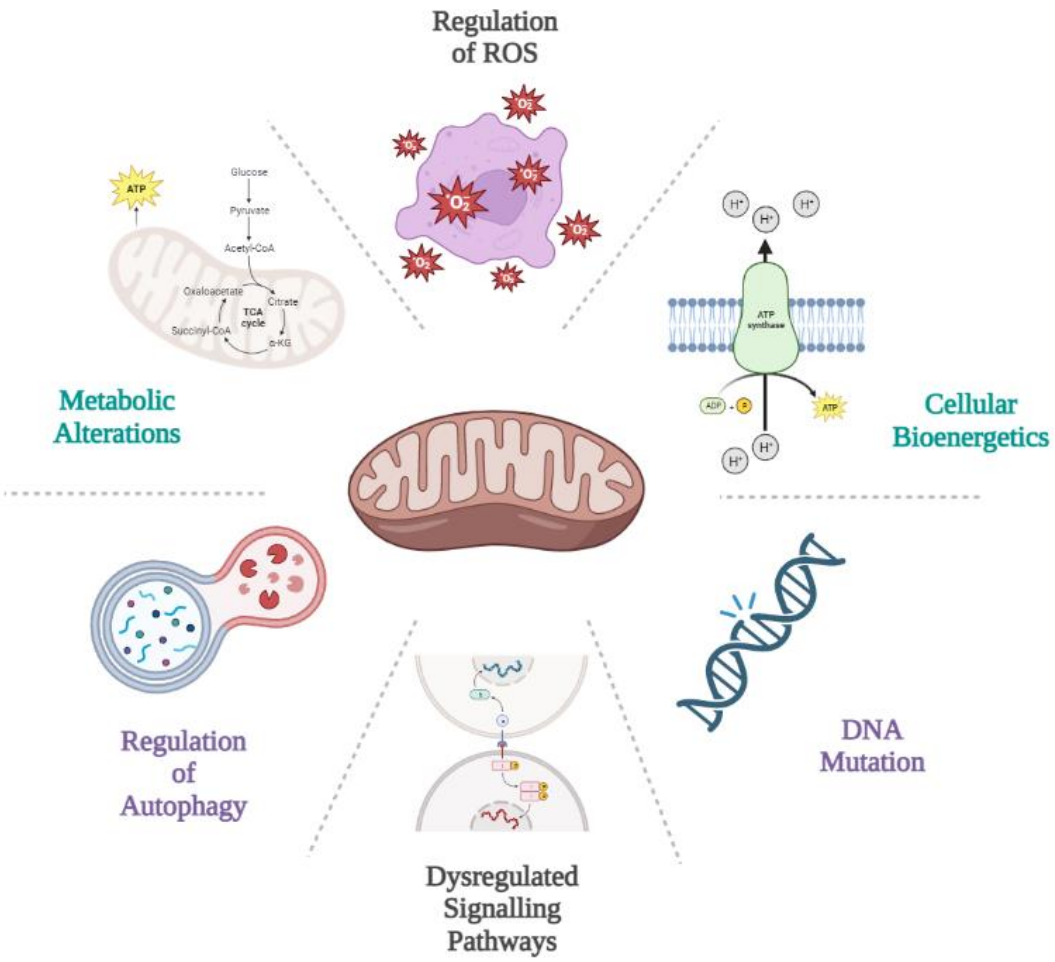

Figure 4. 2: The role of mitochondria in cancer. Mitochondria are involved in many biological processes including, the production/regulation of Reactive Oxygen Species (ROS), Cellular Bioenergetics, DNA mutations, autophagy regulation, and alterations in metabolism. These mechanisms are often critical in tumourigenesis and cancer progression.

4.1.2 Alterations in metabolism and the Warburg effect.

In normal cellular metabolism, glucose is converted to pyruvate and transported to the mitochondrion to enter the Krebs's cycle and undergo oxidative phosphorylation (OxPhos).[260,366,374] Cancer cells are thought to employ aerobic glycolysis described as the "Warburg effect".[250] Despite being highly inefficient compared to OxPhos in terms of ATP production, aerobic glycolysis is substantially faster,[375] thereby fuelling the energy requirements of the rapidly proliferating cancer cells.[242,251,253,260,376]

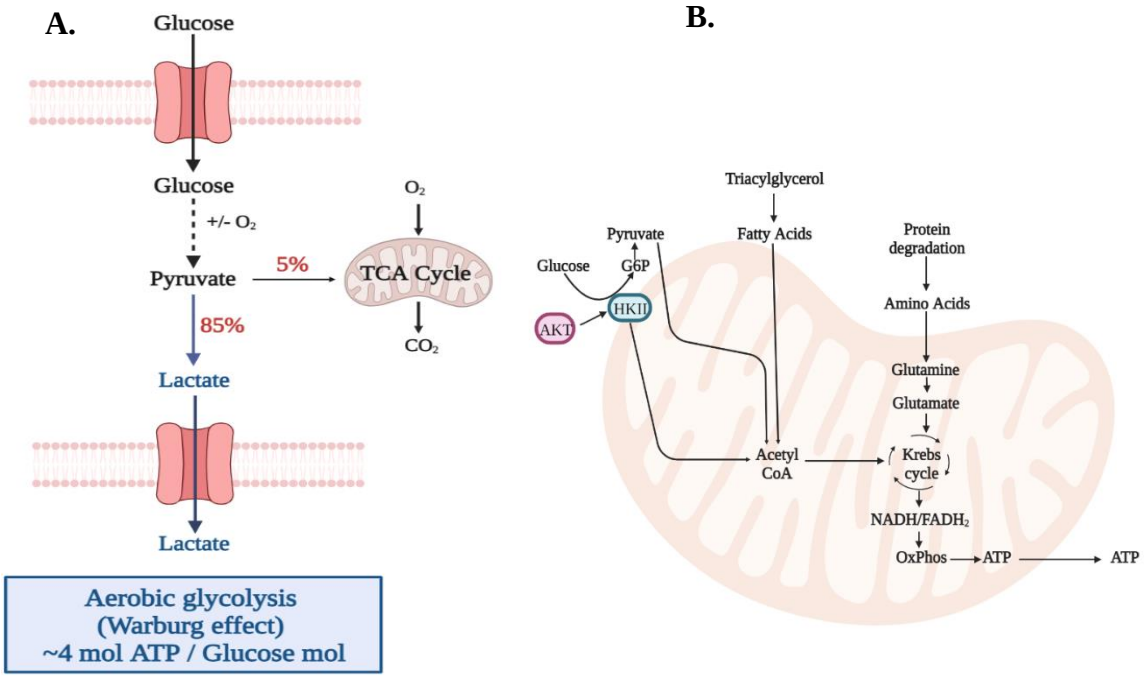

Figure 4. 3: Cellular metabolism: (A.) Warburg Glycolysis; Glucose molecules enter the cell via the GLUT transporters located in the cell membrane. Glucose is converted to pyruvate regardless of the presence of oxygen. Pyruvate is further broken down into lactate (85%) and removed from the cell into the extracellular space. This process of aerobic glycolysis results in lower ATP production with ~4 molecules of ATP / Glucose molecule being produced when compared to the TCA cycle (36 molecules of ATP/glucose). (B) Metabolic pathways within the mitochondria, contributing to ATP production.

Since mitochondria play a key role in driving cellular metabolic processes, cancer cells exploit this to promote growth and proliferation and to provide survival advantage when the cancer cells are exposed to hypoxia, nutrient starvation and during therapeutic treatments .[377] It has also been proposed that cancer cells can alter their metabolic dependencies based on the presence of internal and external stimuli, such as surrounding glucose concentration, which may operate during disease initiation, progression and metastasis.[378]

4.1.3 Mitochondrial Bioenergetics and ROS

Bioenergetics used in the evaluation of the cellular function and health. Cancer cells can alter their bioenergetic requirements to sustain growth and proliferation due to the presence or lack of nutrients, such as glucose, fatty acids, and glutamine.[379] The bioenergetics parameters linking the mitochondrial metabolic reprogramming, the mitochondrial metabolic phenotype, and the cells substrate preference includes the oxygen consumption rate (OCR), which represents the sum of all cellular processes with the ability to consume oxygen.[379,380] It is a good indicator of the health of mitochondria, with high OCR levels indicating a healthy mitochondrion.[379–381]

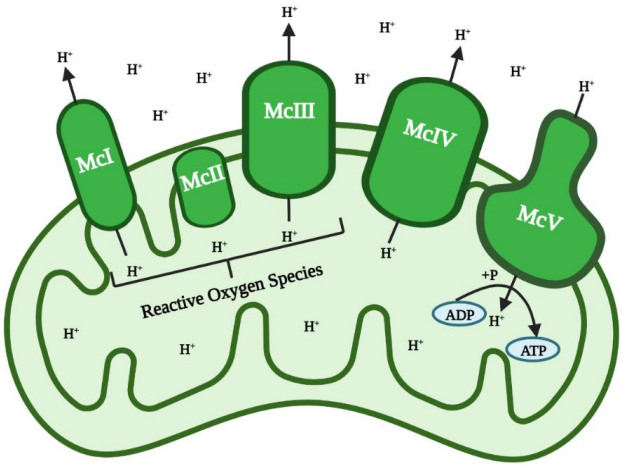

Figure 4. 4: The Mitochondria and its complex transporters for the electron transport chain and ROS production: Mitochondrial Complex I to V are used in the electron transport chain for mitochondrial metabolism. Mitochondrial complex I, II and III are thought to be responsible for the generation of 90% of cellular ROS. Complex V is implicated in the production of ATP from ADP.

Mitochondrial complex I/II/III are the mitochondria's own sources of ROS and are known to contribute to oxidative stress in the mitochondria. ROS production is a regulated process, with an alteration in ROS levels indicating a possible dysfunction of the mitochondria. ROS levels would indicate a dysfunctional mitochondrion, hence the relationship between OCR and ROS levels is a useful tool to determine mitochondrial health.

4.1.4 The role of AR in inducing alterations in metabolic phenotypes and metabolic reprogramming in PCa.

PCa cells display an altered metabolic profile in different stages of cancer development from Prostate Intraepithelial Neoplasia (PIN) to metastatic disease.[244,317] To understand the complexity of prostate metabolism, the role of the androgen receptor (AR) must be considered, as it is an orchestrator of prostate cellular processes. AR promotes both glycolysis and OxPhos, hence its importance as a regulator of early disease establisment and progression.[233] Understanding the link between AR and prostate metabolism is essential in recognizing the metabolic switches that occur during disease progression and in the search for a cure for mCRPC.

The normal prostate epithelium employs AR signalling to maintain its metabolic requirements, and results in the accumulation of Zinc in the mitochondria due to the zinc transporters ZIPI-4 (uptake) and ZnTI-10 (release).[382] This in turn results in the inhibition of m-aconitase (mitochondrial enzyme involved in the citric acid cycle, required for iron concentration regulation) causing the TCA cycle to be cut short, with accretion of citrate.[245,383] AR signalling is responsible for the increase in citrate production by the increase in citrate synthase, OAA and Acetyl Co A in the mitochondria.[233] Normal mammalian cells rely on the TCA cycle for ATP production, resulting in ~38ATP molecules/glucose, however, with the normal prostate epithelium's unique metabolism it is found to produce ~14ATP molecules/glucose.[384] This is characterized by a more glycolytic metabolic phenotype, due to the truncation of the TCA cycle and allows for the sustained secretion of citrate in the seminal fluid.[362]

A drop in Zinc concentrations from the reduction of ZIPI-4 is an early indicator of cancer development, and results in a metabolic shift, with corresponding lower citrate secretion. [28,32] Early prostate adenocarcinoma uses citrate as a substrate for energy production activating the TCA cycle, and this is mediated by AR signalling.[244,245,383] This instigates a metabolic dependency on oxidative phosphorylation and lipogenesis. AR regulates fatty acid (FA) metabolism by the expression of a wide range of enzymes such as fatty acid synthase and acetyl-CoA carboxylase shown to be involved in FA metabolism.[385] The activation of AR in PCa can increase FA synthesis, while its inhibition does the opposite.[385]

AR signalling is present in normal prostate epithelium and continues through to malignancy. [386] However, AR antagonism, with help from cancer associated fibroblasts

(CAFS) and adipocytes, initiate a Warburg phenotype further promoting the androgen independent (AI) disease, with corresponding lactate secretions fuelling further metabolic activities. [244,245,317,365,387,388] Androgen deprivation treatment resistance frequently results in the development in AI disease progression which is linked to Warburg altered metabolism and is incurable.[84,386] Thus highlighting the importance of recognizing the metabolic phentotypes and the androgen status of the different stages of disease progression. The implications of AR on the metabolic processes in the cell is illustrated in Figure 4.5.

4.1.5 The role of glucose and diabetes in PCa pathogenesis.

Metabolic disorders such as altered glucose metabolism and diabetes are linked to the pathogenesis of PCa.[389] The prevalence of diabetes in men (18–99 years) was found to be 8.9% in 2017, with the peak prevalence found to be at the age 65-69 years where the risk of PCa begins to rise dramatically.[390,40] By 2045 this prevalence is expected to rise to 9.9%.[390] Studies suggest that diabetes can have a protective effect to patients with PCa.[391] Overall, it has been found that patients with diabetes have worse outcomes and are of a higher disease risk, however this is often also linked to high apodicticity and obesity, with inferior efficacy of available treatments.[389,7] Literature states that low levels of androgens are a possible risk factor for diabetes in males.[391] We hypothesise that this in turn may affect PCa disease type, depending on its metabolic dependencies.

Blood glucose levels of less than 7.8mM is considered within a normal range, with a reading of more than 11.1mM after 2hrs, considered within a diabetic range. Between 7.8mM and 11.0mM blood glucose is a prediabetic range.[392] With the evaluation of a glucose milieu in this study, biologically relevant concentrations were chosen to represent glucose starvation (zero glucose), ‘normal’ glucose (5.5mM glucose) and prediabetic/diabetic glucose (11mM glucose).

The cellular microenvironment, through its nutrient (glucose, oxygen etc.) gradient and pH, is expected to alter metabolic bioenergetics in cancer cells. The effects of therapeutic intervention in modifying bioenergetics may be mediated by the glucose microenvironment of the cancer cells and is important in understanding the role of both the glucose milieu in this study and the effects of the vitamins and novel compound treatments.

.

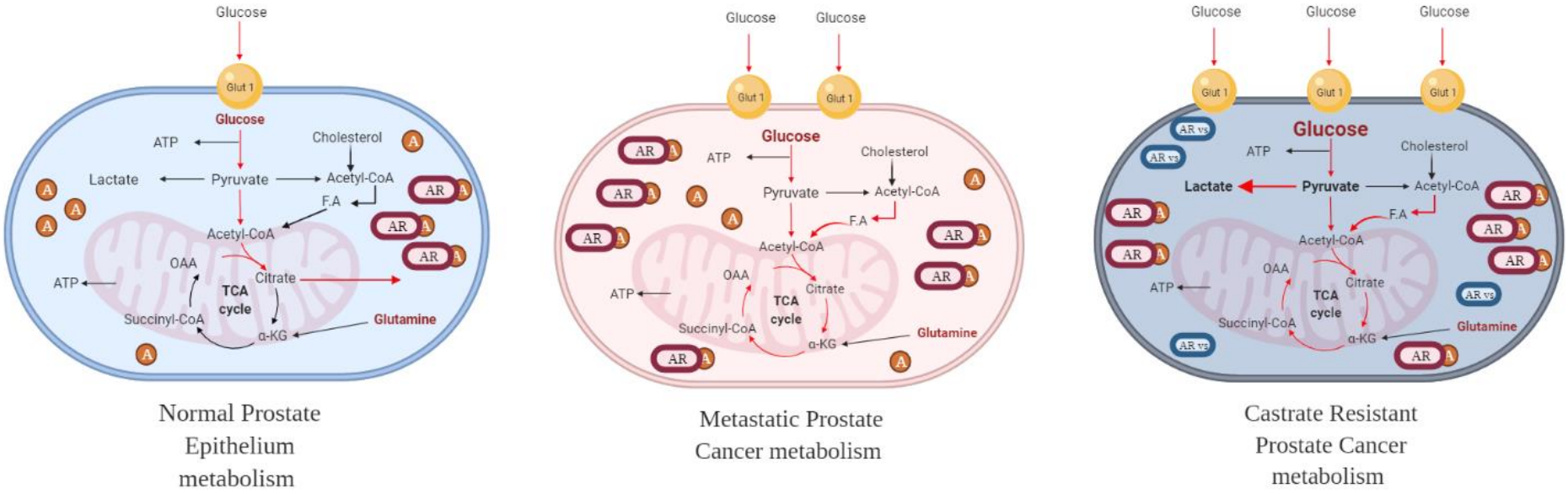

Figure 4. 5: The progression of prostate cancer from oxidative phosphorylation dependent early-stage androgen dependent disease to Warburg dependent late-stage androgen independent disease. (1.) Normal prostate epithelium, here there is high citrate output as the TCA cycle cut is short and a glycolytic metabolic phenotype is observed. (2.) Early-stage adenocarcinoma (androgen dependent), here citrate is used for ATP production for the completion of the TCA cycle. (3.) Late-stage adenocarcinoma (androgen Independent) a switch to a Warburg phenotype is observed here, again with high citrate secretions.

4.2 Aims and Hypothesis

We propose that the cellular bioenergetics of a panel of prostate cell lines can be altered by varying glucose conditions, and with the treatments of Vitamin C, Menadione and TH compounds.

- To determine the metabolic phenotypes and the basal bioenergetic profiles of the PCa cell lines; PNT1a, LNCaP, PC3 and Du145 under zero, 5.5mM and 11mM glucose conditions.
- To determine the metabolic phenotypes and the bioenergetic profiles of the PCa cell lines; PNT1a, LNCaP, PC3 and Du145 when treated with the native vitamins, Menadione and Vitamin C under zero, 5.5mM and 11mM glucose conditions.
- To determine the metabolic phenotypes and the bioenergetic profiles of the PCa cell lines; PNT1a, LNCaP, PC3 and Du145 when treated with two glucose-based TH compounds (TH1, TH4) and one fatty acid TH compound (TH6) under zero, 5.5mM and 11mM glucose conditions.
- To determine if the androgen receptor expression is altered by the varying glucose conditions in the non-malignant and cancer cell lines under zero, 5.5mM and 11mM glucose conditions.

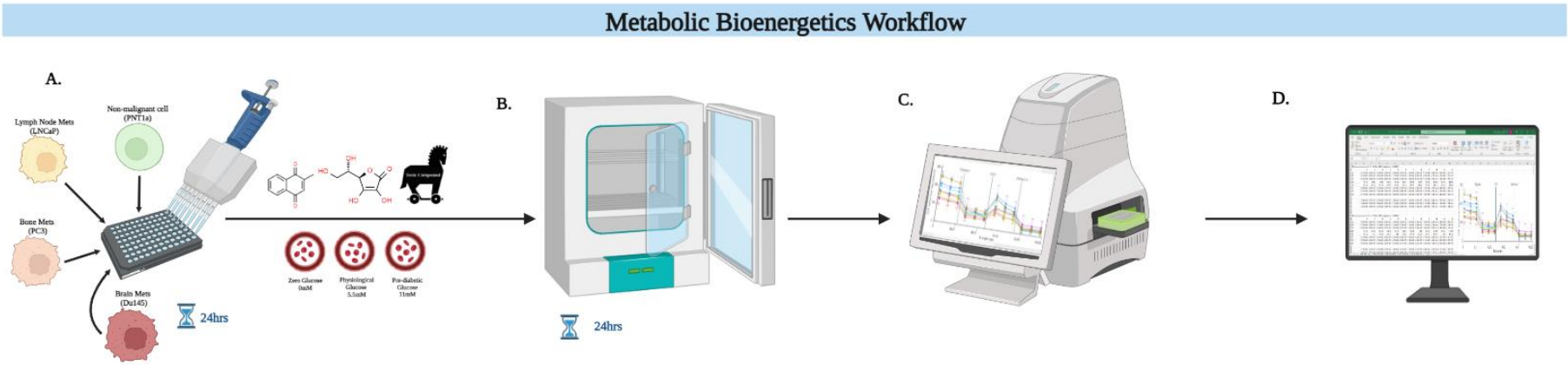

Figure 4. 6: Metabolic bioenergetics workflow .(A.) Non-malignant and malignant prostate cancer cells were cultured to 90% confluency in RPMI-1640 complete culture media. Cells were plated and incubated for 24hrs, then placed in zero, 5.5mM and 11mM glucose media and treated with Vitamin C, Menadione. TH1, TH4 and TH6 respectively. (B.) Cells were incubated for 24hrs prior to performing the assay. (C.) Cells run on the Agilent Seahorse XFe24 with the MitoStress or the ATP rate assay. (D.) Results were analysed on the Agilent online analyser and graphs were generated with GraphPad Prism.

4.3 Methodology

Refer to Chapter 2 for full details of the methods used in this chapter.

4.3.1 Seahorse analysis of the prostate cell lines

The OxPhos in the mitochondria and the rate of ATP production of the prostate cell lines, PNT1a, LNCaP, PC3 and Du145 were determined with the Seahorse XFe24 Analyzer (Agilent Technologies Inc., Santa Clara, CA, US). See Section 2.5 in Chapter 2 for the full methods.

4.3.2 Statistical Analysis

Statistical analysis was performed using GraphPad Prism version 9.0. The results were expressed as mean ± SEM. Parametric one-way analysis of variance (ANOVA) and two tailed t-tests were carried out, using GraphPad Prism version 9.0 and $p < 0.05$ was considered significant, see Table 4.24 for reference.

Table 4.24: Symbols of statistical significance from GraphPad Prism

Symbol	Meaning
Ns	$P > 0.05$
*	$P \leq 0.05$
**	$P \leq 0.01$
***	$P \leq 0.001$
****	$P \leq 0.0001$

4.4 Results

4.4.1 The basal bioenergetic profiles of the prostate cell lines under zero, 5.5mM and 11mM glucose culture media conditions

The effect of the three glucose conditions in the study, were examined to determine the baseline effects on the cell's metabolic phenotypes and bioenergetics. Not only was this to determine how the novel compounds would react in the glucose milieu, but the values chosen were to represent glucose starvation (zero glucose), the 'normal' physiological glucose (5.5mM glucose) and the high pre-diabetic and diabetic glucose (11mM glucose) As aforementioned, patients with PCa tend to be older men where increased likeliness of comorbidities such as diabetes is prevalent.

4.4.1.1 Varying glucose culture media conditions affect rates of ATP production by OxPhos and glycolysis in PNT1a cells

Non-malignant PNT1a cells, cultured in zero glucose conditions, had a total ATP of 24.6pmol/min, of which the majority of the ATP (81.8%) was produced by OxPhos, and the rest was produced by glycolysis (18.2%). In 5.5mM glucose the balance changed to nearly equal ATP production, with 11.4pmol/min of ATP (54.3%) being produced with by OxPhos and 45.7% by glycolysis. In 11mM glucose there were also similar amounts of ATP produced Oxphos (58.6%) and glycolysis (41.4%). In non-malignant PNT1a cells glucose was able to influence glycolysis and OxPhos in a concentration dependent manner (Figure 4.7 **A** and **B)**.

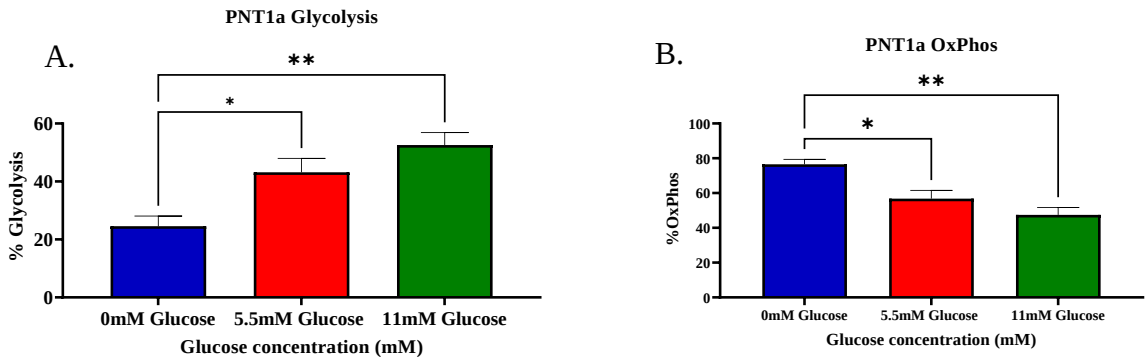

Figure 4. 7: Results of the ATP Rate Assay of non-malignant PNT1a) cells showing the metabolic phenotype of the cell line under zero, 5.5mM and 11mM glucose media conditions. (A.) % ATP production by glycolysis. (B.) % ATP Production by OxPhos. (n=3) 1-way ANOVA). (P > 0.05, ** P ≤ 0.01, *** P ≤ 0.001, **** P ≤ 0.0001)*

4.4.1.2 The zero-glucose conditions increase the mitochondrial endpoints in the non-malignant PNT1a cells

Basal OCR was comparatively higher at 67.8pmol/min in zero media glucose conditions, when compared to OCR rates in 5mM and 11mM media glucose which were 29.9pmol/min and 32.4pmol/min. This was found to be statistically significant (P= 0.03) when OCR values were compared between 5.5mM and zero glucose. The increase in OCR observed is an indication of higher use of OxPhos by the cells under zero glucose conditions.

Proton leak at zero glucose was 6.2pmol/min and decreased by half to 8.6pmol/min at 5.5 mM glucose and 6.5pmol/min at 11mM glucose. These differences in Proton leak were found to be significantly different (P=0.04) between zero and 11mM glucose. An increase in proton leak can be an indication of mitochondrial dysfunction which may be the case due to the lack of glucose in the cell media, but the increase may also be due to the higher reliance on oxphos, increasing mitochondrial metabolic mechanisms, such as proton leak.

Maximal respiration under zero media glucose conditions was found to be 94.5pmol/min. At 5.5mM glucose it was established to be 16.7pmol/min and 22.9pmol/min in the 11mM glucose conditions. On comparing across the three glucose conditions, a significant decrease (P= 0.0006) was observed between the zero glucose conditions versus the cells in the presence of 5.5mM and 11mM glucose, which also indicates the higher use of oxphos by the zero glucose cells.

In the presence of zero glucose, non-mitochondrial respiration was observed to be at 51.9pmol/min and decreased to 35.8pmol/min in 5.5mM media glucose and 6.78pmol/min in 11mM media glucose. This decrease was found to be statistically significant by one-way ANOVA across all three media glucose conditions (P <0.0001). The decrease in non-mitochondrial respiration is interesting here, considering that the cells in the presence of glucose have previously shown to rely on glycolysis which occurs in the cell's cytoplasm.

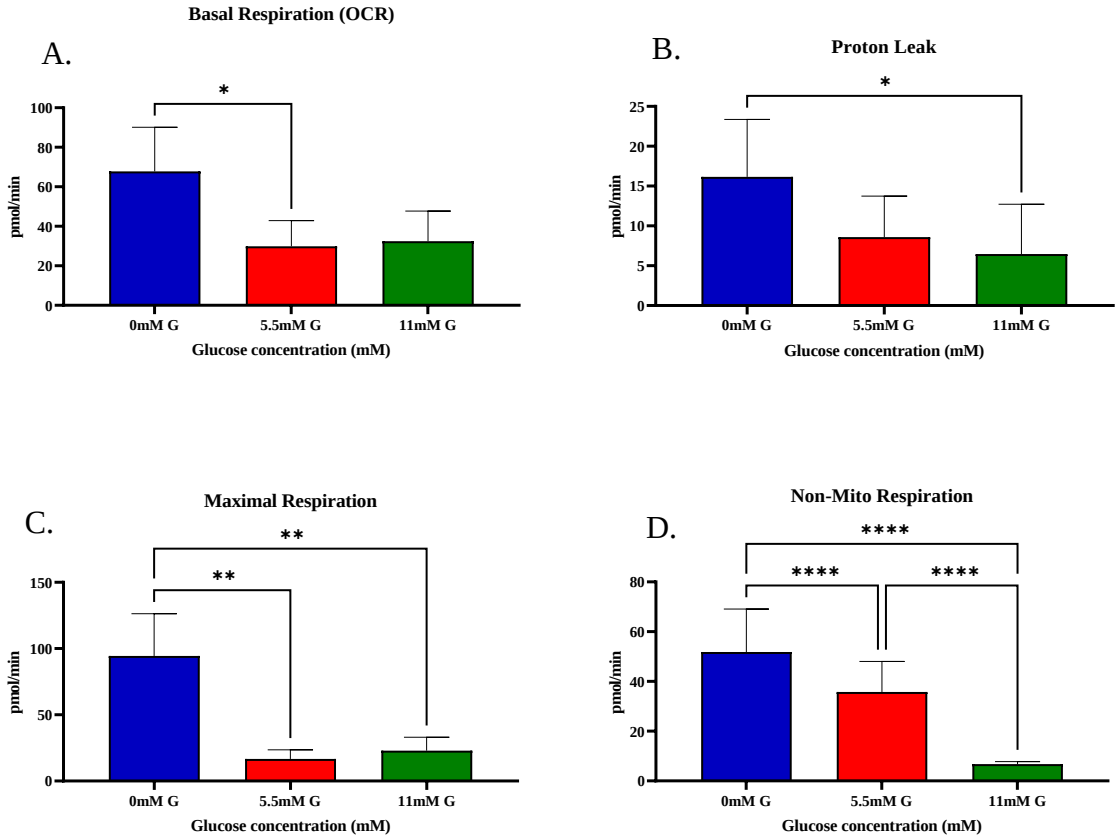

Figure 4. 8: MitoStress Assay of the PNT1a (non-malignant) cell line, in zero, 5.5mM and 11mM glucose media, showing the effects on the; (A) Basal OCR was decreased in the 5.5mM and the 11mM glucose conditions. (B) Proton leak was decreased in the 11mM vs the zero glucose conditions. (C) Maximal respiration was decreased in the 5.5mM and the 11mM glucose compared to the zero glucose cells, and (D) The non-mitochondrial respiration was decreased in the 5.5mM and the 11mM glucose conditions compared to the zero glucose conditions. (n=3) 1-way ANOVA) ($P > 0.05$, ** $P \leq 0.01$, *** $P \leq 0.001$, **** $P \leq 0.0001$).*

4.4.1.3 Increased glucose conditions in the cellular medium increases the rates of ATP production by glycolysis and decreases OxPhos in LNCaP cells

In zero glucose media conditions, ATP production of 200.8pmol/min was observed in the cells with majority (90.1%) being produced by OxPhos and a small proportion (9.9%) by glycolysis. In 5.5mM media glucose conditions, there was a significant decrease in ATP production at 146.2pmol/min, with 76.2% being produced by OxPhos and 23.8% by glycolysis in the 11mM glucose media conditions although there was a slight increase in ATP production at167.4pmol/min with 67.6% being produced by OxPhos and 32.4% by glycolysis the rate of ATP production was lower than that observed for zero glucose conditions. Overall, the ATP production was found to significantly vary across the three glucose conditions (P= 0.004). From these findings it is clear that there is a glucose concentration dependent decrease in OxPhos, and a correlating glucose dependent increase in glycolysis observed in Figure 4.9 **A** and **B** of the LNCaP cells.

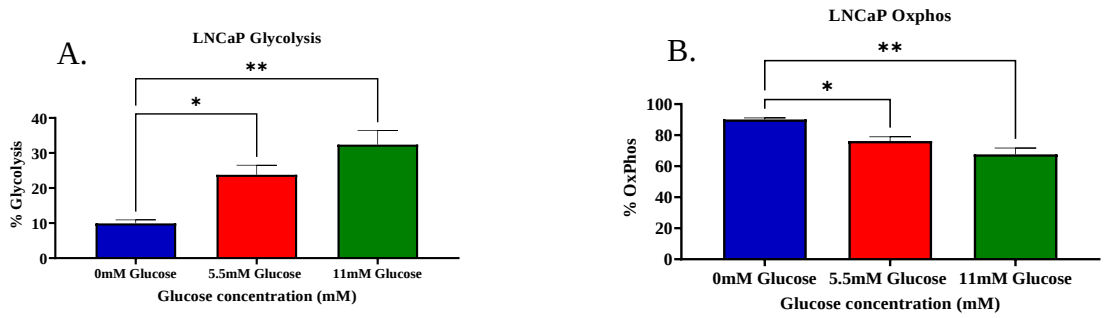

Figure 4. 9: Results of the ATP Rate Assay of LNCaP (early-stage disease) cell line, showing the metabolic phenotype of the cell line under zero, 5.5mM and 11mM glucose media conditions. (A.) % ATP production by glycolysis, was increased in the presence of 5.5mM and 11mM glucose conditions. (B.) % ATP Production by OxPhos was highest in the zero glucose conditions than in the 5.5mM and 11mM glucose conditions. (n=3) 1-way ANOVA). (P > 0.05, ** P ≤ 0.01, *** P ≤ 0.001, **** P ≤ 0.0001)*

4.4.1.4 Varying media glucose conditions do not have an impact on mitochondrial function in LNCaP cells

Basal OCR was found to be highest in zero media glucose conditions at 281.0pmol/min, followed by OCR at 255.0pmol/min in the 11mM glucose conditions and was lowest in 5.5mM media glucose at 233.3pmol/min. The results are presented in Figure 4.10 **A**. the higher levels of OCR in the zero glucose conditions illustrates a greater reliance on OxPhos for energy production in the LNCaP cells.

Proton leak was found to be lower at 80.2pmol/min in zero glucose media conditions when compared to proton leak at 5.5mM and 11mM glucose where it was determined to be 87.1pmol/min and 87.6pmol/min. The results are presented in Figure 4.10 **B**. The similar levels of proton leak are likely due to the LNCaP cell's majority reliance on OxPhos for ATP production, regardless of the glucose concentration present in the cell medium.

Maximal respiration was highest in zero media glucose conditions at 380.1pmol/min, followed by 323.8pmol/min in the 11mM glucose conditions and 303.4pmol/min in the 5.5mM glucose conditions, as shown in Figure 4.10 **C**. No significant changes were observed in the maximal respiration of the LNCaP cells in the three glucose conditions, again likely due to the heavy reliance on OxPhos overall.

Non-mitochondrial respiration was established to be 41.7pmol/min in the zero glucose conditions. In the 5.5mM glucose it was found to be 34.6pmol/min and under 11mM it was determined as 36.4pmol/min. The results are presented in Figure 4.10 **D**. Although a reported increase in glycolysis was established in the LNCaP cells in the presence of glucose the comparable values achieved in the non-mitochondrial respiration indicates that LNCaP is more reliant on other metabolic processes and not glycolysis.

Overall, as per results are presented in Figure 4.10, there was no significant difference for any of the MitoStress endpoints between the three glucose conditions for the LNCaP cells.

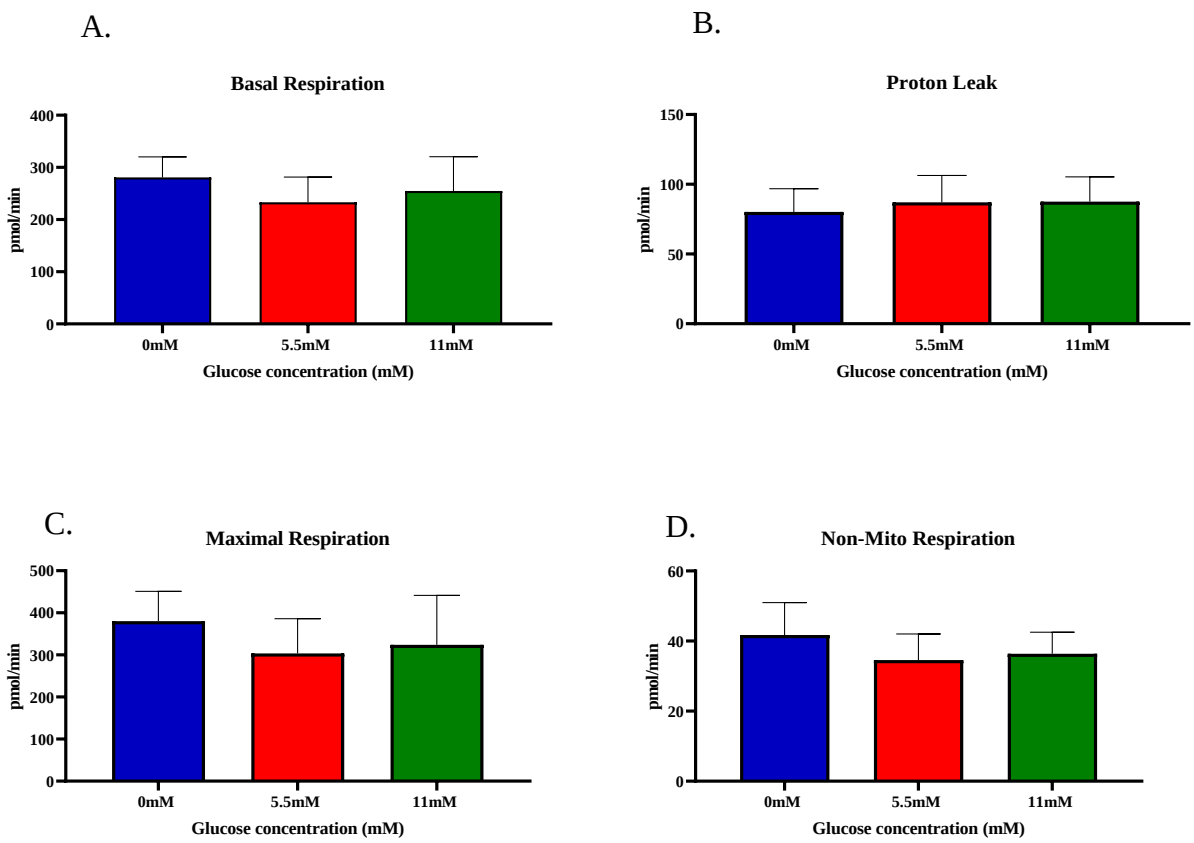

Figure 4. 10: MitoStress Assay of LNCaP cell line, under zero, 5.5mM and 11mM glucose media, showing the effects on the; (A) Basal OCR was unchanged between the glucose conditions, (B) Proton leak was unchanged between the glucose conditions, (C) Maximal respiration was unchanged between the glucose conditions, and (D) The non-mitochondrial respiration was unchanged between the glucose conditions. (n=3) 1-way ANOVA) ($P > 0.05$, ** $P \leq 0.01$, *** $P \leq 0.001$, **** $P \leq 0.0001$).*

4.4.1.5 An increase in glucose in the cell media increases the rated ATP production by glycolysis and decreases the use of OxPhos in the PC3 cells

In Figure 4.11, the PC3 cells, in zero glucose media conditions, ATP production was 50.5pmol/min, with nearly 75.0% being produced by OxPhos and a small proportion 25% by glycolysis. Under media glucose conditions, although ATP production rates similar to those in zero glucose conditions, with ATP production of 51.3pmol/min in 5mM glucose and 49.4pmol/min 11mM glucose, it was interesting to observe that the cells relied heavily on glycolysis for ATP production with 75.2 % of ATP being produced by glycolysis in 5mM glucose conditions and 77.1% by glycolysis in 11mM glucose.

There was a significant increase in ATP production by glycolysis in 5.5mM and 11mM glucose compared to cells in zero glucose (P=0.001). The ATP production rate by OxPhos was significantly decreased, with a correlating increase in glycolysis across the three media glucose conditions (P=0.01). Overall, PC3 cells present with a glucose concentration dependence on glycolysis where the reliance on glycolysis increases in the presence of glucose, and the reliance on OxPhos decreases congruently as glucose concentrations increase in the cell media.

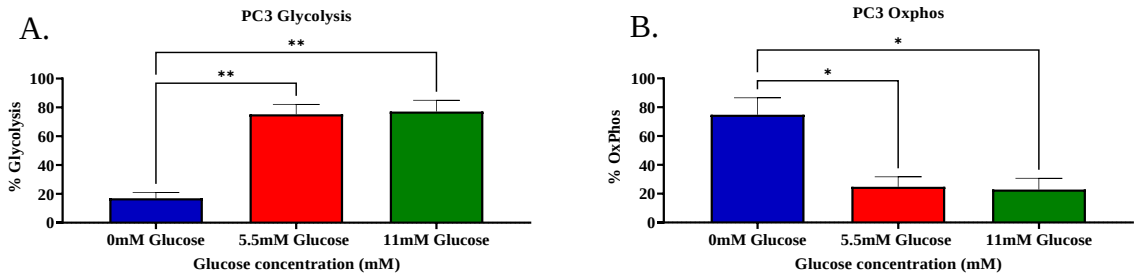

Figure 4. 11: Results of the ATP Rate Assay of PC3 (metastatic androgen independent) cell line, showing the metabolic phenotype of the cell line under zero, 5.5mM and 11mM glucose media conditions. (A.) % ATP production by glycolysis was increased in the 5.5mM and the 11mM glucose conditions. (B.) % ATP Production by OxPhos was decreased in the 5.5mM and the 11mM glucose conditions. (n=3) 1-way ANOVA). (P > 0.05, ** P ≤ 0.01, *** P ≤ 0.001, **** P ≤ 0.0001).*

4.4.1.6 The impact of varying media glucose concentrations on mitochondrial function in PC3 cells

The basal OCR at zero glucose was found to be 67.5pmol/min, at 5.5mM glucose it was 54.1pmol/min and under 11mM glucose, OCR was determined to be significantly increased (P=0.04) to 87.4pmol/min. The increase in OCR determined is possibly due to the increase in fuel for PC3s metabolic processes allowing for its rate of oxygen consumption to increase.

Proton leak in the zero-glucose condition was found to be 24.8pmol/min, in the 5.5mM glucose it was found to be 26.5pmol/min and under 11mM glucose it was increased to 41.7pmol/min. No significance was determined in the proton leak between the three different glucose concentrations in the PC3 cells. the increase in proton leak in the 11mM glucose conditions ins interesting, as PC3 cells are in the optimal conditions for energy production with plenty of glucose substrate to fulfil their metabolic demands. Again, the reliance on OxPhos here is low, which should account for a lower proton leak value determined, however an overall increase in OCR was found in the PC3 cells in the 11mM glucose conditions and may account for this rise in proton leak.

Maximal respiration of the cells in the zero glucose conditions was found to be 156.0pmol/min. Under 5.5mM glucose it was found to be 171.4pmol/min and in the 11mM glucose conditions, the maximal respiration was determined as 235.5pmol/min. No significance was established in the maximal respiration capacity across the three different glucose concentrations in the PC3 cells. the increase in the presence of glucose may allow for the PC3 cells to increase their metabolic capabilities by providing more fuel for their metabolic processes, overall resulting in a glucose dependent increase in maximal respiration.

Non-mitochondrial respiration was found to be 3.46pmol/min under zero glucose. This was significantly increased (P= 0.02) to 20.7pmol/min in the 5.5mM, and 20.4pmol/min and in the 11mM glucose conditions. The glucose concentration dependent increase in non-mitochondrial respiration is likely due to the large increase in reliance on glycolysis for ATP production as seen in Figure 4.12 previously, due to glycolysis occurring outside of the mitochondria.

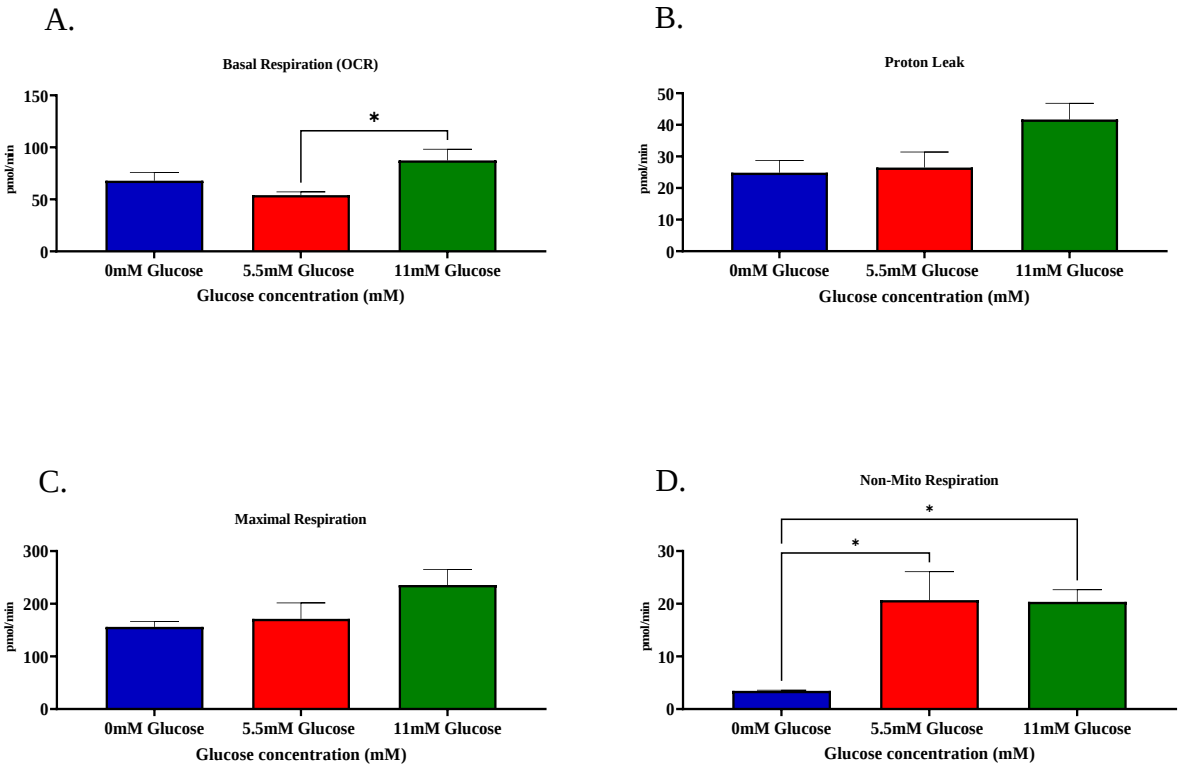

Figure 4. 12: MitoStress Assay of PC3 (malignant and androgen independent) cell line, under zero, 5.5mM and 11mM glucose media, showing the effects on the; (A) Basal OCR was increased in the 11mM glucose versus the 5.5mM glucose conditions, (B) Proton leak was unchanged between the glucose conditions, (C) Maximal respiration was unchanged between the glucose conditions, and (D) The non-mitochondrial respiration was increased in the 5.5mM and 11mM glucose condition versus the zero glucose conditions. (n=3) 1-way ANOVA). ($P > 0.05$, ** $P \leq 0.01$, *** $P \leq 0.001$, **** $P \leq 0.0001$).*

4.4.1.7 Varying media glucose conditions affect rates of ATP production by OxPhos and glycolysis in Du145

In Du145, the cell line representing the metastatic androgen independent disease model ATP production was 113.2pmol/min, with 17.6% by glycolysis and 82.5% by OxPhos under zero glucose media conditions. In the 5.5mM media glucose, cells had an ATP production of 147.1pmol/min, with 71.0% by glycolysis and 30% by OxPhos. For the cells under 11mM media glucose, ATP production was found to be 106.4pmol/min, with 63.0% by glycolysis and 37.0% by OxPhos. Du145 cells displayed a preference for ATP production by OxPhos under zero glucose conditions. They however switched their preference to glycolysis for ATP production in the presence of 5.5mM and 11mM glucose conditions and can be seen in Figure 4.13 **A** and **B**.

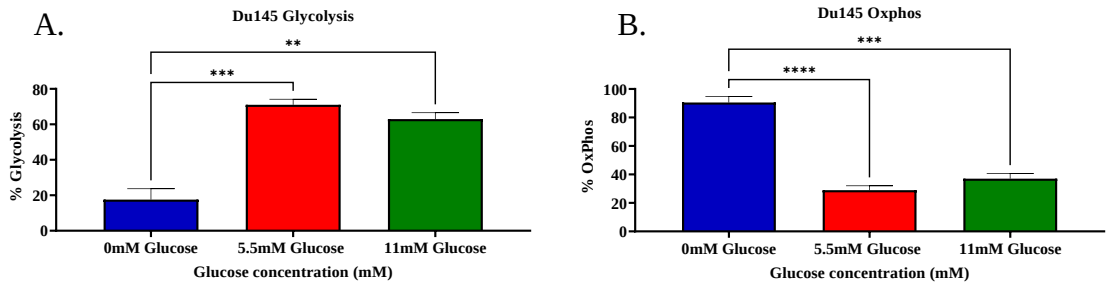

Figure 4. 13: Results of the ATP Rate Assay of Du145 (metastatic androgen independent) cell line, showing the metabolic phenotype of the cell line under zero, 5.5mM and 11mM glucose media conditions. (A.) % ATP production by glycolysis was increased in the 5.5mM and the 11mM glucose conditions. (B.) % ATP Production by OxPhos was decreased in the 5.5mM and the 11mM glucose conditions. (n=3) 1-way ANOVA). (P > 0.05, ** P ≤ 0.01, *** P ≤ 0.001, **** P ≤ 0.0001).*

4.4.1.8 The increase in glucose concentrations in the cell media decreases proton leak and non-mitochondrial respiration and increased maximal respiration in Du145 cells

Basal OCR was found to be 130.47pmol/min under zero glucose media conditions and was quite similar at 137.8pmol/min in 5.5mM glucose and in the 11mM glucose it was found as 124.9pmol/min. Overall, there was no significant change in the OCR across the three glucose conditions. The sustained levels of OCR observed in the Du145 cells across the glucose gradient may be due to the cells in the presence of glucose still relying partially on mitochondrial metabolism for their ATP production.

Proton leak at zero glucose was found to be 41.0pmol/min, in the 5.5mM glucose conditions it was found to be decreased significantly (P=0.004) to 29.4pmol/min and 25.1pmol/min in the 11mM glucose conditions, with the decrease likely due to the decreased reliance on oxphos for ATP production, and less dysfunction to the mitochondria due to the glucose starvation of the cells in the zero glucose conditions.

Maximal respiration of the cells in the zero glucose conditions was 177.76pmol/min. under 5.5mM and 11mM media glucose conditions it increased to 259.4pmol/min and 255.8pmol/min. and was statistically significant (P=0.0006) and illustrates the glucose dependent decrease in reliance on OxPhos by the Du145 cells.

Non-mitochondrial respiration was found to be 19.2pmol/min in zero glucose media with 15.2pmol/min determined in the 5.5mM glucose media and a significant decrease in the 11mM glucose media at 7.9pmol/min (P=0.02).

The MitoStress results are presented in Figure 4.14 below.

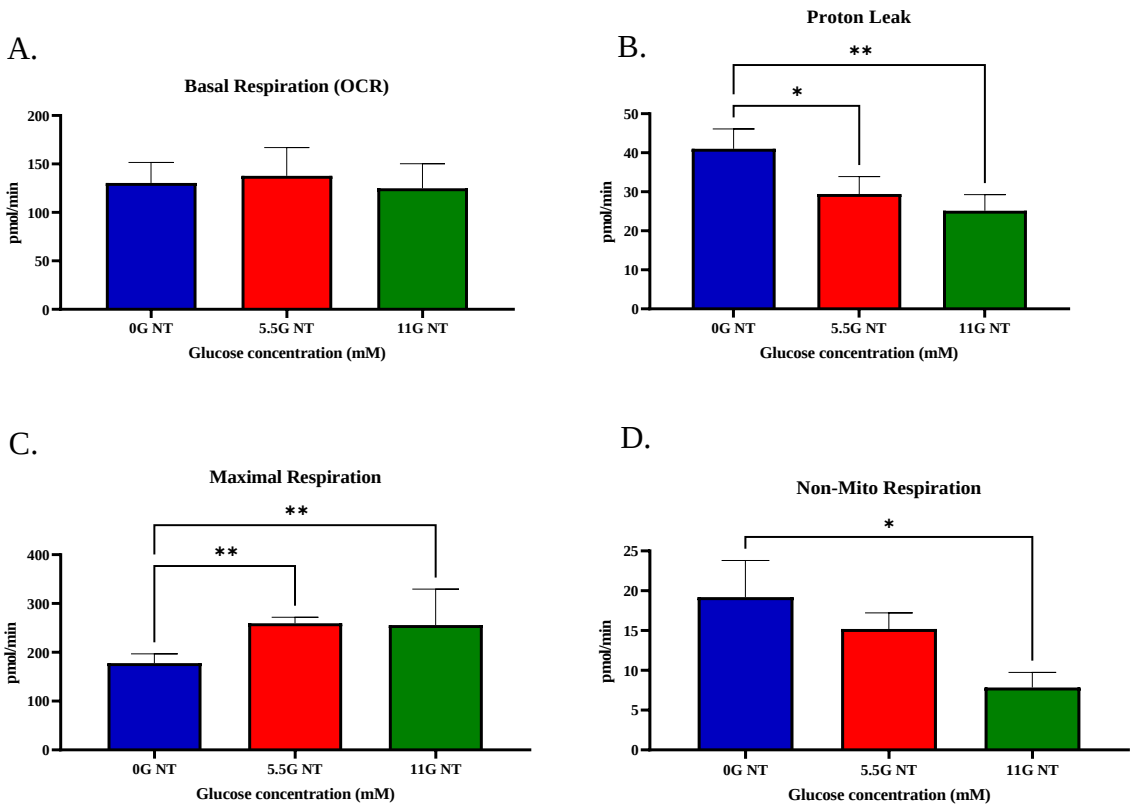

Figure 4. 14: MitoStress Assay of Du145 (metastatic androgen independent) cell line, under zero, 5.5mM and 11mM glucose media, showing the effects on the; (A) Basal OCR was unchanged between the glucose concentrations, (B) Proton leak was decreased in the 5.5mM and 11mM glucose conditions compared to the zero glucose conditions. (C) Maximal respiration was increased in the 5.5mM and 11mM glucose conditions compared to the zero glucose conditions, and (D) The non-mitochondrial respiration was decreased in the 11mM glucose conditions compared to the zero glucose conditions. (n=3) 1-way ANOVA) ($P > 0.05$, ** $P \leq 0.01$, *** $P \leq 0.001$, **** $P \leq 0.0001$).*

4.4.2 The effects of Menadione (macro) and the Novel TH compounds (micro) on the metabolic phenotype of a panel of prostate cell lines under zero, 5.5mM and 11mM glucose conditions

The effect of the macro and micro scale on the metabolic phenotype of the cell lines will allow for the determination of the TH compounds ability to disrupt the Warburg effect, altering the cells reliance on glycolysis. This work was conducted under the glucose gradient to determine if the compounds would have a heightened effect in the different glucose conditions.

Due to no Vitamin C TH compounds being received for this study, the Vitamin C bioenergetics is presented in Appendix 2 to Appendix 37 of the thesis. Overall, Vitamin C increased the proton leak in the cell lines, with the results of significance discussed in the chapter discussion.

4.4.2.1 Treatments with Menadione and the Novel TH compounds did not result in significant alterations to the metabolic phenotype of Prostate cells in 5.5mM glucose conditions.

In zero glucose conditions, the untreated and the Menadione treated PNT1a cells metabolic phenotypes were found to be reliant on OxPhos (80% - 75%). The treatment with the novel TH compounds TH1, TH4 and TH6 did not change the metabolic phenotype for ATP production, as presented in Figure 4.16 **A** and **B**, where the cells remained with a majority reliance on OxPhos.

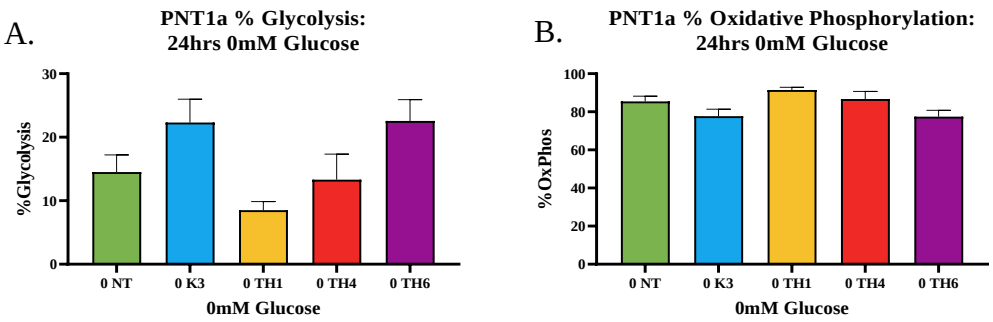

Figure 4. 15: The ATP endpoints of %OxPhos and %Glycolysis for PNT1a cells treated with novel compounds TH1, TH4 and TH6 under zero glucose. (A.) % ATP production by glycolysis was unchanged between the untreated and the treated cells. (B.) % ATP Production by OxPhos was unchanged between the untreated and the treated cells. (n=3) 1-way ANOVA). (* $P > 0.05$, ** $P \leq 0.01$, *** $P \leq 0.001$, **** $P \leq 0.0001$).

LNCaP has a preferential reliance on OxPhos (90%) for its ATP production when in the zero glucose conditions. The treatments of TH1 (87.4%), TH4 (91.0%) and TH6 (73.9%), the ATP production was found to remain within the pathway of OxPhos. Overall, the reliance on glycolysis was found to be low across all treatment groups and the untreated PNT1a cells.

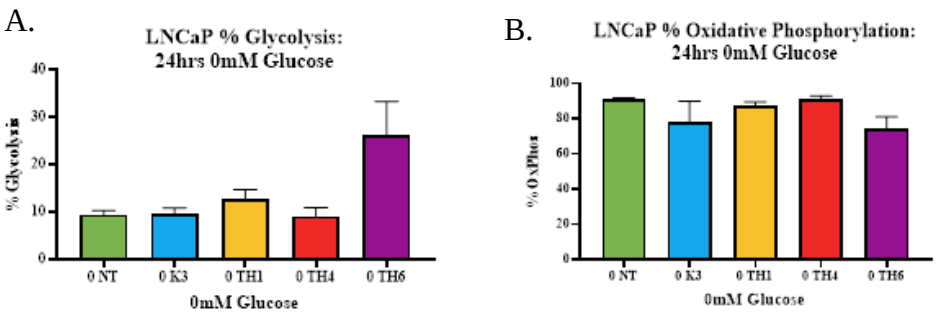

Figure 4. 16: The ATP endpoints of %OxPhos and %Glycolysis for LNCaP cells treated with novel compounds TH1, TH4 and TH6 under zero glucose. (A.) % ATP production by glycolysis was unchanged between the untreated and the treated cells. (B.) % ATP Production by OxPhos was unchanged between the untreated and the treated cells. (n=3) 1-way ANOVA). (* $P > 0.05$, ** $P \leq 0.01$, *** $P \leq 0.001$, **** $P \leq 0.0001$).

PC3 cells present with a metabolic dependency on OxPhos in zero glucose as presented in Figure 4.18 **A** and **B**. This reliance on OxPhos is found to be undisrupted by the treatment with the TH compounds, with all the cells presenting with an ~80% OxPhos reliance.

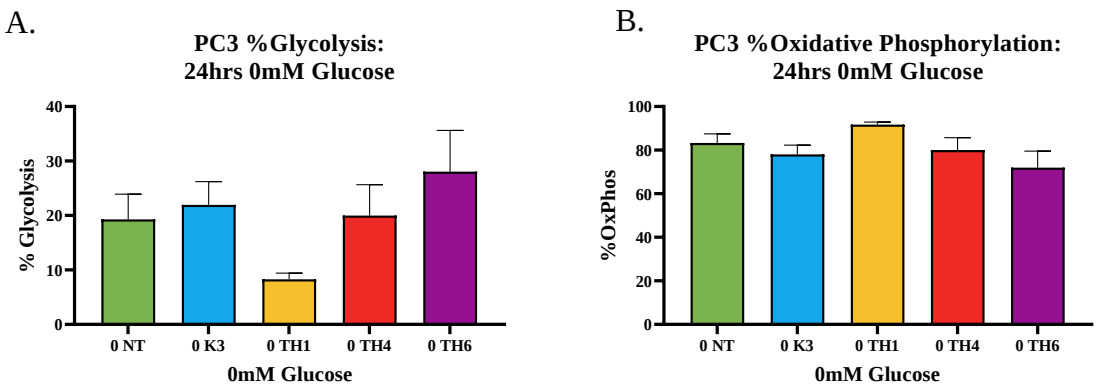

Figure 4. 17: The ATP endpoints of %OxPhos and %Glycolysis for PC3 cells treated with novel compounds TH1, TH4 and TH6 under zero glucose. (A.) % ATP production by glycolysis was unchanged between the untreated and the treated cells. (B.) % ATP Production by OxPhos was unchanged between the untreated and the treated cells. (n=3) 1-way ANOVA). (* $P > 0.05$, ** $P \leq 0.01$, *** $P \leq 0.001$, **** $P \leq 0.0001$).

In the zero glucose conditions, basal Du145 cells express a heavy reliance on OxPhos for ATP production (~80%). This is unchanged with the addition of the novel TH compounds, with the metabolic phenotype maintaining its reliance on OxPhos pathway for energy production also at ~80%. The levels of glycolysis remained low across all the treatment groups, including the untreated Du145 illustrated Figure 4.19 **A** and **B** with no significance achieved between the treatment groups.

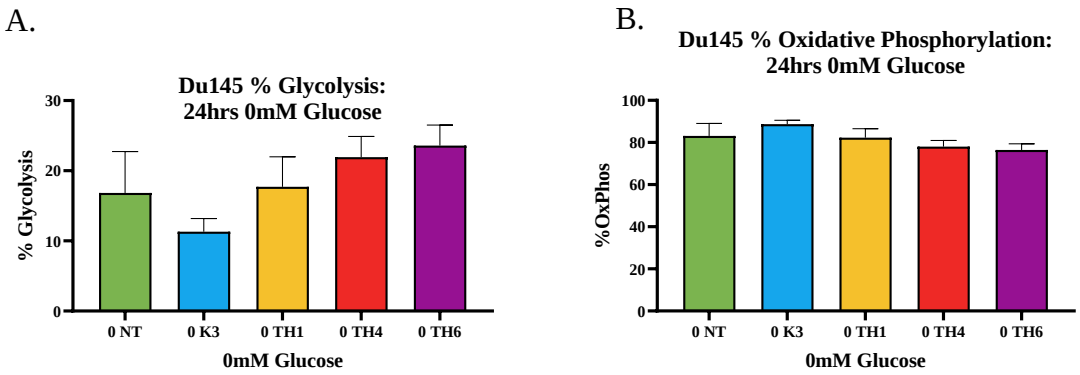

Figure 4. 18: The ATP endpoints of %OxPhos and %Glycolysis for Du145 cells treated with novel compounds TH1, TH4 and TH6 under zero glucose. (A.) % ATP production by glycolysis was unchanged between the untreated and the treated cells. (B.) % ATP Production by OxPhos was unchanged between the untreated and the treated cells. (n=3) 1-way ANOVA). (* $P > 0.05$, ** $P \leq 0.01$, *** $P \leq 0.001$, **** $P \leq 0.0001$).

4.4.2.2 The metabolic reliance on glycolysis and OxPhos was significantly altered across the cell lines in the untreated, and the treated cells in the 5.5mM glucose conditions.

The % glycolysis of the prostate cancer cell lines untreated and treated with menadione, TH1, TH4 and TH6 was compared across the zero glucose conditions. No significant alterations were observed across the cell lines within the treatment groups as illustrated in Figure 4.20. The values obtained for the % glycolysis of the cell lines under 0mM glucose are tabulated in Table 4.2, also showing the similarities in % glycolysis between the cell lines in the different treatment groups.

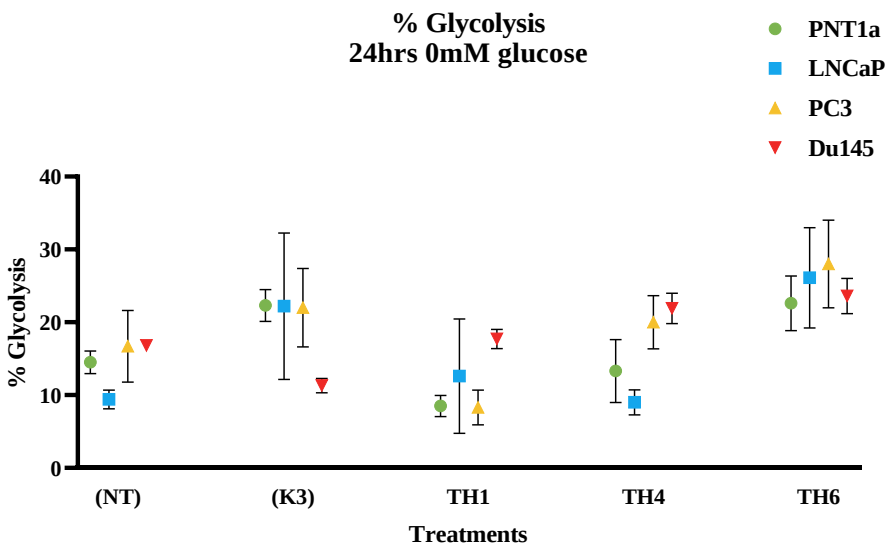

Figure 4. 19: The % glycolysis of the prostate cell lines across the treatment groups in zero glucose conditions where no significant changes were determined between the cell lines in the untreated and the treatments. (n=3) 2-way ANOVA. (P > 0.05, ** P ≤ 0.01, *** P ≤ 0.001, **** P ≤ 0.0001).*

In the zero glucose conditions, all the prostate cell lines display low levels of glycolysis in both the untreated and the treated cells.

Table 4.25: The % Glycolysis determined for the prostate cell lines untreated and when treated with Menadione, TH1, TH4 and TH6 in the zero glucose conditions.

	PNT1a	LNCaP	PC3	Du145
Untreated (NT)	14.5± 2.7	9.4 ± 2.2	16.7 ± 8.5	16.8 ± 0.6
Menadione (K3)	22.3± 3.8	22.2 ± 17.4	22.0 ± 9.3	11.3 ± 1.7
TH1	8.5± 2.5	12.6 ±13.6	8.3 ± 4.1	17.7 ± 2.3
TH4	13.3± 7.5	9.0 ± 3.0	20.0 ± 6.3	21.9 ± 3.6
TH6	22.6± 6.5	26.1 ± 11.9	28.0 ± 10.4	23.6 ± 4.2

The % OxPhos was found to be similar between the cell lines across the treatment groups as shown in Figure 4.21. The values obtained for the % OxPhos of the cell lines under 0mM glucose are tabulated in Table 4.3, also showing the similarities in % OxPhos between the cell lines in the different treatment groups.

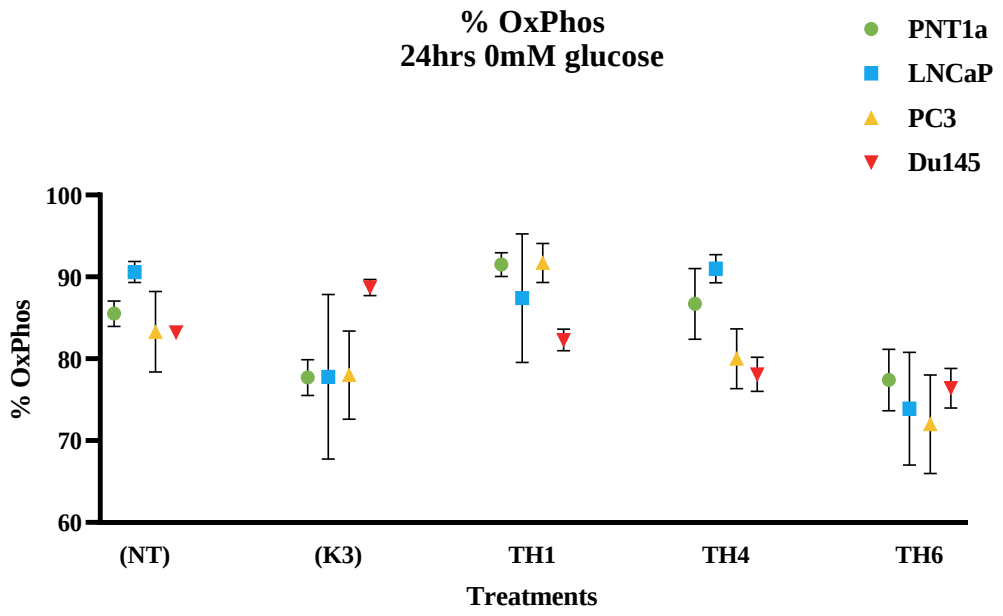

Figure 4. 20: The % oxphos of the prostate cell lines across the treatment groups in zero glucose conditions where no significant changes were determined between the cell lines in the untreated and the treatments. (n=3) 2-way ANOVA. (P > 0.05, ** P ≤ 0.01, *** P ≤ 0.001, **** P ≤ 0.0001).*

The prostate cell lines all present with a high reliance on OxPhos for ATP production in the presence of zero glucose conditions.

Table 4.26: The % OxPhos determined for the prostate cell lines untreated and when treated with Menadione, TH1, TH4 and TH6 in the zero glucose conditions.

	PNT1a	LNCaP	PC3	Du145
Untreated (NT)	85.5 ± 2.7	90.6 ± 2.2	83.3 ± 8.5	83.2 ± 0.6
Menadione (K3)	77.7 ± 3.8	77.8 ± 17.4	78.0 ± 9.3	88.7 ± 1.7
TH1	91.5 ± 2.5	87.4 ± 13.6	91.7 ± 4.1	82.3 ± 2.3
TH4	86.7 ± 7.5	91.0 ± 3.0	80.0 ± 6.3	78.1 ± 3.6
TH6	77.4 ± 6.5	73.9 ± 11.9	72.0 ± 10.4	76.4 ± 4.2

4.4.2.3 Treatments with the Novel Trojan Horse compounds did not significantly alter the metabolic phenotype of the Prostate cells under 5.5M glucose conditions

In the 5.5mM glucose conditions, the PNT1a cells were found to be reliant on glycolysis, however this does decrease with the addition of the novel TH compounds, TH4 and TH6. The treatment with TH4 and TH6 result in a 50:50 reliance on OxPhos and glycolysis for ATP production, whereas the untreated PNT1a show a greater reliance on glycolysis as presented in Figure 4.22 **A** and **B** .

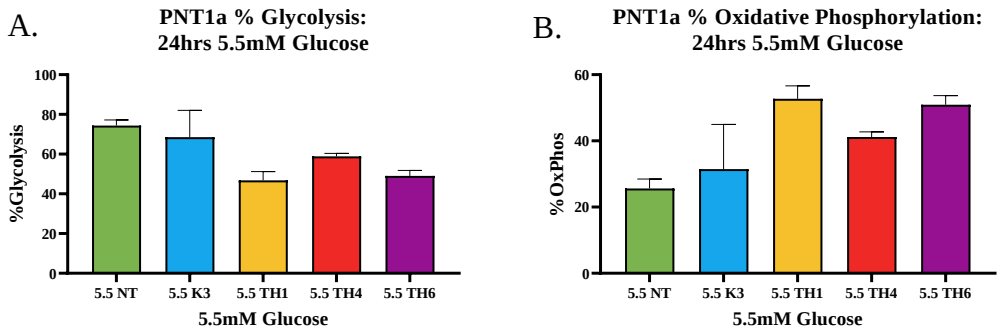

Figure 4. 21: The ATP endpoints of %OxPhos and %Glycolysis for PNT1a cells treated with novel compounds TH1, TH4 and TH6 under zero glucose. (A.) % ATP production by glycolysis was unchanged between the untreated and the treated cells. (B.) % ATP Production by OxPhos was unchanged between the untreated and the treated cells. (n=3) 1-way ANOVA). (* $P > 0.05$, ** $P \leq 0.01$, *** $P \leq 0.001$, **** $P \leq 0.0001$).

In the presence of 5.5mM glucose conditions, LNCaP cell line is found to primarily rely on OxPhos for its ATP production. With the addition of the novel TH compounds, this is found to be unchanged; TH1 (70.0%) TH4 (66.6%) and TH6 (77.1%). The levels of glycolysis reported are low, averaging at around 30% across all the treatment groups as seen in Figure 4.23.

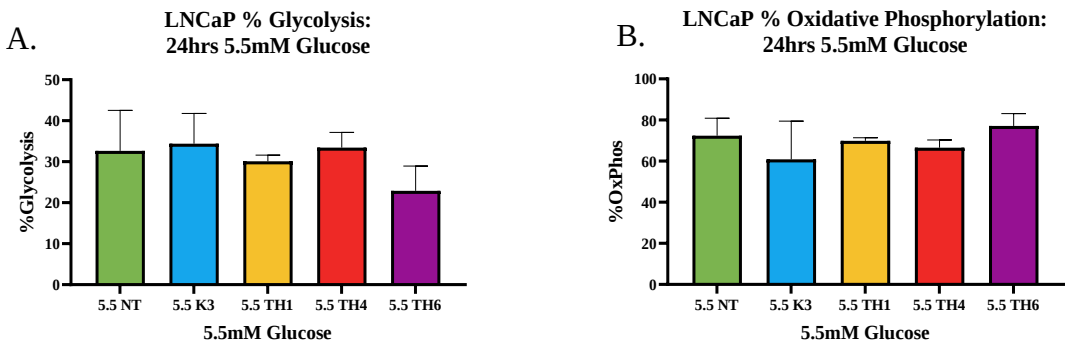

Figure 4. 22: The ATP endpoints of %OxPhos and %Glycolysis for LNCaP cells treated with novel compounds TH1, TH4 and TH6 under 5.5mM glucose. (A.) % ATP production by glycolysis was unchanged between the untreated and the treated cells. (B.) % ATP Production by OxPhos was unchanged between the untreated and the treated cells. (n=3) 1-way ANOVA). (* $P > 0.05$, ** $P \leq 0.01$, *** $P \leq 0.001$, **** $P \leq 0.0001$).

In the presence of 5.5mM glucose, the PC3 cells increase their glycolytic capacity (50.3%). However, the treatment with TH1 (69.2%) and TH6 (69.0%) results in a non-significant increase in glycolysis for ATP production as presented in Figure 4.24.

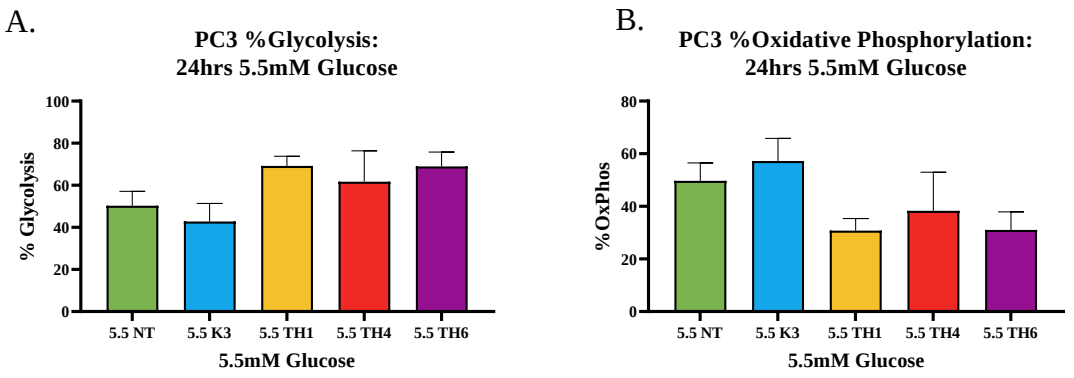

Figure 4. 23: The ATP endpoints of %OxPhos and %Glycolysis for PC3 cells treated with novel compounds TH1, TH4 and TH6 under 5.5mM glucose. (A.) % ATP production by glycolysis was unchanged between the untreated and the treated cells. (B.) % ATP Production by OxPhos was unchanged between the untreated and the treated cells. (n=3) 1-way ANOVA). (* $P > 0.05$, ** $P \leq 0.01$, *** $P \leq 0.001$, **** $P \leq 0.0001$).

The 5.5mM glucose conditions results in a more glycolytic (52.8%) phenotype for the basal Du145 cells. With the novel TH compounds, TH1 (57.7%), TH4 (48.2%) and TH6 (71.7%) treatments, no significant change was observed as in Figure 4.25 below.

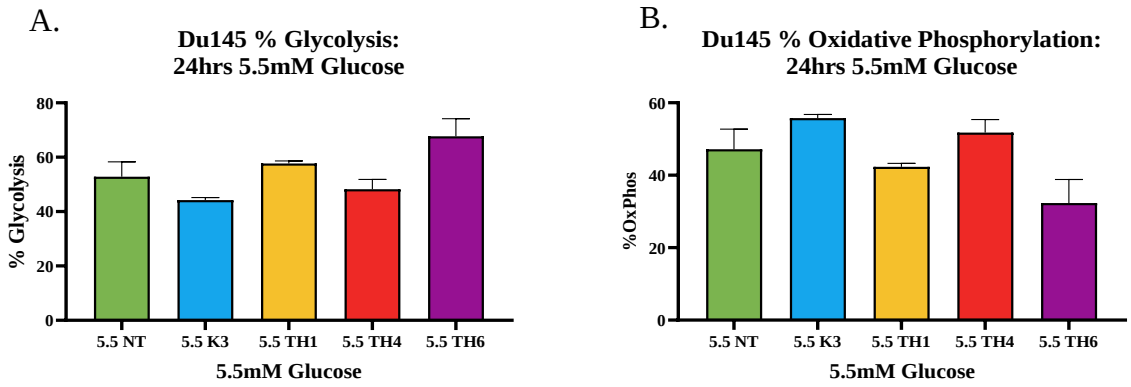

Figure 4. 24: The ATP endpoints of %OxPhos and %Glycolysis for Du145 cells treated with novel compounds TH1, TH4 and TH6 under 5.5mM glucose. (A.) % ATP production by glycolysis was unchanged between the untreated and the treated cells. (B.) % ATP Production by OxPhos was unchanged between the untreated and the treated cells. (n=3) 1-way ANOVA). (* $P > 0.05$, ** $P \leq 0.01$, *** $P \leq 0.001$, **** $P \leq 0.0001$).

4.4.2.4 The metabolic reliance on glycolysis and OxPhos was diverse across the cell lines in the untreated, and the treatment groups in the 5.5mM glucose conditions.

The untreated PNT1a compared to the untreated LNCaP and the Du145 cells showed an increase in glycolysis in the 5.5mM glucose conditions as seen in Figure 4.26. similar levels of glycolysis were seen between the LNCaP, PC3 and Du145 cells treated with Menadione, however an increase in glycolysis is observed in the PNT1a cells. An increase in glycolysis was seen in the PC3 and the Du145 cells treated with TH1 compared to the LNCaP cells treated with TH1. PNT1a, PC3 and Du145 cells showed higher glycolysis as seen in Table 4.4 when treated with TH6 compared to the LNCaP cells treated with TH6. Significance determined for the comparison of the cell lines was *P* <0.0001.

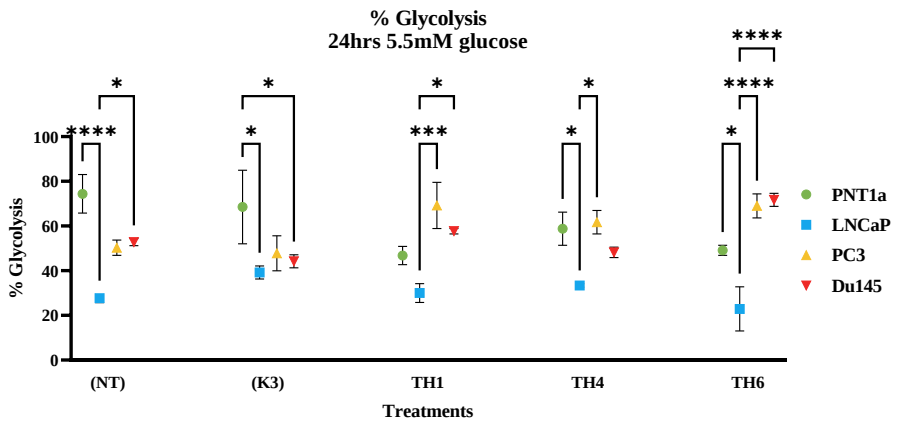

Figure 4. 25: The % glycolysis of the prostate cell lines across the treatment groups in 5.5mM glucose conditions with significance observed between the cell lines in the untreated and the treatment groups. (n=3) 2-way ANOVA. (P > 0.05, ** P ≤ 0.01, *** P ≤ 0.001, **** P ≤ 0.0001).*

Similar levels of glycolysis were determined in the PC3 cells and the Du145 cells in the 5.5mM glucose conditions in the untreated and the treated cells. Overall, LNCaP had the lowest reliance on glycolysis of all the cell lines in 5.5mM glucose conditions as further detailed in Table 4.4 below.

Table 4.27: The % Glycolysis determined for the prostate cell lines untreated and when treated with Menadione, TH1, TH4 and TH6 in the 5.5mM glucose conditions.

	PNT1a	LNCaP	PC3	Du145
Untreated (NT)	74.4 ± 14.9	27.7 ± 3.4	50.3 ± 5.9	52.8 ± 2.8
Menadione (K3)	68.5 ± 28.5	39.2 ± 5.1	47.8 ± 13.6	44.2 ± 5.0
TH1	46.8 ± 7.1	30.0 ± 7.3	69.2 ± 17.9	57.7 ± 2.1
TH4	58.8 ± 12.8	33.4 ± 1.4	61.7 ± 9.1	48.2 ± 4.0
TH6	49.1 ± 3.9	22.9 ± 17.1	69.0± 9.3	71.7 ± 5.0

LNCaP exhibits increased OxPhos in the untreated cells compared to the PNT1a and the Du145 cells in the 5.5mM glucose conditions. Decreased levels of Oxphos was determined in the PNT1a cell line versus the LNCaP and the Du145 cell line all treated with Menadione, with LNCaP, PC3 and Du145 exhibiting a similar level of glycolysis in the Menadione treatment as seen in Figure 4.27 below. PC3 was shown to have lower levels of OxPhos than the LNCaP cells when treated with TH1. In the TH4 treated cells, LNCaP display increased levels of OxPhos compared to the PNT1a and PC3 cells, whereas in the TH6 treated cells, the LNCaP cells had higher oxphos than all three other cell lines. Significance determined for the comparison of the cell lines was P <0.0001.

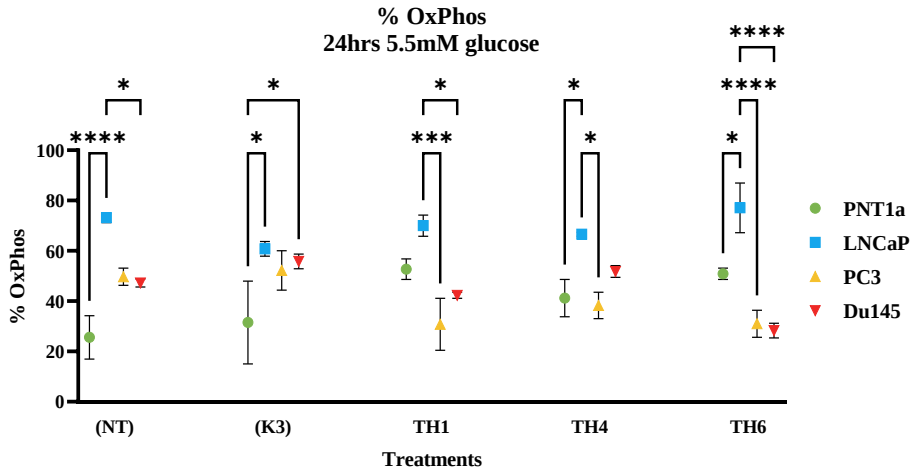

Figure 4. 26: The % oxphos of the prostate cell lines across the treatment groups in 5.5mM glucose conditions with significance observed between the cell lines in the untreated and the treatment groups. (n=3) 2-way ANOVA. (P > 0.05, ** P ≤ 0.01, *** P ≤ 0.001, **** P ≤ 0.0001).*

LNCaP displays the greatest reliance on oxphos across the cell lines, even when treated with Menadione and the TH compounds, with PNT1a and PC3 showing the lowest reliance on OxPhos. The results are further detailed in Table 4.5 below.

Table 4.28: The % OxPhos determined for the prostate cell lines untreated and when treated with Menadione, TH1, TH4 and TH6 in the 5.5mM glucose conditions.

	PNT1a	**LNCaP**	**PC3**	**Du145**
Untreated (NT)	25.6 ± 14.9	72.3 ± 3.4	49.7 ± 5.9	47.2 ± 2.8
Menadione (K3)	31.5 ± 28.5	60.8 ± 5.1	52.2 ± 13.6	55.8 ± 5.0
TH1	52.7 ± 7.1	70.0 ± 7.3	30.8 ± 17.9	42.3 ± 2.1
TH4	41.2 ± 12.8	66.6 ± 1.4	38.3 ± 9.1	51.8 ± 4.0
TH6	50.9 ± 3.9	77.1 ± 17.1	31.0 ± 9.3	28.3 ± 5.0

4.4.2.5 Treatments with Menadione and the Novel TH compounds did not significantly alter the metabolic phenotype of prostate cancer cells under 11mM glucose conditions

The high glucose (11mM) media concentration results in a predominant reliance on glycolysis for ATP production (62.1%). This is found to be unchanged in the treatment with Menadione (47.6%), TH1 (52.3%) and TH4 (62.2%), however, treatment with TH6 resulted in a decrease in glycolytic dependency (24.1%) increasing its OxPhos dependency (75.9%) when compared to the OxPhos (37.9%) levels in the untreated PNT1a cells. Overall, the cells remain with a majority reliance on glycolysis, but treatment with TH6 increased OxPhos.

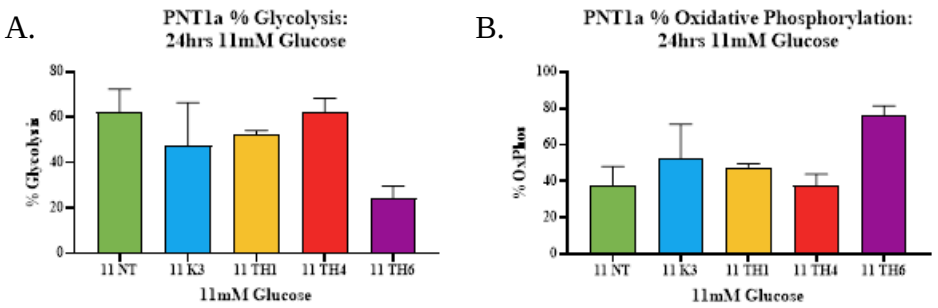

Figure 4. 27: The ATP endpoints of %OxPhos and %Glycolysis for PNT1a cells treated with novel compounds TH1, TH4 and TH6 under zero glucose. (A.) % ATP production by glycolysis was unchanged between the untreated and the treated cells. (B.) % ATP Production by OxPhos was unchanged between the untreated and the treated cells. (n=3) 1-way ANOVA). (* $P > 0.05$, ** $P \leq 0.01$, *** $P \leq 0.001$, **** $P \leq 0.0001$).

In 11mM glucose, LNCaP remains with a predominant reliance on OxPhos (55.5%) as presented in Figure 4.29. This is found to be unchanged in the treatment with Menadione (56.1%), TH1 (66.2%) and TH4 (69.3%). Nevertheless, the treatment of LNCaP with TH6 resulted in a drop in glycolytic dependency and an increase in OxPhos to 81.7%.

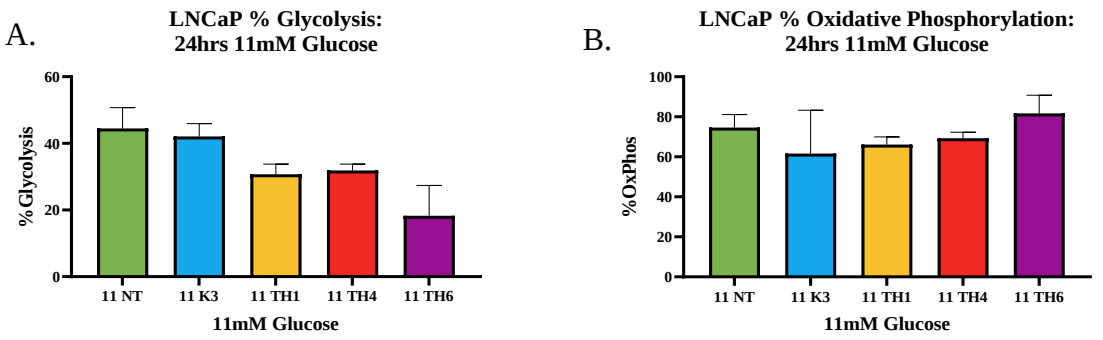

Figure 4. 28: The ATP endpoints of %OxPhos and %Glycolysis for LNCaP cells treated with novel compounds TH1, TH4 and TH6 under 5.5mM glucose . (A.) % ATP production by glycolysis was unchanged between the untreated and the treated cells. (B.) % ATP Production by OxPhos was unchanged between the untreated and the treated cells. (n=3) 1-way ANOVA). (* P > 0.05, ** P ≤ 0.01, *** P ≤ 0.001, **** P ≤ 0.0001).

The 11mM glucose conditions result in a preponderant dependence on glycolysis of 56.0% for the untreated PC3 cells. The PC3 cells are unhindered by treatment with the novel TH compounds and remain in their metabolic phenotypes with a ~60% dependence on glycolysis. The results are presented in Figure 4.30.

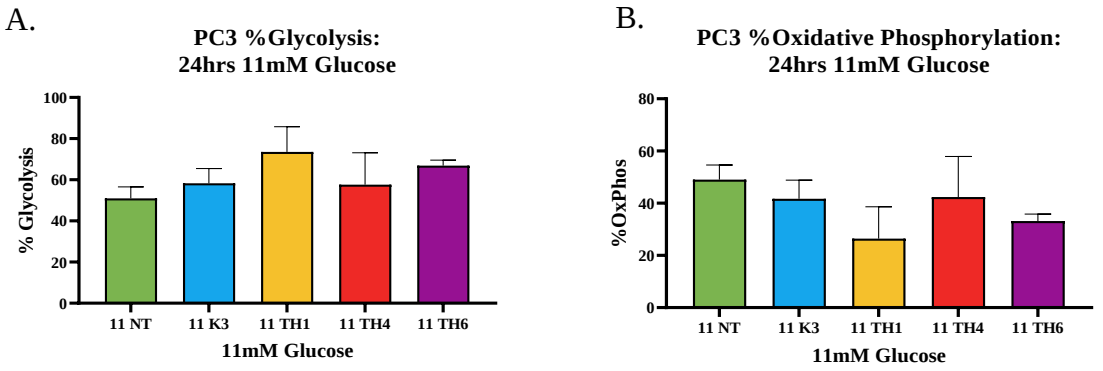

Figure 4. 29: The ATP endpoints of %OxPhos and %Glycolysis for PC3 cells treated with novel compounds TH1, TH4 and TH6 under 11mM glucose. (A.) % ATP production by glycolysis was unchanged between the untreated and the treated cells. (B.) % ATP Production by OxPhos was unchanged between the untreated and the treated cells. (n=3) 1-way ANOVA). (* P > 0.05, ** P ≤ 0.01, *** P ≤ 0.001, **** P ≤ 0.0001).

The 11mM glucose environment shifts the Du145 metabolic phenotype more towards glycolysis (58.6%). All the treatment groups result in Du145 cells maintaining their glycolytic reliance (~55%) for ATP production as shown in Figure 4.31.

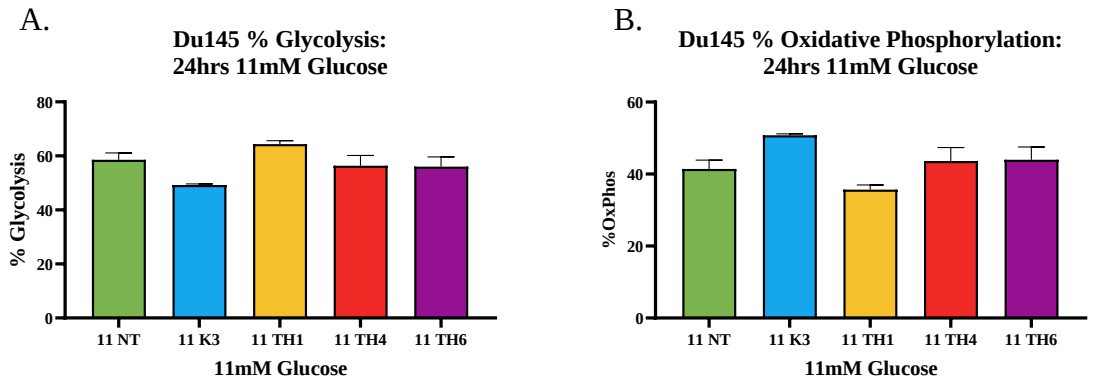

Figure 4. 30: The MitoStress endpoints for Du145 cells treated with novel compounds TH1, TH4 and TH6 under 5.5mM glucose. (A.) % ATP production by glycolysis was unchanged between the untreated and the treated cells. (B.) % ATP Production by OxPhos was unchanged between the untreated and the treated cells. (n=3) 1-way ANOVA). (* P > 0.05, ** P ≤ 0.01, *** P ≤ 0.001, **** P ≤ 0.0001).

4.4.2.6 The metabolic reliance on glycolysis and OxPhos was different across the cell lines in the untreated, and the treatment groups in the 11mM glucose conditions.

An increase in glycolysis was seen in the PC3 and the Du145 cells treated with TH1 compared to the LNCaP cells treated with TH1. In the TH4 treatment group, PC3 cells display a greater reliance on glycolysis compared to the LNCaP cells. The PC3 and Du145 cells present with a higher glycolytic phenotype than PNT1a and PC3 cells when treated with TH6 in the 11mM glucose conditions with results presented in Figure 4.32. Significance for the comparison of the cell lines was P <0.0001.

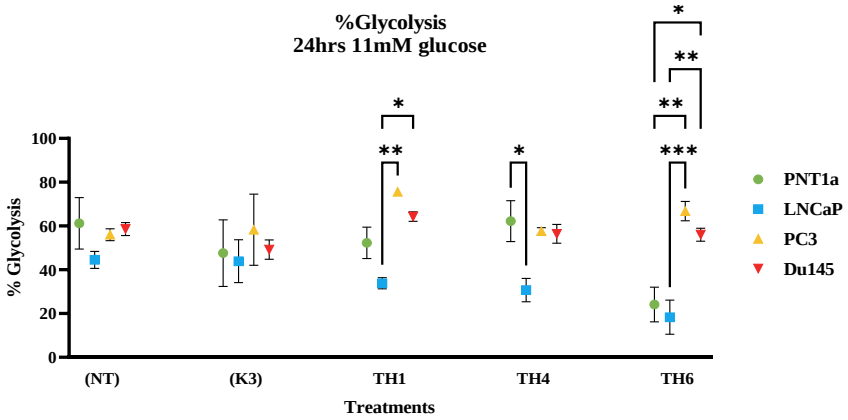

Figure 4. 31: The % glycolysis of the prostate cell lines across the treatment groups in 11mM glucose conditions. Significant alterations were observed across the cell lines in the TH1, TH4 and TH6 treatments. (n=3) 2-way ANOVA. (P > 0.05, ** P ≤ 0.01, *** P ≤ 0.001, **** P ≤ 0.0001).*

Similar levels of glycolysis were determined in the untreated PNT1a, PC3 cells and the Du145 cells in the 11mM, while treatment with Menadione resulted in all the cell lines displaying a comparable glycolytic reliance. However, levels of glycolysis were varied when the cell lines were treated with the novel TH compounds. Once more, even in the presence of glucose LNCaP had the lowest reliance on glycolysis of all the cell lines in the 11mM glucose conditions.

Table 4.29: The % Glycolysis determined for the prostate cell lines untreated and when treated with Menadione, TH1, TH4 and TH6 in the 11mM glucose conditions.

	PNT1a	LNCaP	PC3	Du145
Untreated (NT)	62.1 ± 20.4	44.5 ± 6.7	56.0 ± 4.7	58.6 ± 5.1
Menadione (K3)	47.6 ± 26.3	43.9 ± 17.0	58.3 ± 28.1	49.2 ± 7.6
TH1	52.3 ± 12.4	33.8 ± 4.4	75.6 ± 2.7	64.3 ± 3.7
TH4	62.2 ± 16.2	30.7 ± 9.2	57.6 ± 2.8	56.4 ± 7.4
TH6	24.1 ± 13.7	18.3 ± 13.5	66.8 ± 7.7	56.0 ± 5.1

LNCaP exhibits increased OxPhos in the untreated cells compared to the PNT1a and the Du145 cells in the 5.5mM glucose conditions. Decreased levels of Oxphos was determined in the PNT1a cell line versus the LNCaP and the Du145 cell line all treated with Menadione, with LNCaP, PC3 and Du145 exhibiting a similar level of glycolysis in the Menadione treatment as seen in Figure 4.33 below. PC3 was shown to have lower levels of OxPhos than the LNCaP cells when treated with TH1. In the TH4 treated cells, LNCaP display increased levels of OxPhos compared to the PNT1a and PC3 cells, whereas in the TH6 treated cells, the LNCaP cells had higher oxphos than all three other cell lines. Significance determined for the comparison of the cell lines was P <0.0001.

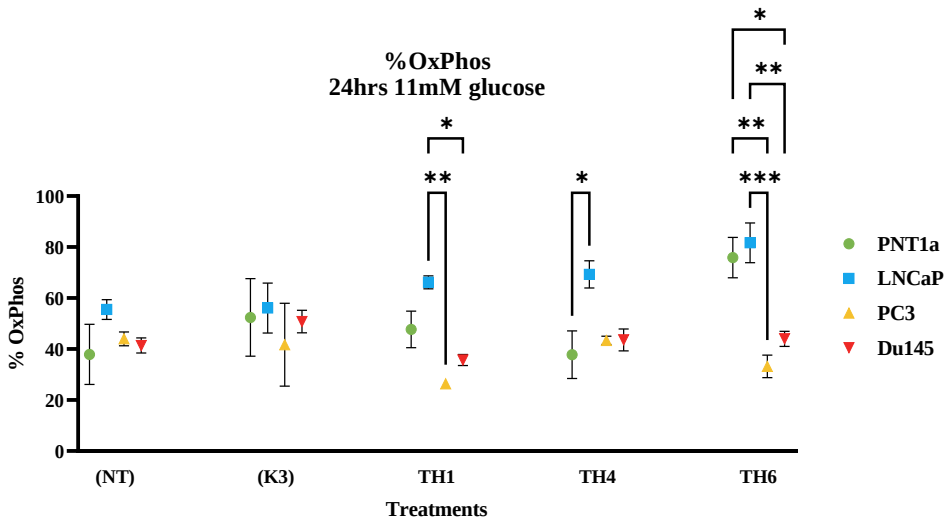

Figure 4. 32: The % OxPhos of the prostate cell lines across the treatment groups in 11mM glucose conditions. Significant alterations were observed across the cell lines in the TH1, TH4 and TH6 treatments. (n=3) 2-way ANOVA. (P > 0.05, ** P ≤ 0.01, *** P ≤ 0.001, **** P ≤ 0.0001).*

The TH treatments resulted in LNCaP to have significantly increased OxPhos compared to the PC3 and Du145 cell lines in the 11mM glucose conditions.

Table 4.30: The % OxPhos determined for the prostate cell lines untreated and when treated with Menadione, TH1, TH4 and TH6 in the 11mM glucose conditions.

	PNT1a	LNCaP	PC3	Du145
Untreated (NT)	37.9 ± 20.4	55.5 ± 6.7	44.0 ± 4.7	41.4 ± 5.1
Menadione (K3)	52.4 ± 26.4	56.1 ± 17.0	41.7 ± 28.1	50.8 ± 7.6
TH1	47.7 ± 12.4	66.2 ± 4.4	26.4 ± 2.7	35.7 ± 3.7
TH4	37.8 ± 16.1	69.3 ± 9.2	43.4 ± 2.8	43.6 ± 7.4
TH6	75.9 ± 13.7	81.7 ± 13.5	33.2 ± 7.7	44.0 ± 5.1

4.4.3 The effects of Menadione (macro) and the Novel TH compounds (micro) on the mitochondrial bioenergetics of a panel of prostate cell lines under zero, 5.5mM and 11mM glucose conditions

The effect of the macro and micro scale on the mitochondrial bioenergetics of the cell lines will allow for insight into the mechanism of cell kill that we have proposed for the compounds. The proposed ROS producing capabilities of the compounds should result in alterations to the mitochondrial bioenergetics, resulting in mitochondrial dysfunction due to oxidative stress. Once more, this work was conducted under the glucose gradient to determine if the compounds would have a heightened effect in the different glucose conditions, and to determine if the glucose conditions will allow for recovery of the cells mitochondrial following treatment and the resulting oxidative stress.

4.4.3.1 Menadione and the TH compounds alter the OCR, proton leak, maximal respiration, and the non-mitochondrial respiration of the panel of prostate cell lines in the zero glucose conditions

The OCR of PNT1a cells (134.4pmol/min) under zero glucose was found to be reduced (P= 0.02) when treated with TH1 (69.5pmol/min) and TH4 (40.8pmol/min), compared to the TH6 treated cells (151.1pmol/min). Otherwise, no significant changes were observed in the mitochondrial metabolism for the PNT1a cells in the presence of zero glucose, between the untreated and the treated cells as presented in Figure 4.34.

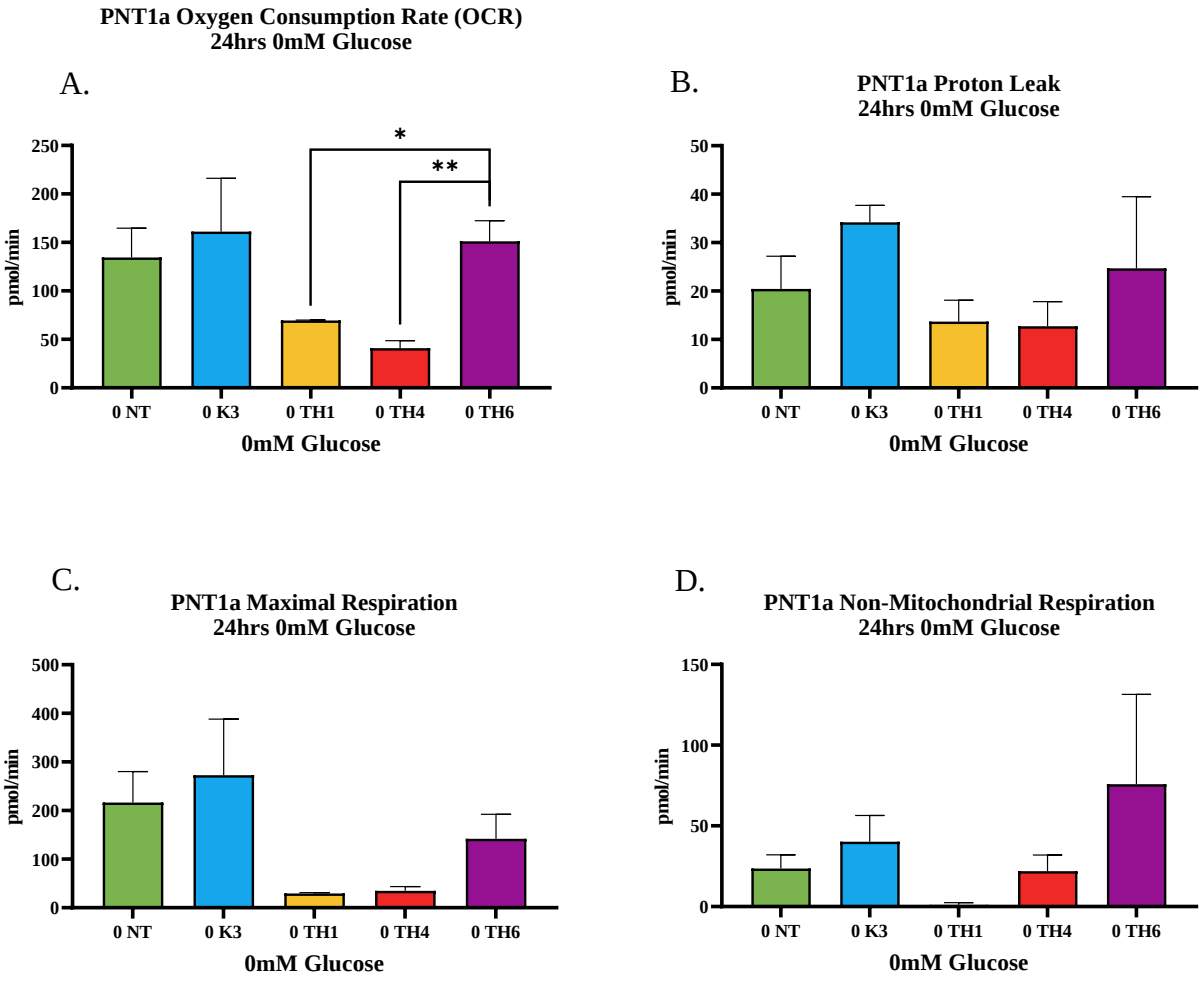

Figure 4. 33: The MitoStress endpoints for PNT1a cells treated with Menadione (K3), TH1, TH4 and TH6 under zero glucose showing the effects on the; (A) Basal OCR, decreased in the TH1 and TH4 treated cells. (B) Proton leak, unchanged across the treatment and the untreated cells. (C) Maximal respiration was unchanged across the treatments and the untreated cells. (D) The non-mitochondrial respiration was unchanged in the untreated and the treated cells. (n=3) 1-way ANOVA). (P > 0.05, ** P ≤ 0.01, *** P ≤ 0.001, **** P ≤ 0.0001).*

The OCR of LNCaP (522.4pmol/min) treated with TH4 showed no change in levels (457.4pmol/min). LNCaP treated with TH1 (237.1pmol/min) TH6 (119.9pmol/min) was found to have a decrease in OCR levels. A significance decrease (P= 0.0002) in OCR was found between Menadione treated LNCaP (469.7pmol/min) and the TH6 treated LNCaP cells. highlighting the compounds' ability to alter the mitochondrial function.

Proton leak for the LNCaP (132.0pmol/min) cells was decreased (P= 0.04) with the TH6 (23.3pmol/min) treatment. Maximal respiration of the LNCaP (647.1pmol/min) cells was decreased (P=0.03) with the TH1 (214.5pmol/min) treatment**.** The non-mitochondrial respiration of LNCaP was found to be unchanged with the novel compound treatments. This highlights the possible dysfunction to the mitochondria, due to the ROS producing TH compounds. The results of the MitoStress test are presented in Figure 4.35.

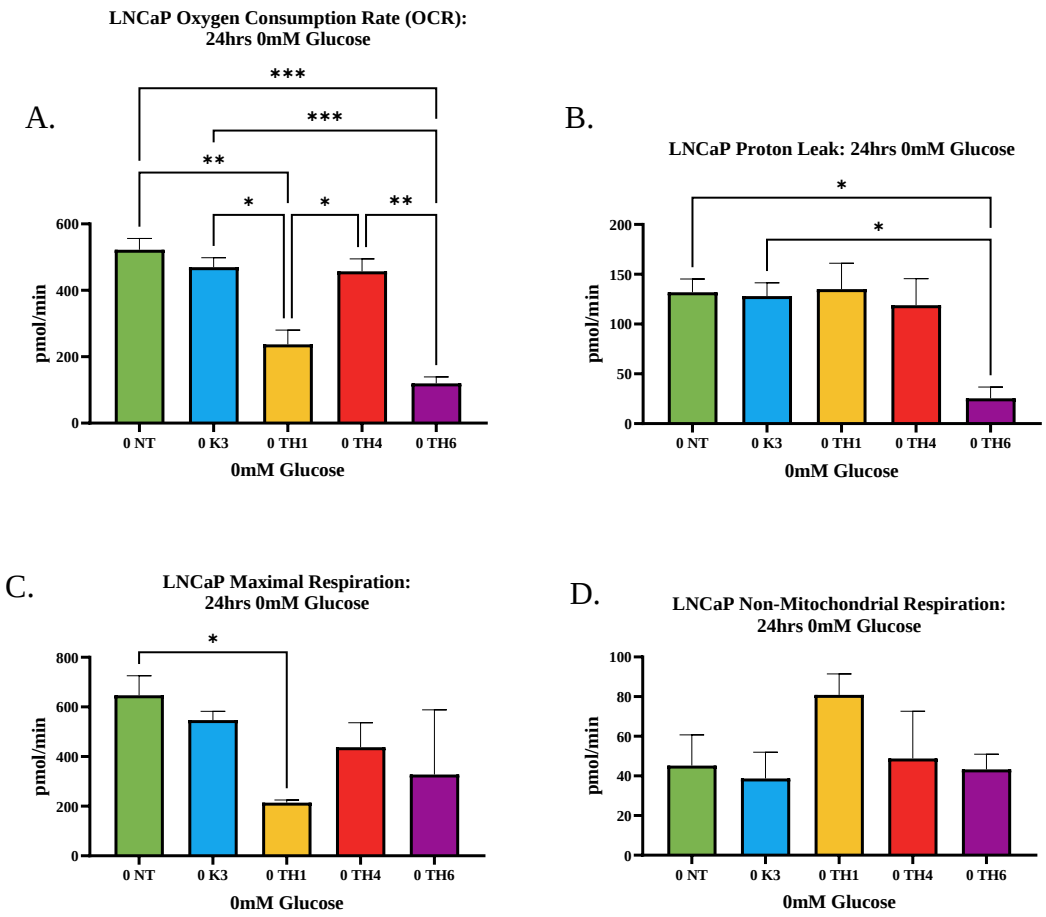

Figure 4. 34: The MitoStress endpoints for LNCaP cells treated with novel compounds TH1, TH4 and TH6 under zero glucose showing the effects on the; (A) Basal OCR was decreased in the TH1 and TH6 treatments. (B) Proton leak was decreased in the cells treated with TH6. (C) Maximal respiration was decreased in the TH1 treated cells. (D) The non-mitochondrial respiration was unchanged between the untreated and the treated cells. (n=3) 1-way ANOVA). (P > 0.05, ** P ≤ 0.01, *** P ≤ 0.001, **** P ≤ 0.0001).*

In zero glucose, the basal OCR of the PC3 cells is unhindered by the treatment with the novel TH compounds. Proton leak was found to be consistent across the treatments to the untreated PC3 cells. No significant alterations were observed in the maximal respiration and the non-mitochondrial respiration of PC3 in the zero glucose and the novel TH treatments, as observed in Figure 4.36.

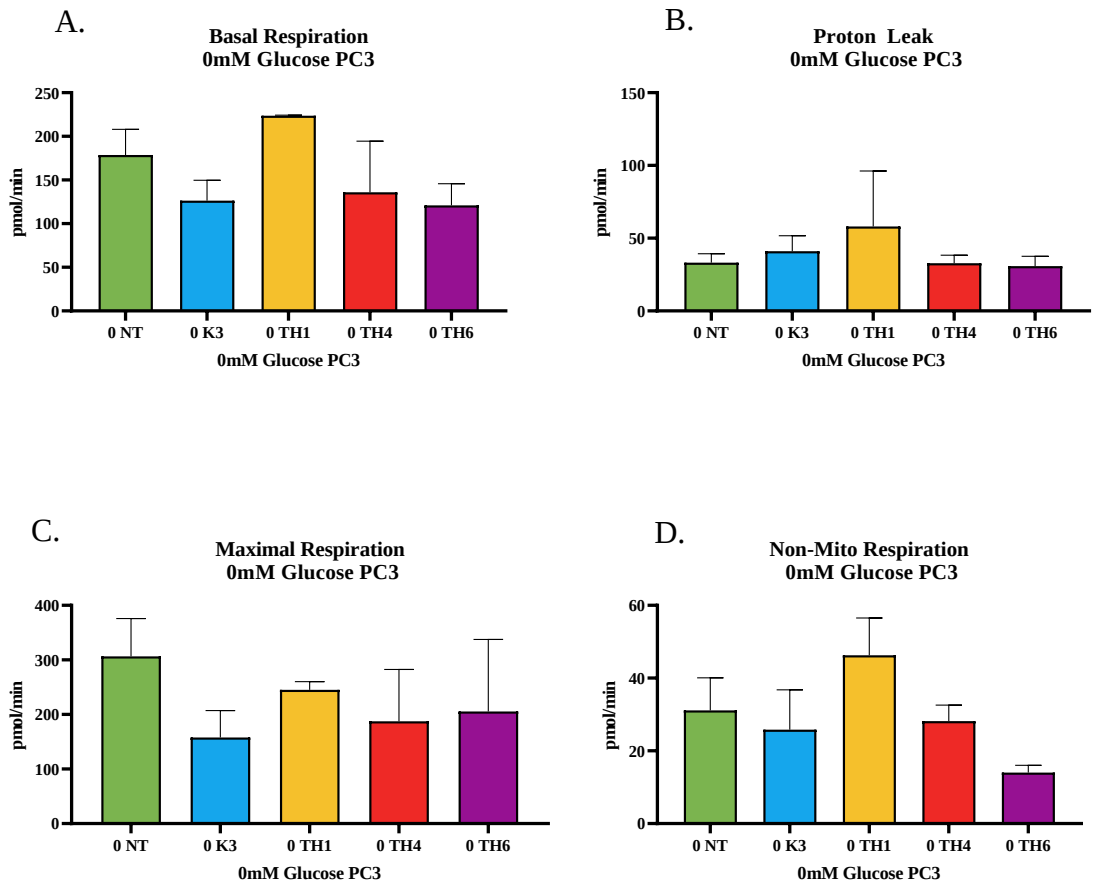

Figure 4. 35: The MitoStress endpoints for PC3 cells treated with novel compounds TH1, TH4 and TH6 under zero glucose showing the effects on the; (A) Basal OCR was unchanged between the untreated and the treated cells. (B) Proton leak was unchanged between the untreated and the treated cells. (C) Maximal respiration was unchanged between the untreated and the treated cells. (D) The non-mitochondrial respiration was unchanged between the untreated and the treated cells (n=3) 1-way ANOVA). ($P > 0.05$, ** $P \leq 0.01$, *** $P \leq 0.001$, **** $P \leq 0.0001$).*

In the zero glucose conditions, the OCR of Du145 was found to be unchanged across the treatment groups. The proton leak was found to be unchanged for the treatment with TH1 and TH4. The treatment with TH6 (44.2pmol/min) resulted in an increase (P=0.02) in the proton leak, compared to the untreated cells (26.2pmol/min). The maximal respiration of Du145 cells were unchanged across the treatment groups, with TH treatments resulting in no significant alteration to the levels recorded. The non-mitochondrial respiration (14.8pmol/min) of the Du145 cells were unchanged with the TH1 (17.6pmol/min) and TH4 (11.8pmol/min) treatments. However, the treatment with TH6 (-7.2pmol/min) resulted in a decrease (P=0.04) in non-mitochondrial respiration. The results reported indicate some alterations to the function of the mitochondria, when treated with the novel TH compounds as seen in Figure 4.37.

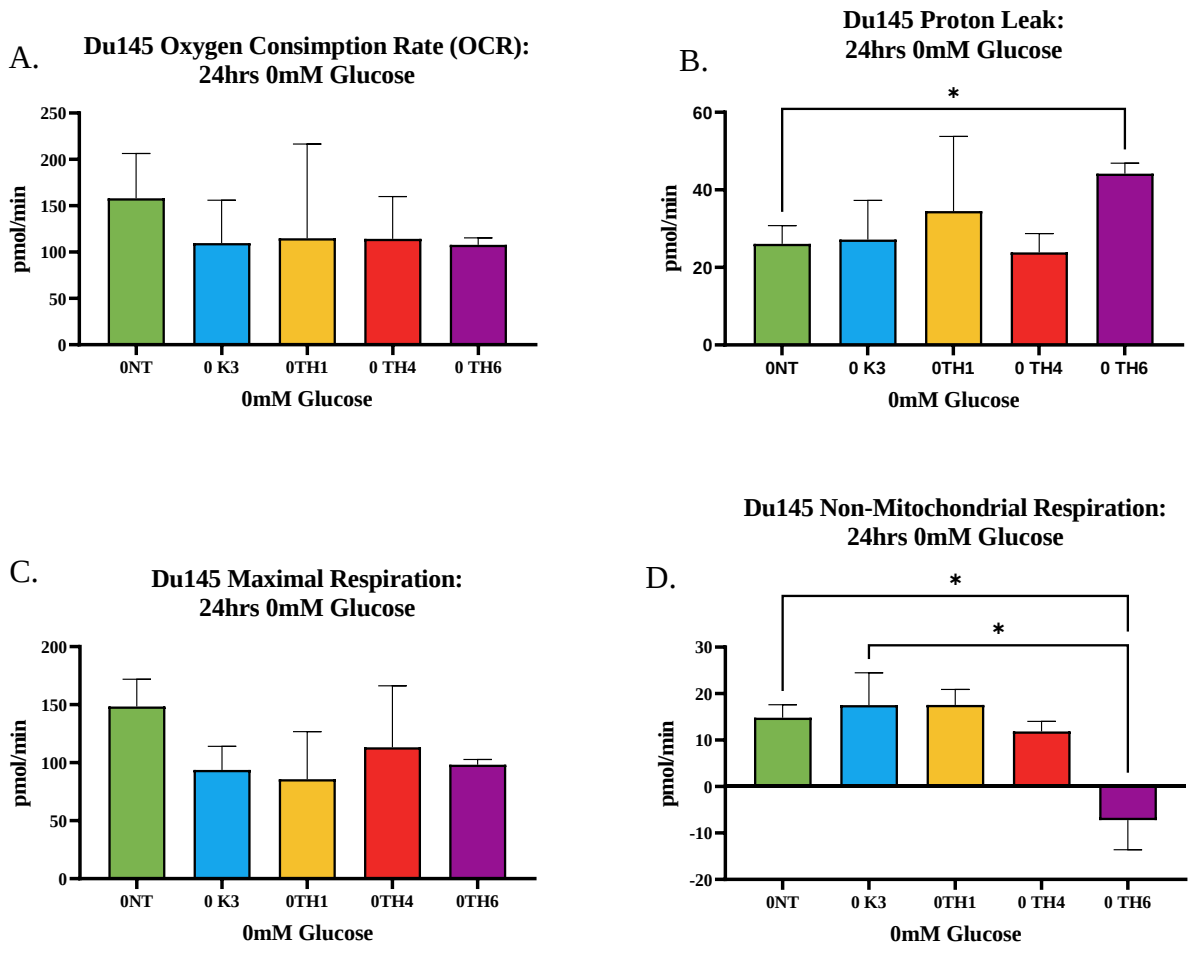

Figure 4. 36: The MitoStress endpoints for Du145 cells treated with novel compounds TH1, TH4 and TH6 under zero glucose showing the effects on the; (A) Basal OCR was unchanged between the untreated and the treated cells. (B) Proton leak was increased in the TH6 treated cells. (C) Maximal respiration was unchanged between the untreated and the treated cells and (D) The non-mitochondrial respiration was decreased in the cells treated with TH6. (n=3) 1-way ANOVA). (P > 0.05, ** P ≤ 0.01, *** P ≤ 0.001, **** P ≤ 0.0001).*

The OCR of the cell lines in zero glucose was highest in the LNCaP cells across the untreated and the Menadione, TH1 and TH4 treated cells ($P \leq 0.0001$), but in the TH6 treated cells, the OCR levels were all similar, with the same trend was observed in the proton leak ($P \leq 0.0001$). Implicating the impact of TH6 on the function of the mitochondria in the cell lines.

LNCaP presents with the highest maximal respiration of the cell lines in the zero-glucose media in all the untreated and treated groups ($P \leq 0.0001$). The untreated, menadione and TH4 treated cells had similar non-mitochondrial respiration levels, while LNCaP treated with TH1 and PNT1a treated with TH6 had the highest levels of non-mitochondrial respiration ($P \leq 0.0001$). The difference in the MitoStress endpoints is found in Figure 4.38 below, illustrating that LNCaP had the highest reliance on oxphos of the cell lines, due to having the highest mitochondrial bioenergetics in the zero glucose conditions.

.

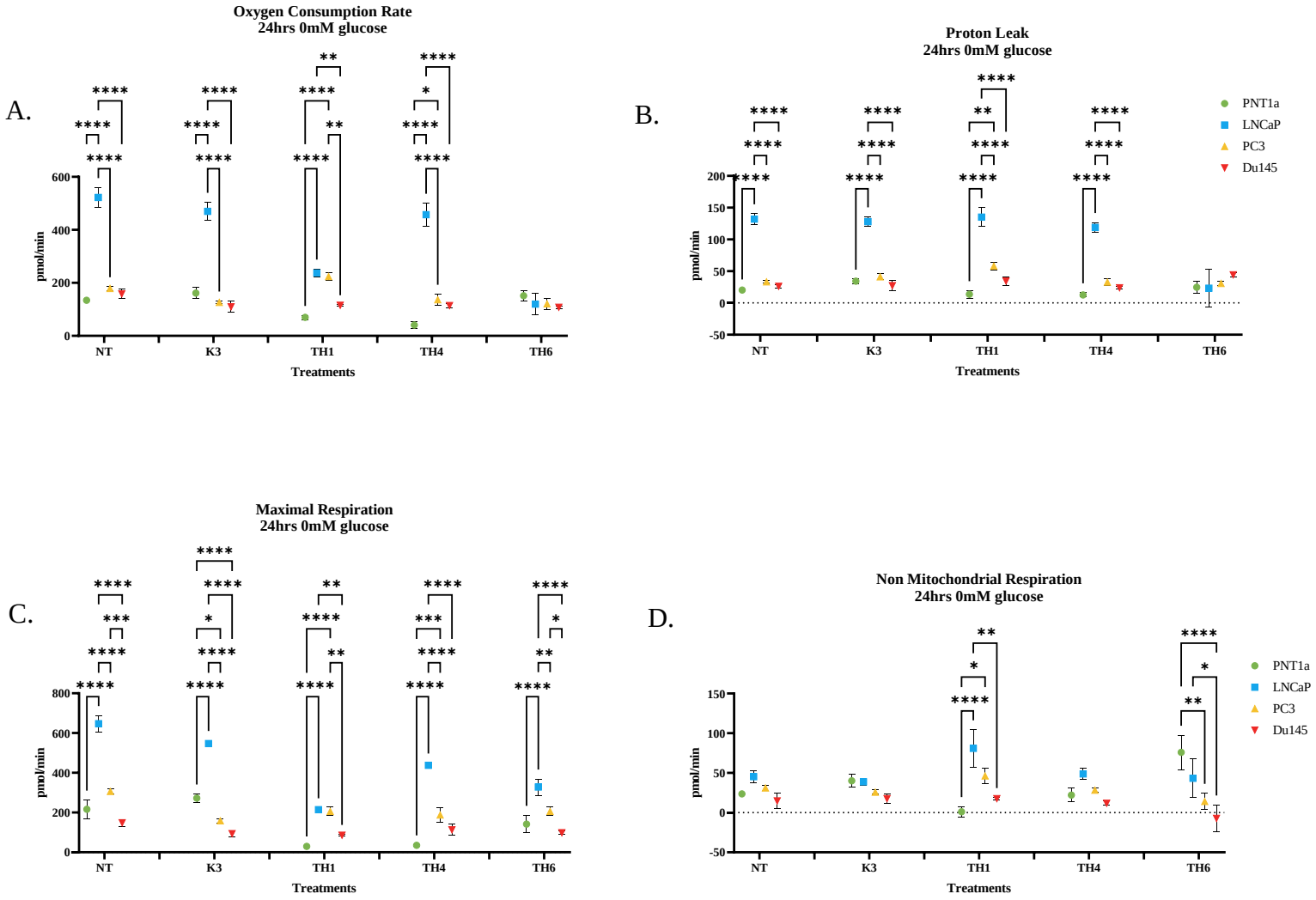

Figure 4. 37: The MitoStress endpoints for PNT1a, LNCaP, PC3 and Du145 cells untreated and treated with Menadione, TH1, TH4 and TH6 under zero glucose showing the effects on the; (A) Basal OCR was highest in the LNCaP cells. (B) Proton highest in the LNCaP cells expect similar levels were found in all cell lines treated with TH6. (C) Maximal respiration was highest in the LNCaP cells and (D) The non-mitochondrial respiration was similar in the cell lines in the untreated, menadione and TH4 treated cells but highest in the TH1 treated LNCaP and highest in the TH6 treated PNT1a cells. (n=3) 1-way ANOVA). ($P > 0.05$, ** $P \leq 0.01$, *** $P \leq 0.001$, **** $P \leq 0.0001$).*

4.4.3.2 Menadione and the TH compounds alter the OCR, proton leak, maximal respiration, and the non-mitochondrial respiration of the panel of prostate cell lines in the 5.5mM glucose conditions

The OCR of the PNT1a cells (240.2pmol/min) under 5.5mM glucose, was reduced (*P*= 0.004) when treated with TH1 (19.7pmol/min) and TH4 (42.3pmol/min) when compared to the Menadione (252.6pmol/min) treated cells as presented in Figure 4.39 **A**. Similar levels of proton leak were observed between the untreated (42.9pmol/min), Menadione (43.1pmol/min) treated and the TH6 (45.5pmol/min) treated PNT1a cells. The OCR was decreased (*P*= 0.004) in the TH1 (2.3pmol/min) and the TH4 (11.0pmol/min) treatments as presented in Figure 4.39 **B**. No significant change was observed in the maximal respiration and non-mitochondrial respiration of the PNT1a cells under 5.5mM glucose. The decrease in OCR and proton leak, may be indicators of alteration to the PNT1a cells mitochondria, following treatment.

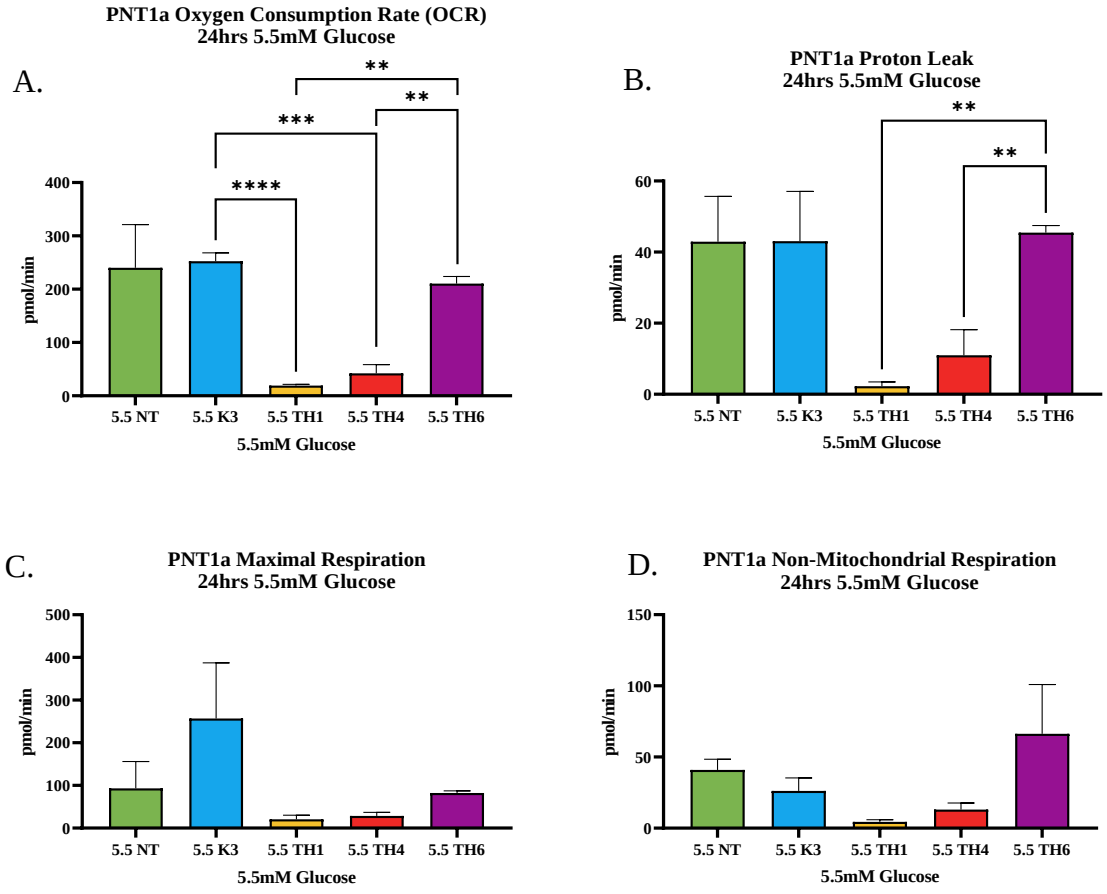

Figure 4. 38: The MitoStress endpoints for PNT1a cells treated with Menadione (K3), TH1, TH4 and TH6 under 5.5mM glucose showing the effects on the; (A) Basal OCR was decreased in the cells treated with TH1 and TH4, (B) Proton leak decreased in the cells treated with TH1 and TH4. (C) Maximal respiration was unchanged between the untreated and the treated cells. (D) The non-mitochondrial respiration was unchanged between the untreated and the treated cells. (n=3) 1-way ANOVA. (P > 0.05, ** P ≤ 0.01, *** P ≤ 0.001, **** P ≤ 0.0001).*

The basal OCR for LNCaP under 5.5mM glucose was found to be at 546.9pmol/min, the treatment with TH1 (57.0pmol/min) TH6 (142.4pmol/min) reduced the OCR levels significantly ($P<0.0001$). The proton leak (160.6pmol/min) was found to be unchanged with the addition of TH4 (107.2pmol/min). The treatment with Menadione (94.2pmol/min), TH1 (35.5pmol/min) TH6 (37.0pmol/min) reduced ($P= 0.0006$) the proton leak. The maximal respiration of LNCaP (761.5pmol/min) was decreased ($P= 0.03$) with the TH1 (42.1pmol/min) and TH6 (95.4pmol/min) treatment. The non-mitochondrial respiration was found to increase with the novel TH4 and TH6 treatments, but not to significance. The results are presented in Figure 4.40 below.

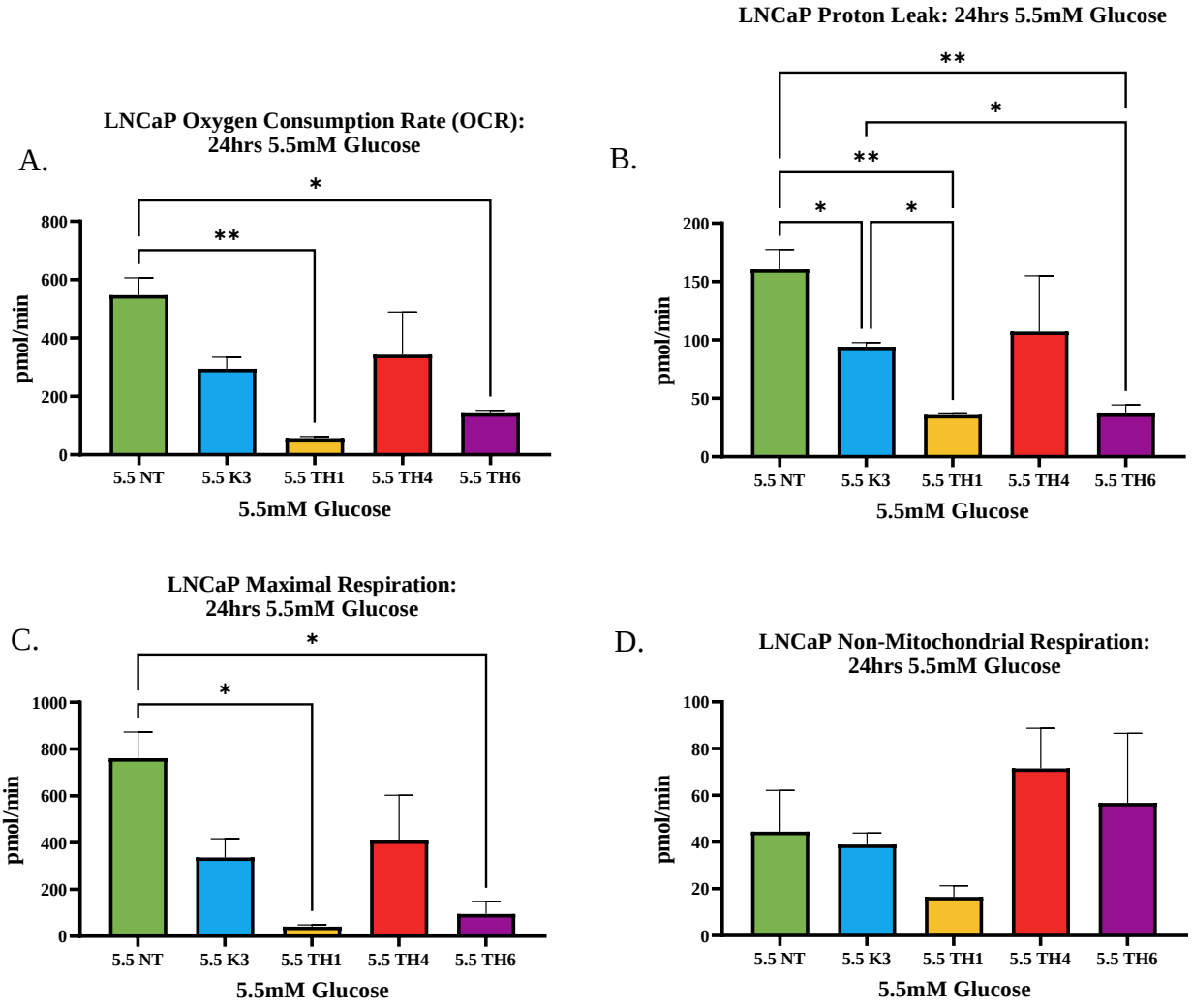

Figure 4. 39: The MitoStress endpoints for LNCaP cells treated with novel compounds TH1, TH4 and TH6 under 5.5mM glucose showing the effects on the; (A) Basal OCR was decreased in the TH1 and the TH6 treated cells. (B) Proton leak was decreased in the Menadione, TH1 and TH6 treated cells. (C) Maximal respiration was decreased in the TH1 and the TH6 treated cells. (D) The non-mitochondrial respiration was unchanged between the untreated and the treated cells. (n=3) 1-way ANOVA). ($P > 0.05$, ** $P \leq 0.01$, *** $P \leq 0.001$, **** $P \leq 0.0001$).*

In the 5.5mM glucose, the PC3 cells basal OCR (262.5pmol/min) saw a reduction in levels, with the novel TH treatments. TH4 (71.8pmol/min) and TH6 (54.3pmol/min) resulted in a significant loss (P= 0.02) of OCR. Proton leak was reduced with the novel compound, TH6 (15.6pmol/min) treatment resulted in a decrease (P=0.0003), compared to the TH4 (43.6pmol/min) treated cells. Maximal respiration saw a reduction observed across the treatment groups, with significance observed in the TH6 treatment group (P=0.03). Non-mitochondrial respiration was unchanged between the untreated cells and the treated cells, with the results presented in Figure 4.41.

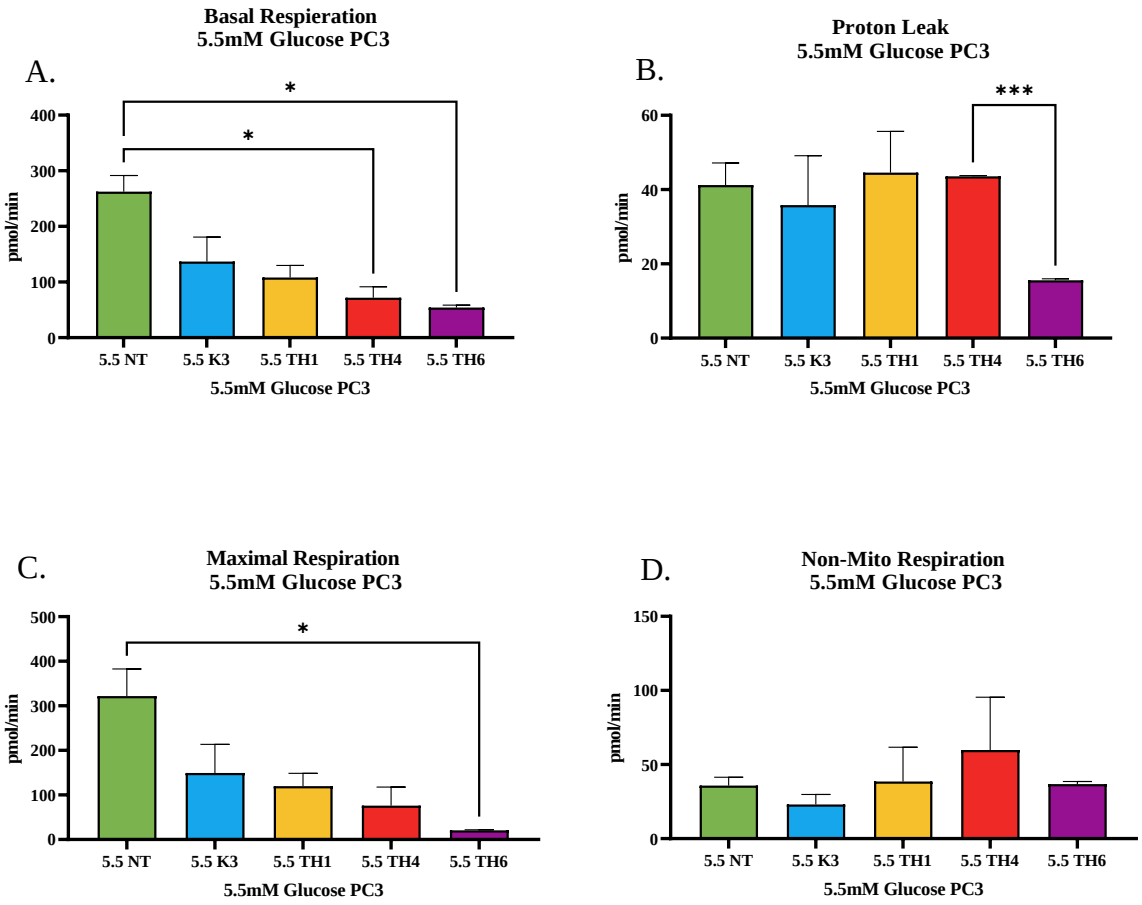

Figure 4. 40: The MitoStress endpoints for PC3 cells treated with novel compounds TH1, TH4 and TH6 under 11mM glucose showing the effects on the; (A) Basal OCR was decreased in the TH4 and TH6 treated cells. (B) Proton leak was decreased in the cells treated with TH6. (C) Maximal respiration was decreased in the cells treated with TH6. (D) The non-mitochondrial respiration was unchanged between the untreated and the treated cells. (n=3) 1-way ANOVA). (P > 0.05, ** P ≤ 0.01, *** P ≤ 0.001, **** P ≤ 0.0001).*

In the presence of 5.5mM glucose condition, the Du145 cells resulted in no change to the OCR (~150pmol/min). The Du145 proton leak (18.9pmol/min) increased with the novel TH treatments, however significance was only reported with the TH6 treatment (40.8pmol/min), (P<0.0001). The maximal respiration (150.1pmol/min) under 5.5mM was unchanged with the TH1 and TH4 treatments. However, the treatment with TH6 (69.3pmol/min) resulted in a decrease (P=0.02) in the maximal respiration. Non-mitochondrial respiration (22.0pmol/min) was increased with the novel TH treatments. TH1 (30.4pmol/min) and TH4 (34.7pmol/min) did not results in a significant increase, however TH6 (45.6pmol/min) has resulted in an increase (P=0.04) of significance. The results are illustrated in Figure 4.42.

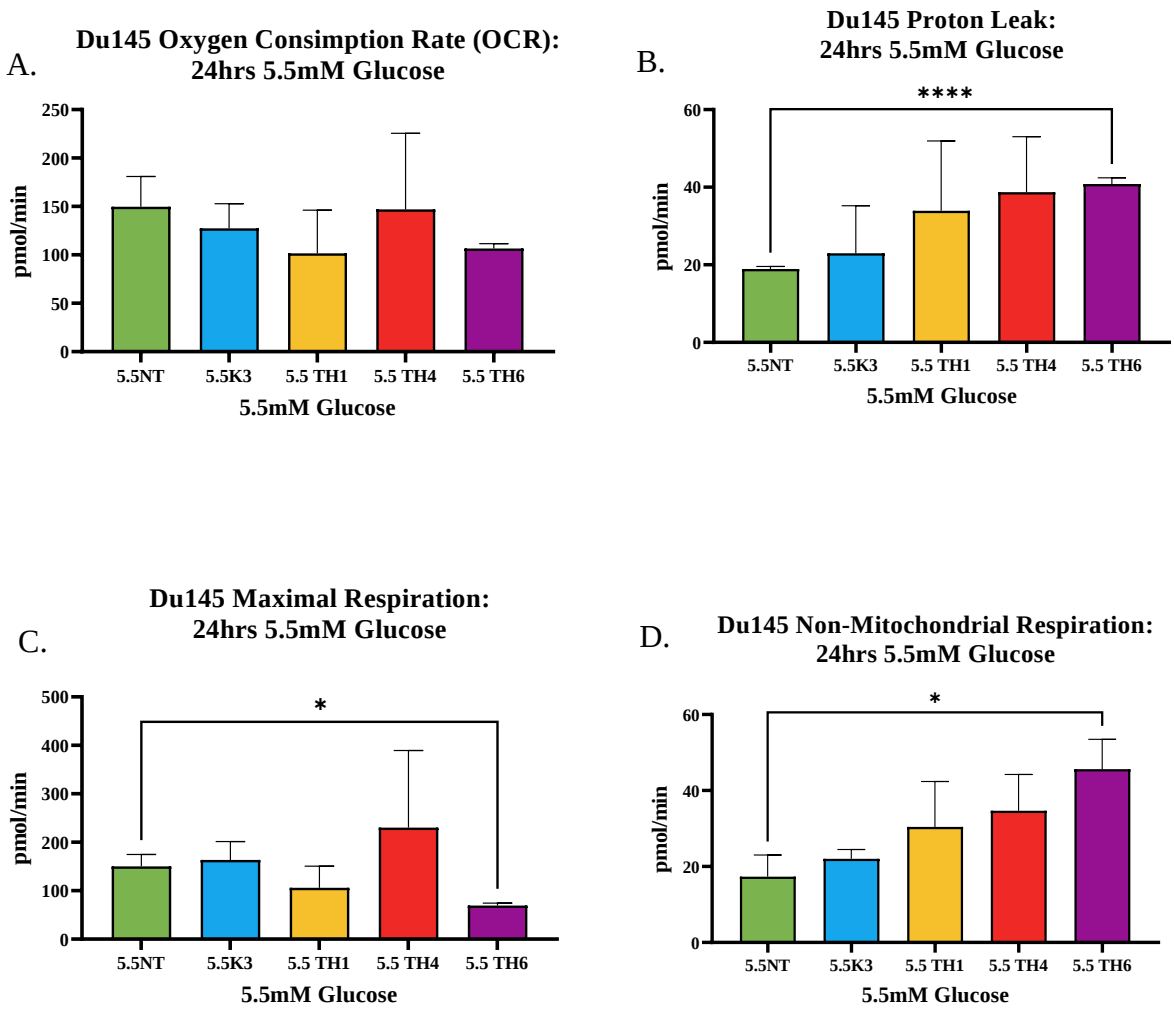

Figure 4. 41: The MitoStress endpoints for Du145 cells treated with novel compounds TH1, TH4 and TH6 under 5.5mM glucose showing the effects on the; (A) Basal OCR was unchanged between the untreated and the treated cells (B) Proton leak was increased in the cells treated with TH6. (C) Maximal respiration was decreased in the TH6 treated cells. (D) The non-mitochondrial respiration was increased in the TH6 treated cells. (n=3) 1-way ANOVA). (P > 0.05, ** P ≤ 0.01, *** P ≤ 0.001, **** P ≤ 0.0001).*

In the prostate cells in the 5.5mM glucose conditions, LNCaP had the highest OCR in the untreated, Menadione and TH4 treated cells ($P<0.0001$), while the cells treated with TH1 all present with similar OCR levels. In the cells treated with TH6, PC3 presented with the highest OCR levels ($P<0.0001$). LNCaP once more had the highest proton leak in the untreated, Menadione, TH1 and TH4 treated cells ($P<0.0001$), where all the cell lines show similar levels of proton leak when treated with TH6, PC3 cells present with the highest maximal respiration in the untreated and TH1 treated cells, with PNT1a cells having the highest levels when treated with Menadione ($P<0.0001$). When cells were treated with TH4, Du145 cells had the highest maximal respiration, where similar readings were reported in all the prostate cell lines when treated with TH6 ($P<0.0001$) as seen in Figure 4.43 below.

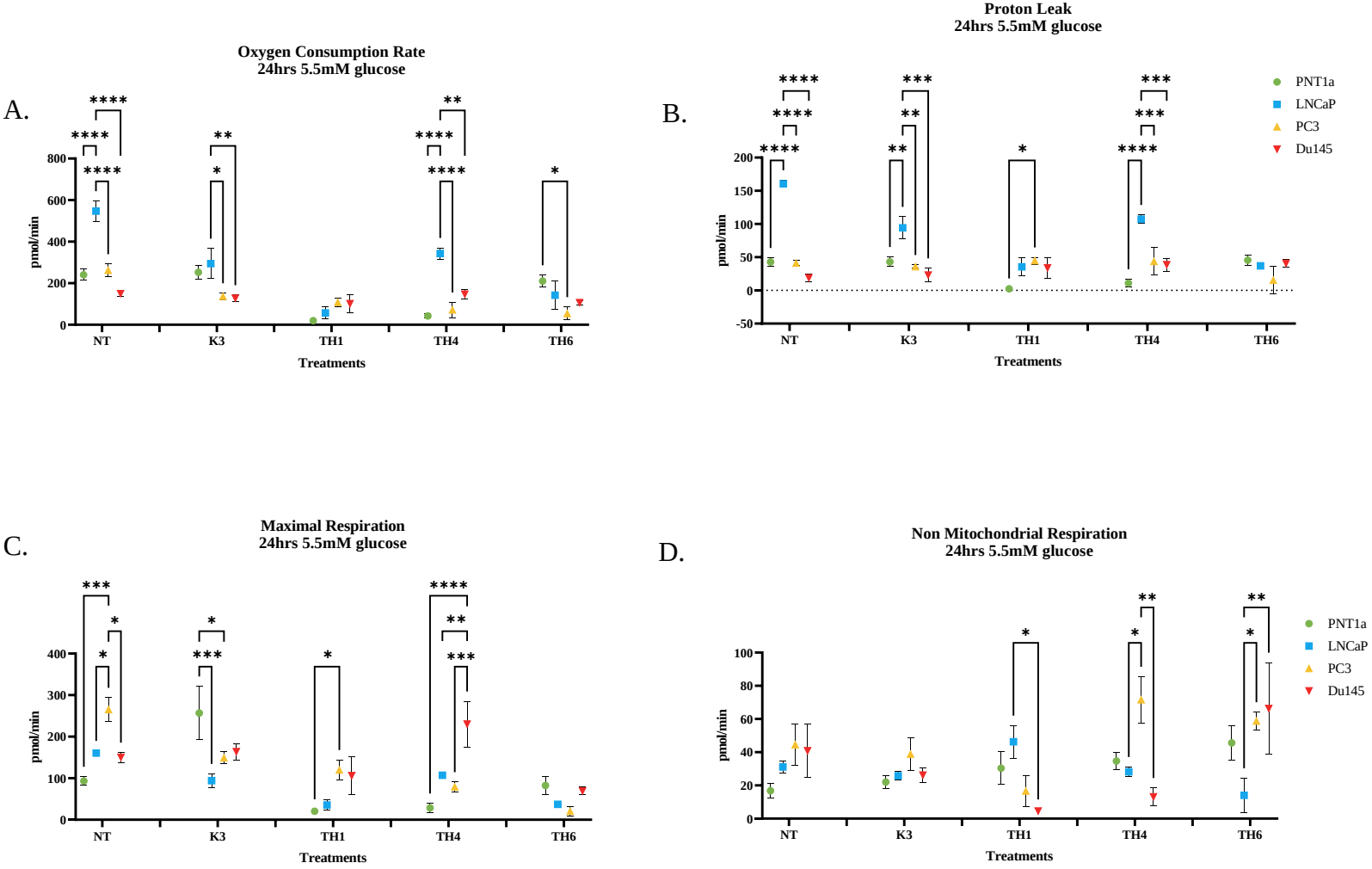

Figure 4. 42: The MitoStress endpoints for PNT1a, LNCaP, PC3 and Du145 cells untreated and treated with Menadione, TH1, TH4 and TH6 under 5.5mM glucose showing the effects on the; (A) Basal OCR was highest in the LNCaP cells in the untreated, menadione and TH4 treated cells, with increased levels in the TH6 treated PC3 cells and similar levels in the TH1 treated cells. (B) Proton highest in the LNCaP cells expect similar levels were found in all cell lines treated with TH6. (C) Maximal respiration was found not to be highest in the LNCaP but was altered in the different treatments. (D) The non-mitochondrial respiration was similar in the cell lines in the untreated, Menadione treated cells but highest in the TH1 treated LNCaP and highest in the TH6 treated PC3 and Du145 cells. (n=3) 1-way ANOVA). ($P > 0.05$, ** $P \leq 0.01$, *** $P \leq 0.001$, **** $P \leq 0.0001$).*

4.4.3.3 Menadione and the TH compounds alter the OCR, proton leak, maximal respiration and the non-mitochondrial respiration of the panel of prostate cell lines in the 11mM glucose conditions

OCR of PNT1a cells under 11mM glucose, was decreased (*P*= 0.001) with the treatments of TH1 (57.5pmol/min) and TH4 (13.3pmol/min) in comparison to the TH6 (252.2pmol/min) treated cells. The proton leak did not significantly change across the untreated and treated cells and the results are presented in Figure 4.44 **B**. No significant change was found in the maximal respiration of the PNT1a cells in the presence of 11mM glucose. The results are presented in Figure 4.44 **C**. The non-mitochondrial respiration was decreased (*P*= 0.02) in the TH1 (-8.5pmol/min) and TH4 (-0.5 pmol/min) when compared to the non-mitochondrial respiration of the cells treated with TH6 (53.7pmol/min).

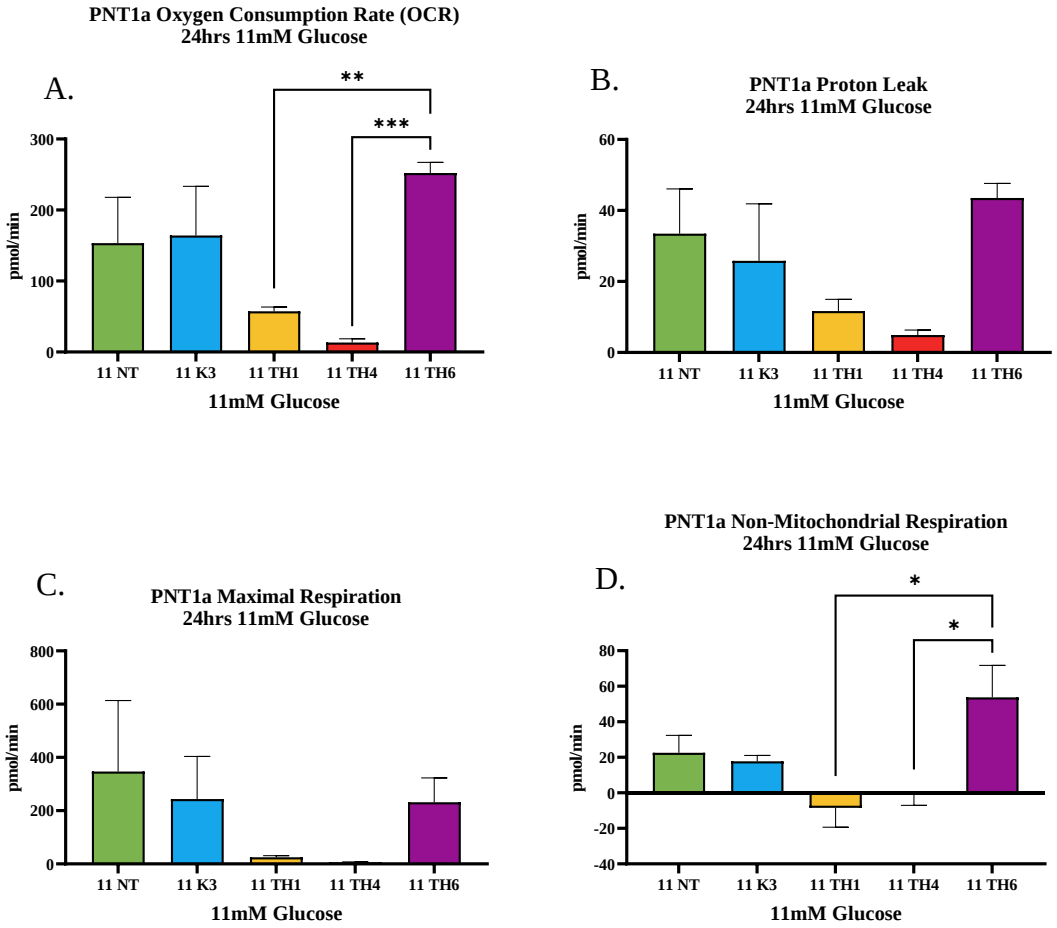

Figure 4. 43: The MitoStress endpoints for PNT1a cells treated with Menadione (K3), TH1, TH4 and TH6 under 5.5mM glucose showing the effects on the; (A) Basal OCR was decreased in the cells treated with TH1 and TH4. (B) Proton leak was unchanged between the untreated and the treated cells. (C) Maximal respiration was unchanged between the untreated and the treated cells. (D) The non-mitochondrial respiration was decreased in the cells treated with TH1 and TH4. (n=3) 1-way ANOVA). (P > 0.05, ** P ≤ 0.01, *** P ≤ 0.001, **** P ≤ 0.0001).*

The OCR of LNCaP under 11mM glucose (541.5pmol/min) was found to decrease (P=0.007) with the treatment with Menadione (170.3pmol/min) and the novel TH compounds; TH1 (52.5pmol/min) and TH6 (80pmol/min). The proton leak of LNCaP (157.7pmol/min) was found to decrease (P=0.001) with the treatment with Menadione (66.3pmol/min) TH1 (17.4pmol/min) and with the treatment of TH6 (43.1pmol/min). The maximal respiration was decreased (P=0.004) with the addition of Menadione (209.1) and the novel TH compounds TH1 (67.1pmol/min) and with TH6 (98.3pmol/min). The non-mitochondrial respiration was found to be unchanged with the addition of novel compounds. The results are presented in Figure 4.45.

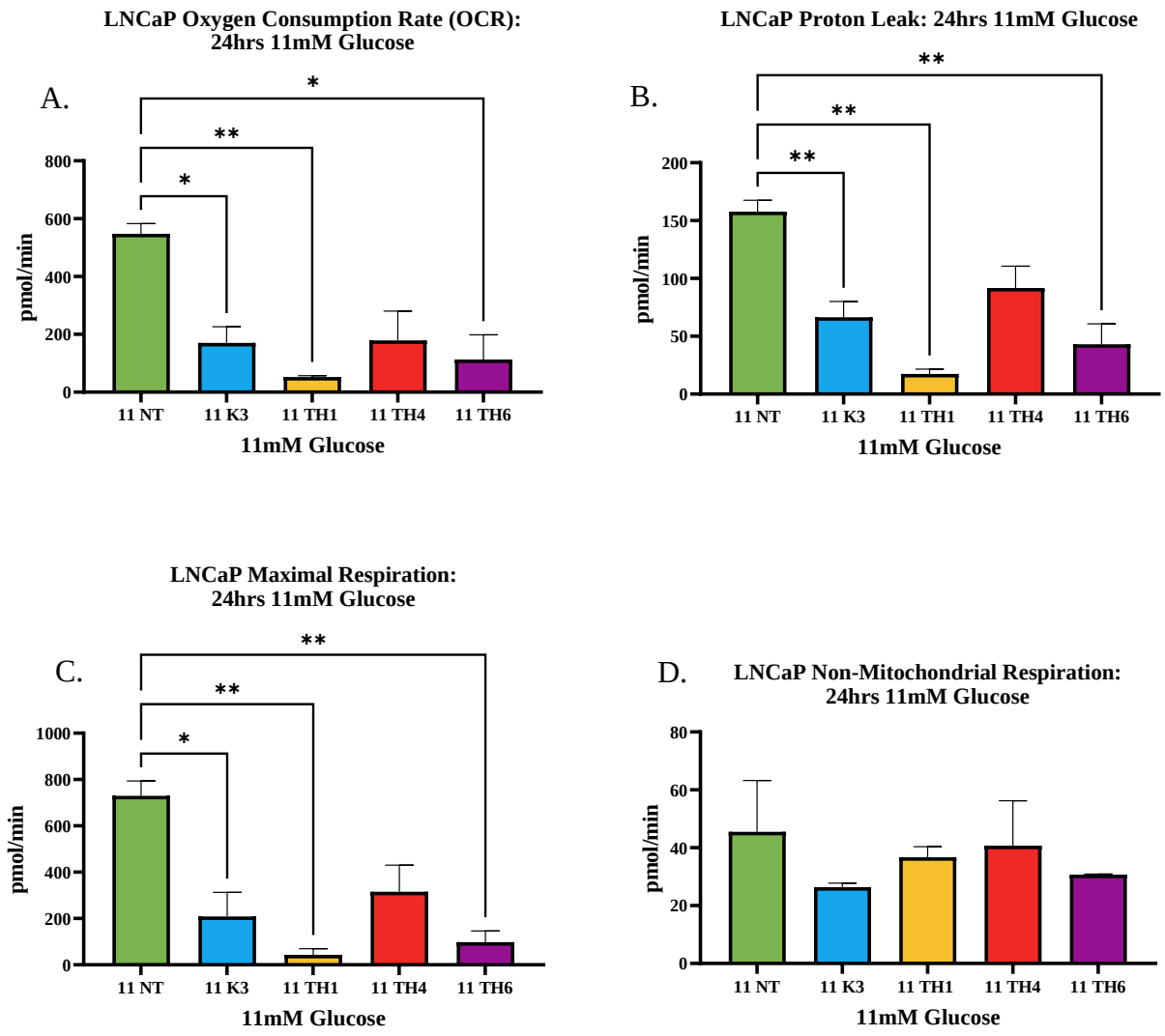

Figure 4. 44:The MitoStress endpoints for LNCaP cells treated with novel compounds TH1, TH4 and TH6 under 11mM glucose showing the effects on the; (A) Basal OCR was decreased in the Menadione, TH1 and TH6 treated cells. (B) Proton leak was decreased in the Menadione, TH1 and TH6 treated cells. (C) Maximal respiration was decreased in the Menadione, TH1 and TH6 treated cells. (D) The non-mitochondrial respiration was unchanged between the untreated and the treated cells. (n=3) 1-way ANOVA). (P > 0.05, ** P ≤ 0.01, *** P ≤ 0.001, **** P ≤ 0.0001).*

Basal OCR (150.8pmol/min) was decreased (P= 0.008) by the treatments with TH4 (28.7pmol/min) and TH6 (37.3mol/min). Proton leak (37.7pmol/min) was decreased with the TH6 (12.8pmol/min) treatments but not to significance (P=0.7). Across all treatments, the maximal respiration decreased in the PC3 cells in comparison to the untreated, with significance (P=0.04) between the untreated (220.6pmol/min) cells and the TH4 (14.1pmol/min) and TH6 (30.1pmol/min) treated PC3 cells. The non-mitochondrial respiration was found to be consistent across the cells examined as seen in Figure 4.46.

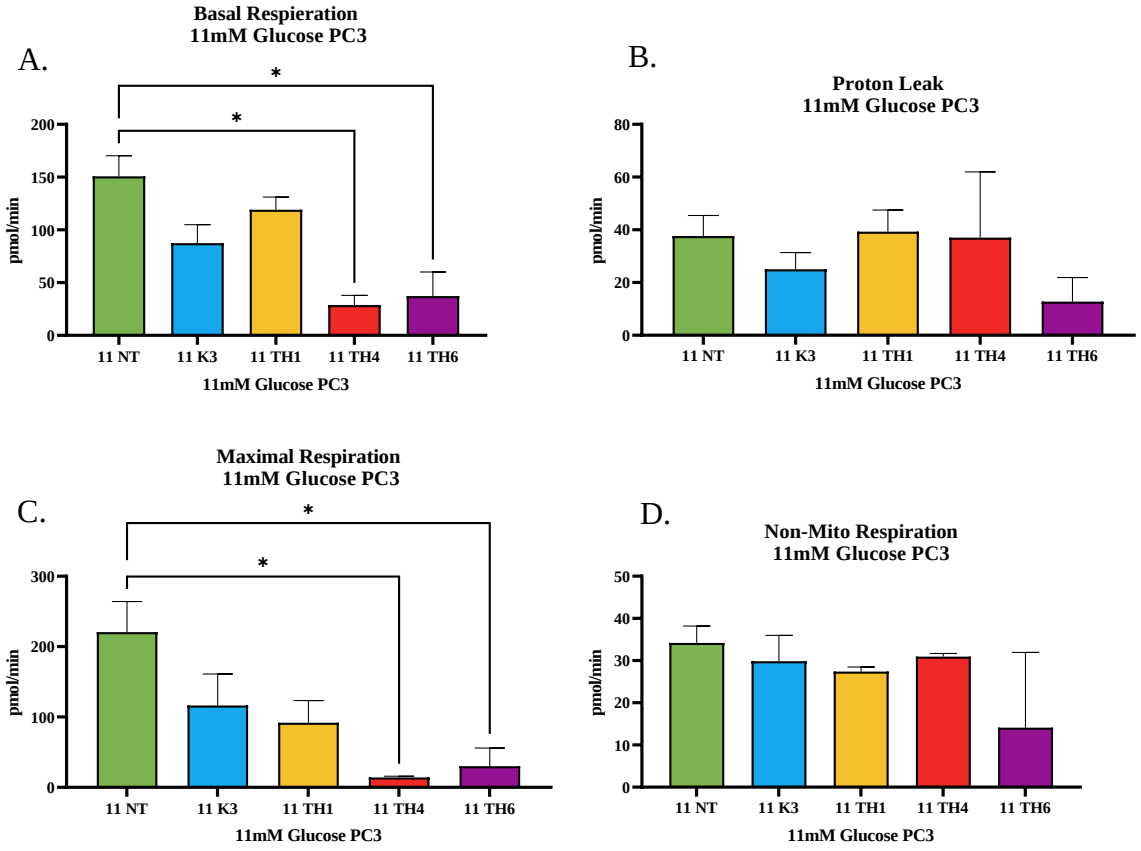

Figure 4. 45: The MitoStress endpoints for PC3 cells treated with novel compounds TH1, TH4 and TH6 under 11mM glucose showing the effects on the; (A) Basal OCR was decreased in the cells treated with TH4 and TH6. (B) Proton leak was unchanged between the untreated and the treated cells. (C) Maximal respiration was decreased in the TH4 and TH6 treated cells. The non-mitochondrial respiration was unchanged between the untreated and the treated cells (n=3) 1-way ANOVA) (P > 0.05, ** P ≤ 0.01, *** P ≤ 0.001, **** P ≤ 0.0001).*

4.4.3.4 Treatments with the Novel Trojan Horse compounds affects the mitochondrial metabolism of Du145 cells under 11mM glucose conditions

The high glucose conditions resulted in the OCR of Du145 to be unchanged across the treatment groups. The proton leak was found to be unaffected by the novel TH treatments. The maximal respiration of the Du145 cells was unchanged by the treatment with TH1 and TH4. However, the treatment with TH6 (47.4pmol/min) resulted in a drop (P=0.04) in the maximal respiration of the Du145 cells (268.2pmol/min). No significant change was observed in the non-mitochondrial respiration of the Du145 cells when treated with the novel TH compounds; TH1, TH4 and TH6. The results are presented in Figure 4.47.

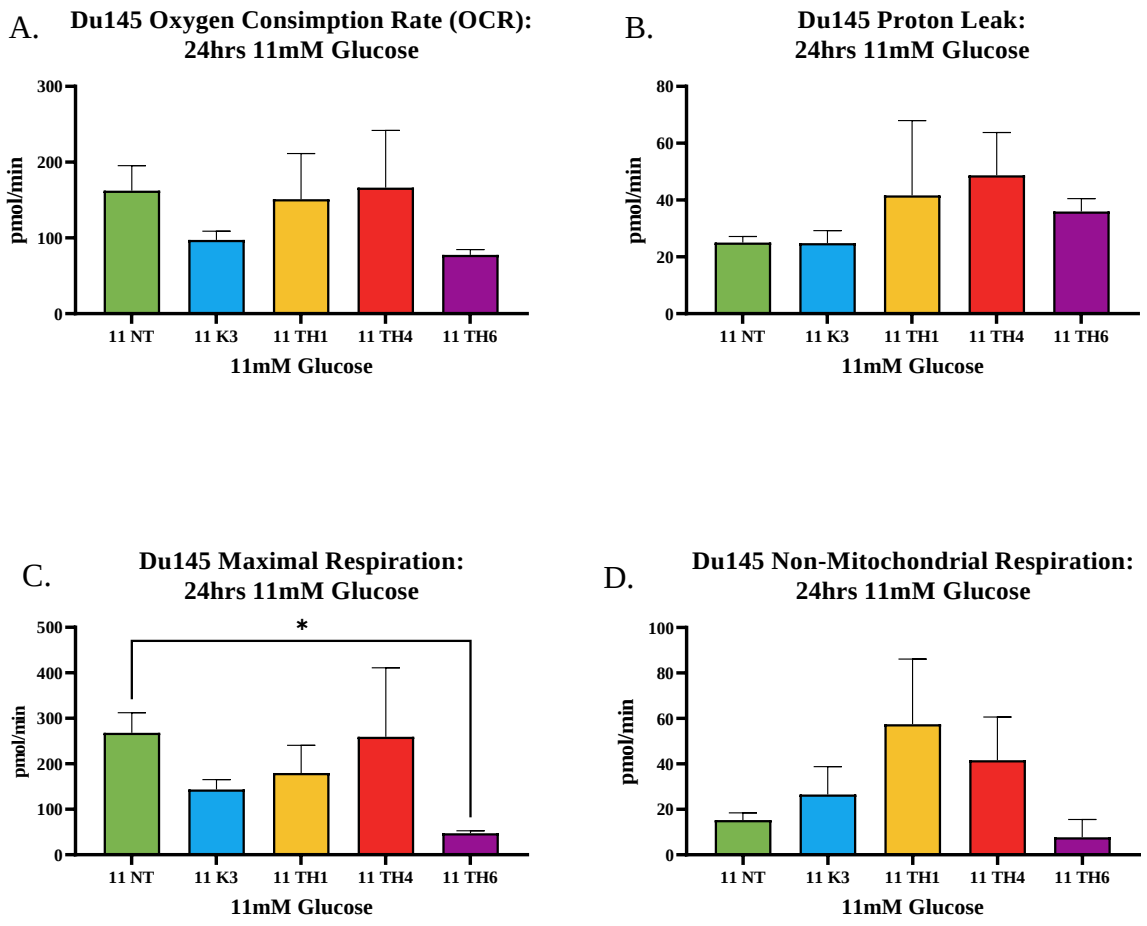

Figure 4. 46: The MitoStress endpoints for Du145 cells treated with novel compounds TH1, TH4 and TH6 under 11mM glucose showing the effects on the; (A) Basal OCR was unchanged between the untreated and the treated cells. (B) Proton leak was unchanged between the untreated and the treated cells. (C) Maximal respiration was decreased in the TH6 treated cells. (D) The non-mitochondrial respiration was unchanged between the untreated and the treated cells. (n=3) 1-way ANOVA). ($P > 0.05$, ** $P \leq 0.01$, *** $P \leq 0.001$, **** $P \leq 0.0001$).*

The untreated prostate cells presented with higher OCR in the LNCaP cell line with similarly high levels of OCR found in the LNCaP and Du145 cells treated with TH4. Du145 cells treated with TH1 had the highest OCR of the cell lines with overall similar levels determined in all the cell lines treated with Menadione. Proton leak was highest in the untreated TH4 and Menadione treated LNCaP cell line, while comparable levels were determined in the TH1 and TH6 treated cells. The maximal respiration of the untreated cells was highest in the LNCaP cell line, and along with Du145 was highest in the TH4 treated cells. In the menadione treated group, the cell lines had similar levels, while Du145 had the highest maximal respiration in the TH1 treatments and PNT1a cells had the highest levels in the TH6 treatment group. Finally, the non-mitochondrial respiration was similar in the untreated cells, PNT1a present with very low levels of non-mitochondrial respiration in the TH1, TH4 and TH6 treated cells compared to the PCa cells. the results of the cell lines are presented in Figure 4.48.

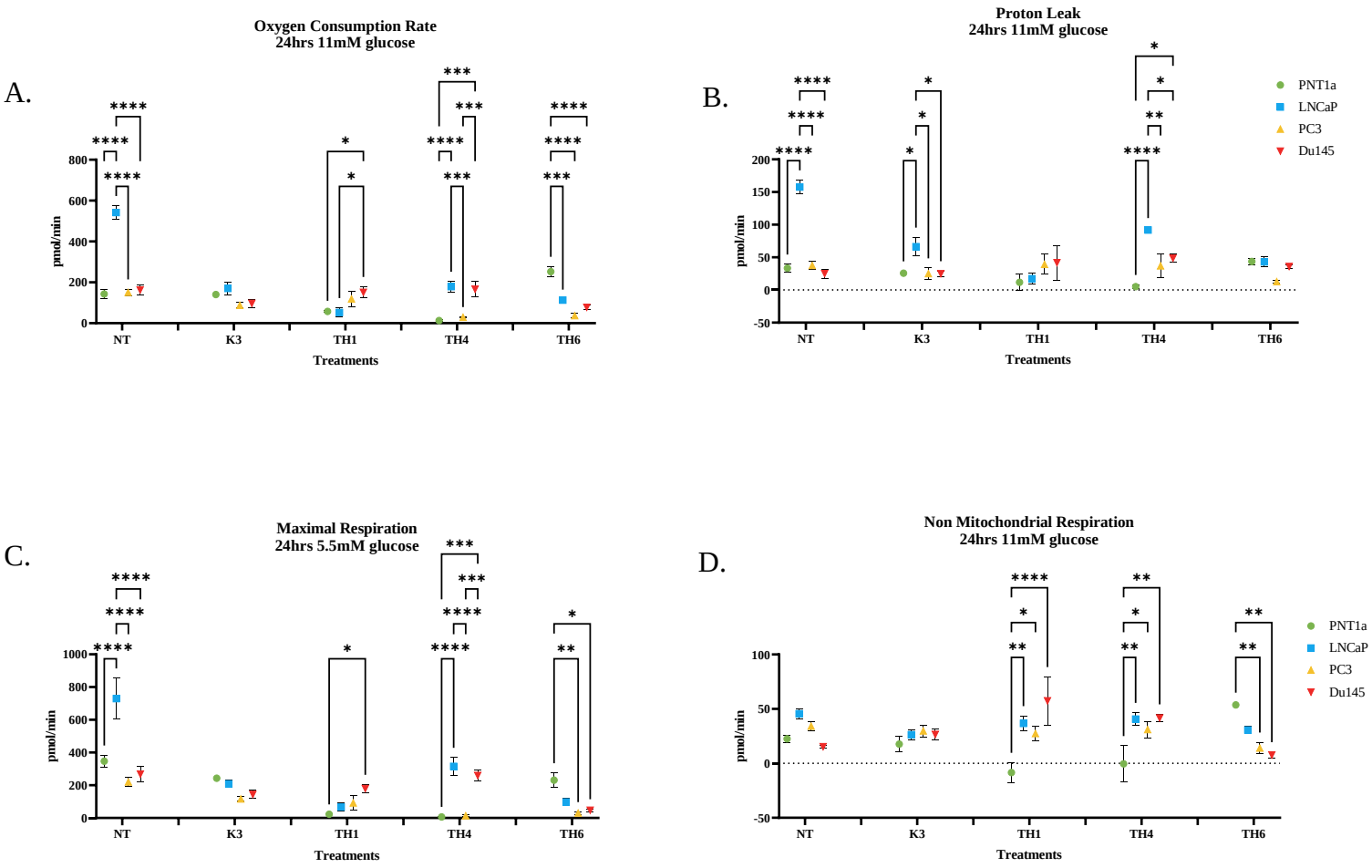

Figure 4. 47: The MitoStress endpoints for PNT1a, LNCaP, PC3 and Du145 cells untreated and treated with Menadione, TH1, TH4 and TH6 under 11mM glucose showing the effects on the; (A) Basal OCR was highest in the LNCaP cells in the untreated, menadione and TH4 treated cells, with increased levels in the TH6 treated PC3 cells and similar levels in the TH1 treated cells. (B) Proton highest in the LNCaP cells expect similar levels were found in all cell lines treated with TH6. (C) Maximal respiration was found not to be highest in the LNCaP but was altered in the different treatments. (D) The non-mitochondrial respiration was similar in the cell lines in the untreated, Menadione treated cells but highest in the TH1 treated LNCaP and highest in the TH6 treated PC3 and Du145 cells. (n=3) 1-way ANOVA). ($P > 0.05$, ** $P \leq 0.01$, *** $P \leq 0.001$, **** $P \leq 0.0001$*

4.5 Summary of Results

Highlights of Chapter 4
• All the prostate cell lines show a glucose dependent reliance on glycolysis and OxPhos, where an increase in glucose on the cell medium increases their reliance on glycolysis simultaneously decreasing their OxPhos reliance. • In the presence of glucose, the PNT1a, PC3 and Du145 cells have a higher reliance on glycolysis than OxPhos for ATP production, with the cells persisting with some reliance on glycolysis even in the zero glucose conditions. • LNCaP remain with a heavy reliance on OxPhos even in high glucose conditions (11mM glucose), with a small reliance on glycolysis as the glucose gradient rises. • Although no significant changes were determined in the metabolic phenotypes of the cell lines, treated with the TH compounds, TH6 reduced the cells glycolytic reliance in the PNT1a cells. • LNCaP have the highest basal reading of all the cell lines in the MitoStress endpoints under all three glucose conditions. • Treatment with the TH compounds resulted in alterations to the mitochondrial bioenergetics, reducing, OCR and maximal respiration and Proton leak in the prostate cells.

.

4.6 Discussion

PCa displays altered metabolism during different stages of disease progression and patients with androgen independent prostate cancer are currently considered incurable. Cancer metabolism is an emerging target for therapeutic action, and with PCa displaying a unique metabolic signature, it is emerging as a disease model of interest for therapeutic targeting.[244] In normal prostate, the TCA cycle is truncated and results in a reliance on other metabolic pathways whereas in early PCa the TCA cycle is thought to be used. The unique metabolism reported in normal prostate, and prostate cancer is thought to be mediated by AR, with AR-mediated metabolic reprogramming in prostate cells increasing in interest.

While AR is a key regulator of prostate cancer progression and was expected to be altered in response to high and low glucose conditions, following 24hr treatments, no alterations in AR expression were observed in the nuclear, cytosol, whole cell lysate or the supernatant fractions under zero, 5.5mM and 11mM glucose conditions. This may be due to the short incubation time under the glucose conditions, not allowing enough time for alterations to occur. Unfortunately, post 24hrs the zero glucose cells tend to show high levels of cell death, making further investigation difficult to achieve. These results could also be linked to the aforementioned AR antagonism mechanism, where the *in vitro* microenvironment is lacking the biological molecules that play a role in altered AR levels across the different glucose milieu.[393–395] Due to these results, it was decided not to continue to examine the AR effects at this time. Nonetheless, worth further investigation in the future.

To the best of our knowledge this study provides the first examination of the implications of a biologically relevant glucose milieu on the mitochondrial bioenergetics and the metabolic phenotype of a panel of prostate cell lines, as well as in examining the effects of Vitamin C, Menadione and vitamin-based compounds on the bioenergetics of prostate cells. Although the bioenergetics of some of the cell lines have been evaluated in the literature, the impacts of the glucose milieu have not presented itself within the literature. This aspect of this study has emerged as an important finding, highlighting the androgen independent cell lines, PC3 and Du145 having an ingrained reliance on glycolysis, even during a period of glucose starvation for 24hrs. Importantly this study highlights how the Warburg effect cannot be quenched in the metastatic androgen independent PCa (PC3 and Du145), even during glucose starvation and even when treated

with metabolic targeting therapies, while the androgen dependent cells (LNCaP) rely primarily on OxPhos for their ATP production. Metabolic reprogramming is a known hallmark of cancer hence the therapeutic targeting of these pathways is of growing interest across the research community.

Metabolic vulnerabilities of cancer cells under glucose starvation are expected, due to the fact that cancer cells are proposed to thrive on glucose for their metabolic processes, such as Warburg glycolysis. We report that during a period of 24hrs cells cultured in zero glucose media, had a substantial reliance on OxPhos for ATP production. This is expected as in the presence of no glucose, cells may be switching to OxPhos, due to the non-availability of glucose molecules. Warburg glycolysis is thought to be 100 times faster than that of OxPhos, thus the high dependence on OxPhos in the zero glucose condition.[251] The LNCaP cells were found to remain in an OxPhos phenotype, even in the presence of the 5.5mM and 11mM glucose conditions. Russell et al and Blajszczak et al have shown in 10mM glucose media that LNCaP cells display a more OxPhos phenotype that that of normal prostate cells, which validates the results that we have achieved in the presence of glucose.[361] What these studies do not address is that the LNCaP cells reliance on oxphos is a glucose gradient dependent, with their reliance on oxphos decreasing with an increase in glucose concentration. However, they do nonetheless still persist with a majority reliance on OxPhos in the high glucose conditions.

Interestingly, although in zero glucose media, the late-stage metastatic disease model (PC3 and Du145) cells present with a high reliance on OxPhos, they do appear to persist with a small reliance on glycolysis, indicating Warburg metabolism is always switched on. A study of the differential utilization of dietary fatty acids in in benign prostate and PCa found that benign prostate epithelial cells (RWPE-1) present with higher glycolytic reliance than LNCaP and PC3 cells through higher levels of glucose consumption and lactate production. This study postulates that the reason for this result of the inhibition of m-aconitase by zinc in the mitochondrial with, an accumulation of citrate reducing the activity of the TCA cycle, known to play a fundamental role in in *vivo* prostate and PCa metabolism. In addition, the study found that BE RWPE-1 cells were less sensitive to glucose starvation than PCa cells.[361] Additionally another study demonstrated that PC3 cells have a slow glycolytic rate in comparison to MCF-7 breast cancer cells with a higher reliance on fatty acid catabolism.[361] While our study did not examine the fatty acid metabolism of the prostate cells, with our focus on targeting the

Warburg effect, from the literature one would expect the TH6 fatty acid compound to have greater effects on the metabolism of the PCa cell lines. TH6 resulted in decreased OCR in the LNCaP cells cell line in all the glucose media conditions and in the presence of 5.5mM and 11mM glucose for the PC3 cells. Further TH6 triggered a decrease in proton leak and maximal respiration in the LNCaP cells across the glucose gradient with alterations in both mitochondrial endpoints observed in the metastatic androgen independent PC3 and Du145 cells in the zero and 5.5mM glucose conditions. The alterations of these mitochondrial bioenergetic endpoints indicate dysfunction to the mitochondria due to the TH6 treatment, and as determined from the literature the PC3 cells have a strong reliance on fatty acid metabolism for their ATP production. Fatty acid metabolism appears to allow the novel TH6 compound to infiltrate the cells and thus affecting their mitochondrial function which would be displayed in their mitochondrial bioenergetics. Further as discussed in Chapter 1 in more detail, the menadione element of the novel TH compounds are thought to produce large levels of endogenous ROS in the cells to overthrow the cancer cells redox homeostasis resulting in oxidative stress. This oxidative stress would result in alterations to the mitochondrial bioenergetics such as the alterations to the proton leak, supporting our hypothesis of ROS related cell death. An increase in ROS would increase proton leak due to proton leakage into the mitochondrial matrix, or electron slippage which leads to the consumption of oxygen without proton translocation further damaging the electron transport chain and the mitochondrial membrane causing an increased proton leak into the mitochondrial matrix, overall altering the mitochondrial bioenergetics.[368,396]

We have proposed that the novel compounds will target the mitochondria, due to the existing literature examining the effects of Menadione *in vitro*, increasing mitochondrial ROS, and oxidative stress in the mitochondria, hence the drop in OCR may support this proposed mechanism.[308,309,342]Alterations to OCR due to therapeutic treatments may in fact be a stress response by the cells with an increase in OCR due to alterations in many factors, including increased ATP turnover, proton leak and non-mitochondrial respiration.[379] Treatments with Vitamin C resulted in a decrease in OCR in all of the cell lines, under varying glucose conditions. Moreover, the glucose Menadione conjugated TH compounds (TH1 and TH4) repeatedly resulted in decreased OCR in the PNT1a, LNCaP and the PC3 cell lines, across the varying glucose conditions. It is reported that decreased OCR is linked to damage to the mitochondria, decreasing ATP

production capabilities of the cells. Thus, a reported decrease in OCR with the novel compounds would be expected to be due to mitochondrial damage. PNT1a, in the presence of zero glucose presents with increased basal OCR, this may be due to the fact that the non-malignant prostate is known to inhibit the Krebs cycle, not employing OxPhos, rather increasing its glycolytic processes for the production of citrate for energy production.[317] However, the lack of glucose, alters its metabolic phenotype to an OxPhos dependency increasing its OCR levels. The metastatic cells, LNCaP, PC3 and Du145 cells OCR appeared unaffected by the zero glucose conditions compared to in the presence of glucose. Some studies propose that increased OCR is proportional to increased ROS, due to ROS being a product of OxPhos.[368,380] However, high levels of ROS are known to lead to mitochondrial damage and cell death mechanisms such as mitophagy, autophagy and apoptosis, hence why cancer cells often shift their metabolic processes to glycolysis or fatty acid oxidation to avoid this oxidative damage.[386] This in turn may also result in decreased OCR levels seen in the cells treated with the ROS producing Menadione and the Menadione based TH compounds. These findings would support the hypothesis of the thesis, with the compounds increasing cellular ROS causing alterations to the cells metabolism though increasing oxidative stress, by shifting the redox homeostasis of the cells by overthrowing their antioxidant mechanisms.

Ultimately, the adaptation of cancer cells to their microenvironment and nutrient deprivation displays the metabolic plasticity of cancer cells, allowing them to switch between OxPhos, glycolysis and fatty acid oxidation, although, the LNCaP cell line was not able to do this but the other cancer cell lines (PC3 and Du145) were more adaptable, which could contribute to their metastatic potential. This metabolic reprogramming allows the energy requirements for the cancer cells to be fulfilled for growth and proliferation. Changes to the nutrient environment during metastasis will result in changes to cellular metabolic demands to promote the cells survival. While cancer cells require several key nutrients as they develop, intrinsic and microenvironment factors will determine their nutrient dependencies throughout progression, shifting their nutrient demand and altering their metabolism for survival during the starvation of a nutrient substrate, in this case, glucose. The shift to fatty acid, amino-acid, or glutamine metabolism would be expected during this time of nutrient stress, which could influx the utilisation of other metabolic pathways for ATP production.[175,317,365] We see this shift in the PC3 and Du145, metastatic androgen independent cells, where during the glucose

deprivation (zero glucose) conditions, they switch to a more mitochondrial metabolic phenotype, limiting their levels of glycolysis due to the lack of glucose to fuel the high glycolytic demands, this proving that the cells can reprogramme their metabolism during nutrient stress, utilising other substrates to fuel their metabolism, whereas this metabolic reprogramming is less evident in the LNCaP cells, remaining with an OxPhos reliance. This may be in part linked to the androgen status of the cell lines, with LNCaP being androgen dependent, impacting their metastatic potential compared to their androgen independent counterpart. Given that, the androgen independent disease is said to use citrate as a substrate for energy production activating the TCA cycle mediated by AR signalling prompting a metabolic dependency on oxidative phosphorylation.[244,245,383] This may account for the androgen independent LNCaP cells inherent use of OxPhos, regardless of their nutrient environment.

A hallmark of the tumour microenvironment is nutrient deprivation, as the core of a tumour will develop a nutrient deprived microenvironment due to a poor blood supply, highlighting the importance of evaluating the effect of the glucose milieu on the metabolic activity of the prostate cell lines to replicate the possible in *vivo* action of the cell's metabolism and their reactions to the novel TH compounds. Existing studies have highlighted that nutrient deprivation can control the behaviour of cancer cells; thus the modulation of their metabolism is vital to understand for this work and to determine the effects and cells mechanisms of adaptation to encourage metastasis progression.[397,398] Determining and examining the biological mechanisms involved in the metastatic process and how they can be altered is essential in finding therapeutic intervention success.

Chapter 5. The effect of novel Trojan horse compounds on mitochondrial function and ROS production in prostate tumour cells

5.1 Introduction

In Chapter 4, the effect of the novel Trojan Horse (TH) compounds on the metabolic bioenergetics was examined across the panel of non-malignant prostate cells and prostate cancer cells. In this Chapter, we delve deeper into the investigation of the possible cause of the observed mitochondrial dysfunction by the novel compounds.

The mitochondrial membrane potential (MMP) is used as a marker of cell and mitochondrial health and function.[399,400] MMP is generated via the action of a series of proton pumps (Complexes I, III and IV) and plays a vital role in energy storage during oxidative phosphorylation (OxPhos) and occurs as a result of redox transformations associated the Krebs cycle.[373] The mitochondrial membrane allows for the transport of ions and molecules in and out of the mitochondria, required for that of metabolic processes, thus regulation of MMP is vital for this to occur efficiently.[400,401] Perturbations in MMP has been shown to associate with cancer cell malignancy, tumorigenesis and cellular differentiation.[402] MMP is typically found to be stabilised within the cell, with sustained alterations in basal MMP used as an indicator of mitochondrial dysfunction, often resulting in a reduction in cell viability and overall health.[373] MMP is associated in mitochondrial self-regulation though the eradication of unhealthy or dysfunctional mitochondria, and is linked to cell viablility.[373] Studies have shown that prostate carcinoma has higher basal MMP than that of normal epithelial cells and the elevated MMP is linked to higher rates of cell division and tumour formation.[373,402] MMP contributes to the assessment of mitochondrial bioenergetics, due to its ability to reflect OxPhos and the electron transport chains functionality.[399,403] Due to these the links between MMP and oxphos, the alterations in the mitochondrial endpoints in Chapter 4, highlights the importance of determining the effects on the MMP in the panel of cell lines in the study.

The electron transport chain activity within the mitochondrial results in ROS production. Mitochondria are major contributors to cellular ROS, as they are produced from metabolic reactions.[404,405] Some ROS are free radical molecules that essentially exist with an unfulfilled valency, with one unpaired electron in the valence orbital of the oxygen component, causing them to be highly reactive, superoxide and hydroxyl are two examples of free radicals with unpaired electrons.[406,407] Other forms of ROS such as H_2O_2 and OONO- are not free radicals but are reactive oxygen species. ROS are typically by-

products of aerobic metabolism, from the mitochondria with this mechanism detailed in Figure 5.1.[407]

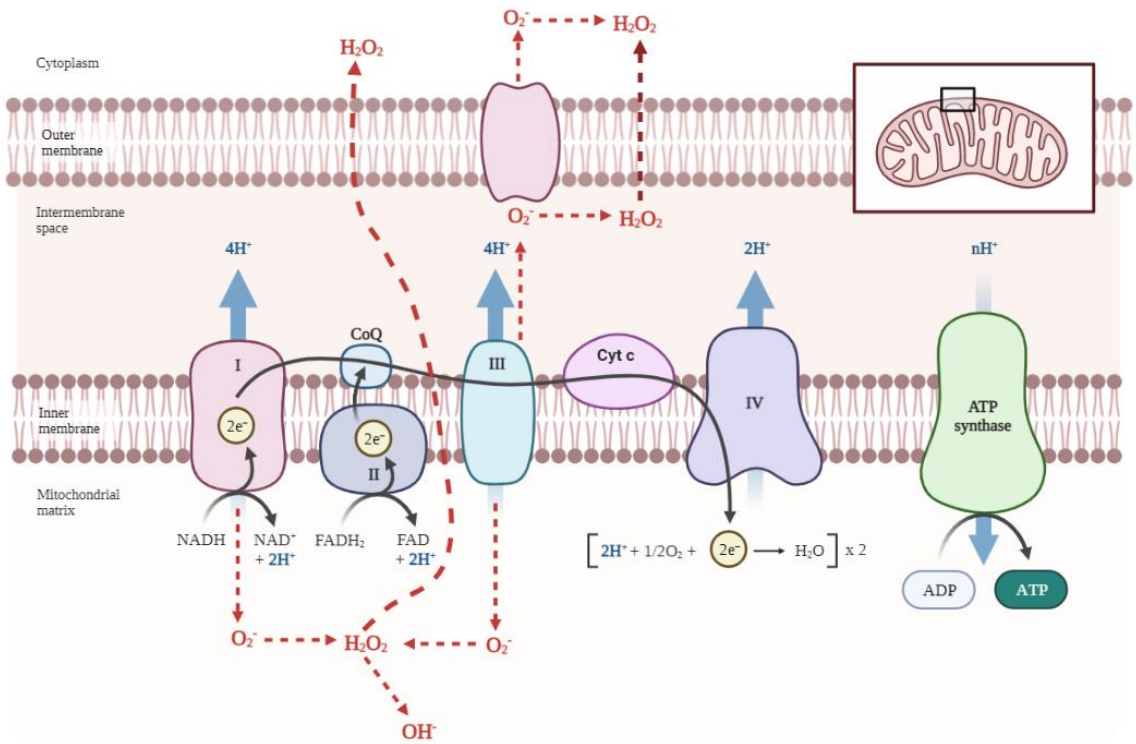

Figure 5. 1: Mitochondrial ROS production through the electron transport chain . Superoxide (O_2^-)produced by mitochondrial complex I and III is converted to hydrogen peroxide (H_2O_2)by superoxide dismutase. H_2O_2 can pass through the mitochondrial membranes and convert to hydroxyl radicals (OH^-) by Fenton/Haber-Weiss reactions. O_2^- produced by mitochondrial III, diffuses through the mitochondrial membranes through the voltage dependent anion channel into the cytoplasm where here it is also converted to H_2O_2 as cytoplasmic ROS.[408] Image created in Biorender.

Oxidative stress is a hallmark of cancer and has been well established.[239] Oxidative stress occurs when high concentrations of ROS overwhelm the endogenous antioxidant systems resulting in damage of cellular macromolecules.[327] The redox status of a cell is defined as the reduction potential of all antioxidant molecules in the cell and is maintained towards a negative redox potential value due to the activity of cellular homeostasis mechanisms.[409] This cellular redox balance be altered by fluctuations in physiological conditions based upon the concentrations of cellular antioxidants.[409] Studies suggest that cells utilise ROS to stimulate proliferation required for the progression of tumours, through amplification of genomic instability which can evokes increased oxidative stress, which in turn can cause a vulnerability in the cancer cells to ROS stimulating therapeutic action.[15,16] From this, it appears that ROS is both required for cancer cell malignancy progression, viability, and death.[413] The activation of transcription

factors such as nuclear factor kappa-light-chain-enhancer of activated B cells [NF-κB], activator protein-1 (AP-1), hypoxia-inducible factor-1α (HIF-1α), and signal transducer and activator of transcription 3 ((STAT)-3), by ROS results in the expression of proteins that control cellular processes like inflammation, cancer cell proliferation and invasion, angiogenesis, and metastasis and cellular transformation.[318] Remarkably, ROS has also been shown to regulate the expression of tumour suppressor genes p53, Rb, and PTEN.[318] The levels of ROS within a cell are dependent of its redox status, which is derived from the concentration of oxidised and reduced forms of proteins, enzymes, and ROS itself.[414,415] Redox balance is dependent on the formation and eradication of exogenous and endogenous ROS. High ROS concentrations are due to the uncontrolled production of ROS, resulting in oxidative stress and cytotoxicity.[414–416]

Some tumour cells have been found to increase production in antioxidant proteins to counteract the increased ROS generated.[413,417] There are various enzymatic systems and factors that maintain the redox status of cells, these antioxidant defence mechanisms are complex, regulating cytoplasmic, mitochondrial, and nuclear levels of ROS in the cell.[377,404,413,417] The mitochondria are equipped with many antioxidant pathways to counteract the ROS production including superoxide dismutase (SOD2); a biological enzyme that catalyses the dismutation of superoxide radicals, glutathione; antioxidant molecules, thioredoxin; small redox proteins and peroxiredoxins; cysteine-dependent peroxidase enzymes to regulate peroxide concentrations.[377] High concentrations of ROS produce oxidative damage within DNA resulting in mutations, linked to cancer, where hydroxyl radicals are known to react with purines and pyrimidines in DNA resulting in base alterations. Due to mitochondrial DNA's proximity to the electron transport chain components, it is in the high risk of damage and therefore inducing cell death.[404,418–420]

This chapter examines the basal mitochondrial dysfunction and how this is altered by the novel mitochondrial targeting TH compounds, and to determine if the mechanism of action includes the production of high levels of ROS resulting in cell death.

5.2 Hypothesis and Aims

We hypothesise that the treatment of a panel of PCa and non-malignant prostate cell lines with novel TH compounds will trigger a significant increase in endogenous ROS production, to levels high enough to evade cellular antioxidant processes, resulting in mitochondrial damage and cell death.

- To determine the endogenous ROS production, MMP levels and apoptotic states in the panel of prostate cell lines; PNT1a, LNCaP, PC3 and Du145 cells in the zero, 5.5mM and 11mM glucose conditions.

- To determine the endogenous ROS production, MMP levels and apoptotic states in the panel of prostate cell lines; PNT1a, LNCaP, PC3 and Du145 cells treated with Menadione, TH4 and TH6 in the zero, 5.5mM and 11mM glucose conditions.

- To compare the endogenous ROS production, MMP levels and apoptotic states between the panel of prostate cell lines; PNT1a, LNCaP, PC3 and Du145 cells treated with Menadione, TH4 and TH6 in the zero, 5.5mM and 11mM glucose conditions, in order to determine the cell line with the most optimal response to the novel compounds.

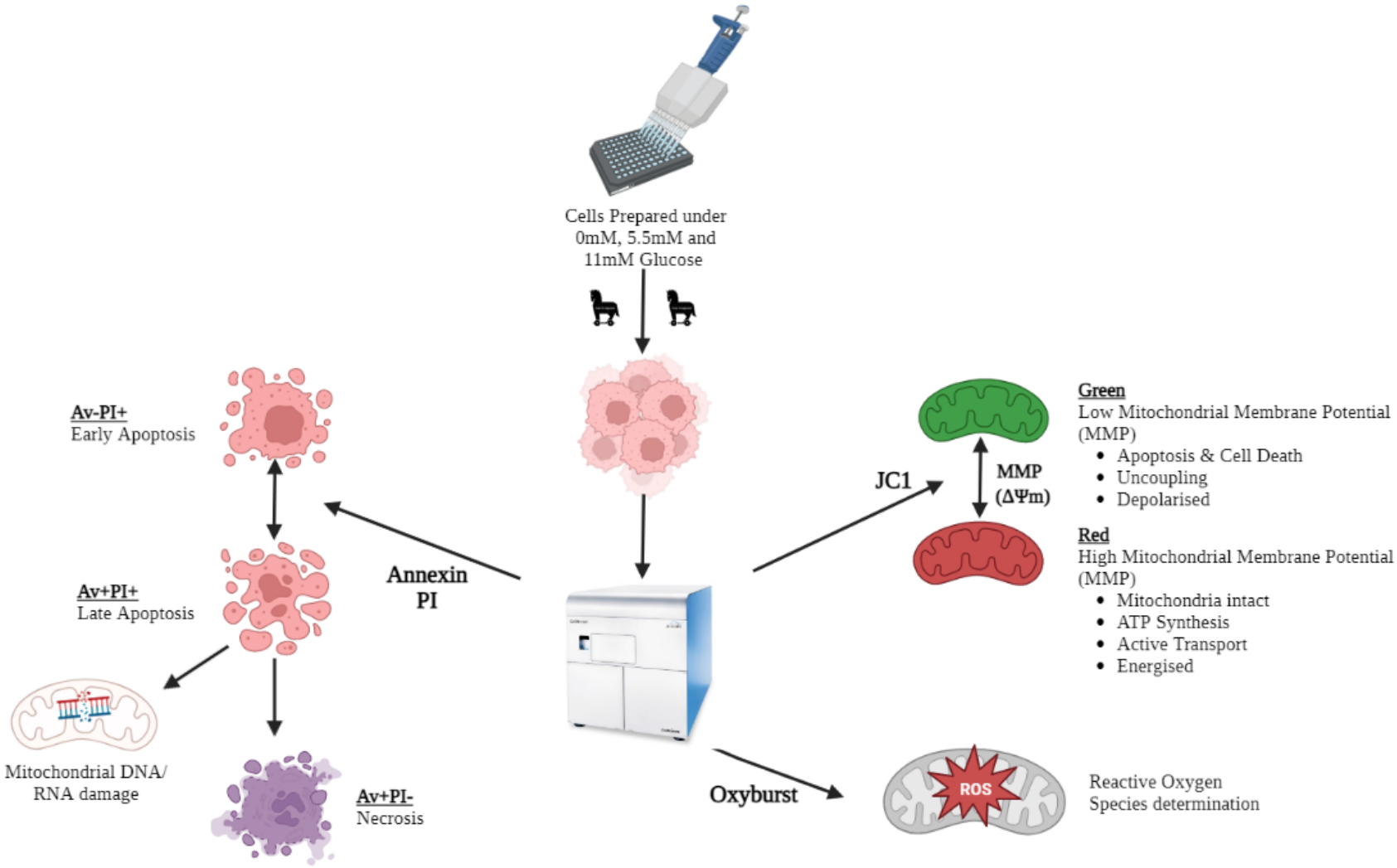

Figure 5. 2: Chapter methodology. Determination of the impact on the MMP, ROS production and Apoptosis by the Novel TH Compounds. The prostate cells are plated for 24hrs in complete RPMI 1640 for 24hrs. Following this, the cells are placed in the zero, 5.5mM and 11mM glucose media conditions, with the required treatments (untreated, Menadione, TH4, TH6) respectively, for 24hrs incubation. The day of the assay, the fluorescent markers are added to the cells. AvPI indicating apoptosis and DNA damage, JC1 indicating MMP, and Oxyburst indicating cellular ROS production.

5.3 Methods

The flow cytometry protocols are detailed further in Chapter 2, Section 2.8. Representative histograms of the flowcytometry markers used are presented in Appendix 51.

5.3.1 Statistical analysis

Statistical analysis was conducted using GraphPad Prism 9 Software [GraphPad Software, CA, USA]. All data is presented as mean ± SEM. Statistical test used include One-way ANOVA and two-tailed t-test. Statistical significance was considered at $P<0.05$.

5.4 Results

5.4.1 Representative fluorocytograms of endogenous ROS, the MMP and apoptosis analysis of prostate non-malignant and PCa cells across the zero, 5.5mM and 11mM glucose conditions

The following representative fluorocytograms show the endogenous ROS, the MMP and apoptosis analysis of prostate non-malignant and PCa cells across the zero, 5.5mM and 11mM glucose conditions, illustrated in Figure 5.3 – Figure 5.5.

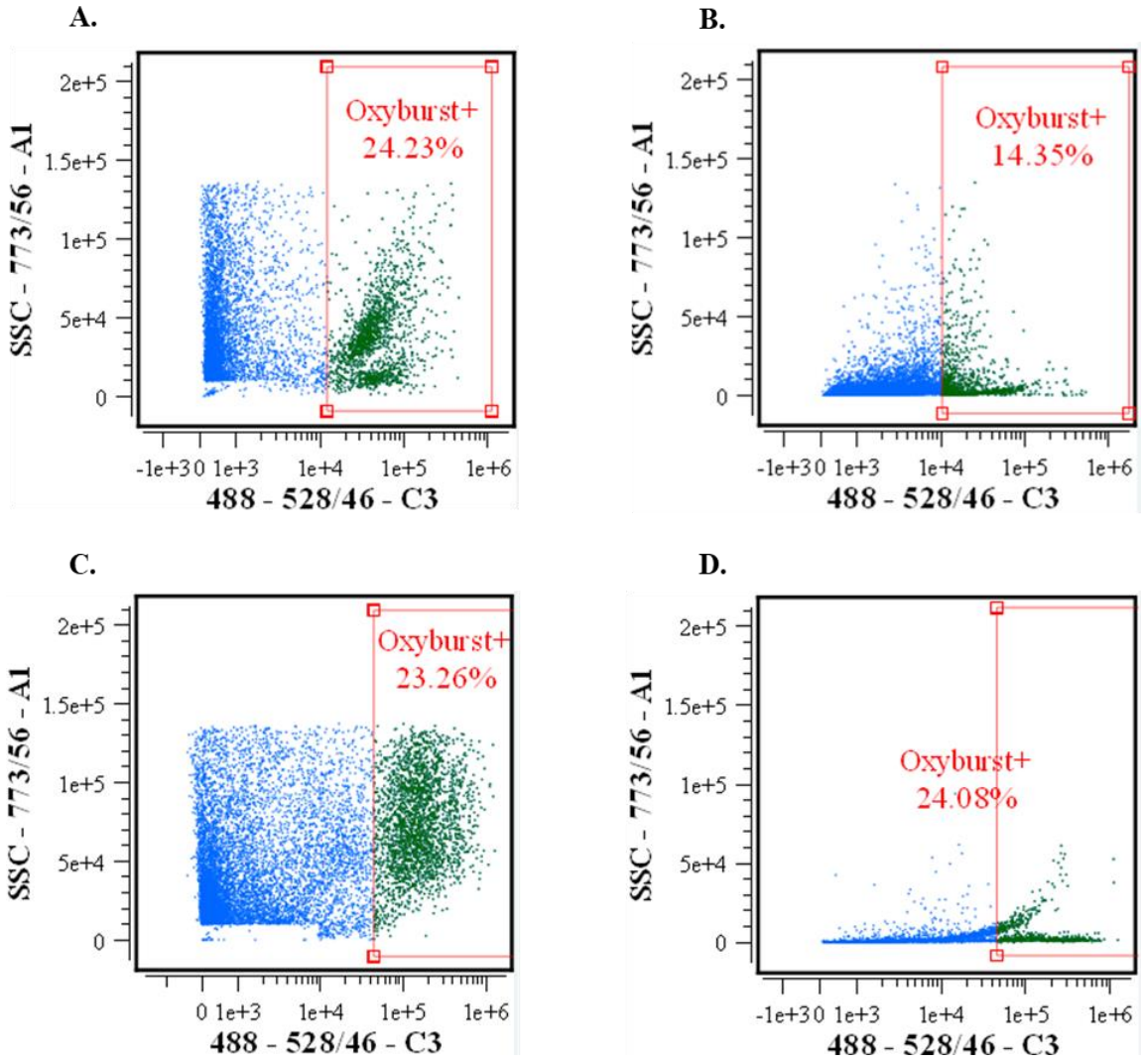

Figure 5. 3: Representative fluorocytograms of ROS analysis of PNT1a, LNCaP, PC3 and Du145 cells in the 5.5mM glucose.

(A) PNT1a untreated cells in the presence of 5.5mM glucose conditions. (B) LNCaP untreated cells in the presence of 5.5mM glucose conditions. (C) PC3 untreated cells in the presence of 5.5mM glucose conditions. (D) Du145 untreated cells in the presence of 5.5mM glucose conditions. Following 24hr incubation, cells were placed into 5.5mM glucose media for a further 24hrs. All cells were collected and stained with Oxyburst and analysed by flow cytometry. The Oxyburst negative cells are in the left quadrant (blue) and the Oxyburst positive cells are in the right quadrant (green). The data from the 5.5mM untreated conditions are shown here in all 4 cell lines used.

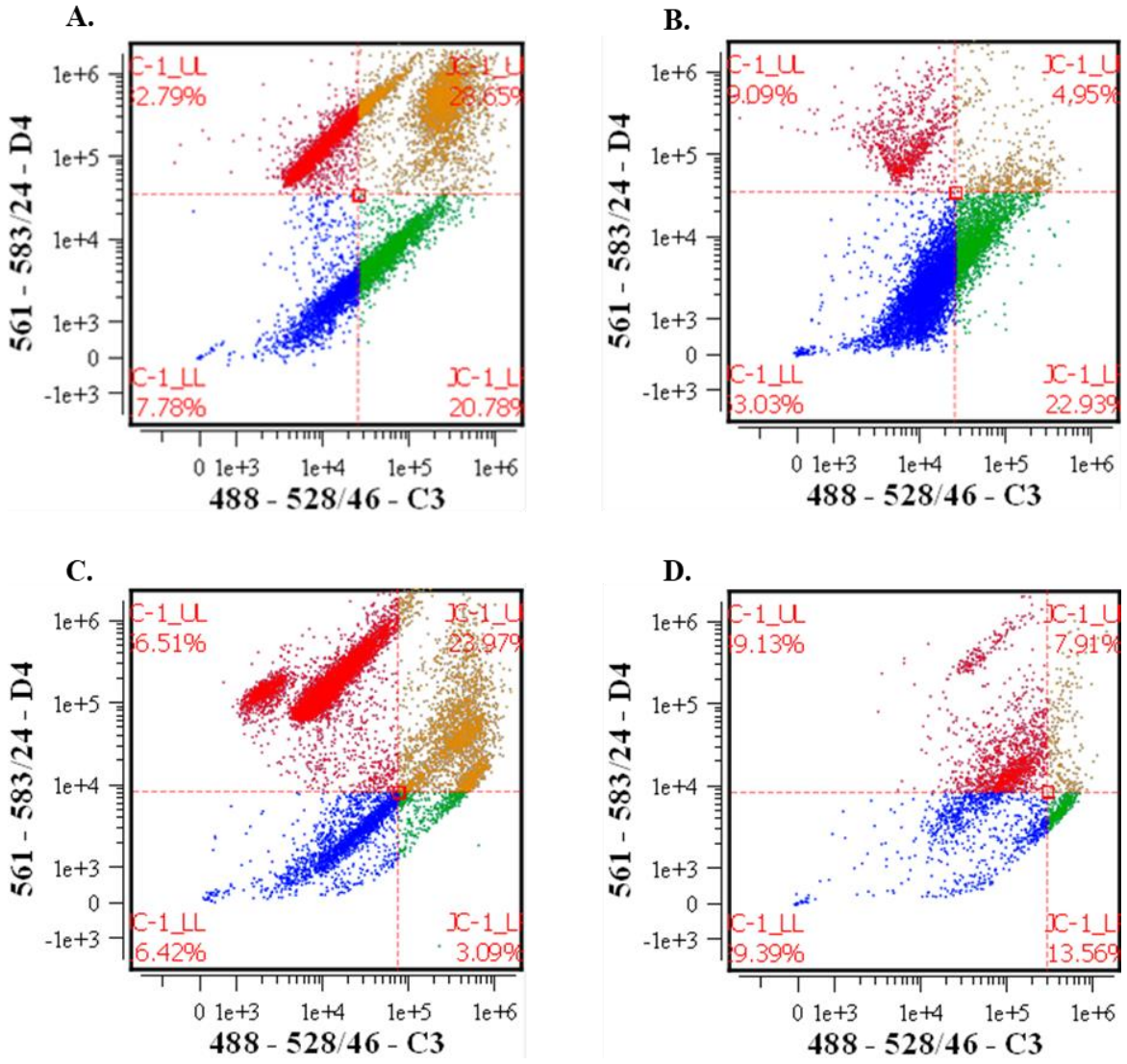

Figure 5. 4: Representative fluorocytograms of MMP analysis of PNT1a, LNCaP, PC3 and Du145 cells in the 5.5mM glucose.

(A) PNT1a untreated cells in the presence of 5.5mM glucose conditions. (B) LNCaP untreated cells in the presence of 5.5mM glucose conditions. (C) PC3 untreated cells in the presence of 5.5mM glucose conditions. (D) Du145 untreated cells in the presence of 5.5mM glucose conditions. Following 24hr incubation, cells were placed into 5.5mM glucose media for a further 24hrs. All cells were collected and stained with JC-1 and analysed by flow cytometry. Viable/healthy cells are in the lower left quadrant (blue). Cells with healthy and or high MMP are in the upper left quadrant (red). Cells with dual staining of JC-1 are in the upper right quadrant (yellow). The cells with unhealthy/ low MMP are in the lower right quadrant (green). The data from the 5.5mM untreated conditions are shown here in all 4 cell lines used.

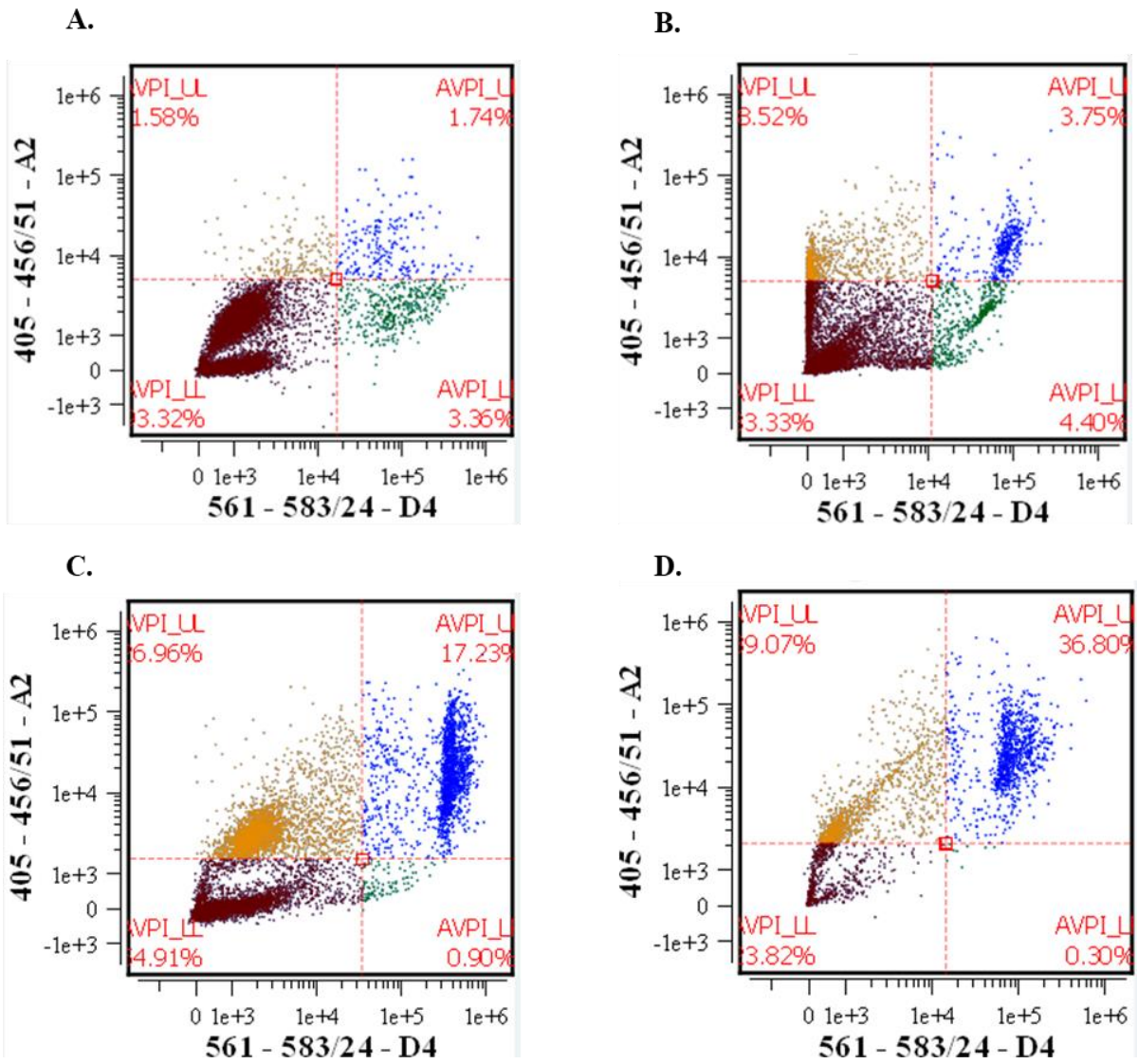

Figure 5. 5: Representative fluorocytograms of Apoptosis analysis of PNT1a, LNCaP, PC3 and Du145 cells in the 5.5mM glucose.

(A) PNT1a untreated cells in the presence of 5.5mM glucose conditions. (B) LNCaP untreated cells in the presence of 5.5mM glucose conditions. (C) PC3 untreated cells in the presence of 5.5mM glucose conditions. (D) Du145 untreated cells in the presence of 5.5mM glucose conditions. Following 24hr incubation, cells were placed into 5.5mM glucose media for a further 24hrs. All cells were collected and stained with Av PI and analysed by flow cytometry. Viable/healthy cells are in the lower left quadrant (brown). Necrotic cells are in the upper left quadrant (yellow). Cells in late apoptosis are in the upper right quadrant (blue). The cells in early apoptosis are in the lower right quadrant (green). The data from the 5.5mM untreated conditions are shown here in all 4 cell lines used.

5.4.2 Endogenous ROS and the mitochondrial effects across the zero, 5.5mM and 11mM glucose conditions of the PNT1a, LNCaP, PC3 and Du145 cell lines.

In the PNT1a cells, compared to the zero glucose, increased Oxyburst expression was observed in the presence of glucose, 5.5mM and 11mM glucose (P=0.005). The high MMP was increased in the 5.5mM glucose conditions (P=0.02). The JC-1 double positive quadrant resulted in no change between the glucose conditions. Low MMP expression resulted in decreased levels in the 5.5mM glucose group (P=0.002). Necrosis marker resulted in no change between the different glucose milieus. Late apoptosis was found to decrease between the 5.5mM and the 11mM glucose cells (P=0.03). No change was found between the glucose milieu in the healthy cells. No change was found between the glucose conditions in the early apoptosis group. The results are presented in Figure 5.6 **I**.

Necrosis was increased in LNCaP 11mM glucose (P=0.024) compared to the 5.5mM glucose conditions (5.6 **I** (E)) . Although this is found at very low levels with almost 100% of cells with no indicators of apoptosis or DNA damage as presented in Figure 5.6 **II** (G). Decreased early apoptosis was observed in the 11mM LNCaP cells (P=0.044).

Oxyburst expression did not change across the different glucose conditions for PC3 cells. High MMP was found to decrease in the 11mM glucose condition (P=0.04), with no change between the zero and 5.5mM conditions. No change was found for the double positive JC-1 across the glucose conditions. The low MMP was unchanged across the varied glucose milieu. Necrosis was found to be reduced in the 11mM glucose condition (P=0.01) compared to the zero and the 5.5mM glucose conditions. The healthy PC3 cells increased in the 11mM glucose in comparison to the 5.5mM glucose cells (P=0.04). Finally, early apoptosis was unchanged across the PC3 cells in the varied glucose conditions. The results are presented in Figure 5.6 **III**.

Du145 cells had consistent results across the glucose milieu of zero, 5.5mM and 11mM glucose, no significant change was found across all the flowcytometry panels examined as seen in Figure 5.6 **IV**.

I

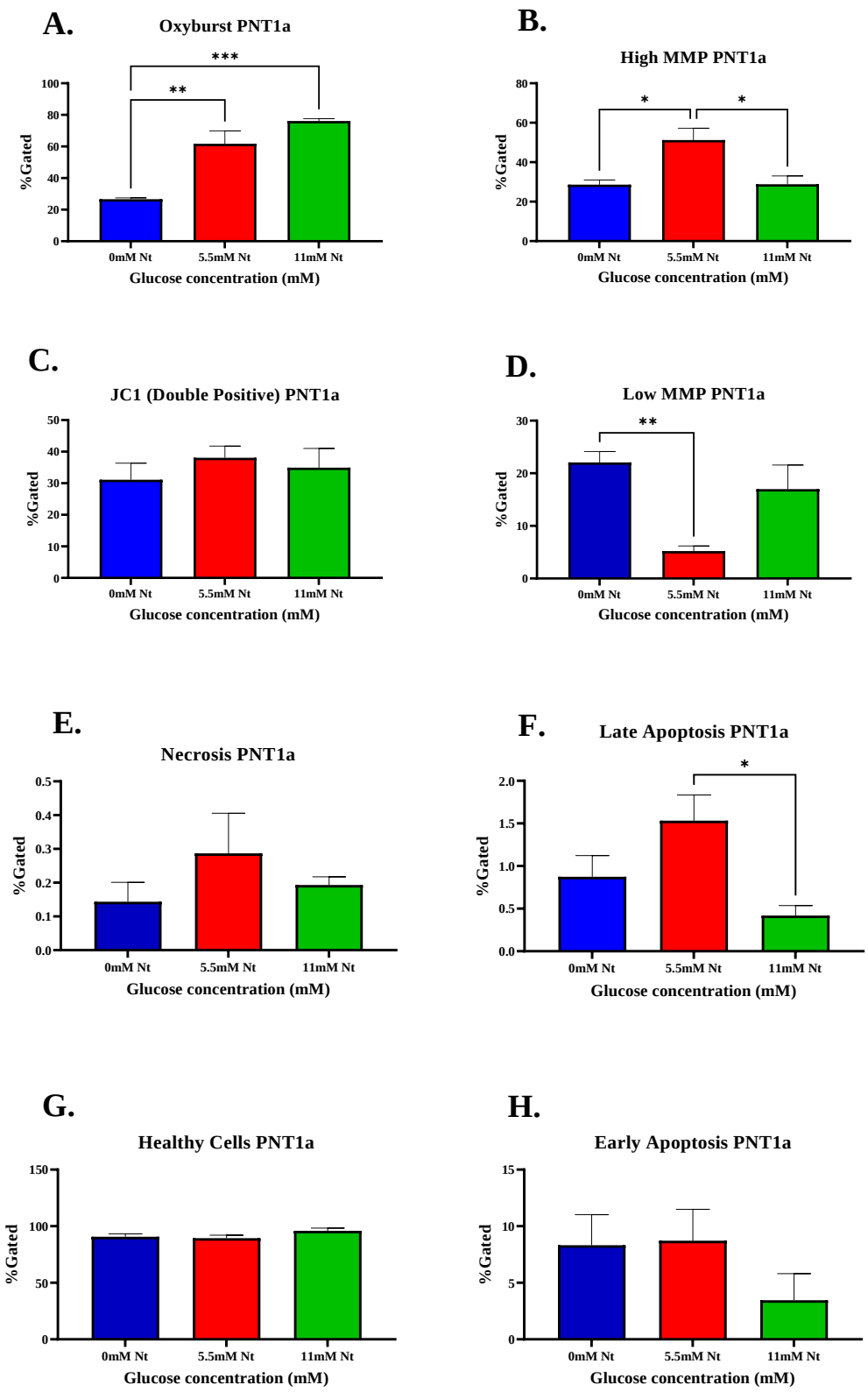
A.
Oxyburst PNT1a
***
**
%Gated
0mM Nt
5.5mM Nt
11mM Nt
Glucose concentration (mM)
B.
High MMP PNT1a
*
*
%Gated
0mM Nt
5.5mM Nt
11mM Nt
Glucose concentration (mM)
C.
JC1 (Double Positive) PNT1a
%Gated
0mM Nt
5.5mM Nt
11mM Nt
Glucose concentration (mM)
D.
Low MMP PNT1a
**
%Gated
0mM Nt
5.5mM Nt
11mM Nt
Glucose concentration (mM)
E.
Necrosis PNT1a
%Gated
0mM Nt
5.5mM Nt
11mM Nt
Glucose concentration (mM)
F.
Late Apoptosis PNT1a
*
%Gated
0mM Nt
5.5mM Nt
11mM Nt
Glucose concentration (mM)
G.
Healthy Cells PNT1a
%Gated
0mM Nt
5.5mM Nt
11mM Nt
Glucose concentration (mM)
H.
Early Apoptosis PNT1a
%Gated
0mM Nt
5.5mM Nt
11mM Nt
Glucose concentration (mM)

II

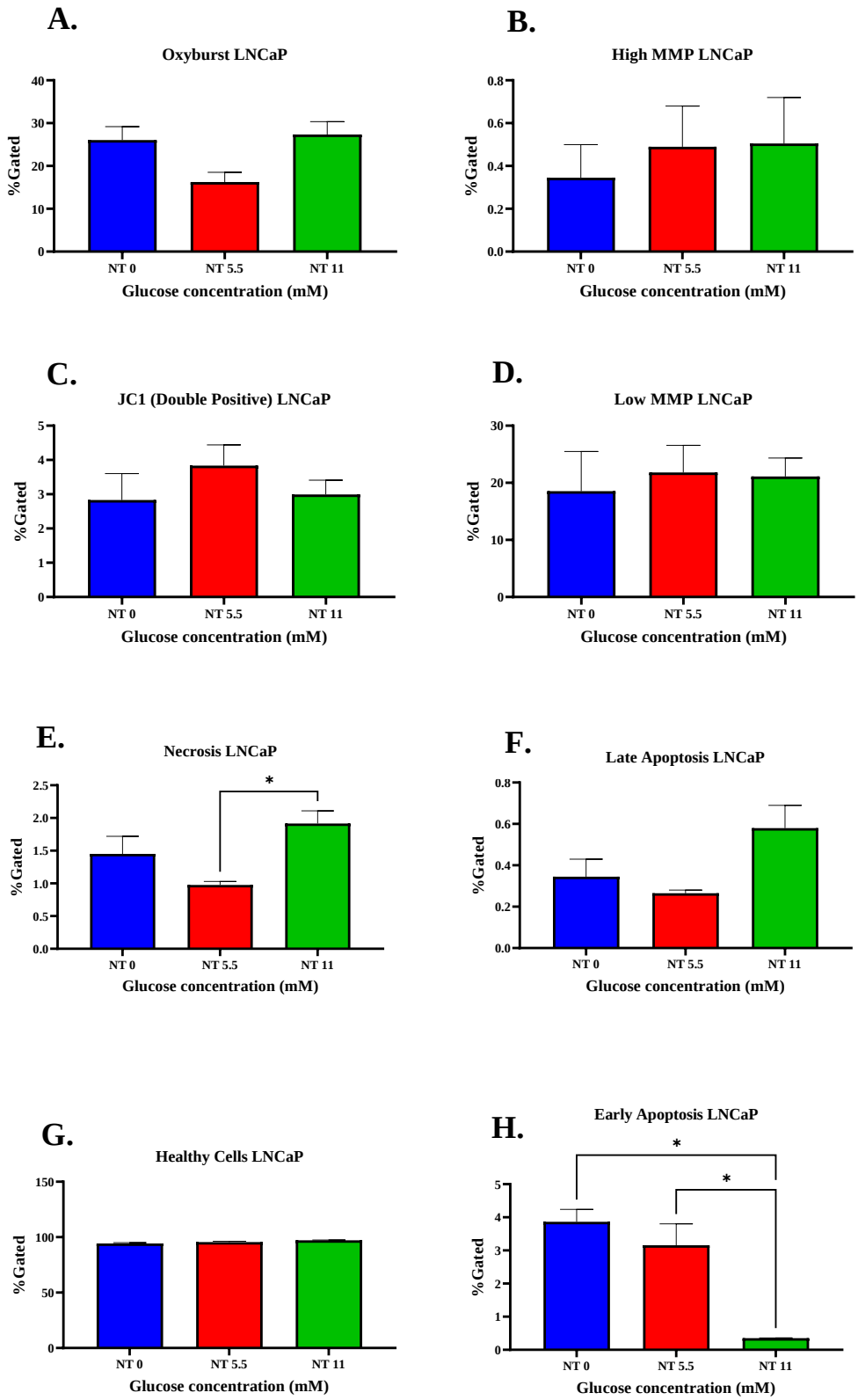
A.
Oxyburst LNCaP
%Gated
40
30
20
10
0
NT 0
NT 5.5
NT 11
Glucose concentration (mM)
B.
High MMP LNCaP
%Gated
0.8
0.6
0.4
0.2
0.0
NT 0
NT 5.5
NT 11
Glucose concentration (mM)
C.
JC1 (Double Positive) LNCaP
%Gated
5
4
3
2
1
0
NT 0
NT 5.5
NT 11
Glucose concentration (mM)
D.
Low MMP LNCaP
%Gated
30
20
10
0
NT 0
NT 5.5
NT 11
Glucose concentration (mM)
E.
Necrosis LNCaP
*
%Gated
2.5
2.0
1.5
1.0
0.5
0.0
NT 0
NT 5.5
NT 11
Glucose concentration (mM)
F.
Late Apoptosis LNCaP
%Gated
0.8
0.6
0.4
0.2
0.0
NT 0
NT 5.5
NT 11
Glucose concentration (mM)
G.
Healthy Cells LNCaP
%Gated
150
100
50
0
NT 0
NT 5.5
NT 11
Glucose concentration (mM)
H.
Early Apoptosis LNCaP
*
*
%Gated
5
4
3
2
1
0
NT 0
NT 5.5
NT 11
Glucose concentration (mM)

III

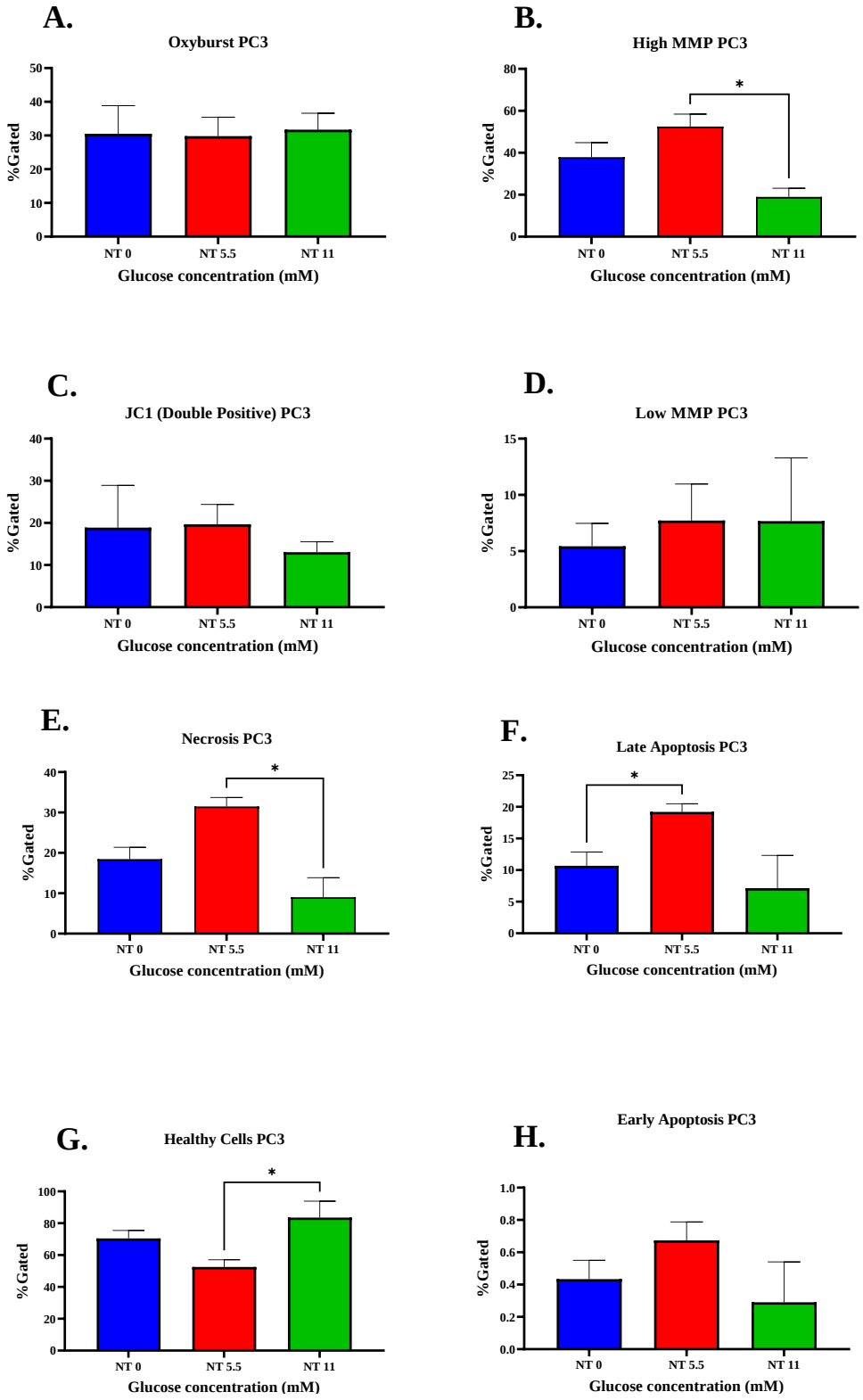
A.
Oxyburst PC3
%Gated
0
10
20
30
40
50
NT 0
NT 5.5
NT 11
Glucose concentration (mM)
B.
High MMP PC3
%Gated
0
20
40
60
80
*
NT 0
NT 5.5
NT 11
Glucose concentration (mM)
C.
JC1 (Double Positive) PC3
%Gated
0
10
20
30
40
NT 0
NT 5.5
NT 11
Glucose concentration (mM)
D.
Low MMP PC3
%Gated
0
5
10
15
NT 0
NT 5.5
NT 11
Glucose concentration (mM)
E.
Necrosis PC3
%Gated
0
10
20
30
40
*
NT 0
NT 5.5
NT 11
Glucose concentration (mM)
F.
Late Apoptosis PC3
%Gated
0
5
10
15
20
25
*
NT 0
NT 5.5
NT 11
Glucose concentration (mM)
G.
Healthy Cells PC3
%Gated
0
20
40
60
80
100
*
NT 0
NT 5.5
NT 11
Glucose concentration (mM)
H.
Early Apoptosis PC3
%Gated
0.0
0.2
0.4
0.6
0.8
1.0
NT 0
NT 5.5
NT 11
Glucose concentration (mM)

IV

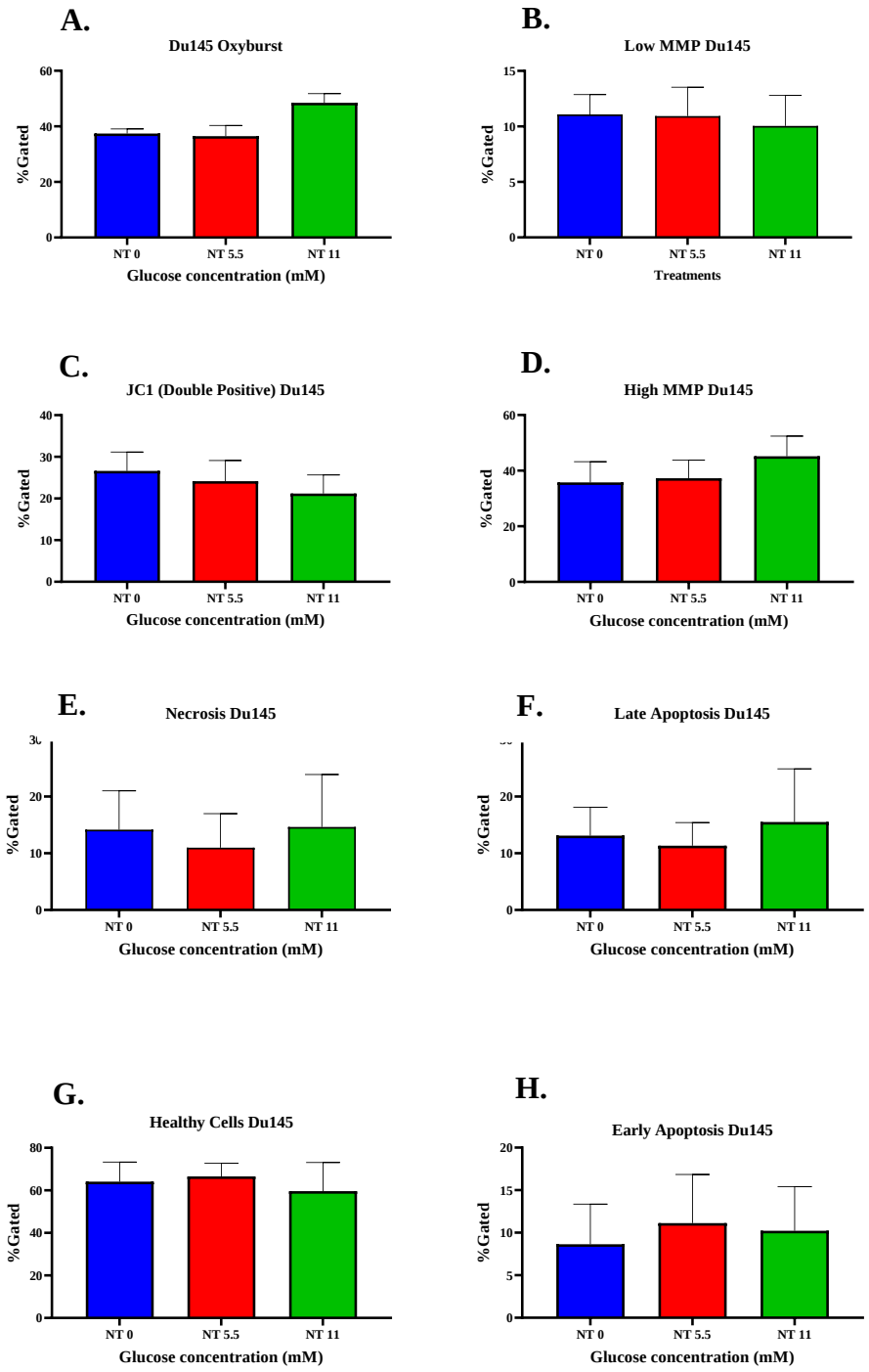

Figure 5. 6: ***(I.)****PNT1a % gated cells;****(II.)*** *LNCaP %gated cells;* ***(III.)*** *PC3 %gated cells and* ***(IV.)*** *Du145 %gated in the zero, 5.5mM and 11mM glucose conditions. (n=3) by one-way ANOVA.* ***(A)*** *Oxyburst expression, represents the endogenous ROS determined in the live cell.* ***(B)*** *JC-1 Red, is an indicator of high MMP, which indicates, intact mitochondria and complete ATP synthesis.* ***(C)*** *JC-1 Double positive, cells presenting double positive for JC1.* ***(D)*** *JC-1 Green; indicates low MMP, along with apoptosis and cell death, uncoupling of mitochondrial metabolic processes and a depolarised mitochondrion.* ***(E)*** *Av positive, PI negative is an indicator of necrosis.* ***(F)*** *Av positive and PI positive is an indication of late apoptosis.* ***(G)*** *Av negative and PI negative indicates healthy cells.* ***(H)*** *Av negative PI positive is an indicator of early apoptosis.*

5.4.3 Endogenous ROS and the mitochondrial effects across the zero, 5.5mM and 11mM glucose conditions in the PNT1a cells treated with Menadione and TH compounds

In the zero glucose conditions, Oxyburst expression in the PNT1a cells treated with the novel TH compounds did appear to increase however did not reach significance (P=0.1). The MMP expression was unchanged across the treatments in the presence of zero glucose conditions. The high MMP, was found to be approaching significance (P=0.07), although was found to be nonsignificant. Necrosis expression resulted in no change across the treatment groups in the presence of zero glucose. Overall, with low levels of necrosis observed. Late apoptosis was found to be unchanged between the untreated PNT1a cells and the TH treated cells. However, cells treated with Menadione increased the late apoptosis expression (P=0.004) in the PNT1a cells. The healthy cell expression was unchanged between all the treatment groups, as was the early apoptosis. The results are presented in Figure 5.7 **I**.

An increase in ROS production was found between the PNT1a untreated and the TH4 treated cells (P=0.03). No change was observed within the MMP in the 5.5mM glucose conditions. Necrosis expression resulted in no change across the treatment groups in the presence of 5.5mM glucose. Late apoptosis was found to be unchanged between the untreated PNT1a cells and the TH treated cells. However, cells treated with Menadione increased the late apoptosis expression in the PNT1a cells (P=0.05). The healthy cell expression was unchanged between all the treatment groups, as was the early apoptosis. The results are presented in Figure 5.17 **II**.

PNT1a Oxyburst expression was found to be increased with the TH treatments in the 11mM glucose milieu (P=0.005). A significant increase was found in the high MMP with the treatment with Menadione compared to that of the untreated PNT1a cells (P=0.02). TH6 treated cells also resulted in an increase in high MMP (P=0.04). The TH4 treated cells resulted in similar high MMP expression to that of the Menadione group and are approaching significance. Late apoptosis is increased with the Menadione treatment in the 11mM glucose PNT1a cells (P=0.04). No change was reported in the low MMP or the apoptotic markers in the 11mM glucose milieu, with the results presented in Figure 5.7 **III**.

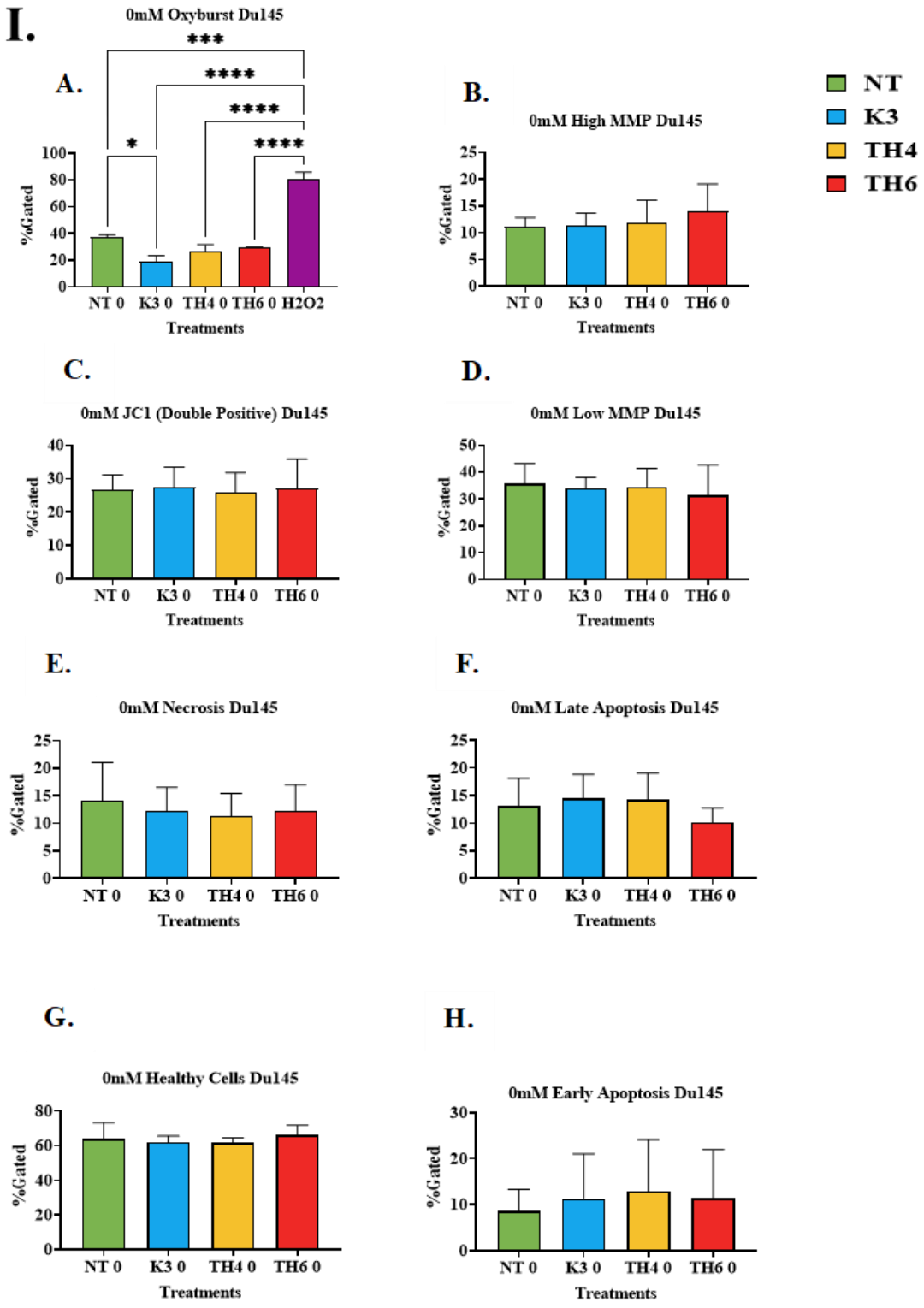
I.
A.
0mM Oxyburst Du145
***
****
****
****
*
%Gated
100
80
60
40
20
0
NT 0
K3 0
TH4 0
TH6 0
H2O2
Treatments
B.
0mM High MMP Du145
%Gated
25
20
15
10
5
0
NT 0
K3 0
TH4 0
TH6 0
Treatments
NT
K3
TH4
TH6
C.
0mM JC1 (Double Positive) Du145
%Gated
40
30
20
10
0
NT 0
K3 0
TH4 0
TH6 0
Treatments
D.
0mM Low MMP Du145
%Gated
50
40
30
20
10
0
NT 0
K3 0
TH4 0
TH6 0
Treatments
E.
0mM Necrosis Du145
%Gated
25
20
15
10
5
0
NT 0
K3 0
TH4 0
TH6 0
Treatments
F.
0mM Late Apoptosis Du145
%Gated
25
20
15
10
5
0
NT 0
K3 0
TH4 0
TH6 0
Treatments
G.
0mM Healthy Cells Du145
%Gated
80
60
40
20
0
NT 0
K3 0
TH4 0
TH6 0
Treatments
H.
0mM Early Apoptosis Du145
%Gated
30
20
10
0
NT 0
K3 0
TH4 0
TH6 0
Treatments

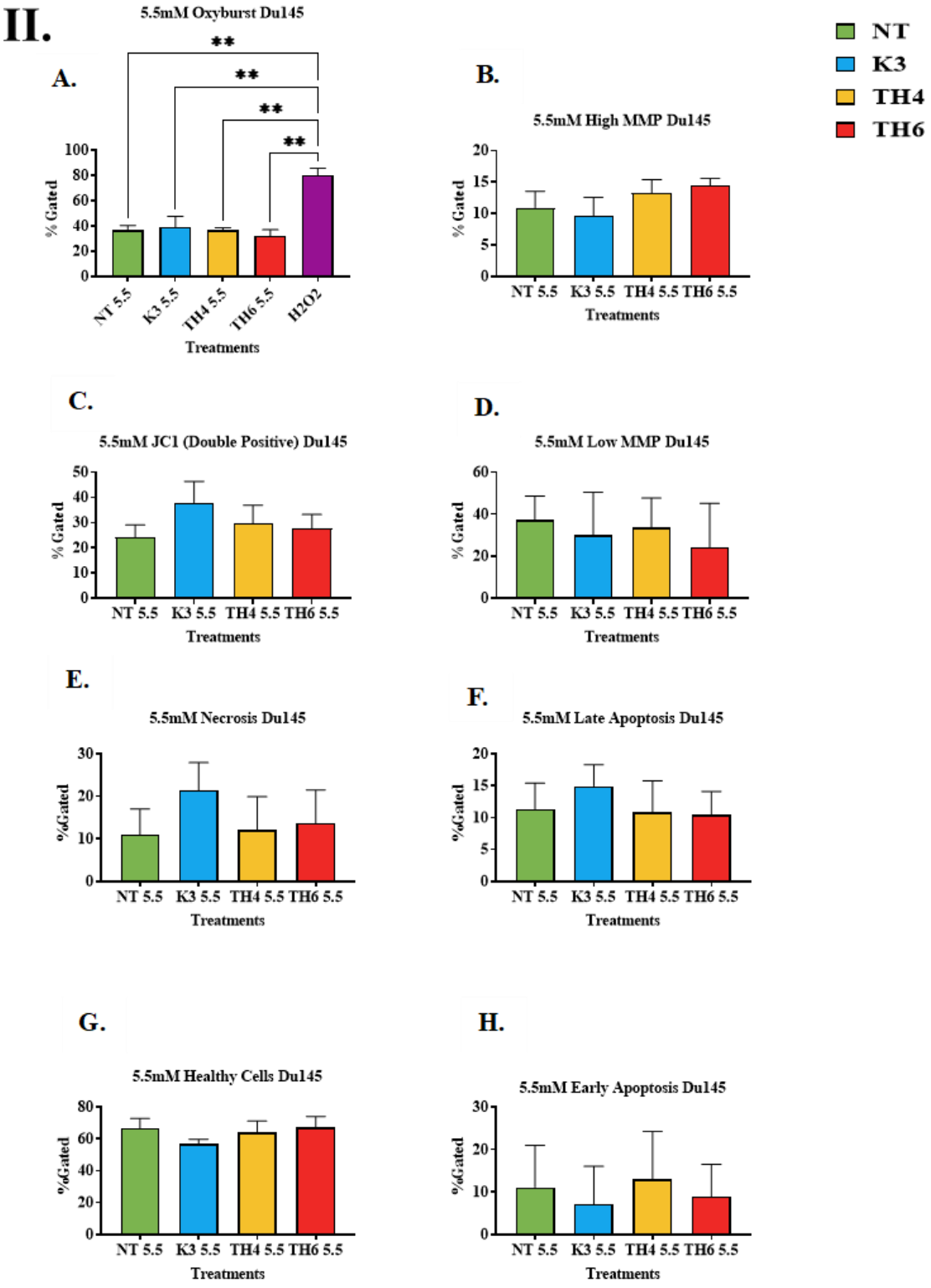
II.
A.
5.5mM Oxyburst Du145
**
**
**
**
% Gated
100
80
60
40
20
0
NT 5.5
K3 5.5
TH4 5.5
TH6 5.5
H2O2
Treatments
B.
5.5mM High MMP Du145
% Gated
20
15
10
5
0
NT 5.5
K3 5.5
TH4 5.5
TH6 5.5
Treatments
NT
K3
TH4
TH6
C.
5.5mM JC1 (Double Positive) Du145
% Gated
50
40
30
20
10
0
NT 5.5
K3 5.5
TH4 5.5
TH6 5.5
Treatments
D.
5.5mM Low MMP Du145
% Gated
60
40
20
0
NT 5.5
K3 5.5
TH4 5.5
TH6 5.5
Treatments
E.
5.5mM Necrosis Du145
%Gated
30
20
10
0
NT 5.5
K3 5.5
TH4 5.5
TH6 5.5
Treatments
F.
5.5mM Late Apoptosis Du145
%Gated
20
15
10
5
0
NT 5.5
K3 5.5
TH4 5.5
TH6 5.5
Treatments
G.
5.5mM Healthy Cells Du145
%Gated
80
60
40
20
0
NT 5.5
K3 5.5
TH4 5.5
TH6 5.5
Treatments
H.
5.5mM Early Apoptosis Du145
%Gated
30
20
10
0
NT 5.5
K3 5.5
TH4 5.5
TH6 5.5
Treatments

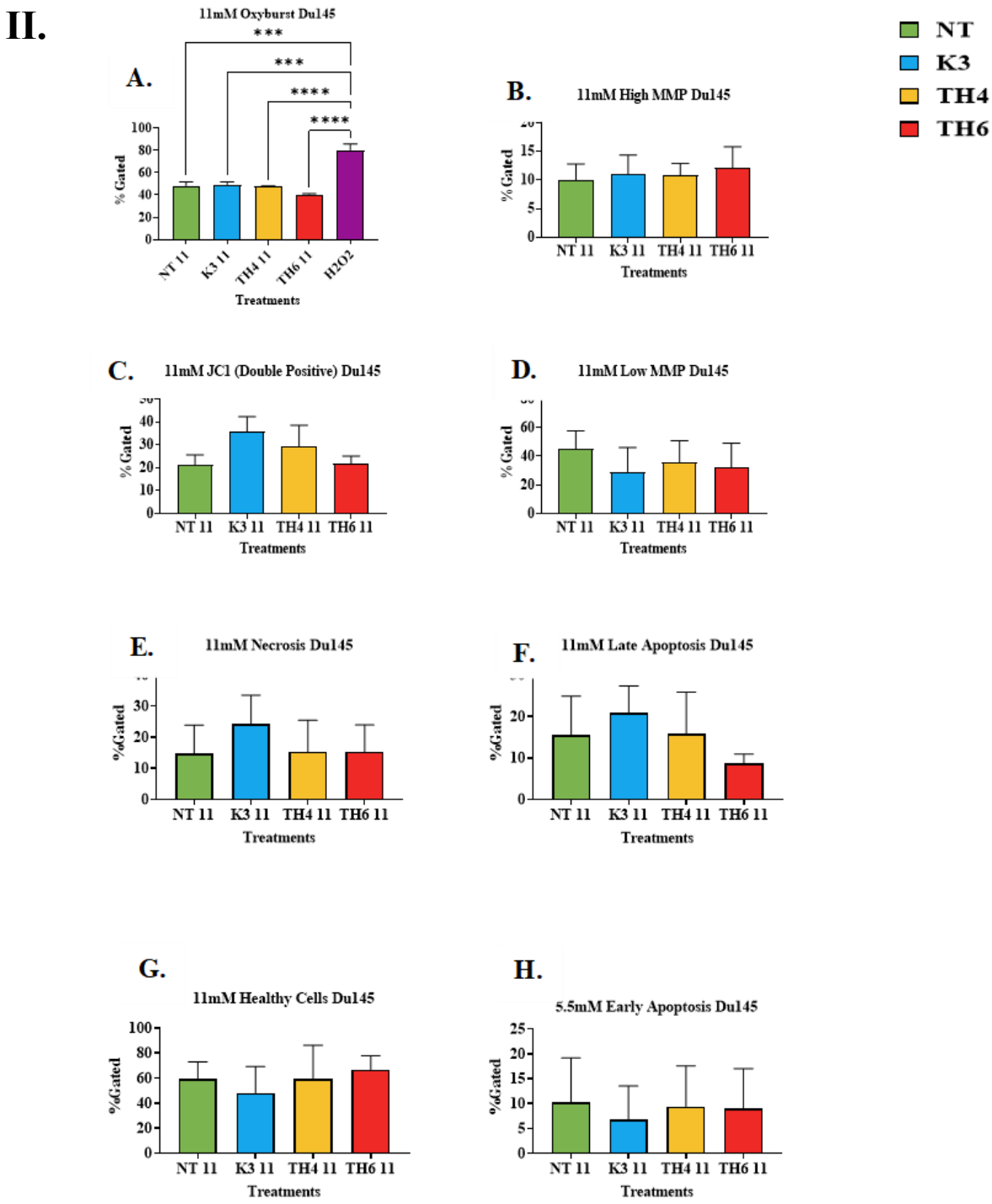

*Figure 5. 7: PNT1a Cells treated with Menadione, TH4 and TH6 CellStream data in the **(I.)** zero glucose conditions **(II.)** 5.5mM glucose conditions **(III.)** 11mM glucose conditions. (n=3) by one-way ANOVA (A-I) . PNT1a Cells treated with Menadione, TH4 and TH6 CellStream data in the 11mM Glucose conditions (n=3) by one-way ANOVA (A-I). (**A**) Oxyburst expression, represents the endogenous ROS determined in the live cell. (**B**) JC-1 Red, is an indicator of high MMP, which indicates, intact mitochondria and complete ATP synthesis. (**C**) JC-1 Double positive, cells presenting double positive for JC1. (**D**) JC-1 Green; indicates low MMP, along with apoptosis and cell death, uncoupling of mitochondrial metabolic processes and a depolarised mitochondrion. (**E**) Av positive, PI negative is an indicator of necrosis. (**F**) Av positive and PI positive is an indication of late apoptosis. (**G**) Av negative and PI negative indicates healthy cells. (**H**) Av negative PI positive is an indicator of early apoptosis*

5.4.3.1 The effects of the Menadione and TH treatments on the mitochondrial depolarisation in the PNT1a cell line in zero, 5.5mM and 11mM glucose conditions.

Mitochondrial depolarisation is calculated as a ratio of the JC1 red to JC1 green expression in the cells and is shown in Figure 5.8. A drop in mitochondrial depolarisation in the treatments, versus the untreated cells, is considered to indicate mitochondrial dysfunction. No significance was found between the treatment groups, or between the glucose conditions as presented in Figure 5.8.

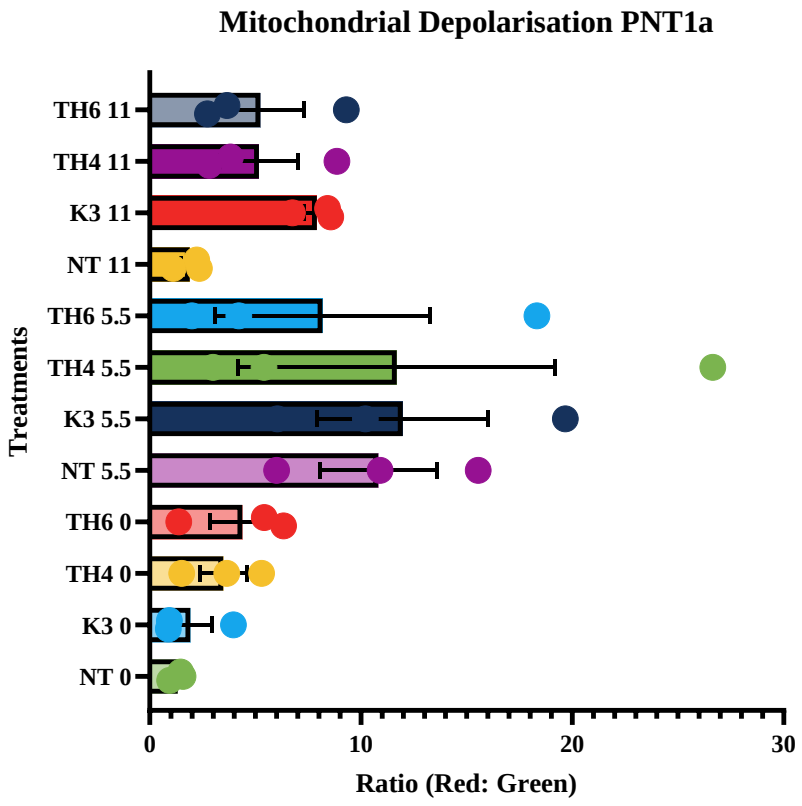

Figure 5. 8: Mitochondrial depolarisation of PNT1a cells un-treated and treatment with Menadione, TH4 and TH6 CellStream data in the zero, 5.5mM and 11mM Glucose conditions (n=3) by two-way ANOVA.

.

5.4.4 Endogenous ROS and the mitochondrial effects across the zero, 5.5mM and 11mM glucose conditions in the LNCaP cells treated with Menadione and TH compounds

No significance was observed across all the flowcytometry panels except for an increase in early apoptosis in the zero glucose untreated cells as shown in Figure 5.9 **I.** (H.) in comparison to the treated zero LNCaP cells.

No significant changes were found across the Oxyburst and MMP markers for the 5.5mM treated and untreated LNCaP cells, Figure 5.9**II** (A.-E). However, an increase in necrosis was observed with Menadione (P=0.004) and TH6 (P=0.0005) treatments for LNCaP 5.5mM, as observed in Figure 5.9 **II** (F.). Further, an increase in late apoptosis is present in the LNCaP cells treated with TH6 (P=0.05) as seen in Figure 5.9 **II** (G.). The majority of the LNCaP cells reported high levels of healthy cells. Finally, the untreated LNCaP cells had increased early apoptosis, in comparison to the treated groups (P=0.01).

The Oxyburst levels determined for LNCaP in the 11mM glucose conditions, resulted in no change between treatment groups (P=0.9). No change was reported in the high MMP for the LNCaP cells. JC-1 double positive was found to have significant change, with a decrease for the TH6 treated cells versus the untreated and Menadione treated cells. No changes were seen in the levels of necrosis present in the untreated and treated LNCaP cells. However, TH6 treatment, versus the untreated is trending towards significance (P=0.06). The Late apoptosis marker appears higher in the TH6 treated cells, but not to significance (P=0.1). The majority of the LNCaP cells presented with no marker of apoptosis or DNA damage as seen in Figure 5.9 **III** (H.). Early apoptosis was increased in the TH6 treated LNCaP cells (P<0.0001).

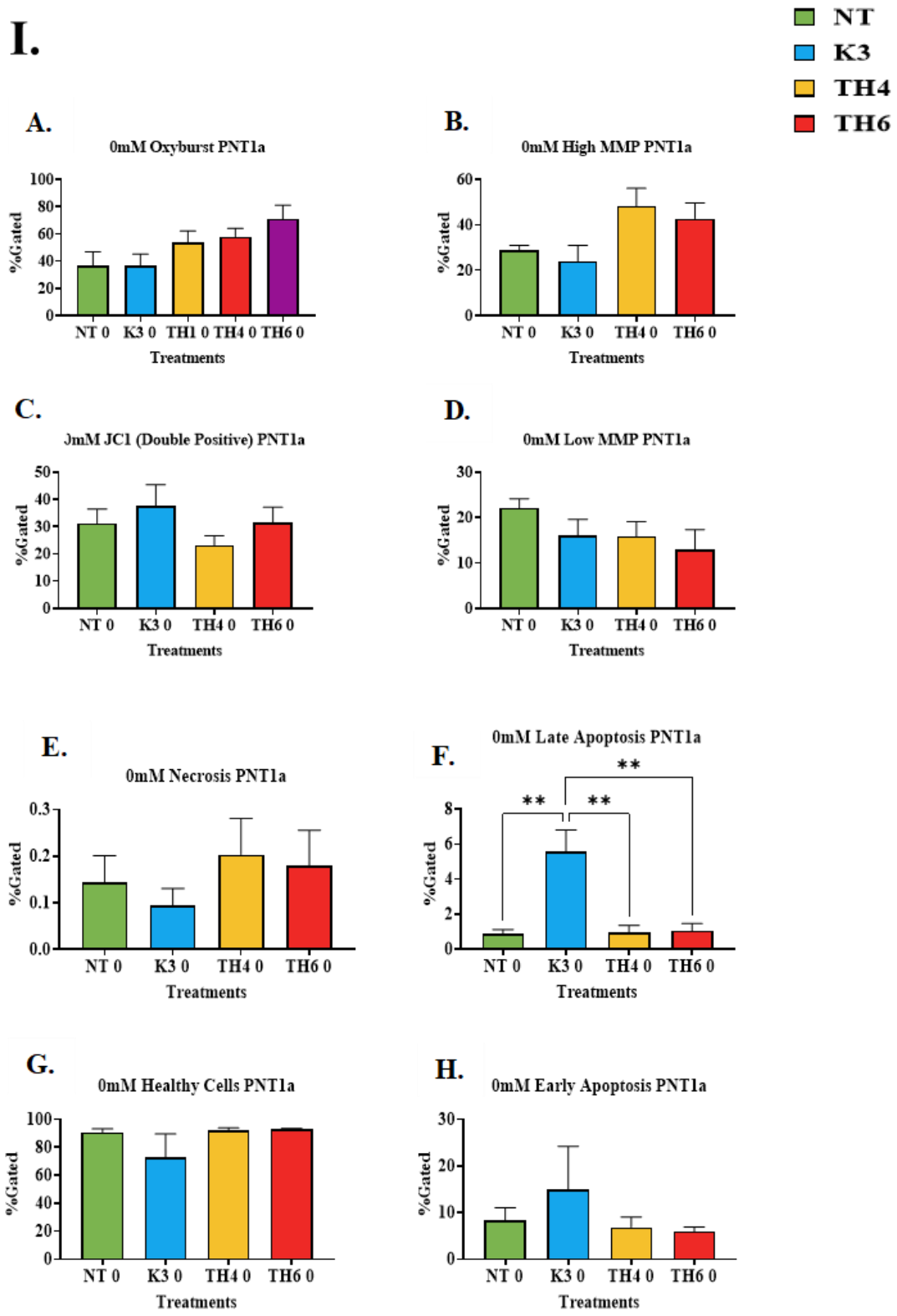
I.
NT
K3
TH4
TH6
A.
0mM Oxyburst PNT1a
%Gated
NT 0
K3 0
TH1 0
TH4 0
TH6 0
Treatments
B.
0mM High MMP PNT1a
%Gated
NT 0
K3 0
TH4 0
TH6 0
Treatments
C.
JmM JC1 (Double Positive) PNT1a
%Gated
NT 0
K3 0
TH4 0
TH6 0
Treatments
D.
0mM Low MMP PNT1a
%Gated
NT 0
K3 0
TH4 0
TH6 0
Treatments
E.
0mM Necrosis PNT1a
%Gated
NT 0
K3 0
TH4 0
TH6 0
Treatments
F.
0mM Late Apoptosis PNT1a
**
**
**
%Gated
NT 0
K3 0
TH4 0
TH6 0
Treatments
G.
0mM Healthy Cells PNT1a
%Gated
NT 0
K3 0
TH4 0
TH6 0
Treatments
H.
0mM Early Apoptosis PNT1a
%Gated
NT 0
K3 0
TH4 0
TH6 0
Treatments

II.

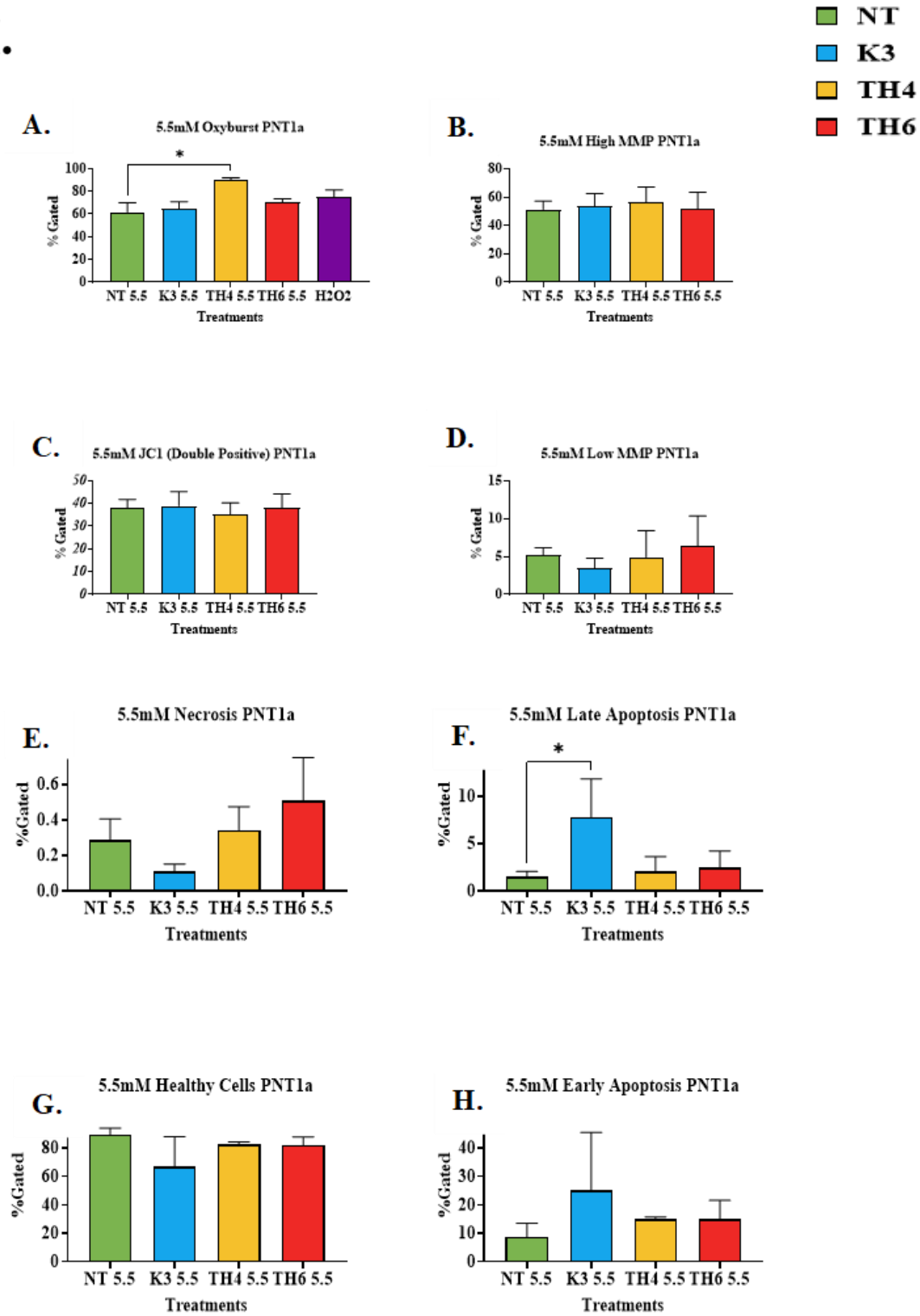
NT
K3
TH4
TH6
A.
5.5mM Oxyburst PNT1a
% Gated
NT 5.5 K3 5.5 TH4 5.5 TH6 5.5 H2O2
Treatments
B.
5.5mM High MMP PNT1a
% Gated
NT 5.5 K3 5.5 TH4 5.5 TH6 5.5
Treatments
C.
5.5mM JC1 (Double Positive) PNT1a
% Gated
NT 5.5 K3 5.5 TH4 5.5 TH6 5.5
Treatments
D.
5.5mM Low MMP PNT1a
% Gated
NT 5.5 K3 5.5 TH4 5.5 TH6 5.5
Treatments
E.
5.5mM Necrosis PNT1a
%Gated
NT 5.5 K3 5.5 TH4 5.5 TH6 5.5
Treatments
F.
5.5mM Late Apoptosis PNT1a
%Gated
NT 5.5 K3 5.5 TH4 5.5 TH6 5.5
Treatments
G.
5.5mM Healthy Cells PNT1a
%Gated
NT 5.5 K3 5.5 TH4 5.5 TH6 5.5
Treatments
H.
5.5mM Early Apoptosis PNT1a
%Gated
NT 5.5 K3 5.5 TH4 5.5 TH6 5.5
Treatments

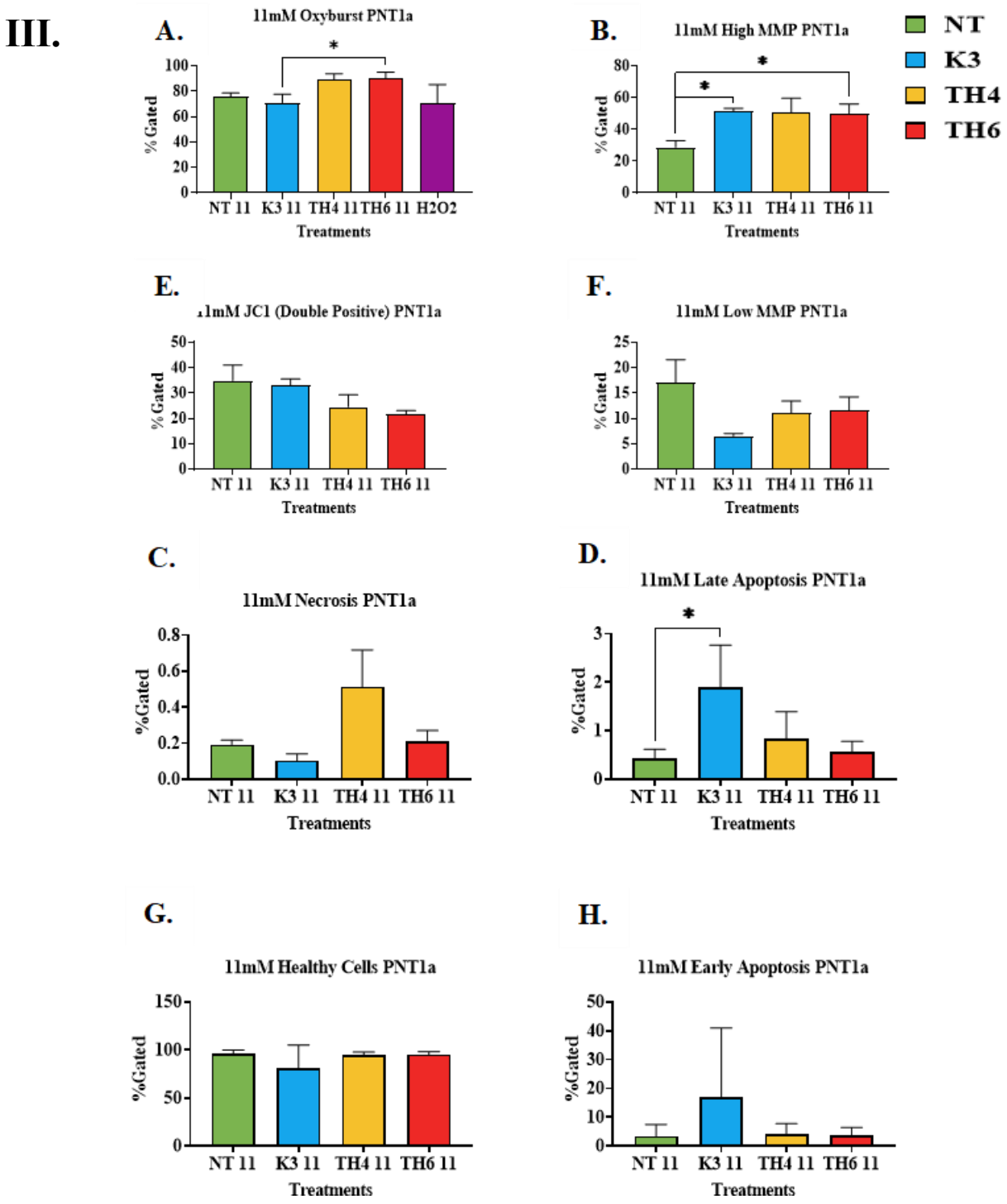

*Figure 5. 9: LNCaP treated %gated in the **(I.)** zero glucose; **(II.)** 5.5mM glucose and **(III.)** 11mM glucose conditions. (n=3) by one-way ANOVA (A-I (**A**) Oxyburst expression, represents the endogenous ROS determined in the live cell. (**B**) JC-1 Red, is an indicator of high MMP, which indicates, intact mitochondria and complete ATP synthesis. (**C**) JC-1 Double positive, cells presenting double positive for JC1. (**D**) JC-1 Green; indicates low MMP, along with apoptosis and cell death, uncoupling of mitochondrial metabolic processes and a depolarised mitochondrion. (**E**) Av positive, PI negative is an indicator of necrosis. (**F**) Av positive and PI positive is an indication of late apoptosis. (**G**) Av negative and PI negative indicates healthy cells. (**H**) Av negative PI positive is an indicator of early apoptosis.*

5.4.4.1 The effects of the Menadione and TH treatments on the mitochondrial depolarisation in the LNCaP cell line in zero, 5.5mM and 11mM glucose conditions.

Mitochondrial depolarisation of LNCaP is shown in Figure 5.10. In the presence of zero glucose, the mitochondrial depolarisation of LNCaP is increased when treated with Menadione versus the zero untreated LNCaP (*P*=0.02) and the 11mM Menadione treated LNCaP (*P*=0.002).

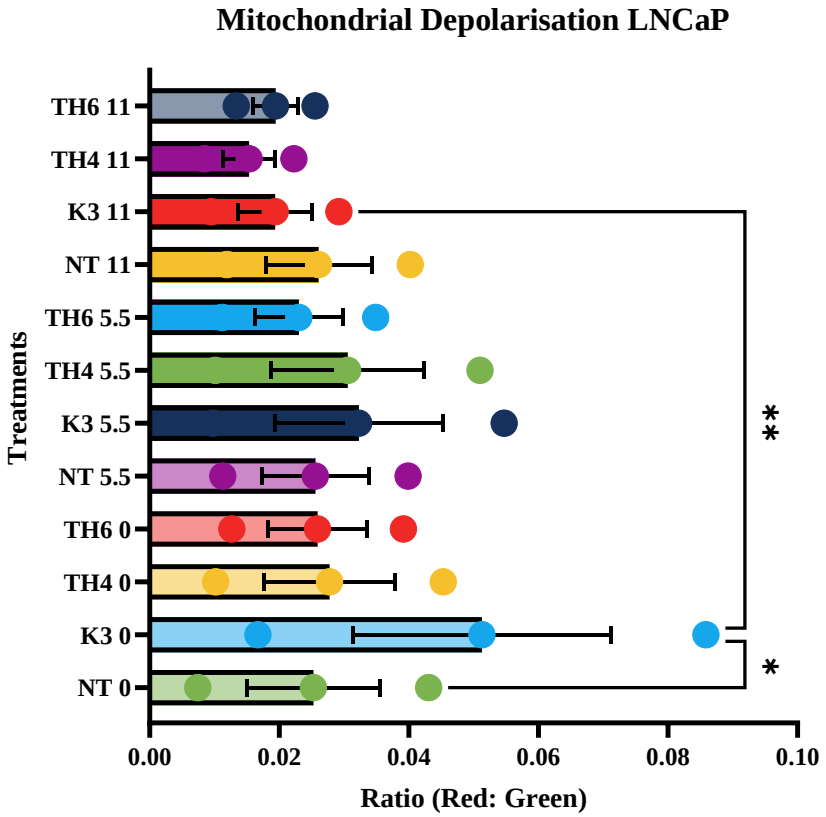

Figure 5.10: Mitochondrial Depolarisation of LNCaP cells un-treated and treatment with Menadione, TH4 and TH6 CellStream data in the zero, 5.5mM and 11mM Glucose conditions (n=3) by two-way ANOVA.

5.4.5 Endogenous ROS and the mitochondrial effects across the zero, 5.5mM and 11mM glucose conditions in the PC3 cells treated with Menadione and TH compounds

No significant change was found within any the zero PC3 evaluation. However, the late apoptosis in Figure 5.11 **I** (**G.)** between the untreated PC3 and TH6 treated PC3 is trending towards significance (P=0.06).

No significant changes were found in the cells in the 5.5mM glucose for the Oxyburst and MMP evaluation. Early apoptosis was found to be unchanged between the treatment groups (P=0.4). Late apoptosis was increased in the TH4 treated PC3 cells compared to the untreated cells (P=0.008). The lack of apoptosis and DNA damage found in the untreated cells was illustrated in Figure 5.11 **II** (H.), where higher levels of healthy cells were found in the untreated cells (P=0.01). DNA damage was consistent across all the PC3 cells in the 5.5mM glucose.

No significant changes were found in the cells in the 11mM glucose for the Oxyburst, MMP and apoptosis evaluation, as presented in Figure 5.11 **III**.

I.

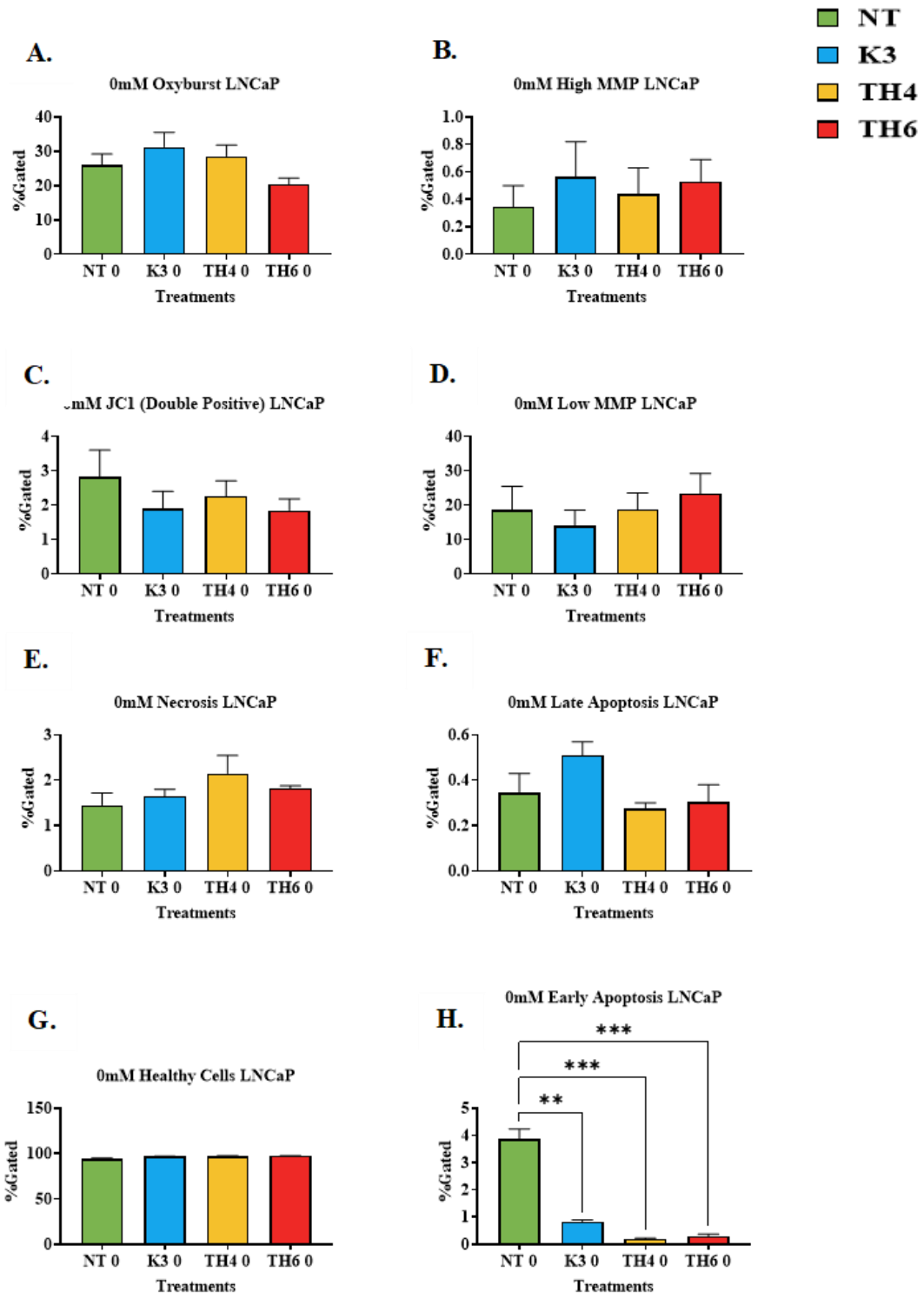
NT
K3
TH4
TH6
A.
0mM Oxyburst LNCaP
%Gated
Treatments
NT 0
K3 0
TH4 0
TH6 0
B.
0mM High MMP LNCaP
C.
mM JC1 (Double Positive) LNCaP
D.
0mM Low MMP LNCaP
E.
0mM Necrosis LNCaP
F.
0mM Late Apoptosis LNCaP
G.
0mM Healthy Cells LNCaP
H.
0mM Early Apoptosis LNCaP
***
***
**

II.

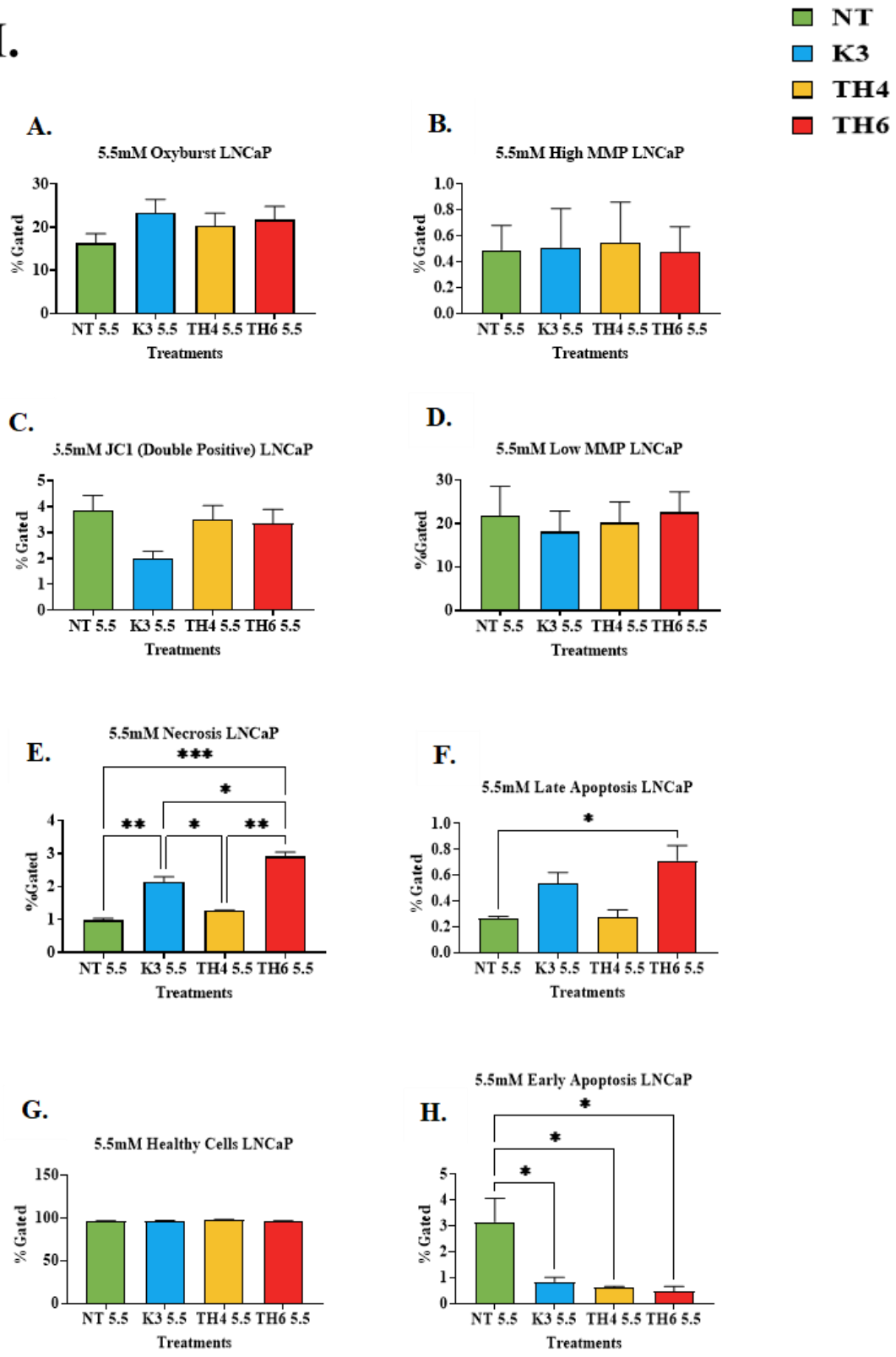
NT
K3
TH4
TH6
A.
5.5mM Oxyburst LNCaP
% Gated
NT 5.5 K3 5.5 TH4 5.5 TH6 5.5
Treatments
B.
5.5mM High MMP LNCaP
% Gated
NT 5.5 K3 5.5 TH4 5.5 TH6 5.5
Treatments
C.
5.5mM JC1 (Double Positive) LNCaP
% Gated
NT 5.5 K3 5.5 TH4 5.5 TH6 5.5
Treatments
D.
5.5mM Low MMP LNCaP
%Gated
NT 5.5 K3 5.5 TH4 5.5 TH6 5.5
Treatments
E.
5.5mM Necrosis LNCaP
%Gated
NT 5.5 K3 5.5 TH4 5.5 TH6 5.5
Treatments
F.
5.5mM Late Apoptosis LNCaP
% Gated
NT 5.5 K3 5.5 TH4 5.5 TH6 5.5
Treatments
G.
5.5mM Healthy Cells LNCaP
% Gated
NT 5.5 K3 5.5 TH4 5.5 TH6 5.5
Treatments
H.
5.5mM Early Apoptosis LNCaP
% Gated
NT 5.5 K3 5.5 TH4 5.5 TH6 5.5
Treatments

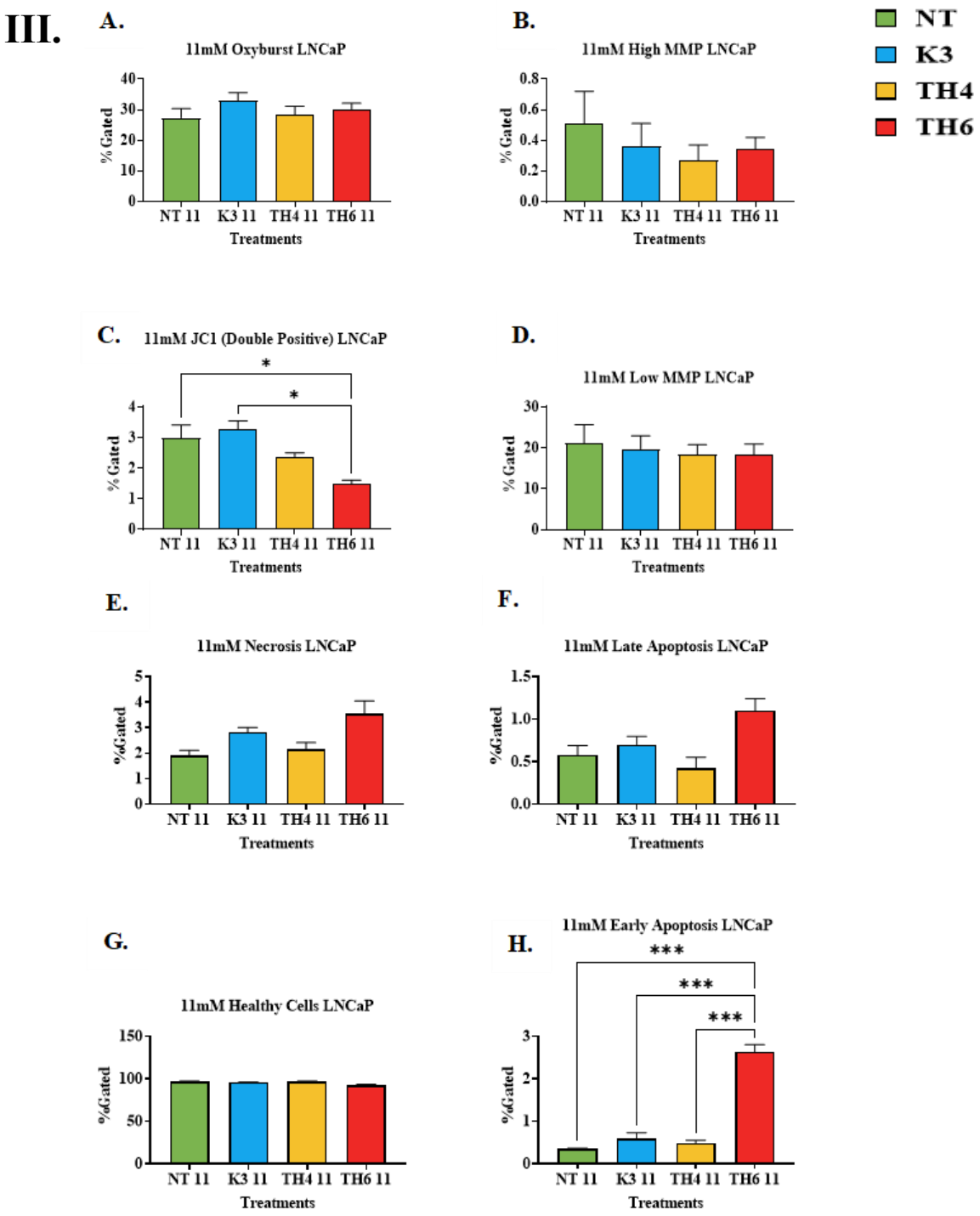

*Figure 5. 11: PC3 untreated vs treated %gated in the **(I.)** zero glucose; **(II.)** 5.5mM glucose and **(III.)** 11mM glucose conditions. (n=3) by one-way ANOVA . (**A**) Oxyburst expression, represents the endogenous ROS determined in the live cell. (**B**) JC-1 Red, is an indicator of high MMP, which indicates, intact mitochondria and complete ATP synthesis. (**C**) JC-1 Double positive, cells presenting double positive for JC1. (**D**) JC-1 Green; indicates low MMP, along with apoptosis and cell death, uncoupling of mitochondrial metabolic processes and a depolarised mitochondrion. (**E**) Av positive, PI negative is an indicator of necrosis. (**F**) Av positive and PI positive is an indication of late apoptosis. (**G**) Av negative and PI negative indicates healthy cells. (**H**) Av negative PI positive is an indicator of early apoptosis.*

5.4.5.1 The effects of the Menadione and TH treatments on the mitochondrial depolarisation in the PC3 cell line in zero, 5.5mM and 11mM glucose conditions.

Mitochondrial depolarisation of PC3 is shown in Figure 5.12. The mitochondrial depolarisation of PC3 treated with TH4 was increased significantly in the presence of 11mM glucose (P=0.001) versus the untreated, Menadione, and TH6 cells. No significance was found between the TH4 treatments across the glucose conditions.

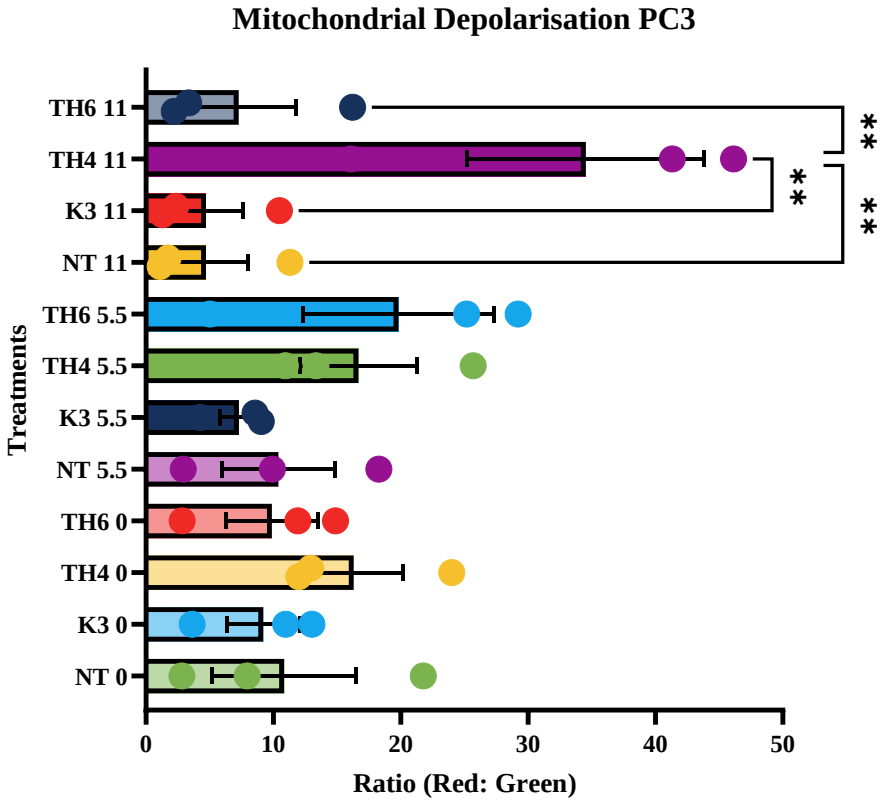

Figure 5. 12: Mitochondrial Depolarisation of PC3 cells un-treated and treatment with Menadione, TH4 and TH6 CellStream data in the zero, 5.5mM and 11mM glucose conditions (n=3) by two-way ANOVA.

5.4.6 Endogenous ROS and the mitochondrial effects across the zero, 5.5mM and 11mM glucose conditions in the Du145 cells treated with Menadione and TH compounds

In the zero glucose, Oxyburst expression was decreased when cells were treated with Menadione versus the untreated Du145 cells ($P<0.0001$). The H_2O_2 control exhibited high levels of ROS in the Du145 cells. No other significant changes were expressed across the flowcytometry panels examined in the zero glucose for the Du145 cells. Results are presented in Figure 5.13 **I**.

In the presence of 5.5mm glucose, the H_2O_2 control exhibited high levels of ROS in the Du145 cells. No other significant changes were expressed across the flowcytometry panels examined for the Du145 cells in the 5.5mM glucose conditions as presented in Figure 5.13 **II.** (**A**.).

Once more, the H_2O_2 control exhibited high levels of ROS in the Du145 cells in the 11mM glucose conditions. No other significant changes were observed for the Du145 cells as seen in Figure 5.13 **III**.

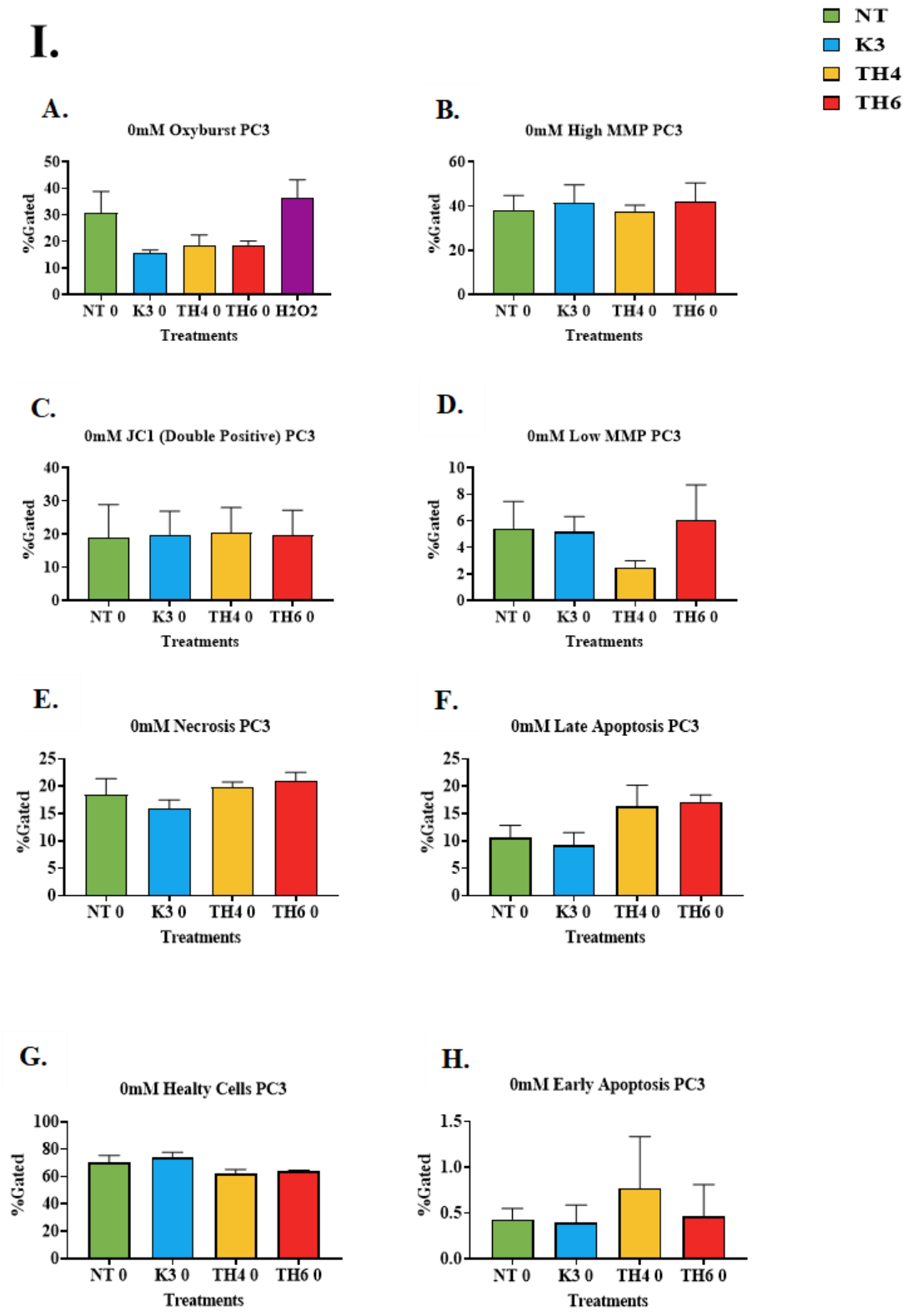
I.
NT
K3
TH4
TH6
A.
0mM Oxyburst PC3
%Gated
NT 0
K3 0
TH4 0
TH6 0
H2O2
Treatments
B.
0mM High MMP PC3
C.
0mM JC1 (Double Positive) PC3
D.
0mM Low MMP PC3
E.
0mM Necrosis PC3
F.
0mM Late Apoptosis PC3
G.
0mM Healty Cells PC3
H.
0mM Early Apoptosis PC3

II.

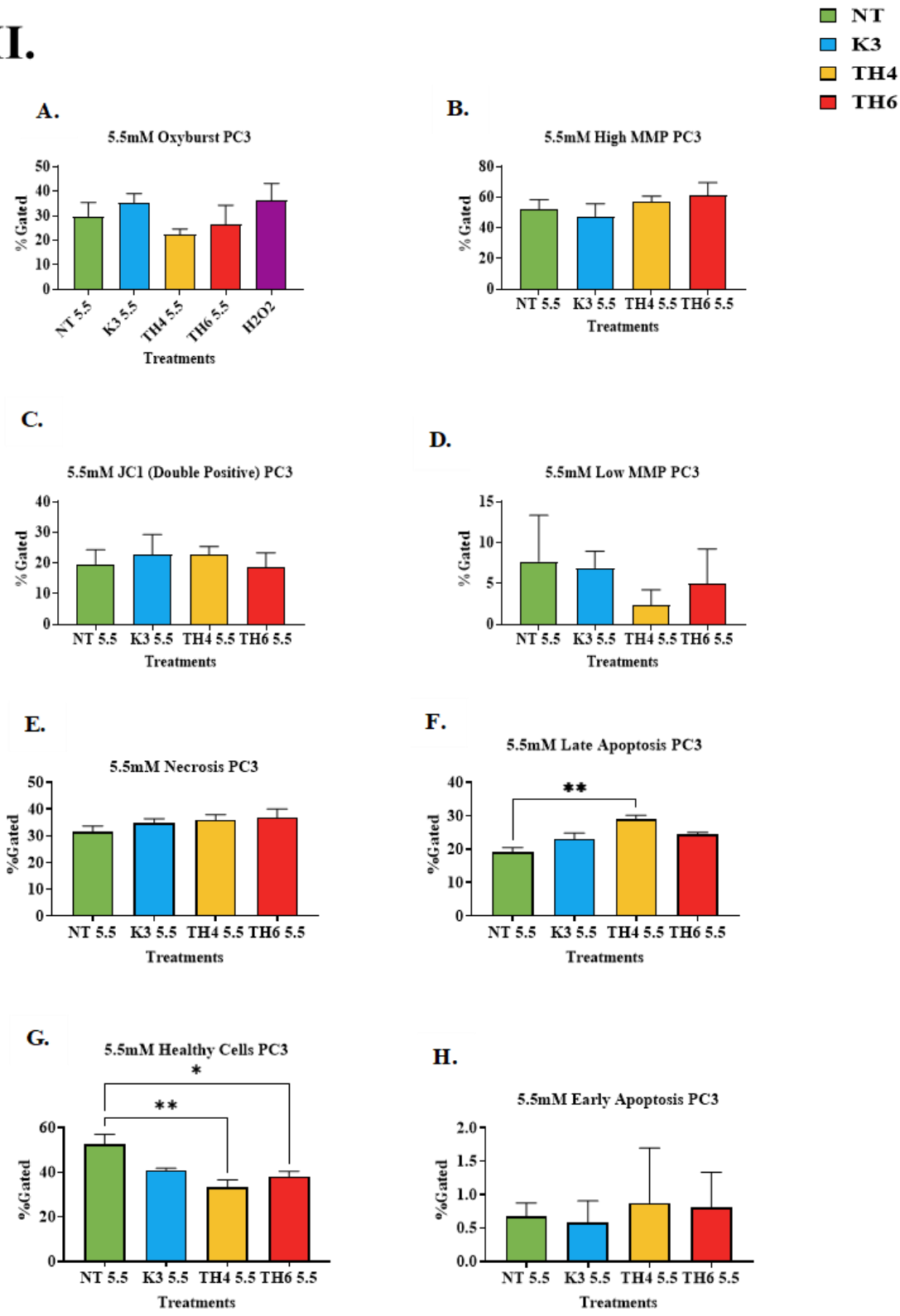
NT
K3
TH4
TH6
A.
5.5mM Oxyburst PC3
% Gated
NT 5.5
K3 5.5
TH4 5.5
TH6 5.5
H2O2
Treatments
B.
5.5mM High MMP PC3
% Gated
NT 5.5
K3 5.5
TH4 5.5
TH6 5.5
Treatments
C.
5.5mM JC1 (Double Positive) PC3
% Gated
NT 5.5
K3 5.5
TH4 5.5
TH6 5.5
Treatments
D.
5.5mM Low MMP PC3
% Gated
NT 5.5
K3 5.5
TH4 5.5
TH6 5.5
Treatments
E.
5.5mM Necrosis PC3
%oGated
NT 5.5
K3 5.5
TH4 5.5
TH6 5.5
Treatments
F.
5.5mM Late Apoptosis PC3
**
%oGated
NT 5.5
K3 5.5
TH4 5.5
TH6 5.5
Treatments
G.
5.5mM Healthy Cells PC3
*
**
%oGated
NT 5.5
K3 5.5
TH4 5.5
TH6 5.5
Treatments
H.
5.5mM Early Apoptosis PC3
%oGated
NT 5.5
K3 5.5
TH4 5.5
TH6 5.5
Treatments

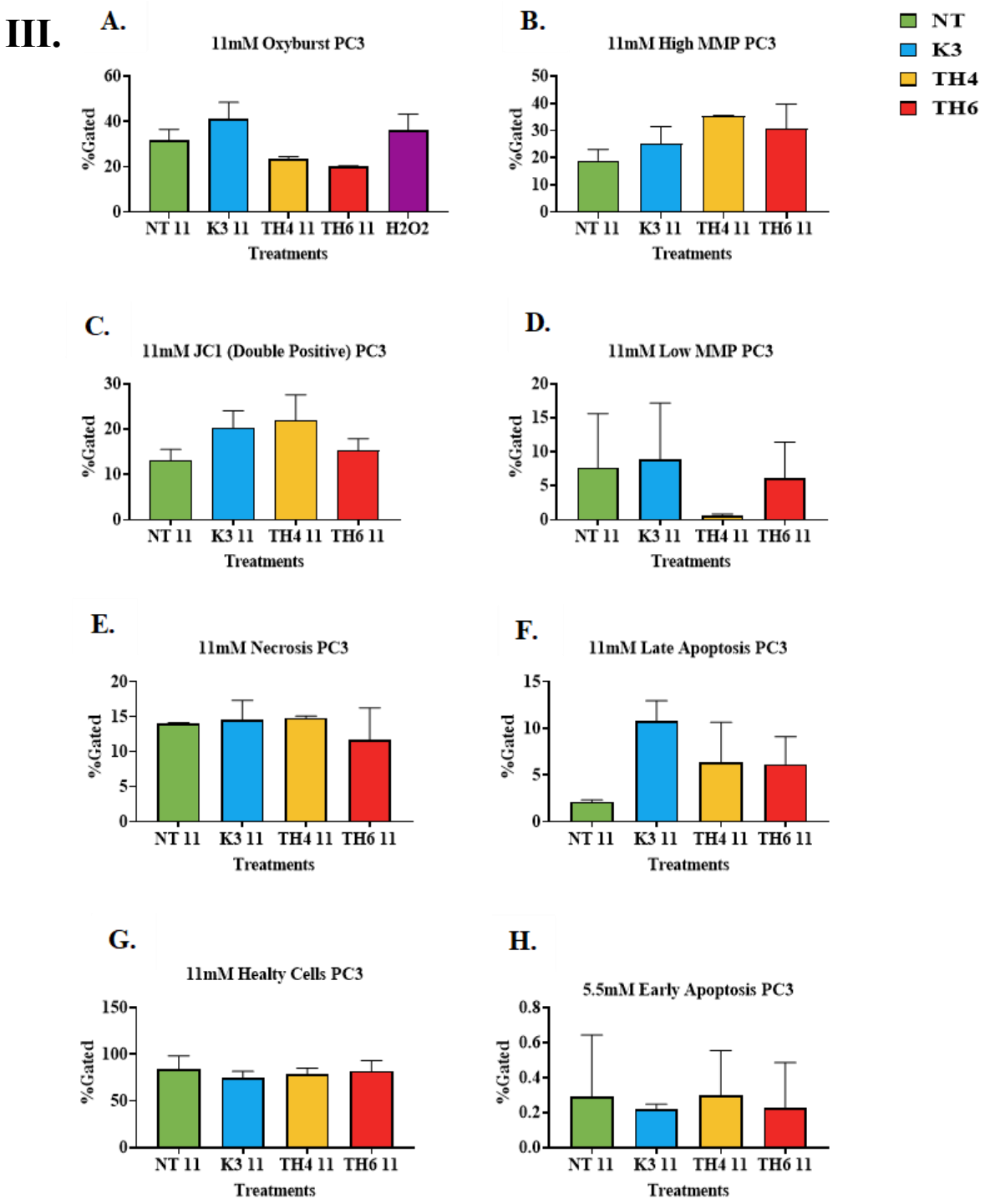

*Figure 5. 13: Du145 treated %gated in the **(I.)** Zero glucose **(II.)** 5.5mM glucose and **(III.)** 11mM glucose conditions (n=3) by one-way ANOVA . **(A)** Oxyburst expression, represents the endogenous ROS determined in the live cell. **(B)** JC-1 Red, is an indicator of high MMP, which indicates, intact mitochondria and complete ATP synthesis. **(C)** JC-1 Double positive, cells presenting double positive for JC1. **(D)** JC-1 Green; indicates low MMP, along with apoptosis and cell death, uncoupling of mitochondrial metabolic processes and a depolarised mitochondrion. **(E)** Av positive, PI negative is an indicator of necrosis. **(F)** Av positive and PI positive is an indication of late apoptosis. **(G)** Av negative and PI negative indicates healthy cells. **(H)** Av negative PI positive is an indicator of early apoptosis.*

5.4.6.1 The effects of the Menadione and TH treatments on the mitochondrial depolarisation in the Du45 cell line in zero, 5.5mM and 11mM glucose conditions.

Mitochondrial depolarisation of Du145 is shown in Figure 5.14. No significance was found between the treatment groups, or between the glucose conditions.

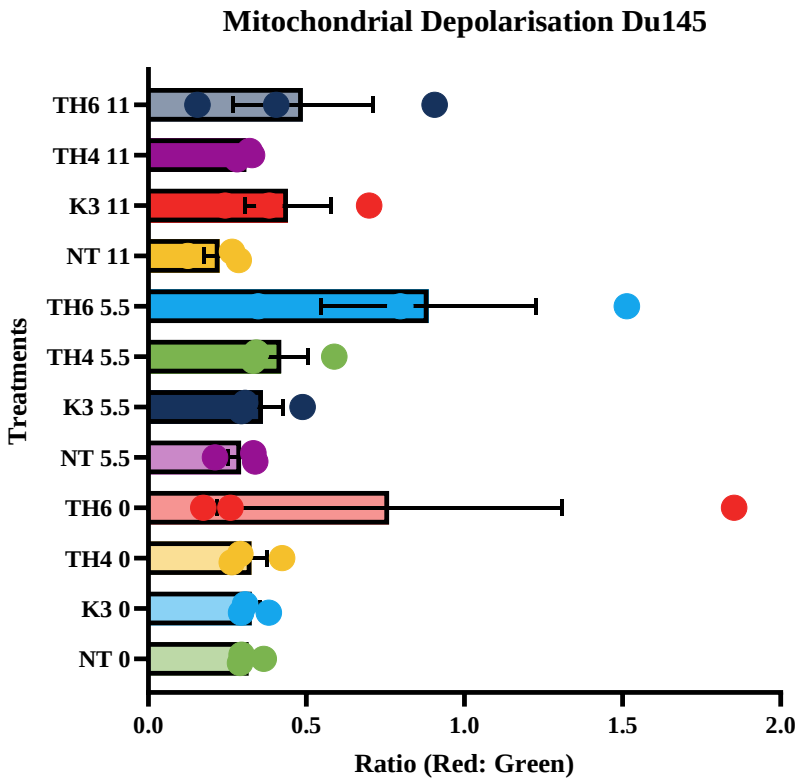

Figure 5. 14: Mitochondrial Depolarisation of Du145 cells un-treated and treatment with Menadione, TH4 and TH6 CellStream data in the zero, 5.5mM and 11mM Glucose conditions (n=3) by two-way ANOVA.

5.4.7 Comparing the Endogenous ROS across the PNT1a, LNCaP, PC3 and Du145 cell lines in the zero, 5.5mM and 11mM glucose conditions treated with Menadione and TH compounds

No change was found in the ROS production across the cell lines when treated with Menadione in the zero, 5.5mM and the 11mM glucose media conditions as highlighted through the Oxyburst expression. Here the % gated cells positive for Oxyburst is presented, with the mean fluorescent intensity (MFI) presented in Appendix 50.

The results shown in Appendix 50 shows that the MFI of Oxyburst was decreased in the TH6 treated LNCaP cells in the zero glucose conditions, and that the MFI was overall higher in the zero glucose cells, both in the untreated and the treated LNCaP cells.

ROS expression was decreased in the PC3 and Du145 cells treated with TH4 compared to the PNT1a cells treated with TH4 in the zero glucose conditions. The ROS production was increased in the PNT1a cells treated with TH4 when compared to the untreated group, whereas the TH4 treated PC3 cells ROS expression was decreased in compared to the PNT1a cell line, in the presence of 5.5mM glucose.

The ROS production was increased in the PNT1a and the PC3 cell lines treated with TH6 in the presence of 11mM glucose. This was decreased in the Du145 cells. The ROS production was increased in the TH6 treated PNT1a cells when compared to the untreated group, whereas the TH6 treated PC3 and Du145 ROS expression was decreased in compared to the PNT1a cell line, in the presence of zero glucose. No change was observed when comparing the cell lines in the 5.5mM glucose conditions when treated with TH6. The ROS production was increased in the PNT1a, LNCaP and the PC3 cell lines treated with TH6 in the presence of 11mM glucose, whereas Du145 expression was reduced, as illustrated in Figure 5.15.

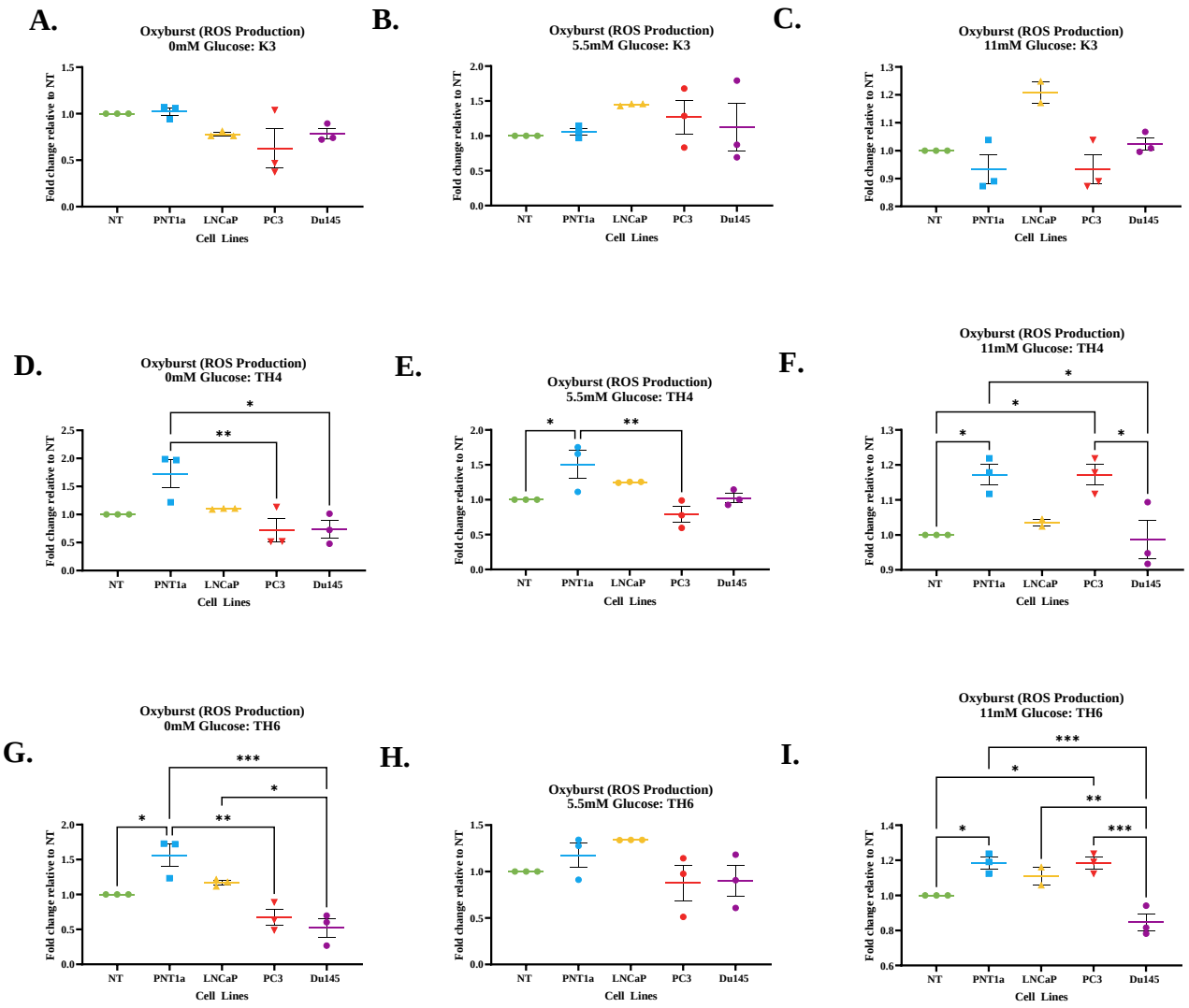

*Figure 5. 15: the Endogenous ROS across the PNT1a, LNCaP, PC3 and Du145 cell lines in the zero, 5.5mM and 11mM glucose conditions treated with Menadione and TH compounds (n=3) by two-way ANOVA . (**A**) ROS production by Menadione Treated cell lines in the zero Glucose. (**B**) ROS production by Menadione Treated cell lines in the 5.5mM Glucose. (**C**) ROS production by Menadione Treated cell lines in the 11mM Glucose. (**D**) ROS production by TH4 Treated cell lines in the zero Glucose. (**E**) ROS production by TH4 Treated cell lines in the 5.5mM Glucose.(**F**) ROS production by TH4 Treated cell lines in the 11mM Glucose. (**G**) ROS production by TH6 Treated cell lines in the zero Glucose. (**H**) ROS production by TH6 Treated cell lines in the 5.5mM Glucose. (**I**) ROS production by TH6 Treated cell lines in the 11mM Glucose.*

5.4.8 Comparing the levels of Apoptosis across the PNT1a, LNCaP, PC3 and Du145 cell lines in the zero, 5.5mM and 11mM glucose conditions treated with Menadione and TH compounds

In the presence of 5.5mM glucose, necrosis was increased in LNCaP cells treated with Menadione ($P<0.0001$). Necrosis was also increased in the Du145 cells in comparison to the PNT1a cells ($P=0.04$) in the 5.5mM glucose. No change was found in the zero and 11mM glucose cells treated with Menadione.

Necrosis was decreased in Du145 cells ($P=0.01$) when treated with TH4 in the presence of zero glucose. No change was found in the levels of necrosis in the 5.5mM and the 11mM glucose conditions, when treated with TH4.

Necrosis was increased in LNCaP in the 5.5mM ($p <0.0001$) and 11mM ($P=0.0004$) glucose when treated with TH6. Overall TH6 had the most impact on LNCaP with increased necrosis observed when in the presense of glucose (5.5mM and 11mM glucose) as presented in Figure 5.16.

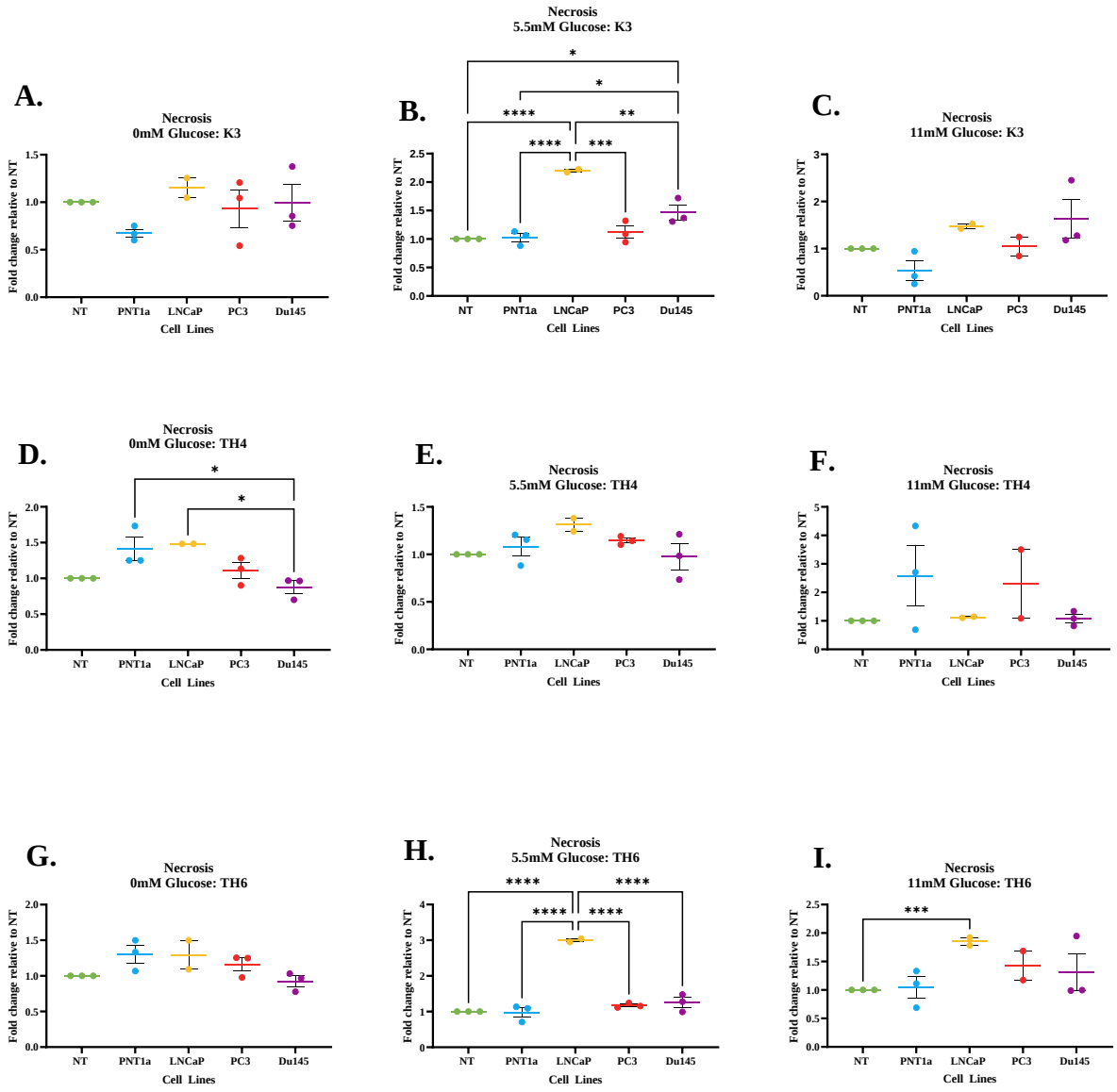

*Figure 5. 16: The Necrosis levels across the PNT1a, LNCaP, PC3 and Du145 cell lines in the zero, 5.5mM and 11mM glucose conditions treated with Menadione and TH compounds (n=3) by two-way ANOVA. (**A**) Necrosis levels by Menadione Treated cell lines in the zero glucose. (**B**) Necrosis levels by Menadione Treated cell lines in the 5.5mM glucose. (**C**) Necrosis levels by Menadione Treated cell lines in the 11mM Glucose. (**D**) Necrosis levels by TH4 Treated cell lines in the zero Glucose. (**E**) Necrosis levels by TH4 Treated cell lines in the 5.5mM glucose.(**F**) Necrosis levels by TH4 Treated cell lines in the 11mM glucose. (**G**) Necrosis levels by TH6 Treated cell lines in the zero Glucose. (**H**) Necrosis levels by TH6 Treated cell lines in the 5.5mM Glucose. (**I**) Necrosis levels by TH6 Treated cell lines in the 11mM Glucose.*

Late apoptosis was increased in PNT1a in the zero glucose (P=0.01) and 11mM glucose (P=0.0006) when trerated with Menadione, Figure 5.17 (**A and C**). PC3, Du145 and LNCaP had similar levels to that of the untreated cells across the glucose conditions when treated with Menadione.

No change was reported across the glucose conditons and the cell lines when treated with novel TH4 as illustrated in Figure 5.17 (**D-F**).

Late apoptosis was unchanged in the zero glucose across the cell lines examined, when treated with TH6. However, late apoptosis was increased in the presence of 5.5mM glucose (P=0.009) and 11mM glucose (0.002) with the LNCaP cell line as shown in Figure 5.17 (**H- I**).

Menadione caused greater apoptotic effects in the non-malignant PNT1a cell line,than the malignant cell lines. Overall TH6 had the most impact on LNCaP with increase late apoptosis observed in the presense of glucose.

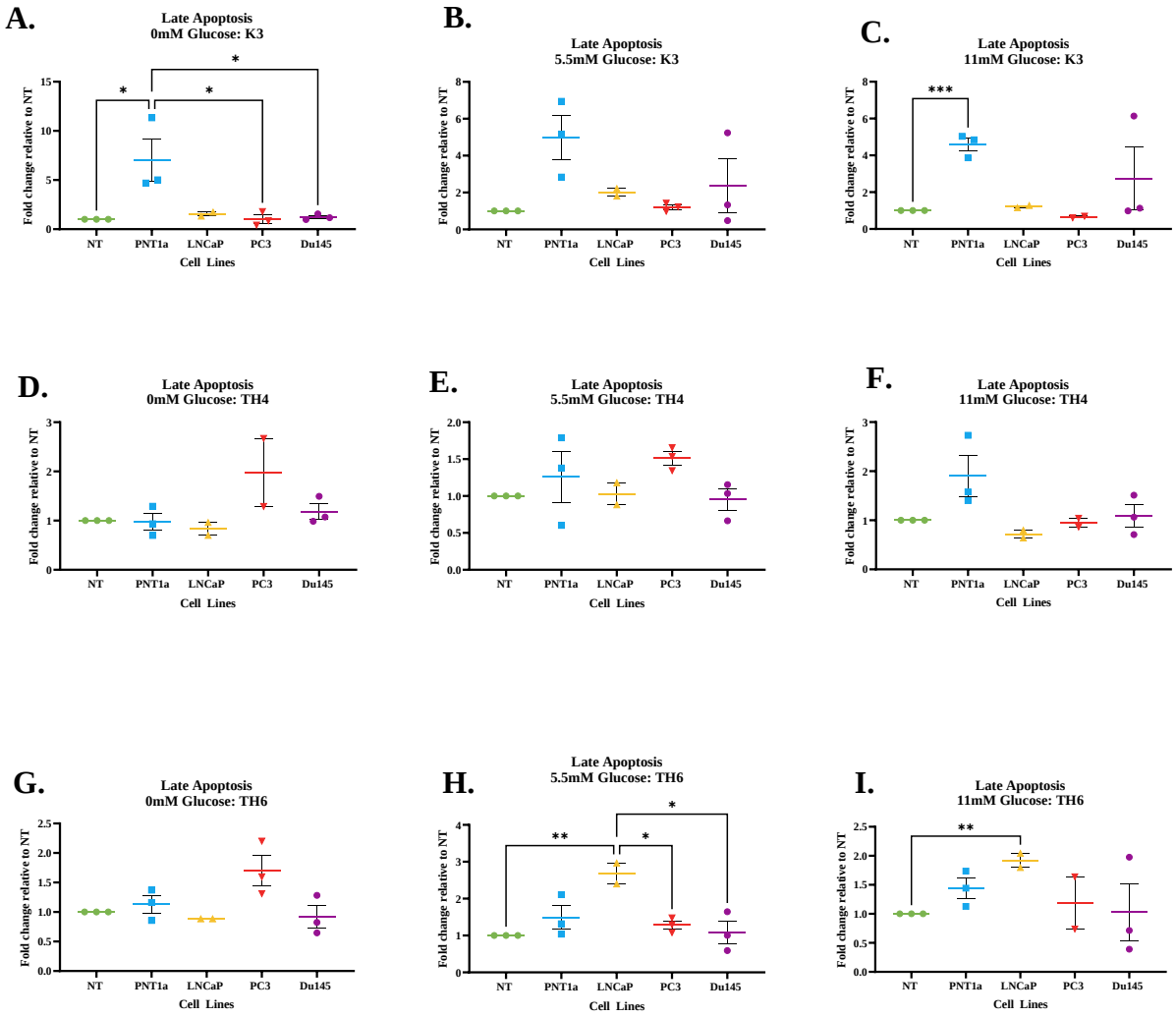

*Figure 5. 17: The Late apoptosis levels across the PNT1a, LNCaP, PC3 and Du145 cell lines in the zero, 5.5mM and 11mM glucose conditions treated with Menadione and TH compounds (n=3) by two-way ANOVA. (**A**) Late apoptosis levels by Menadione Treated cell lines in the zero Glucose. (**B**) Late apoptosis levels by Menadione Treated cell lines in the 5.5mM Glucose. (**C**) Late apoptosis levels by Menadione Treated cell lines in the 11mM Glucose. (**D**) Late apoptosis levels by TH4 Treated cell lines in the zero Glucose. (**E**) Late apoptosis levels by TH4 Treated cell lines in the 5.5mM Glucose.(**F**) Late apoptosis levels by TH4 Treated cell lines in the 11mM Glucose. (**G**) Late apoptosis levels by TH6 Treated cell lines in the zero Glucose. (**H**) Late apoptosis levels by TH6 Treated cell lines in the 5.5mM Glucose. (**I**) Late apoptosis levels by TH6 Treated cell lines in the 11mM Glucose.*

Early apoptosis was increased in the PNT1a cell line in the 5.5mM (P=0.0009) and 11mM (P= 0.01) glucose, when treated with Menadione Figure 5.18 (**B-C**).

In the presence of 5.5mM glucose, LNCaP early apoptosis was decreased when treated with TH4, when compared to PNT1a (P=0.05). In the 11mM glucose conditions, early apoptosis was decreased in Du145 when treated with TH4 (P=0.04).

In the 5.5mM glucose, early apoptosis was decreased in the LNCaP cell line, when treated with TH6 (P=0.01), conversely in the 11mM glucose condition early apoptosis was increased in the LNCaP cells in comparison to all the other cell lines ($p < 0.0001$).

PNT1a had the greatest response to the Menadione treatment. However, of the novel compounds, LNCaP showed higher levels of early apoptosis when treated with TH6 in the 11mM glucose as presented in Figure 5.18.

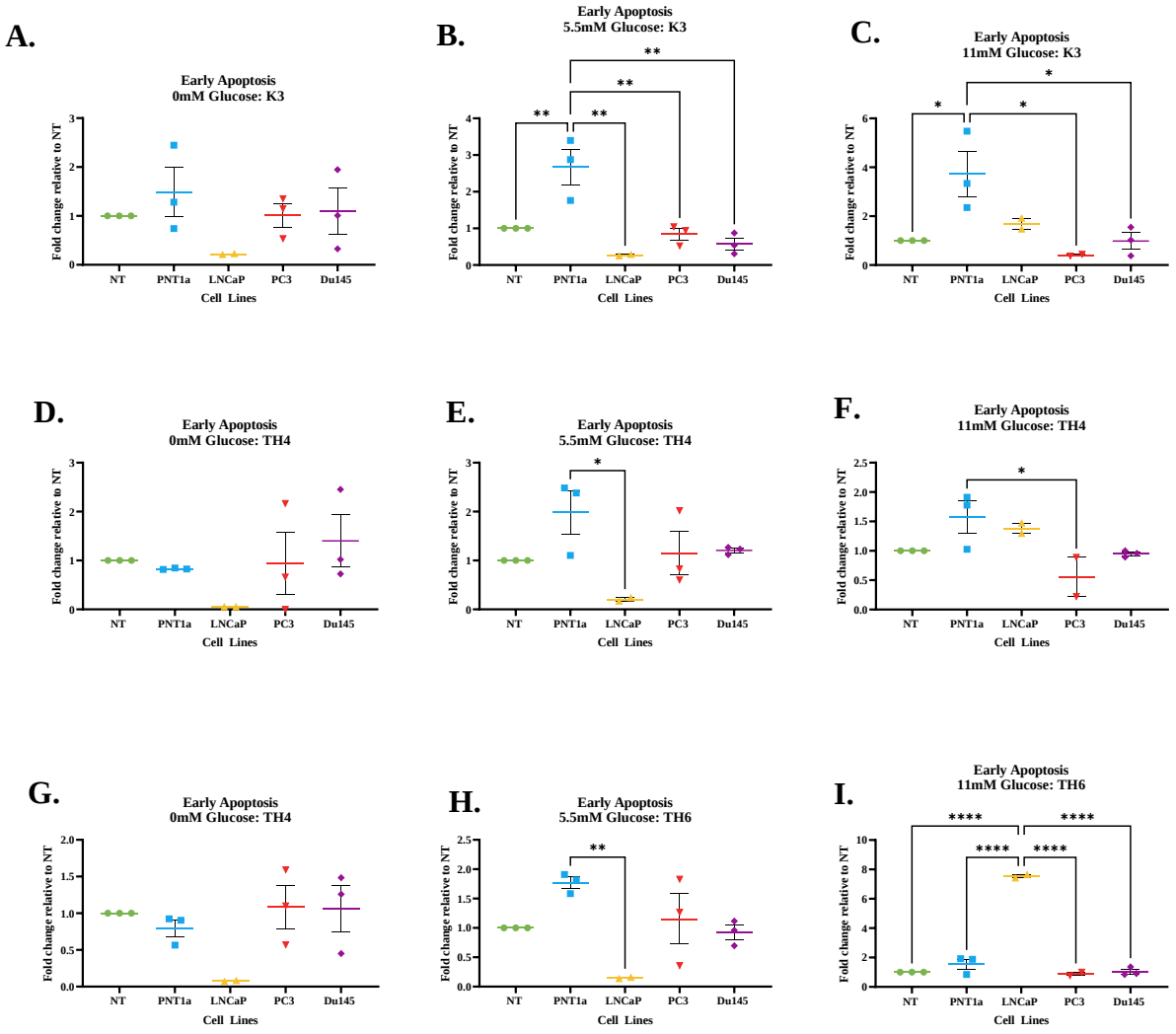

*Figure 5. 18: The early apoptosis levels across the PNT1a, LNCaP, PC3 and Du145 cell lines in the zero, 5.5mM and 11mM glucose conditions treated with Menadione and TH compounds(n=3) by two-way ANOVA. (**A**) Early apoptosis levels by Menadione Treated cell lines in the zero Glucose. (**B**) Early apoptosis levels by Menadione Treated cell lines in the 5.5mM Glucose. (**C**) Early apoptosis levels by Menadione Treated cell lines in the 11mM Glucose. (**D**) Early apoptosis levels by TH4 Treated cell lines in the zero Glucose. (**E**) Early apoptosis levels by TH4 Treated cell lines in the 5.5mM Glucose.(**F**) Early apoptosis levels by TH4 Treated cell lines in the 11mM Glucose. (**G**) Early apoptosis levels by TH6 Treated cell lines in the zero Glucose. (**H**) Early apoptosis levels by TH6 Treated cell lines in the 5.5mM Glucose. (**I**) Early apoptosis levels by TH6 Treated cell lines in the 11mM Glucose*

5.4.9 Comparing the levels of MMP across the PNT1a, LNCaP, PC3 and Du145 cell lines in the zero, 5.5mM and 11mM glucose conditions treated with Menadione and TH compounds

As presented in Figure 5.19, high MMP levels were found in the LNCaP cells when treated with Menadione in the zero glucose (P=0.02). In the 11mM glucose, the PNT1a, high MMP was reported when treated with Menadione (P=0.002).

High MMP levels were lower in the LNCaP cells when treated with TH4 in the 11mM glucose conditions (P=0.009). No differences in MMP were observed between the cell lines in the zero and 5.5mM glucose when treated with TH4 and TH6. However, in the TH6 treated cells in presence of 11mM glucose, high MMP was higher in the PNT1a (P=0.002) and PC3 (P=0.01) when compared to the untreated control, and LNCaP had reduced levels compared to that of the PNT1a cells and the PC3 cells (P=0.001).

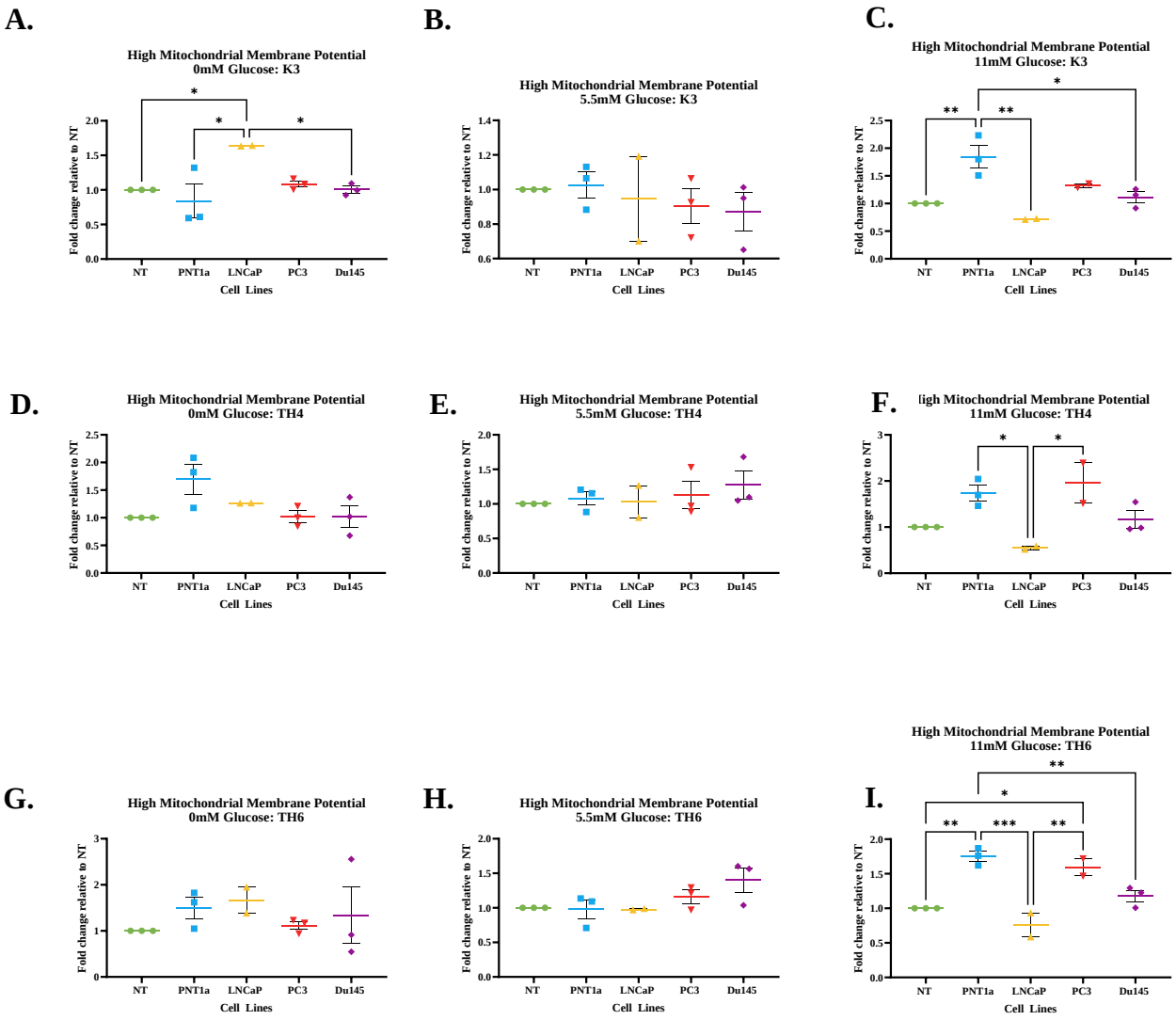

*Figure 5. 19: The high MMP levels across the PNT1a, LNCaP, PC3 and Du145 cell lines in the zero, 5.5mM and 11mM glucose conditions treated with Menadione and TH compounds (n=3) by two-way ANOVA. (**A**) High MMP levels by Menadione Treated cell lines in the zero Glucose. (**B** High MMP levels by Menadione Treated cell lines in the 5.5mM Glucose. (**C**) High MMP levels by Menadione Treated cell lines in the 11mM Glucose. (**D**) High MMP levels by TH4 Treated cell lines in the zero Glucose. (**E**) High MMP levels by TH4 Treated cell lines in the 5.5mM Glucose.(**F**) High MMP levels by TH4 Treated cell lines in the 11mM Glucose. (**G**) High MMP levels by TH6 Treated cell lines in the zero Glucose. (**H**) High MMP levels by TH6 Treated cell lines in the 5.5mM Glucose. (**I**) High MMP levels by TH6 Treated cell lines in the 11mM Glucose.*

Low MMP levels were further reduced in the PNT1a and Du145 cells when treated with Menadione in the zero glucose (P=0.003).

No change was found across the cell lines in the zero, 5.5mM and 11mM glucose conditions when treated with TH4.

No change was found across the cell lines in the zero and 11mM glucose conditions when treated with TH6. However, in the 5.5mM glucose PNT1a had further reduced MMP in comparison to the untreated control and the LNCaP MMP (P=0.03). The results are presented in Figure 5.20 below.

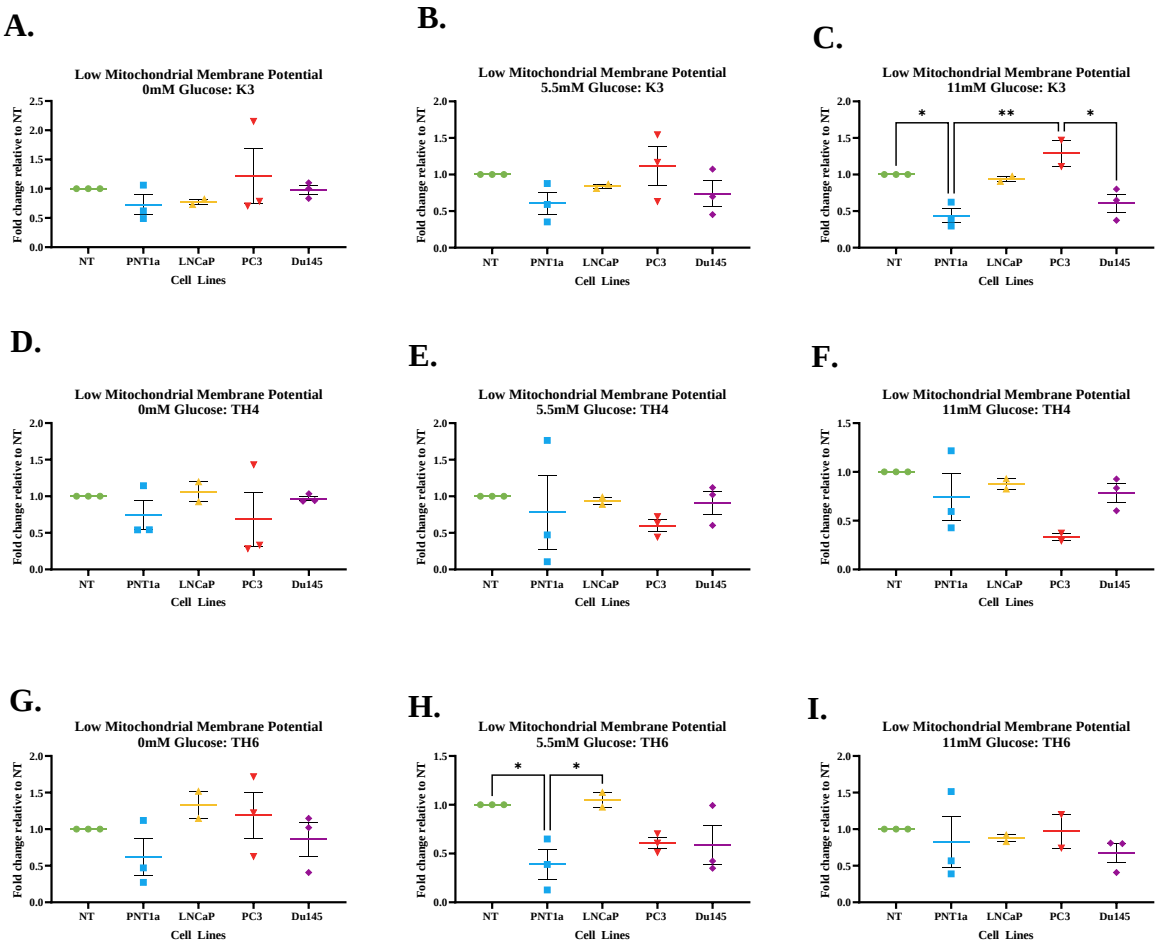

*Figure 5. 20: The low MMP levels across the PNT1a, LNCaP, PC3 and Du145 cell lines in the zero, 5.5mM and 11mM glucose conditions treated with Menadione and TH compounds (n=3) by two-way ANOVA. (**A**) Low MMP levels by Menadione Treated cell lines in the zero Glucose. (**B** Low MMP levels by Menadione Treated cell lines in the 5.5mM Glucose. (**C**) Low MMP levels by Menadione Treated cell lines in the 11mM Glucose. (**D**) Low MMP levels by TH4 Treated cell lines in the zero Glucose. (**E**) Low MMP levels by TH4 Treated cell lines in the 5.5mM Glucose.(**F**) Low MMP levels by TH4 Treated cell lines in the 11mM Glucose. (**G**) Low MMP levels by TH6 Treated cell lines in the zero Glucose. (**H**) Low MMP levels by TH6 Treated cell lines in the 5.5mM Glucose. (**I**) Low MMP levels by TH6 Treated cell lines in the 11mM Glucose*

5.5 Summary of results

Chapter 5 highlights	
PNT1a	• PNT1a cells show lower levels of Oxyburst in zero glucose conditions when compared to expression in 5.5 mM and 11mM glucose conditions. • The levels of high MMP were increased in 5.5mM glucose PNT1a cells, with similar levels in the 11mM and zero cells, respectively. • Increased late apoptosis was observed in the 5.5mM PNT1a cells, but overall levels were low. • In the zero glucose conditions, PNT1a cells treated with Menadione increase late apoptosis markers. In the 5.5mM glucose treatment, PNT1a cells treated with TH4 show increase ROS expression and increased late apoptosis with Menadione treatment. • TH4 and TH6 result in increased ROS for the PNT1a cells in the 11mM glucose conditions, again with increased late apoptosis with Menadione treatment.
LNCaP	• The LNCaP cells in the zero glucose showed no impact with the novel treatments. • In the 5.5mM glucose LNCaP showed increased necrosis with Menadione and TH6 treatments with increased late apoptosis also observed with TH6. • In the presence of zero glucose, the mitochondrial depolarisation of LNCaP is increased when treated with Menadione versus the zero untreated LNCaP (P=0.018) and the 11mM Menadione treated LNCaP (P=0.002).
PC3	• PC3 cells showed no significance across all flowcytometry panels and treatments, except for an increase in late apoptosis in the TH4 treated cells in the 5.5mM glucose. • The mitochondrial depolarisation of PC3 treated with TH4 was increased significantly in the presence of 11mM glucose (P=0.0012).
Du145	• No significant alterations were found in the novel treatments across the glucose conditions.

5.6 Discussion

Our unique approach which aims to target specific niches of the cancer metabolome by employing a 'Trojan horse' metabolic targeting event involves the use of Menadione, complexed to simple sugars and lipids with aims to show significant ROS activity, resulting in the direct killing of cancer cells, with little to no effect on non-malignant cells. The use of natural moieties in new therapeutics is preferred if they can achieve selective cell kill towards malignant cells, rather than normal cells. Many studies have shown the success of the native Menadione, illustrating cytotoxic effects in cell lines and in patient studies, through their ROS generating capabilities and our study was designed based upon these results.[349,421,422] To note, the exploration of Vitamin C was halted at this point, as it was apparent that we would not receive a Vitamin C based novel compound in the time of the study completion.

The examination into the impact of the novel TH compounds on the mitochondria of the non-malignant and cancer cell lines, was conducted by examining the ROS production, apoptosis markers and the mitochondrial membrane potential of the untreated and treated cells.

The Oxyburst examination into the ROS production by the cells allowed a baseline level of ROS to be determined in the cell lines across a varying glucose milieu, as Menadione is a known ROS producing molecule at high concentrations. However overall, no significant effect on the ROS production was noted across the malignant cell lines when treated with the novel TH compounds, whereas under 5.5mM and 11mM glucose the PNT1a cells treated with TH4 and TH6 showed an increase ROS as shown in Figure 5.15. The results obtained in this chapter were less convincing of our theory, where ROS would be increased in the metastatic cells following treatment. However, the results may also suggest that metastatic cells have a higher antioxidant profile that deals with the ROS stimulation provided by the TH compounds. This may be an adaptation of the metastatic cells to overcome high levels of ROS to increase cell survival. In Chapter 6, the effects of the compounds on the cell's metabolome is further investigated, where these effects have been further evaluated.

The key to this study was to allow high enough concentrations of Menadione to enter the cell to remove antioxidant enzymes capability to eliminate ROS and to result in redox related cell death.[295] Antioxidants such as glutathione, catalase, and superoxide dismutase are known quenchers, and are known to decrease the oxidative stress

capabilities of Menadione reducing its anticancer effects.[308,342] Thus, to accomplish the levels of endogenous ROS for this study to achieve cancer cell death, the concentrations of intracellular Menadione needs to be high. We proposed the coupling of the Menadione to glucose would allow this to be achieved, again due to their metabolic processes as aforementioned. Clinical *in vivo* studies of Menadione have suggested that at high concentrations of Menadione to be tolerable and safe for patients wither in combination with traditional therapies or alone, however results are varied on its success *in vivo*.[310, 311]

We proposed that Menadione would enter the mitochondria where through Fenton's reactions would produce hydroxyl and hydroperoxyl radicals and result in DNA damage and cell death.[309,423] The goal was to overthrow the possible ROS scavengers such as glutathione and antioxidant enzymes; catalase and superoxide dismutase from quenching the ROS produced from the novel compounds, by allowing high levels of Menadione to enter the cell. Studies have shown Menadione to decrease oncogenic superoxide which is reported to allow for apoptosis through the generation of onco-suppressive hydroperoxides and hydroxyl radicals, which can result in DNA strand breaks.[254,306] Cancer cells that have genetic abnormalities or mutations often present with increased levels of ROS than that of a normal, healthy cells.[318] Thus, one could hypothesise that due to the ability of ROS to trigger cell death, that treating cells with ROS stimulating compounds would be an effective cancer-specific therapy.[318] A consequence of the excess ROS produced in the cancer cells, include damages to amino acids, particularly in the presence of Cu^{2+} and Fe^{2+}, trace metals which are known to mediate ROS production, overall resulting in metabolic changes to the cancer cells.[409,424] An increase in cellular antioxidants would prevent redox damage associated with cancer development. During oxidative stress cells will increase their antioxidant enzymes and molecules to avoid damage to their cellular proteins, lipids, and DNA, through the reduction of hydrogen donors or quenching singlet oxygen which delays oxidative reactions in the growing cancer cells.[318] With this, cancer cells have been shown to have higher concentrations of ROS scavenging enzymes to mop up excess ROS that is produced by the cancer cells rapid proliferation, compared to normal cells. However, if high enough concentrations of Menadione could be infiltrated into the cell under disguise of a sugar, or lipid required by the cell, we could achieve redox related death in the cancer cell. It is known that Menadione mechanisms in vitro, have been identified to increase the expression of pro-apoptotic proteins and a simultaneous decrease in anti- apoptotic

proteins in different forms of human cancer cells. The primary mechanism of cell death by Menadione is thought to be due to its redox cycling capabilities, forming mitochondrial ROS at high concentration and inducing oxidative stress.[422] Menadione is shown to cause alteration in redox alteration in cell, resulting in membrane damage, DNA damage, inhibition of blood vessel formation, altered proliferation, cell shrinkage, and the activation of capsase-3.[297,422,425] Interestingly some current chemotherapies and γ-radiation therapies in cancer treatment, mediate their therapeutic effects through the production of ROS with an increased interest in the use of ROS mediating nutraceuticals from natural products.[318]

Oxyburst is a molecular probe that offers derivatives of reduced fluorescein and calcein as cell-permeant indicators for reactive oxygen species, where the fluorescent emission indicates the oxidization by ROS in the cell.[161] The 2′,7′-dichlorofluorescein (DCF) and calcein within the molecular probe do not fluoresce until the acetate groups on the probe are removed by intracellular esterase with oxidation occurring within the cell resulting in the ROS mediated fluorescent emission.[161] The Oxyburst probe measures the whole cell ROS production and the mechanism proposed in this thesis would be an influx in mitochondrial ROS. Oxyburst is commonly used to measure whole cellular ROS, however we aim to evaluate the mitochondrial ROS changes. With this, isolating the cells mitochondria through subcellular fractionation may allow for us to quantify and monitor the ROS production within the mitochondria, isolated from the non-malignant prostate and the cancer cells.[424] This may result in more specific results applicable to our study and may yield an increase in ROS when the cells are treated with the TH compounds.

Of the cancer cells, LNCaP showed the best response to the novel compounds, with alterations observed with the TH6 treatments (Figure 5.16). Increased levels of the apoptotic markers were seen across the TH6 treatments, with increases in necrosis, late apoptosis, and early apoptosis respectively in the various glucose conditions. Under 5.5mM glucose, LNCaP showed increased necrosis with Menadione and TH6 treatments, with an increase in late apoptosis also observed with TH6 treatments. This may be linked to the metabolic phenotype of the early stage PCa disease thought to rely on, oxphos and fatty acid oxidation.[15,34,35] LNCaP in Chapter 4 showed great reliance on oxphos for its ATP production, with further work required to determine its reliance on fatty acid oxidation. For the metastatic cell lines, PC3 exhibited an increase in late apoptosis in the TH4 treated cells under 5.5mM glucose, however Du145 cells showed no apoptotic

response to the TH compounds. This could be due to the aforementioned deficiency in ROS observed within the cell lines, resulting in lower levels of apoptosis.

Overall, the MMP levels were maintained across all the cell lines in both the treated and untreated cells. The levels of high MMP were increased in the basal 5.5mM glucose PNT1a cells, with similar levels in the 11mM and zero cells, respectively. Sustained alterations in MMP is considered an indicator of mitochondrial dysfunction.[402] As aforementioned, prostate carcinoma is known to have high basal levels of MMP, thus the determination of the baseline levels was vital in the exploration of the mitochondrial health.[373] Studies have shown that decreased MMP are indicators of apoptosis and mitochondrial depolarisation, thus the treated cells were compared to the untreated to determine the alterations in the MMP.[399,401]

We hypothesised that the treatment of prostate cell lines with novel TH compounds would induce a significant increase in endogenous ROS production, to levels high enough to evade cellular antioxidant processes, resulting in mitochondrial damage and cell death. The method used for the ROS determination may require a more specified method such as mitochondrial probes or the isolation of the mitochondria to detect the increase of ROS by the TH compounds. In this chapter the use of the Oxyburst molecular probe may not have been the most optimal method for measuring ROS, allowing future examinations of mitochondrial ROS to be considered. Furthermore, the evaluation of the alterations to the cancer cell metabolome in Chapter 6 may further enlighten the reason for the minimal alterations in whole cell ROS production we expected to find.

Chapter 6. Metabolomic investigations of the effects of the Trojan Horse compounds

6.1 Introduction

The final step of this study was to examine the effects of the novel TH compounds on a metabolite level. The metabolites of significance are discussed in this chapter, with hopes of aiding in the understanding of how the novel TH compounds are performing within the cell lines. In this chapter Menadione, TH4 and TH6 were taken forward for further analysis as they had shown the most promise in earlier experimental analysis.

6.1.1 Amino acid metabolism in cancer

Amino acid metabolism is upregulated in many cancer types, as it supports the proliferation and survival of cancer cells under stress, such as oxidative or nutrient stress.[426] Known to have extensive effects in cancer cell metabolism and mitochondrial health through both tumour suppression and tumorigenic processes such as; glutamine providing ATP for the TCA cycle, biosynthesis of nucleotides, regulation of ROS and epigenetic regulation of acetylation and methylation in cancer.[427]

Amino acid metabolism plays a role in the production of essential amino acids for protein biosynthesis, glucose and lipid conversions and the production of purines and pyrimidines for nucleic acid synthesis.[428] Amino acids generate α-ketoacid, used in the TCA cycle and OxPhos during ATP production and contributes to the homeostasis of cellular ROS levels due to the synthesis of non-enzymatic antioxidants such as cysteine, taurine and glutathione.[428, 429] Alterations in basal amino acid metabolism would provide useful knowledge in establishment of the novel TH compounds efficacy, as amino acid metabolism holds a strong prevalence throughout many aspects of cancer biology.

6.1.2 Biogenic amines in cancer

Biogenic amines, also referred to as polyamines are polycationic compounds consisting of a nitrogenous base with a minimum of two positive charged amino groups to enable electrostatic binding to macromolecules with negative charges, such as DNA, RNA, proteins and phospholipids.[430,431] Some of the most important biogenic amines include, spermine, spermidine and the precursor putrescine, all involved in the amine biosynthetic and metabolic pathways.[431,432]

Biogenic amines are involved in cellular processes including cell cycle regulation, cell signal transduction, differentiation and gene expression.[433,434] The biosynthetic pathways of these amines have been found to be very active in cancer cells, with accumulations found in rapidly proliferating cancer cells, generally with higher amine levels in cancer cells, than that of normal cells.[434, 432] High levels of these amines have

been linked to the progression of several cancers including, prostate, breast, gastric and colorectal cancers.[431, 388,435] However, a decrease in biogenic amines in the cell by pharmacological intervention, has been shown to lead to cancer cell senescence and apoptosis.[431]

6.1.3 Ceramides and sphingolipids in cancer

Ceramides are sphingolipids composed of an 18-carbon unsaturated amino alcohol hydrocarbon chain, conjugated to a fatty acid by an amide group, with this fatty acyl group often determining the biological relevance of the ceramide.[436] Sphingolipids are complex lipids that are implicated in many cellular processes.[437] They provide cell membrane structural integrity and their metabolism is known to regulate proliferation, apoptosis and senescence.[435]

Ceramides are typically known as tumor suppressor lipids due to their abilities to induce apoptosis, however some are known to regulate proliferation through blocking cell cycle transition.[438–440] The dichotomy in ceramide function highlights them as a possible target for therapeutic action in cancer drug discovery.[438]

6.1.4 Carboxylic acids in cancer

Carboxylic acids are multi-faceted molecules across cellular biology comprising of many biologically relevant molecules including, amino-acids, short, medium, and long chain fatty acids, bile acids, and metabolites of the TCA cycle.[441]

Lactic acids is a prevalent carboxylic acid in cancer cell biology, with influx in lactate production detected in the cell being a marker for Warburg metabolism.[243] This altered metabolism in cancer cells, producing increased lactate is linked to angiogenesis through increased production of interleukin 8, leading to autocrine stimulation of endothelial cell proliferation and the maturation of new blood vessels.[441] The output of lactic acid determined in the PCa cell lines will aid in the establishment of the metabolic phenotype of the cell lines, and possibly indicate mitochondrial dysfunction by treatment with the novel compounds as it may be indicative of circumvention of mitochondrial metabolism.

Overall, the implications of the metabolites determined will lead to a greater understanding of the impact of the glucose conditions and the TH compound on the cell's metabolome.

6.2 Hypothesis and Aims

We hypothesise that the metabolome of the PNT1a, LNCaP, PC3 and Du145 cells will be affected by the presence glucose conditions, zero, 5.5mM and 11mM glucose, as well as by the treatment with Menadione, TH4 and TH6.

- To determine the alterations to the metabolome of the PNT1a cells by the zero, 5.5mM and 11mM glucose, as well as from the treatments with Menadione, TH4 and TH6.
- To determine the alterations to the metabolome of the LNCaP cells by the zero, 5.5mM and 11mM glucose and from the treatments with Menadione, TH4 and TH6.
- To determine the alterations to the metabolome of the PC3 cells from the zero, 5.5mM and 11mM glucose, and the treatments with Menadione, TH4 and TH6.
- To determine the alterations to the metabolome of the Du145 cells from the zero, 5.5mM and 11mM glucose, and following the treatments with Menadione, TH4 and TH6.

6.3 Methods

The methods used in this chapter are detailed in full in Chapter 2, Section 2.9.

6.4 Results

6.4.1 LCMS-MS analysis of PNT1a cells in the zero, 5.5mM and 11mM glucose conditions following treatment with Menadione, TH4 and TH6.

PNT1a LCMS-MS analysis was performed in the zero, 5.5mM and 11mM glucose conditions following treatment with menadione, TH4 and TH6. The analytes of significance are presented in Figure 6.1 – Figure 6.4.

The metabolites of significance between treatment groups and glucose conditions are presented in Table 6.1 below, where the concentrations of each metabolite is presented as the mean value and in the micro molar scale.

Table 6. 1: PNT1a Metabolomics outcomes of significance in the zero, 5.5mM and 11mM glucose, untreated and treated with Menadione, TH4 and TH6 . All concentrations in µM, with data represented as mean (n=3).

Metabolites (µM)	Zero Glucose				5.5mM Glucose				11mM Glucose			
	NT	K3	TH4	TH6	NT	K3	TH4	TH6	NT	K3	TH4	TH6
Alanine	55.9	123.4	110.1	203.7	361.7	13.5	257.0	280.0	30.8	95.1	102.4	56.3
Asparagine	204	361.7	13.5	257	280.0	30.8	95.1	102.4	56.3	26.5	31.5	110.4
Cystine	362	13.5	257	280	30.8	95.1	102.4	56.3	26.5	31.5	110.4	31.6
Glutamine	13.5	257	280	30.8	95.1	102.4	56.3	26.5	31.5	110.4	31.6	66.6
Histidine	30.8	95.1	102.4	56.3	26.5	31.5	110.4	31.6	66.6	7.8	37.7	47.8
Methionine	0.01	0.008	0.04	0.007	0.01	4.2	12.6	31.8	19.7	6.8	0.5	510.3
Proline	0.04	0.007	0.005	4.2	12.6	31.8	19.7	6.8	0.5	510.3	4.7	3.9
Serine	0.01	0.005	4.2	12.6	31.8	19.7	6.8	0.5	510.3	4.7	3.9	0.1
Trptophan	4.2	12.6	31.8	19.7	6.8	0.5	510.3	4.7	3.9	0.1	0.1	1.3
Asymmetric dimethylhistidine	4.7	3.9	0.2	0.08	1.3	0.01	0.02	0.05	0.1	0.01	0.02	0.03
Cytisine	0.08	1.3	0.005	0.02	0.05	0.1	0.01	0.02	0.03	0.1	0.01	0.1
Metionine Sulfoxide	0.02	0.05	0.1	0.009	0.02	0.0	0.1	0.0	0.1	0.1	0.3	0.4
Acetryornithine	0.05	0.1	0.009	0.02	0.03	0.1	0.01	0.1	0.1	0.3	0.4	0.1
Phenylacetyglycine	0.1	0.009	0.02	0.03	0.1	0.01	0.1	0.1	0.3	0.4	0.1	0.0
Symmetric dimethylhistidine	0.01	0.02	0.037	0.1	0.01	0.1	0.1	0.3	0.4	0.1	0.002	1.8
t4-OH-Pro	0.02	0.03	0.1	0.01	0.1	0.1	0.3	0.4	0.1	0.002	1.8	12.9
taurine	0.03	0.1	0.01	0.1	0.1	0.3	0.4	0.1	0.002	1.8	12.9	0.5
Beta-alanine	####	1.8	12.9	0.5	0.3	0.04	0.9	0.3	0.1	0.1	0.1	0.1
γ-Aminobutyric acid	1.8	12.9	0.5	0.3	0.04	0.9	0.3	0.1	0.1	0.1	0.1	0.1
Putrescine	12.9	0.5	0.3	0.04	0.9	0.3	0.1	0.1	0.1	0.1	0.1	0.1
Spermidine	0.5	0.3	0.04	0.9	0.3	0.1	0.1	0.1	0.1	0.1	0.1	0.3
Spermine	0.3	0.04	0.9	0.3	0.1	0.1	0.1	0.1	0.1	0.1	0.3	1.0
Lactic Acid	4.6	0.3	0.4	0.4	0.5	0.2	0.1	0.1	0.1	0.1	0.2	0.5
3-Hydroxyglutaric acid	1.8	0.2	0.5	0.6	0.3	0.1	0.1	0.1	0.1	0.1	0.2	0.6
Succinate	2.2	0.2	0.6	0.5	0.3	0.1	0.1	0.1	0.1	0.1	0.2	0.7
Cer(d18:1/22:0)	2.8	0.2	0.5	0.5	0.3	0.1	0.1	0.1	0.1	0.1	0.2	0.6
Cer(d18:2/20:0)	2.3	0.2	0.5	0.5	0.3	0.1	0.1	0.1	0.1	0.1	0.2	0.6

6.4.1.1 The effects on amino acids in the PNT1a cells under zero, 5.5mM and 11mM glucose conditions, treated with Menadione, TH4 and TH6.

Alanine concentration was increased in the 5.5mM glucose untreated cells, in comparison to the zero and 11mM untreated cells and the 5.5mM glucose Menadione treated cells. Alanine as also increased in the 5.5mM versus the 11mM glucose TH6 treated cells ($P<0.0001$).

Aspartate was found to be increased in the zero glucose untreated cells in comparison to the zero glucose TH4 treated cells. the zero glucose Menadione treated cells showed increased aspartate in comparison to the Menadione treated cells under 5.5mM and 11mM glucose respectively. Lastly, the untreated PNT1a cells in the 5.5mM glucose had increased aspartate in comparison to the 5.5mM glucose Menadione, TH4 and TH6 treated cells and the 11mM glucose untreated cells ($P<0.0001$).

The cystine concentrations were increased in the untreated zero glucose conditions versus the Menadione treated zero glucose cells, and the 5.5mM and 11mM glucose untreated cells. The zero glucose TH4 treated cells had increased cystine concentrations in comparison to the TH4 treated 5.5mM and 11mM glucose condition cells. TH6 treated cells in the zero glucose have increased cystine concentrations than that of the 5.5mM and 11mM TH6 treated cells ($P<0.0001$).

Glutamine concentrations were increased in the zero glucose Menadione treated PNT1a cells versus the zero untreated cells and the 5.5mM and 11mM glucose Menadione cells. The zero glucose TH4 treated PNT1a cells had increased glutamine concentrations versus the 5.5mM and 11mM glucose TH4 treated cells. The untreated PNT1a cells in the zero glucose has higher glutamine concentrations than the 5.5mM glucose untreated cells, where the 5.5mM glucose untreated cells have higher concentrations than the 5.5mM glucose TH6 cells and the 11mM glucose untreated cells. The 11mM glucose Menadione treated cells have increased glutamine versus the 11mM glucose untreated cells ($P<0.0001$).

Histidine concentrations were found to be increased in the zero Menadione treated PNT1a cells, when compared to the zero glucose untreated cells and the 5.5mM and 11mM glucose Menadione treated cells. TH4 treated cells in the zero glucose, had higher concentrations of histidine than the zero untreated cells and the 11mM TH4 treated

PNT1a cells. In the 5.5mM glucose, TH4 treated cells had higher histidine than the 5.5mM glucose untreated cells and the 11mM glucose TH4 treated cells. The 11mM glucose untreated PNT1a cells have higher histidine than the 11mM Menadione treated cells, the 11mM glucose TH4 cells and the 5.5mM untreated cells ($P<0.0001$).

In the 11mM glucose conditions, PNT1a cells treated with TH6 had higher levels of methionine than the 11mM glucose untreated cells and TH6 treated cells in the zero and 5.5mM glucose ($P<0.003$).

Proline concentrations were found to be higher in 11mM glucose Menadione treated cells, versus the 11mM glucose untreated cells and the zero and 5.5mM glucose Menadione treated cells ($P<0.003$).

Serine was increased in the 11mM untreated cells in comparison to the 11mM Menadione, TH4 and TH6 treated cells and in the zero and 5.5mM glucose untreated cells ($P<0.003$).

Increased tryptophan was seen in the 5.5mM glucose TH4 treated PNT1a cells versus the zero and 11mM glucose TH4 cells, as well as the 5.5mM glucose untreated cells ($P<0.003$).

In the zero glucose, the untreated cells had higher asymmetric dimethyl arginine than the TH4 and TH6 treated cells in the the same glucose conditions. The untreated zero glucose cells had higher concentrations than the 5.5mM and 11mM glucose untreated cells. Menadione treated cells in the zero glucose, have increased asymmetric dimethyl arginine than in 5.5mM and 11mM glucose cells ($P<0.0001$).

Methionine sulfoxide was increased in the TH6 treated cells in the 11mM glucose conditions, versus the zero and 5.5mM glucose conditions ($P<0.003$).

Acetylornithine was found to be decreased in the zero and 5.5mM glucose cells treated with TH6 in comparison to the 11mM glucose treated TH6 PNT1a cells ($P<0.004$).

Phenylacetyl glycine was decreased in the zero and 5.5mM glucose cells treated with Menadione in comparison to the 11mM glucose Menadione treated cells ($P<0.004$).

Symmetric dimethyl arginine was increased in the TH6 treated 11mM glucose cells versus the 11mM untreated cells and in comparison, to the zero and 5.5mM glucose TH6 treated cells($P<0.0001$).

Increased Trans-4-hydroxyproline was found in the 11mM glucose cells, treated with TH6 in comparison to the 11mM untreated cells and the TH6 treated PNT1a in the zero and 5.5mM glucose conditions ($P<0.0001$).

The final amino acid found to have significance was taurine, which was increased in the 11mM glucose TH4 treated cells versus the 11mM untreated cells and the TH4 treated cells in the presence of zero and 5.5mM glucose conditions ($P<0.0001$).

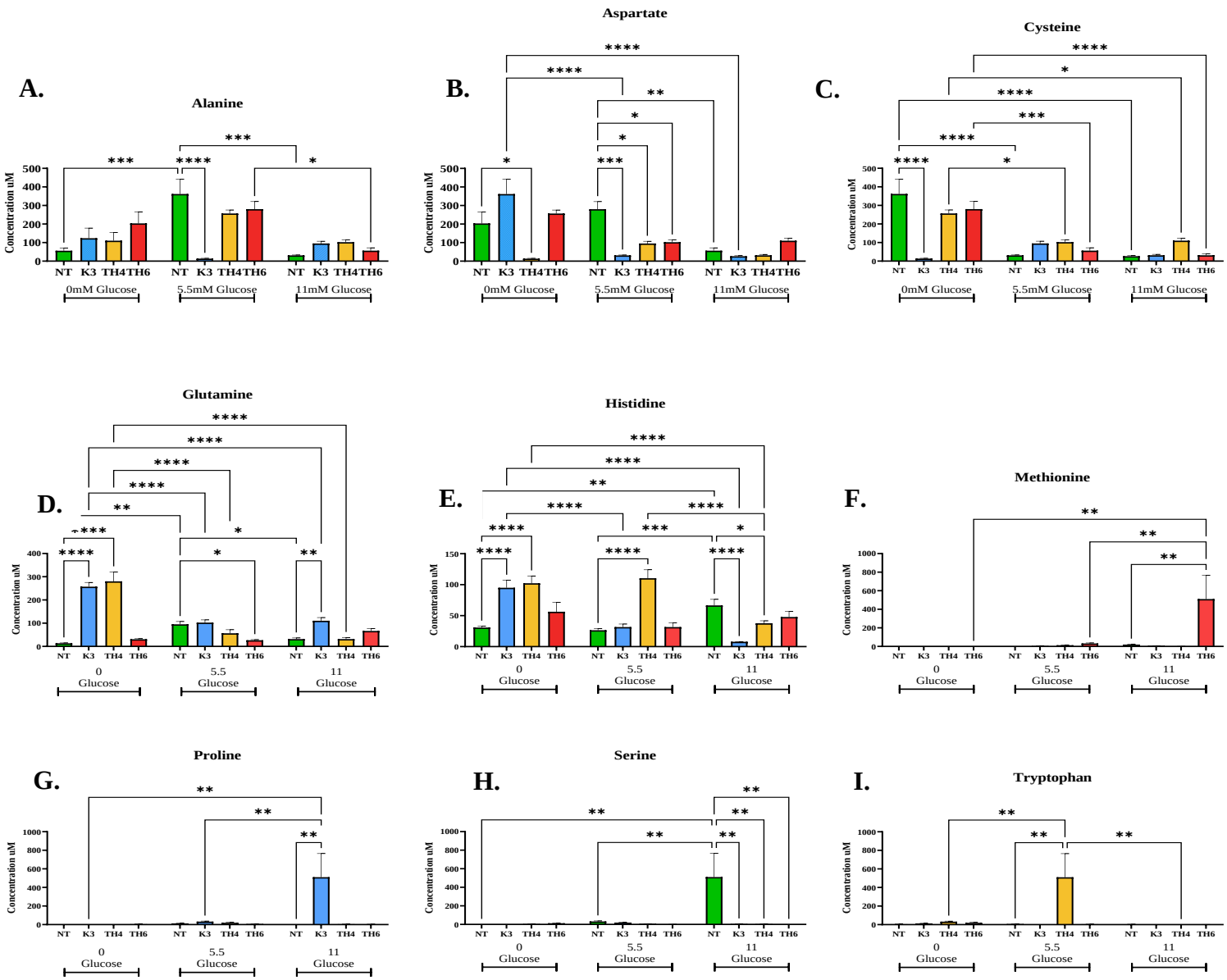
A.
Alanine
B.
Aspartate
C.
Cysteine
D.
Glutamine
E.
Histidine
F.
Methionine
G.
Proline
H.
Serine
I.
Tryptophan
Concentration uM
NT K3 TH4 TH6
0mM Glucose
5.5mM Glucose
11mM Glucose
0 Glucose
5.5 Glucose
11 Glucose

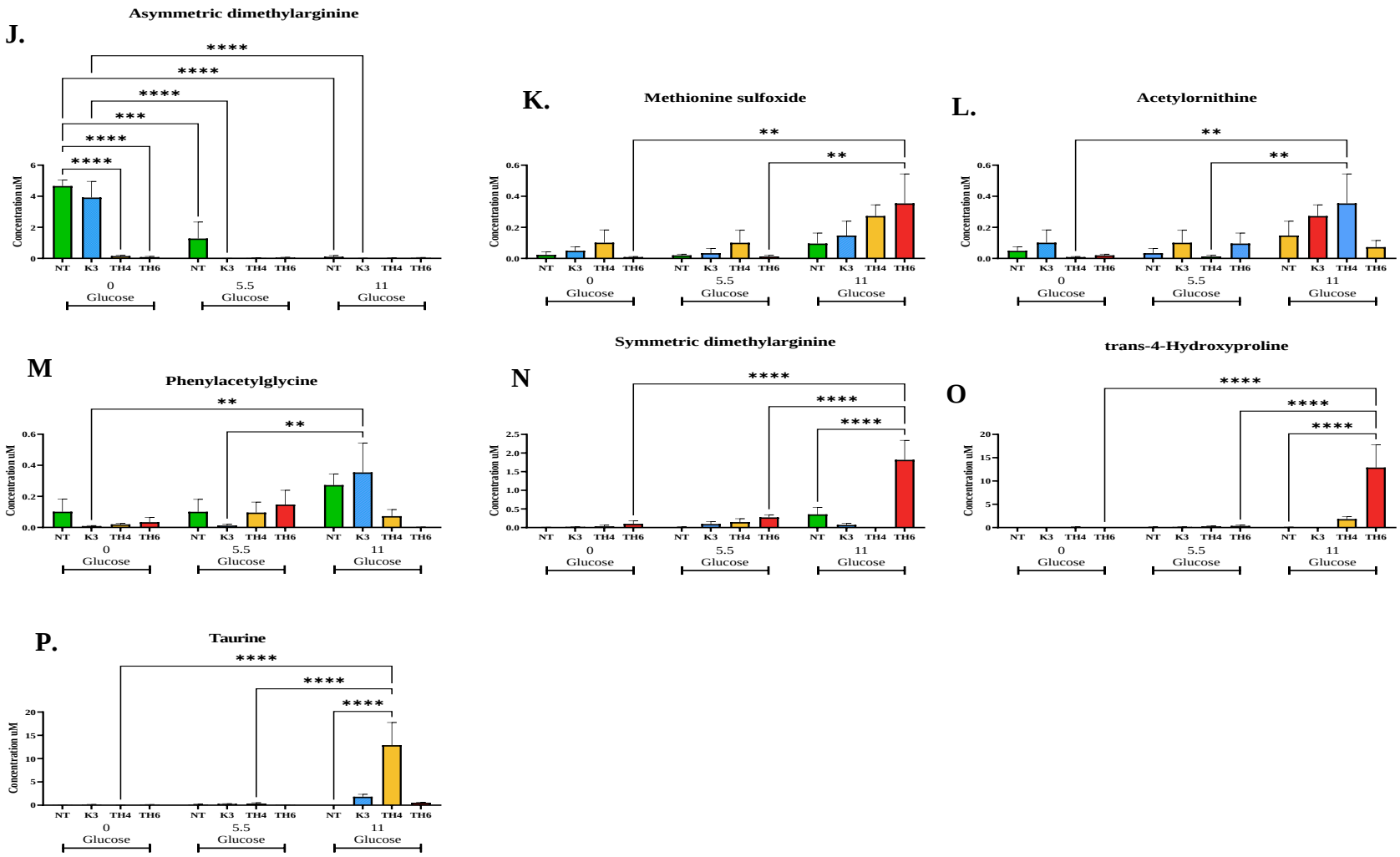

Figure 6. 1: PNT1a Metabolomics outcomes of significance in the zero, 5.5mM and 11mM glucose, untreated and treated with Menadione, TH4 and TH6 (Amino Acids) : (A.) Alanine concentrations. (B.) Aspartate concentrations. (C.) Cystine concentrations. (D.) Glutamine concentrations. (E.) Histidine concentrations. (F.) Methionine concentrations. (G.) Proline concentration. (H.) Serine concentrations. (I.) Tryptophan concentrations. (J.) Asymmetric dimethylarginine concentrations. (K.) Methionine Sulfoxide concentrations. (L.) Acetylornithine concentrations. (M.) phenylacetyl glycine concentrations. (N.) Symmetric dimethylarginine concentrations. (O.) Trans-4-hydroxyproline concentration. (P.) taurine concentrations. All concentrations in µM, with data represented as mean ± SEM (n=3).

6.4.1.2 The effects on biogenic amines in the PNT1a cells under zero, 5.5mM and 11mM glucose conditions, treated with Menadione, TH4 and TH6.

Alterations in biogenic amines were observed in the LCMS-MS evaluation of the PNT1a cells.

β-alanine was increased in the zero glucose TH4 treated cells compared to the zero glucose untreated PNT1a cells, and to the 5.5mM and 11mM glucose cells, treated with TH4 ($P<0.0001$).

γ-Aminobutyric acid was increased in the PNT1a cells treated with Menadione in the zero glucose in comparison to the untreated cells, as well as the 5.5mM and 11mM glucose cells treated with Menadione ($P<0.0001$).

Increased putrescine was found in the zero untreated PNT1a cells, in comparison to the Menadione, TH4 and TH6 treated cells in the zero glucose as well as the untreated 5.5mM and 11mM glucose cells ($P<0.0001$).

Spermidine was increased in the zero untreated PNT1a cells, versus the 11mM glucose untreated and the zero glucose TH4 treated cells. A decrease was found in the zero glucose untreated cells, when compared to the zero glucose TH6 treated cells. While the increase in zero glucose TH6 was observed versus the 5.5mM and 11mM glucose cells treated with TH6 ($P<0.0001$).

Spermine concentrations were higher in zero glucose TH4 treated cells in comparison to the zero untreated cells and the 5.5mM glucose TH4 treated cells. The PNT1a cells treated with TH6 in the 11mM glucose, had increased spermine than the zero and 5.5mM glucose TH6 treated cells and the 11mM untreated cells ($P<0.0001$).

The results for the biogenic amines of significance are presented in Figure 6.2.

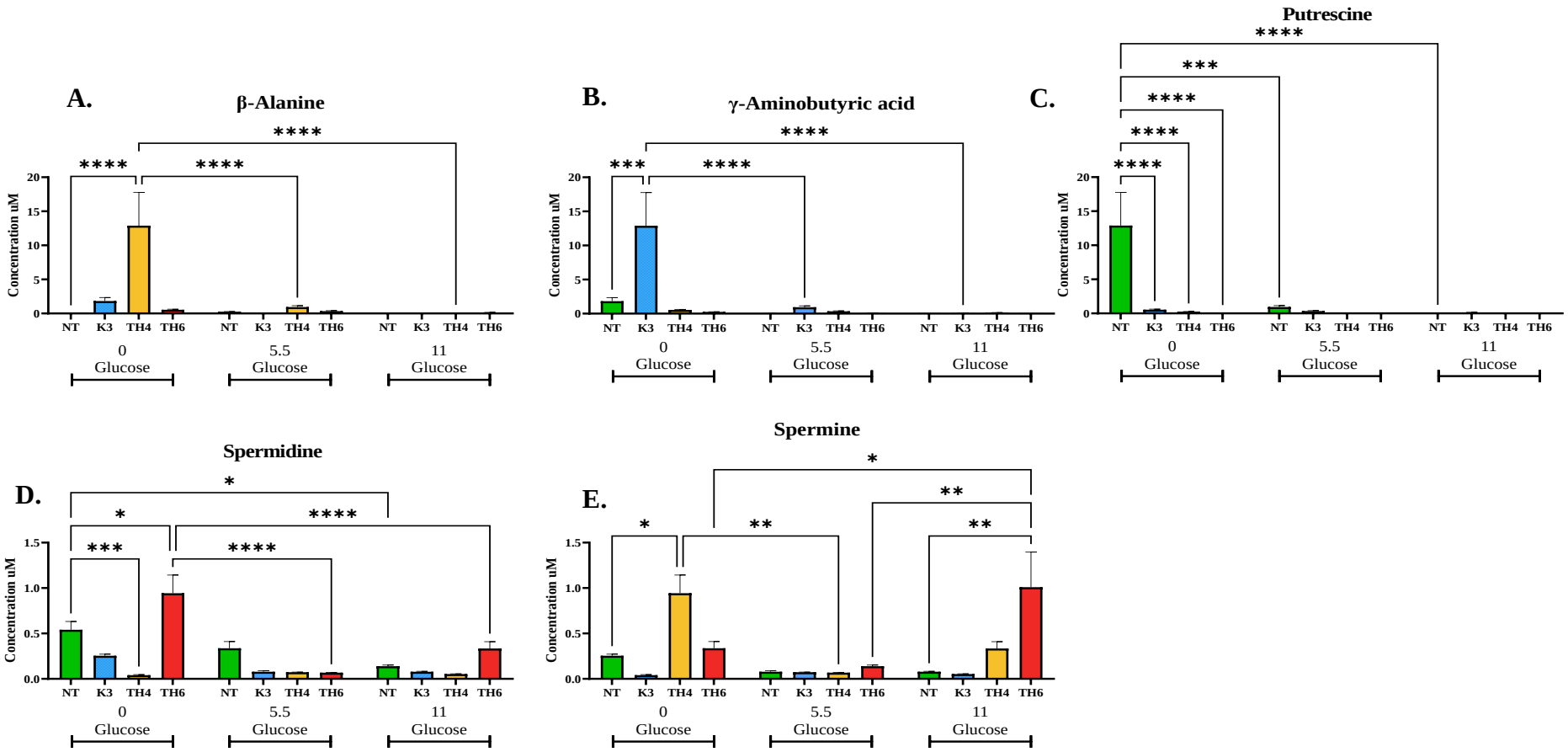

Figure 6.2: PNT1a Metabolomics outcomes of significance in the zero, 5.5mM and 11mM glucose, untreated and treated with Menadione, TH4 and TH6 (Biogenic Amines): (A.) β-alanineconcentrations. (B.) γ-Aminobutyric acid concentrations. (C.) Putrescine concentrations. (D.) Spermidine concentrations. (E.) Spermine concentrations. All concentrations in µM, with data represented as mean ± SEM (n=3).

6.4.1.3 The effects on carboxylic acids in the PNT1a cells under zero, 5.5mM and 11mM glucose conditions, treated with Menadione, TH4 and TH6.

Lactic acid was increased in the 11mM glucose TH6 treated cells versus the 11mM glucose untreated and the zero and 5.5mM glucose TH6 treated cells (P=0.0008).

Increased 3-Hydroxy glutaric acid was observed in the 11mM glucose cells treated with TH4 in comparison to the 11mM untreated cells (P=0.0005).

In the 11mM glucose PNT1a cells treated with Menadione were found to have higher succinate than that of the untreated, in the same glucose conditions and to the zero and 5.5mM glucose PNT1a cells treated with Menadione (P=0.0005).

6.4.1.4 The effects on ceramides in the PNT1a cells under zero, 5.5mM and 11mM glucose conditions, treated with Menadione, TH4 and TH6.

The ceremide Cer(d18:1/22:0) was increased in the TH6 treated PNT1a cells in the 11mM glucose, in comparison to the zero and 5.5mM cells treated with TH6 (P=0.0009).

Cer(d18:2/20:0) was also increased in the TH6 treated cells, but in the 5.5mM glucose and in compared to the zero glucose cells (P=0.002).

The results for the carboxylic acids and ceramides of significance are presented in Figure 6.3 and Figure 6.4 respectively, with pathway mapping based on the metabolites of significance in the PNT1a cells presented in Figure 6.5, performed with Metaboanalyst 5.0.

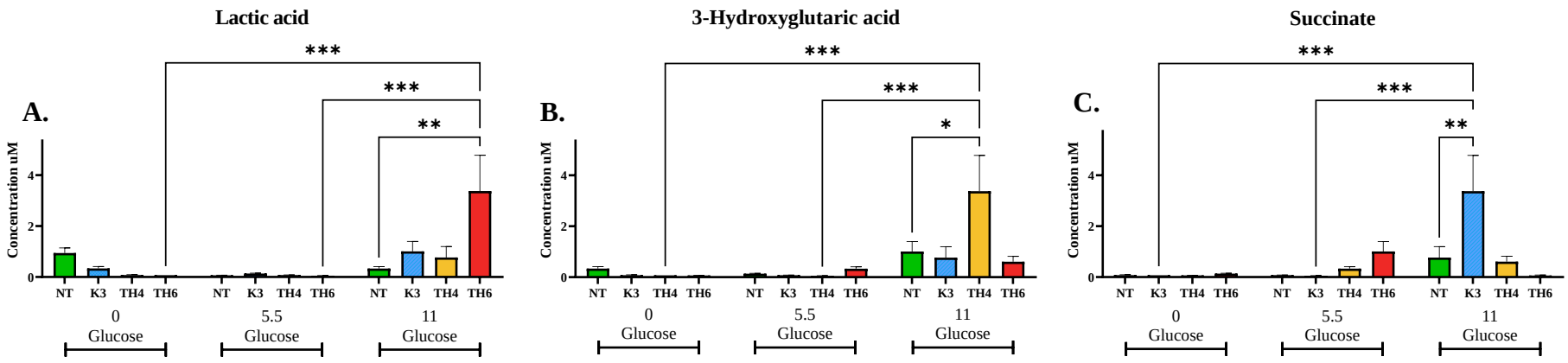

Figure 6. 3: PNT1a Metabolomics outcomes of significance in LNCaP cells in the zero, 5.5mM and 11mM glucose, untreated and treated with Menadione, TH4 and TH6 (Carboxylic Acids): (A.) Lactic Acid concentrations. (B.)3-Hydroxyglutaric acid concentrations. (C.) Succinate concentrations. All concentrations in µM, with data represented as mean ± SEM (n=3).

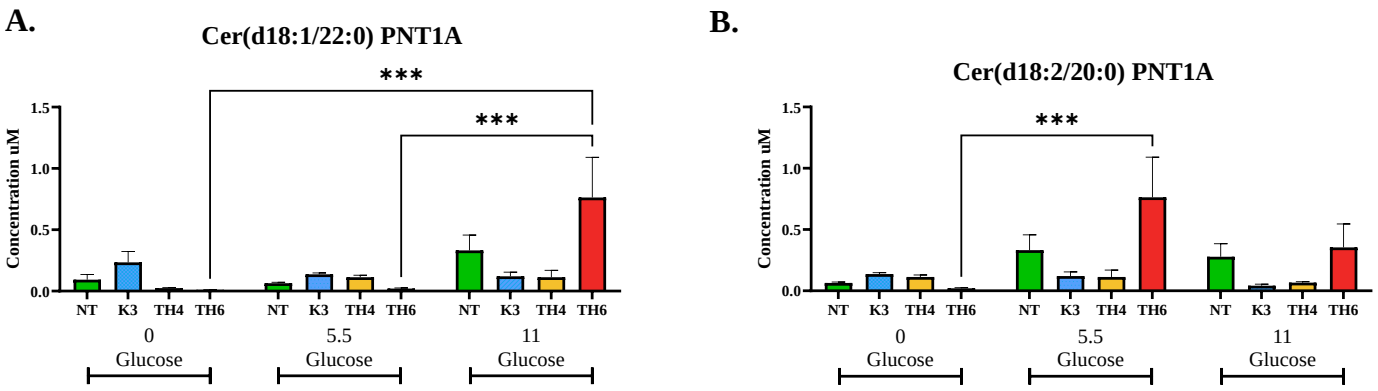

Figure 6. 4: PNT1a Metabolomics outcomes of significance in the zero, 5.5mM and 11mM glucose, untreated and treated with Menadione, TH4 and TH6 (Ceramides) : (A.) Cer(d18:1/22:0) concentrations. (B.) Cer(d18:2/20:0) concentrations. All concentrations in µM, with data represented as mean ± SEM (n=3).

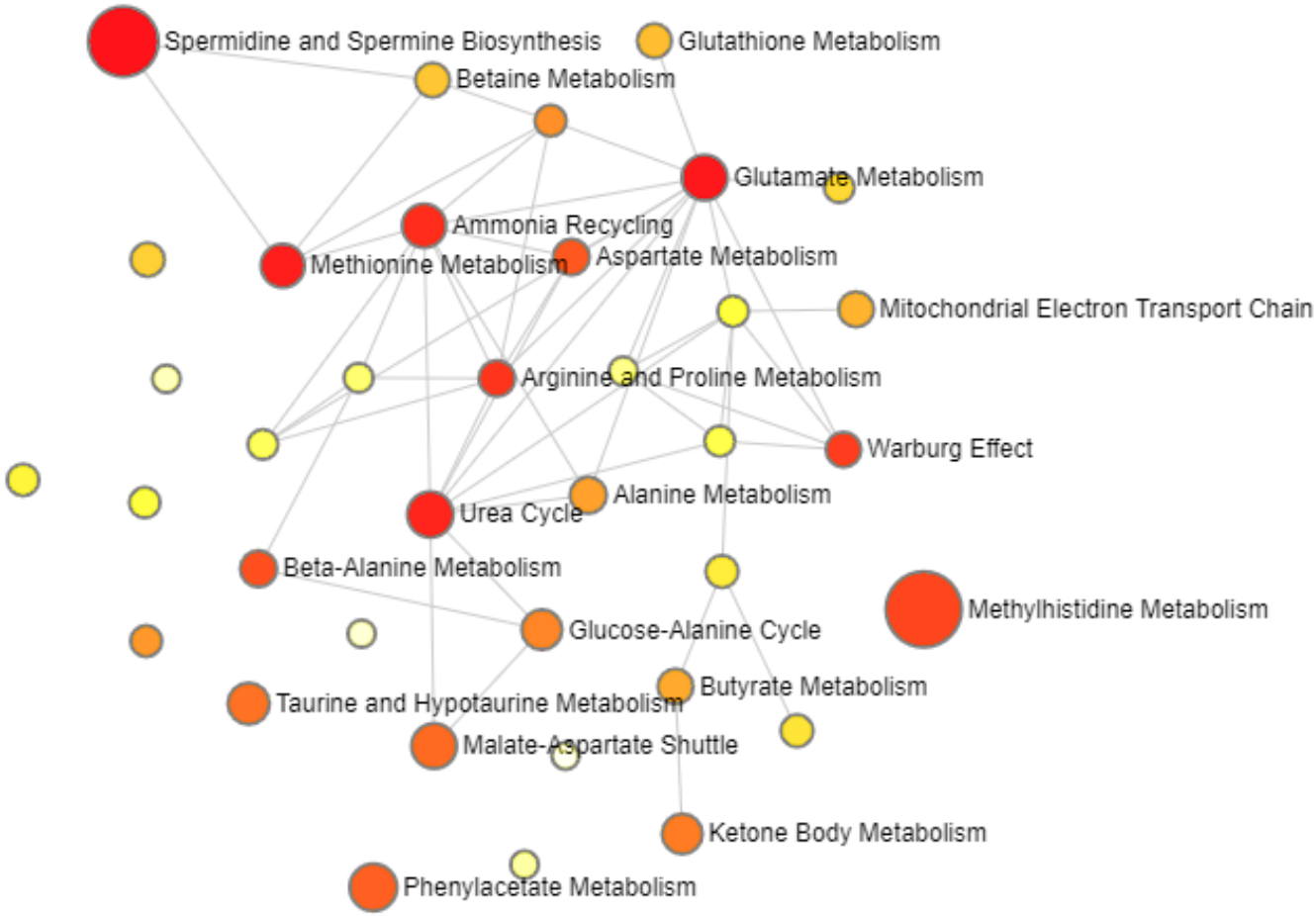

Figure 6. 5:Pathway analysis of the significant metabolites present in the PNT1a cell line , indicating the possible pathways of relevance in the cell line. Small yellow dots indicate pathways of less significance, with the larger red dots indicating pathways of higher significance. Connected dots indicate pathway connections. Pathways were determined by the number of metabolites present within each pathway based on the human metabolome database (HMDB) and matched to metabolic pathways by MetaboAnalyst 5.0.

6.4.2 LCMS-MS analysis of LNCaP cells in the zero, 5.5mM and 11mM glucose conditions, treated with Menadione, TH4 and TH6.

LNCaP LCMS-MS analysis was performed in the zero, 5.5mM and 11mM glucose conditions respectively with untreated and treated cells were examined with the significant analytes presented in Figure 6.6.

The metabolites of significance between treatment groups and glucose conditions are presented in Table 6.2 below, where the concentrations of each metabolite is presented as the mean value and in the micro molar scale.

Table 6. 2: LNCaP Metabolomics outcomes of significance in the zero, 5.5mM and 11mM glucose, untreated and treated with Menadione, TH4 and TH6 . All concentrations in µM, with data represented as mean (n=3).

Metabolites (µM)	Zero Glucose				5.5mM Glucose				11mM Glucose			
	NT	K3	TH4	TH6	NT	K3	TH4	TH6	NT	K3	TH4	TH6
Alanine	81.5	223.3	120.7	903.3	194.5	379.3	491.3	23.6	53.9	61.2	49.2	20.0
3-Methylhistidine	0.1	382.3	5.8	17.1	0.1	0.02	0.6	0.006	0.01	0.02	0.02	0.003
Carnosine	0.02	0.6	0.006	0.01	0.02	0.02	0.003	0.006	0.004	0.008	0.1	0.02
Cystine	0.6	0.006	0.01	0.02	0.02	0.003	0.006	0.004	0.008	0.1	0.024	0.1
Phenylacetyglycine	0.003	0.01	0.004	0.01	0.1	0.02	0.1	0.1	0.2	0.1	0.003	0.7
Beta alanine	0.7	8.2	0.8	0.3	0.03	0.8	0.3	0.2	0.2	0.1	0.2	0.1

6.4.2.1 The effects on amino acids in the LNCaP cells under zero, 5.5mM and 11mM glucose conditions, treated with Menadione, TH4 and TH6.

Alanine concentrations were increased in the TH6 treated LNCaP cells in the zero glucose, when compared to the untreated zero glucose and to the 5.5mM and 11mM glucose TH6 expression (P=0.001). 3-Methylhistidine was increased in zero glucose Menadione treated cells, versus the untreated zero glucose, the 5.5mM glucose and 11mM glucose Menadione treatments (P=0.002).

Carnosine concentrations were increased in zero glucose Menadione treated cells, versus the untreated zero glucose, the 5.5mM glucose and 11mM glucose Menadione treatments (P<0.0001). Cysteine was increased in the zero untreated cells, in comparison to all of the untreated cells (5.5mM and 11mM glucose) and all of the treatments in the zero glucose (P<0.0001).

Phenylacetyl glycine was increased in the 11mM glucose condition of the untreated LNCaP, in comparison to the zero glucose untreated cells. Along with being increased in the 11mM glucose TH6 treatment, versus the untreated 11mM glucose and the zero and the 5.5mM glucose TH6 treatments ($P<0.0001$).

6.4.2.2 The effects on biogenic amines in the LNCaP cells under zero, 5.5mM and 11mM glucose conditions, treated with Menadione, TH4 and TH6.

β- alanine was increased in zero glucose Menadione treated cells, versus the untreated zero, the 5.5mM and 11mM glucose Menadione treated cells ($P<0.0001$).

The results for the amino acids and biogenic amines of significance are presented in Figure 6.6 with pathway mapping based on the metabolites of significance in the LNCaP cells presented in Figure 6.7.

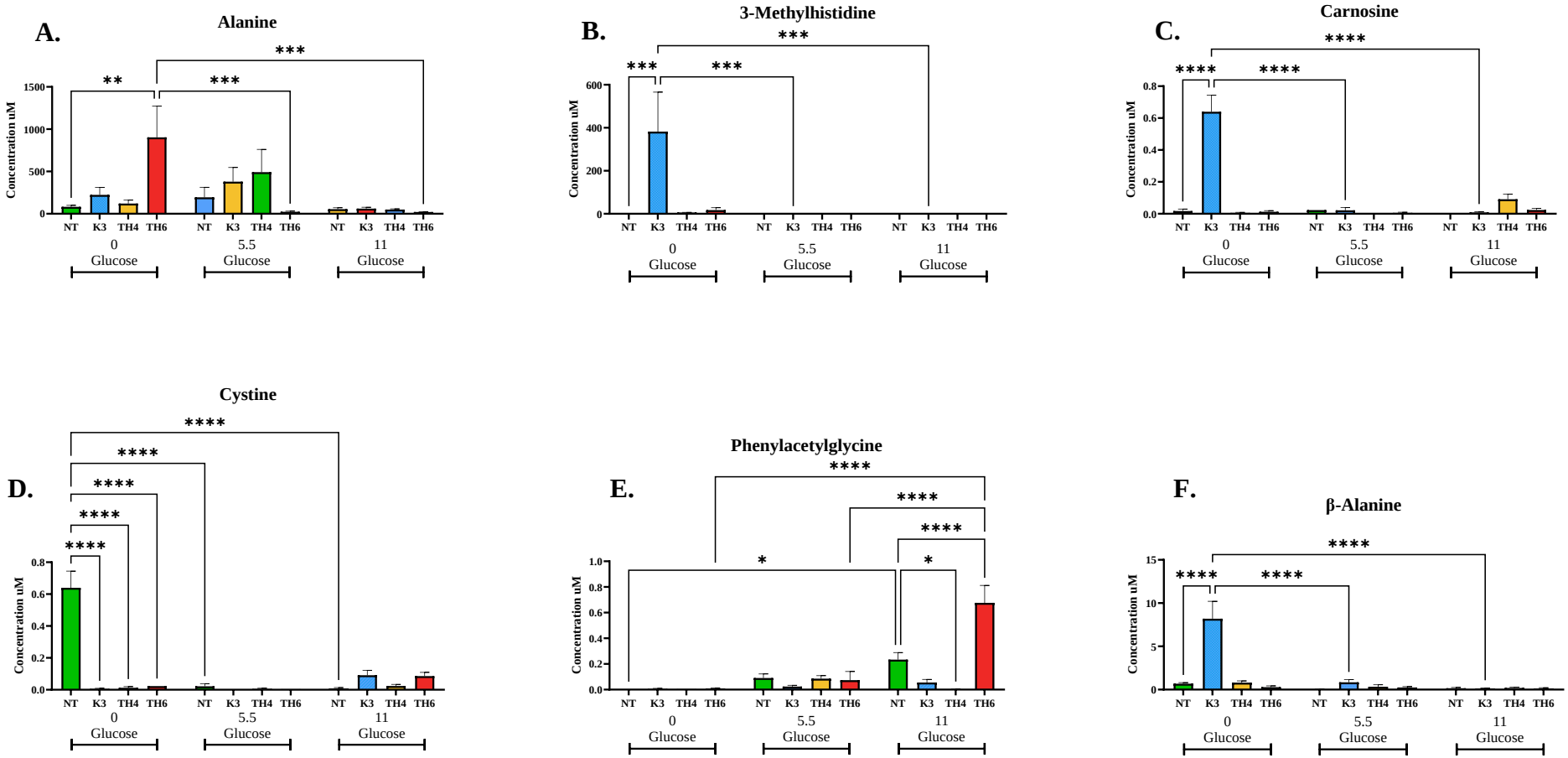

Figure 6. 6: LNCaP Metabolomic outcomes of significance in LNCaP cells in the zero, 5.5mM and 11mM glucose, untreated and treated with Menadione, TH4 and TH6. (A.) Alanine amino acid concentrations. (B.) 3-Methylhistidine concentrations. (C.) Carnosine concentrations. (D.) Cystine concentration. (E.) Phenylacetyl glycine concentrations. (F.) β-Alanine concentrations. All concentrations in µM, with data represented as mean ± SEM (n=3).

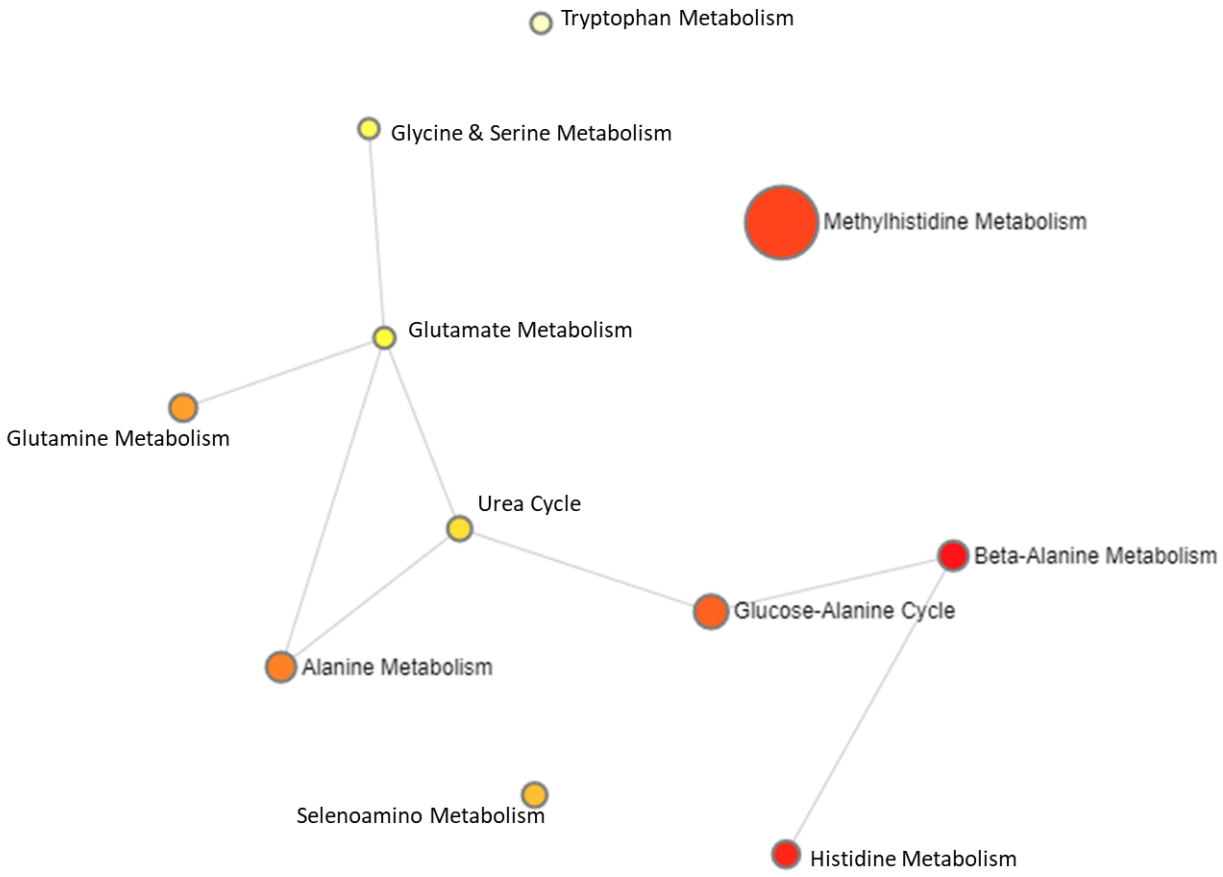

Figure 6. 7: Pathway analysis of the significant metabolites present in the LNCaP cell line , indicating the possible pathways of relevance in the cell line. Small yellow dots indicate pathways of less significance, with the larger red dots indicating pathways of higher significance. Connected dots indicate pathway connections. Pathways determined by the number of metabolites present within each pathway based on the HMDB and matched to metabolic pathways by MetaboAnalyst 5.0.

6.4.3 LCMS-MS analysis of PC3 cells in the zero, 5.5mM and 11mM glucose conditions, treated with Menadione, TH4 and TH6.

The metabolites of significance between treatment groups and glucose conditions are presented in Table 6.3 below, where the concentrations of each metabolite is presented as the mean value and in the micro molar scale.

Table 6. 3: PC3 Metabolomics outcomes of significance in the zero, 5.5mM and 11mM glucose, untreated and treated with Menadione, TH4 and TH6 . All concentrations in µM, with data represented as mean (n=3).

Metabolites (µM)	Zero Glucose				5.5mM Glucose				11mM Glucose			
	NT	K3	TH4	TH6	NT	K3	TH4	TH6	NT	K3	TH4	TH6
Alanine	23.8	112.5	45.6	51.8	395.3	11.8	74.2	95.4	16.1	48.3	57.0	53.2
Asparagine	45.6	51.8	395.3	11.8	74.2	95.4	16.1	48.3	57.0	53.2	14.6	17.3
Cystine	11.8	74.2	95.4	16.1	48.3	57.0	53.2	14.6	17.3	42.4	36.4	30.4
Glutamine	0.05	0.01	0.01	3.2	1.7	1.4	21.3	5.8	0.6	609.7	3.9	2.8
3-Methylhistidine	5.8	0.6	609.7	3.9	2.8	0.1	0.1	1.6	0.01	0.1	0.1	0.1
5 Aminovaleric acid	0.6	609.7	3.9	2.8	0.1	0.1	1.6	0.01	0.1	0.1	0.1	0.04
Asymmetric dimethylhistidine	3.9	2.8	0.1	0.1	1.6	0.01	0.1	0.1	0.1	0.04	0.02	0.02
Betaine	2.8	0.1	0.1	1.6	0.0	0.1	0.1	0.1	0.04	0.02	0.02	0.03
Carnosine	0.1	0.1	1.6	0.01	0.1	0.1	0.1	0.04	0.02	0.02	0.03	63.3
Metionine Sulfoxide	0.1	0.1	0.1	0.04	0.02	0.02	0.03	63.3	0.03	0.2	0.3	0.4
Symmetric dimethylhistidine	0.04	0.02	0.02	0.03	63.3	0.03	0.2	0.3	0.4	0.2	0.004	1.8
Taurine	0.02	0.03	63.3	0.03	0.2	0.3	0.4	0.2	0.004	1.8	11.5	0.5
Beta Alanine	0.004	1.8	11.5	0.5	0.4	0.04	0.8	0.7	0.1	0.1	0.1	0.2
γ-Aminobutyric acid	1.8	11.5	0.5	0.4	0.04	0.8	0.7	0.1	0.1	0.1	0.2	0.1
Putrescine	11.5	0.5	0.4	0.04	0.8	0.7	0.1	0.1	0.1	0.2	0.1	0.1
Spermidine	0.5	0.4	0.04	0.8	0.7	0.1	0.1	0.1	0.2	0.1	0.1	0.2
Lactic Acid	0.8	0.7	0.1	0.1	0.1	0.2	0.1	0.1	0.2	0.5	0.4	2.5
3-Hydroxyglutaric acid	0.7	0.1	0.1	0.1	0.2	0.1	0.1	0.2	0.5	0.4	2.5	0.4
Cer(d18:1/20:0(OH))	0.2	0.1	0.1	0.2	0.5	0.4	2.5	0.4	0.04	7.1	1.3	0.2
Cer(d18:1/26:1)	0.4	2.5	0.4	0.04	7.1	1.3	0.2	0.1	2.0	2.9	0.6	0.7
Cer(d18:20:0)	0.4	2.5	0.4	0.04	7.1	1.3	0.2	0.1	2.0	2.9	0.6	0.7

6.4.3.1 The effects on amino acids in the PC3 cells under zero, 5.5mM and 11mM glucose conditions, treated with Menadione, TH4 and TH6.

Alterations in the amino acid pathways were observed in the PC3 cells. Alanine was decreased in the untreated 5.5mM glucose versus the zero and 11mM glucose cells. Increased concentrations were observed in the 5.5mM untreated cells versus the corresponding Menadione, TH4 and TH6 treated cells. Increased alanine was found in the zero glucose Menadione treated cells compared to the same in the 5.5mM glucose cells ($P<0.0001$).

Asparagine was increased in the zero glucose TH4 treated cells versus zero glucose untreated and the TH4 treated 5.5mM and 11mM glucose cells ($P<0.0001$).

Glutamine was increased in the zero glucose cells treated with Menadione and TH4 when compared to the untreated and the corresponding treatments in the 5.5mM and 11mM glucose. Decreased concentrations were determined in the 5.5mM glucose TH6 treated cells versus their untreated. A reduction in glutamine was found in the zero and 11mM glucose untreated cells than in the 5.5mM glucose cells. Increased levels were found in the 11mM Menadione treated PC3 cells compared to their untreated ($P<0.0001$).

Proline was higher in the 11mM glucose Menadione treated cells compared to the untreated, and the zero and 5.5mM glucose Menadione treated cells ($P<0.0001$).

3-Methylhistidine was increased in the zero glucose TH4 treated cells versus the untreated and the TH4 treated cells in the 5.5mM and 11mM glucose conditions ($P<0.0001$).

5-Aminovaleric acid was increased in the zero glucose Menadione treated PC3 cells, versus the zero glucose untreated and the Menadione treated in the 5.5mM and 11mM glucose ($P<0.0001$).

Asymmetric-dimethyl arginine was increased in the zero untreated cells, compared to the TH4 and TH6 treatments in the zero glucose, as well as the 11mM untreated cells. Concentrations were decreased in the 5.5mM and 11mM glucose, Menadione treated cells compared to the zero glucose Menadione treated cells ($P<0.0003$).

Betaine was increased in the zero glucose untreated cells, compared to the Menadione and TH4 treated cells of the same glucose conditions. It was also increased versus the 5.5mM and 11mM glucose untreated cells ($P<0.0001$).

Carnosine was found to be increased in the 11mM glucose cells treated with TH6, compared to that of the untreated and the TH6 treated cells in 5.5mM and 11mM glucose conditions ($P<0.0001$).

Methionine sulfoxide was increased in the 5.5mM glucose TH6 treated cells compared to its corresponding untreated cells, and the TH6 treated cells in the zero and 11mM glucose conditions ($P<0.0001$).

Symmetric-dimethyl arginine was increased in the untreated 5.5mM glucose cells, compared to the Menadione, TH4, TH6 treated and the untreated cells in the zero and 11mM glucose conditions ($P<0.0001$).

Increased taurine was detected in the TH4 treated cells in the zero glucose versus the corresponding zero glucose untreated cells, and the TH4 treated cells in the 5.5mM and 11mM glucose conditions. The 11mM glucose TH4 treated cells had higher concentrations of taurine than its corresponding 11mM glucose untreated cells ($P<0.0001$).

The results for the amino acids of significance are presented in Figure 6.8.

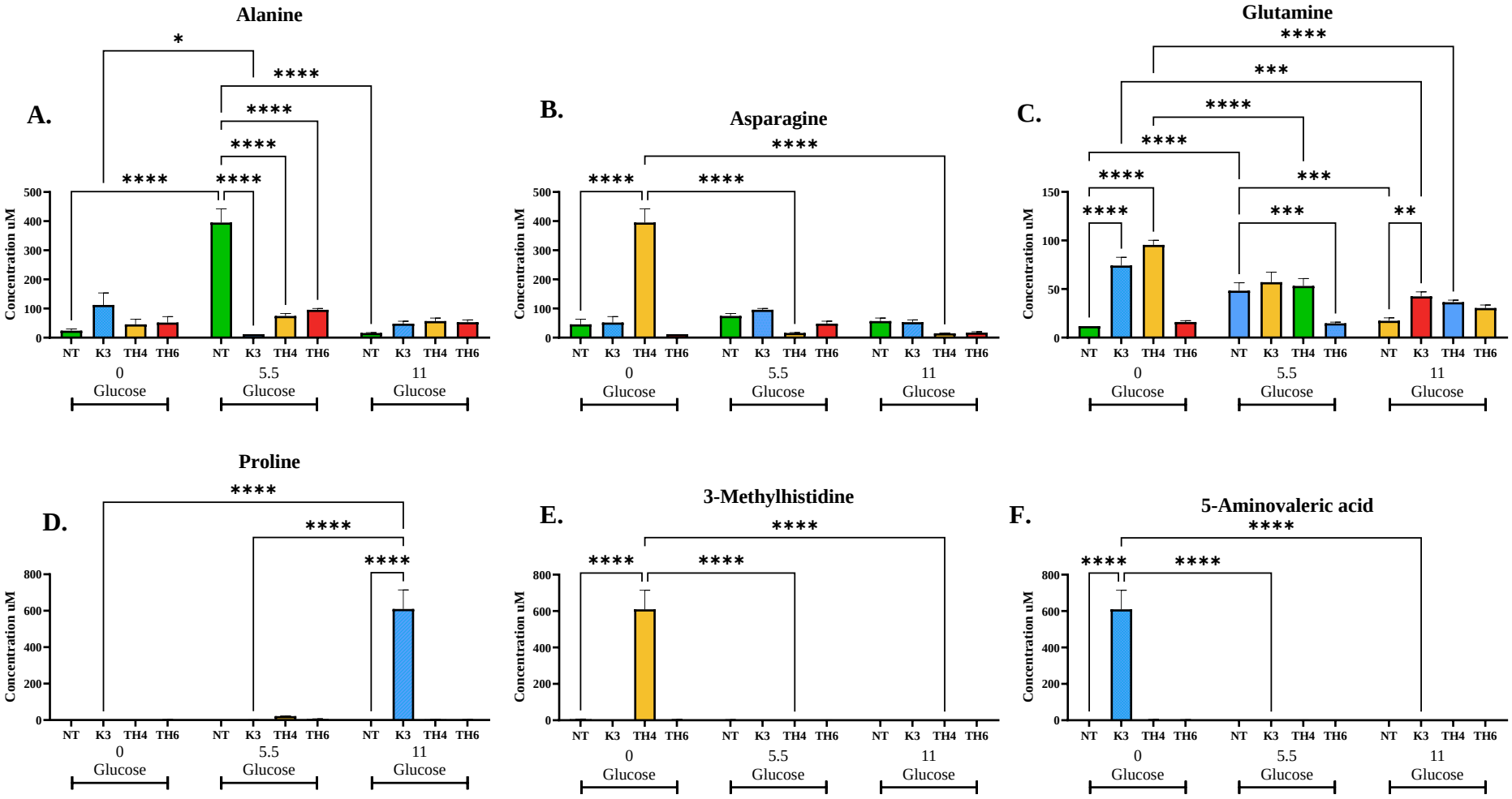
A.
Alanine
B.
Asparagine
C.
Glutamine
D.
Proline
E.
3-Methylhistidine
F.
5-Aminovaleric acid
Concentration uM
NT K3 TH4 TH6
0 Glucose
5.5 Glucose
11 Glucose

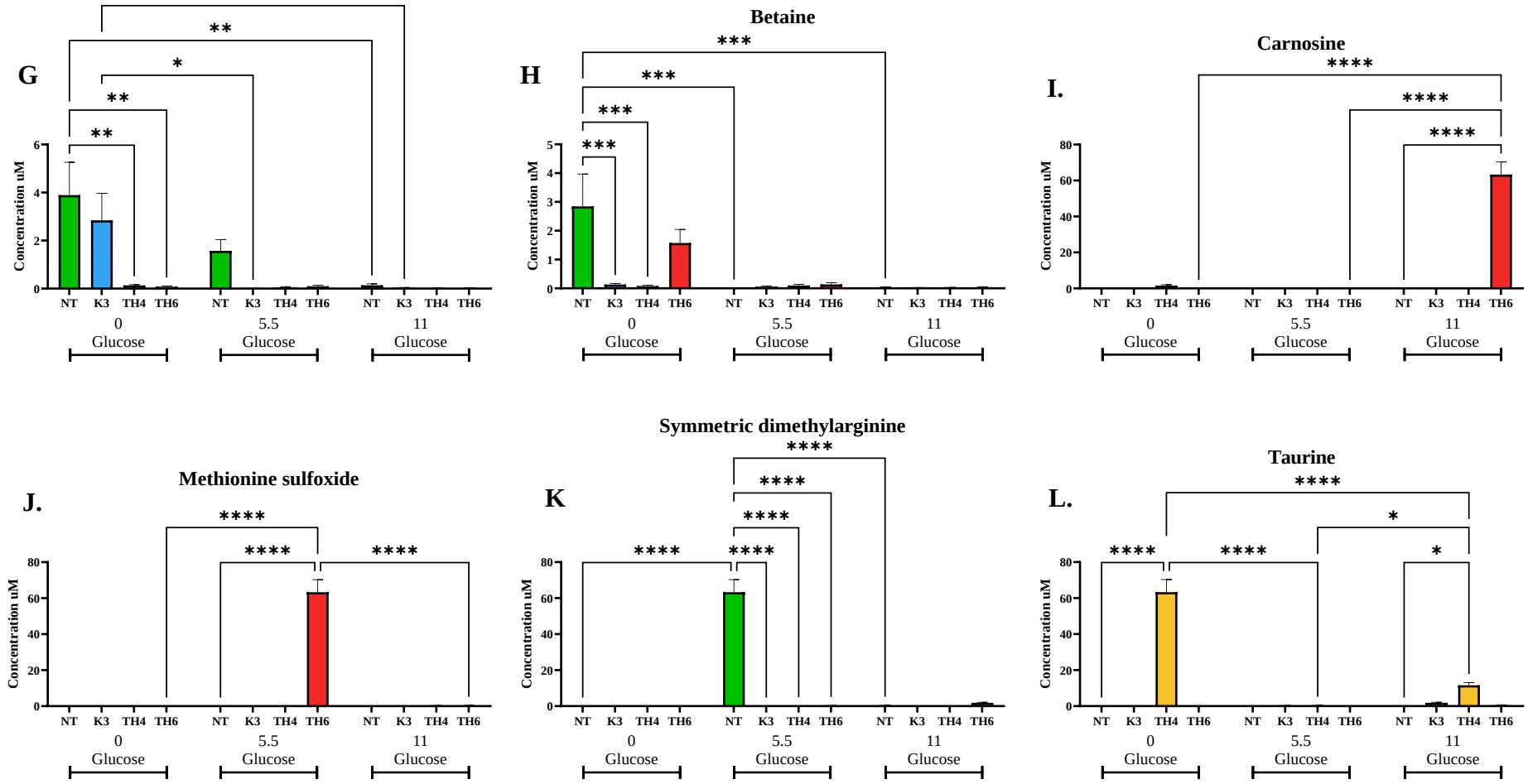

Figure 6. 8: PC3 Metabolomics outcomes of significance in the zero, 5.5mM and 11mM glucose, untreated and treated with Menadione, TH4 and TH6 (Amino Acids) : (A.) Alanine concentrations. (B.) Asparagine concentrations. (C.) Glutamine concentrations. (D.) Proline concentrations. (E.) 3-Methylhistidine concentrations. (F.) 5-Aminovaleric acid concentrations. (G.) Asymmetric dimethylarginine concentrations. (H.) Betaine concentrations. (I.) Carnosine concentration. (J.) Methionine Sulfoxide concentrations. (K.) Acetylornithine concentrations. (L.) Taurine concentrations. All concentrations in µM, with data represented as mean ± SEM (n=3).

6.4.3.2 The effects on biogenic amines in the PC3 cells under zero, 5.5mM and 11mM glucose conditions, treated with Menadione, TH4 and TH6.

β- alanine was increased in the TH4 treated cells in the presence of zero glucose conditions, compared to the zero untreated and the 5.5mM and 11mM glucose TH4 treated cells ($P<0.0001$). γ-Aminobutyric acid was increased in the zero glucose Menadione treated cells compared to the zero untreated and the 5.5mM and 11mM glucose Menadione treated PC3 cells ($P<0.0001$).

A decrease in putrescine was found in all of the treatments in the zero glucose versus the untreated cells. This decrease was also observed in the untreated in the 5.5mM and 11mM glucose versus the zero glucose untreated ($P<0.0001$).

Spermidine was reduced in the TH4 treated cells versus the untreated cell in the presence of zero glucose. Concentrations were increased in the TH6 treated cells versus the untreated in the zero glucose as well as the TH6 treated in the 5.5mM and 11mM glucose. All of the treated (Menadione, TH4 and TH6) cells had reduced spermidine than the corresponding untreated cells in the 5.5mM glucose, as did the 11mM untreated cells ($P<0.0001$).

The results for the biogenic amines of significance are presented in Figure 6.9.

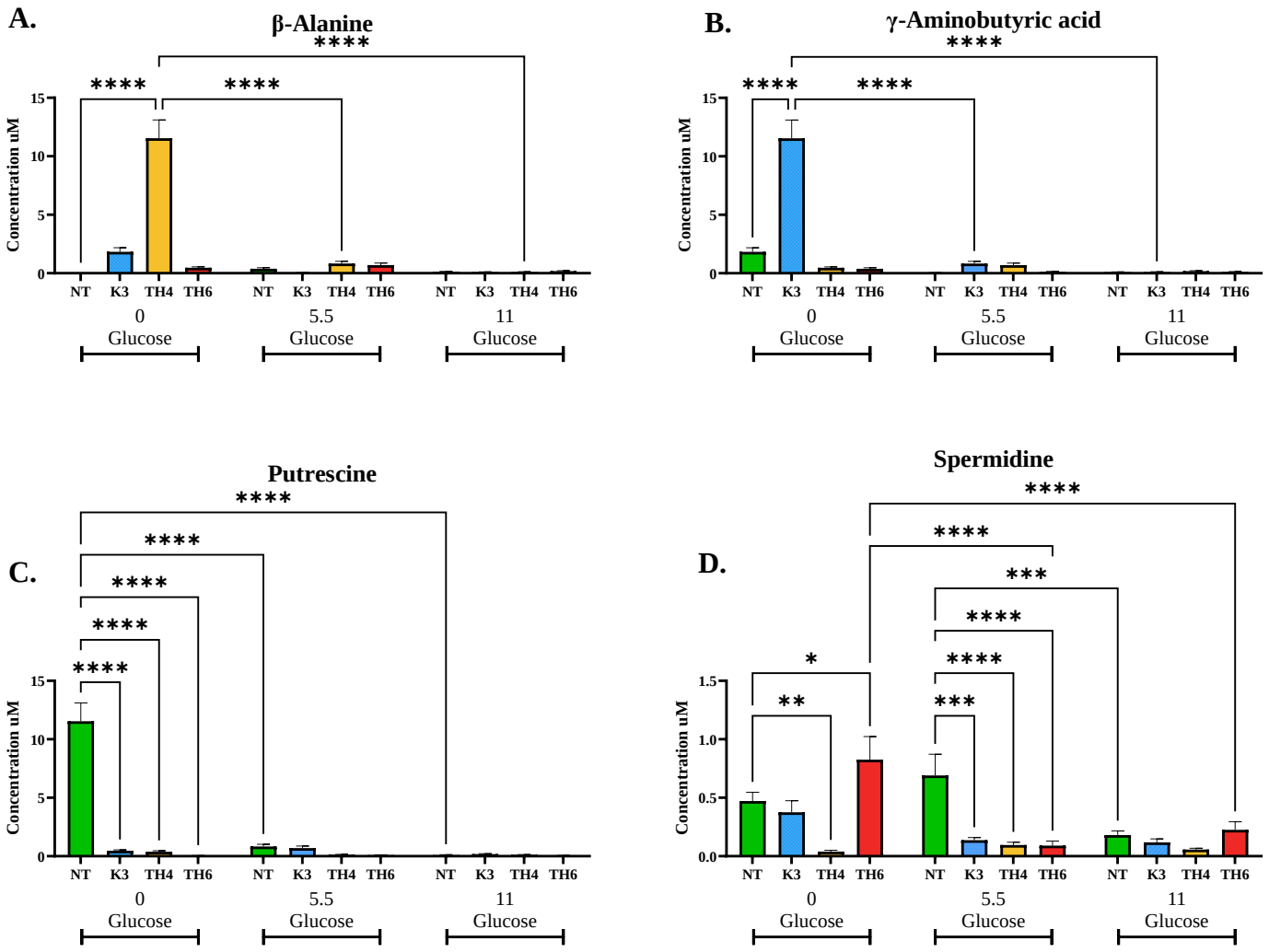

Figure 6. 9: PC3 Metabolomics outcomes of significance in the zero, 5.5mM and 11mM glucose, untreated and treated with Menadione, TH4 and TH6 (Biogenic Amines) : (A.) β-alanineconcentrations. (B.) γ-Aminobutyric acid concentrations. (C.) Putrescine concentrations. (D.) Spermidine concentrations. All concentrations in µM, with data represented as mean ± SEM (n=3).

6.4.3.3 The effects on carboxylic acids in the PC3 cells under zero, 5.5mM and 11mM glucose conditions, treated with Menadione, TH4 and TH6.

Lactic acid concentrations were increased it the 11mM glucose TH6 treated cells compared to the corresponding untreated cells of the same glucose conditions and that of the 5.5mM and zero glucose conditions (P=0.001).

3-Hydroxyglutaric acid was increased in the TH4 treated cells in the presence of 11mM glucose versus the untreated (P=0.001).

6.4.3.4 The effects on ceramides in the PC3 cells under zero, 5.5mM and 11mM glucose conditions, treated with Menadione, TH4 and TH6.

Cer(d18:1/20:0(OH)) was increased in the 11mM glucose Menadione treated cells versus the 11mM untreated and the zero and 5.5mM glucose Menadione treated cells (P=0.003).

Cer(d18:1/26:1) was increased in the 5.5mM untreated cells compared to the zero and 11mM glucose untreated cells. Concentrations were decreased in the 5.5mM glucose cells treated with Menadione, TH4 and TH6 compared the 5.5mM glucose untreated cells (P=0.003).

Cer(d18:2/20:0) was increased in the zero glucose cells treated with TH6 compared to the TH6 treatments in the 5.5mM and 11mM glucose conditions (P=0.003).

The results for the carboxylic acids and ceramides of significance are presented in Figure 6.10 and Figure 6.11 respectively. The pathway mapping based on the metabolites of significance in the PC3 cells is presented in Figure 6.12.

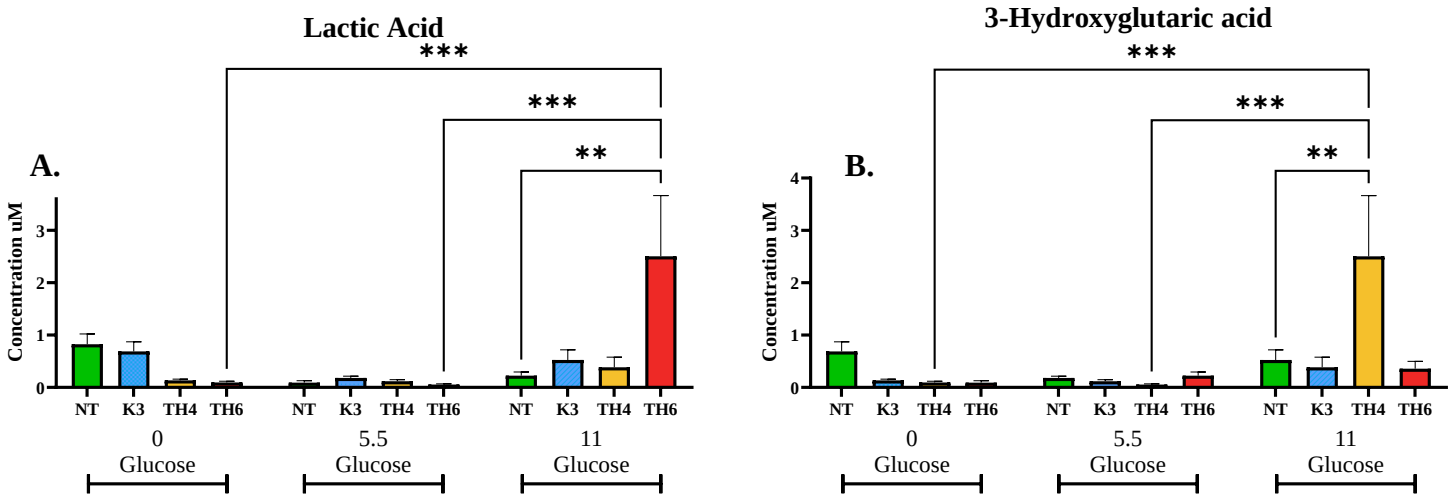

Figure 6. 10: PC3 Metabolomics outcomes of significance in the zero, 5.5mM and 11mM glucose, untreated and treated with Menadione, TH4 and TH6 (Carboxylic Acids) : (A.) Lactic acid concentrations. (B.) 3-Hydroxyglutaric acid concentrations. All concentrations in µM, with data represented as mean ± SEM. (n-3).

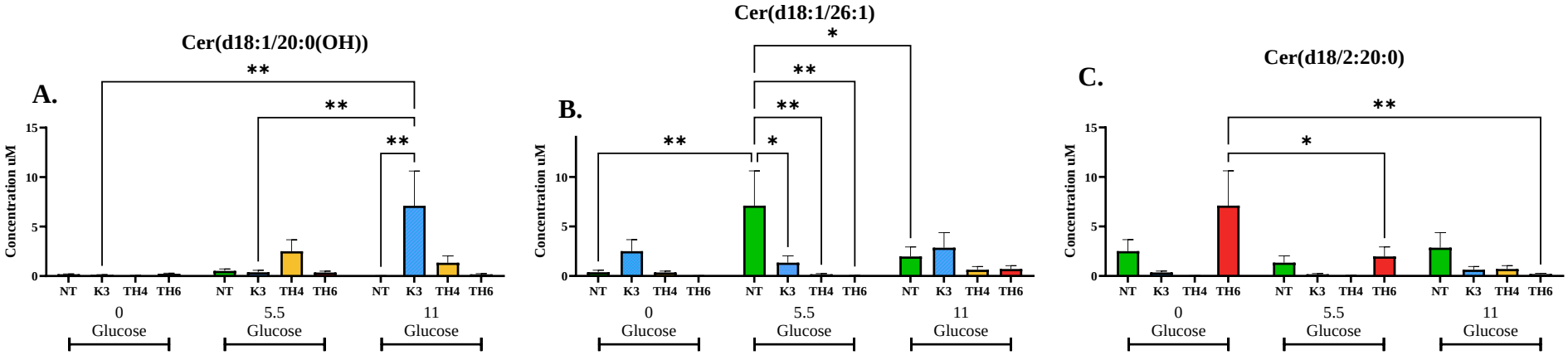

Figure 6. 11: PC3 Metabolomics outcomes of significance in the zero, 5.5mM and 11mM glucose, untreated and treated with Menadione, TH4 and TH6 (Ceramides) : (A.) Cer(d18:1/20:0(OH)) concentrations. (B.) Cer(d18:1/26:1) concentrations. (C.) Cer(d18/2:20:0) concentrations. All concentrations in µM, with data represented as mean ± SEM. (n=3).

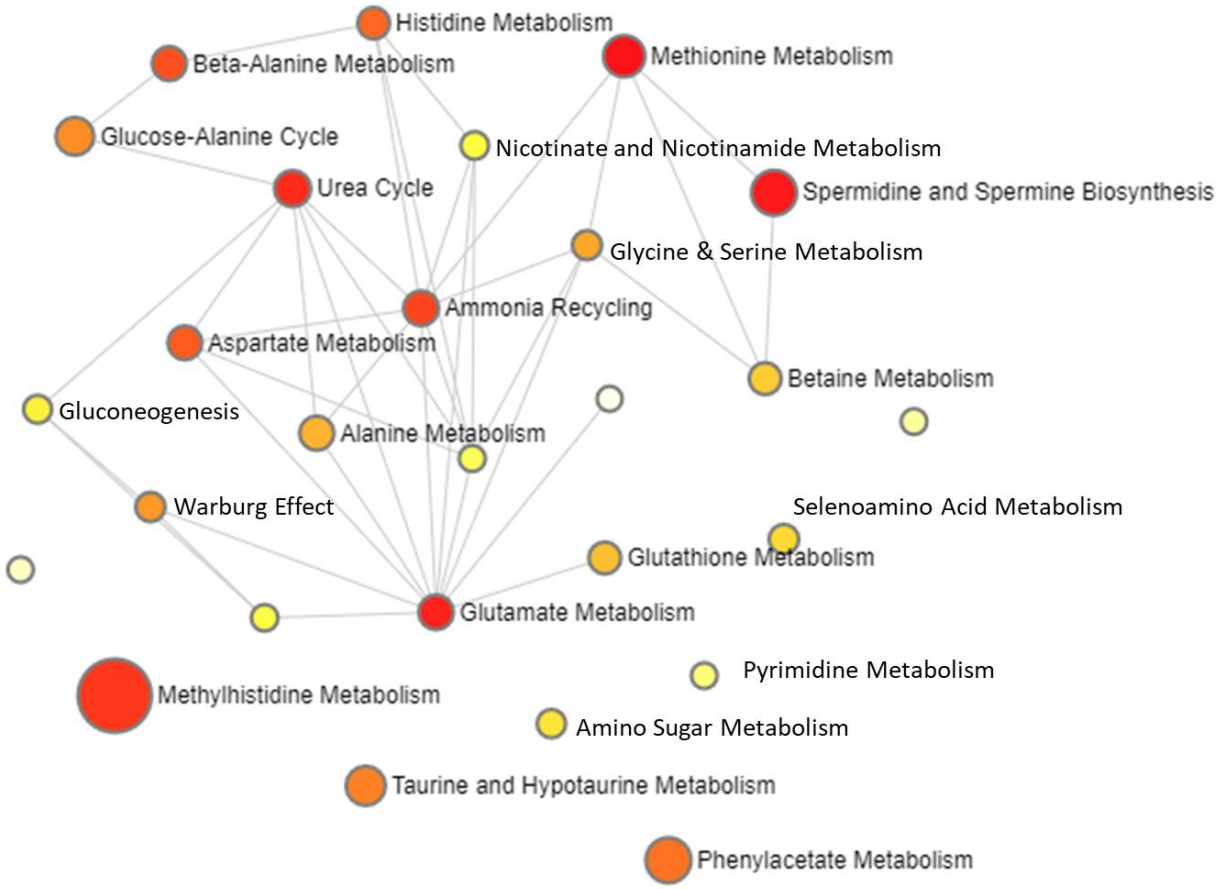

Figure 6. 12:Pathway analysis of the significant metabolites present in the PC3 cell line , indicating the possible pathways of relevance in the cell line. Small yellow dots indicate pathways of less significance, with the larger red dots indicating pathways of higher significance. Connected dots indicate pathway connections. Pathways determined by the number of metabolites present within each pathway based on the HMDB and matched to metabolic pathways by MetaboAnalyst 5.0.

6.4.4 LCMS-MS analysis of Du145 cells in the zero, 5.5mM and 11mM glucose conditions, treated with Menadione, TH4 and TH6.

Alterations in amino acids, biogenic amines and carboxylic acids were found in the LCMS-MS analysis of the Du145 cells in the zero, 5.5mM and 11mM glucose, both treated and untreated.

The metabolites of significance between treatment groups and glucose conditions are presented in Table 6.4 below, where the concentrations of each metabolite is presented as the mean value and in the micro molar scale.

Table 6. 4: Du145 Metabolomics outcomes of significance in the zero, 5.5mM and 11mM glucose, untreated and treated with Menadione, TH4 and TH6 . All concentrations in µM, with data represented as mean (n=3).

Metabolites (µM)	**Zero Glucose**				**5.5mM Glucose**				**11mM Glucose**			
	NT	**K3**	**TH4**	**TH6**	**NT**	**K3**	**TH4**	**TH6**	**NT**	**K3**	**TH4**	**TH6**
Alanine	25.0	132.3	59.9	47.0	325.7	22.5	237.2	101.2	12.9	40.3	53.0	39.6
Phenylalanine	0.01	0.04	0.01	0.01	5.3	2.5	3.0	14.7	4.3	0.1	447.0	5.7
Methylhistidine	4.3	0.1	447.0	5.7	3.6	0.1	0.03	0.6	0.01	0.04	0.1	0.1
Asymmetric dimethylargenine	5.7	3.6	0.1	0.03	0.6	0.01	0.04	0.1	0.1	0.01	0.01	0.01
γ-Aminobutyric acid	1.4	11.7	0.4	0.3	0.0	0.6	0.7	0.1	0.2	0.1	0.3	0.2
Putrescine	11.7	0.4	0.3	0.0	0.6	0.7	0.1	0.2	0.1	0.3	0.2	0.1
Lactic acid	11.7	0.4	0.3	0.0	0.6	0.7	0.1	0.2	0.1	0.3	0.2	0.1
3-Hydroxyglutaric acid	0.7	0.1	0.2	0.1	0.3	0.2	0.1	0.3	1.0	1.0	3.3	0.5

6.4.4.1 The effects on amino acids in the Du145 cells under zero, 5.5mM and 11mM glucose conditions, treated with Menadione, TH4 and TH6.

Alanine was found to be decreased in the 5.5mM glucose Menadione treated cells compared to that of the equivalent untreated cells. The expression in the 5.5mM untreated cells was greater than that of the untreated cells in the the zero and 11mM glucose concentrations (P=0.02).

Phenylalanine was increased in the TH4 treated cells versus the untreated cells in the 11mM glucose conditions. It was also found to be higher in the zero glucose TH4 treated cells versus the 5.5mM and 11mM glucose TH4 treated cells (P<0.0001).

3-Methylhistidine was increased in the TH4 treated cells versus the untreated in the presence of zero glucose, its was also higher than in the 5.5mM and 11mM glucose cells treated with TH4 (P<0.0001).

Asymmetric-dimethyl arginine was found to be increased in the zero glucose untreated versus the TH4 and TH6 treated PC3 cells, it was also higher than that of the 5.5mM and 11mM glucose untreated cells. the zero glucose Menadione treated cells had higher asymmetric-dimethyl arginine than that of the 5.5mM and 11mM glucose Menadione treated cells (P<0.0001).

The results for the amino acids of significance are presented in Figure 6.13.

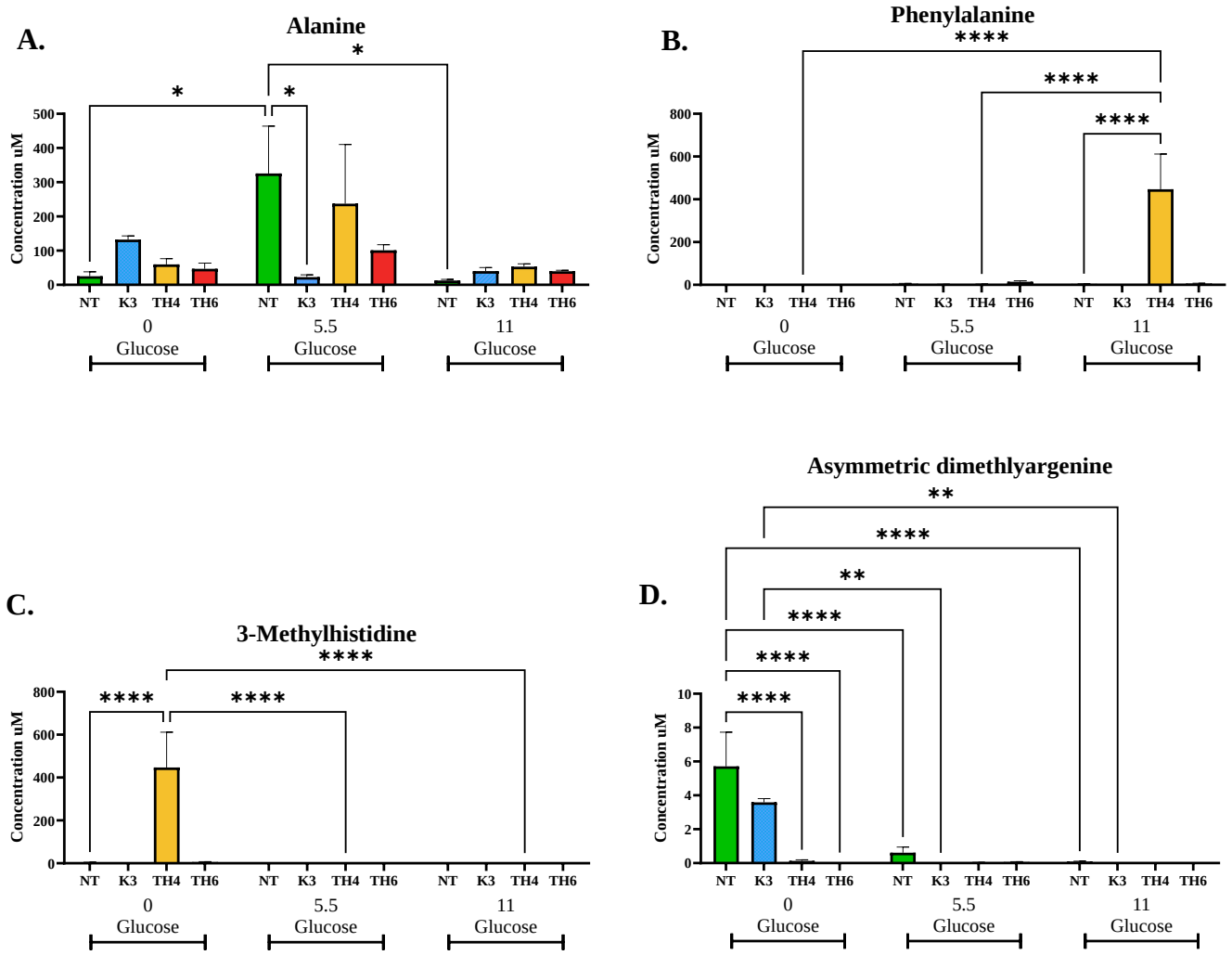

Figure 6. 13: Du145 Metabolomics outcomes of significance in the zero, 5.5mM and 11mM glucose, untreated and treated with Menadione, TH4 and TH6 (Amino Acids) : (A.) Alanine concentrations. (B.) Asparagine concentrations. (C.) Glutamine concentrations. (D.) Proline concentrations. All concentrations in µM, with data represented as mean ± SEM (n=3).

The results for the biogenic amines and carboxylic acids of significance are presented in Figure 6.14 and Figure 6.15 respectively. The pathway mapping based on the metabolites of significance in the Du145 cells is presented in Figure 6.16.

6.4.4.2 The effects on biogenic amines in the Du145 cells under zero, 5.5mM and 11mM glucose conditions, treated with Menadione, TH4 and TH6.

The biogenic amine, γ-Aminobutyric acid was found to be increased in the zero glucose Menadione treated cells versus the zero glucose untreated cells as well as the 5.5mM and 11mM glucose Menadione treated cells ($P<0.0001$).

Putrescine was decreased in the Menadione, TH4 and TH6 treated cells compared to the untreated cells in the zero glucose. It was also reduced in the 5.5mM and 11mM glucose untreated cells ($P<0.0001$).

6.4.4.3 The effects on carboxylic acids in the Du145 cells under zero, 5.5mM and 11mM glucose conditions, treated with Menadione, TH4 and TH6.

Lactic acid was increased in the TH6 treated cells in the 11mM glucose compared to TH6 treated 5.5mM glucose cells ($P=0.09$).

3-Hydroxyglutaric acid was increased in the TH4 treated cells in the 11mM glucose versus that of the 5.5mM glucose TH4 treated cells ($P=0.09$).

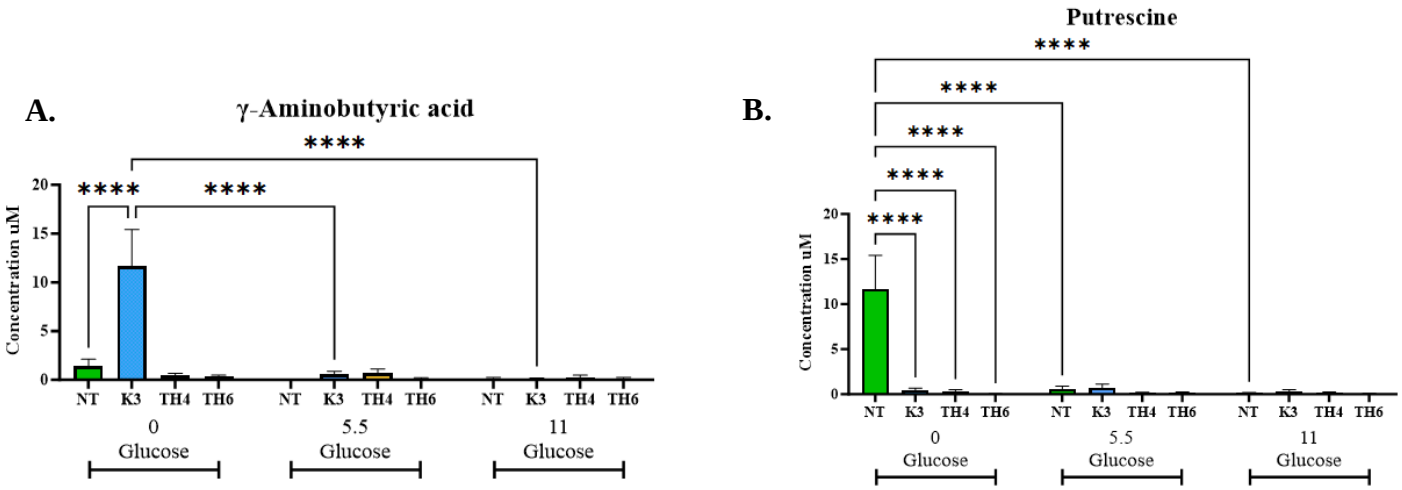

Figure 6. 14: Du145 Metabolomics outcomes of significance in the zero, 5.5mM and 11mM glucose, untreated and treated with Menadione, TH4 and TH6 (Biogenic Amines) : (A.) β-alanineconcentrations. (B.) γ-Aminobutyric acid concentrations. All concentrations in µM, with data represented as mean ± SEM (n=3).

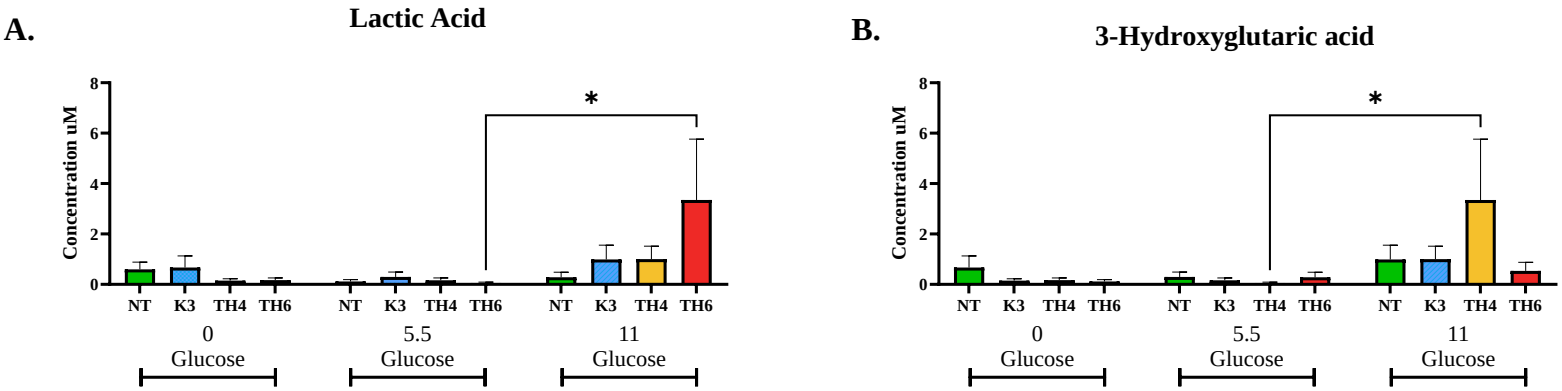

Figure 6. 15: Du145 Metabolomics outcomes of significance in the zero, 5.5mM and 11mM glucose, untreated and treated with Menadione, TH4 and TH6 (Carboxylic Acids) : (A.) Lactic acid concentrations. (B.) 3-Hydroxyglutaric acid concentrations. All concentrations in µM, with data represented as mean ± SEM (n=3).

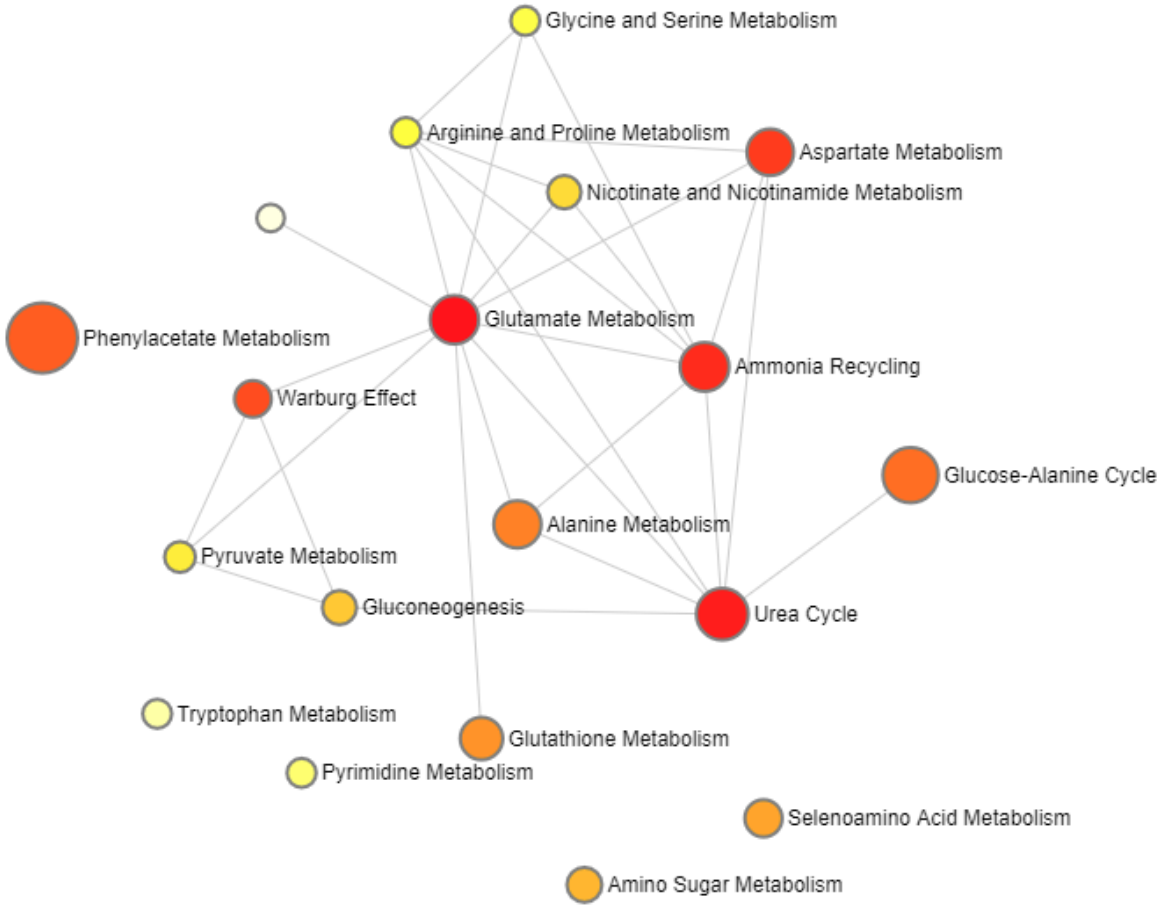

Figure 6. 16: Pathway analysis of the significant metabolites present in the Du145 cell line , indicating the possible pathways of relevance in the cell line. Small yellow dots indicate pathways of less significance, with the larger red dots indicating pathways of higher significance. Connected dots indicate pathway connections. Pathways determined by the number of metabolites present within each pathway based on the HMDB and matched to metabolic pathways by MetaboAnalyst 5.0.

6.5 Summary of results

Chapter 6 highlights
• Alterations in amino acids, biogenic amines, carboxylic acids and ceramides were observed in the PNT1a cells in the the presence of zero, 5.5mM and 11mM when treated with Menadione and the novel TH compounds, TH4 and TH6. • Alterations in amino acids, and biogenic amines were observed in the LNCaP cells in the the presence of zero, 5.5mM and 11mM when treated with Menadione and the novel TH compounds, TH4 and TH6. • Alterations in amino acids, biogenic amines, carboxylic acids, and ceramides were observed in the PC3 cells in the the presence of zero, 5.5mM and 11mM when treated with Menadione and the novel TH compounds, TH4 and TH6. • Alterations in amino acids, biogenic amines, and carboxylic acids were observed in the Du145 cells in the the presence of zero, 5.5mM and 11mM when treated with Menadione and the novel TH compounds, TH4 and TH6.

6.6 Results

In this chapter, thirty-three metabolites of significance are discussed across the cell lines and the treatments with Menadione and the novel TH4 and TH6 compounds. Twenty-one amino acids, five biogenic acids, three carboxylic acids and four ceramides of interest were identified as altered by either the glucose concentrations in which the cells were cultured or by the treatment with Menadione and the TH compounds.

Amino acid metabolism has extreme extensive effects in cancer cells and their metabolome. For instance, glutamine, leucine, valine, and other amino acids are used in the TCA cycle in the mitochondria, while aspartate and glutamine are used in purine biosynthesis as carbon and nitrogen donors.

Glutamate metabolism was identified in the pathway mapping of the PNT1a and PC3 cell lines from the metabolites of significance. The relevant metabolites involved in this metabolic pathway identified in the cells include glutamine, γ-Aminobutyric acid, and alanine. Glutamate is produced from glutamine, 5-oxoproline and α-ketoglutarate (α-KG).[429] Mitochondrial dysfunction often found in cancer, can lead to α-KG in the cell then undergoing carboxylation reduction to form isocitrate, then converted to citrate to fuel metabolic functions.[442] Glutamine itself produces this α-ketoglutarate through the anaplerotic metabolism of glutamine, providing fuel to the TCA cycle through glutaminolysis, identified in the LNCaP pathway mapping.[426]

Similar levels of glutamine were observed in both cell lines with PNT1a having 13.5uM in the zero glucose, 95.6uM in the 5.5mM glucose and 31.5uM in the 11mM glucose. PC3 cells presented with 11.8uM in the zero, 48.3uM in the 5.5mM and 17.1uM in the 11mM glucose. PNT1a cells present with higher levels of glutamine in the presence of glucose, than that of the PC3 cells, with both showing increased concentrations of glutamine when treated with the novel TH compounds, especially in the zero glucose conditions. Conversely an existing study on PNT1a and PC3 cells have found increased levels of glutamine in the PC3 cell lines, however this study was only conducted in media glucose conditions.[442]

Metabolites linked to Warburg Metabolism were identified through the pathway mapping, where glutamine with lactic acid is implicated. Lactic Acid was identified in the PNT1a, PC3 and Du145 cells, with increased levels seen in the 11mM glucose TH6 treatments. Lactic acid has been linked to Warburg glycolysis by Otto Warburg, where

glucose is converted to lactic acid in the cytoplasm.[317,428,443–445] Lactic acidosis is often observed in late-stage metastatic prostate cancer patients, this involves accumulation of lactate and protons within the patient.[446–449] Acidosis favors metastasis, angiogenesis and immunosuppression, associated with poor patient prognosis.[446] Thus, the presence of lactic acid as a metabolite of significance is an indicator of Warburg glycolysis and an important marker or severe PCa disease.

Cysteine, carnosine, and proline are all amino acids linked to oxidative stress management.[450–452] Cysteine, carnosine and proline are scavengers of ROS, during oxidative stress.[450,451,453,454] Cystine, carnosine and proline were found in the PNT1a, LNCaP and PC3 cells. Cystine was increased in the untreated zero glucose LNCaP cells. It is well established that cancer cells have higher baseline level of ROS than normal cells and thus are more susceptible to oxidative stress mechanisms, thus cell in the presence of low glucose may be in the additional stress due to nutrient deprivation increasing the cystine present in the cells.[296,451] Heightened levels of cystine was also observed in the zero glucose PNT1a cells. these cells were treated with Menadione and Menadione conjugated compounds, so again the treatment may increase the requirement for ROS scavengers in the cell, inducing increased cystine, from cystine pools in the cells.[426,451] Carnosine was increased in the Menadione treated LNCaP cells in the zero glucose. PC3 cells in the 11mM glucose treated with TH6 also had increased concentrations of carnosine. Menadione is a known ROS generator, thus the increased carnosine observed may be linked to this increased endogenous ROS.[296,452,453] In the LNCaP and the PC3 cells, proline was increased in the 11mM Menadione treated cells, this again is perhaps due to the ROS scavenging capabilities of proline, cleaning up the excess ROS that would be produced by the treatment with Menadione.[294,295,297, 455]

Betaine was increased in the untreated PC3 cells in the zero glucose conditions, while methionine was not significant in the cell line. Methionine was increased in the PNT1a 11mM glucose TH6 treated cells. Again, both amino acids are linked to redox homeostasis in the cell and thus may be in higher concentrations to remove excess ROS produced by the novel compounds or regulate the high baseline levels established in cancer cells.[456] Most amino acids are known to be susceptible to oxidation by ROS and reactive nitrogen species (RNS) in the cell, with the amino acid methionine known to be particularly sensitive to this.[457] A study on the amino acid betaine in prostate cancer found it to suppress proliferation by increasing oxidative stress related apoptosis and

inflammation in Du145 cells.[458] The study found that oxidant status of the cells was increased with betaine treatment versus the control.[458] Betaine is a methyl donor on the synthesis of methionine.[459] Methionine is an essential amino acid in protein synthesis, one-carbon metabolism, sulfur metabolism, epigenetic modification, and redox maintenance in the cell.[427, 457]

Aspartate was found to be significant in the PNT1a cells with increased levels in the zero and 5.5mM glucose conditions. Aspartate is a nonessential amino acid found to supplements the TCA cycle with NAD+/NADH homeostasis.[456,460] It is linked in nucleotide biosynthesisand is important in cell proliferation when the electron transport chain is impaired.[456,460] The observed increase may be due to nutrient stress caused by the glucose deprivation in the zero glucose conditions. Perhaps impacting the electron transport chain resulting in overall mitochondrial dysfunction, with aspartate supporting energy production for the nutrient deprived cells.

Symmetric and asymmetric dimethylarginine (SDMA and ADMA) are methyl arginine derivatives, produced during hydrolytic protein turnover, with the degradation of methylated proteins.[457] ADMA was found to be increased in the PNT1a zero glucose untreated, and Menadione treated cells, while SDMA was increased in the 11mM glucose TH6 treated cells. In the PC3 cells, ADMA was also increased in the zero-glucose untreated, and Menadione treated cells, with high levels of SDMA in the 5.5mM untreated PC3 cells. The Du145 cells presented with the same trend, with high ADMA concentrations in the zero glucose untreated, and Menadione treated cells. ADMA has been found to be elevated in cancer patient plasma, with the cause of this elevation still not conclusive.[457] Increased ADMA found in prostate cancer cells (LNCaP and PC3 cell lines) is associated with reduced angiogenesis and metastasis, while in studies of other cancers, the increase ADMA is linked to increased metastasis.[461,462] ADMA is known to inhibit nitric oxide synthesis by competitive inhibition of nitric oxide synthase, while SDMA may impact nitric oxide production through the suppression of L-arginine.[463]

Phenylacetyl glycine was increased in the PNT1a cells treated with Menadione in zero glucose conditions and in the LNCaP cells in 11mM glucose conditions, treated with TH6. Studies have shown phenylacetylglycine to be increased in urine of PCa patients.[464] Increased phenylacetylglycine in urine has been linked to mitochondrial toxicity in drug induced phospholipidosis.[464] The increase in phenylacetylglycine was found to be an

indicator of mitochondrial dysfunction due to a metabolic switch to anaerobic metabolism or by the disruption to the urea cycle, with toxicity thought to be due to the impairment of the proton motor force and alteration of fatty acid catabolism.[464] Thus the lipid backbone of the TH6 compound may be linked to this increase in phenylacetylglycine in the LNCaP cells.

Histidine was found to be quite prevalent in the PNT1a cells. This may be from the supplementation of the cell medium with FBS, which would include histidine, as histidine is common in dietary animal products.[465,466] Histidine is an amino acid that cannot be made in the body and thus is required through nutritional supplementation.[467] It is important for its role in the active site of enzymes, protein synthesis and nitrogen balance.[466,467]

Tryptophan was increased in the PNT1a cells in the 5.5mM glucose, treated with TH4. An essential amino acid. Tryptophan metabolism has been shown to promote tumour progression, by the immunosuppressant environment caused throughout its mechanisms, such as triggering autophagy and inhibiting mTORC1 (mTOR complex 1, a regulator of growth and metabolism) in tumor cell lines *in vitro* [436] Tryptophan catabolism results in the in metabolites; kynurenine, and rate-limiting step enzymes in the kynurenine pathway, which are essential in immune cells survival.[427] Studies have noted that ratio of kynurenine to tryptophan is correlated with a PD-1 blockade resistance that is associated with poorer survival if increased in the cancer cells and has been reported in some tumour types.[427]

5 Biogenic amines were identified with significant alterations from the panel of metabolites examined. β-alanine and γ-aminobutyric acid present with significant changes within most of the cell lines. β-alanine was increased in the PNT1a cells in the zero glucose conditions treated with TH4. The same was seen in the PC3 cells in the zero glucose conditions treated with TH4, having increased concentrations of β-alanine. The non-essential amino acid β-alanine, is a known intracellular buffer and is metabolized into carnosine. Interestingly, diet supplementation with β-alanine has been linked to delayed lactate accumulation during exercise through its buffering abilities.[464] PNT1a cells present with higher concentrations of γ-aminobutyric acid in the Menadione treated cells in the zero glucose conditions. The same was seen in both the PC3 and the Du145 cells, with Menadione treated cells in zero glucose, presenting with increased γ-aminobutyric

acid. γ-Aminobutyric acid, has been known to increase proliferation and cellular invasiveness of prostate cancer, with γ-aminobutyric acid emerging as a tumor signaling molecule.[464] Studies have shown that γ-aminobutyric acid was increased in the prostates of cancer patients with metastasis, compared to that of patients without metastasis.[468]

The most common polyamines are putrescine, spermidine and spermine, which are major regulators of proliferation.[464] Spermidine, spermine and putrescine, are all implicated in the spermidine and spermine biosynthesis pathway. Spermine was increased in the zero glucose TH4 and the 11mM glucose TH6 treated PNT1a cells. Spermidine was increased in the zero glucose untreated and TH6 treated PNT1a cells. Putrescine was highest in the zero glucose untreated PNT1a cells. Putrescine was high in the untreated zero cells while spermidine was high in the TH6 treated zero glucose cells and the 5.5mM glucose untreated cells, in the PC3 cell line. Putrescine was present in the untreated Du145 cells in the zero glucose. The dysregulation of polyamine metabolism is seen in some cancers where the levels of spermidine, spermine and putrescine are increased, resulting in crosstalk between their metabolism and oncogenic pathways (mTOR and RAS pathways).[431,432,469]

Succinate was found to be increased in the PNT1a cells treated with Menadione in the 11mM glucose. Succinate is important in cellular metabolism as it is a link between the Krebs cycle and the mitochondrial respiratory chain, thus is important in mitochondrial metabolism.[436] PNT1a cells show a 50:50 split between oxphos and glycolysis, thus the increase in succinate may be utilised here to mediate this split metabolic preference.

Some ceramides of interest were identified to be increased in the PNT1a and PC3 treated cells. In the PNT1a cells, ceramides were increased with the TH treatments. Cer(d18:1/22:0) concentrations were found to be increased in the 11mM glucose PNT1a cells treated with TH6, while Cer(d18:2/20:0) was increased in the 5.5mM glucose cells treated with TH6. In the PC3 cells, Cer(d18:1/20:0(OH)) concentrations were increased in the Menadione treated cells in the 11mM glucose, with Cer(d18:1/26:1) concentrations increased in the 5.5mM glucose untreated cells. Cer(d18/2:20:0) was increased in the zero glucose TH6 treated PC3 cells. Ceramides are known to play a role in cellular invasion, metastasis, mitophagy and apoptosis in cancer cells, with cellular stress inducing the generation of ceramides to mediate these processes.[470,471] Cancer cells have been found to

subvert these processes through the dysregulation of enzymes in sphingolipid metabolism.[470] Ceramide with a carbon chain of 16 (C(16)-ceramide) are linked to proliferation, whereas C(18)-ceramides mediate cell death in cancer cells.[438] However, cancer cells have been shown to downregulate these pro cell death ceramides to support their proliferation and metastasis.[470] Cer(d18) are synthesized from serine and palmitate in a de novo pathway and are regarded as important cellular signals for inducing apoptosis.[472] Thus the presence of these ceramides in the treated PNT1a and PC3 cell lines, are likely indicators of apoptosis.

Overall, many alterations were identified across the metabolome of the prostate cell lines, with significance found in amino acids, biogenic amines, carboxylic acids and ceramides. Of greatest significance was the influx of ROS scavenging amino acids which would likely account for the modest increases of ROS observed, when the cells were treated with the TH compounds. Cancer cells are likely increasing their antioxidant capabilities to evade cell death by the TH treatments. The results achieved with the LCMS-MS analysis accounts for the ROS results achieved in Chapter 5.

Chapter 7. Overall Discussion

7.1 Overall Discussion

With PCa being one of the most prevalent cancers in males globally, developments in treatment and knowledge of the disease are vital to reduce burden on global healthcare systems, to improve patient care and overall health outcomes. Studies have shown PCa cells to hold an altered metabolic phenotype, with the early disease relying on OxPhos, the intermediate/late disease then switching to fatty acid oxidation and Warburg metabolism.[317,365] This work lends a hand to the TH strategy by setting a baseline understanding of the PCa metabolic processes which could be targeted for treatment. This work is a proof of concept and an early examination and design process of metabolic targeting compounds and shows promise for our TH strategy. In this study we aimed to examine early prototypes of the novel compounds. This work will pave the way for further improvements in the compound design to achieve a successful set of novel treatments, with improved selectivity, low cytotoxicity in the non-malignant cells and a high cytotoxicity in cancer cells, by targeting cancers unrelenting need for fuel. These types of early studies are vital in the drug discovery process, a long and laborious process, often with poor success outcomes. We are determined to design a set of successful novel TH compounds, comprised of a basic fuel molecule, conjugated to a non-toxic vitamin moity, to improve patient outcomes and their quality of life.

Our compounds are of a novel design, so the literature provided little insight into the success of this study, with reliance on existing work that examines the impacts of the native vitamins in cancer treatment and current knowledge of PCa metabolism, guiding the way through the experimental design. Our hypothesis of the TH compounds anticipated the malignant cells to have a higher uptake of the glucose conjugated TH compounds than that of Menadione, due to the well-established principle of Warburg's glycolysis requiring glucose 100 times faster than that of a non-malignant cell.[473,249,347] However as presented in Chapter 3, this was not the case. The concentrations of Menadione resulting cytotoxicity were in fact far lower than that of the TH compounds, although in some cases the SI was slightly improved. Menadione has been studied both in vitro and in vivo to examine its anticancer effects alone and in combination with conventional cancer therapies. These studies have shown some benefits and high tolerance (in *vivo*). For the TH compounds, two methods of conjugation were used for the attachment of Menadione to the metabolic moity (sugar or lipid). With the aim to improve the selective cytotoxicity of the compounds in the cancer cells versus the normal cells.

From this, the best cytotoxicity and selectivity was determined in the TH4 and TH6 compounds, but unfortunately still yielding low SI values. Of the glucose-Menadione compounds, TH4 resulted in greater SI than that of TH1 across the cell lines and the glucose conditions. These compounds differed only by their conjugation group, where TH1 is comprised of an amine linker group, and TH4 of an aryl linker chain. The differing chemistry of these compounds allowed for TH4 to show greater selectivity towards the metastatic cells than that of the non-malignant cell, indicating the importance of examining not only the active elements of the compounds (the Menadione and the glucose), but the efficacy of the linker groups also. With the method of compound synthesis being that of click chemistry, limits are placed on the linker group composition, possibly implying the need for using other methods of compound conjugation, even with the known and aforementioned benefits of click chemistry in therapeutic synthesis. Overall, the highest SI determined was 2.0 with the TH6 treatment in the metastatic Du145 cells. In the development of new cancer therapeutics, a high SI is required to be deemed suitable for therapeutic efficacy, the standard SI must be 10.0 and higher to be deemed safe for use in *vivo*.[353] With the SI values achieved for the TH compounds examined in this study, further development is required to achieve higher SI values, which would be optimal for future in *vivo* work safety. With Menadiones success in existing studies, alterations to the linker group and the metabolic substrate used may improve the overall selectivity of the compounds.

Mannose has shown success in disrupting the proliferation and progression of metastatic cancer, where mannose is shown to impact tumours through the suppression of cellular metabolism and enhancing the efficacy of some chemotherapeutic agents.[474] Mannose is transported by the glucose transporters but accumulates in the cell as mannose-6-phosphate, which has been shown to impair metabolic processes such as glycolysis, the TCA cycle, the pentose phosphate pathway and glycan synthesis.[475] Coupling mannose to the Menadione instead of glucose with the more effective aryl linker group, may improve the anticancer mechanisms of the TH compounds by adding an additional threat to the cancer cells. For example, in triple negative breast cancer (TNBC) with resistance to immunotherapy and radiotherapy, D-mannose was found to promote the degradation of PD-L1 and improved immunotherapy and radiotherapy outcomes in patients.[476] Mannose has been successful in *vitro* and in mouse models, with truncated tumour growth shown in many cancer types.[475] In the animal models, oral

administration of mannose improved the therapeutic action of conventional chemotherapies without affecting the animal's overall heath.[475] The existing literature would highlight mannose as a substate of interest for the further examinations of the composition of the TH compounds.

The efficacy of 6-azidohexanoic acid as a fatty acid substrate could be improved with, the use of biologically relevant fatty acids. 6-azidohexanoic acid is useful in the synthesis of chemical probes, and other bioconjugation strategies. However, its biological relevance otherwise is unknown.[353] The use of fatty acids such as pyruvate may be a more biologically viable substrate and improve cellular response to the novel compounds. Pyruvate plays an essential role in cellular metabolism, being a product of glycolysis. It is used as a fuel source in the mitochondria for the TCA cycle and carbon flux for ATP production. Thus, the conjugating menadione to this biologically relevant fatty acid, may improve the SI and cytotoxicity of the fatty acid-Menadione TH compounds.

Treatment resistance in cancer is an issue, with many studies currently investigating ways to evade cellular mechanisms of resistance. The plasticity of cancer cells plays a huge role in this method of evasion, where cancer cells can shift to a differentiated state, with limited tumorigenic potential which aids their continued growth and proliferation.[384,477] This study aimed to target this plasticity in cancer cells with a treatment that would target multiple aspects of cancer cell biology, through targeting the Warburg effect, and ultimately triggering redox related cell death through the infiltration of menadione into the cell. Some efforts have aimed to target the metastatic process of the cell through glycoconjugation of natural substrates and known chemotherapies but remain unsuccessful to date.[351,352] With this we wanted to establish the effect of glucose on the cell lines to determine if a varied glucose milieu could in fact alter the metabolism and in turn if the metastatic potential of the cells could be changed with our TH targeting event.

The basal bioenergetic evaluation of the cell lines is very important finding throughout this study. The metabolic phenotype of the cell lines under the varied glucose conditions demonstrates the impact of the nutrient environment on in *vitro* culturing of cell lines. This work has highlighted the impact of the range of glucose concentration on the biochemistry of the cells before treatment and how this may impact overall experimental results. From the results obtained in Chapter 4, one would expect that with the changes in metabolic status of the cells that the metastatic potential of the cells may

be altered. The prostate cells behave differently when placed in media of different glucose concentrations significantly altering their metabolic dependencies, with all the cells relying on OxPhos when in zero glucose with all of the cells increasing glycolysis in a glucose dependent manner. This could result in alterations to other aspects of the in *vitro* model, where some changes were seen in the metabolite expression, ROS production and MMP between the prostate cells in the different glucose conditions, highlighting the importance of the nutritional cellular environment on experimental outcomes. Most studies conduct their experiments under "normal" media glucose, which can range from zero to 11mM glucose and higher with supplementation. Thus, it may be important to consider the glucose conditions in which work is undertaken and how that may impact experimental outcomes. Moreover, this work has highlighted the inherent need of the metastatic androgen independent PCa cells to maintain even low levels of Warburg glycolysis for their ATP production, showing that even under glucose starvation the metastatic androgen independent disease cannot shut off the Warburg effect. This appears to be ingrained in their biology and is a very important finding. Warburg glycolysis is linked to poor prognosis and advanced disease in many cancers.[317] In addition, acidosis in PCa patients is linked to increased lactic acid from Warburg glycolysis and is frequently observed in the late-stage metastatic disease, with a correlation to poor prognosis.[447,449] Thus the presence of lactic acid from the Warburg effect is an important marker or severe PCa disease and will impact metabolic based therapeutic approaches.[446]

We postulated that treatment with the TH compounds may result in a metabolic switching event within the PCa cells, reversing Warburg metabolism by collapsing their glycolytic abilities, regressing the disease. This was not observed in the TH treated cells in this study, however it became very clear that the androgen independent metastatic PCa cells remain switched on to the Warburg effect, even after nutrient deprivation and the novel treatments, highlighting the importance of the Warburg effect in PCa. Pertega-Gomes et al have described the metabolic heterogeneity of PCa and its clinical relevance, while illustrating that the advanced stages of prostate cancer, both in *vitro*, and in *vivo* present with an increased glycolytic phenotype, and how it is linked to poorer patient prognosis.[387] Their work showed increase glucose consumption in PC3 cells along with increased OCR and ECAR overall highlighting their metabolic plasticity.[387] Metabolites linked to Warburg metabolism in our work was identified through pathway mapping of the metabolites determined in the androgen independent metastatic PCa PC3 and Du145

cells, where glutamine with lactic acid is implicated. Increased lactic acid is an indicator of Warburg glycolysis [317,428,443–445] The metabolic phenotypes of the PC3 and the Du145 cells display a preferential use of glycolysis for ATP production in the presence of 5.5mM and 11mM glucose conditions, this finding was supported by the levels of lactic acid determined in the cell lines. Increases were observed in the TH treatments in the presence of glucose, however the cells showed low reliance on glycolysis in the zero glucose conditions. The LNCaP cells showed negligible reliance on glycolysis across the glucose milieu, with its predominant OxPhos phenotype. As aforementioned, in other works, LNCaP has been found to have a strong reliance on OxPhos, where this work has highlighted that even under a varied nutrient environment, this remains. All these findings lead to questioning if the Warburg phenotype could be reversed and the androgen independent cells could be returned to the same metabolic programming as the androgen dependent LNCaP cells, it may be possible to prevent treatment resistance in PCa disease.

Although no significant changes were observed in the metabolic phenotypes of the cells when treated with the vitamins or the TH compounds, alterations were observed in the mitochondrial bioenergetics. The cells treated with the novel compounds across the glucose conditions presented at times with increased proton leak, maximal respiration, basal OCR, and non-mitochondrial respiration all linked to alterations in the mitochondria and possible mitochondrial dysfunction. Mitochondrial health was further examined through the MMP and mitochondrial depolarisation. The link between mitochondrial bioenergetics and MMP are noted frequently in the literature, with increased mitochondrial depolarisation and a sustained shift in MMP indicating mitochondrial dysfunction overall impacting OxPhos in the mitochondria, then impacting the cells OCR. A decrease in mitochondrial depolarisation was not found in any of the cell lines in the study, however alterations in MMP was found in the cells treated with menadione and TH6. Although, the androgen independent metastatic disease (Du145 cells) did not present with any alterations to their MMP or mitochondrial depolarisation. However, the alterations that were observed in the mitochondrial bioenergetics were anticipated to likely be due to heightened ROS levels in the cells due to the treatment with the novel compounds.[309]

We posited that the mitochondrial dysfunction seen in the bioenergetic profiles of the cell lines was due to an increase in endogenous ROS due to the proposed mechanism of cell death through oxidative stress by the Menadione in the TH compounds.

Menadione is thought to result in a decrease in oncogenic superoxide leading to apoptosis through the generation of onco-suppressive hydroperoxides and cytotoxic hydroxyl radicals.[295,297] ROS scavengers and antioxidants quench ROS, decreasing the oxidative stress capabilities of Menadione overall reducing its anticancer effects.[305,307–309] However, if high enough concentrations of Menadione are achieved, the capability of antioxidant enzymes to eliminate ROS is exceeded and results in redox related death.[305,307–309] The ROS determination of the cells was unexpected, with little increases in ROS observed in both the %gated and the %MFI of the cancer cells treated with Menadione and the TH compounds. In the continuation of the study, the metabolomics of the cell lines expressed increased levels of ROS scavenging amino acids in the cells treated with the novel compounds. Cysteine, carnosine, and proline are all amino acids linked to oxidative stress management and are known ROS scavengers increased in times of oxidative stress.[450–452] The three amino acids were found in the PNT1a, LNCaP and PC3 cells treated with the novel compounds, which may account for the lack of ROS determined through the Oxyburst assay by flowcytometry. Betaine and Methionine are also implicated in redox homeostasis, the influx in these amino acids may remove excess ROS produced by the TH compounds. The metabolomic evaluation of the cell lines tied all the pieces together giving light as to why high levels of ROS was not observed in the cells treated with Menadione and the TH compounds. The amino acids are creating a dynamic balance between the ROS produced by the compounds and the cell's ability to produce ROS scavenging molecules to maintain ROS homeostasis, illustrated in Figure 7.1 below. Surprisingly, we did still observe metabolic alterations in the cells through the cellular bioenergetics even with ROS scavenging observed which may be an effort by the cells to alter their metabolism to increase amino acid production as a protective effect against ROS.

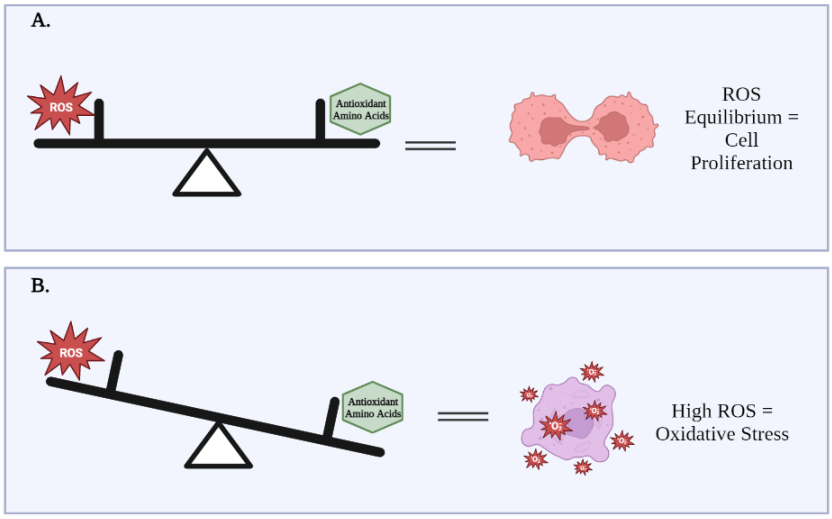

Figure 7. 1: Redox Equilibrium: (A) As seen in this study, increased levels of ROS produced by the Menadione and TH compounds is balanced out by the influx of antioxidant amino acids produced by the mitochondria, allowing for cells to continue to grow and proliferate. (B) What we aim to achieve, to increase the levels of endogenous ROS to overthrow the ROS scavenging mechanisms of the mitochondria resulting in oxidative stress and cell death. Images created in Biorender online.

From this, the metabolic reprogramming of the disease back to its earlier disease phase may be possible with therapeutic intervention, however there are many biological modulators that must be considered. Regulators of the cellular homeostasis, nutrient sensing, and metabolic homeostasis may play a role in the metabolic outcomes of the metastatic cells, with growing interest in the implications of the endosomal, lysosomal pathways on the metastatic journey and metabolic programming of cancer cells.[478] The regulation of the glucose transporter, GLUT4 trafficking is an examples of endosomal metabolic regulation. Cellular glucose uptake is mediated in part by the insulin-dependent recruitment of GLUT4 from the intracellular storage vesicles.[479] Once internalized by the cell, GLUT4 moves through the endosomal system where Rab proteins such as Rab 4 and Rab 5. Rab 4 is responsible for the transport of cellular cargo from the early endosomes to the recycling endosomes, whereas Rab 5 plays a role in the regulation of early endocytosis where it employs its effectors to early endosomes to orchestrate the transport of endosomes.[480] Rab 5 has been shown to impact the membrane receptor internalisation, trafficking, and related signalling pathways of a cell, highlighting how the endosomal system may impact the metabolome of the cell through its glucose uptake regulation through GLUT4.[480] Mutations in endosomal genes have also been found in metabolic diseases like diabetes, highlighting the impacts of the endosomal system on disease pathology.[478] From these findings one could hypothesise that the glucose milieu examined and the TH compounds may impact the cells endosomal system and their metabolic outcome, leading one to propose if the endosomal lysosomal system could be targeted for therapeutic action or used to determine disease severity.

Amino acid metabolism was found to be altered in the TH treated cells with the influx in antioxidant amino acids observed. Studies have linked androgen in activating amino acid metabolism in PCa, and while we observed no alterations in the basal AR expression of the cells across the glucose milieu, it may be worth investigating if treatment would alter the AR expression in the cell lines, which may assist in the metabolic alterations of the cell lines.[442,481] Putluri et al found an influx in pathways associated with amino acid metabolism in androgen treated PCa cells, implicating the possible role of androgen signalling in metabolic regulation.[481] Again, with an interest in reversing the androgen independent metastatic phenotype by perturbing the Warburg effect, may also impact the androgen status of the cancer. Many chemotherapeutics of

PCa target androgen, thus it's reasonable to consider that this phenotype reversal would have huge implications on the clinical outcomes of currently untreatable PCa patients.[478]

Interestingly throughout this study, PC3 cells have shown themselves to be the most resilient of the PCa cell lines, with very high levels of novel compounds required for cell death, as determined in Chapter 3, along with their capabilities to adapt to the zero glucose conditions with ease with high levels of ATP production still found even when under nutritional stress. This may play a role in the results observed, with the PC3 cancer model allowing for any limitations of the novel compounds to be observed and allowing for further work to be conducted in the compound design, to improve the mechanism of action as well as the uptake of the novel compounds. Existing studies on the PC3 cell line, have established its similarity to clinical CRPC and highlights its suitability as a model of the intermediate androgen-independent disease.[252,482,483] PC3 in the presence of 11mM glucose showed increased ROS, when treated with TH4. This is encouraging as the IC_{50} values required for cell kill in PC3 was far higher than that of the other cell lines, seen in Table 3.31 of Chapter 3. This perhaps indicates that the levels of TH compounds required to cause an increase in ROS production is far higher than previously thought. Additionally, increased levels of ROS scavenging amino acids were observed in the PC3 cells treated with the TH compounds, which may account for the lower levels of ROS observed than we had proposed.

Our work identifies that the Warburg effect cannot be easily perturbed in androgen independent cells, which leads to the question if the metabolic status of the cells impacts the cells metastatic levels and if the novel compounds can push the cells back to an earlier metastatic metabolic phenotype, resulting in easier disease treatment. Perhaps the cancer cells metastatic journey is highly precarious where nutrients like glucose and maybe even oxygen in the bloodstream may alter the cell's metastasis, leading one to consider the impacts of hypoxia and if the cells can learn to survive without these vital nutritional substrates. Ultimately, if the PCa disease phenotype can be reversed with future iterations of these compounds, it would be incredibly important for patient outcomes and further reduce the burden of untreatable disease on our health care system. The impacts of cancer research on the patient is paramount, with endless studies eager to improve the life of people suffering with the disease. Throughout this study and through my personal experiences with cancer during this project, the importance of the patient has

become my principal driver to ensure my work is my best, with my hope that my research can one day help improve the life of even one person with cancer.

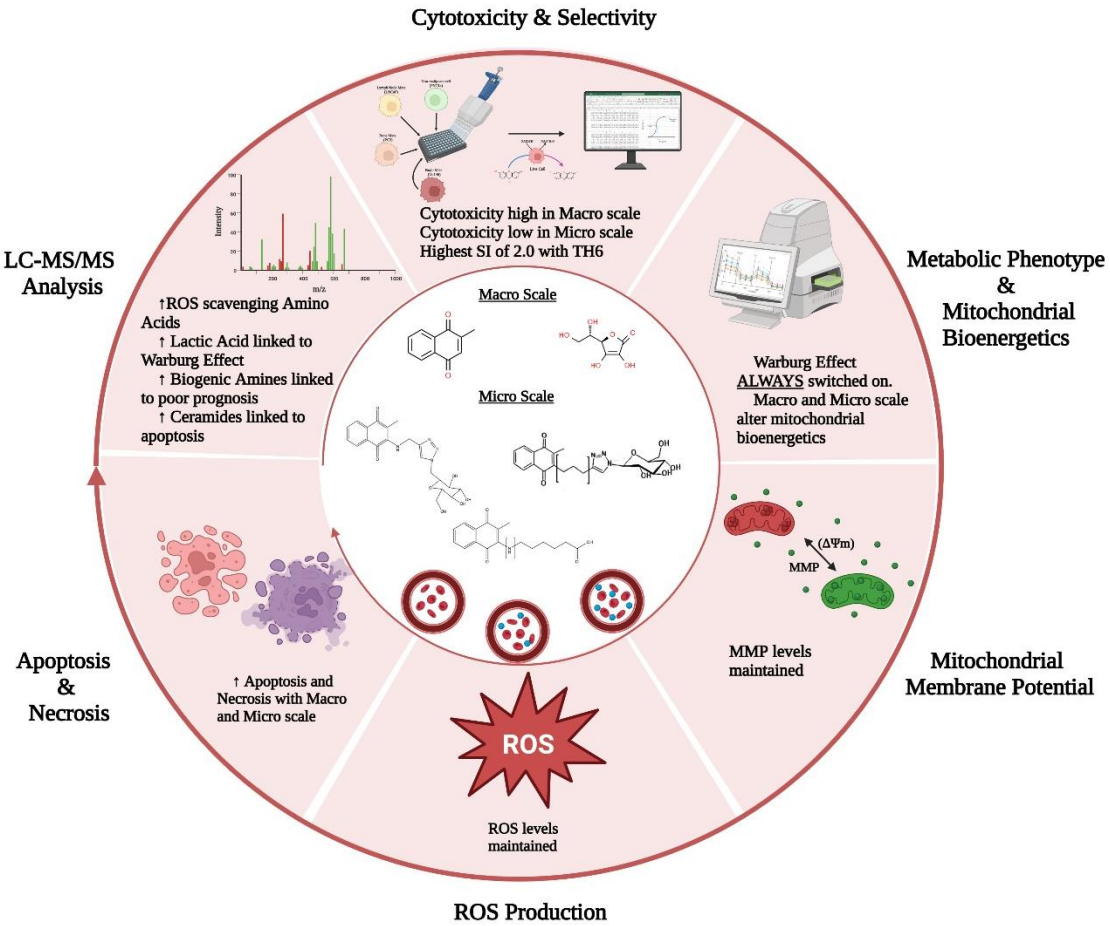

Figure 7. 2: Summary of Results : the panel of prostate non-malignant (PNT1a) and PCa (LNCaP, PC3 and Du145) cells were used to represent the different stages of PCa disease. The cells were evaluated under a varying glucose milieu and treated with menadione, Vitamin C and novel TH compounds. TH6 showed the greatest cytotoxic selectivity of the TH compound, even presenting with a higher SI than Menadione in some cases. The Warburg effect appear to not be quenched even in the zero glucose conditions and when treated with the TH compounds in the androgen independent cells (PC3 and Du145), although alteration in mitochondrial bioenergetics was apparent in the prostate cells treated with the TH compounds. Alterations in MMP were not significant in the TH treated cells, nor was ROS however increased apoptosis and necrosis was observed in the treatment groups. Finally, the LCMSMS analysis showed an increase in ROS scavenging amino acids such as proline and carnosine in the TH and Menadione treated cells, which may account for the small alterations observed in ROS expression. Images created in Biorender online.

7.2 Future Directions:

The work in this study shows promise for the TH strategy, will cell death observed in the cells treated with the TH compounds. As discussed, alterations to the metabolic substrates used in the TH compounds to the likes of mannose and pyruvate may increase the selectivity of the novel compounds which may overall improve the technique. Since the effect of the nutrient environment has been examined in this work the effect of hypoxia is of interest. Hypoxia is known to affect the metabolism of cancer with oxygen deprivation often found in the tumour core. As we have determined the effect of the nutrient glucose on the cell, the effect of varying oxygen concentrations may also be enlightening.

Determining the glucose uptake in the cell lines across the glucose milieu and how this would affect the uptake of the TH compounds would certainly add to the study. Establishing if the compounds are in fact up taken by GLUT in the cells would also be helpful with imaging of this uptake of the glucose compounds, which would require fluorescent tagging of the novel compounds. Further on with this GLUT uptake, the emergence of the endosomal system in the regulation of GLUT (especially GLUT4) may pose an interest in evaluating the effects of the glucose milieu and the TH compounds on the endosomal system in the cell, if the novel compounds are in fact up taken by GLUT. Aside from glucose, fatty acid metabolism is important in PCa thus evaluating the basal fatty acid metabolism of the cells and if this would be altered by the TH treatment is emerging of interest, as existing in *vivo* studies have shown metastatic PCa to hold a large reliance on fatty acid metabolism for energy production throughout their metastatic progression. Overall, further examinations into the effects of the nutrient cellular environment and the TH compounds uptake mechanism would be of interest in the future of this work.

Examining the effect of the glucose milieu and of the novel compounds on cell invasion and migration would inform further as to the effectiveness of the novel compounds and how the cells behave across the glucose conditions. Due to the similarities observed in the PC3 and Du145 cell lines metabolic bioenergetic profiles, this further investigation may enlighten the difference in aggressiveness of the two cell lines which may further inform which cell line a better model for use in cell line based investigations.

Further evaluation of the ROS scavengers, glutathione and superoxide dismutase would allow for further understanding of the ROS results achieved with the compounds, along with the use of more specific ROS determination experiments. We believe this TH strategy to have great potential in causing selective redox related cell death in the cancer cells.

Finally, once TH compounds with greater SI values are established, this work could be continued in other cancer types with further expansion into organoids, orthotopic cancer models and maybe even animal work in the future.

7.3 Conclusions:

In conclusion, we achieved or aim of delivering a set of novel TH compounds that combined fuel substrates to vitamin moieties in the hopes of targeting PCa metabolism. Overall cytotoxicity was achieved with the compound treatments in the panel of prostate cell lines, but low selectivity was achieved. The compounds were found to impact the mitochondria, through alterations in OCR, proton leak, maximal and non-mitochondrial respiration of the cells along with alterations to MMP and increased levels of apoptosis and necrosis observed, but with little significance found in the cellular ROS production. To end, the LCMS-MS analysis of the cells tied the study together with increased ROS scavenging amino acids, present in the TH treated cells indicating that the lack of endogenous ROS observed may in fact be as a result of this influx of amino acids to counteract the effects of the increase ROS. To add to these findings, we also observed in the androgen independent metastatic PCa cell lines, hold a fundamental reliance on Warburg glycolysis for ATP production that cannot be easily quenched. Furthering the understanding of PCa disease metabolism and biology will improve future work in overcoming cancers resistance to treatment. Overall, the findings indicate that the TH compounds play a role in targeting the different niches of PCa metabolism and the mitochondria.

Chapter 8. Bibliography

1. Bray F, Ferlay J, Soerjomataram I, Siegel RL, Torre LA, Jemal A. Global cancer statistics 2018: GLOBOCAN estimates of incidence and mortality worldwide for 36 cancers in 185 countries. *CA Cancer J Clin*. 2018. doi:10.3322/caac.21492

2. Rawla P. Epidemiology of Prostate Cancer. *World J Oncol*. 2019;10(2):63-89. doi:10.14740/wjon1191

3. Pernar CH, Ebot EM, Wilson KM, Mucci LA. The Epidemiology of Prostate Cancer. *Cold Spring Harb Perspect Med*. 2018. doi:10.1101/cshperspect.a030361

4. Patel AR, Klein EA. Risk factors for prostate cancer. *Nat Clin Pract Urol*. 2009. doi:10.1038/ncpuro1290

5. National Cancer Registry Ireland. *Cancer Factsheet Prostate*. Dublin; 2018. https://www.ncri.ie/sites/ncri/files/factsheets/Factsheet prostate.pdf.

6. Perdana NR, Mochtar CA, Umbas R, Hamid ARA. The Risk Factors of Prostate Cancer and Its Prevention: A Literature Review. *Acta Med Indones*. 2016.

7. O'Connell F, O'Sullivan J. Help or hindrance: The obesity paradox in cancer treatment response. *Cancer Lett*. 2021;522. doi:10.1016/j.canlet.2021.09.021

8. Divella R, De Luca R, Abbate I, Naglieri E, Daniele A. Obesity and cancer: The role of adipose tissue and adipo-cytokines-induced chronic inflammation. *J Cancer*. 2016. doi:10.7150/jca.16884

9. De Pergola G, Silvestris F. Obesity as a major risk factor for cancer. *J Obes*. 2013. doi:10.1155/2013/291546

10. Fujita K, Hayashi T, Matsushita M, Uemura M, Nonomura N. Obesity, inflammation, and prostate cancer. *J Clin Med*. 2019;8(2). doi:10.3390/jcm8020201

11. Adesunloye BA. Mechanistic insights into the link between obesity and prostate cancer. *Int J Mol Sci*. 2021;22(8). doi:10.3390/ijms22083935

12. Wilson RL, Taaffe DR, Newton RU, Hart NH, Lyons-Wall P, Galvão DA. Obesity and prostate cancer: A narrative review. *Crit Rev Oncol Hematol*. 2022;169. doi:10.1016/j.critrevonc.2021.103543

13. Egan AM, Dinneen SF. What is diabetes? *Med (United Kingdom)*. 2022;50(10). doi:10.1016/j.mpmed.2022.07.001

14. Zhu D, Toker M, Shyr W, Fram E, Watts KL, Agalliu I. Association of Obesity and Diabetes With Prostate Cancer Risk Groups in a Multiethnic Population. *Clin Genitourin Cancer*. 2022;20(3). doi:10.1016/j.clgc.2022.01.016

15. Leitzmann MF, Ahn J, Albanes D, et al. Diabetes mellitus and prostate cancer risk in the Prostate, Lung, Colorectal, and Ovarian Cancer Screening Trial. *Cancer Causes Control*. 2008;19(10). doi:10.1007/s10552-008-9198-6

16. Miller EA, Pinsky PF. Examining the relationship between diabetes and prostate cancer through changes in screening guidelines. *Cancer Causes Control*. 2020;31(12). doi:10.1007/s10552-020-01347-4

17. Di Sebastiano KM, Pinthus JH, Duivenvoorden WCM, Mourtzakis M. Glucose impairments and insulin resistance in prostate cancer: the role of obesity, nutrition and exercise. *Obes Rev*. 2018;19(7). doi:10.1111/obr.12674

18. Hsing AW, Sakoda LC, Chua SC. Obesity, metabolic syndrome, and prostate cancer. In: *American Journal of Clinical Nutrition*. ; 2007. doi:10.1093/ajcn/86.3.843s

19. Pérez-Hernández AI, Catalán V, Gómez-Ambrosi J, Rodríguez A, Frühbeck G. Mechanisms linking excess adiposity and carcinogenesis promotion. *Front Endocrinol (Lausanne)*. 2014;5(MAY). doi:10.3389/fendo.2014.00065

20. özçelik melike. Impact of Diabetes on Clinical Outcomes of Prostate Cancer. *Eurasian J Med Adv*. 2022. doi:10.14744/ejma.2022.72792

21. Lee J, Giovannucci E, Jeon JY. Diabetes and mortality in patients with prostate cancer: a meta-analysis. *Springerplus*. 2016;5(1). doi:10.1186/s40064-016-3233-y

22. Buschemeyer WC, Freedland SJ. Obesity and Prostate Cancer: Epidemiology and Clinical Implications{A figure is presented}. *Eur Urol*. 2007. doi:10.1016/j.eururo.2007.04.069

23. Nelles JL, Hu WY, Prins GS. Estrogen action and prostate cancer. *Expert Rev Endocrinol Metab*. 2011;6(3). doi:10.1586/eem.11.20

24. Bosland MC. The role of estrogens in prostate carcinogenesis: a rationale for chemoprevention. *Rev Urol*. 2005;7 Suppl 3.

25. Dobbs RW, Malhotra NR, Greenwald DT, Wang AY, Prins GS, Abern MR.

Estrogens and prostate cancer. *Prostate Cancer Prostatic Dis*. 2019;22(2). doi:10.1038/s41391-018-0081-6

26. Härkönen PL, Mäkelä SI. Role of estrogens in development of prostate cancer. *J Steroid Biochem Mol Biol*. 2004;92(4). doi:10.1016/j.jsbmb.2004.10.016

27. Leitzmann MF, Rohrmann S. Risk factors for the onset of prostatic cancer: Age, location, and behavioral correlates. *Clin Epidemiol*. 2012. doi:10.2147/CLEP.S16747

28. Mistry T, Digby JE, Desai KM, Randeva HS. Obesity and Prostate Cancer: A Role for Adipokines. *Eur Urol*. 2007. doi:10.1016/j.eururo.2007.03.054

29. Baillargeon J, Rose DP. Obesity, adipokines, and prostate cancer (review). *Int J Oncol*. 2006. doi:10.3892/ijo.28.3.737

30. Olson OC, Quail DF, Joyce JA. Obesity and the tumor microenvironment. *Science (80-)*. 2017. doi:10.1126/science.aao5801

31. Wang M, Zhao J, Zhang L, et al. Role of tumor microenvironment in tumorigenesis. *J Cancer*. 2017. doi:10.7150/jca.17648

32. Kuhajda FP. Fatty Acid Metabolism and Cancer. In: *Encyclopedia of Biological Chemistry: Second Edition*. ; 2013. doi:10.1016/B978-0-12-378630-2.00037-2

33. Moore SC, Leitzmann MF, Albanes D, et al. Adipokine genes and prostate cancer risk. *Int J Cancer*. 2009;124(4). doi:10.1002/ijc.24043

34. Baillargeon J, Rose DP. Obesity, adipokines, and prostate cancer (review). *Int J Oncol*. 2006;28(3). doi:10.3892/ijo.28.3.737

35. Gann PH, Hennekens CH, Ma J, Longcope C, Stampfer MJ. Prospective study of sex hormone levels and risk of prostate cancer. *J Natl Cancer Inst*. 1996;88(16). doi:10.1093/jnci/88.16.1118

36. Diaz-Arjonilla M, Schwarcz M, Swerdloff RS, Wang C. Obesity, low testosterone levels and erectile dysfunction. *Int J Impot Res*. 2009;21(2). doi:10.1038/ijir.2008.42

37. Ma Y, Liang D, Liu J, et al. SHBG Is an Important Factor in Stemness Induction of Cells by DHT In Vitro and Associated with Poor Clinical Features of Prostate Carcinomas. *PLoS One*. 2013;8(7). doi:10.1371/journal.pone.0070558

38. Håheim LL. Metabolic syndrome and prostate cancer. *Expert Rev Endocrinol Metab*. 2007. doi:10.1586/17446651.2.5.633

39. Allott EH, Masko EM, Freedland SJ. Obesity and prostate cancer: Weighing the evidence. *Eur Urol*. 2013. doi:10.1016/j.eururo.2012.11.013

40. The Gobal Cancer Organisation. *Prostate:GLOBCAN 2018*.; 2018. https://gco.iarc.fr/today/data/factsheets/cancers/27-Prostate-fact-sheet.pdf.

41. Brawley OW, Knopf K, Thompson I. The epidemiology of prostate cancer Part II: The risk factors. *Semin Urol Oncol*. 1998.

42. Attard G, Parker C, Eeles RA, et al. Prostate cancer. *Lancet*. 2016. doi:10.1016/S0140-6736(14)61947-4

43. Xu J, Meyers D, Freije D, et al. Evidence for a prostate cancer susceptibility locus on the X chromosome. *Nat Genet*. 1998;20(2). doi:10.1038/2477

44. Schrijvers D. Androgen-independent prostate cancer. *Prostate Cancer*. 2007. doi:10.1200/jco.2003.05.117

45. Loeb S, Partin AW. Single nucleotide polymorphisms and prostate cancer susceptibility. *Rev Urol*. 2008;10(4):304-305. https://pubmed.ncbi.nlm.nih.gov/19145275.

46. Cao SY, Zhou CH, Wang JY, et al. Association between single nucleotide poymorphisms on chromosome 17q and prostate cancer in chinese population. *Chin J Cancer*. 2011;30(10). doi:10.5732/cjc.011.10070

47. Kenfield SA, Stampfer MJ, Chan JM, Giovannucci E. Smoking and prostate cancer survival and recurrence. *JAMA - J Am Med Assoc*. 2011. doi:10.1001/jama.2011.879

48. Ecke TH, Schlechte HH, Schiemenz K, et al. TP53 gene mutations in prostate cancer progression. In: *Anticancer Research*. Vol 30. ; 2010.

49. Ittmann M. Anatomy and histology of the human and murine prostate. *Cold Spring Harb Perspect Med*. 2018. doi:10.1101/cshperspect.a030346

50. Tyekucheva S, Bowden M, Bango C, et al. Stromal and epithelial transcriptional map of initiation progression and metastatic potential of human prostate cancer. *Nat Commun*. 2017. doi:10.1038/s41467-017-00460-4

51. Heidenreich A, Aus G, Bolla M, et al. EAU Guidelines on Prostate Cancer. *Eur Urol*. 2008. doi:10.1016/j.eururo.2007.09.002

52. Bladou F, Fogaing C, Levental M, Aronson S, Alameldin M, Anidjar M. Transrectal ultrasound-guided biopsy for prostate cancer detection: Systematic and/or magnetic-resonance imaging-targeted. *Can Urol Assoc J*. 2017;11(9). doi:10.5489/cuaj.4308

53. Heidenreich A, Bastian PJ, Bellmunt J, et al. EAU guidelines on prostate cancer. Part II: Treatment of advanced, relapsing, and castration-resistant prostate cancer. *Eur Urol*. 2014. doi:10.1016/j.eururo.2013.11.002

54. Nelson AW, Shah N. Prostate cancer. *Surg (United Kingdom)*. 2019. doi:10.1016/j.mpsur.2019.07.006

55. Gleason DF. Histologic grading and clinical staging of prostatic carcinom. *Urol Pathol prostate , M Tann Ed Philadelphia, PA Lea Febiger*. 1977.

56. Chan TY. World Health Organization classification of tumours: Pathology & genetics of tumours of the urinary system and male genital organs. *Urology*. 2005. doi:10.1016/j.urology.2004.09.048

57. Chen N, Zhou Q. The evolving gleason grading system. *Chinese J Cancer Res*. 2016. doi:10.3978/j.issn.1000-9604.2016.02.04

58. Humphrey PA, Moch H, Cubilla AL, Ulbright TM, Reuter VE. The 2016 WHO Classification of Tumours of the Urinary System and Male Genital Organs—Part B: Prostate and Bladder Tumours. *Eur Urol*. 2016. doi:10.1016/j.eururo.2016.02.028

59. Gordetsky J, Epstein J. Grading of prostatic adenocarcinoma: Current state and prognostic implications. *Diagn Pathol*. 2016. doi:10.1186/s13000-016-0478-2

60. Al-Maghrabi JA, Bakshi NA, Farsi HMA. Gleason grading of prostate cancer in needle core biopsies: A comparison of general and urologic pathologists. *Ann Saudi Med*. 2013. doi:10.5144/0256-4947.2013.40

61. Heidenreich A, Aus G, Bolla M, et al. EAU Guidelines on Prostate Cancer. *Eur Urol*. 2008. doi:10.1016/j.eururo.2007.09.002

62. Hayes JH, Ollendorf DA, Pearson SD, et al. Active surveillance compared with initial treatment for men with low-risk prostate cancer: A decision analysis. *JAMA -*

J Am Med Assoc. 2010. doi:10.1001/jama.2010.1720

63. Chen RC, Bryan Rumble R, Andrew Loblaw D, et al. Active surveillance for the management of localized prostate cancer (Cancer Care Ontario guideline): American society of clinical oncology clinical practice guideline endorsement. *J Clin Oncol*. 2016. doi:10.1200/JCO.2015.65.7759

64. Schoots IG, Petrides N, Giganti F, et al. Magnetic resonance imaging in active surveillance of prostate cancer: A systematic review. *Eur Urol*. 2015. doi:10.1016/j.eururo.2014.10.050

65. Romero-Otero J, García-Gómez B, Duarte-Ojeda JM, et al. Active surveillance for prostate cancer. *Int J Urol*. 2016. doi:10.1111/iju.13016

66. Klotz L, Vesprini D, Sethukavalan P, et al. Long-term follow-up of a large active surveillance cohort of patients with prostate cancer. *J Clin Oncol*. 2015. doi:10.1200/JCO.2014.55.1192

67. Dall'Era MA, Albertsen PC, Bangma C, et al. Active surveillance for prostate cancer: A systematic review of the literature. *Eur Urol*. 2012. doi:10.1016/j.eururo.2012.05.072

68. Donovan JL, Hamdy FC, Lane JA, et al. Patient-reported outcomes after monitoring, surgery, or radiotherapy for prostate cancer. *N Engl J Med*. 2016. doi:10.1056/NEJMoa1606221

69. Ghilezan M, Yan D, Martinez A. Adaptive Radiation Therapy for Prostate Cancer. *Semin Radiat Oncol*. 2010. doi:10.1016/j.semradonc.2009.11.007

70. Jones CU, Hunt D, McGowan DG, et al. Radiotherapy and short-term androgen deprivation for localized prostate cancer. *N Engl J Med*. 2011. doi:10.1056/NEJMoa1012348

71. Parker CC, James ND, Brawley CD, et al. Radiotherapy to the primary tumour for newly diagnosed, metastatic prostate cancer (STAMPEDE): a randomised controlled phase 3 trial. *Lancet*. 2018. doi:10.1016/S0140-6736(18)32486-3

72. Hospital SJ. *National Medicine Information Centre*.; 2012. http://www.stjames.ie/GPsHealthcareProfessionals/Newsletters/NMICBulletins/NMICBulletins2012/NMIC PROSTATE CANCER DECEMBER 2012_final.pdf.

73. Albertsen PC. Re: 10-Year Outcomes After Monitoring, Surgery or Radiotherapy for Localized Prostate Cancer. *Eur Urol*. 2017. doi:10.1016/j.eururo.2017.05.045

74. Schrijvers D. Androgen-independent prostate cancer. *Recent Results Cancer Res*. 2007. doi:10.1007/978-3-642-27841-9_267-2

75. Koukourakis G, Kelekis N, Armonis V, Kouloulias V. Brachytherapy for prostate cancer: A systematic review. *Adv Urol*. 2009. doi:10.1155/2009/327945

76. Demanes DJ, Ghilezan MI. High-dose-rate brachytherapy as monotherapy for prostate cancer. *Brachytherapy*. 2014. doi:10.1016/j.brachy.2014.03.002

77. Chin J, Rumble RB, Kollmeier M, et al. Brachytherapy for patients with prostate cancer: American Society of Clinical Oncology/Cancer Care Ontario joint guideline update. *J Clin Oncol*. 2017. doi:10.1200/JCO.2016.72.0466

78. Zaorsky NG, Davis BJ, Nguyen PL, et al. The evolution of brachytherapy for prostate cancer. *Nat Rev Urol*. 2017. doi:10.1038/nrurol.2017.76

79. Mayles P, Rosenwald JC. Brachytherapy. *Handb Radiother Phys Theory Pract*. 2007. doi:10.5005/jp/books/13101_27

80. Lane JA, Donovan JL, Davis M, et al. Active monitoring, radical prostatectomy, or radiotherapy for localised prostate cancer: Study design and diagnostic and baseline results of the ProtecT randomised phase 3 trial. *Lancet Oncol*. 2014. doi:10.1016/S1470-2045(14)70361-4

81. Brenner DJ, Curtis RE, Hall EJ, Ron E. Second malignancies in prostate carcinoma patients after radiotherapy compared with surgery. *Cancer*. 2000. doi:10.1002/(SICI)1097-0142(20000115)88:2<398::AID-CNCR22>3.0.CO;2-V

82. Sriprasad S, Feneley MR, Thompson PM. History of prostate cancer treatment. *Surg Oncol*. 2009. doi:10.1016/j.suronc.2009.07.001

83. Resnick MJ, Koyama T, Fan KH, et al. Long-term functional outcomes after treatment for localized prostate cancer. *N Engl J Med*. 2013. doi:10.1056/NEJMoa1209978

84. Sharifi N, Gulley JL, Dahut WL. Androgen deprivation therapy for prostate cancer. *J Am Med Assoc*. 2005. doi:10.1001/jama.294.2.238

85. Warde P, Mason M, Ding K, et al. Combined androgen deprivation therapy and radiation therapy for locally advanced prostate cancer: A randomised, phase 3 trial. *Lancet*. 2011. doi:10.1016/S0140-6736(11)61095-7

86. Pagliarulo V. Androgen deprivation therapy for prostate cancer. In: *Advances in Experimental Medicine and Biology*. Vol 1126. Springer New York LLC; 2018:1-30. doi:10.1007/978-3-319-99286-0_1

87. Litwin MS, Tan HJ. The diagnosis and treatment of prostate cancer: A review. *JAMA - J Am Med Assoc*. 2017. doi:10.1001/jama.2017.7248

88. Harrington JM, Schwenke DC, Epstein DR, Bailey DE. Androgen-deprivation therapy and metabolic syndrome in men with prostate cancer. *Oncol Nurs Forum*. 2014;41(1). doi:10.1188/14.ONF.21-29

89. Saylor PJ, Smith MR. Metabolic complications of androgen deprivation therapy for prostate cancer. *J Urol*. 2013;189(1 SUPPL). doi:10.1016/j.juro.2012.11.017

90. Saylor PJ, Smith MR. Metabolic Complications of Androgen Deprivation Therapy for Prostate Cancer. *J Urol*. 2009;181(5). doi:10.1016/j.juro.2009.01.047

91. Braga-Basaria M, Dobs AS, Muller DC, et al. Metabolic syndrome in men with prostate cancer undergoing long-term androgen-deprivation therapy. *J Clin Oncol*. 2006;24(24). doi:10.1200/JCO.2006.05.9741

92. Yuan J qi, Xu T, Zhang X wei, et al. Metabolic syndrome and androgen deprivation therapy in metabolic complications of prostate cancer patients. *Chin Med J (Engl)*. 2012;125(20). doi:10.3760/cma.j.issn.0366-6999.2012.20.023

93. Wu YH, Jhan JH, Ke HL, et al. Risk of developing hypertension after hormone therapy for prostate cancer: a nationwide propensity score-matched longitudinal cohort study. *Int J Clin Pharm*. 2020;42(6). doi:10.1007/s11096-020-01143-9

94. Yunusova N V., Kondakova I V., Kolomiets LA, Afanas'ev SG, Kishkina AY, Spirina L V. The role of metabolic syndrome variant in the malignant tumors progression. *Diabetes Metab Syndr Clin Res Rev*. 2018;12(5). doi:10.1016/j.dsx.2018.04.028

95. Toohey K, Hunter M, Paterson C, Mortazavi R, Singh B. Exercise Adherence in Men with Prostate Cancer Undergoing Androgen Deprivation Therapy: A

Systematic Review and Meta-Analysis. *Cancers (Basel)*. 2022;14(10). doi:10.3390/cancers14102452

96. Shao W, Zhang H, Qi H, Zhang Y. The effects of exercise on body composition of prostate cancer patients receiving androgen deprivation therapy: An update systematic review and meta-analysis. *PLoS One*. 2022;17(2 February). doi:10.1371/journal.pone.0263918

97. Phillips CK, Petrylak DP. Docetaxel. In: *Drug Management of Prostate Cancer*. ; 2010. doi:10.1007/978-1-60327-829-4_12

98. Scott E. Chemohormonal therapy in metastatic hormone-sensitive prostate cancer. *Urol Oncol Semin Orig Investig*. 2017. doi:10.1016/j.urolonc.2016.12.021

99. James ND, Sydes MR, Clarke NW, et al. Addition of docetaxel, zoledronic acid, or both to first-line long-term hormone therapy in prostate cancer (STAMPEDE): Survival results from an adaptive, multiarm, multistage, platform randomised controlled trial. *Lancet*. 2016. doi:10.1016/S0140-6736(15)01037-5

100. Sweeney CJ, Chen YH, Carducci M, et al. Chemohormonal therapy in metastatic hormone-sensitive prostate cancer. *N Engl J Med*. 2015. doi:10.1056/NEJMoa1503747

101. Corcoran C, Rani S, O'Brien K, et al. Docetaxel-Resistance in Prostate Cancer: Evaluating Associated Phenotypic Changes and Potential for Resistance Transfer via Exosomes. *PLoS One*. 2012. doi:10.1371/journal.pone.0050999

102. Attard G, Sydes MR, Mason MD, et al. Combining enzalutamide with abiraterone, prednisone, and androgen deprivation therapy in the STAMPEDE trial. *Eur Urol*. 2014. doi:10.1016/j.eururo.2014.05.038

103. Fizazi K, Scher HI, Molina A, et al. Abiraterone acetate for treatment of metastatic castration-resistant prostate cancer: Final overall survival analysis of the COU-AA-301 randomised, double-blind, placebo-controlled phase 3 study. *Lancet Oncol*. 2012. doi:10.1016/S1470-2045(12)70379-0

104. Harland S, Staffurth J, Molina A, et al. Effect of abiraterone acetate treatment on the quality of life of patients with metastatic castration-resistant prostate cancer after failure of docetaxel chemotherapy. In: *European Journal of Cancer*. ; 2013.

doi:10.1016/j.ejca.2013.07.144

105. Ryan CJ, Molina A, Li J, et al. Serum androgens as prognostic biomarkers in castration-resistant prostate cancer: Results from an analysis of a randomized phase III trial. In: *Journal of Clinical Oncology*. ; 2013. doi:10.1200/JCO.2012.45.4595

106. Antonarakis ES, Lu C, Wang H, et al. AR-V7 and resistance to enzalutamide and abiraterone in prostate cancer. *N Engl J Med*. 2014. doi:10.1056/NEJMoa1315815

107. Scher HI, Fizazi K, Saad F, et al. Increased survival with enzalutamide in prostate cancer after chemotherapy. *N Engl J Med*. 2012. doi:10.1056/NEJMoa1207506

108. Hussain M, Fizazi K, Saad F, et al. Enzalutamide in men with nonmetastatic, castration-resistant prostate cancer. *N Engl J Med*. 2018. doi:10.1056/NEJMoa1800536

109. Beer TM, Armstrong AJ, Rathkopf DE, et al. Enzalutamide in metastatic prostate cancer before chemotherapy. *N Engl J Med*. 2014. doi:10.1056/NEJMoa1405095

110. Mateo J, Carreira S, Sandhu S, et al. DNA-Repair Defects and Olaparib in Metastatic Prostate Cancer. *N Engl J Med*. 2015;373(18). doi:10.1056/nejmoa1506859

111. National Cancer Institute. Cabazitaxel. National Cancer Institute.

112. Kreis K, Horenkamp-Sonntag D, Schneider U, Zeidler J, Glaeske G, Weissbach L. Safety and survival of docetaxel and cabazitaxel in metastatic castration-resistant prostate cancer. *BJU Int*. 2022;129(4). doi:10.1111/bju.15542

113. National Institutes of Health & U.S. National Library of Medicine. JEVTANA-cabazitaxel kit.

114. Kaufman B, Shapira-Frommer R, Schmutzler RK, et al. Olaparib monotherapy in patients with advanced cancer and a germline BRCA1/2 mutation. *J Clin Oncol*. 2015. doi:10.1200/JCO.2014.56.2728

115. Mateo J, Lord CJ, Serra V, et al. A decade of clinical development of PARP inhibitors in perspective. *Ann Oncol*. 2019. doi:10.1093/annonc/mdz192

116. de Bono J, Mateo J, Fizazi K, et al. Olaparib for Metastatic Castration-Resistant Prostate Cancer. *N Engl J Med*. 2020. doi:10.1056/nejmoa1911440

117. Clarke N, Wiechno P, Alekseev B, et al. Olaparib combined with abiraterone in

patients with metastatic castration-resistant prostate cancer: a randomised, double-blind, placebo-controlled, phase 2 trial. *Lancet Oncol*. 2018. doi:10.1016/S1470-2045(18)30365-6

118. Goodall J, Mateo J, Yuan W, et al. Circulating cell-free DNA to guide prostate cancer treatment with PARP inhibition. *Cancer Discov*. 2017. doi:10.1158/2159-8290.CD-17-0261

119. Martin GA, Chen AH, Parikh K. A Novel Use of Olaparib for the Treatment of Metastatic Castration-Recurrent Prostate Cancer. *Pharmacotherapy*. 2017. doi:10.1002/phar.2027

120. Syed YY. Rucaparib: First Global Approval. *Drugs*. 2017. doi:10.1007/s40265-017-0716-2

121. Brand DH, Tree AC, Ostler P, et al. Intensity-modulated fractionated radiotherapy versus stereotactic body radiotherapy for prostate cancer (PACE-B): acute toxicity findings from an international, randomised, open-label, phase 3, non-inferiority trial. *Lancet Oncol*. 2019;20(11). doi:10.1016/S1470-2045(19)30569-8

122. Bruner DW, Pugh SL, Lee WR, et al. Quality of Life in Patients with Low-Risk Prostate Cancer Treated with Hypofractionated vs Conventional Radiotherapy: A Phase 3 Randomized Clinical Trial. *JAMA Oncol*. 2019;5(5). doi:10.1001/jamaoncol.2018.6752

123. Siva S, Bressel M, Murphy DG, et al. Stereotactic Abative Body Radiotherapy (SABR) for Oligometastatic Prostate Cancer: A Prospective Clinical Trial. *Eur Urol*. 2018;74(4). doi:10.1016/j.eururo.2018.06.004

124. Hölscher T, Baumann M, Kotzerke J, et al. Toxicity and Efficacy of Local Ablative, Image-guided Radiotherapy in Gallium-68 Prostate-specific Membrane Antigen Targeted Positron Emission Tomography-staged, Castration-sensitive Oligometastatic Prostate Cancer: The OLI-P Phase 2 Clinical Trial. *Eur Urol Oncol*. 2022;5(1). doi:10.1016/j.euo.2021.10.002

125. Emmett L, Willowson K, Violet J, Shin J, Blanksby A, Lee J. Lutetium 177 PSMA radionuclide therapy for men with prostate cancer: a review of the current literature and discussion of practical aspects of therapy. *J Med Radiat Sci*. 2017;64(1).

doi:10.1002/jmrs.227

126. Hofman MS, Emmett L, Violet J, et al. TheraP: a randomized phase 2 trial of 177Lu-PSMA-617 theranostic treatment vs cabazitaxel in progressive metastatic castration-resistant prostate cancer (Clinical Trial Protocol ANZUP 1603). *BJU Int*. 2019. doi:10.1111/bju.14876

127. McBean R, O'Kane B, Parsons R, Wong D. Lu177-PSMA therapy for men with advanced prostate cancer: Initial 18 months experience at a single Australian tertiary institution. *J Med Imaging Radiat Oncol*. 2019. doi:10.1111/1754-9485.12891

128. Hofman MS, Violet J, Hicks RJ, et al. [177 Lu]-PSMA-617 radionuclide treatment in patients with metastatic castration-resistant prostate cancer (LuPSMA trial): a single-centre, single-arm, phase 2 study. *Lancet Oncol*. 2018. doi:10.1016/S1470-2045(18)30198-0

129. Emmett L, Crumbaker M, Ho B, et al. Results of a Prospective Phase 2 Pilot Trial of 177 Lu–PSMA-617 Therapy for Metastatic Castration-Resistant Prostate Cancer Including Imaging Predictors of Treatment Response and Patterns of Progression. *Clin Genitourin Cancer*. 2019. doi:10.1016/j.clgc.2018.09.014

130. Morgenstern A, Apostolidis C, Kratochwil C, Sathekge M, Krolicki L, Bruchertseifer F. An Overview of Targeted Alpha Therapy with 225 Actinium and 213 Bismuth . *Curr Radiopharm*. 2018. doi:10.2174/1874471011666180502104524

131. A. Scheinberg D, R. McDevitt M. Actinium-225 in Targeted Alpha-Particle Therapeutic Applications. *Curr Radiopharm*. 2012. doi:10.2174/1874471011104040306

132. Borchardt PE, Yuan RR, Miederer M, McDevitt MR, Scheinberg DA. Targeted actinium-225 in vivo generators for therapy of ovarian cancer. *Cancer Res*. 2003.

133. Feuerecker B, Knorr K, Beheshti A, et al. Safety and Efficacy of Ac-225-PSMA-617 in mCRPC after Failure of Lu-177-PSMA. *J Med Imaging Radiat Sci*. 2019;50(1):S20-S21. doi:10.1016/j.jmir.2019.03.066

134. Turner PG, Jain S, Cole A, et al. Toxicity and efficacy of concurrent androgen deprivation therapy, pelvic radiotherapy, and radium-223 in patients with De Novo metastatic hormone-sensitive prostate cancer. *Clin Cancer Res*. 2021;27(16).

doi:10.1158/1078-0432.CCR-21-0685

135. Drake CG. Prostate cancer as a model for tumour immunotherapy. *Nat Rev Immunol*. 2010. doi:10.1038/nri2817

136. Di Lorenzo G, Buonerba C, Kantoff PW. Immunotherapy for the treatment of prostate cancer. *Nat Rev Clin Oncol*. 2011. doi:10.1038/nrclinonc.2011.72

137. Modena A, Ciccarese C, Iacovelli R, et al. Immune Checkpoint Inhibitors and Prostate Cancer: A New Frontier? *Oncol Rev*. 2016;10(1):293. doi:10.4081/oncol.2016.293

138. Wada S, Jackson CM, Yoshimura K, et al. Sequencing CTLA-4 blockade with cell-based immunotherapy for prostate cancer. *J Transl Med*. 2013. doi:10.1186/1479-5876-11-89

139. Gerritsen WR. The evolving role of immunotherapy in prostate cancer. In: *Annals of Oncology*. ; 2012. doi:10.1093/annonc/mds259

140. Karan D, Van Veldhuizen P. Combination immunotherapy with prostate GVAX and ipilimumab: Safety and toxicity. *Immunotherapy*. 2012. doi:10.2217/imt.12.53

141. Beer TM, Kwon ED, Drake CG, et al. Randomized, double-blind, phase III trial of ipilimumab versus placebo in asymptomatic or minimally symptomatic patients with metastatic chemotherapy-naive castration-resistant prostate cancer. *J Clin Oncol*. 2017. doi:10.1200/JCO.2016.69.1584

142. Cabel L, Loir E, Gravis G, et al. Long-term complete remission with Ipilimumab in metastatic castrate-resistant prostate cancer: Case report of two patients. *J Immunother Cancer*. 2017. doi:10.1186/s40425-017-0232-7

143. Goswami S, Aparicio A, Subudhi SK. Immune Checkpoint Therapies in Prostate Cancer. *Cancer J*. 2016;22(2):117-120. doi:10.1097/PPO.0000000000000176

144. Fay AP, Antonarakis ES. Blocking the PD-1/PD-L1 axis in advanced prostate cancer: are we moving in the right direction? *Ann Transl Med*. 2019;7(Suppl 1):S7-S7. doi:10.21037/atm.2019.01.37

145. Alsaab HO, Sau S, Alzhrani R, et al. PD-1 and PD-L1 Checkpoint Signaling Inhibition for Cancer Immunotherapy: Mechanism, Combinations, and Clinical

Outcome . *Front Pharmacol* . 2017;8:561. https://www.frontiersin.org/article/10.3389/fphar.2017.00561.

146. Isaacsson Velho P, Antonarakis ES. PD-1/PD-L1 pathway inhibitors in advanced prostate cancer. *Expert Rev Clin Pharmacol*. 2018;11(5):475-486. doi:10.1080/17512433.2018.1464388

147. Guo ZS, Lu B, Guo Z, et al. Vaccinia virus-mediated cancer immunotherapy: Cancer vaccines and oncolytics. *J Immunother Cancer*. 2019. doi:10.1186/s40425-018-0495-7

148. Cheever MA, Higano CS. PROVENGE (sipuleucel-T) in prostate cancer: The first FDA-approved therapeutic cancer vaccine. *Clin Cancer Res*. 2011. doi:10.1158/1078-0432.CCR-10-3126

149. Anassi E, Ndefo UA. Sipuleucel-T (Provenge) injection the first immunotherapy agent (Vaccine) for hormone-refractory prostate cancer. *P T*. 2011.

150. Schellhammer PF, Chodak G, Whitmore JB, Sims R, Frohlich MW, Kantoff PW. Lower baseline prostate-specific antigen is associated with a greater overall survival benefit from sipuleucel-T in the immunotherapy for prostate adenocarcinoma treatment (IMPACT) trial. *Urology*. 2013. doi:10.1016/j.urology.2013.01.061

151. Small EJ, Schellhammer PF, Higano CS, et al. Placebo-controlled phase III trial of immunologic therapy with Sipuleucel-T (APC8015) in patients with metastatic, asymptomatic hormone refractory prostate cancer. *J Clin Oncol*. 2006. doi:10.1200/JCO.2005.04.5252

152. Kantoff PW, Higano CS, Shore ND, et al. Sipuleucel-T immunotherapy for castration-resistant prostate cancer. *N Engl J Med*. 2010. doi:10.1056/NEJMoa1001294

153. Gulley JL, Arlen PM, Madan RA, et al. Immunologic and prognostic factors associated with overall survival employing a poxviral-based PSA vaccine in metastatic castrate-resistant prostate cancer. *Cancer Immunol Immunother*. 2010. doi:10.1007/s00262-009-0782-8

154. Sonpavde G, Kantoff PW. Immunotherapy for Castration-Resistant Prostate Cancer. *Urol Clin North Am*. 2012. doi:10.1016/j.ucl.2012.07.004

155. Kantoff PW, Schuetz TJ, Blumenstein BA, et al. Overall survival analysis of a phase II randomized controlled trial of a poxviral-based PSA-targeted immunotherapy in metastatic castration-resistant prostate cancer. *J Clin Oncol*. 2010. doi:10.1200/JCO.2009.25.0597

156. Gulley JL, Borre M, Vogelzang NJ, et al. Phase III Trial of PROSTVAC in Asymptomatic or Minimally Symptomatic Metastatic Castration-Resistant Prostate Cancer. *J Clin Oncol*. 2019;37(13):1051-1061. doi:10.1200/JCO.18.02031

157. Singh P, Pal SK, Alex A, Agarwal N. Development of PROSTVAC immunotherapy in prostate cancer. *Futur Oncol*. 2015. doi:10.2217/fon.15.120

158. Ford WCL, Harrison A. The role of citrate in determining the activity of calcium ions in human semen. *Int J Androl*. 1984. doi:10.1111/j.1365-2605.1984.tb00777.x

159. Kothari RP, Chaudhari AR. Zinc levels in seminal fluid in infertile males and its relation with serum free testosterone. *J Clin Diagnostic Res*. 2016. doi:10.7860/JCDR/2016/14393.7723

160. Timms BG. Prostate development: A historical perspective. *Differentiation*. 2008. doi:10.1111/j.1432-0436.2008.00278.x

161. Invitrogen™. OxyBURST™ Green H2DCFDA, SE. Thermo Fisher Scientific Inc. Webpage. https://www.thermofisher.com/order/catalog/product/D2935. Published 2006. Accessed January 31, 2023.

162. Corn PG. The tumor microenvironment in prostate cancer: Elucidating molecular pathways for therapy development. *Cancer Manag Res*. 2012;4(1). doi:10.2147/CMAR.S32839

163. Brawer MK. Prostatic intraepithelial neoplasia: an overview. *Rev Urol*. 2005;7 Suppl 3.

164. Corn PG. The tumor microenvironment in prostate cancer: Elucidating molecular pathways for therapy development. *Cancer Manag Res*. 2012. doi:10.2147/CMAR.S32839

165. American Cancer Society. Prostate Cancer What is prostate cancer ? *Am Cancer Soc*. 2016.

166. Martinez-Outschoorn UE, Peiris-Pagés M, Pestell RG, Sotgia F, Lisanti MP. Cancer metabolism: a therapeutic perspective. *Nat Rev Clin Oncol*. 2017. doi:10.1038/nrclinonc.2016.60

167. Datta K, Muders M, Zhang H, Tindall DJ. Mechanism of lymph node metastasis in prostate cancer. *Futur Oncol*. 2010. doi:10.2217/fon.10.33

168. Cheng L, Montironi R, Bostwick DG, Lopez-Beltran A, Berney DM. Staging of prostate cancer. *Histopathology*. 2012. doi:10.1111/j.1365-2559.2011.04025.x

169. Nathanson SD. Insights into the mechanisms of lymph node metastasis. *Cancer*. 2003. doi:10.1002/cncr.11464

170. Hughes C, Murphy A, Martin C, Sheils O, O'Leary J. Molecular pathology of prostate cancer. *J Clin Pathol*. 2005. doi:10.1136/jcp.2002.003954

171. Jin JK, Dayyani F, Gallick GE. Steps in prostate cancer progression that lead to bone metastasis. *Int J Cancer*. 2011. doi:10.1002/ijc.26024

172. Bubendorf L, Schöpfer A, Wagner U, et al. Metastatic patterns of prostate cancer: An autopsy study of 1,589 patients. *Hum Pathol*. 2000. doi:10.1053/hp.2000.6698

173. Muruganandan S, Sinal CJ. The impact of bone marrow adipocytes on osteoblast and osteoclast differentiation. *IUBMB Life*. 2014;66(3). doi:10.1002/iub.1254

174. Mundy GR. Metastasis to bone: Causes, consequences and therapeutic opportunities. *Nat Rev Cancer*. 2002. doi:10.1038/nrc867

175. Green SM, Mostaghel EA, Nelson PS. Androgen action and metabolism in prostate cancer. *Mol Cell Endocrinol*. 2012. doi:10.1016/j.mce.2011.09.046

176. Culig Z, Klocker H, Bartsch G, Steiner H, Hobisch A. Androgen receptors in prostate cancer. *J Urol*. 2003. doi:10.1210/er.2002-0032

177. Formaggio N, Rubin MA, Theurillat JP. Loss and revival of androgen receptor signaling in advanced prostate cancer. *Oncogene*. 2021;40(7). doi:10.1038/s41388-020-01598-0

178. Lonergan P, Tindall D. Androgen receptor signaling in prostate cancer development and progression. *J Carcinog*. 2011;10. doi:10.4103/1477-3163.83937

179. Edwards J, Krishna NS, Grigor KM, Bartlett JMS. Androgen receptor gene

amplification and protein expression in hormone refractory prostate cancer. *Br J Cancer*. 2003;89(3). doi:10.1038/sj.bjc.6601127

180. McAllister MJ, Underwood MA, Leung HY, Edwards J. A review on the interactions between the tumor microenvironment and androgen receptor signaling in prostate cancer. *Transl Res*. 2019;206. doi:10.1016/j.trsl.2018.11.004

181. Visakorpi T, Hyytinen E, Koivisto P, et al. In vivo amplification of the androgen receptor gene and progression of human prostate cancer. *Nat Genet*. 1995;9(4). doi:10.1038/ng0495-401

182. Merson S, Yang ZH, Brewer D, et al. Focal amplification of the androgen receptor gene in hormone-naive human prostate cancer. *Br J Cancer*. 2014;110(6). doi:10.1038/bjc.2014.13

183. Brooke G, Bevan C. The Role of Androgen Receptor Mutations in Prostate Cancer Progression. *Curr Genomics*. 2009;10(1). doi:10.2174/138920209787581307

184. Klocker H, Culig Z, Hobisch A, et al. Androgen receptor mutations in prostate cancer. In: *Molecular Biology of Prostate Cancer*. ; 2013. doi:10.1515/9783110807271.81

185. Hay CW, McEwan IJ. The impact of point mutations in the human androgen receptor: Classification of mutations on the basis of transcriptional activity. *PLoS One*. 2012;7(3). doi:10.1371/journal.pone.0032514

186. Morova T, McNeill DR, Lallous N, et al. Androgen receptor-binding sites are highly mutated in prostate cancer. *Nat Commun*. 2020;11(1). doi:10.1038/s41467-020-14644-y

187. Krušlin B, Škara L, Vodopić T, et al. Genetics of Prostate Carcinoma. *Acta Med Acad*. 2021;50(1). doi:10.5644/ama2006-124.327

188. Barbieri CE. Introduction to “Molecular drivers of prostate cancer development, progression, and resistance to therapy.” *Urol Oncol Semin Orig Investig*. 2018;36(8). doi:10.1016/j.urolonc.2018.06.003

189. Zhu Y, Luo J. Regulation of androgen receptor variants in prostate cancer. *Asian J Urol*. 2020;7(3). doi:10.1016/j.ajur.2020.01.001

190. Lee YR, Chen M, Pandolfi PP. The functions and regulation of the PTEN tumour suppressor: new modes and prospects. *Nat Rev Mol Cell Biol*. 2018;19(9). doi:10.1038/s41580-018-0015-0

191. Bazzichetto C, Conciatori F, Pallocca M, et al. PTEN as a Prognostic/Predictive Biomarker in Cancer: An Unfulfilled Promise? *Cancers (Basel)*. 2019;11(4). doi:10.3390/cancers11040435

192. Jamaspishvili T, Berman DM, Ross AE, et al. Clinical implications of PTEN loss in prostate cancer. *Nat Rev Urol*. 2018. doi:10.1038/nrurol.2018.9

193. Wise HM, Hermida MA, Leslie NR. Prostate cancer, PI3K, PTEN and prognosis. *Clin Sci*. 2017. doi:10.1042/CS20160026

194. Chalhoub N, Baker SJ. PTEN and the PI3-Kinase Pathway in Cancer. *Annu Rev Pathol Mech Dis*. 2009. doi:10.1146/annurev.pathol.4.110807.092311

195. Zhou X, Yang X, Sun X, et al. Effect of PTEN loss on metabolic reprogramming in prostate cancer cells. *Oncol Lett*. 2019. doi:10.3892/ol.2019.9932

196. Sansal I, Sellers WR. The biology and clinical relevance of the PTEN tumor suppressor pathway. *J Clin Oncol*. 2004. doi:10.1200/JCO.2004.02.141

197. Imada EL, Sanchez DF, Dinalankara W, et al. Transcriptional landscape of PTEN loss in primary prostate cancer. *BMC Cancer*. 2021;21(1). doi:10.1186/s12885-021-08593-y

198. McCabe N, Kennedy RD, Prise KM. The role of PTEN as a cancer biomarker. *Oncoscience*. 2016. doi:10.18632/oncoscience.296

199. Vidotto T, Saggioro FP, Jamaspishvili T, et al. PTEN-deficient prostate cancer is associated with an immunosuppressive tumor microenvironment mediated by increased expression of IDO1 and infiltrating FoxP3+ T regulatory cells. *Prostate*. 2019. doi:10.1002/pros.23808

200. Saini S. PSA and beyond: alternative prostate cancer biomarkers. *Cell Oncol*. 2016. doi:10.1007/s13402-016-0268-6

201. Mulholland DJ, Tran LM, Li Y, et al. Cell autonomous role of PTEN in regulating castration-resistant prostate cancer growth. *Cancer Cell*. 2011.

doi:10.1016/j.ccr.2011.05.006

202. Lo U-G, Yang D, Hsieh J-T. The role of microRNAs in prostate cancer progression. *Transl Androl Urol*. 2013;2(3):228-241. doi:10.3978/j.issn.2223-4683.2013.08.01

203. Dillon LM, Miller TW. Therapeutic targeting of cancers with loss of PTEN function. *Curr Drug Targets*. 2014;15(1):65-79. doi:10.2174/1389450114666140106100909

204. Hoey C, Ahmed M, Fotouhi Ghiam A, et al. Circulating miRNAs as non-invasive biomarkers to predict aggressive prostate cancer after radical prostatectomy. *J Transl Med*. 2019. doi:10.1186/s12967-019-1920-5

205. Peng Y, Croce CM. The role of microRNAs in human cancer. *Signal Transduct Target Ther*. 2016. doi:10.1038/sigtrans.2015.4

206. Zhang B, Pan X, Cobb GP, Anderson TA. microRNAs as oncogenes and tumor suppressors. *Dev Biol*. 2007. doi:10.1016/j.ydbio.2006.08.028

207. Andl T, Ganapathy K, Bossan A, Chakrabarti R. MicroRNAs as guardians of the prostate: Those who stand before cancer. what do we really know about the role of microRNAs in prostate biology? *Int J Mol Sci*. 2020;21(13). doi:10.3390/ijms21134796

208. Sreekumar A, Saini S. Role of MicroRNAs in Neuroendocrine Prostate Cancer. *Non-coding RNA*. 2022;8(2). doi:10.3390/ncrna8020025

209. Li T, Li D, Sha J, Sun P, Huang Y. MicroRNA-21 directly targets MARCKS and promotes apoptosis resistance and invasion in prostate cancer cells. *Biochem Biophys Res Commun*. 2009;383(3). doi:10.1016/j.bbrc.2009.03.077

210. Bonci D, Coppola V, Patrizii M, et al. A microRNA code for prostate cancer metastasis. *Oncogene*. 2016;35(9). doi:10.1038/onc.2015.176

211. Chiyomaru T, Yamamura S, Zaman MS, et al. Genistein suppresses prostate cancer growth through inhibition of oncogenic MicroRNA-151. *PLoS One*. 2012;7(8). doi:10.1371/journal.pone.0043812

212. Nip H, Dar AA, Saini S, et al. Oncogenic microRNA-4534 regulates PTEN pathway in prostate cancer. *Oncotarget*. 2016;7(42). doi:10.18632/ONCOTARGET.12031

213. Bidarra D, Constâncio V, Barros-Silva D, et al. Circulating MicroRNAs as

Biomarkers for Prostate Cancer Detection and Metastasis Development Prediction. *Front Oncol*. 2019. doi:10.3389/fonc.2019.00900

214. Teyssonneau D, Margot H, Cabart M, et al. Prostate cancer and PARP inhibitors: progress and challenges. *J Hematol Oncol*. 2021;14(1). doi:10.1186/s13045-021-01061-x

215. Risdon EN, Chau CH, Price DK, Sartor O, Figg WD. PARP Inhibitors and Prostate Cancer: To Infinity and Beyond BRCA . *Oncologist*. 2021;26(1). doi:10.1634/theoncologist.2020-0697

216. Mekonnen N, Yang H, Shin YK. Homologous Recombination Deficiency in Ovarian, Breast, Colorectal, Pancreatic, Non-Small Cell Lung and Prostate Cancers, and the Mechanisms of Resistance to PARP Inhibitors. *Front Oncol*. 2022;12. doi:10.3389/fonc.2022.880643

217. Crocetto F, Barone B, Caputo VF, Fontana M, de Cobelli O, Ferro M. Brca germline mutations in prostate cancer: The future is tailored. *Diagnostics*. 2021;11(5). doi:10.3390/diagnostics11050908

218. Boussios S, Rassy E, Moschetta M, et al. BRCA Mutations in Ovarian and Prostate Cancer: Bench to Bedside. *Cancers (Basel)*. 2022;14(16). doi:10.3390/cancers14163888

219. Sishc BJ, Davis AJ. The role of the core non-homologous end joining factors in carcinogenesis and cancer. *Cancers (Basel)*. 2017;9(7). doi:10.3390/cancers9070081

220. Zhang W, van Gent DC, Incrocci L, van Weerden WM, Nonnekens J. Role of the DNA damage response in prostate cancer formation, progression and treatment. *Prostate Cancer Prostatic Dis*. 2020;23(1). doi:10.1038/s41391-019-0153-2

221. Karanika S, Karantanos T, Li L, Corn PG, Thompson TC. DNA damage response and prostate cancer: Defects, regulation and therapeutic implications. *Oncogene*. 2015;34(22). doi:10.1038/onc.2014.238

222. Hessels D, Schalken JA. The use of PCA3 in the diagnosis of prostate cancer. *Nat Rev Urol*. 2009. doi:10.1038/nrurol.2009.40

223. Auprich M, Bjartell A, Chun FKH, et al. Contemporary role of prostate cancer

antigen 3 in the management of prostate cancer. *Eur Urol*. 2011. doi:10.1016/j.eururo.2011.08.003

224. Alford A V, Brito JM, Yadav KK, Yadav SS, Tewari AK, Renzulli J. The Use of Biomarkers in Prostate Cancer Screening and Treatment. *Rev Urol*. 2017. doi:10.3909/riu0772

225. Filella X, Fernández-Galan E, Bonifacio RF, Foj L. Emerging biomarkers in the diagnosis of prostate cancer. *Pharmgenomics Pers Med*. 2018. doi:10.2147/PGPM.S136026

226. Tan ME, Li J, Xu HE, Melcher K, Yong EL. Androgen receptor: Structure, role in prostate cancer and drug discovery. *Acta Pharmacol Sin*. 2015. doi:10.1038/aps.2014.18

227. Zhou Y, Bolton EC, Jones JO. Androgens and androgen receptor signaling in prostate tumorigenesis. *J Mol Endocrinol*. 2015;54(1):R15-R29. doi:10.1530/JME-14-0203

228. Xiong X, Schober M, Tassone E, et al. KLF4, A Gene Regulating Prostate Stem Cell Homeostasis, Is a Barrier to Malignant Progression and Predictor of Good Prognosis in Prostate Cancer. *Cell Rep*. 2018;25(11). doi:10.1016/j.celrep.2018.11.065

229. Ghaleb AM, Yang VW. Krüppel-like factor 4 (KLF4): What we currently know. *Gene*. 2017;611:27-37. doi:10.1016/j.gene.2017.02.025

230. Dai C, Heemers H, Sharifi N. Androgen Signaling in Prostate Cancer. *Cold Spring Harb Perspect Med*. 2017;7(9):a030452. doi:10.1101/cshperspect.a030452

231. Karantanos T, Evans CP, Tombal B, Thompson TC, Montironi R, Isaacs WB. Understanding the mechanisms of androgen deprivation resistance in prostate cancer at the molecular level. *Eur Urol*. 2015. doi:10.1016/j.eururo.2014.09.049

232. Sun Y, Wang BE, Leong KG, et al. Androgen deprivation causes epithelial-mesenchymal transition in the prostate: Implications for androgen- deprivation therapy. *Cancer Res*. 2012. doi:10.1158/0008-5472.CAN-11-3004

233. Green SM, Mostaghel EA, Nelson PS. Androgen action and metabolism in prostate cancer. *Mol Cell Endocrinol*. 2012. doi:10.1016/j.mce.2011.09.046

234. Shafi AA, Yen AE, Weigel NL. Androgen receptors in hormone-dependent and castration-resistant prostate cancer. *Pharmacol Ther*. 2013. doi:10.1016/j.pharmthera.2013.07.003

235. Pienta KJ, Bradley D. Mechanisms underlying the development of androgen-independent prostate cancer. *Clin Cancer Res*. 2006. doi:10.1158/1078-0432.CCR-06-0067

236. Feldman BJ, Feldman D. The development of androgen-independent prostate cancer. *Nat Rev Cancer*. 2001. doi:10.1038/35094009

237. Craft N, Shostak Y, Carey M, Sawyers CL. A mechanism for hormone-independent prostate cancer through modulation of androgen receptor signaling by the HER-2/neu tyrosine kinase. *Nat Med*. 1999. doi:10.1038/6495

238. Grossmann ME, Huang H, Tindall DJ. Androgen receptor signaling in androgen-refractory prostate cancer. *J Natl Cancer Inst*. 2001. doi:10.1093/jnci/93.22.1687

239. Fouad YA, Aanei C. Revisiting the hallmarks of cancer. *Am J Cancer Res*. 2017;7(5).

240. Hanahan D, Weinberg RA. Hallmarks of cancer: The next generation. *Cell*. 2011. doi:10.1016/j.cell.2011.02.013

241. Silvia Licciulli. New Dimensions in Cancer Biology: Updated Hallmarks of Cancer Published. American Association of Cancer Research. https://www.aacr.org/blog/2022/01/21/new-dimensions-in-cancer-biology-updated-hallmarks-of-cancer-published/. Published January 21, 2022. Accessed February 19, 2023.

242. Schwartz L, Supuran C, Alfarouk K. The Warburg Effect and the Hallmarks of Cancer. *Anticancer Agents Med Chem*. 2017. doi:10.2174/1871520616666161031143301

243. Seyfried TN, Shelton LM. Cancer as a metabolic disease. *Nutr Metab*. 2010. doi:10.1186/1743-7075-7-7

244. Eidelman E, Twum-Ampofo J, Ansari J, Siddiqui MM. The Metabolic Phenotype of Prostate Cancer. *Front Oncol*. 2017. doi:10.3389/fonc.2017.00131

245. Costello LC, Franklin RB. The clinical relevance of the metabolism of prostate cancer; zinc and tumor suppression: Connecting the dots. *Mol Cancer*. 2006. doi:10.1186/1476-4598-5-17

246. Dang C V. Links between metabolism and cancer. *Genes Dev*. 2012. doi:10.1101/gad.189365.112

247. Vander Heiden MG. Targeting cancer metabolism: A therapeutic window opens. *Nat Rev Drug Discov*. 2011. doi:10.1038/nrd3504

248. DeBerardinis RJ, Lum JJ, Hatzivassiliou G, Thompson CB. The Biology of Cancer: Metabolic Reprogramming Fuels Cell Growth and Proliferation. *Cell Metab*. 2008. doi:10.1016/j.cmet.2007.10.002

249. Xu XD, Shao SX, Jiang HP, et al. Warburg effect or reverse warburg effect? a review of cancer metabolism. *Oncol Res Treat*. 2015. doi:10.1159/000375435

250. Venkatesh K V., Darunte L, Bhat PJ. Warburg Effect. In: *Encyclopedia of Systems Biology*. ; 2013. doi:10.1007/978-1-4419-9863-7_703

251. Liberti M V., Locasale JW. The Warburg Effect: How Does it Benefit Cancer Cells? *Trends Biochem Sci*. 2016. doi:10.1016/j.tibs.2015.12.001

252. Li X, Zhong Y, Lu J, et al. MtDNA depleted PC3 cells exhibit Warburg effect and cancer stem cell features. *Oncotarget*. 2016;7(26). doi:10.18632/oncotarget.9610

253. Heiden MG Vander, Cantley LC, Thompson CB. Understanding the warburg effect: The metabolic requirements of cell proliferation. *Science (80-)*. 2009. doi:10.1126/science.1160809

254. Karanam B, Schmitt D, Arora R, Yates C, Dean-Colomb W, Tan M. Inhibition of the Warburg effect with a natural compound reveals a novel measurement for determining the metastatic potential of breast cancers. *Oncotarget*. 2015;6(2). doi:10.18632/oncotarget.2689

255. Gogvadze V, Zhivotovsky B, Orrenius S. The Warburg effect and mitochondrial stability in cancer cells. *Mol Aspects Med*. 2010. doi:10.1016/j.mam.2009.12.004

256. Heiden M Vander, Cantley L, Thompson C. Understanding the Warburg Effect : Cell Proliferation. *Science (80-)*. 2009. doi:10.1126/science.1160809

257. Brinkkoetter PT, Bork T, Salou S, et al. Anaerobic Glycolysis Maintains the Glomerular Filtration Barrier Independent of Mitochondrial Metabolism and Dynamics. *Cell Rep*. 2019;27(5). doi:10.1016/j.celrep.2019.04.012

258. Melkonian EA, Schury MP. *Biochemistry, Anaerobic Glycolysis*.; 2019.

259. Wu W, Zhao S. Metabolic changes in cancer: Beyond the Warburg effect. *Acta Biochim Biophys Sin (Shanghai)*. 2013. doi:10.1093/abbs/gms104

260. Hsu PP, Sabatini DM. Cancer cell metabolism: Warburg and beyond. *Cell*. 2008. doi:10.1016/j.cell.2008.08.021

261. Lu J, Tan M, Cai Q. The Warburg effect in tumor progression: Mitochondrial oxidative metabolism as an anti-metastasis mechanism. *Cancer Lett*. 2015;356(2). doi:10.1016/j.canlet.2014.04.001

262. Du J, Cullen JJ, Buettner GR. Ascorbic acid: Chemistry, biology and the treatment of cancer. *Biochim Biophys Acta - Rev Cancer*. 2012. doi:10.1016/j.bbcan.2012.06.003

263. Padayatty SJ, Katz A, Wang Y, et al. Vitamin C as an Antioxidant: Evaluation of Its Role in Disease Prevention. *J Am Coll Nutr*. 2003. doi:10.1080/07315724.2003.10719272

264. Ngo B, Van Riper JM, Cantley LC, Yun J. Targeting cancer vulnerabilities with high-dose vitamin C. *Nat Rev Cancer*. 2019;19(5):271-282. doi:10.1038/s41568-019-0135-7

265. Reczek CR, Chandel NS. Revisiting vitamin C and cancer. *Science (80-)*. 2015. doi:10.1126/science.aad8671

266. Chen Q, Espey MG, Sun AY, et al. Ascorbate in pharmacologic concentrations selectively generates ascorbate radical and hydrogen peroxide in extracellular fluid in vivo. *Proc Natl Acad Sci U S A*. 2007. doi:10.1073/pnas.0702854104

267. Lane DJR, Richardson DR. The active role of vitamin C in mammalian iron metabolism: Much more than just enhanced iron absorption! *Free Radic Biol Med*. 2014. doi:10.1016/j.freeradbiomed.2014.07.007

268. Carr AC, Shaw GM, Fowler AA, Natarajan R. Ascorbate-dependent vasopressor

synthesis: A rationale for vitamin C administration in severe sepsis and septic shock? *Crit Care*. 2015. doi:10.1186/s13054-015-1131-2

269. Chen Q, Espey MG, Krishna MC, et al. Pharamacologic ascorbic acid concentrations selectively kill cancer cells: Action as a pro-drug to deliver hydrogen peroxide to tissuse. *Proc Natl Acad Sci U S A*. 2005. doi:10.1073/pnas.0506390102

270. Vollbracht C, Schneider B, Leendert V, Weiss G, Auerbach L, Beuth J. Intravenous vitamin C administration improves quality of life in breast cancer patients during chemo-/radiotherapy and aftercare: Results of a retrospective, multicentre, epidemiological cohort study in Germany. *In Vivo (Brooklyn)*. 2011.

271. Padayatty SJ, Riordan HD, Hewitt SM, Katz A, Hoffer LJ, Levine M. Intravenously administered vitamin C as cancer therapy: Three cases. *CMAJ*. 2006. doi:10.1503/cmaj.050346

272. Taper HS, Jamison JM, Gilloteaux J, Gwin CA, Gordon T, Summers JL. In vivo reactivation of DNases in implanted human prostate tumors after administration of a vitamin C/K3combination. *J Histochem Cytochem*. 2001. doi:10.1177/002215540104900111

273. Padayatty SJ, Sun H, Wang Y, et al. Vitamin C Pharmacokinetics: Implications for Oral and Intravenous Use. *Ann Intern Med*. 2004. doi:10.7326/0003-4819-140-7-200404060-00010

274. Padayatty SJ, Sun AY, Chen Q, Espey MG, Drisko J, Levine M. Vitamin C: Intravenous use by complementary and alternative medicine practitioners and adverse effects. *PLoS One*. 2010. doi:10.1371/journal.pone.0011414

275. Pei Z, Wu K, Li Z, et al. Pharmacologic ascorbate as a pro-drug for hydrogen peroxide release to kill mycobacteria. *Biomed Pharmacother*. 2019. doi:10.1016/j.biopha.2018.11.078

276. Niki E. Action of ascorbic acid as a scavenger of active and stable oxygen radicals. In: *American Journal of Clinical Nutrition*. ; 1991. doi:10.1093/ajcn/54.6.1119s

277. Valko M, Rhodes CJ, Moncol J, Izakovic M, Mazur M. Free radicals, metals and antioxidants in oxidative stress-induced cancer. *Chem Biol Interact*. 2006. doi:10.1016/j.cbi.2005.12.009

278. Yun J, Mullarky E, Lu C, et al. Vitamin C selectively kills KRAS and BRAF mutant colorectal cancer cells by targeting GAPDH. *Science (80-)*. 2015. doi:10.1126/science.aaa5004

279. Chen P, Yu J, Chalmers B, et al. Pharmacological ascorbate induces cytotoxicity in prostate cancer cells through ATP depletion and induction of autophagy. *Anticancer Drugs*. 2012. doi:10.1097/CAD.0b013e32834fd01f

280. Abeshouse A, Ahn J, Akbani R, et al. The Molecular Taxonomy of Primary Prostate Cancer. *Cell*. 2015. doi:10.1016/j.cell.2015.10.025

281. Fischer AP, Miles SL. Ascorbic acid, but not dehydroascorbic acid increases intracellular vitamin C content to decrease Hypoxia Inducible Factor -1 alpha activity and reduce malignant potential in human melanoma. *Biomed Pharmacother*. 2017;86:502-513. doi:https://doi.org/10.1016/j.biopha.2016.12.056

282. Uetaki M, Tabata S, Nakasuka F, Soga T, Tomita M. Metabolomic alterations in human cancer cells by Vitamin C-induced oxidative stress. *Sci Rep*. 2015. doi:10.1038/srep13896

283. Padayatty SJ, Riordan HD, Hewitt SM, Katz A, Hoffer LJ, Levine M. Intravenously administered vitamin C as cancer therapy: Three cases. *CMAJ*. 2006. doi:10.1503/cmaj.050346

284. Ohno S, Ohno Y, Suzuki N, Soma GI, Inoue M. High-dose vitamin C (ascorbic acid) therapy in the treatment of patients with advanced cancer. In: *Anticancer Research*. ; 2009. doi:29/3/809 [pii]

285. Wilson MK, Baguley BC, Wall C, Jameson MB, Findlay MP. Review of high-dose intravenous vitamin C as an anticancer agent. *Asia Pac J Clin Oncol*. 2014. doi:10.1111/ajco.12173

286. Vissers MCM, Das AB. Potential mechanisms of action for vitamin C in cancer: Reviewing the evidence. *Front Physiol*. 2018. doi:10.3389/fphys.2018.00809

287. Jonas SK, Riley P a, Willson RL. Hydrogen peroxide cytotoxicity. Low-temperature enhancement by ascorbate or reduced lipoate. *Biochem J*. 1989. doi:10.1042/bj2640651

288. Kurbacher CM, Wagner U, Kolster B, Andreotti PE, Krebs D, Bruckner HW.

Ascorbic acid (vitamin C) improves the antineoplastic activity of doxorubicin, cisplatin, and paclitaxel in human breast carcinoma cells in vitro. *Cancer Lett*. 1996. doi:10.1016/0304-3835(96)04212-7

289. Tarumoto T, Nagai T, Ohmine K, et al. Ascorbic acid restores sensitivity to imatinib via suppression of Nrf2-dependent gene expression in the imatinib-resistant cell line. *Exp Hematol*. 2004. doi:10.1016/j.exphem.2004.01.007

290. Li Y, Schellhorn HE. New Developments and Novel Therapeutic Perspectives for Vitamin C. *J Nutr*. 2007. doi:10.1093/jn/137.10.2171

291. Tian W, Wang Y, Xu Y, et al. The Hypoxia-inducible factor renders cancer cells more sensitive to Vitamin C-induced toxicity. *J Biol Chem*. 2014. doi:10.1074/jbc.M113.538157

292. Hassan GS. Menadione. In: *Profiles of Drug Substances, Excipients and Related Methodology*. ; 2013. doi:10.1016/B978-0-12-407691-4.00006-X

293. Thijssen HHW, Vervoort LMT, Schurgers LJ, Shearer MJ. Menadione is a metabolite of oral vitamin K. *Br J Nutr*. 2006. doi:10.1079/bjn20051630

294. Shearer MJ, Newman P. Metabolism and cell biology of vitamin K. *Thromb Haemost*. 2008. doi:10.1160/TH08-03-0147

295. Lamson DW, Plaza SM. The anticancer effects of vitamin K. *Altern Med Rev*. 2003.

296. Dasari S, Ali SM, Zheng G, et al. Vitamin K and its analogs: Potential avenues for prostate cancer management. *Oncotarget*. 2017;8(34). doi:10.18632/oncotarget.17997

297. Ivanova D, Zhelev Z, Getsov P, et al. Vitamin K: Redox-modulation, prevention of mitochondrial dysfunction and anticancer effect. *Redox Biol*. 2018. doi:10.1016/j.redox.2018.03.013

298. Jamison JM, Gilloteaux J, Taper HS, Calderon PB, Summers JL. Autoschizis: A novel cell death. *Biochem Pharmacol*. 2002. doi:10.1016/S0006-2952(02)00904-8

299. Criddle DN, Gillies S, Baumgartner-Wilson HK, et al. Menadione-induced reactive oxygen species generation via redox cycling promotes apoptosis of murine pancreatic acinar cells. *J Biol Chem*. 2006. doi:10.1074/jbc.M607704200

300. Gilloteaux J, Jamison JM, Arnold D, Taper HS, Summers JL. Ultrastructural aspects of autoschizis: A new cancer cell death induced by the synergistic action of ascorbate/menadione on human bladder carcinoma cells. *Ultrastruct Pathol*. 2001. doi:10.1080/019131201300343810

301. Gilloteaux J, Jamison JM, Neal D, Summers JL. Synergistic antitumor cytotoxic actions of ascorbate and menadione on human prostate (DU145) cancer cells in Vitro: Nucleus and other injuries preceding cell death by autoschizis. *Ultrastruct Pathol*. 2014. doi:10.3109/01913123.2013.852645

302. Gilloteaux J, Jamison JM, Arnold D, Taper HS, Von Gruenigen VE, Summers JL. Microscopic aspects of autoschizic cell death in human ovarian carcinoma (2774) cells following vitamin C, vitamin K3 or vitamin C:K 3 treatment. *Microsc Microanal*. 2003. doi:10.1017/S1431927603030125

303. Gant TW, Ramakrishna Rao DN, Mason RP, Cohen GM. Redox cycling and sulphydryl arylation; Their relative importance in the mechanism of quinone cytotoxicity to isolated hepatocytes. *Chem Biol Interact*. 1988. doi:10.1016/0009-2797(88)90052-X

304. Xing G, Miller CJ, Ninh Pham A, Jones AM, Waite TD. Oxidant Generation Resulting from the Interaction of Copper with Menadione (Vitamin K3)–a Model for Metal-mediated Oxidant Generation in Living Systems. *J Inorg Biochem*. 2018. doi:10.1016/j.jinorgbio.2018.08.007

305. Castro FAV, Mariani D, Panek AD, Eleutherio ECA, Pereira MD. Cytotoxicity mechanism of two naphthoquinones (menadione and plumbagin) in Saccharomyces cerevisiae. *PLoS One*. 2008. doi:10.1371/journal.pone.0003999

306. Bissell MJ, Inman J. Reprogramming stem cells is a microenvironmental task. *Proc Natl Acad Sci U S A*. 2008. doi:10.1073/pnas.0808457105

307. Armstrong JS, Steinauer KK, Hornung B, et al. Role of glutathione depletion and reactive oxygen species generation in apoptotic signaling in a human B lymphoma cell line. *Cell Death Differ*. 2002. doi:10.1038/sj.cdd.4400959

308. Di Monte D, Bellomo G, Thor H, Nicotera P, Orrenius S. Menadione-induced cytotoxicity is associated with protein thiol oxidation and alteration in intracellular

Ca2+ homeostasis. *Arch Biochem Biophys*. 1984. doi:10.1016/0003-9861(84)90207-8

309. Loor G, Kondapalli J, Schriewer JM, Chandel NS, Vanden Hoek TL, Schumacker PT. Menadione triggers cell death through ROS-dependent mechanisms involving PARP activation without requiring apoptosis. *Free Radic Biol Med*. 2010. doi:10.1016/j.freeradbiomed.2010.09.021

310. Tareen B, Summers JL, Jamison JM, et al. A 12 week, open label, phase I/IIa study using apatone for the treatment of prostate cancer patients who have failed standard therapy. *Int J Med Sci*. 2008;5(2):62-67. doi:10.7150/ijms.5.62

311. Tetef M, Margolin K, Ahn C, et al. Mitomycin C and menadione for the treatment of lung cancer: a phase II trial. *Invest New Drugs*. 1995. doi:10.1007/BF00872865

312. Gilloteaux J, Jamison JM, Neal DR, Loukas M, Doberzstyn T, Summers JL. Cell damage and death by autoschizis in human bladder (RT4) carcinoma cells resulting from treatment with ascorbate and menadione. In: *Ultrastructural Pathology*. ; 2010. doi:10.3109/01913121003662304

313. J. G, JM. J, D. A, et al. Cancer cell necrosis by autoschizis: synergism of antitumor activity of vitamin C: vitamin K3 on human bladder carcinoma T24 cells. *Scanning*. 1998.

314. Gilloteaux J, Jamison JM, Arnold D, Summers JL. Autoschizis: another cell death for cancer cells induced by oxidative stress. *Ital J Anat Embryol*. 2001.

315. Verrax J, Cadrobbi J, Delvaux M, et al. The association of vitamins C and K3 kills cancer cells mainly by autoschizis, a novel form of cell death. Basis for their potential use as coadjuvants in anticancer therapy. *Eur J Med Chem*. 2003. doi:10.1016/S0223-5234(03)00082-5

316. Gilloteaux J, Jamison JM, Neal DR. Cell death by autoschizis in TRAMP prostate carcinoma cells as a result of treatment by ascorbate: Menadione combination. In: *Ultrastructural Pathology*. ; 2005. doi:10.1080/01913120590951239

317. Cutruzzolà F, Giardina G, Marani M, et al. Glucose metabolism in the progression of prostate cancer. *Front Physiol*. 2017. doi:10.3389/fphys.2017.00097

318. STEMCELL Technologies. Using a hemocytometer for cell counting protocol.

STEMCELL Technologies. https://www.stemcell.com/how-to-count-cells-with-a-hemocytometer.html. Published March 2020. Accessed March 20, 2023.

319. Agilent Technologies. Agilent Seahorse XF Cell Mito Stress Test Kit. User Guide. Kit 103015-100. User Guide. https://www.agilent.com/cs/library/usermanuals/public/XF_Cell_Mito_Stress_Test_Kit_User_Guide.pdf. Published 2019.

320. Agilent Technologies I. *Agilent Seahorse XFp Real-Time ATP Rate Assay Kit*. Santa Clara, CA; 2018. https://www.agilent.com/cs/library/usermanuals/public/103591-400_Seahorse_XFp_ATP_Rate_Assay_Kit_User_Guide.pdf.

321. *Measuring the Metabolic Switch in Cancer Cells Metabolic Profile Provides New Insight into Choices of Therapeutic Intervention Application Brief*. https://www.agilent.com/cs/library/applications/metabolic_switch_cancer.pdf. Accessed February 18, 2019.

322. Luminex. Amnis® CellStream® Flow Cytometers. Luminex Webpage. https://www.luminexcorp.com/cellstream-flow-cytometers/#overview. Accessed March 20, 2023.

323. Thermo Fisher Scientific Inc. JC-1 Dye for Mitochondrial Membrane Potential. Thermo Fisher Scientific Inc. Webpage. https://www.thermofisher.com/uk/en/home/life-science/cell-analysis/cell-viability-and-regulation/apoptosis/mitochondria-function/jc-1-dye-mitochondrial-membrane-potential.html. Published 2006. Accessed January 31, 2023.

324. SCIEX. QTRAP® 6500 LC-MS/MS System. https://sciex.com/products/mass-spectrometers/qtrap-systems/qtrap-6500-system.

325. Zaro JL. Lipid-Based Drug Carriers for Prodrugs to Enhance Drug Delivery. *AAPS J*. 2014. doi:10.1208/s12248-014-9670-z

326. Chakraborty S, Shukla D, Mishra B, Singh S. Lipid - An emerging platform for oral delivery of drugs with poor bioavailability. *Eur J Pharm Biopharm*. 2009. doi:10.1016/j.ejpb.2009.06.001

327. Schieber M, Chandel NS. ROS function in redox signaling and oxidative stress. *Curr Biol*. 2014. doi:10.1016/j.cub.2014.03.034

328. Xu H, Jones LH. Click chemistry patents and their impact on drug discovery and chemical biology. *Pharm Pat Anal*. 2015;4(2). doi:10.4155/ppa.14.59

329. Agalave SG, Maujan SR, Pore VS. Click chemistry: 1,2,3-triazoles as pharmacophores. *Chem - An Asian J*. 2011;6(10):2696-2718. doi:10.1002/asia.201100432

330. Chaturvedi P, Chaturvedi N, Gupta S, Mishra A, Singh M, Siddhartha T. Click chemistry: A new approach for drug discovery. *Int J Pharm Sci Rev Res*. 2011;10(2).

331. Takayama Y, Kusamori K, Nishikawa M. Click chemistry as a tool for cell engineering and drug delivery. *Molecules*. 2019;24(1). doi:10.3390/molecules24010172

332. Yi G, Son J, Yoo J, Park C, Koo H. Application of click chemistry in nanoparticle modification and its targeted delivery. *Biomater Res*. 2018;22(1). doi:10.1186/s40824-018-0123-0

333. Ferreira LMR. Cancer metabolism: The Warburg effect today. *Exp Mol Pathol*. 2010. doi:10.1016/j.yexmp.2010.08.006

334. Gonzalez-Menendez P, Hevia D, Alonso R, Gonzalez-Pola I, Mayo JC, Sainz RM. GLUT1/GLUT4 balance is a marker of androgen-insensitivity in prostate cancer. *Eur J Cancer*. 2016;61. doi:10.1016/s0959-8049(16)61134-6

335. Gonzalez-Menendez P, Hevia D, Alonso-Arias R, et al. GLUT1 protects prostate cancer cells from glucose deprivation-induced oxidative stress. *Redox Biol*. 2018;17. doi:10.1016/j.redox.2018.03.017

336. Gonzalez-Menendez P, Hevia D, Rodriguez-Garcia A, Mayo JC, Sainz RM. Regulation of GLUT transporters by flavonoids in androgen-sensitive and-insensitive prostate cancer cells. *Endocrinol (United States)*. 2014;155(9). doi:10.1210/en.2014-1260

337. Wanjari UR, Mukherjee AG, Gopalakrishnan AV, et al. Role of Metabolism and Metabolic Pathways in Prostate Cancer. *Metabolites*. 2023;13(2). doi:10.3390/metabo13020183

338. Cham J, Venkateswaran AR, Bhangoo M. Targeting the PI3K-AKT-mTOR Pathway in Castration Resistant Prostate Cancer: A Review Article. *Clin Genitourin Cancer*.

2021;19(6). doi:10.1016/j.clgc.2021.07.014

339. Tortorella E, Giantulli S, Sciarra A, Silvestri I. AR and PI3K/AKT in Prostate Cancer: A Tale of Two Interconnected Pathways. *Int J Mol Sci*. 2023;24(3). doi:10.3390/ijms24032046

340. Chen JY, Wang FB, Xu H, et al. High glucose promotes prostate cancer cells apoptosis via Nrf2/ARE signaling pathway. *Eur Rev Med Pharmacol Sci*. 2019;23(3). doi:10.26355/EURREV_201908_18647

341. Coller HA. Is cancer a metabolic disease? 9582978472. *Am J Pathol*. 2014. doi:10.1016/j.ajpath.2013.07.035

342. Gilloteaux J, Jamison JM, Neal D, Summers JL. Synergistic antitumor cytotoxic actions of ascorbate and menadione on human prostate (DU145) cancer cells in Vitro: Nucleus and other injuries preceding cell death by autoschizis. *Ultrastruct Pathol*. 2014. doi:10.3109/01913123.2013.852645

343. Damiani E, Solorio JA, Doyle AP, Wallace HM. How reliable are in vitro IC50 values? Values vary with cytotoxicity assays in human glioblastoma cells. *Toxicol Lett*. 2019;302. doi:10.1016/j.toxlet.2018.12.004

344. Rampersad SN. Multiple applications of alamar blue as an indicator of metabolic function and cellular health in cell viability bioassays. *Sensors (Switzerland)*. 2012;12(9). doi:10.3390/s120912347

345. Erikstein BS, Hagland HR, Nikolaisen J, et al. Cellular stress induced by resazurin leads to autophagy and cell death via production of reactive oxygen species and mitochondrial impairment. *J Cell Biochem*. 2010;111(3). doi:10.1002/jcb.22741

346. Venugopal M, Jamison JM, Gilloteaux J, et al. Synergistic antitumour activity of vitamins C and K3 against human prostate carcinoma cell lines. *Cell Biol Int*. 1996. doi:10.1006/cbir.1996.0102

347. Shaw RJ. Glucose metabolism and cancer. *Curr Opin Cell Biol*. 2006. doi:10.1016/j.ceb.2006.10.005

348. Smirnoff N. Ascorbic acid: Metabolism and functions of a multi-facetted molecule. *Curr Opin Plant Biol*. 2000. doi:10.1016/S1369-5266(00)00069-8

349. Osada S, Tomita H, Tanaka Y, et al. The utility of vitamin K3 (menadione) against pancreatic cancer. *Anticancer Res*. 2008.

350. Zadziński R, Fortuniak A, Biliński T, Grey M, Bartosz G. Menadione toxicity in saccharomyces cerevisiae cells: Activation by conjugation with glutathione. *Biochem Mol Biol Int*. 1998. doi:10.1080/15216549800201792

351. Ciuleanu TE, Pavlovsky A V., Bodoky G, et al. A randomised Phase III trial of glufosfamide compared with best supportive care in metastatic pancreatic adenocarcinoma previously treated with gemcitabine. *Eur J Cancer*. 2009;45(9). doi:10.1016/j.ejca.2008.12.022

352. Annunziata A, Cucciolito ME, Esposito R, et al. A highly efficient and selective antitumor agent based on a glucoconjugated carbene platinum(ii) complex. *Dalt Trans*. 2019;48(22). doi:10.1039/c9dt01614g

353. Sigma Aldrich. 6-Azidohexanoic acid. Sigma Aldrich Webpage. https://www.sigmaaldrich.com/IE/en/product/aldrich/900930. Accessed March 10, 2023.

354. Lu H, Mei C, Yang L, et al. PPM-18, an Analog of Vitamin K, Induces Autophagy and Apoptosis in Bladder Cancer Cells Through ROS and AMPK Signaling Pathways. *Front Pharmacol*. 2021;12. doi:10.3389/fphar.2021.684915

355. Pelageev DN, Dyshlovoy SA, Pokhilo ND, et al. Quinone-carbohydrate nonglucoside conjugates as a new type of cytotoxic agents: Synthesis and determination of in vitro activity. *Eur J Med Chem*. 2014;77. doi:10.1016/j.ejmech.2014.03.006

356. Lu J-J, Bao J-L, Wu G-S, et al. Quinones Derived from Plant Secondary Metabolites as Anti-cancer Agents. *Anticancer Agents Med Chem*. 2013;13(3). doi:10.2174/1871520611313030008

357. Gul S, Maqbool MF, Maryam A, et al. Vitamin K: A novel cancer chemosensitizer. *Biotechnol Appl Biochem*. 2022;69(6). doi:10.1002/bab.2312

358. Davis-Yadley AH, Malafa MP. Vitamins in pancreatic cancer: A review of underlying mechanisms and future applications. *Adv Nutr*. 2015;6(6). doi:10.3945/an.115.009456

359. Lu H, Mei C, Yang L, et al. PPM-18, an Analog of Vitamin K, Induces Autophagy and Apoptosis in Bladder Cancer Cells Through ROS and AMPK Signaling Pathways. *Front Pharmacol*. 2021;12. doi:10.3389/fphar.2021.684915

360. Morales P, Vara D, Goméz-Cañas M, et al. Synthetic cannabinoid quinones: Preparation, in vitro antiproliferative effects and in vivo prostate antitumor activity. *Eur J Med Chem*. 2013;70:111-119. doi:10.1016/j.ejmech.2013.09.043

361. Dyshlovoy SA, Pelageev DN, Hauschild J, et al. Successful targeting of thewarburg effect in prostate cancer by glucose-conjugated 1,4-naphthoquinones. *Cancers (Basel)*. 2019;11(11). doi:10.3390/cancers11111690

362. Bader DA, McGuire SE. Tumour metabolism and its unique properties in prostate adenocarcinoma. *Nat Rev Urol*. 2020;17(4):214-231. doi:10.1038/s41585-020-0288-x

363. Sreekumar A, Poisson LM, Rajendiran TM, et al. Metabolomic profiles delineate potential role for sarcosine in prostate cancer progression. *Nature*. 2009. doi:10.1038/nature07762

364. Trock BJ. Application of metabolomics to prostate cancer. *Urol Oncol Semin Orig Investig*. 2011;29(5):572-581. doi:10.1016/j.urolonc.2011.08.002

365. Wu X, Daniels G, Lee P, Monaco ME. Lipid metabolism in prostate cancer. *Am J Clin Exp Urol*. 2014.

366. Pavlova NN, Thompson CB. The Emerging Hallmarks of Cancer Metabolism. *Cell Metab*. 2016. doi:10.1016/j.cmet.2015.12.006

367. Renner K, Singer K, Koehl GE, et al. Metabolic hallmarks of tumor and immune cells in the tumor microenvironment. *Front Immunol*. 2017. doi:10.3389/fimmu.2017.00248

368. Hill BG, Benavides GA, Lancaster JJR, et al. Integration of cellular bioenergetics with mitochondrial quality control and autophagy. In: *Biological Chemistry*. Vol 393. ; 2012. doi:10.1515/hsz-2012-0198

369. Freya TG, Mannellab CA. The internal structure of mitochondria. *Trends Biochem Sci*. 2000;25(7). doi:10.1016/S0968-0004(00)01609-1

370. Xue C, Pasolli HA, Piscopo I, et al. Mitochondrial structure alteration in human prostate cancer cells upon initial interaction with a chemopreventive agent phenethyl isothiocyanate. *Cancer Cell Int*. 2014;14(1). doi:10.1186/1475-2867-14-30

371. Frey TG, Renken CW, Perkins GA. Insight into mitochondrial structure and function from electron tomography. *Biochim Biophys Acta - Bioenerg*. 2002;1555(1-3). doi:10.1016/S0005-2728(02)00278-5

372. Papaliagkas V, Anogianaki A, Anogianakis G, Ilonidis G. The proteins and the mechanisms of apoptosis: A mini-review of the fundamentals. *Hippokratia*. 2007;11(3).

373. Ljubava D Zorova 1, Vasily A Popkov 2, Egor Y Plotnikov 3, Denis N Silachev 3, Irina B Pevzner 3, Stanislovas S Jankauskas 3, Valentina A Babenko 2, Savva D Zorov 4, Anastasia V Balakireva 5, Magdalena Juhaszova 6, Steven J Sollott 6 DBZ 7. Mitochondrial membrane potential. *Anal Biochem*. 2018;1(552):50-59. doi:10.1016/j.ab.2017.07.009.

374. Porporato PE, Filigheddu N, Pedro JMBS, Kroemer G, Galluzzi L. Mitochondrial metabolism and cancer. *Cell Res*. 2018. doi:10.1038/cr.2017.155

375. Heiden MG Vander. Understanding the Warburg Effect. *Science (80-)*. 2009. doi:10.1126/science.1160809

376. Heiden M Vander, Cantley L, Thompson C. Understanding the Warburg Effect : Cell Proliferation. *Science (80-)*. 2009. doi:10.1126/science.1160809

377. Vyas S, Zaganjor E, Haigis MC. Mitochondria and Cancer. *Cell*. 2016. doi:10.1016/j.cell.2016.07.002

378. Lynam-Lennon N, Maher SG, Maguire A, et al. Altered mitochondrial function and energy metabolism is associated with a radioresistant phenotype in oesophageal adenocarcinoma. *PLoS One*. 2014;9(6). doi:10.1371/journal.pone.0100738

379. Kalyanaraman B, Cheng G, Hardy M, et al. A review of the basics of mitochondrial bioenergetics, metabolism, and related signaling pathways in cancer cells: Therapeutic targeting of tumor mitochondria with lipophilic cationic compounds. *Redox Biol*. 2018;14. doi:10.1016/j.redox.2017.09.020

380. Cheng J yan, Yang J bo, Liu Y, et al. Profiling and targeting of cellular mitochondrial

bioenergetics: inhibition of human gastric cancer cell growth by carnosine. *Acta Pharmacol Sin*. 2019;40(7). doi:10.1038/s41401-018-0182-8

381. Kalyanaraman B, Cheng G, Hardy M, et al. Corrigendum to 'A review of the basics of mitochondrial bioenergetics, metabolism, and related signaling pathways in cancer cells: Therapeutic targeting of tumor mitochondria with lipophilic cationic compounds' [REDOX 14C (2017) 316–327] (S2213231717306614) (10.1016/j.redox.2017.09.020)). *Redox Biol*. 2018;16. doi:10.1016/j.redox.2018.03.001

382. Hara N, Nishiyama T. Androgen Metabolic Pathway Involved in Current and Emerging Treatment for Men with Castration Resistant Prostate Cancer: Intraprostatic Androgens as Therapeutic Targets and Endocrinological Biomarkers. *Curr Drug Targets*. 2014. doi:10.2174/1389450115666141024114736

383. Costello LC, Franklin RB. Novel role of zinc in the regulation of prostate citrate metabolism and its implications in prostate cancer. *Prostate*. 1998. doi:10.1002/(SICI)1097-0045(19980601)35:4<285::AID-PROS8>3.0.CO;2-F

384. Uo T, Sprenger CC, Plymate SR. Androgen Receptor Signaling and Metabolic and Cellular Plasticity During Progression to Castration Resistant Prostate Cancer. *Front Oncol*. 2020;10:2275. doi:10.3389/fonc.2020.580617

385. Swinnen J V., Heemers H, Van De Sande T, et al. Androgens, lipogenesis and prostate cancer. *J Steroid Biochem Mol Biol*. 2004;92(4):273-279. doi:10.1016/j.jsbmb.2004.10.013

386. Massie CE, Lynch A, Ramos-Montoya A, et al. The androgen receptor fuels prostate cancer by regulating central metabolism and biosynthesis. *EMBO J*. 2011. doi:10.1038/emboj.2011.158

387. Pertega-Gomes N, Felisbino S, Massie CE, et al. A glycolytic phenotype is associated with prostate cancer progression and aggressiveness: A role for monocarboxylate transporters as metabolic targets for therapy. *J Pathol*. 2015. doi:10.1002/path.4547

388. McDunn JE, Li Z, Adam KP, et al. Metabolomic signatures of aggressive prostate cancer. *Prostate*. 2013;73(14):1547-1560. doi:10.1002/pros.22704

389. Grossmann M, Wittert G. Androgens, diabetes and prostate cancer. *Endocr Relat Cancer*. 2012;19(5). doi:10.1530/ERC-12-0067

390. Cho NH, Shaw JE, Karuranga S, et al. IDF Diabetes Atlas: Global estimates of diabetes prevalence for 2017 and projections for 2045. *Diabetes Res Clin Pract*. 2018;138. doi:10.1016/j.diabres.2018.02.023

391. Selvin E, Feinleib M, Zhang L, et al. Androgens and diabetes in men: Results from the Third National Health and Nutrition Examination Survey (NHANES III). *Diabetes Care*. 2007;30(2). doi:10.2337/dc06-1579

392. Mayo Clinic. Diabetes. https://www.mayoclinic.org/diseases-conditions/diabetes/diagnosis-treatment/drc-20371451#:~:text=A blood sugar level less,mmol%2FL) indicates prediabetes. Published 2020. Accessed January 11, 2020.

393. Li Z, Sun C, Qin Z. Metabolic reprogramming of cancer-associated fibroblasts and its effect on cancer cell reprogramming. *Theranostics*. 2021;11(17). doi:10.7150/THNO.62378

394. Wanandi SI, Ningsih SS, Asikin H, Hosea R, Neolaka GMG. Metabolic interplay between tumour cells and cancer-associated fibroblasts (CAFs) under hypoxia versus normoxia. *Malaysian J Med Sci*. 2018;25(3). doi:10.21315/mjms2018.25.3.2

395. Eisenberg L, Eisenberg-Bord M, Eisenberg-Lerner A, Sagi-Eisenberg R. Metabolic alterations in the tumor microenvironment and their role in oncogenesis. *Cancer Lett*. 2020;484. doi:10.1016/j.canlet.2020.04.016

396. Jastroch M, Divakaruni AS, Mookerjee S, Treberg JR, Brand MD. Mitochondrial proton and electron leaks. *Essays Biochem*. 2010;47. doi:10.1042/BSE0470053

397. Altea-Manzano P, Cuadros AM, Broadfield LA, Fendt S. Nutrient metabolism and cancer in the in vivo context: a metabolic game of give and take . *EMBO Rep*. 2020;21(10). doi:10.15252/embr.202050635

398. Ahmadiankia N, Bagheri M, Fazli M. Nutrient deprivation modulates the metastatic potential of breast cancer cells. *Reports Biochem Mol Biol*. 2019;8(2).

399. Esteras N, Adjobo-Hermans MJW, Abramov AY, Koopman WJH. Visualization of mitochondrial membrane potential in mammalian cells. *Methods Cell Biol*. 2020;155:221-245. doi:10.1016/BS.MCB.2019.10.003

400. Rovini A, Heslop K, Hunt EG, et al. Quantitative analysis of mitochondrial membrane potential heterogeneity in unsynchronized and synchronized cancer cells. *FASEB J*. 2021;35(1). doi:10.1096/fj.202001693R

401. Momcilovic M, Jones A, Bailey ST, et al. In vivo imaging of mitochondrial membrane potential in non-small-cell lung cancer. *Nature*. 2019;575(7782). doi:10.1038/s41586-019-1715-0

402. Zhang B bei, Wang D gang, Guo F fen, Xuan C. Mitochondrial membrane potential and reactive oxygen species in cancer stem cells. *Fam Cancer*. 2015;14(1). doi:10.1007/s10689-014-9757-9

403. Lee Y-X, Lin P-H, Rahmawati E, Ma Y-Y, Chan C, Tzeng C-R. Mitochondria Research in Human Reproduction. *The Ovary*. January 2019:327-335. doi:10.1016/B978-0-12-813209-8.00020-0

404. Apel K, Hirt H. Reactive oxygen species: metabolism, oxidative stress, and signal transduction. *Annu Rev Plant Biol*. 2004. doi:10.1146/annurev.arplant.55.031903.141701

405. Zorov DB, Juhaszova M, Sollott SJ. Mitochondrial reactive oxygen species (ROS) and ROS-induced ROS release. *Physiol Rev*. 2014;94(3). doi:10.1152/physrev.00026.2013

406. Held P. *An Introduction to Reactive Oxygen Species Measurement of ROS in Cells*. Vermont, USA; 2012. http://www.biotek.com/resources/articles/reactive-oxygen-species.html.

407. Kowaltowski AJ, de Souza-Pinto NC, Castilho RF, Vercesi AE. Mitochondria and reactive oxygen species. *Free Radic Biol Med*. 2009. doi:10.1016/j.freeradbiomed.2009.05.004

408. Fogg VC, Lanning NJ, MacKeigan JP. Mitochondria in cancer: At the crossroads of life and death. *Chin J Cancer*. 2011;30(8). doi:10.5732/cjc.011.10018

409. George S, Abrahamse H. Redox potential of antioxidants in cancer progression and prevention. *Antioxidants*. 2020;9(11). doi:10.3390/antiox9111156

410. Irani K. Reactive oxygen species. In: *Endothelial Biomedicine*. ; 2007. doi:10.1017/CBO9780511546198.043

411. Circu ML, Aw TY. Reactive oxygen species, cellular redox systems, and apoptosis. *Free Radic Biol Med*. 2010. doi:10.1016/j.freeradbiomed.2009.12.022

412. Murphy MP. How mitochondria produce reactive oxygen species. *Biochem J*. 2008. doi:10.1042/bj20081386

413. Liou G-Y, Storz P. Reactive oxygen species in cancer. *Free Radic Res*. 2010. doi:10.3109/10715761003667554

414. Sena LA, Chandel NS. Physiological roles of mitochondrial reactive oxygen species. *Mol Cell*. 2012. doi:10.1016/j.molcel.2012.09.025

415. Schumacker PT. Reactive oxygen species in cancer cells: Live by the sword, die by the sword. *Cancer Cell*. 2006. doi:10.1016/j.ccr.2006.08.015

416. Circu ML, Aw TY. Reactive oxygen species, cellular redox systems, and apoptosis. *Free Radic Biol Med*. 2010. doi:10.1016/j.freeradbiomed.2009.12.022

417. Breheny D. Environmental reactive oxygen species and cancer. In: *Systems Biology of Free Radicals and Antioxidants*. ; 2012. doi:10.1007/978-3-642-30018-9_119

418. Turrens JF. Mitochondrial formation of reactive oxygen species. *J Physiol*. 2003. doi:10.1113/jphysiol.2003.049478

419. Kopinski PK, Singh LN, Zhang S, Lott MT, Wallace DC. Mitochondrial DNA variation and cancer. *Nat Rev Cancer*. 2021;21(7). doi:10.1038/s41568-021-00358-w

420. Fruehauf JP, Meyskens FL. Reactive oxygen species: A breath of life or death? *Clin Cancer Res*. 2007. doi:10.1158/1078-0432.CCR-06-2082

421. Di Monte D, Ross D, Bellomo G, Eklöw L, Orrenius S. Alterations in intracellular thiol homeostasis during the metabolism of menadione by isolated rat hepatocytes. *Arch Biochem Biophys*. 1984. doi:10.1016/0003-9861(84)90206-6

422. Criddle DN, Gillies S, Baumgartner-Wilson HK, et al. Menadione-induced reactive oxygen species generation via redox cycling promotes apoptosis of murine pancreatic acinar cells. *J Biol Chem*. 2006. doi:10.1074/jbc.M607704200

423. Caricchio R, Kovalenko D, Kaufmann WK, Cohen PL. Apoptosis provoked by the oxidative stress inducer menadione (vitamin K3) is mediated by the Fas/Fas ligand

system. *Clin Immunol*. 1999. doi:10.1006/clim.1999.4757

424. Wolff G, Toborek M. Targeting the therapeutic effects of exercise on redox-sensitive mechanisms in the vascular endothelium during tumor progression. *IUBMB Life*. 2013;65(7). doi:10.1002/iub.1169

425. Ray PD, Huang BW, Tsuji Y. Reactive oxygen species (ROS) homeostasis and redox regulation in cellular signaling. *Cell Signal*. 2012. doi:10.1016/j.cellsig.2012.01.008

426. Wei Z, Liu X, Cheng C, Yu W, Yi P. Metabolism of Amino Acids in Cancer. *Front Cell Dev Biol*. 2021;8. doi:10.3389/fcell.2020.603837

427. Yoo HC, Han JM. Amino acid metabolism in cancer drug resistance. *Cells*. 2022;11(1). doi:10.3390/cells11010140

428. Strmiska V, Michalek P, Eckschlager T, et al. Prostate cancer-specific hallmarks of amino acids metabolism: Towards a paradigm of precision medicine. *Biochim Biophys Acta - Rev Cancer*. 2019;1871(2):248-258. doi:10.1016/j.bbcan.2019.01.001

429. Vučetić M, Cormerais Y, Parks SK, Pouysségur J. The central role of amino acids in cancer redox homeostasis: Vulnerability points of the cancer redox code. *Front Oncol*. 2017;7(DEC). doi:10.3389/fonc.2017.00319

430. Nakanishi S, Cleveland JL. Polyamine Homeostasis in Development and Disease. *Med Sci*. 2021;9(2). doi:10.3390/medsci9020028

431. Novita Sari I, Setiawan T, Seock Kim K, Toni Wijaya Y, Won Cho K, Young Kwon H. Metabolism and function of polyamines in cancer progression. *Cancer Lett*. 2021;519:91-104. doi:10.1016/j.canlet.2021.06.020

432. Miller-Fleming L, Olin-Sandoval V, Campbell K, Ralser M. Remaining Mysteries of Molecular Biology: The Role of Polyamines in the Cell. *J Mol Biol*. 2015;427(21):3389-3406. doi:10.1016/j.jmb.2015.06.020

433. Agostinelli E, Tempera G, Molinari A, et al. The physiological role of biogenic amines redox reactions in mitochondria. New perspectives in cancer therapy. *Amino Acids*. 2007;33(2). doi:10.1007/s00726-007-0510-7

434. Toninello A, Pietrangeli P, De Marchi U, Salvi M, Mondovì B. Amine oxidases in apoptosis and cancer. *Biochim Biophys Acta - Rev Cancer*. 2006;1765(1). doi:10.1016/j.bbcan.2005.09.001

435. Tsoi TH, Chan CF, Chan WL, et al. Urinary polyamines: A pilot study on their roles as prostate cancer detection biomarkers. *PLoS One*. 2016;11(9). doi:10.1371/journal.pone.0162217

436. Liu X han, Zhai X yue. Role of tryptophan metabolism in cancers and therapeutic implications. *Biochimie*. 2021;182:131-139. doi:10.1016/j.biochi.2021.01.005

437. Companioni O, Mir C, Garcia-Mayea Y, LLeonart ME. Targeting Sphingolipids for Cancer Therapy. *Front Oncol*. 2021;11. doi:10.3389/fonc.2021.745092

438. Saddoughi SA, Ogretmen B. Diverse Functions of Ceramide in Cancer Cell Death and Proliferation. In: *Advances in Cancer Research*. Vol 117. ; 2013. doi:10.1016/B978-0-12-394274-6.00002-9

439. Huang W-C, Chen C-L, Lin Y-S, Lin C-F. Apoptotic Sphingolipid Ceramide in Cancer Therapy. *J Lipids*. 2011;2011. doi:10.1155/2011/565316

440. Li Z, Zhang L, Liu D, Wang C. Ceramide glycosylation and related enzymes in cancer signaling and therapy. *Biomed Pharmacother*. 2021;139. doi:10.1016/j.biopha.2021.111565

441. Bian X, Qian Y, Tan B, et al. In-depth mapping carboxylic acid metabolome reveals the potential biomarkers in colorectal cancer through characteristic fragment ions and metabolic flux. *Anal Chim Acta*. 2020;1128. doi:10.1016/j.aca.2020.06.064

442. Arslan E, Koyuncu I. Comparison of amino acid metabolisms in normal prostate (pnt-1a) and cancer cells (pc-3). *Oncologie*. 2021;23(1). doi:10.32604/ONCOLOGIE.2021.014764

443. Kracklauer M. Molecular Cancer. *Mol Cancer*. 2010. doi:10.1186/1476-4598-6-81

444. Yu L, Chen X, Wang L, Chen S. The sweet trap in tumors: aerobic glycolysis and potential targets for therapy. *Oncotarget*. 2016. doi:10.18632/oncotarget.7676

445. Bader DA, McGuire SE. Tumour metabolism and its unique properties in prostate adenocarcinoma. *Nat Rev Urol*. 2020;17(4). doi:10.1038/s41585-020-0288-x

446. de la Cruz-López KG, Castro-Muñoz LJ, Reyes-Hernández DO, García-Carrancá A, Manzo-Merino J. Lactate in the Regulation of Tumor Microenvironment and Therapeutic Approaches. *Front Oncol*. 2019;9. doi:10.3389/fonc.2019.01143

447. Fabyan K, Holtzclaw A, Sherner J. PROSTATE LACTATE: A CASE OF SEVERE LACTIC ACIDOSIS WITH AN INTERESTING MECHANISM OF ACTION. *Chest*. 2019;156(4). doi:10.1016/j.chest.2019.08.2050

448. Munoz J, Mohd Khushman MK, Amr Hanbali AH, Stoltenberg M. Severe lactic acidosis in a patient with metastatic prostate cancer. *J Cancer Res Ther*. 2011;7(2). doi:10.4103/0973-1482.82925

449. Van Der Mijn JC, Kuiper MJ, Siegert CEH, Wassenaar AE, Van Noesel CJM, Ogilvie AC. Lactic acidosis in prostate cancer: Consider the warburg effect. *Case Rep Oncol*. 2017;10(3). doi:10.1159/000485242

450. D'Aniello C, Patriarca EJ, Phang JM, Minchiotti G. Proline Metabolism in Tumor Growth and Metastatic Progression. *Front Oncol*. 2020;10. doi:10.3389/fonc.2020.00776

451. Bonifácio VDB, Pereira SA, Serpa J, Vicente JB. Cysteine metabolic circuitries: druggable targets in cancer. *Br J Cancer*. 2020. doi:10.1038/s41416-020-01156-1

452. Turner MD, Sale C, Garner AC, Hipkiss AR. Anti-cancer actions of carnosine and the restoration of normal cellular homeostasis. *Biochim Biophys Acta - Mol Cell Res*. 2021;1868(11). doi:10.1016/j.bbamcr.2021.119117

453. Prakash MD, Fraser S, Boer JC, Plebanski M, de Courten B, Apostolopoulos V. Anti-cancer effects of carnosine—a dipeptide molecule. *Molecules*. 2021;26(6). doi:10.3390/molecules26061644

454. Phang JM, Liu W, Hancock CN, Fischer JW. Proline metabolism and cancer: Emerging links to glutamine and collagen. *Curr Opin Clin Nutr Metab Care*. 2015;18(1). doi:10.1097/MCO.0000000000000121

455. Phang JM. Proline metabolism in cell regulation and cancer biology: Recent advances and hypotheses. *Antioxidants Redox Signal*. 2019;30(4). doi:10.1089/ars.2017.7350

456. Yoo HC, Han JM. Amino acid metabolism in cancer drug resistance. *Cells*.

2022;11(1). doi:10.3390/cells11010140

457. Lee BC, Gladyshev VN. The biological significance of methionine sulfoxide stereochemistry. *Free Radic Biol Med*. 2011;50(2). doi:10.1016/j.freeradbiomed.2010.11.008

458. Kar F, Hacioglu C, Kacar S, Sahinturk V, Kanbak G. Betaine suppresses cell proliferation by increasing oxidative stress–mediated apoptosis and inflammation in DU-145 human prostate cancer cell line. *Cell Stress Chaperones*. 2019;24(5). doi:10.1007/s12192-019-01022-x

459. Ueland PM, Holm PI, Hustad S. Betaine: A key modulator of one-carbon metabolism and homocysteine status. *Clin Chem Lab Med*. 2005;43(10). doi:10.1515/CCLM.2005.187

460. Birsoy K, Wang T, Chen WW, Freinkman E, Abu-Remaileh M, Sabatini DM. An Essential Role of the Mitochondrial Electron Transport Chain in Cell Proliferation Is to Enable Aspartate Synthesis. *Cell*. 2015;162(3). doi:10.1016/j.cell.2015.07.016

461. Chen Y-L, Lowery AkT, Lin S, Walker AM, Chen K-HE. Tumor cell-derived asymmetric dimethylarginine regulates macrophage functions and polarization. *Cancer Cell Int*. 2022;22(1):351. doi:10.1186/s12935-022-02769-7

462. Kami Reddy KR, Dasari C, Vandavasi S, et al. Novel Cellularly Active Inhibitor Regresses DDAH1 Induced Prostate Tumor Growth by Restraining Tumor Angiogenesis through Targeting DDAH1/ADMA/NOS Pathway. *ACS Comb Sci*. 2019. doi:10.1021/acscombsci.8b00133

463. Chachaj A, Wiśniewski J, Rybka J, et al. Asymmetric and symmetric dimethylarginines and mortality in patients with hematological malignancies—A prospective study. *PLoS One*. 2018;13(5). doi:10.1371/journal.pone.0197148

464. Abdul M, Mccray SD, Hoosein NM. Expression of gamma-aminobutyric acid receptor (subtype A) in prostate cancer. *Acta Oncol (Madr)*. 2008;47(8):1546-1550. doi:10.1080/02841860801961265

465. Holeček M. Histidine in health and disease: Metabolism, physiological importance, and use as a supplement. *Nutrients*. 2020;12(3). doi:10.3390/nu12030848

466. Moro J, Tomé D, Schmidely P, Demersay TC, Azzout-Marniche D. Histidine: A

systematic review on metabolism and physiological effects in human and different animal species. *Nutrients*. 2020;12(5). doi:10.3390/nu12051414

467. Brosnan ME, Brosnan JT. Histidine metabolism and function. *J Nutr*. 2020;150:2570S-2575S. doi:10.1093/jn/nxaa079

468. Azuma H, Inamoto T, Sakamoto T, et al. Gamma-aminobutyric acid as a promoting factor of cancer metastasis; induction of matrix metalloproteinase production is potentially its underlying mechanism. *Cancer Res*. 2003;63(23):8090-8096.

469. Casero RA, Marton LJ. Targeting polyamine metabolism and function in cancer and other hyperproliferative diseases. *Nat Rev Drug Discov*. 2007;6(5):373-390. doi:10.1038/nrd2243

470. Sheridan M, Ogretmen B. The role of ceramide metabolism and signaling in the regulation of mitophagy and cancer therapy. *Cancers (Basel)*. 2021;13(10). doi:10.3390/cancers13102475

471. Ogretmen B. Sphingolipid metabolism in cancer signalling and therapy. *Nat Rev Cancer*. 2017;18(1). doi:10.1038/nrc.2017.96

472. Human Metabolome Data Base. Metabocard for Cer(d18:1/22:0) (HMDB0004952). Human Metabolome Database. https://hmdb.ca/metabolites/HMDB0004952. Accessed February 13, 2023.

473. Zhao Y, Butler EB, Tan M. Targeting cellular metabolism to improve cancer therapeutics. *Cell Death Dis*. 2013. doi:10.1038/cddis.2013.60

474. Nan F, Sun Y, Liang H, Zhou J, Ma X, Zhang D. Mannose: A Sweet Option in the Treatment of Cancer and Inflammation. *Front Pharmacol*. 2022;13. doi:10.3389/fphar.2022.877543

475. Gonzalez PS, O'Prey J, Cardaci S, et al. Mannose impairs tumour growth and enhances chemotherapy. *Nature*. 2018. doi:10.1038/s41586-018-0729-3

476. Zhang R, Yang Y, Dong W, et al. D-mannose facilitates immunotherapy and radiotherapy of triple-negative breast cancer via degradation of PD-L1. *Proc Natl Acad Sci U S A*. 2022;119(8). doi:10.1073/pnas.2114851119

477. Tiwari R, Manzar N, Ateeq B. Dynamics of Cellular Plasticity in Prostate Cancer

Progression. *Front Mol Biosci*. 2020;7. doi:10.3389/fmolb.2020.00130

478. Jurasz P, Alonso-Escolano D, Radomski MW. Platelet-cancer interactions: Mechanisms and pharmacology of tumour cell-induced platelet aggregation. *Br J Pharmacol*. 2004. doi:10.1038/sj.bjp.0706013

479. Gilleron J, Gerdes JM, Zeigerer A. Metabolic regulation through the endosomal system. *Traffic*. 2019;20(8). doi:10.1111/tra.12670

480. Mohrmann K, Gerez L, Oorschot V, Klumperman J, Van Der Sluijs P. rab4 function in membrane recycling from early endosomes depends on a membrane to cytoplasm cycle. *J Biol Chem*. 2002;277(35). doi:10.1074/jbc.M203064200

481. Putluri N, Shojaie A, Vasu VT, et al. Metabolomic profiling reveals a role for androgen in activating amino acid metabolism and methylation in prostate cancer cells. *PLoS One*. 2011;6(7). doi:10.1371/journal.pone.0021417

482. Hu J, Lei H, Fei X, et al. NES1/KLK10 gene represses proliferation, enhances apoptosis and down-regulates glucose metabolism of PC3 prostate cancer cells. *Sci Rep*. 2015;5. doi:10.1038/srep17426

483. Ferreri C, Sansone A, Buratta S, et al. The n-10 fatty acids family in the lipidome of human prostatic adenocarcinoma cell membranes and extracellular vesicles. *Cancers (Basel)*. 2020;12(4). doi:10.3390/cancers12040900

Chapter 9. Appendix

Appendix 1: Agilent Seahorse MitoStress and ATP Rate Test endpoints. Mean ± SD results for PNT1a, LNCaP, PC3 and Du145 cell lines (n=3) 1-way ANOVA). Values calculated by the Agilent Wave online results analyser

Cell Lines	Glucose Concentration	Basal Respiration (OCR)	H^+ leak	Maximal Respiration	Non-mitochondrial respiration	ATP Production	%OxPhos	% Glycolysis
PNT1a	0mM	67.8 ± 28.5	16.2 ± 5.6	94.5 ± 35.5	51.9 ± 4.3	24.6± 15.7	76.5 ± 11.7	24.4 ± 11.7
	5.5mM	29.9 ± 10.5	8.6 ±3.1	16.7 ± 5.4	35.8 ±3.1	11.4± 3.7	56.8 ±12.4	43.2 ± 12.4
	11mM	32.4 ± 6.2	6.5 ± 3.4	22.9 ± 7.9	6.8 ± 3.0	15.7± 5.1	47.4 ± 9.9	52.6 ± 9.9
LNCaP	0mM	281.0 ± 47.8	80.2 ± 21.6	380.1 ± 46.1	41.7 ± 7.2	200.8± 34.8	90.1 ± 2.2	9.9 ± 2.2
	5.5mM	233.3 ± 68	87.1 ± 31.2	303.42 ± 62.5	34.6 ± 10.3	146.2± 32.7	76.2 ± 3.4	23.8 ± 3.4
	11mM	255.0 ± 30.1	87.6 ± 19.3	323.78 ± 32.8	36.4 ± 5.9	167.4± 24.9	67.6 ± 3.9	32.4 ± 3.9
PC3	0mM	67.5 ± 15.8	24.8 ± 1.2	156.0 ± 11.2	3.5 ± 0.6	50.5± 18.3	74.8 ± 4.8	25.2 ± 4.8
	5.5mM	54.1 ± 9.3	26.5 ± 4.9	171.4 ±15.3	20.7 ± 4.2	51.3± 21.6	24.8 ± 23.8	75.2 ± 23.8
	11mM	87.4 ± 4.5	41.7 ± 3.7	235.51 ±18.9	20.4 ± 5.6	49.4± 15.8	22.9 ± 17.7	77.1 ± 17.7
Du145	0mM	130.5 ± 14.7	41.0 ± 5.3	177.8 ± 15.3	19.2 ± 1.5	113.2± 7.5	82.5 ± 3.9	17.5 ± 3.9
	5.5mM	137.8 ± 28.9	29.4 ± 9.4	259.4 ± 10.5	15.2 ± 4.9	147.1± 18.9	29.0 ± 9.4	71.0 ± 9.4
	11mM	124.9 ± 26.0	25.1 ± 4.8	255.8 ± 11.2	7.9 ± 6.2	106.4± 12.8	37.0 ± 3.9	63.0 ± 3.9

.

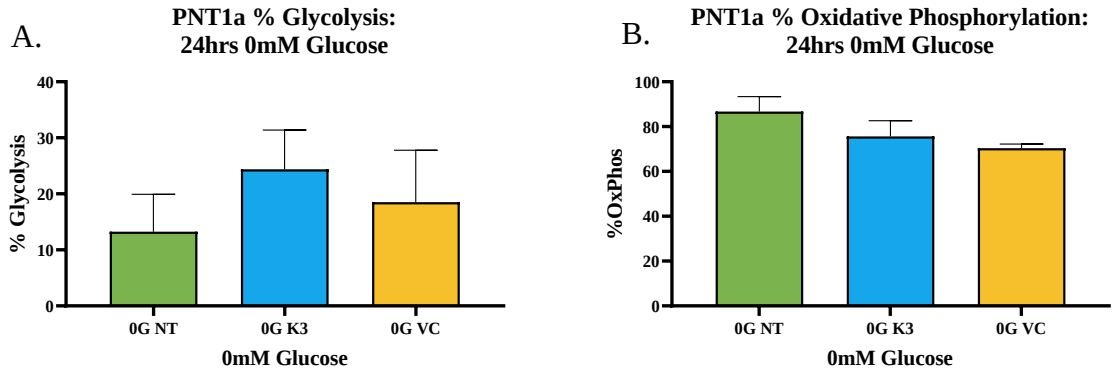

Appendix 2: The ATP endpoints of %OxPhos and %Glycolysis for PNT1a cells treated with Menadione (K3) and Vitamin C (VC) under zero glucose. (A.) % ATP production by glycolysis was unchanged between the untreated and the treated cells. (B.) % ATP Production by OxPhos was unchanged between the untreated and the treated cells. (n=3) 1-way ANOVA)

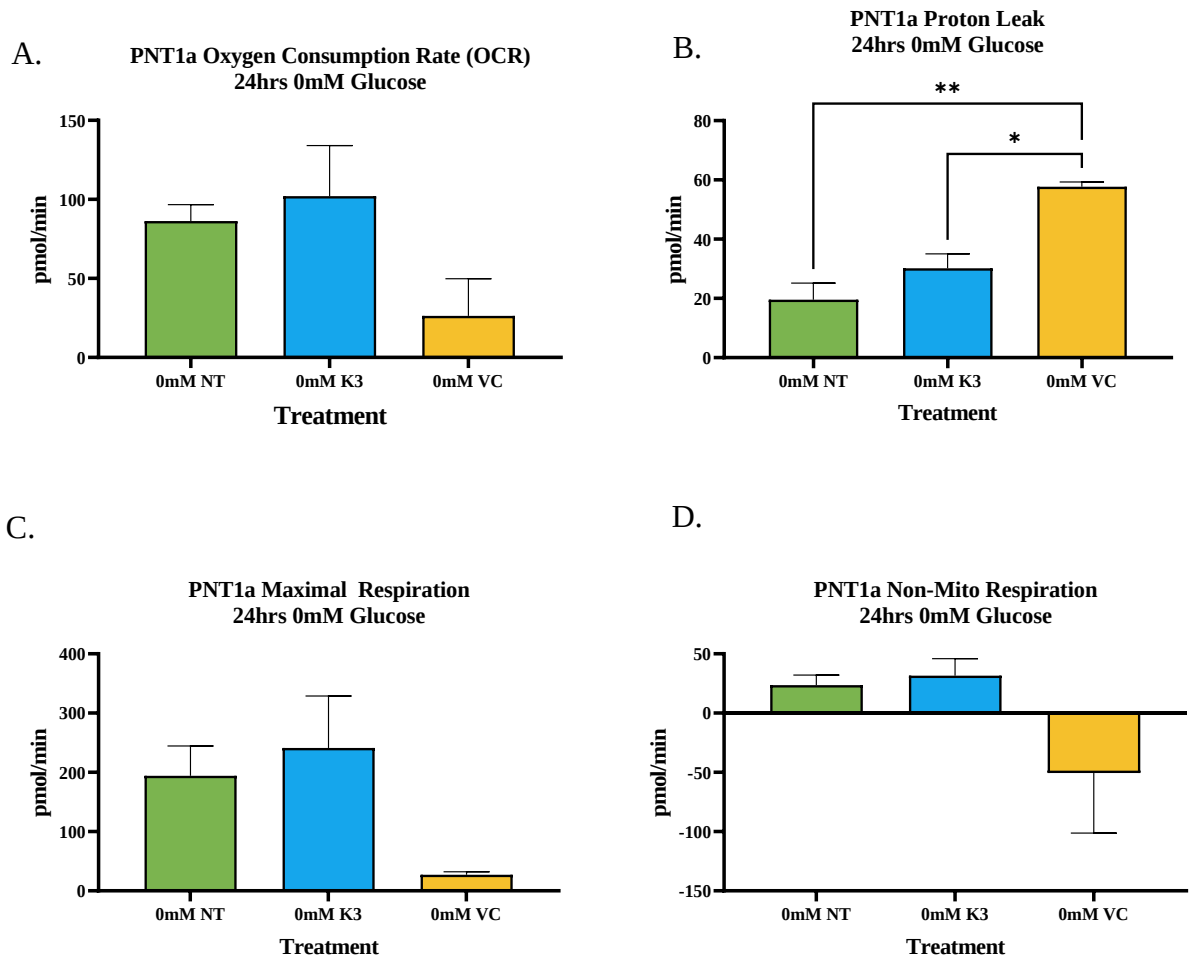

Appendix 3: The MitoStress endpoints for PNT1a cells treated with Menadione (K3) and Vitamin C (VC) under zero glucose showing the effects on the; (A) Basal OCR was unchanged between the untreated and the treated cells., (B) Proton leak was increased in the Vitamin C treated cells. (C) Maximal respiration was unchanged between the untreated and the treated cells, and (D) The non-mitochondrial respiration was unchanged between the untreated and the treated cells. (n=3) 1-way ANOVA).

Appendix 4: Agilent Seahorse MitoStress and ATP Rate Test mean results for PNT1a cells treated Menadione and Vitamin C under 0mM glucose. (n=3) 1-way ANOVA).

Treatments	Basal OCR	Proton (H+) Leak	Maximal Respiration	Non-mitochondrial respiration	ATP Production	% OxPhos	% Glycolysis
No Treatment	86.31 ± 2.9	20.4 ± 3.1	114.7 ± 6.7	23.6 ± 4.3	114 ± 17.2	86.7± 7.7	13.3 ± 7.7
Menadione (K3)	102.1 ± 32.6	34.2 ± 5.9	124.9 ± 21.4	35.8 ± 14.1	139.1 ± 31.1	75.62 ± 13.6	24.4 ± 13.6
Vitamin C	26.3 ± 8	59.3 ± 8.7	27.3 ±24.3	-50.6 ± 24.5	159.8 ± 4.9	70.4 ± 13	18.5 ± 13

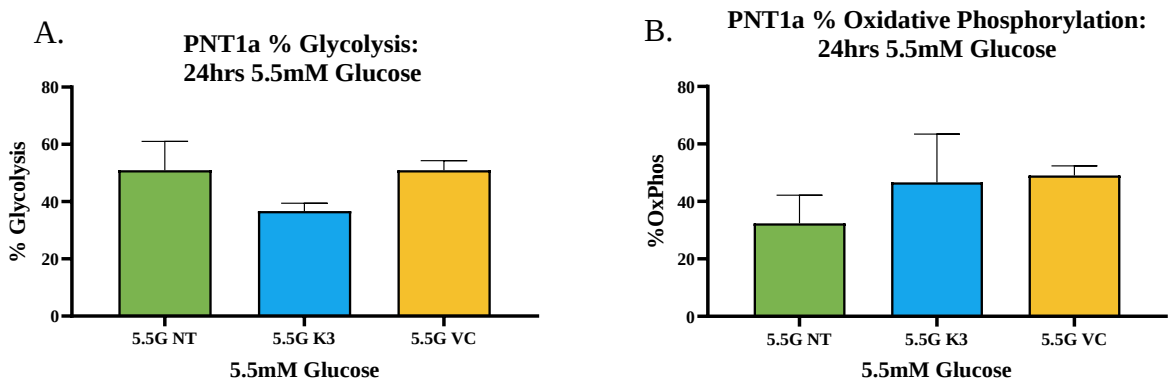

Appendix 5: The ATP endpoints of %OxPhos and %Glycolysis for PNT1a cells treated with Menadione (K3) and Vitamin C (VC) under 5.5mM Glucose (n=3) 1-way ANOVA). (A.) % ATP production by glycolysis was unchanged between the untreated and the treated cells. (B.) %ATP Production by OxPhos was unchanged between the untreated and the treated cells

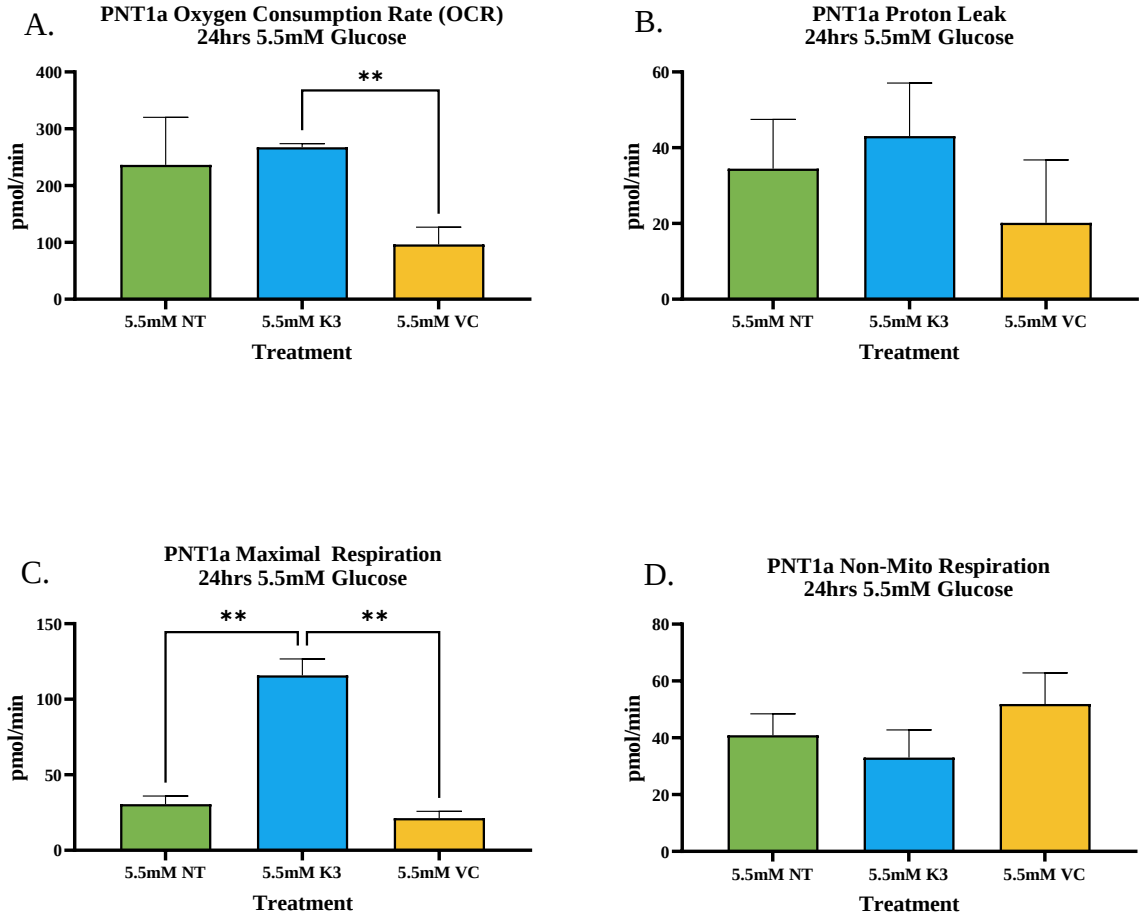

Appendix 6: The MitoStress endpoints for PNT1a cells treated with Menadione (K3) and Vitamin C (VC) under 5.5mM glucose showing the effects on the; (A) Basal OCR was decreased in the Vitamin C treated cells versus the Menadione treated cells. (B) Proton leak was unchanged between the untreated and the treated cells. (C) Maximal respiration was increased in the Menadione treated cells compared to the untreated, and the Vitamin C treated cells. and (D) The non-mitochondrial respiration was unchanged between the untreated and the treated cells. (n=3) 1-way ANOVA).

Appendix 7: Agilent Seahorse MitoStress and ATP Rate Test mean results for PNT1a cells treated Menadione and Vitamin C under 5.5mM glucose. (n=3) 1-way ANOVA).

Treatments	**Basal OCR**	**Proton (H+) Leak**	**Maximal Respiration**	**Non-mitochondrial respiration**	**ATP Production**	**% OxPhos**	**% Glycolysis**
No Treatment	236.5 ± 53.9	42.9 ± 10.7	30.6 ± 13.2	40.9 ±28.0	174.7 ± 12.3	51 ± 9.6	49 ± 9.6
Menadione (K3)	267.4 ± 53.1	43.1 ± 12.7	115.8 ± 68.5	33.0 ± 18.6	128.6 ± 56.7	36.7 ± 27.6	63.3±27.6
Vitamin C	47.0 ± 20.8	36.8 ± 1.1	21.3 ± 24.7	51.93 ± 20.1	79.8 ± 6.24	51± 20.4	49 ± 20.4

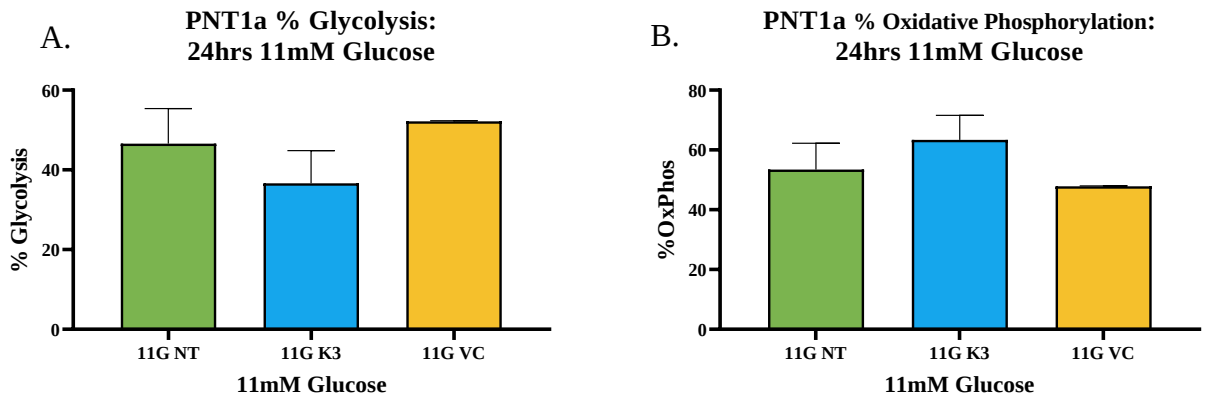

Appendix 8:The ATP endpoints of %OxPhos and %Glycolysis for PNT1a cells treated with Menadione (K3) and Vitamin C (VC) under 11mM Glucose. (A.) % ATP production by glycolysis was unchanged between the untreated and the treated cells. (B.) % ATP Production by OxPhos was unchanged between the untreated and the treated cells. (n=3) 1-way ANOVA).

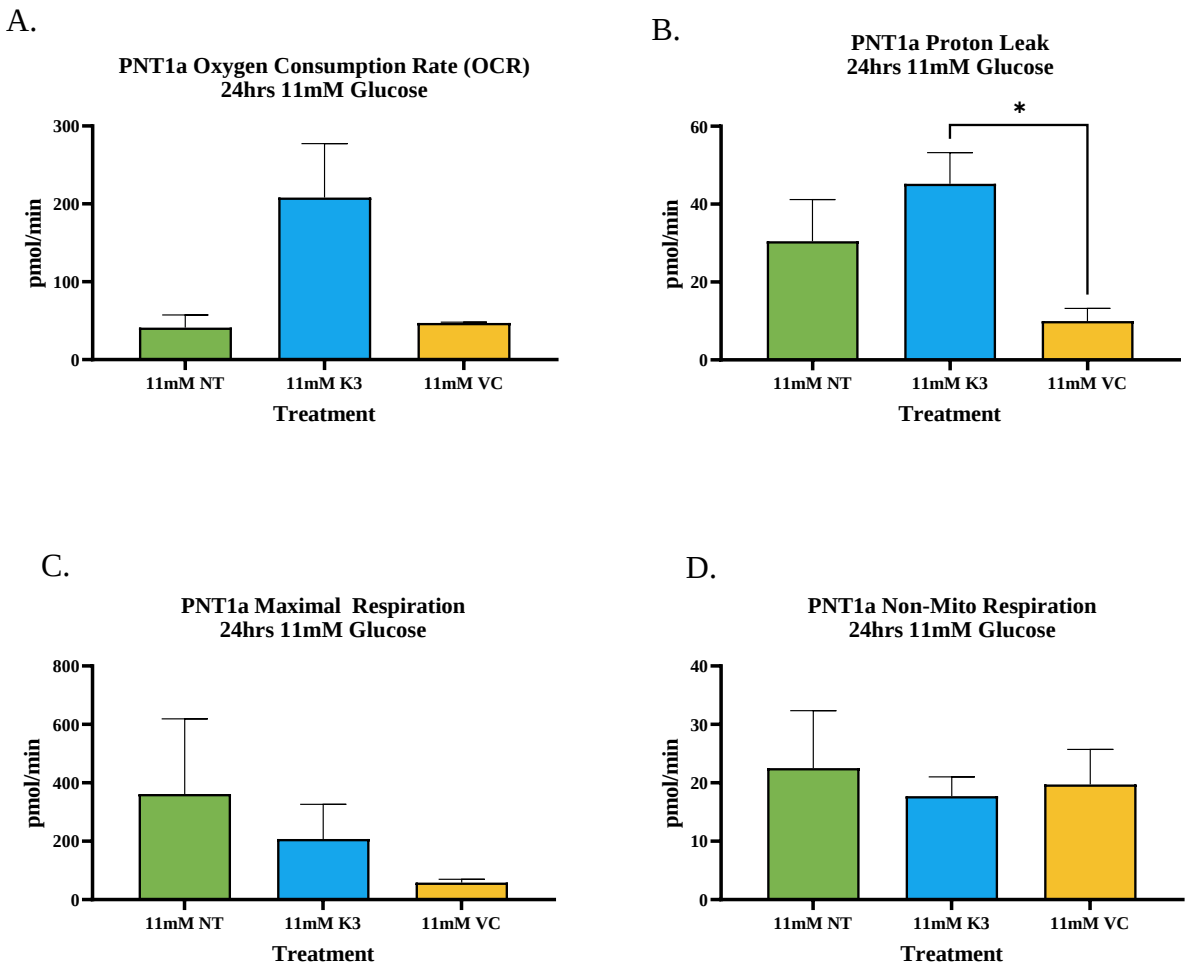

Appendix 9: The MitoStress endpoints for PNT1a cells treated with Menadione (K3) and Vitamin C (VC) under 11mM glucose showing the effects on the; (A) Basal OCR was unchanged between the untreated and the treated cells., (B) Proton leak was decreased in the Vitamin C treated cells compared to the Menadione treated cells. (C) Maximal respiration was unchanged between the untreated and the treated cells. and (D) The non-mitochondrial respiration was unchanged between the untreated and the treated cells. (n=3) 1-way ANOVA)

Appendix 10: Agilent Seahorse MitoStress and ATP Rate Test mean results for PNT1a cells treated Menadione and Vitamin C under 11mM glucose. (n=3) 1-way ANOVA).

Treatments	Basal OCR	Proton (H+) Leak	Maximal Respiration	Non-mitochondrial respiration	ATP Production	% OxPhos	% Glycolysis
No Treatment	73.7 ± 14.8	33.5 ± 10.2	465.9 ± 69.9	22.0 ± 5.6	152.7 ± 29.1	46.6 ± 13.4	53.4 ± 13.4
Menadione (K3)	208.1 ± 20.2	51.1 ± 4.3	561.0 ± 65.1	14.8 ± 12.5	123.0 ± 15.3	36.6 ± 30.7	63.4 ± 30.7
Vitamin C	47.0 ± 38.8	13.2 ± 15.3	583.0 ± 54.1	19.7 ± 31.8	43.8 ± 30.3	52.2 ± 2.8	47.8 ± 2.8

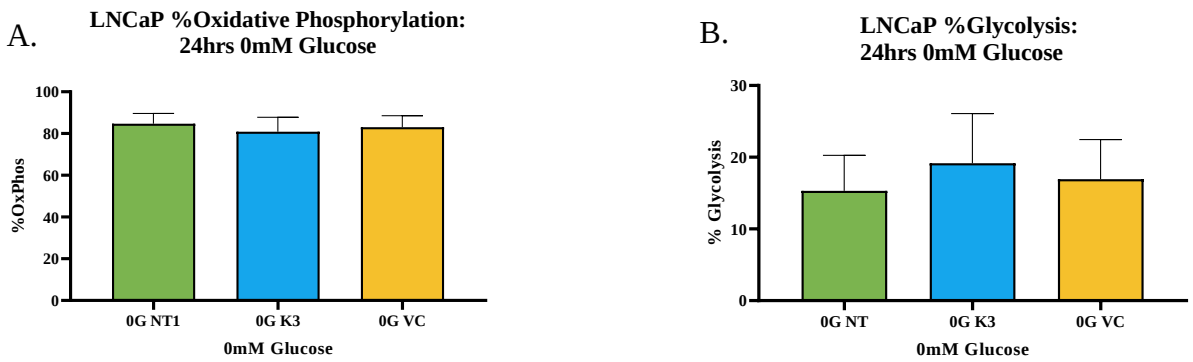

Appendix 11: The ATP endpoints of %OxPhos and %Glycolysis for LNCaP cells treated with Menadione (K3) and Vitamin C (VC) under zero glucose (A.) % ATP production by glycolysis was unchanged between the untreated and the treated cells. (B.) % ATP Production by OxPhos was unchanged between the untreated and the treated cells. (n=3) 1-way ANOVA).The impact of Vitamin C and Menadione treatment on the mitochondrial function of LNCaP cells in zero glucose conditions.

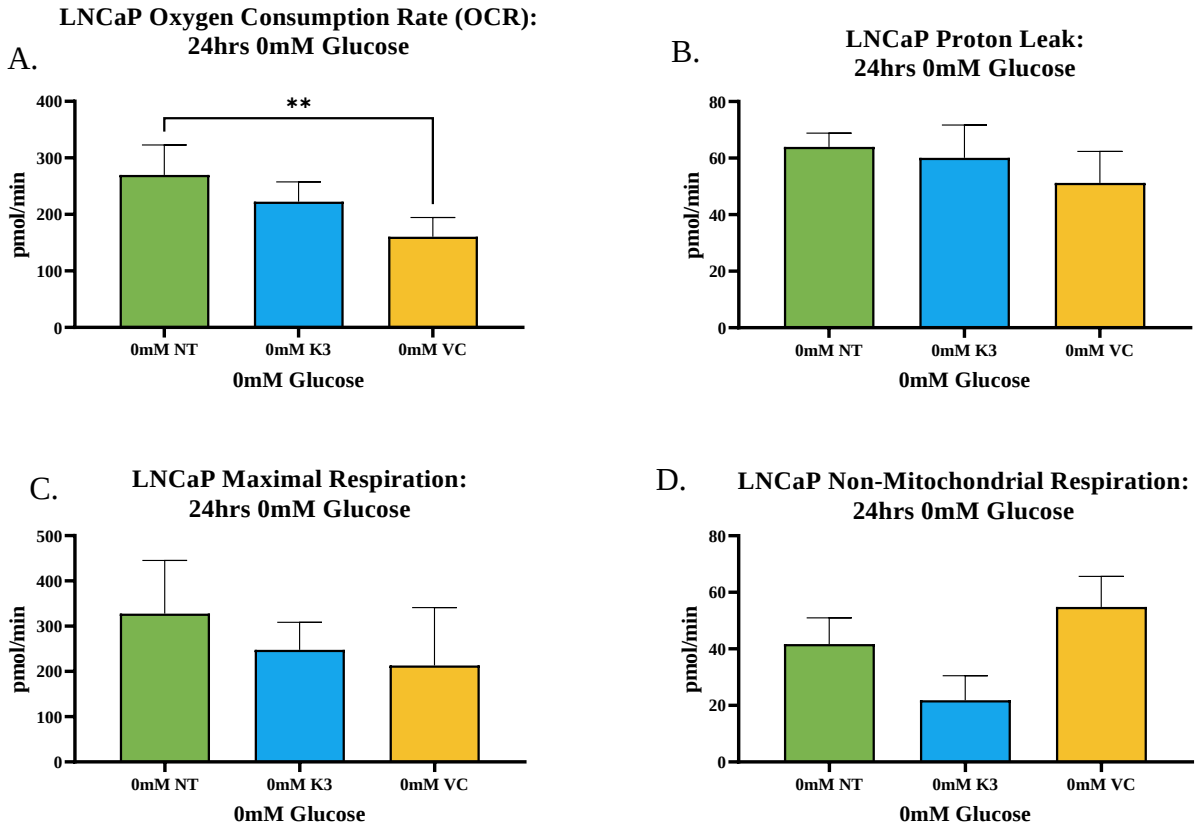

Appendix 12: The MitoStress endpoints for LNCaP cells treated with Menadione (K3) and Vitamin C (VC) under zero glucose showing the effects on the; (A) Basal OCR was decreased in the Vitamin C treated cells compared to the untreated cells. (B) Proton leak was unchanged between the untreated and the treated cells. (C) Maximal respiration was unchanged between the untreated and the treated cells. (D) The non-mitochondrial respiration was unchanged between the untreated and the treated cells. (n=3) 1-way ANOVA).

Appendix 13: Agilent Seahorse MitoStress and ATP Rate Test mean ± SD results for LNCaP cells treated Menadione and Vitamin C under 0mM glucose. (n=3) 1-way ANOVA).

Treatments	Basal OCR	Proton (H+) Leak	Maximal Respiration	Non-mitochondrial respiration	ATP Production	% OxPhos	% Glycolysis
No Treatment	269.7 ± 33.7	63.9 ± 11.5	327.7 ± 94.4	41.7 ± 7.2	200.8 ± 34.8	84.7 ± 8.6	15.3 ± 8.6
Menadione (K3)	222.7 ± 35.9	60.1 ± 9.7	247.6 ± 15.0	21.8 ± 6.7	162.5 ± 7.1	80.8 ± 8.3	19.2 ± 8.3
Vitamin C	160.5 ± 28.6	51.2 ± 44.2	212.9 ± 49.7	54.8 ± 52.1	155.2 ± 26.0	83.1 ± 8.2	16.9 ± 8.2

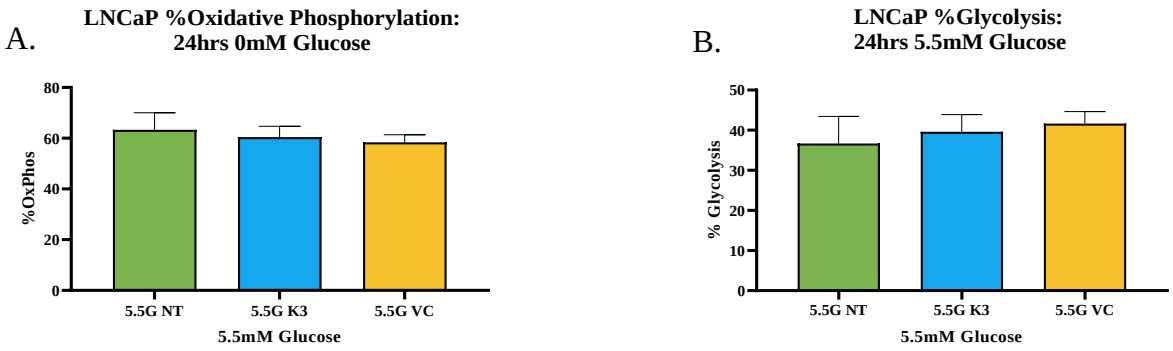

Appendix 14: The ATP endpoints of %OxPhos and %Glycolysis for LNCaP cells treated with Menadione (K3) and Vitamin C (VC) under 5.5mM Glucose. (A.) % ATP production by glycolysis was unchanged between the untreated and the treated cells. (B.) % ATP Production by OxPhos was unchanged between the untreated and the treated cells. (n=3) 1-way ANOVA).

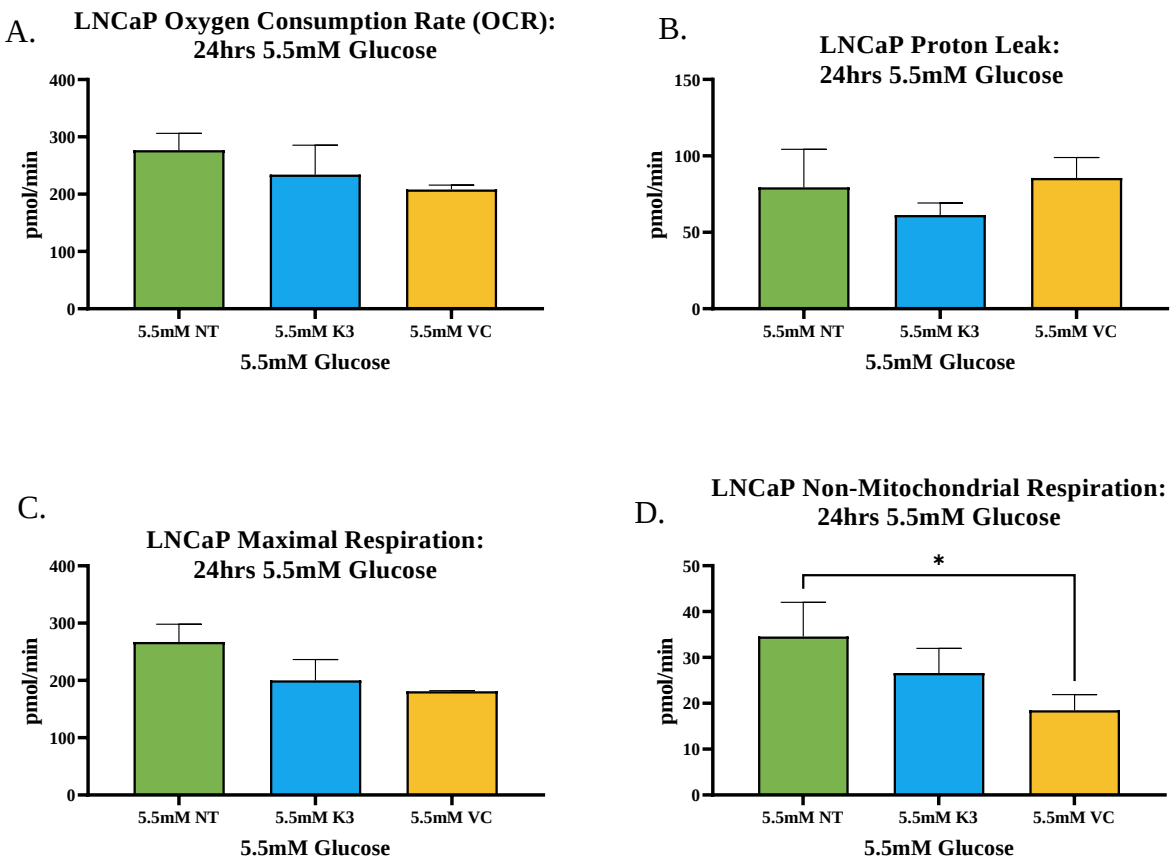

Appendix 15: The MitoStress endpoints for LNCaP cells treated with Menadione (K3) and Vitamin C (VC) under 5.5mM glucose showing the effects on the; (A) Basal OCR was unchanged between the untreated and the treated cells. (B) Proton leak was unchanged between the untreated and the treated cells. (C) Maximal respiration was unchanged between the untreated and the treated cells. (D) The non-mitochondrial respiration was decreased in the Vitamin C treated cells compared to the untreated cells. (n=3) 1-way ANOVA).

Appendix 16: Agilent Seahorse MitoStress and ATP Rate Test mean ± SD results for LNCaP cells treated Menadione and Vitamin C under 5.5mM glucose. (n=3) 1-way ANOVA).

Treatments	Basal OCR	Proton (H+) Leak	Maximal Respiration	Non-mitochondrial respiration	ATP Production	% OxPhos	% Glycolysis
No Treatment	276.8 ± 34.7	79.5 ± 31.3	267.2 ± 34.2	34.6 ± 10.4	146.2 ± 54.4	63.3 ± 4.0	36.7 ± 4.0
Menadione (K3)	234.2 ± 52.8	60.1 ± 9.7	200.2 ± 31.4	26.6 ± 2.3	199.5 ± 1.6	60.4 ± 17.5	39.6 ± 17.5
Vitamin C	208.1 ± 63.6	85.5 ± 31.5	181.1 ± 51.8	18.5 ± 6.0	125.4 ± 30.0	58.3 ± 13.7	49.1 ± 6.6

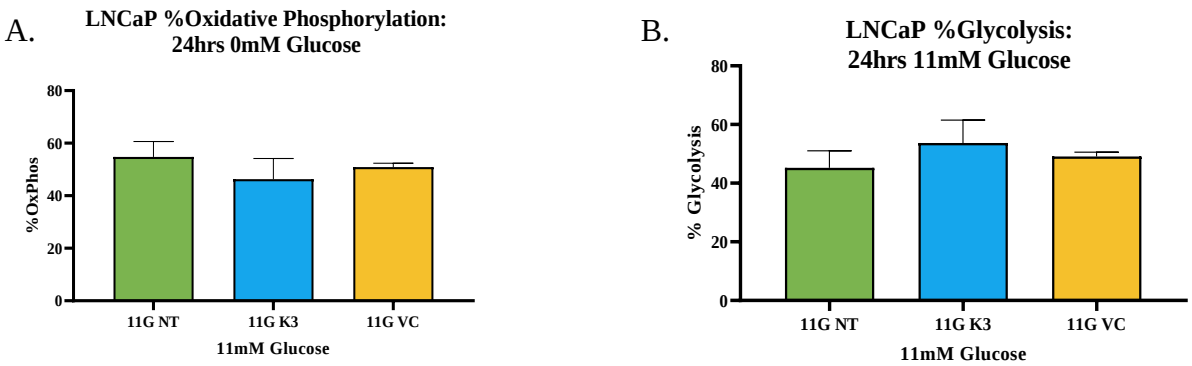

Appendix 17:The ATP endpoints of %OxPhos and %Glycolysis for PC3 cells treated with Menadione (K3) and Vitamin C (VC) under 11mM Glucose . (A.) % ATP production by glycolysis was unchanged between the untreated and the treated cells. (B.) % ATP Production by OxPhos was unchanged between the untreated and the treated cells. (n=3) 1-way ANOVA).

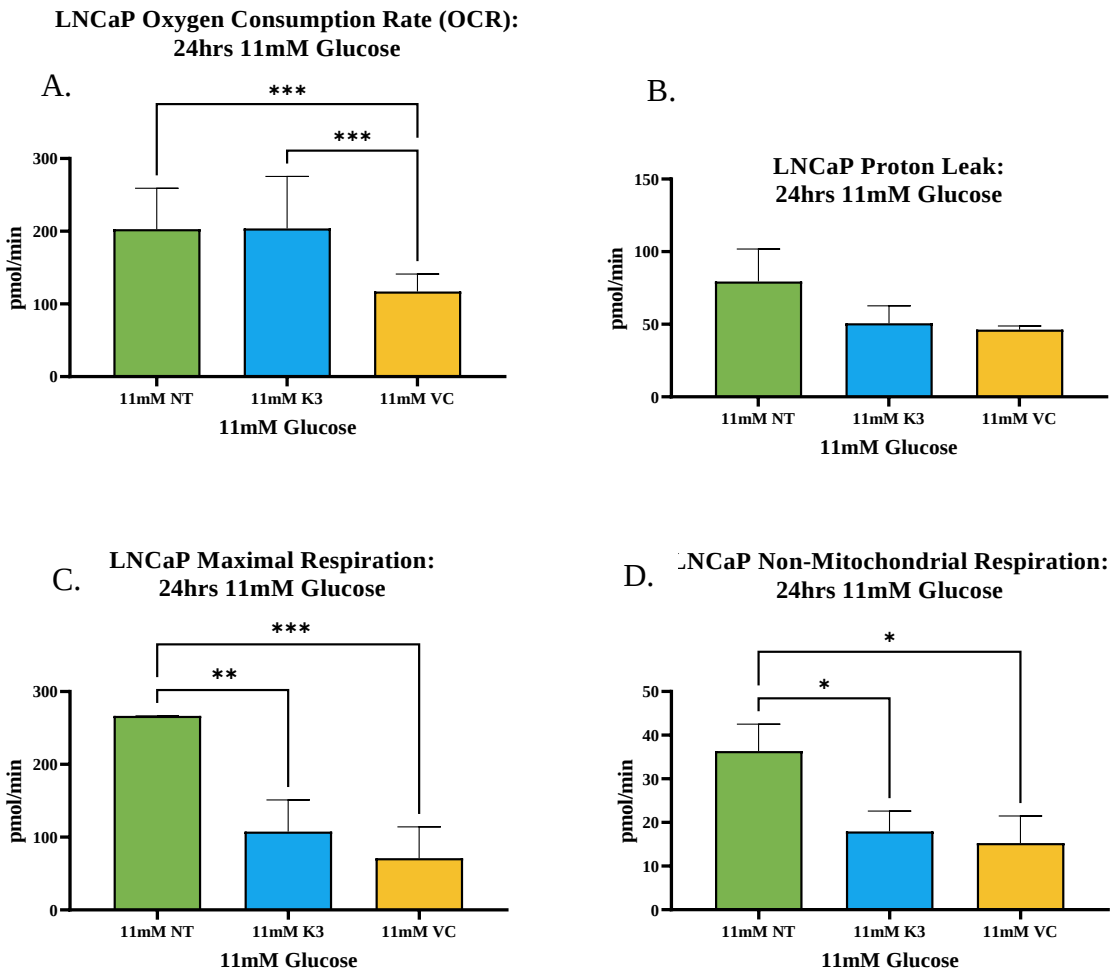

Appendix 18: The MitoStress endpoints for PC3 cells treated with Menadione (K3) and Vitamin C (VC) under 11mM glucose showing the effects on the; (A) Basal OCR was reduced in the Vitamin C treated cells compared to the untreated and the Menadione treated cells. (B) Proton leak was unchanged between the untreated and the treated cells. (C) Maximal respiration was increased in the untreated cells compared to the Menadione and the Vitamin C treated cells. and (D) The non-mitochondrial respiration was increased in the untreated cells compared to the Menadione and the Vitamin C treated cells. (n=3) 1-way ANOVA).

Appendix 19: Agilent Seahorse MitoStress and ATP Rate Test mean ± SD results for LNCaP cells treated Menadione and Vitamin C under 11mM glucose. (n=3) 1-way ANOVA).

Treatments	Basal OCR	Proton (H+) Leak	Maximal Respiration	Non-mitochondrial respiration	ATP Production	% OxPhos	% Glycolysis
No Treatment	202.9 ± 32.6	79.5 ± 19.3	266.5 ± 79.8	36.4 ± 5.9	167.4 ± 24.9	54.8 ± 3.3	45.2 ± 3.3
Menadione (K3)	204.0 ± 37.8	50.7 ± 22.6	107.5 ± 46.8	17.9 ± 4.2	124.9 ± 18.2	46.3 ± 4.8	53.7 ± 4.8
Vitamin C	117.1 ± 22.7	46.3 ± 40.9	71.0 ± 16.0	15.3 ± 15.4	81.6 ± 33.1	50.9 ± 6.6	49.1 ± 6.6

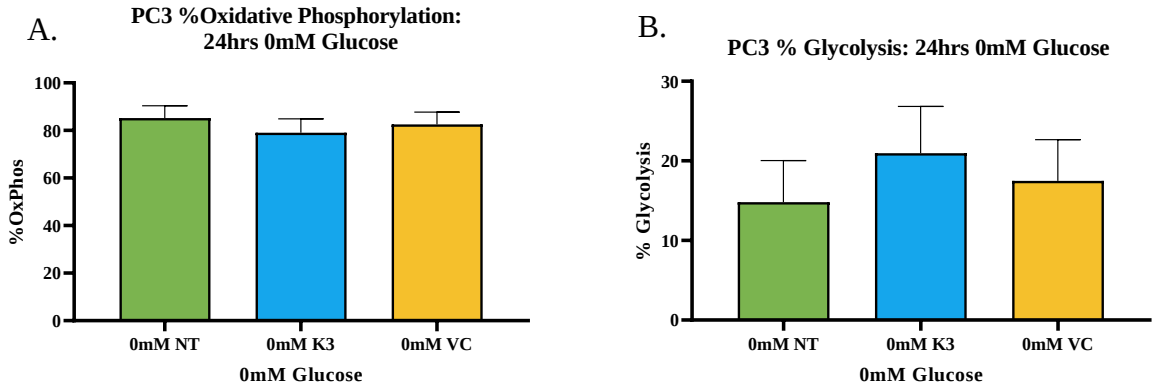

Appendix 20: The ATP endpoints of %OxPhos and %Glycolysis for PC3 cells treated with Menadione (K3) and Vitamin C (VC) under zero glucose. (A.) % ATP production by glycolysis was unchanged between the untreated and the treated cells. (B.) % ATP Production by OxPhos was unchanged between the untreated and the treated cells. (n=3) 1-way ANOVA).

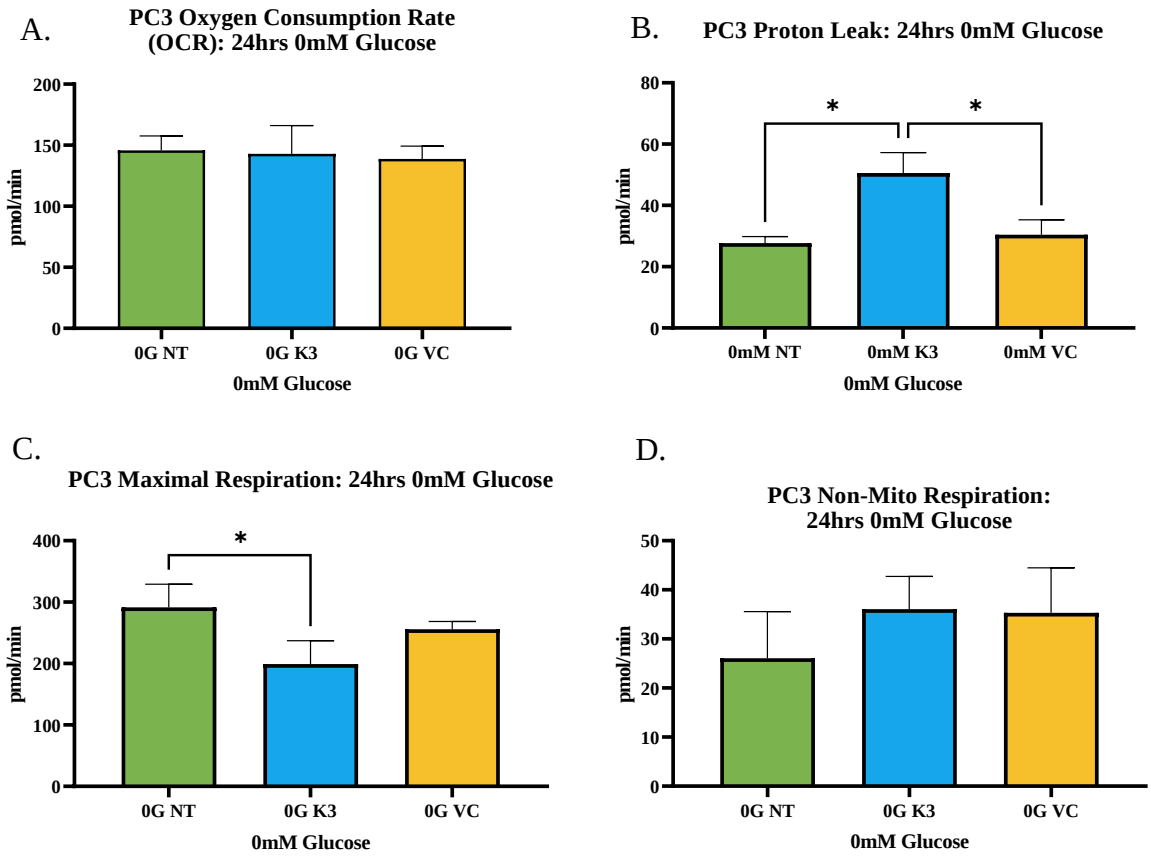

Appendix 21: The MitoStress endpoints for PC3 cells treated with Menadione (K3) and Vitamin C (VC) under zero glucose showing the effects on the; (A) Basal OCR was unchanged between the untreated and the treated cells. (B) Proton leak was increased in the Menadione treated cells compared to the untreated and the Vitamin C treated cells. (C) Maximal respiration was decreased in the Menadione treated cells versus the untreated cells. and (D) The non-mitochondrial respiration was unchanged between the untreated and the treated cells. (n=3) 1-way ANOVA).

Appendix 22: Agilent Seahorse MitoStress and ATP Rate Test mean results for PC3 cells treated Menadione and Vitamin C under 0mM glucose. (n=3) 1-way ANOVA)

Treatments	Basal OCR	Proton (H+) Leak	Maximal Respiration	Non-mitochondrial respiration	ATP Production	% OxPhos	% Glycolysis
No Treatment	147.1 ± 9.6	27.0 ± 4.7	307.1 ± 13	35.6 ± 3.1	120.1 ± 4.9	85.2 ± 9.4	14.8 ± 9.4
Menadione (K3)	137.6 ± 11.2	53.0 ±6.8	189.0± 28	42.7 ± 3.1	84.6 ± 11.5	79.1 ± 9.6	20.9 ± 9.6
Vitamin C	147.1 ±16.1	34.9 ± 11.2	265.4 ± 65.2	44.5 ± 10.1	112.2 ± 24.7	82.5 ± 8.2	17.5 ± 8.2

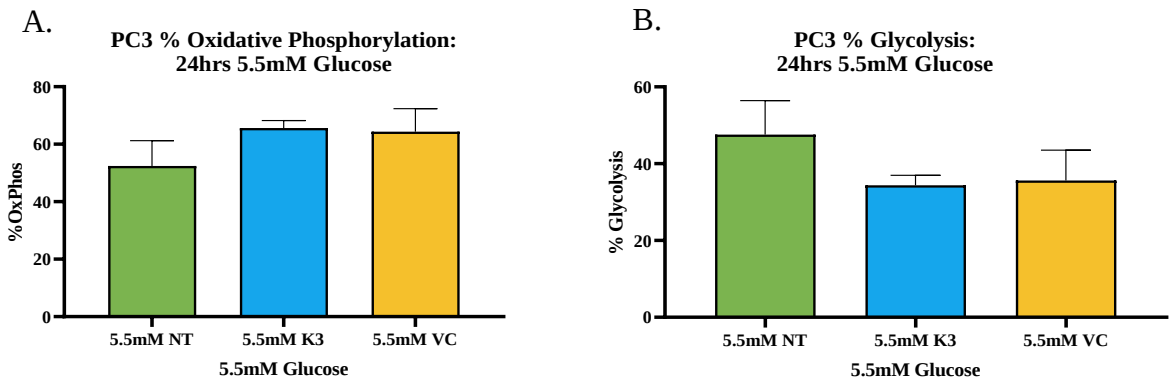

Appendix 23: The ATP endpoints of %OxPhos and %Glycolysis for PC3 cells treated with Menadione (K3) and Vitamin C (VC) under 5.5mM glucose . (A.) % ATP production by glycolysis was unchanged between the untreated and the treated cells. (B.) % ATP Production by OxPhos was unchanged between the untreated and the treated cells. (n=3) 1-way ANOVA).

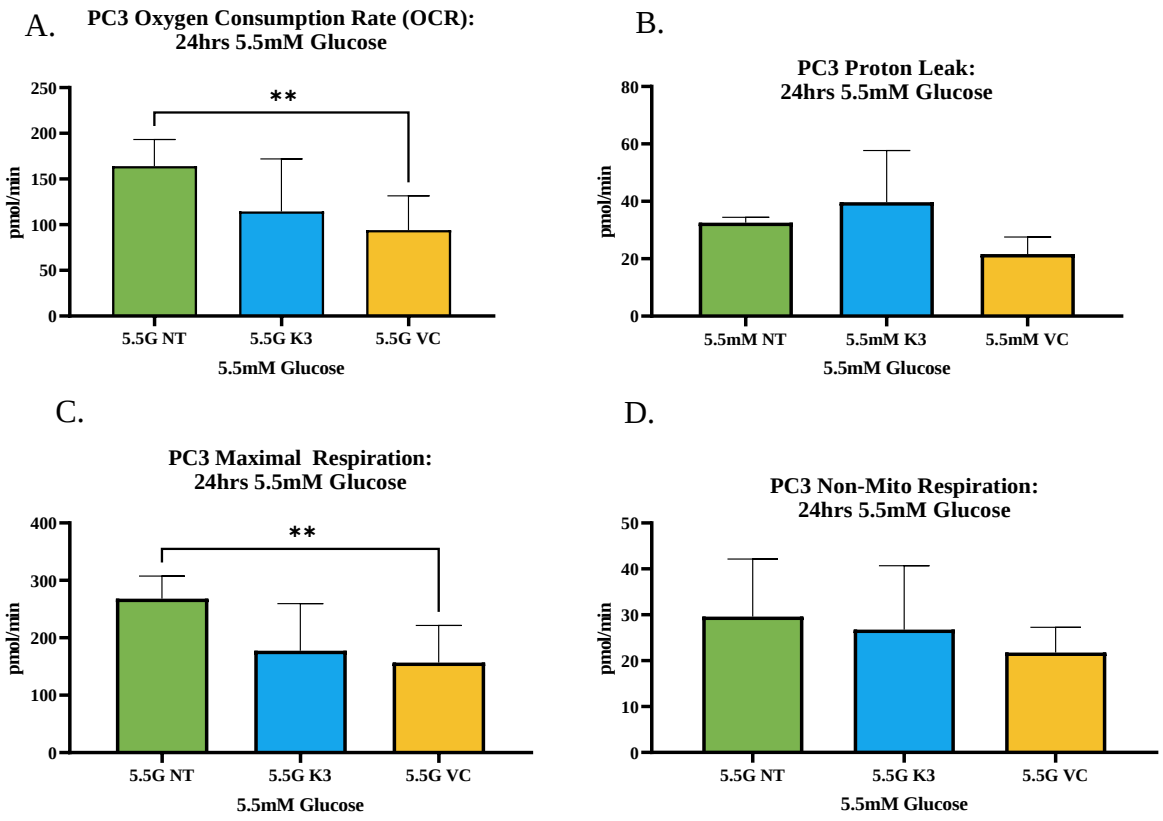

Appendix 24: The MitoStress endpoints for PC3 cells treated with Menadione (K3) and Vitamin C (VC) under 5.5mM glucose showing the effects on the; (A) Basal OCR was reduced in the Vitamin C treated cells versus the untreated cells. (B) Proton leak was unchanged between the untreated and the treated cells. (C) Maximal respiration was decreased in the Vitamin C treated cells compared to the untreated cells. and (D) The non-mitochondrial respiration was unchanged between the untreated and the treated cells. (n=3) 1-way ANOVA).

Appendix 25: Agilent Seahorse MitoStress and ATP Rate Test mean results for PC3 cells treated Menadione and Vitamin C under 5.5mM glucose. (n=3) 1-way ANOVA)

Treatments	Basal OCR	Proton (H+) Leak	Maximal Respiration	Non-mitochondrial respiration	ATP Production	% OxPhos	% Glycolysis
No Treatment	164.4 ± 35.3	33.2 ± 4.6	282 ± 56.2	29.6 ± 1.9	131.2 ± 33.3	52.4 ± 7.7	47.6 ± 7.7
Menadione (K3)	137.6 ± 11.2	49.1 ± 5.1	195.9 ± 20.1	26.8 ± 1.3	78.8 ± 18.7	65.6 ± 17.2	34.4 ± 17.2
Vitamin C	80.3 ± 10.1	34.9 ± 11.2	129.8 ± 19	21.8 ± 3.5	58.8 ± 6.4	64.4 ± 14.1	35.6 ± 14.1

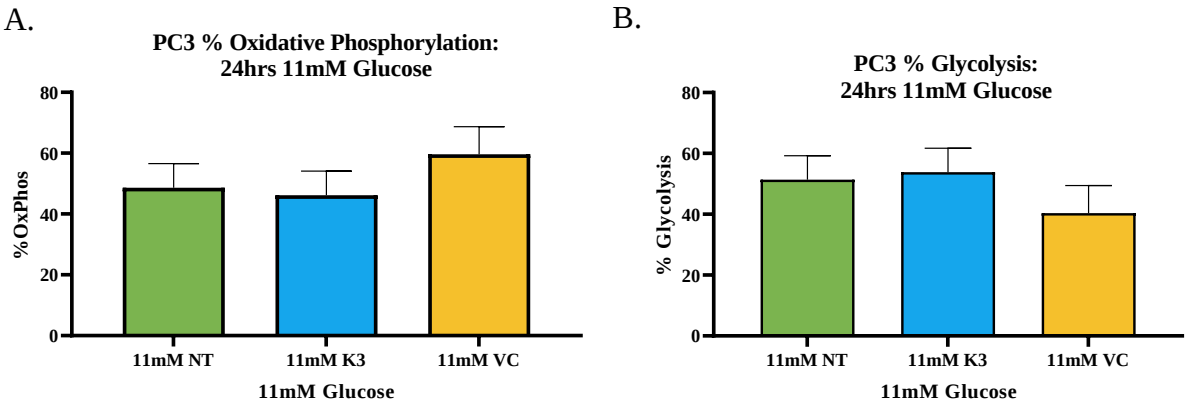

Appendix 26:The ATP endpoints of %OxPhos and %Glycolysis for PC3 cells treated with Menadione (K3) and Vitamin C (VC) under 11mM Glucose. (A.) % ATP production by glycolysis was unchanged between the untreated and the treated cells. (B.) % ATP Production by OxPhos was unchanged between the untreated and the treated cells. (n=3) 1-way ANOVA).

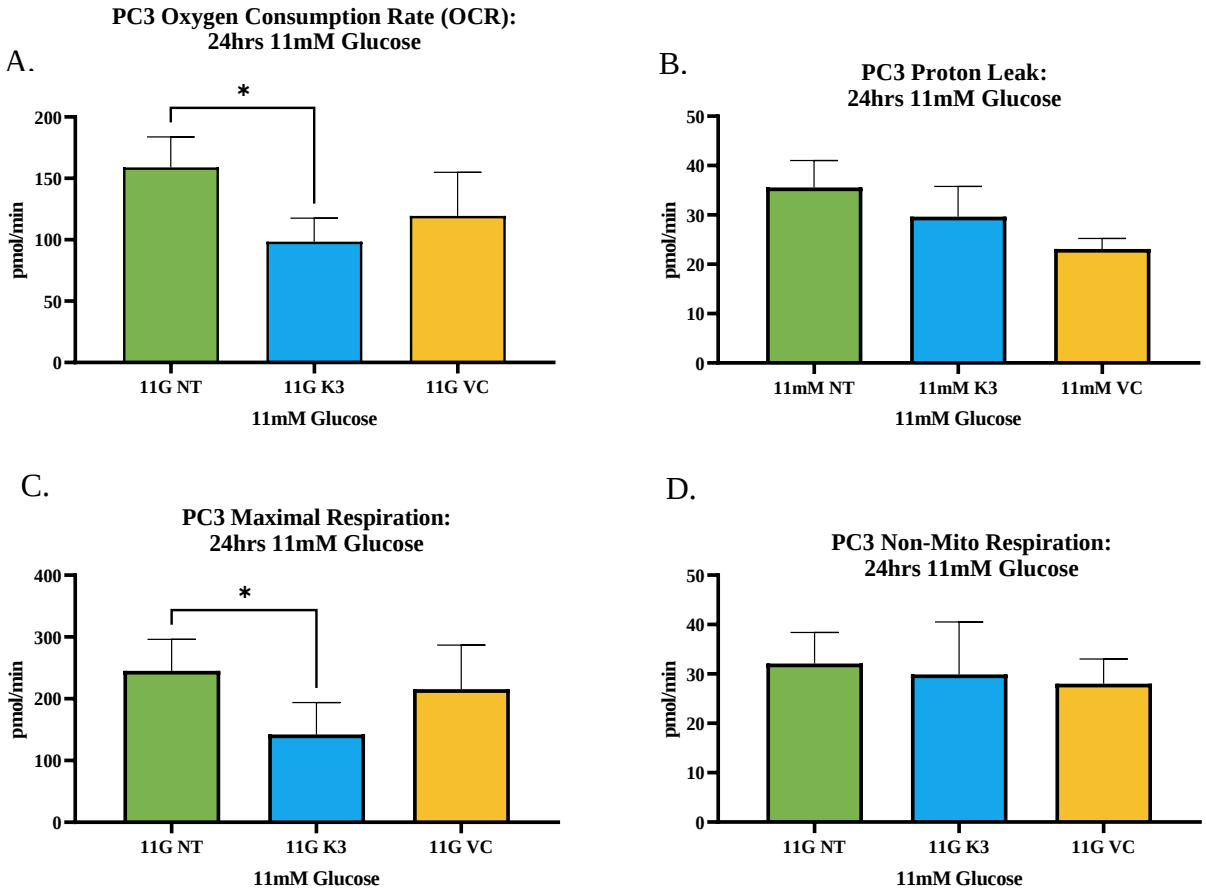

Appendix 27: The MitoStress endpoints for PC3 cells treated with Menadione (K3) and Vitamin C (VC) under 11mM glucose showing the effects on the; (A) Basal OCR was decreased in the Menadione treated cells compared to the untreated. (B) Proton leak was unchanged between the untreated and the treated cells, (C) Maximal respiration was decreased in the Menadione treated cells compared to the untreated. (D) The non-mitochondrial respiration was unchanged between the untreated and the treated cells. (n=3) 1-way ANOVA).

Appendix 28: Agilent Seahorse MitoStress and ATP Rate Test mean results for PC3 cells treated Menadione and Vitamin C under 11mM glucose. (n=3) 1-way ANOVA)

Treatments	Basal OCR	Proton (H+) Leak	Maximal Respiration	Non-mitochondrial respiration	ATP Production	% OxPhos	% Glycolysis
No Treatment	177.2 ± 27.1	40.9 ± 9.4	269.5 ± 68.6	32.1 ± 7.2	136.3 ± 17.6	48.7 ± 4.6	51.4 ± 4.6
Menadione (K3)	110.5 ± 46.9	32.6 ± 22.6	144.5 ± 30.2	29.9 ± 3.2	206.7 ± 12.1	46.2 ± 35.5	53.8 ± 35.5
Vitamin C	114.7 ± 35.8	23.1 ± 9.7	204.9 ± 63.6	28.0 ± 2.2	91.6 ± 26.2	59.6 ± 6.1	40.4 ± 6.1

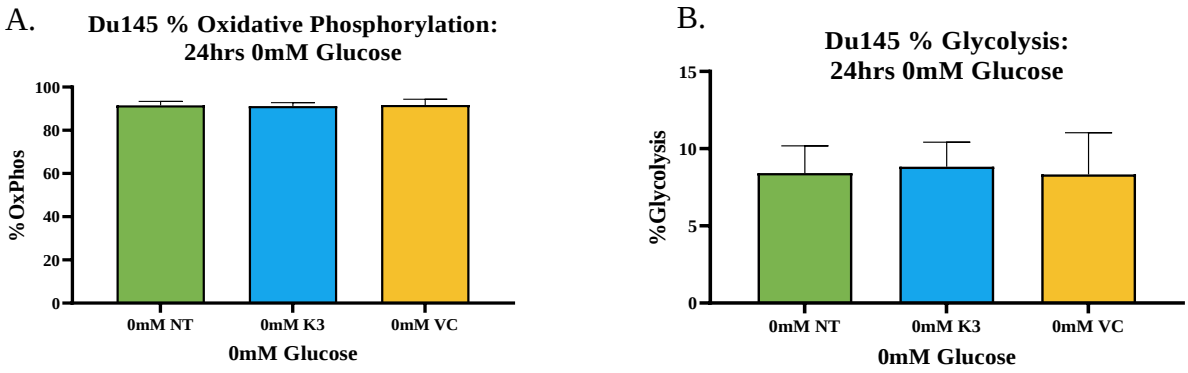

Appendix 29: The ATP endpoints of %OxPhos and %Glycolysis for Du145 cells treated with Menadione (K3) and Vitamin C (VC) under zero glucose. (A.) % ATP production by glycolysis was unchanged between the untreated and the treated cells. (B.) % ATP Production by OxPhos was unchanged between the untreated and the treated cells. (n=3) 1-way ANOVA).

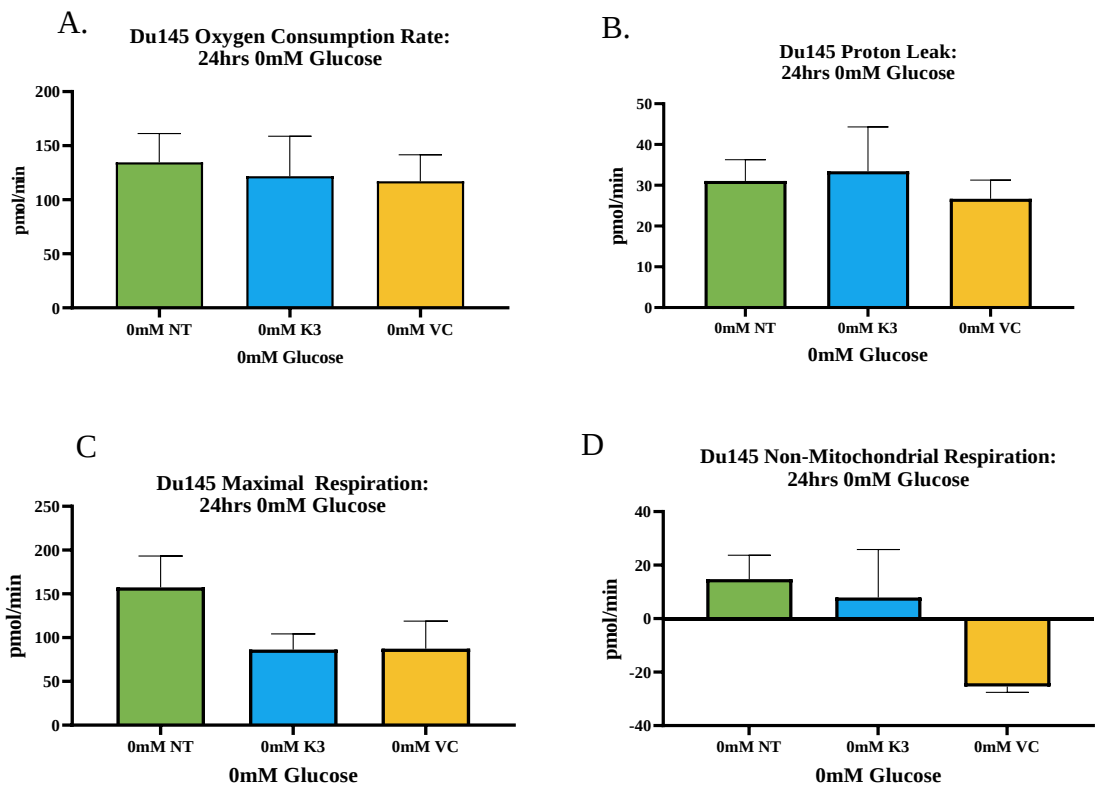

Appendix 30: The MitoStress endpoints for Du145 cells treated with Menadione (K3) and Vitamin C (VC) under glucose showing the effects on the; (A) Basal OCR was unchanged between the untreated and the treated cells. (B) Proton leak was unchanged between the untreated and the treated cells. (C) Maximal respiration was unchanged between the untreated and the treated cells. (D) The non-mitochondrial respiration was unchanged between the untreated and the treated cells. (n=3) 1-way ANOVA).

Appendix 31: Agilent Seahorse MitoStress and ATP Rate Test mean results for Du145 cells treated Menadione and Vitamin C under 0mM glucose. (n=3) 1-way ANOVA)

Treatments	Basal OCR	Proton (H+) Leak	Maximal Respiration	Non-mitochondrial respiration	ATP Production	% OxPhos	% Glycolysis
No Treatment	134.7 ± 33.8	31.0 ± 23.7	157.4 ± 40.7	14.79 ± 2.0	103.6 ± 47.1	91.6 ± 1.2	8.4 ± 0.9
Menadione (K3)	132.3 ± 76.2	33.5 ± 15.9	86.4 ± 63.4	35.4 ± 23.9	88.3 ± 59.2	91.2 ± 4.5	8.8 ± 4.5
Vitamin C	125.4 ± 32.6	26.7 ± 26.1	87.3 ± 94	-25.38 ± 3.6	80.9 ± 49.3	91.7 ± 5.2	8.3 ± 5.2

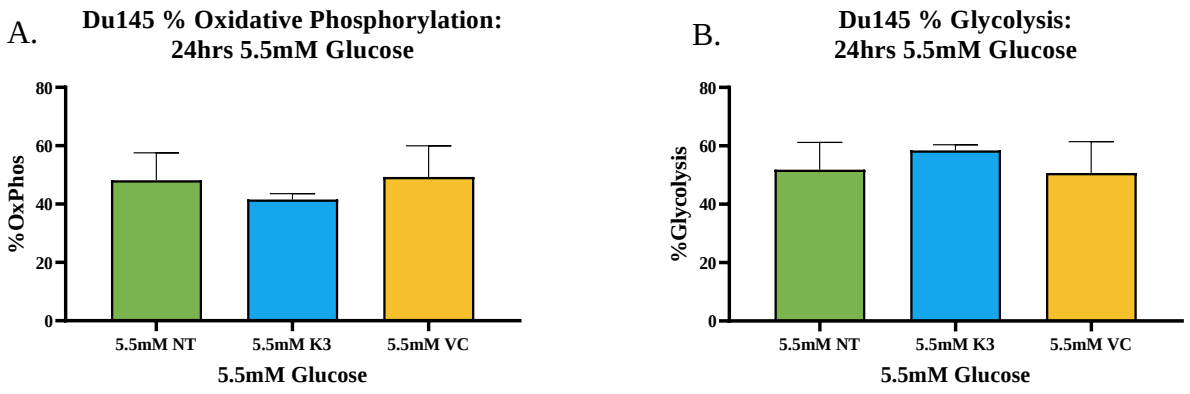

Appendix 32: The ATP endpoints of %OxPhos and %Glycolysis for PC3 cells treated with Menadione (K3) and Vitamin C (VC) under 5.5mM glucose was unchanged between the untreated and the treated cells. (A.) % ATP production by glycolysis. (B.) % ATP Production by OxPhos was unchanged between the untreated and the treated cells. (n=3) 1-way ANOVA).

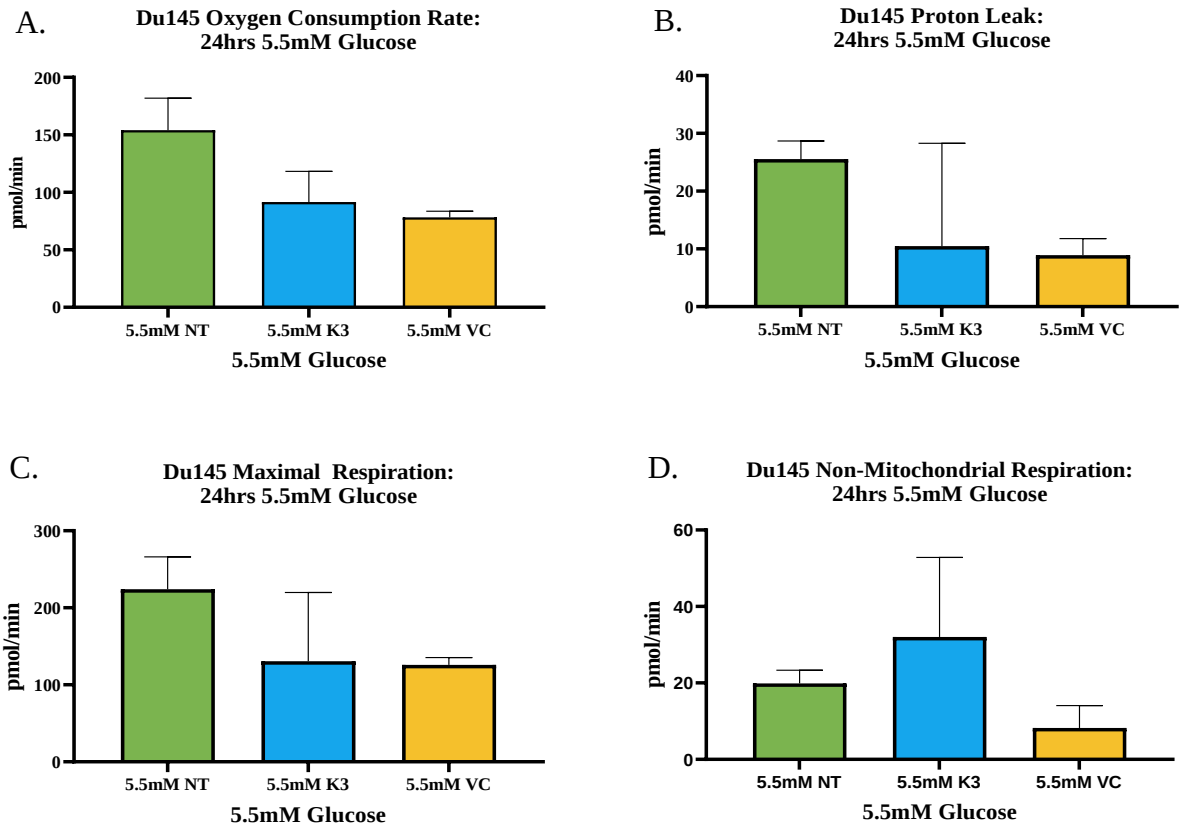

Appendix 33: The MitoStress endpoints for Du145 cells treated with Menadione (K3) and Vitamin C (VC) under 5.5mM glucose showing the effects on the; (A) Basal OCR was unchanged between the untreated and the treated cells. (B) Proton leak was unchanged between the untreated and the treated cells. (C) Maximal respiration was unchanged between the untreated and the treated cells. (D) The non-mitochondrial respiration was unchanged between the untreated and the treated cells. (n=3) 1-way ANOVA

Appendix 34: Agilent Seahorse MitoStress and ATP Rate Test mean results for Du145 cells treated Menadione and Vitamin C under 5.5mM glucose. (n=3) 1-way ANOVA)

Treatments	Basal OCR	Proton (H+) Leak	Maximal Respiration	Non-mitochondrial respiration	ATP Production	% OxPhos	% Glycolysis
No Treatment	114.0 ± 43.1	25.5 ± 11.5	224.2 ± 89.8	19.9 ± 7.2	128.6 ± 41.7	48.2 ± 5.2	51.8% ± 5.2
Menadione (K3)	113.8 ± 60.5	10.5 ± 18.0	130.6 ± 54.1	32.1 ± 24.6	53.9 ± 24.2	41.6 ± 10.8	58.4 ± 10.8
Vitamin C	84.5 ± 43.8	8.9 ± 17.8	125.8 ± 50.5	8.2 ± 23.0	63.0 ± 24.6	49.3 ± 9.8	50.7 ± 9.8

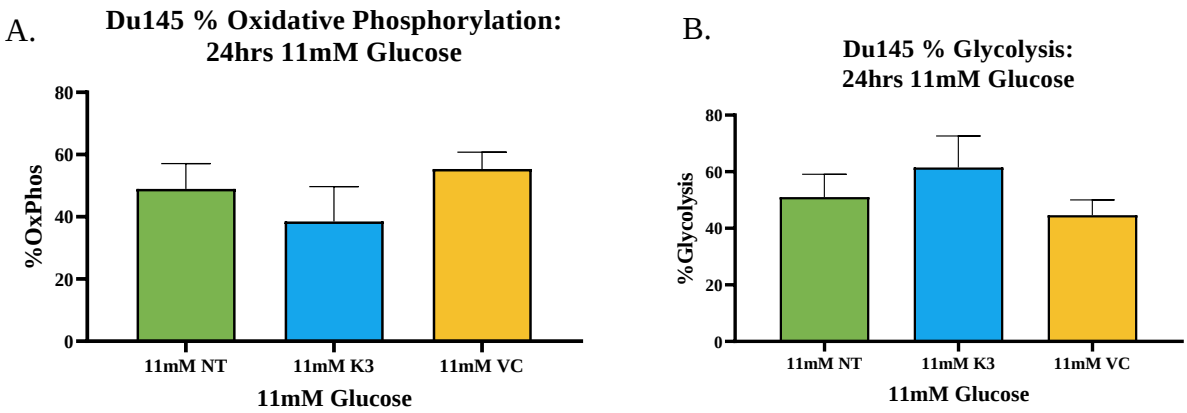

Appendix 35:The ATP endpoints of %OxPhos and %Glycolysis for Du145 cells treated with Menadione (K3) and Vitamin C (VC) under 11mM Glucose . (A.) % ATP production by glycolysis was unchanged between the untreated and the treated cells. (B.) % ATP Production by OxPhos was unchanged between the untreated and the treated cells. (n=3) 1-way ANOVA)

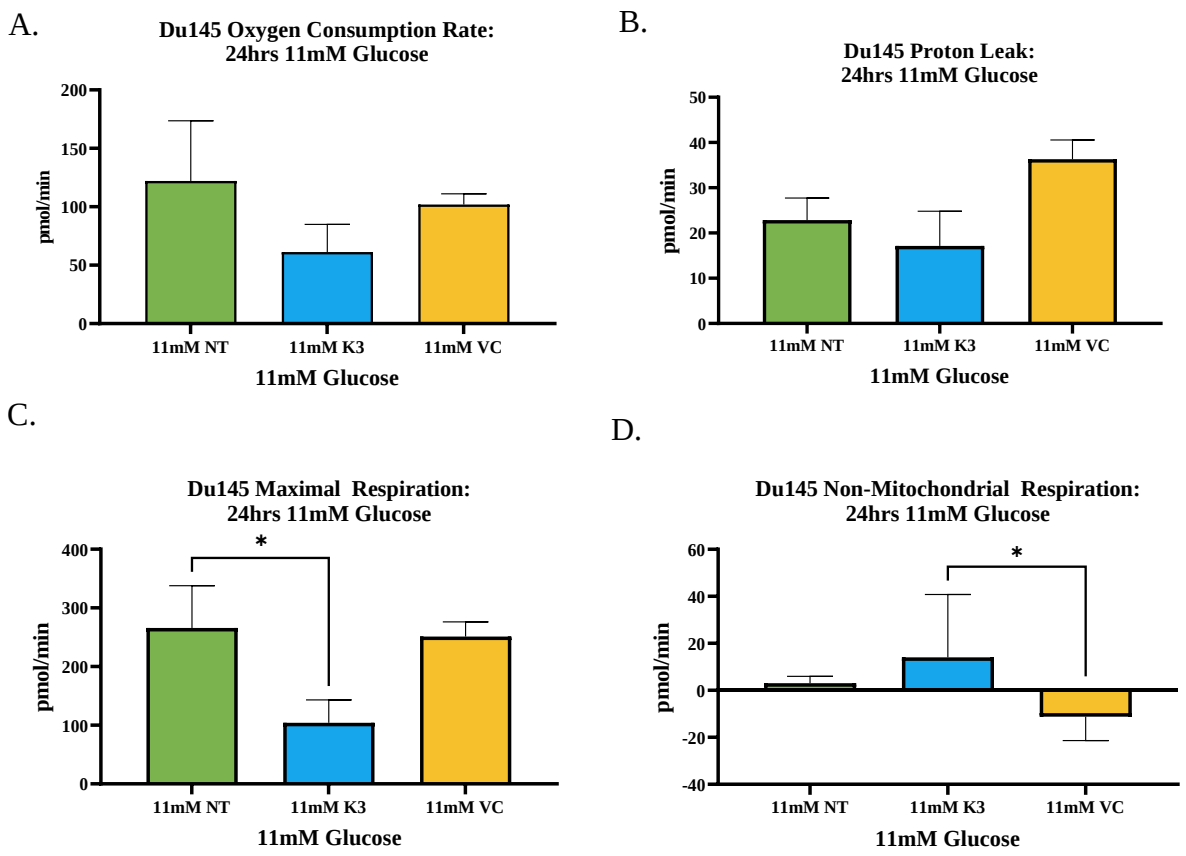

Appendix 36: The MitoStress endpoints for Du145 cells treated with Menadione (K3) and Vitamin C (VC) under 11mM glucose showing the effects on the; (A) Basal OCR was unchanged between the untreated and the treated cells (B) Proton leak was unchanged between the untreated and the treated cells. (C) Maximal respiration was decreased in the Menadione treated cells compared to the untreated cells. (D) The non-mitochondrial respiration was decreased in the Vitamin C treated cells compared to the Menadione treated cells. (n=3) 1-way ANOVA).

Appendix 37: Agilent Seahorse MitoStress and ATP Rate Test mean results for Du145 cells treated Menadione and Vitamin C under 11mM glucose. (n=3) 1-way ANOVA)

Treatments	Basal OCR	Proton (H+) Leak	Maximal Respiration	Non-mitochondrial respiration	ATP Production	% OxPhos	% Glycolysis
No Treatment	122.2 ± 76.3	22.9 ± 11.1	273.5 ± 16.81	3.0 ± 8	99.3 ± 11.8	49.0 ± 8.9	51.0 ± 7.0
Menadione (K3)	62.1 ± 11	17.1 ± 6.0	104.0 ± 32.3	14.1 ± 16.0	44.1 ± 11.1	38.5 ± 2.1	61.5 ± 2.1
Vitamin C	125.4 ± 32.6	36.3 ± 21.0	246.6 ± 61.5	-11.2 ± 12.5	71.4 ± 14.7	55.4 ± 3.4	44.6 ± 3.4

Appendix 38: Agilent Seahorse MitoStress and ATP Rate Test mean ± SD results for PNT1a cells treated with novel compounds TH1, TH4 and TH6 under 0mM glucose. (n=3) 1-way ANOVA

Treatments	Basal OCR	Proton (H+) Leak	Maximal Respiration	Non-mitochondrial respiration	ATP Production	% OxPhos	% Glycolysis
No Treatment	134.4 ± 19.7	20.4 ± 3.1	216.6 ± 80.54	23.6 ± 5.2	134.0 ± 17.1	85.5 ± 2.7	14.5± 2.7
Menadione (K3)	161.3 ± 37.1	34.2 ± 5.9	272.6 ± 36.46	40.1 ± 14.4	139.1 ± 31.1	77.7 ± 3.8	22.3± 3.8
TH 1 (TH1)	69.5± 13.2	13.7 ± 10.1	29.4 ± 5.5	1.01 ± 11.67	54.9 ± 8.3	91.5 ± 2.5	8.5± 2.5
TH 4 (TH4)	40.83± 20.1	12.7 ± 5.8	34.7 ± 5.7	22.0 ± 15.0	37.4 ± 4.0	86.7 ± 7.5	13.3± 7.5
TH 6 (TH6)	151.1 ± 32.2	24.7 ± 17.1	141.8 ± 77.2	75.9 ± 37.7	140.3 ± 31.0	77.4 ± 6.5	22.6± 6.5

Appendix 39: Agilent Seahorse MitoStress and ATP Rate Test mean ± SD results for LNCaP cell lines treated with novel compounds TH1, TH4 and TH6 under 0mM glucose. (n=3) 1-way ANOVA)

Treatments	Basal OCR	Proton (H+) Leak	Maximal Respiration	Non-mitochondrial respiration	ATP Production	% OxPhos	% Glycolysis
No Treatment	522.4 ± 64.5	132.0 ± 14.9	647.1 ± 71.4	45.2 ± 13.6	390.5 ± 49.6	90.6 ± 2.2	9.4 ± 2.2
Menadione (K3)	469.7 ± 59.8	128.0 ± 13.3	547.2 ± 27.7	38.7 ± 8.2	341.9 ± 46.5	77.8 ± 17.4	22.2 ± 17.4
TH1	237.1 ± 26.4	135.1 ±25.9	214.5 ± 16.6	80.9 ± 40.6	143.3 ±16.1	87.4 ± 13.6	12.6 ±13.6
TH4	457.4 ± 75.4	118.9 ± 13.7	437.6 ± 21.3	48.8 ± 12.7	338.5 ± 33.7	91.0 ± 3.0	9.0 ± 3.0
TH6	119.9 ± 71.9	23.3 ± 51.7	328.0 ± 70.7	43.3 ± 41.8	97.4 ± 18.0	73.9 ± 11.9	26.1 ± 11.9

Appendix 40: Agilent Seahorse MitoStress and ATP Rate Test mean ± SD results for PC3 cell lines treated with novel compounds TH1, TH4 and TH6 under 0mM glucose. (n=3) 1-way ANOVA)

Treatments	Basal OCR	Proton (H+) Leak	Maximal Respiration	Non-mitochondrial respiration	ATP Production	% OxPhos	% Glycolysis
No Treatment	178.7 ±12.0	33.2 ± 3.1	306.5 ± 22.2	31.1 ± 6.3	145.5 ± 9.6	83.3 ± 8.5	16.7 ± 8.5
Menadione (K3)	126.3 ± 9.4	41.1 ± 8.1	158.0 ± 19.9	25.8 ± 4.5	76.9 ± 13.6	78.0 ± 9.3	22.0 ± 9.3
TH1	223.6 ± 23.3	58.1 ± 11.1	205.6 ± 37.1	46.3 ± 17.0	128.1 ± 29.7	91.7 ± 4.1	8.3 ± 4.1
TH4	136.0 ± 36.5	32.8 ± 9.7	187.6 ± 61.1	28.2 ± 5.2	103.1 ±26.9	80.0 ± 6.3	20.0 ± 6.3
TH6	120.9 ± 37.3	30.8 ± 6.3	205.6 ± 37.1	14.0 ± 17.9	90.1 ± 7.7	72.0 ± 10.4	28.0 ± 10.4

Appendix 41: Agilent Seahorse MitoStress and ATP Rate Test mean results for Du145 cell lines under 0mM glucose (n=3) 1-way ANOVA)

Treatments	Basal OCR	Proton (H+) Leak	Maximal Respiration	Non-mitochondrial respiration	ATP Production	% OxPhos	% Glycolysis
No Treatment	158.1 ± 31.5	26.2 ± 4.3	148.3 ± 29.7	14.8 ± 17.4	390.5 ± 25.8	83.2 ± 0.6	16.8 ± 0.6
Menadione (K3)	109.7 ± 37.9	27.2 ± 14.4	93.8 ± 25.6	17.6 ± 10.2	341.9 ± 13.6	88.7 ± 1.7	11.3 ± 1.7
TH 1	115.0 ± 4.9	34.5 ± 12.0	85.7 ± 7.9	17.6 ± 2.7	145.3 ± 16.1	82.3 ± 2.3	17.7 ± 2.3
TH 4	114.4 ± 14.1	23.9 ± 3.0	113.3 ± 48.2	11.8 ± 4.5	338.5 ± 103.8	78.1 ± 3.6	21.9 ± 3.6
TH 6	107.8 ± 9.5	44.2 ± 5.5	98.2 ± 16.5	-7.2 ± 29.4	97.4 ±18.0	76.4 ± 4.2	23.6 ± 4.2

Appendix 42: Agilent Seahorse MitoStress and ATP Rate Test mean ± SD results for PNT1a cells treated with novel compounds TH1, TH4 and TH6 under 5.5mM glucose. (n=3) 1-way ANOVA)

Treatments	Basal OCR	Proton (H+) Leak	Maximal Respiration	Non-mitochondrial respiration	ATP Production	% OxPhos	% Glycolysis
No Treatment	240.2 ± 45.9	42.9 ± 10.7	93.2 ± 18.2	40.9 ± 28.0	174.7 ± 12.3	25.6 ± 14.9	74.4 ± 14.9
Menadione (K3)	252.6 ± 54.3	43.1 ± 12.7	256.9 ± 111.1	26.2 ± 7.9	96.5 ± 5.6	31.5 ± 28.5	68.5 ± 28.5
TH 1 (TH1)	19.7 ± 5.9	2.3 ± 1.7	20.5 ± 8.61	4.5 ± 1.9	12.33 ± 1.9	52.7 ± 7.1	46.8 ± 7.1
TH 4 (TH4)	42.3 ± 16.1	11.0 ± 10.2	28.4 ± 19.1	13.1 ± 9.4	31.3 ± 9.421	41.2 ± 12.8	58.8 ± 12.8
TH 6 (TH6)	210.5 ± 49.6	45.5 ± 13.8	82.4 ± 38.2	66.3 ± 48.0	152.3 ± 7.3	50.9 ± 3.9	49.1 ± 3.9

Appendix 43: Agilent Seahorse MitoStress and ATP Rate Test mean ± SD results for LNCaP cell lines treated with novel compounds TH1, TH4 and TH6 under 5.5mM glucose. (n=3) 1-way ANOVA)

Treatments pmol/min	Basal OCR	Proton (H+) Leak	Maximal Respiration	Non-mitochondrial respiration	ATP Production	% OxPhos	% Glycolysis
No Treatment	546.9 ± 84.6	160.6 ± 9.7	761.5 ± 48.2	44.5 ± 21.7	386.3 ± 39.3	72.3 ± 3.4	27.7 ± 3.4
Menadione (K3)	294.6 ± 125.1	94.2 ± 29	336.9 ± 26.0	38.9 ± 16.9	200.4 ± 15.0	60.8 ± 5.1	39.2 ± 5.1
TH1	57.0 ± 49.2	35.5 ± 22.7	42.1 ± 30.26	16.6 ± 15.9	178.0 ± 1.72	70.0 ± 7.3	30.0 ± 7.3
TH4	343.0 ± 47.3	107.2 ± 11.7	409.46 ± 99.7	71.6 ± 24.1	253.7 ± 36.3	66.6 ± 1.4	33.4 ± 1.4
TH6	142.4 ± 118.5	37.0 ± 4.9	95.4 ± 38.0	58.8 ± 9.3	134.9 ± 15.4	77.1 ± 17.1	22.9 ± 17.1

Appendix 44: Agilent Seahorse MitoStress and ATP Rate Test mean ± SD results for PC3 cell lines treated with novel compounds TH1, TH4 and TH6 under 5.5mM glucose. (n=3) 1-way ANOVA)

Treatments	Basal OCR	Proton (H+) Leak	Maximal Respiration	Non-mitochondrial respiration	ATP Production	% OxPhos	% Glycolysis
No Treatment	262.5 ± 52.1	41.2 ±7.0	265.1 ± 49.8	31.1 ± 6.3	171.7 ± 27.4	49.7 ± 5.9	50.3 ± 5.9
Menadione (K3)	136.7 ± 26.7	35.8 ± 4.4	149.3 ± 26.3	25.8 ± 4.5	74.4 ± 14.7	57.2 ± 13.6	47.8 ± 13.6
TH1	108.2 ± 35.3	44.6 ± 9.2	119.8 ± 42.1	46.3 ± 17.0	63.6 ± 26.1	30.8 ± 17.9	69.2 ± 17.9
TH4	71.8 ± 63.6	43.6 ± 35.8	79.1 ± 20.5	28.2 ± 5.2	28.2 ± 27.9	38.3 ± 9.1	61.7 ± 9.1
TH6	54.3 ± 54.2	15.6 ± 35	20.5 ± 18.7	14.0 ± 18.0	55.3 ± 35.4	31.0 ± 9.3	69.0± 9.3

Appendix 45: Agilent Seahorse MitoStress and ATP Rate Test mean results for Du145 cell lines under 11mM glucose (n=3) 1-way ANOVA)

Treatments	Basal OCR	Proton (H+) Leak	Maximal Respiration	Non-mitochondrial respiration	ATP Production	% OxPhos	% Glycolysis
No Treatment	162.3 ± 45.0	25.1 ± 11.8	268.2 ± 78.3	15.3 ± 2.3	389.8 ± 48.0	41.4 ± 5.1	58.6 ± 5.1
Menadione (K3)	97.3 ± 34.3	24.8 ± 7.9	143.6 ± 44.3	26.5 ± 8.3	103.9 ± 26.6	50.8 ± 7.6	49.2 ± 7.6
TH 1	151.0 ± 48.0	41.7 ± 46.4	179.8 ± 43.6	57.4 ± 38.4	12.8 ± 7.9	35.7 ± 3.7	64.3 ± 3.7
TH 4	166.5 ± 67.1	48.7 ± 11.5	259.3 ± 54.9	41.7 ± 6.2	173.9 ± 4.3	43.6 ± 7.4	56.4 ± 7.4
TH 6	77.7 ± 15.9	36.0 ± 4.7	47.4 ± 13.3	7.7 ± 4.9	71.9 ± 5.0	44.0 ± 5.1	56.0 ± 5.1

Appendix 46: Agilent Seahorse MitoStress and ATP Rate Test mean ± SD results for PNT1a cells treated with novel compounds TH1, TH4 and TH6 under 11mM glucose. (n=3) 1-way ANOVA)

Treatments	Basal OCR	Proton (H+) Leak	Maximal Respiration	Non-mitochondrial respiration	ATP Production	% OxPhos	% Glycolysis
No Treatment	143.2 ± 36.7	33.5 ± 10.2	346.9 ± 64.4	22.5 ± 5.2	152.8 ± 29.1	37.9 ± 20.4	62.1 ± 20.4
Menadione (K3)	140.4 ± 15.2	25.8 ±5.8	243.3 ± 27.4	17.7 ± 11.9	123. ± 15.3	52.4 ± 26.4	47.6 ± 26.3
TH1	57.45 ± 8.6	11.66 ±21.8	23.0 ± 0.6	-8.5 ± 16.2	31.3 ± 33.4	47.7 ± 12.4	52.3 ± 12.4
TH4	13.3 ± 4.8	5.0 ± 5.7	6.5 ± 4.5	-0.5 ± 29	9.7 ± 3.9	37.8 ± 16.1	62.2 ± 16.2
TH6	252.2 ± 43.9	43.6 ± 8.9	231.4 ±76.4	53.7 ± 4.2	216.4 ± 21.5	75.9 ± 13.7	24.1 ± 13.7

Appendix 47: Agilent Seahorse MitoStress and ATP Rate Test mean ± SD results for LNCaP cell lines under treated with novel compounds TH1, TH4 and TH6 under 11mM glucose. (n=3) 1-way ANOVA)

Treatments	Basal OCR	Proton (H+) Leak	Maximal Respiration	Non-mitochondrial respiration	ATP Production	% OxPhos	% Glycolysis
No Treatment	541.5 ± 58.1	157.7 ± 18.6	729.2 ± 217.0	45.5 ± 8.4	389.8 ± 27.5	55.5 ± 6.7	44.5 ± 6.7
Menadione (K3)	170.3 ± 52.5	66.3 ± 25.0	209.1 ± 35.5	26.3 ± 7.5	103.9 ± 26.5	56.1 ± 17.0	43.9 ± 17.0
TH1	52.5 ± 40.1	17.4 ± 15.1	67.1 ± 43.0	36.7 ± 12.1	12.8 ± 7.9	66.2 ± 4.4	33.8 ± 4.4
TH4	178.7 ± 44.6	91.7 ± 6.2	315.7 ± 93.8	40.7 ± 10.4	173.9 ± 4.28	69.3 ± 9.2	30.7 ± 9.2
TH6	113.3 ± 6.7	43.1 ± 13.1	98.3 ± 43.1	30.7 ± 5.9	71.9 ± 8.0	81.7 ± 13.5	18.3 ± 13.5

Appendix 48: Agilent Seahorse MitoStress and ATP Rate Test mean ± SD results for PC3 cell lines treated with novel compounds TH1, TH4 and TH6 under 11mM glucose. (n=3) 1-way ANOVA)

Treatments	Basal OCR	Proton (H+) Leak	Maximal Respiration	Non-mitochondrial respiration	ATP Production	% OxPhos	% Glycolysis
No Treatment	150.8 ± 27.5	37.7 ± 10.0	220.6 ± 52.9	34.2 ± 7.2	147.8 ±18.3	44.0 ± 4.7	56.0 ± 4.7
Menadione (K3)	87.5 ± 23.8	25.0 ± 14.8	116.28 ± 26.6	29.8 ± 9.4	126.8 ± 8.4	41.7 ± 28.1	58.3 ± 28.1
TH1	119.0 ± 65.9	39.3 ± 26.6	91.9 ± 75.3	27.4 ± 12.2	59.5 ± 8.6	26.4 ± 2.7	75.6 ± 2.7
TH4	28.7 ± 5.5	37.0 ± 31.8	14.1 ± 6.6	31.0 ± 13.2	7.1 ± 4.8	43.4 ± 2.8	57.6 ± 2.8
TH6	37.3 ± 20.4	12.8 ± 3.3	30.1 ± 13.1	14.1 ± 9.2	28.2 ± 22.16	33.2 ± 7.7	66.8 ± 7.7

Appendix 49: Agilent Seahorse MitoStress and ATP Rate Test mean results for Du145 cell lines under 5.5mM glucose (n=3) 1-way ANOVA)

Treatments	Basal OCR	Proton (H+) Leak	Maximal Respiration	Non-mitochondrial respiration	ATP Production	% OxPhos	% Glycolysis
No Treatment	149.8 ± 26.2	18.9 ± 9.8	150.1 ± 20.5	16.8 ± 7.8	386.3 ± 39.3	47.2 ± 2.8	52.8 ± 2.8
Menadione (K3)	127.4 ± 27.3	23.0 ± 18.0	163.7 ± 33.4	22.0 ± 6.5	200.4 ± 15.0	55.8 ± 5.0	44.2 ± 5.0
TH 1	101.5 ± 72.6	33.9 ± 27.1	106.1 ± 80.2	30.4 ± 17.1	17.8 ± 17.5	42.3 ± 2.1	57.7 ± 2.1
TH 4	146.9 ± 41.5	38.7 ± 16.8	230.1 ± 95.5	34.7 ± 9.3	235.7 ± 36.3	51.8 ± 4.0	48.2 ± 4.0
TH 6	106.6 ± 19.4	40.8 ± 10.7	69.3 ± 15.7	45.6 ± 18.1	134.9 ± 15.4	28.3 ± 5.0	71.7 ± 5.0

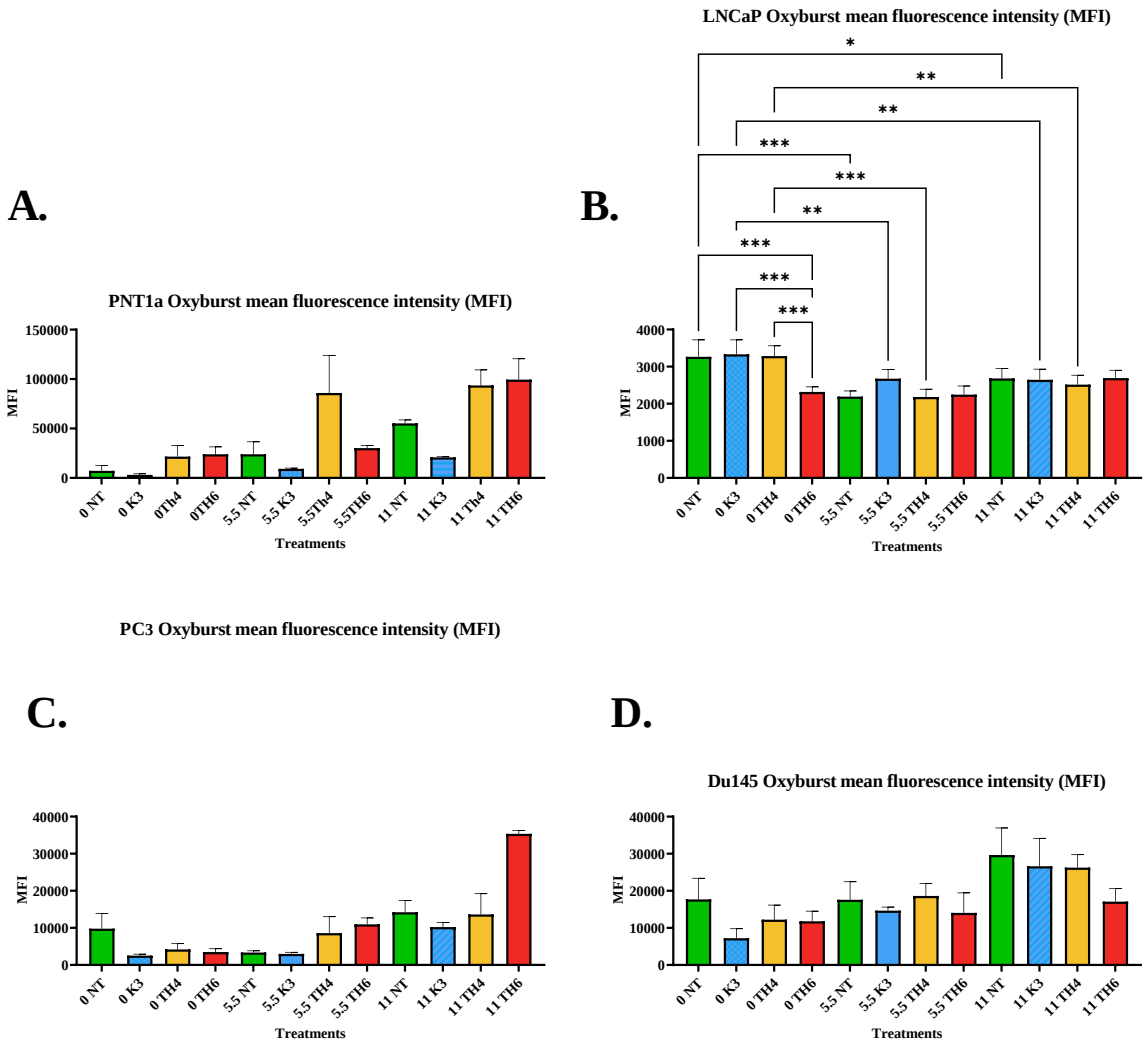

Appendix 50: Oxyburst Mean Fluorescence Intensity (MFI) in the prostate cell lines under the varied glucose milieu. (A.) PNT1a cells Oxyburst MFI in the zero, 5.5mM and 11mM glucose conditions, with no significance found. (B.) LNCaP cells Oxyburst MFI in the zero, 5.5mM and 11mM glucose conditions, with increased Oxyburst expression in the zero glucose conditions compared to the 5.5mM and the 11mM glucose conditions. (C.) PC3 cells Oxyburst MFI in the zero, 5.5mM and 11mM glucose conditions, with no significance found. (D.) Du145 cells Oxyburst MFI in the zero, 5.5mM and 11mM glucose conditions, with no significance found

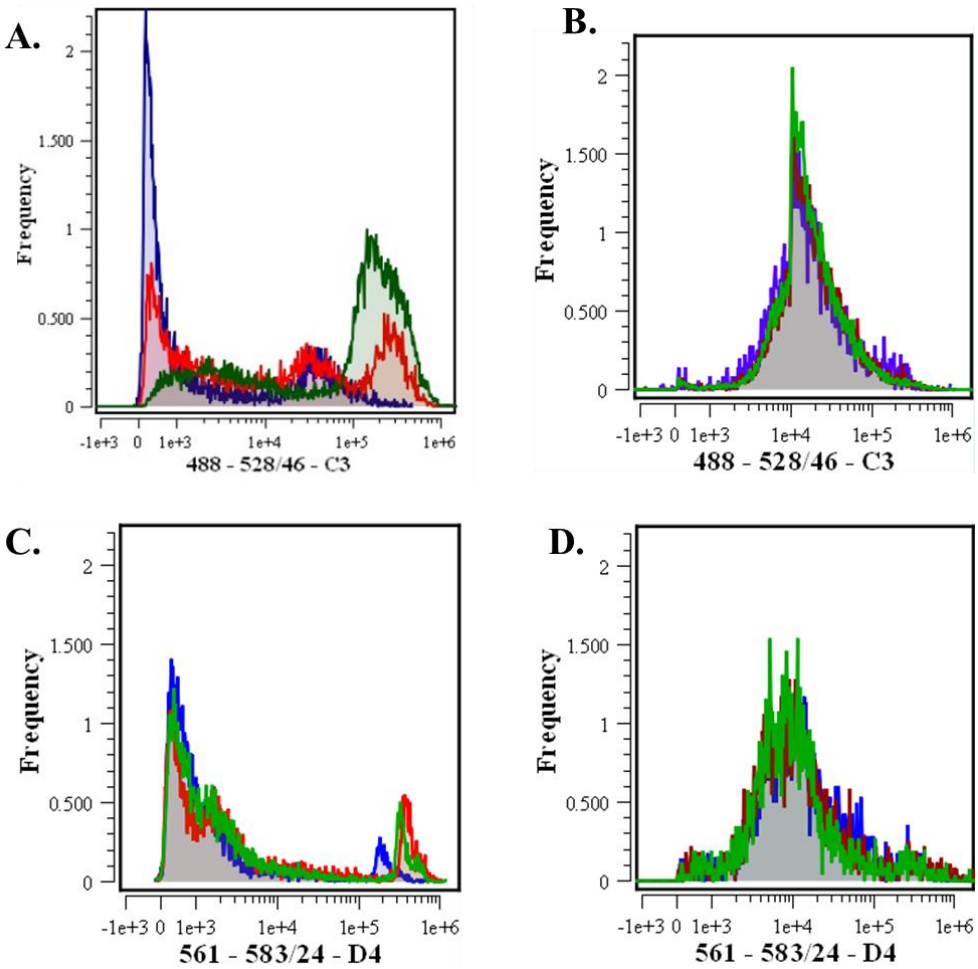

Appendix 51: (A.) Frequency histogram showing the Oxyburst frequency spread of PNT1a. cells in the zero (blue), 5.5mM (red) and 11mM (green) glucose media . (B.) JC-1 (green) Frequency histogram showing the frequency spread of the LNCaP cell line in the zero (blue), 5.5mM (red) and 11mM (green) glucose media. (C.) Av Frequency histogram showing the frequency spread of the basal PC3 cell line in the zero (blue), 5.5mM (red) and 11mM (green) glucose media. (D.) JC-1 (red) frequency histogram of the MMP spread of the Du145 cell line in the zero (blue), 5.5mM (red) and 11mM (green) glucose media.